

Faculty of Science and Engineering
Department of Spatial Sciences

Remote Sensing of West Africa's Water Resources
Using Multi-Satellites and Models

Ndehedehe, Christopher Edet

This thesis is presented for the Degree of
Doctor of Philosophy
of
Curtin University

September 2017

To the best of my knowledge and belief this thesis contains no material previously published by any other person except where due acknowledgement has been made. This thesis contains no material which has been accepted for the award of any other degree or diploma in any university.

Christopher E. Ndehedehe

A handwritten signature in blue ink, appearing to read 'Christopher E. Ndehedehe', with a stylized flourish at the end.

5th September, 2017

“I can do all things through Christ which strengtheneth me.”
- Philippians 4:13

Acknowledgements

I am very grateful to the Almighty God who through His Son, Jesus Christ, my Redeemer and personal Saviour, gave me abundant life and preserved me to see this reality. My sincere gratitude also goes to my lead supervisor A/Prof Joseph L. Awange and the two Associate Supervisors, Dr Robert J. Corner and A/Prof Richard O. Anyah (University of Connecticut, USA) for their support and guidance during the period of this study. Apart from his wealth of experience that was brought to bear, A/Prof Joseph Awange has been a great inspiration to me, and it is heartening that his advice, suggestions, and motivations were really helpful. A/Prof Michael Kuhn (Curtin University) is also acknowledged for his contributions towards this research. I deeply appreciate the support and every moment spent with my colleague, Nathan O. Agutu in the geodesy lab, and also to Dr Khandu Nakhap (Landgate, Perth) for his support during the early stages of my candidature. My colleagues Dr Onuwa Okwuashi and Dr Richard Ajah of the University of Uyo, Nigeria, are also appreciated for their advice and encouragement.

Special thanks to Curtin University for the funding received through the Curtin Strategic International Research Scholarship (CSIRS) programme, which supported my PhD work during the entire period. Am deeply appreciative of the CSIRS funding and initiative, which i will forever remain grateful to Curtin University and to God for making me a recipient. My sincere gratitude also goes to the University of Uyo for the study leave, which was accompanied by the support from the TETFUND project. I would also like to appreciate the Department of Spatial Sciences for the research facilities, conducive and enabling research environment that were provided.

My deepest appreciation goes to my beloved family. To my wife and special love, Mmayen Ndehedehe, her understanding, patience, and support during the period are invaluable. To my son, Koabasi (six years old), who at about the midnight of 17th January 2016 asked me “What’s so important about getting a PhD, is it more like you get more money when you have a PhD?”, i say thanks and God bless you. I also appreciate my two adorable and beautiful daughters, Kenderabasi (five years old) and Kereseabasi (three years old) for the joy and love they brought to my life that sustained me during the struggle. These daughters of Zion are two special people that i will forever remain grateful to God for bringing them my way. I thank my parents Mr Edet John Ndehedehe and Mrs Mmayen Edet Ndehedehe for their fervent prayers and love. My siblings, Emmanuel, Grace, and Believe are also appreciated for all their concerns and prayers.

List of Publications

Published peer reviewed journal papers

This PhD thesis is a combination of 8 peer-reviewed journal papers. These papers (6 published and 2 revised and resubmitted) summarise the significant findings of the thesis during the period of candidature (2014 – 2017). The respective thesis chapters and objectives covered by these papers are indicated in Table 1.1. Other cross-sectoral collaborations indirectly related to the thesis and in which our multi-variate techniques, machine learning, and remote sensing skills were deployed in region specific and country-level studies are also listed below. Details on copyright permissions/authorization and author and coauthor contributions to the published papers adapted for the thesis are indicated in Appendices A and B, respectively.

- (1) **Christopher Ndehedehe**, Joseph Awange, Nathan Agutu, Michael Kuhn, and Bernhard Heck (2016). Understanding changes in terrestrial water storage over West Africa between 2002 and 2014. *Advances in Water Resources*, 88, 211–230, dx.doi.org/10.1016/j.advwatres.2015.12.009.
- (2) S.A. Andam-Akorful, V.G. Ferreira **C.E. Ndehedehe** & J.A. Quaye-Ballard (2017). An investigation into the freshwater variability in West Africa during 1979 – 2010. *International Journal of Climatology*, 37(S1), 333–349, dx.doi.org/10.1002/joc.5006.
- (3) **Christopher E. Ndehedehe**, Joseph L. Awange, Michael Kuhn, Nathan O. Agutu, and Yoichi Fukuda (2017). Analysis of hydrological variability over the Volta river basin using in-situ data and satellite observations. *Journal of Hydrology: Regional Studies*, 12, 88-110, dx.doi.org/10.1016/j.ejrh.2017.04.005.
- (4) **Christopher E. Ndehedehe**, Joseph L. Awange, Michael Kuhn, Nathan Agutu, and Yoichi Fukuda (2017). Influence of climate teleconnections on West Africa’s terrestrial water storage. *Hydrological Processes*, 31(18), 3206-3224, dx.doi.org/10.1002/hyp.11237.
- (5) **Christopher E. Ndehedehe**, Joseph L. Awange, Nathan O. Agutu, and Onuwa Okwuashi (2017). Changes in hydro-meteorological conditions over Sub-Saharan Africa (1980 – 2015) and links to global climate. *Revised and resubmitted to Global and Planetary Change*.
- (6) **Christopher E. Ndehedehe**, Nathan Agutu, Onuwa Okwuashi, Vagner G. Ferreira (2016). Spatio-temporal variability of droughts and terrestrial water storage over Lake Chad Basin using independent component analysis. *Journal of Hydrology*, 540, 106 – 128, dx.doi.org/10.1016/j.jhydrol.2016.05.068.
- (7) **Christopher E. Ndehedehe**, Joseph L. Awange, Robert J. Corner, Michael Kuhn and Onuwa H. Okwuashi (2016). On the potentials of multiple climate

variables in assessing the spatio-temporal characteristics of hydrological droughts over the Volta Basin. *Science of the Total Environment*, 557 – 558, 819 – 837, dx.doi.org/10.1016/j.scitotenv.2016.03.004.

- (8) **Christopher E. Ndehedehe**, Joseph L. Awange, Michael Kuhn, and Nathan O. Agutu (2017). Hydrological controls on surface vegetation dynamics over Sub-Sahara Africa using GRACE satellite Observations. *Revised and submitted to Journal of Arid Environments*.

Other cross-sectoral collaborations indirectly related to this thesis are

- (9) **Christopher E. Ndehedehe**, Nathan O. Agutu & Onuwa Okwuashi (2017). Is terrestrial water storage a useful indicator in assessing the impacts of climate variability on crop yield in semi-arid ecosystems. Manuscript in final stage of acceptance for publication in *Ecological Indicators*.
- (10) Onuwa Okwuashi & **Christopher Ndehedehe** (2017). Prototype logistic regression based cellular automata methodology for modelling future urban land use change. Manuscript in final stage of acceptance for publication in *Journal of Land Use Science*.
- (11) Nathan O. Agutu, Joseph L. Awange, A. Zerihun, **Christopher E. Ndehedehe**, Michael Kuhn, and Yoichi Fukuda (2017). Assessing multi-satellite remote sensing, reanalysis, and land surface models' products in characterizing agricultural drought in East Africa. *Remote Sensing of Environment*, 194, 287-302, dx.doi.org/10.1016/j.rse.2017.03.041.
- (12) Onuwa Okwuashi & **Christopher Ndehedehe** (2016). Tide modelling using support vector machine regression. *Journal of Spatial Science*, 62(1), 29-46, dx.doi.org/10.1080/14498596.2016.1215272.
- (13) Onuwa Okwuashi & **Christopher Ndehedehe** (2015). Digital terrain model height estimation using support vector machine regression. *South African Journal of Science*, 111(9/10), 5 pages. dx.doi.org/10.17159/sajs.2015/20140153.
- (14) Onuwa Okwuashi & **Christopher E. Ndehedehe** (2017). A novel prototype supervised semivariogram classifier: an example-based methodology for the classification of a multispectral remote sensing image. Manuscript under review in *Remote Sensing of Environment*.

Abstract

The preponderance of evidence show that the warming of the climate system affects natural systems, leading to accelerations in the global hydrological cycle. In Africa, changes in the climate system have enormous impacts on freshwater resources, weather systems, agriculture, health, and much of the continent's remarkable biodiversity. These impacts will continue to grow with negative consequences that will hamper economic development and demean the standard of living of the world's poorest continent. Despite these deleterious impacts of climate variations, in West Africa, there are still considerable gaps however, in the knowledge of how global changes in climate impact on the region's freshwater systems. Not only is hydrology poorly understood, the knowledge of large scale temporal and spatial dynamics in land water storage, and a suitable framework to characterize key hydrological metrics and extreme weather events are lacking. West Africa play key roles in global climate and shows one of the strongest variations in climatic conditions and water resources systems. As it turns out, the region is apparently under-represented in the literature when it comes to significant discussions on terrestrial hydrology. This prominent gap is largely precipitated by increasing number of constraints such as lack of considerable and robust investments in gauge measurements for meteorological and hydrological applications amongst other factors. To improve our contemporary understanding of West Africa's terrestrial water systems and address the aforementioned issues, this thesis explored a suite of some relatively new remote sensing, global reanalysis, model, and satellite gravity data, to primarily investigate the spatio-temporal characteristics of terrestrial water storage (TWS). A new statistical-based framework to improve drought characterisation and the understanding of hydrological variability, physical characteristics, and the impacts of climate variability on eco-hydrological processes in West Africa is studied. This is achieved through a number of specific objectives that also employ, in addition, a range of multivariate techniques to analyse a suite of multi-resolution data and Gravity Recovery and Climate Experiment (GRACE) observations. This thesis outlines thoroughly documented protocols in the practical monitoring and comprehensive assessment of hydrological processes, influence of global climate and large reservoir systems on the regional dynamics of TWS. GRACE-TWS in West Africa is principally driven by rainfall unlike the Congo basin where river discharge provides the dominant control. A fourth-order cumulant statistics is introduced as novel method to support drought regionalisation and characterisation. Low frequency climate oscillations and quasi-periodic phenomena play key roles in drought characteristics and in the temporal and spatial distribution of West Africa's TWS. Contemporary and complementary perspectives on GRACE-TWS hydrological controls on surface vegetation dynamics over West Africa are also presented. In practical terms, this thesis shows that GRACE observations will continue to provide considerable leverage and unparalleled perspectives in (i) large scale hydrological studies, (ii) assessing the impacts of global climate change, and (iii) evaluating ecosystem performance in West Africa. This research has ignited a plethora of scientific findings that are not only informative but instructive and useful for public policy and management decisions related to water resources.

Contents

Acknowledgements	iv
List of Publications	v
Abstract	vii
1 Introduction	1
1.1 Global terrestrial water systems	1
1.2 West African perspective	3
1.3 Impacts of climate change on hydrological cycle	5
1.3.1 Extreme hydro-climatic conditions	8
1.3.2 Ecosystem dynamics	9
1.4 Anthropogenic interventions on hydrology	10
1.5 Earth observations and model simulations in terrestrial hydrology	12
1.6 Knowledge gaps and hydrological challenges	15
1.7 Research objectives	19
1.8 Thesis outline	20
2 Terrestrial water storage over West Africa	22
3 The impacts of reservoir systems on terrestrial water storage	61
4 The influence of climate variability on terrestrial water storage	85
5 A new method for spatio-temporal drought analysis	161
6 Hydrological controls on surface vegetation dynamics	205
7 Conclusion	242
References	245

Appendix A Copyright Permission Statements	266
Appendix B Statements of Contribution by Others	294
List of Figures	297
List of Tables	298

1 Introduction

1.1 Global terrestrial water systems

Available freshwater resources in the form of lakes, reservoirs, groundwater, and river systems are not only variable and unpredictable, but extremely limited and yet critical for terrestrial life and ecosystem services. Whereas only 2.5 % of the world's total water supply of about 1,386 million cubic kilometers is freshwater, only 29.9% and 0.26% of the total freshwater represent groundwater resources and surface waters concentrated in lakes, reservoirs, and river systems (see, [Shiklomanov, 2000](#)). Global freshwater assessments show that its availability and variability are driven mostly by human, climatic, and physiographic factors; unevenly distributed and scarce; and withdrawals are increasingly dynamic (e.g., [Alcamo et al., 2003](#); [Shiklomanov, 2000](#); [Gleick, 2000](#)). Freshwater is apparently a life-sustaining resource, an essential component of human life that plays key roles in all ecological and societal activities such as agriculture, health, ecosystem management, socio-economic development, and security. Because freshwater is limited, and greatly essential for the survival of humanity and ecosystems, its demand is increasingly multi-sectorial with agriculture not just being in strong competition, but the biggest consumer of global water resources compared to other sectors that use freshwater resources (e.g., [Brauman et al., 2016](#)). Nevertheless, as some documentary evidence suggests, water shortages (or rather scarcity) will be one of the world's most pressing challenges in the 21st century (e.g., [Freitas, 2013](#); [Rijsberman, 2006](#); [Vörösmarty et al., 2005](#); [Kuylenstierna et al., 1997](#); [Alcamo et al., 1997](#)).

Due to increasing global population, rapid urbanisation and industrialisation, the demand for freshwater is inevitably expected to rise. For example, a large number of river basins that makes up 12% of the total global area of basins with limited annual available water are already under pressure because of increased water withdrawals ([Alcamo et al., 1997](#)). While water availability is more likely to restrict economic development in these basins, a study on water balance of global aquifers reveal that an estimated 1.7 billion people live in regions where groundwater resources and groundwater dependent ecosystems are under threat ([Gleeson et al., 2012](#)). Groundwater extraction have tripled and depletion rates have doubled between 1960 and 2000 in Asia and north America ([Gleick, 2000](#)). Some new metrics based on the framework of the Inter-Sectoral Impact Model Intercomparison Project (ISI-MIP) suggest a 40% increase in the number of people living under absolute water scarcity, up from 15% of the global population with a severe decrease in water resources ([Schewe et al., 2013](#)). Whereas humanity in general takes water for granted owing to its obvious simplicity (see, [Falken-](#)

mark and Lundqvist, 1998), future simulations of freshwater availability are generally somewhat consistent and show increased water stress in the coming decades owing to population rise and the impacts of unmitigated climate change. For instance, as at the year 2000, total water withdrawals amounted to 8.4% of global water resources, and this amount is expected to increase up to 12.2% (i.e., between 4600 – 5800 km³/yr) by 2025 (Shiklomanov, 2000). In a study of global water resources, Vörösmarty et al. (2000) combined outputs from climate models with other socio-economic data to examine future availability of freshwater. Their projected estimate of global water use by 2025 is cautiously moderate and puts the value at 4700 km³/yr. Water scarcity projections based on Water Gap Model and criticality ratio estimate that about 57% and 69% of the world's population will be living in countries facing high water stress by 2025 and 2075, respectively (Alcamo et al., 1997). Although Gleick (2000) argued that these values may be somewhat too high, Kuylenstierna et al. (1997) had previously confirmed that considerable portion of the world's population will face water stress by 2025, be it moderate or severe. This essentially, suggests the need for more scientific conversations to help raise awareness not just on freshwater variability but on the susceptibility of global water resources to climate change and human-induced factors.

Numerical projections and perspectives on water scarcity and anticipated future use underscores threats to food production and livelihood. With freshwater projections of an amount less than 1000 m³/capita/yr in the world's densely populated arid areas, for example, water scarcity will likely be a major restriction to agricultural development in the coming decades (Rijsberman, 2006). About 25% of people living in Africa are already experiencing water stress while an estimated 13% are direct recipients of drought-related stress once each generation (see, Vörösmarty et al., 2005). These indicators of water stress will have significant impact on a considerable proportion of Africa's agricultural biomes, which are mostly found in arid regions. Because of such concerns and the cumulative impacts of climate variability on water availability, stormwater harvesting has recently (see, Fisher-Jeffes et al., 2017) been suggested in South Africa as possible alternative water resource that could supplement traditional urban water supplies and improve water security. Water scarcity by itself represents one of the characteristics (e.g., degree of scarcity) that could make water a potential source of strategic rivalry (Gleick, 1993). This is true for Texas, Africa, and other regions where water-related conflicts and the impacts of water scarcity on national security have been identified (Freitas, 2013; Gleick, 2000, 1993). As further mentioned in Freitas (2013), the increasing pressure on Sub-Sahara Africa's water resources is a potential source of local agitations and inter-state tensions that may eventually lead to armed conflicts. The enormous shared freshwater resources of Sub-Sahara Africa, which has reduced considerably in the past two decades (e.g., Freitas, 2013), may

exacerbate local tensions due to growing water scarcity and increased competition amongst riparian countries.

However, the underlying issues on global terrestrial water systems are three fold; (i) the impacts of climate change and/or indices of climate variability (e.g., El-Niño Southern Oscillation-ENSO), which contribute significantly to rapid changes in terrestrial water cycle (i.e., hydrological cycle) in many parts of the world (e.g., [Ndehedehe et al., 2017d](#); [Prudhomme et al., 2014](#); [Schewe et al., 2013](#); [Phillips et al., 2012](#); [Hurkmans et al., 2009](#); [Malhi and Wright, 2004](#); [Vörösmarty et al., 2000](#); [Gleick, 1989](#)), (ii) the various forms of human actions (e.g., groundwater extraction, land use change, etc), especially in the era of the Anthropocene, that alter flows and freshwater stocks thereby affecting the availability of water in a human-influenced catchments (e.g., [Konar et al., 2016](#); [Van Loon et al., 2016](#)), and (iii) poor understanding of large scale dynamics in terrestrial water systems due to insufficient observational networks for its monitoring (e.g., [Hall et al., 2014](#); [Alsdorf et al., 2007](#); [Alsdorf and Lettenmaier, 2003](#); [Alsdorf et al., 2003](#); [Vörösmarty et al., 2001](#)). As terrestrial water systems are likely to be impacted upon by global climates, such impacts will inevitably trickle down to agriculture and other sectors that depend on freshwater.

1.2 West African perspective

In Africa, hydrological variability and human modified-droughts resulting from unmitigated climate change and human activities have amazingly large negative impacts on freshwater resources, biodiversity, food security, and health amongst other factors. These deleterious impacts hampers economic development (e.g., gross domestic product-GDP) and contributes to increased poverty in one of the world's poorest continent. Despite the sweeping, recurrent climatic, hydrological, and environmental changes that affect the stability of regional income, little is known about the terrestrial water systems of West Africa. As further explored in some segments of this thesis, an increasing number of constraints (e.g., lack of robust investments in gauge measurements, political instability, government bureaucracies, etc.) combine to restrict the availability of in-situ observations for large scale hydrological research in West Africa. These problems can only be more intense with implications on water resources development, given the region's lack of preparedness, resources, and plausible policy responses.

Despite advancements in space agency programmes, developments in Earth observation and its growing applications in hydrology, West Africa's terrestrial hydrology is conspicuously under-represented in the literature. As oppose to other regions of the

world with detailed diverse applications of remote sensing data to study hydrological processes (e.g., McCabe et al., 2017; Alsdorf et al., 2016), discipline specific studies that delivers on the terrestrial hydrology and impacts of climate variability on water resources are undeniably limited and somewhat lacking for West Africa. The massive changes in land cover and land use patterns of West Africa in the last 5 decades as mentioned in Li et al. (2007) have had significant impacts on its terrestrial hydrology causing an imbalance in water budget and complex hydrological processes (Favreau et al., 2009; Séguis et al., 2004; Li et al., 2007; Leduc et al., 1997). Understanding the interactions between changes in land use practices and hydrological conditions of the region is critical for predicting future climate scenarios. However, the dwindling available freshwater resources of West Africa (e.g., Ndehedehe et al., 2017c; Freitas, 2013; Wald, 1990) and the growing pressure on water resources caused by anthropogenic activities and climate change in the region is a clarion call to remotely sensed, large scale terrestrial hydrology-focused investigation. Considering that most drainage basins in West Africa are located in hydrologically unfavourable environments (see, Anyadike, 1992), understanding the impacts of global climate change on regional dynamics in terrestrial water cycle is warranted.

West Africa is one of the world's poorest regions with increasing population and intensity in climate extremes. That population growth and freshwater variability are now significant measures of economic development (see, Hall et al., 2014; Brown and Lall, 2006), West Africa, under a climate change scenario, perhaps could be the most vulnerable to severe water stress and human-modified drought in the nearest future. As most agricultural goods are produced in regions that are vulnerable to water-related impacts, this will have massive implications not just on the economy of West Africa but other regions of the world that indirectly consume the water resources of West Africa. This arguably emphasizes the strategic importance of West African countries in global food production chain. In addition, it also suggests that the scale of the problem is global. Therefore, this thesis provides contemporary perspectives that advance our knowledge base on water resources and hydrological processes in West Africa. Given the scarcity of hydrologic information, large scale hydrological study will improve our understanding of the impacts of climate variability on the region's terrestrial water systems. In order to strengthen infrastructure and management initiatives on water resources development in West Africa, this thesis articulates new and impressive perspectives on the characterisation of space-time evolutions of extreme weather events and key hydrological metrics.

1.3 Impacts of climate change on hydrological cycle

Discussions on greenhouse effect and its implications continue to predominate the world's science and policy agenda on global change because of the growing evidence of warming in the climate system and the human influence that exacerbates it. Despite an increasing number of climate change mitigation policies, the 2014 IPCC report (IPCC, 2015) confirms that anthropogenic emissions of greenhouse gases (GHG) are the highest in history, reaching $49 \pm 4.5 \text{ GtCO}_2\text{-eq/yr}^3$ in 2010. These GHG alters the radiative equilibrium of the atmosphere, causing increase in temperature and strong changes in other components of the hydrological cycle (e.g., Gleick, 1989). The notorious GHG emissions are the principal driver of global warming, which is expected to be a major constraint on freshwater availability in the years to come. Warming of the climate system through anthropogenic GHG emissions and other multiple strings of human activities (e.g., deforestation, land use changes, etc.) affects natural systems, leading to accelerations and alterations in the global hydrological cycle. At the global scale, the weight of evidence show an ongoing acceleration of the water cycle (see, Wild et al., 2008; Huntington, 2006, and the references therein).

It has been shown that global hydrological models forced by GHG concentration and climate models indicate a considerable rise in regional and global water scarcity (Schewe et al., 2013). As mentioned in another recent report (Prudhomme et al., 2014), the increase in global severity of hydrological drought towards the end of the 21st century has been linked to the impacts of climate change. The impacts of anthropogenic-induced climate change on water resources in China however, are still unclear owing to the uncertainty of global climate models in providing realistic scenarios of the rising GHG concentrations, and the poor response of regional climate models to aerosols and ozone forcing (Paolino et al., 2012). But the countries in Africa are typical examples of regions in the world where dangerous climate thresholds exists. Clearly, multiple lines of evidence from considerable case studies in West Africa (see, e.g., Ndehedehe et al., 2016b; Hua et al., 2016; Diatta and Fink, 2014; Nicholson, 2013; Mohino et al., 2011; Paeth et al., 2012; Bader and Latif, 2011; Joly and Voldoire, 2010; Losada et al., 2010; Ali and Lebel, 2009; Boone et al., 2009; Giannini et al., 2008; Reason and Rouault, 2006; Nicholson and Grist, 2001; Nicholson et al., 2000; Janicot, 1994) show that changes in climate through perturbations of the tropical oceans, mesoscale convective systems, indices of climate variability (e.g., ENSO, Pacific Decadal Oscillation, etc.), and the West African monsoon, impact strongly on precipitation patterns. This influence on precipitation patterns arguably results in considerable changes in land water storage and increased acceleration of the hydrological cycle (see, e.g., Ndehedehe et al., 2016a; Todd et al., 2011).

One important aspect of the hydrological cycle that shows an increasing acceleration owing to climate change is precipitation. As the climate warms, the hydrological cycle accelerates, causing an increase in the spatio-temporal variability of precipitation and also in the duration and intensity of extreme events (e.g., droughts, storms, and floods). The increase in extreme weather events have implications (e.g., loss of biodiversity, increased risk of flood, soil erosion, etc.) that will affect the sustainability of water resources, hydrological systems, human health, management of storm runoff, and agriculture (Ojo et al., 2004; Gleick, 1989; Huntington, 2006, and the references therein). Historical climate records have shown West Africa's continued increased propensity towards extreme climatic conditions. The 2012 report of the World Meteorological Organization (WMO, WMO, 2013), for example, show significant climate thresholds, indicating that about 3 million people in West Africa were affected by severe flood. This flood destroyed properties and caused outbreaks of cholera and other diseases in the region. Another WMO statement in 2013 (WMO, 2015) also highlighted an extreme rainfall conditions that affected nearly all West African countries, resulting in loss of human lives, destruction of farmlands and properties. These recurring floods are obvious intensification of the hydrological cycle resulting from the impacts of climate change and or variability. In water-limited ecosystems, precipitation deficits and drought frequencies are more likely to reduce forest productivity and ecosystem services. For some regions, there may be a growing uncertainty regarding the impacts of climate change on the hydrological cycle due to contrasting results (e.g., Piao et al., 2010). However, the 'dry gets drier and wet gets wetter' paradigm is reinforced for about 10.8% of global land areas (Greve et al., 2014).

Rainfall variability in West Africa remains a profound challenge to the availability of freshwater for agriculture, hydropower generation, and other ecosystem services. The temporal and spatial dynamics of rainfall in West Africa have been heavily documented (see, e.g., Nkiaka et al., 2017; Sanogo et al., 2015; Otto et al., 2013; Paeth et al., 2012; Frappart et al., 2009; Ali and Lebel, 2009; Barbe et al., 2002; Lebel et al., 2000; Nicholson et al., 2000; Janicot, 1992), and show that rainfall is highly variable at inter-annual (year to year) and intra-annual (seasonal) time scales. In a study analysing rainfall and extensive river flow records (1931-1990) in Sub-Saharan Africa-SSA, for instance, Conway et al. (2009) found that in West Africa, rainfall variability was high and explained 40% – 60% and 60% – 80% of the changes in river flows during the periods of 1931 – 1960 and 1961 – 1990, respectively. In the central Sahel, a more extreme climate was observed as the proportion of annual rainfall linked to extreme rainfall increased from 17% during 1970 – 1990 to 21% in the 2001 – 2010 period (Panthou et al., 2014). During the period of 1968-1997 in West Africa, Nicholson et al. (2000) noted that rainfall has been on average about 15% to 40% lower compared to the 1931–1960 period. Based on coefficient of variance, Li et al. (2005) showed that

rainfall is a principal driver of water fluxes (river discharge and evapotranspiration) in West Africa and that hydrological variability is relatively higher in dry period than wet period. [Conway et al. \(2009\)](#) also confirmed this for SSA, but in addition indicated that river basin physiography and human interventions provide some form of control on inter-annual and inter-decadal variability in river flows. The West African climate has been linked to the West African Monsoon (WAM) system, a significant element of the regional climate that brings about 70% of the annual rainfall (e.g., [Sultan and Gaetani, 2016](#); [Janicot, 1992](#)). Apart from the WAM system, sea surface temperature (SST) forcings, land surface conditions, quasi-periodic phenomena (e.g., ENSO), and other low frequency global ocean signals however, play key roles in the strong inter-annual and multi-decadal variability of West African rainfall.

More recently, [Andam-Akorful et al. \(2017\)](#) analysed net-precipitation and other water budget quantities (e.g., rainfall) over West Africa during the 1979 – 2010 period using wavelet power transforms and coherence analysis. One significant aspects of the findings of the study is that observed decreasing rate of available freshwater (net-precipitation) is highly coupled to a low frequency modulating El-Niño activity that induced lower changes in rainfall variance, as well as higher evaporation variance. In the Congo basin and much of Central Africa, the hydrological conditions are even more complex owing to the local influence of SST, atmospheric circulation features and mesoscale convective systems, which regulate rainfall through their control on the rain belt (e.g., [Farnsworth et al., 2011](#); [Balas et al., 2007](#)). Whereas the recent study by [Ndehedehe et al. \(2016a\)](#) show that rainfall drives terrestrial water storage (TWS) in West Africa, drivers of hydrological variability is somewhat unclear in the Congo basin (i.e., much of Equatorial Africa). The drying trends observed in the northern Congolese forest were found to be generally consistent with declines in rainfall, TWS, and aboveground woody and leaf biomass ([Zhou et al., 2014](#)). But observed declines in TWS in three sub-basins (Congo, Ubangi, and Sangha) of the Congo river basin during the 2003 – 2012 period were attributed to deforestation ([Ahmed et al., 2014](#)). The Congo basin is an epic biodiversity that houses the world’s second largest rainforest. As highlighted by [Washington et al. \(2013\)](#), the basin is among the three prominent convective regions on Earth that dominates global rainfall climatology during transition seasons. Its hydrological characteristics, nonetheless, are less reported compared to the Amazon basin where a relatively large inventory of hydrology-related studies exist ([Alsdorf et al., 2016](#)). Hence, more studies will be required to build a concrete contemporary understanding of hydrological processes, climate feedbacks, and interactions in the region’s biophysical systems. That said, the strong inter-annual and intra-annual variability in rainfall that characterises the climate system of West Africa presents significant challenges to sustainable water resources management and economic growth.

1.3.1 Extreme hydro-climatic conditions

Population change and global warming play key roles in water scarcity. Whereas numerical experiments show that by 2025 population growth will impact global water systems more than the influence of greenhouse warming (Vörösmarty et al., 2000), Schewe et al. (2013) argue that global climate change will fundamentally continue to amplify water scarcity. In West Africa, the highly variable climatic conditions poses more threat to the numerous water and ecological resources in the region, amongst other factors (e.g., population). Since the inception of meteorological measurements, the narrative of unusual climatic thresholds and extreme climatic events (droughts and floods) in the region are apparent indications that West Africa is one of the most vulnerable regions to the impact of global climate change. For example, the spatial extent of Lake Chad, a prominent freshwater body in the world's largest interior drainage basin, declined from 24,000 km² in the 1950's to approximately 1700 km² in recent times (see, e.g., Ndehedehe et al., 2016b; Wald, 1990; Birkett, 2000; Coe and Foley, 2001; Leblanc et al., 2003; Lemoalle et al., 2012). This historic and dramatic decline of Lake Chad's surface area (Fig. 1.1) is the aftermath of the persistent and long drought episodes of the 1960s and 1980s. These severe drought episodes were continental in nature and have been linked by some diagnostic studies (e.g., Bader and Latif, 2011; Giannini et al., 2003; Fontaine and Bigot, 1993; Janicot, 1992) to large scale climatological shifts and modifications in global SST. In the Volta basin, fluctuation in food production was attributed to high variability in rainfall distribution pattern (Kasei et al., 2010) while hydrological drought years were characterised by strong decline in the water levels of Lake Volta (see, Ndehedehe et al., 2016c; Bekoe and Logah, 2013). The long term drying observed in the Central Equatorial Africa has been linked to SST variations and circulation changes associated with a weaker West African monsoon (Hua et al., 2016).

Whereas droughts contribute to food scarcity, famine, hydropower failure, and loss of biodiversity amongst others (e.g., Mpelasoka et al., 2018; Ndehedehe et al., 2016c; Zhou et al., 2014; Shiferaw et al., 2014; Bekoe and Logah, 2013), excess water such as the most recent floods across the globe (US, India, Bangladesh, Nepal, and Nigeria) could even be more devastating. Because of the epic flood caused by Hurricane Harvey in the US, Texas for instance, received about 19 trillion gallons of rainfall in four days, the highest from a tropical system (<http://mashable.com/2017/08/29/harvey-houston-flood-by-the-numbers-worst-flood/>). A total of 25 million gallons of rainfall is nonetheless, anticipated in Texas when the tropical storm dissipates, and so far, more than 17,000 people have been displaced, in addition to power outages and other catastrophic footprint of physical damages in the region. Unlike the US where such devastating flood seldom occurs, floods of this magnitude are somewhat frequent phe-

nomena and even more catastrophic in some regions of West Africa. For example, it was mentioned in [Basu \(2009\)](#) that the 2007 severe flood caused by a sequence of above normal precipitation affected about 800,000 people in West Africa. A climatological diagnostics of this anomalous flood by [Paeth et al. \(2012\)](#) indicated that it was caused by La-Niña event in the Pacific and a heightened activity of African easterly waves, amongst other factors. In 2009, torrential rains and floods affected an estimated 600,000 people in 16 West African countries, killing an estimated 159 people ([Basu, 2009](#)).

Furthermore, severe floods ravaged West Africa in 2012 and 2013; destroying human lives, farmlands, properties; and causing outbreaks of cholera and other diseases ([WMO, 2015, 2013](#)). The latest in the strings of multiple extreme wet events in the region is the recent mudslides and torrential flooding in Freetown, the capital city of Sierra Leone. According to several online reports, for example, the American Broadcasting Company (<http://abcnews.go.com/International/wireStory/official-200-dead-sierra-leone-floods-49204542>), more than 400 people died in Sierra Leone while at least 3000 people were rendered homeless as a result of this torrential flood and mudslides. Intense rainfall, deforestation, and other forms of human activities have been identified as immediate and preliminary factors for this deadly disaster (<http://news.nationalgeographic.com/2017/08/sierra-leone-mudslide-deadly-video-spd/>). As recently chronicled in West Africa ([Ndehedehe et al., 2016b](#); [Nka et al., 2015](#)), wet conditions and flood phenomenon in some Sahelian catchments are becoming more frequent and severe. The recovery of monsoon rainfall and continued increase in the occurrence of extreme weather events will unavoidably trigger large changes in the region's TWS. As part of the findings of this thesis, [Ndehedehe et al. \(2017c\)](#) suggest that the recent decline in GRACE-derived TWS and water budget quantities (2002 – 2014) within the vicinity of the lower Volta basin in West Africa are strong indications of the impacts of natural climate variations.

1.3.2 Ecosystem dynamics

Africa is generally one of the least represented regions in studies of ecosystem dynamics and the impacts of climate variability (e.g., [Hély et al., 2006](#)). As it stands, there is an increasing evidence of some level of ecosystem disturbance due to the impacts of climate variability on the region's rich biodiversity. The decline of primary production, widespread desertification, and land degradation are, for example, well known fall-outs of unprecedented droughts and water deficit conditions in the region (e.g., [Knauer et al., 2014](#); [Shiferaw et al., 2014](#); [Bader and Latif, 2011](#); [Tucker et al., 1991](#)). A recent study on Sahelian annual vegetation growth and phenology by [Pierre et al. \(2016\)](#) show

that drought shortened the mean vegetation cycle and reduced its amplitude. They argued further that despite the recovery of rainfall in the 1990s, the current conditions for green and dry vegetation are still below pre-drought conditions. It is mentioned in [Lovett et al. \(2005\)](#) that climate change will have major impacts on biodiversity with increased social consequences arising from ecological disturbance. This, as they have further highlighted, will have considerable implications on the continent's readiness to alleviate poverty and meet the Millennium Goals (Social Development Goals). Given the volume of peer-reviewed scholarly scientific articles on climate science, it is no longer novel that Africa as a whole is the most vulnerable continent to the impacts of climate variability and change. Large segments of the West African region are heavily reliant on rainfed agriculture, making the impacts of climate variability on freshwater, vegetation dynamics, and weather conditions more deleterious and devastating in the region. As it turns out, economic development is hampered by strong hydrological variability caused by the impacts of climate variability in the region (e.g., [Brown and Lall, 2006](#)). This apparently leads to critical water infrastructure needs to help mitigate the impacts of hydrological variability on food production and livelihood. Overall, in West Africa, a plethora of other case studies (e.g., [Andam-Akorful et al., 2017](#); [Panthou et al., 2014](#); [Phillips et al., 2012](#); [Todd et al., 2011](#); [Sheffield and Wood, 2008](#); [Malhi and Wright, 2004](#)) converge on the roles of climate change and indices of climate variability on precipitation changes, hydrological conditions and ecosystem dynamics.

1.4 Anthropogenic interventions on hydrology

Anthropogenic factors such as land use change and dam constructions have contributed to freshwater variability. For example, reservoirs and dams constructed along most of the world's major rivers have dramatically changed the seasonal flow rates and trends in stream flow rates (e.g., [Dai et al., 2009](#); [Yang et al., 2004](#); [Lammers et al., 2001](#)). Human induced changes in the ecosystem, accompanied by long term rise in water tables and increase in recharge were reported for south-east Australia and south-west US (see, [Scanlon et al., 2005](#); [Allison et al., 1990](#)). In West Africa, despite the severe drought conditions of the 1970s and 1980s, extensive network of well observations revealed that groundwater resources and water table in Niger increased tremendously ([Favreau et al., 2009](#); [Leduc et al., 1997, 2001](#)). This hydrological paradox was attributed to a change in land clearing and changes in land use, which caused an increase in runoff ([Descroix et al., 2009](#); [Favreau et al., 2009](#); [Séguis et al., 2004](#)). Although [Descroix et al. \(2009\)](#), in addition, argued from a hydrological perspective that this observed anomaly could possibly emanate from the hydraulic conductivity of the soil and its infiltration capacity, [Li et al. \(2007\)](#) confirmed the impacts of land use change on the hydrological regimes of Niger and Lake Chad basins. They showed that complete deforestation

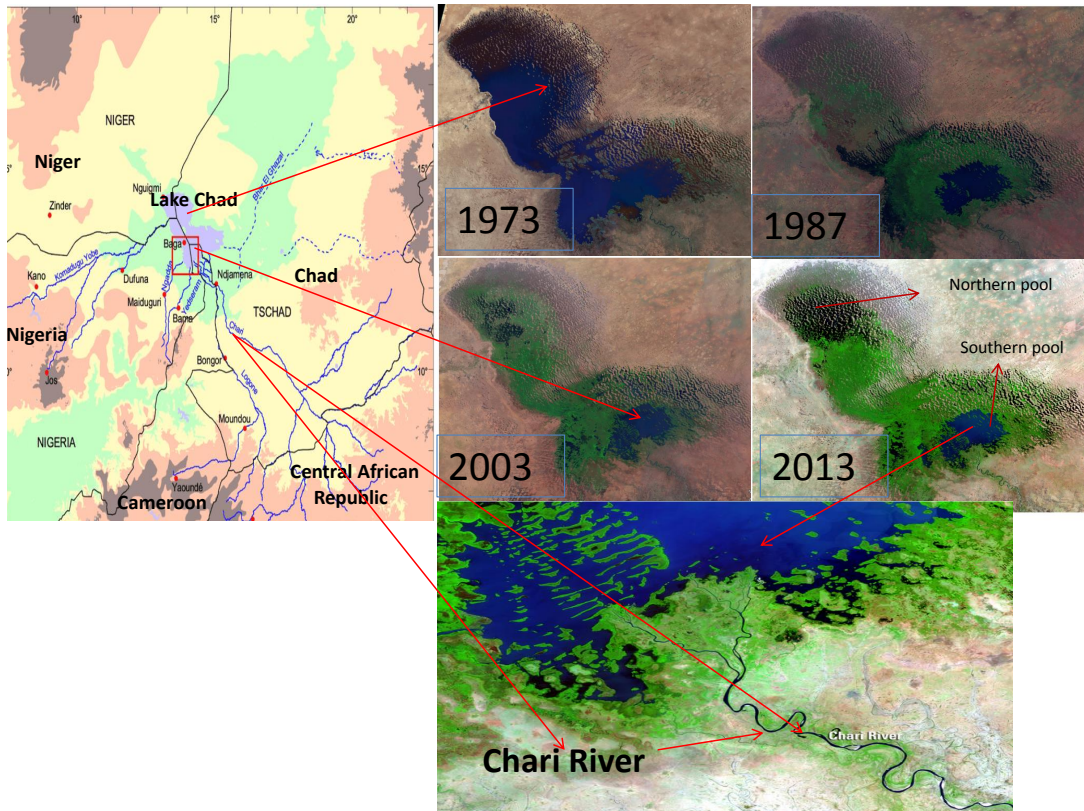


Figure 1.1: The spatial and temporal changes of Lake Chad's surface area as shown by Landsat imageries for 1973, 1987, 2003, and 2013. The blue lines on the map (left) show the river networks within the basin. The present Lake Chad shows two segmented pools with the northern pool completely dried up during drought periods (right). Map is adapted from [Ndehedehe et al. \(2016b\)](#).

increased simulated runoff ratio from 0.15 to 0.44 and annual stream flow by 35-65%. Interestingly, another study on the influence of agricultural water use on global water system ([Rost et al., 2008](#)) reported that land use change reduced global evapotranspiration by 2.8% and increased discharge by 5.0% (1764 km³/yr), while irrigation increased evapotranspiration by about 1.9% and decreased discharge by at least 0.5%. The extraction of fossil groundwater decreased TWS over the Saharan aquifers while TWS increased in the Volta basin despite a significant decline in precipitation during the same period (see, e.g., [Ndehedehe et al., 2017c](#); [Moore and Williams, 2014](#); [Ahmed et al., 2014](#)), suggesting the implications of water management strategies adopted for these regions. The contribution of this thesis to water resources development in West Africa has extended the literature on the role of human interventions on hydrological variability. For instance, [Ndehedehe et al. \(2017c\)](#) recently found that water ponding by the Akosombo dam in the Lake Volta accounted for about 41% of the increasing trend in GRACE-TWS despite an apparent significant decline in precipitation between 2002 and 2014. With the rapid evolution of water resources in Senegal, [Ngom et al. \(2016\)](#) believes that as opposed to the 1980s when the water cycle of the region was representative of natural conditions, it is now intensely modified and largely modulated

by human activities, probably due to the installations of hydraulic infrastructures.

The contraction of the Lake Chad's surface area was primarily caused by strong declines in regional precipitation patterns, restricting inflow from Chari-Logone river systems, which provides about 95% freshwater of the Lake. However, as indicated in several studies (see, e.g., Ndehedehe et al., 2016b; Birkett, 2000; Coe and Foley, 2001), water withdrawals from the Lake for irrigation purposes during water deficit periods compounded the effects of extreme droughts, resulting in about 90% decline of the Lake's surface area (Fig. 1.1). Apparently, this underscores the role of human activities in not only exacerbating the impacts of climate variability but in also reshaping the stability of Lake's ecosystem. The human-modified droughts of the Lake Chad basin is typical of the Anthropocene, where various forms of human activities impacts on catchment storage, soil properties, and hydrological processes, thereby modifying hydrological drought severity. Van Loon et al. (2016), for example, argued generally, that urbanisation impacts on recharge and infiltration rates while soil moisture is influenced by deforestation, afforestation, desertification, and agricultural practices through evapotranspiration. In view of the aforementioned case studies, it can be reconciled that the combine effects of climate variations and human interventions, conjugated with the well known strong land-atmosphere coupling in the region (e.g., Boone et al., 2009; Koster et al., 2004), will unarguably result in strong and profound influence on water resources systems and hydrological processes.

1.5 Earth observations and model simulations in terrestrial hydrology

The advent of space science in the last four decades has contributed immensely to the progress in earth system science, making it possible for the frequent observations of large scale, key water budget quantities. Advances in remote sensing hydrology evidenced in new space-borne measurements in particular has made it possible to provide reliable estimates of precipitation, soil moisture, streamflow, lakes, soil moisture, glaciers and Ice sheets, etc., from orbiting platforms (see, e.g., Petropoulos et al., 2015; Alsdorf et al., 2007; Lettenmaier, 2005). Numerous studies (see, e.g., Agutu et al., 2017; Okwuashi and Ndehedehe, 2017; Carrao et al., 2016; Funk et al., 2015; Dardel et al., 2014; Chen et al., 2014; Zhou et al., 2014; Du et al., 2013; Wagner et al., 2009; Sheffield et al., 2009; Tucker et al., 1991) have demonstrated the innate potentials of satellite data obtained from several remote sensing platforms such as optical, thermal, and microwave, in drought monitoring, land use change, regional water balance, and hydrological applications. Global reanalysis (e.g., Modern-Era Retrospective Analy-

sis for Research and Applications-MERRA) and model data (e.g., WaterGap Global Hydrology Model-WGHM, CPC soil moisture, Global Land Data Assimilation System-GLDAS, etc.) driven by observed meteorological forcing data have also been introduced in understanding global changes in climates and hydrological cycle (see, e.g., [Döll et al., 2014](#); [Rienecker et al., 2011](#); [Rodell et al., 2004](#); [Fan and Dool, 2004](#); [Dirmeyer et al., 2004](#)). The WGHM model data provides estimates of groundwater recharge from surface water bodies in semi-arid and arid regions ([Döll et al., 2014](#)) while global reanalysis such as the MERRA data provide atmospheric fields, water fluxes, and global estimates of soil moisture, which are very useful in land surface hydrological studies ([Rienecker et al., 2011](#); [Reichle et al., 2011](#)). With the rapid upsurge in wireless and smartphone technologies; unmanned drones, aerial vehicles, and tethered balloons, scientists can now archive estimates of daily average rainfall, temperatures, floods; map snow depths; and monitor other critical hydrological quantities such as channel depth ([McCabe et al., 2017](#)). These sophisticated sensing platforms provide the remote sensing community and hydrologists a plethora of opportunities to develop new frameworks that advances and facilitate our understanding of global changes in hydro-climatic conditions.

Be it satellite, model or reanalysis data, their applications have enhanced and revolutionised our knowledge of hydrological cycle, water availability and global change. For example, using a model soil moisture driven by a hybrid reanalysis-observation forcing dataset, [Sheffield and Wood \(2008\)](#) reported a small wetting trend in global soil moisture (1950 – 2000) that was attributed to increasing precipitation. Based on new data from the WaterGAP integrated global water resources model, [Brauman et al. \(2016\)](#) recently found periodic water shortage in 71% of world irrigated areas and 47% of large cities suggesting that water security depends largely on reducing society's vulnerability to water shortages. Multiple satellites and model data have been combined to produce a comprehensive indicator that provides balance for characterisation while reflecting aspects of meteorological, agricultural, and hydrological drought information (e.g., [Mishra et al., 2015](#); [Niu et al., 2015](#); [Du et al., 2013](#); [Vicente-Serrano et al., 2012](#); [Corzo Perez et al., 2011](#); [Sheffield and Wood, 2008](#)). A new multivariate framework for drought monitoring by [Ndehedehe et al. \(2016c\)](#), based on a fourth order cumulant statistics also demonstrated the potentials of integrating multiple climate variables (in-situ, model, and satellite data) in hydrological drought characterisation, contributing to a broad framework of existing methods. Even in a more recent collaboration in East Africa ([Agutu et al., 2017](#)), a suite of remote sensing, land surface models, and reanalysis products showed strong potential for agricultural drought characterisation, providing alternatives for the in-situ data deficient region. These are some indications of the opportunities that exist for large scale hydro-climatic research that leverage on satellite programmes and other multi-resolution data.

The Gravity Recovery and Climate Experiment (GRACE, [Tapley et al., 2004](#)) is a

sophisticated and the latest of satellite gravity mission in the list of space geodetic programmes such as the European Space Agency's Gravity field and Ocean Circulation Explorer (GOCE), amongst others. GRACE has given an unparalleled perspective to global terrestrial hydrology by providing quantitative estimates of monthly changes in TWS (soil moisture; groundwater; surface water-lakes, rivers, wetlands; snow; and canopy) over large spatial scales. Because of its spatial resolution (200,000 km³), the dynamics in multi-layered land water storage (i.e., all aspects of TWS) can be measured at global or regional scales with an accuracy of 1.5 cm equivalent water height (Famiglietti and Rodell, 2013). Apart from its broad applications in droughts, floods, terrestrial water budget, and ecosystem assessments (see, e.g., Zhang et al., 2016; Ndehedehe et al., 2016c; A et al., 2015; Thomas et al., 2014; Long et al., 2014; Reager et al., 2014; Yang et al., 2014; Long et al., 2013; Houborg et al., 2012; Chen et al., 2010; Sheffield et al., 2009; Yirdaw et al., 2008; Wouters et al., 2014, and the references therein), it is now one of the most vital tools in hydrological research, specifically in monitoring sub-surface water storage, aquifer system processes, evaluating groundwater resources, and as a useful hydrological indicator in assessing the impacts of climate variability on annual crop yields (see, e.g., Chen et al., 2016; Ndehedehe et al., 2017a; Castellazzi et al., 2016; Famiglietti et al., 2015; Alley and Konikow, 2015; Senay et al., 2014; Döll et al., 2014; Famiglietti, 2014; Gonçálves et al., 2013; Famiglietti and Rodell, 2013; Alsdorf et al., 2010; Henry et al., 2011; Tiwari et al., 2009; Swenson and Wahr, 2007). The developments and evolutions of GRACE-derived TWS over West Africa as highlighted in the author's peer-reviewed published papers (see Table 1.1) and other previous reports suggest complex hydrological processes for the humid parts due to the presence of surface waters, wetlands, and a considerably strong inter-annual rainfall (see, Ndehedehe et al., 2017c; Ferreira and Asiah, 2015; Moore and Williams, 2014; Ahmed et al., 2014). GRACE-based hydrological studies are relatively few in West Africa and the Congo basin (e.g., Ndehedehe et al., 2016a, 2017d; Lee et al., 2011; Henry et al., 2011; Crowley et al., 2006). Some validation studies (Nahmani et al., 2012; Grippa et al., 2011; Hinderer et al., 2009) however, have been reported in the region and more studies will be required to deploy GRACE observations in hydro-geological, ecological, and climatological studies in the region. This thesis also presents an array of novel findings and interesting insights in the aforementioned areas that advance essential aspects of research in remote sensing hydrology (Chapters 2-6). Further, in non-industrialised regions where hydrological infrastructures and observational networks are in decline, non-operational or sparse (e.g., Alsdorf et al., 2003; Alsdorf and Lettenmaier, 2003), GRACE observations and its Follow-On (GRACE-FO) mission, which is scheduled for launch soonest would be the only operational, state-of-the-art, and most sophisticated gravity mission that would benefit hydrological and climate research tremendously. The finer spatial resolution of GRACE-FO mission (< 50,000 km²) would allow not just the quantification of the terrestrial water

budget components but the closure of water balance with limited uncertainties. In addition to the GRACE-FO, the scheduled launch of Surface Water and Ocean Topography (SWOT) mission by 2020 as published by National Aeronautics and Space Administration (NASA, www.jpl.nasa.gov/missions/surface-water-and-ocean-topography-swot) is expected to provide detailed measurements of surface water storage variations (i.e., wetlands, lakes, or reservoirs), complementing the GRACE mission.

Other sustained investments in satellite geodetic programmes have provided large coverage of dynamics in terrestrial water bodies. For example, measurements obtained from interferometric synthetic aperture radar (InSAR), radar altimetry (TOPEX/Poseidon), ERS satellites, Envisat and Jason1 missions, Ice, Cloud and land elevation satellite (ICESat), Shuttle Radar Topography Mission (SRTM), Global positioning System (GPS), Japan's Advance Land Observing Satellite (ALOS), amongst others have proved to be useful in understanding the impacts of climate variability on the temporal and spatial dynamics of surface water resources (e.g., [Tourian et al., 2017](#); [Ndehedehe et al., 2017c](#); [Lee et al., 2014](#); [Alsdorf et al., 2007](#); [Frappart et al., 2006](#); [Lettenmaier, 2005](#); [Alsdorf et al., 2003](#); [Birkett, 1995, 2000](#); [Alsdorf et al., 2001](#)). All of these satellite programmes and global land surface schemes have ignited a plethora of scientific findings that are not only informative but useful for public policy and management decisions related to water resources.

1.6 Knowledge gaps and hydrological challenges

Reoccurring drought episodes of the 1970s and 1980s, and the incessant impacts of climate variability on the socio-economic systems of West Africa are major triggers that led to the plenitude of climate research in the region. The various aspects of these studies focused mainly on analysing multiple climate variables such as precipitation, runoff, soil moisture, temperature, and zonal winds, amongst others. Moreover, historical gauge data, outputs from global and regional climate models (i.e., GCMs and RCMs), and a host of optical remote sensing data have been widely used in several hydro-climatic research at all levels (county level, region-specific, and large scales) in the region. These studies as highlighted in previous sections, have heavily explored and diagnosed the mechanisms of meteorological patterns and how they drive other fluxes (runoff and evapotranspiration) and land state variables (soil moisture). However, there are still knowledge gaps, particularly in areas regarding large scale temporal and spatial dynamics of TWS, and the impacts of both climate change and water resources development (e.g., irrigation schemes and dam constructions for hydropower) on the hydrological systems of West Africa. From a hydrological stand point, water development schemes (e.g., Lake Volta) impacts on natural hydrological variabilities making

it difficult to understand the impacts of climate on hydrological conditions. Further, as outlined in previous sections, several scientific reports have outlined exhaustively the influence of global climate and some oceanic hot spots on precipitation changes in West Africa. Nonetheless, the influence of climate variability and low-frequency variability that are connected to slow oceanic and climate oscillations from global SST anomaly on the region's TWS, is largely unknown. Such influence modulate hydrological processes and arguably, would provide significant controls on the spatial and temporal distributions of regional changes in TWS and other water budget quantities (e.g., runoff).

Moreover, poor understanding of hydrological variability poses significant challenge to risk management and the prediction of extreme weather events (Hall et al., 2014). The knowledge of hydrological variability in this most financially and climatically challenged region of the world is critical. This is true as variations in hydrology have been identified as one of the key variables causing disparity in the level of economic growth amongst nations, given that it represents a significant challenge to food security and infrastructure development in the world's poorest regions (see, Hall et al., 2014; Brown and Lall, 2006). In West Africa, water-related knowledge and innovative technologies are not in the front lines of academic research institutions and government agenda, owing to poor funding and other disincentives. Consequently, the vulnerability of the region to the impacts of climate change will continue to grow with ripple effects through its socio-economic systems. Observed devastating extremes in the climate of West Africa raises some concerns not just for water availability but also for a number of issues that include, for example, food security, health, policy and risk management strategies, and socio-economic challenges (e.g., migration, GDP, etc.). The trajectory of future changes in hydrological conditions and water management practices are complex and will influence agricultural systems in terms of adaptation measures and mitigation strategies (see, e.g., Paolino et al., 2012; Roudier et al., 2011; Falloon and Betts, 2010). Despite the tragedies of frequent extremes in climatic conditions of West Africa, understanding hydrological variability is a wise choice that could unlock sustainable pathways that can help mitigate the impacts of hydrological changes on economic growth.

Knowledge gaps in large scale TWS dynamics and the impacts of climate on the hydrology of West Africa exists, primarily because of limited or lack of observational networks to provide the current state of hydrologic information. Gauge stations for rainfall and river discharge measurements are in decline globally (e.g., Alsdorf et al., 2007; Alsdorf and Lettenmaier, 2003; Lettenmaier, 2005). It is even worse in non-industrialised nations such as the African sub-region where the gauge networks are not just extremely sparse, discontinuous and lacking, but their density falls far below the WMO guidelines (e.g., Vörösmarty et al., 2001). As further mentioned in Vörösmarty

[et al. \(2005\)](#), the routine reporting of African river discharge to relevant climate agencies such as the WMO declined by 90% since 1990. Despite some investments in gauge measurements for meteorological and hydrological applications in some parts of West Africa, many sub-regions have little or no history of hydrological measurements. This is largely attributed to incessant political instabilities, unfavourable government policies, and the costs and logistics implications for the installation of gauges to characterise flow dynamics.

The lack of capacity to face the future challenges of climate change impact on water resources, owing to sparse observational records in some gauged river basins, is intensified by political concerns, legal and institutional constraints that have hindered the acquisition of existing data for scientific purposes. Research institutions find it difficult to engage in regional water management and trans-boundary water sharing conversations because hydro-climatic data from national archives and government repositories are frequently withheld, mostly for political and security reasons. This could only be more damaging for West African countries where water sharing across political boundaries is vastly enormous. Further, the African Monsoon Multidisciplinary Analysis-Couplage Atmosphere Tropicale Cycle Hydrologique (AMMA-CATCH, e.g., [Lebel et al., 2009](#)) and Gravity and Hydrology in Africa (GHYRAF, [Hinderer et al., 2009](#)) projects are few among the significant initiatives that are primarily dedicated to studying land surface conditions in West Africa and other African regions through monitoring of hydro-climatological and ecological changes. However, whereas the AMMA-CATCH networks are highly insufficient with presence in only three countries of West Africa, the GHYRAF project is sandwiched between poor funding and trans-boundary issues. Increased observational networks are critical for the proper initialization of numerical weather prediction models and monitoring climate variability in West Africa ([Jenkins et al., 2002](#)). But as indicated in some reports (see, e.g., [Ndehedehe et al., 2016a](#); [Todd et al., 2011](#); [Farnsworth et al., 2011](#); [Conway et al., 2009](#)), the paucity of high quality base line data remains a major constraint to understanding the climatic influence on changes in the hydrological cycle over the region.

As argued by [Alsdorf et al. \(2007\)](#), gauge observations such as those from river stage are incapable of large scale monitoring of hydrological conditions. This is because of the physics of water flow across floodplains and wetlands, and since gauge networks essentially provide a one spatial dimension information about the spatial dynamics of surface water extent. For some of these reasons and those presented by [Alsdorf et al. \(2003\)](#) in a related study, large scale dynamics in surface waters (lakes, wetlands, rivers, reservoirs) are generally unknown. Understanding changes in the hydrological cycle over West Africa would not be possible without large scale measurements that allow the estimations of the temporal and spatial dynamics of hydrological quantities. Apparently, developments in climate models (GCMs and RCMs, e.g., [Erfanian et al.,](#)

2016; Washington et al., 2013; Otto et al., 2013; Mohino et al., 2011; Cook and Vizu, 2006; Li et al., 2005; Koster et al., 2004; Giannini et al., 2003; Lebel et al., 2000), land-surface parameterization schemes and hydrological models (e.g., Sheffield et al., 2014; Thiemiig et al., 2013; Lemoalle et al., 2012; Todd et al., 2011; Boone et al., 2009; Li et al., 2007; Schuol and Abbaspour, 2006) have shown some prospects as they have been widely employed to forecast and study the West African climatology and large scale variability in the varied components of the hydrological cycle. Global hydrological models (GHMs) forced by global climate models and the latest GHG concentration scenarios and atmospheric general circulation models (AGCM) have also shown potentials in global water assessment of droughts and water resources (e.g., Prudhomme et al., 2014; Schewe et al., 2013; Nakaegawa et al., 2013; Corzo Perez et al., 2011). However, the skills of these models (GHMs, GCMs, and RCMs) are restricted due to (i) their poor representation of surface water balance (e.g., Alsdorf et al., 2007), (ii) bias and conceptual model uncertainties (e.g., Todd et al., 2011; Schuol and Abbaspour, 2006; Lebel et al., 2000), (iii) dependence on computational estimates (e.g., Koster et al., 2004), (iv) lack of feedback processes involving anthropogenic impacts (e.g., Piao et al., 2010; Alsdorf and Lettenmaier, 2003), and (v) model physics and choice of parameterisations (e.g., Oettli et al., 2011). Considerable progress is therefore required for the improved estimates of land-atmosphere impacts for GCM climate scenarios (Boone et al., 2009). But given the inherent problems of GCM in simulating primary aspects of the West African monsoon (e.g., Cook and Vizu, 2006), and uncertainties in satellite estimates of some key hydrological fluxes globally (Lettenmaier, 2005), then the implication of the problem is global.

Furthermore, the lack of a suitable framework to improve the characterisation of space-time evolutions of hydrological quantities and extreme weather events is another problem that limits climate forecasting systems, understanding of TWS dynamics, and the holistic assessment of key hydrological metrics (e.g., magnitude, frequency, duration, predictability, etc.). The impacts of climate variability and other processes of oceanic inter-annual variability (e.g., ENSO, Pacific Decadal Oscillation-PDO, etc) in West Africa may result in contrasting outcomes on hydrological regimes. One of such example is the debate on rainfall recovery over West Africa. Nicholson (2005) and Lebel and Ali (2009) have contrasting cases of recovery possibly due to different reference periods. But essentially, they both show that while recovery was marked in some areas, rainfall deficit continued unabated in other Sahelian areas. The failure of rainfall regime in one region does not translate to failure in other sub-regions (e.g., Ndehedehe et al., 2016c; Owusu and Waylen, 2009), probably owing to different drivers of rainfall, local and land surface conditions. Assuming drought and wet conditions vary in space and time, then the existing methods (e.g., van Huijgevoort, 2014; Panthou et al., 2014; Lebel and Ali, 2009; Rouault and Richard, 2003; Nicholson et al., 2000) used to

analyse extreme weather events and hydrological conditions are insufficient, warranting further studies. It was elaborated further in [Ndehedehe et al. \(2016c\)](#), that regional average time series of drought indices such as, effective drought index (EDI), standardised precipitation index (SPI), groundwater drought index (GWI), and palmer drought severity index (PDSI), amongst several other indices (see, e.g., [Li and Rodell, 2015](#); [Kasei et al., 2010](#); [Ali and Lebel, 2009](#); [Laux, 2009](#); [Vicente-Serrano, 2006](#); [Heim, 2002](#); [McKee et al., 1993](#)) hide the underlying spatial variability of the index, and may lead to generalisations of wet and dry regimes. As the outcome of such drought indices is likely to be skewed, this may not be very helpful for predicting ecological responses, adequate evaluation of drought impacts, crafting of drought policies, and in the fostering of campaign on regional adaptation strategies. Hence, a spatio-temporal drought framework based on the regionalisation and localisation of drought signals over the region of interest would adequately improve our knowledge of hydrological variability. This approach would ultimately be significant to understanding the oceanic hot spots, climate oscillations, and tropospheric effects associated with the characteristics of extreme weather events in the region.

1.7 Research objectives

This thesis addresses the knowledge gaps identified in Section 1.6 by exploring a suite of remotely sensed data from optical and gravity missions, global reanalysis, and model data to primarily, investigate spatio-temporal variations and characteristics of land water storage over West Africa and the impacts of global climate. New methods and framework to assess extreme weather events and improve understanding of key hydrological metrics are studied. The specific objectives of study are:

- (i) Investigate the spatial and temporal dynamics of GRACE-derived TWS and its relation to precipitation. The study examines the inter-annual and seasonal variability of GRACE-derived TWS changes, satellite altimetry-derived lake height variations of water reservoirs, and precipitation patterns. The hydrological characteristics of West Africa are explored using GRACE-derived TWS (2002 – 2014) and net-precipitation (i.e., the maximum available freshwater flux) during the 1979 – 2010 period.
- (ii) Examine the impacts of reservoir systems on hydrological variability based on spherical harmonic synthesis and statistical decomposition technique. Here, the aim is to understand the spatial and temporal dynamics of GRACE-derived TWS over the Volta basin after removing the hydrological signal induced by Lake Volta water level changes. The contributions of Lake Volta to the overall trends in

GRACE-derived TWS over the Volta basin during the 2002 – 2014 period and the impacts of climate variability on the freshwater systems of the Volta basin are also investigated.

- (iii) Investigate the impacts of global climate on changes in TWS. In this context, the influence of prominent climate teleconnections and global sea surface temperature fields on TWS derived from GRACE (2002 – 2014) and global reanalysis (1980 – 2015) products are explored using canonical correlation analysis and a range of statistical decomposition methods. Further, by employing a suite of multi-resolution data, long term changes in rainfall, soil moisture, TWS, and groundwater over West Africa and parts of the Congo basin (1980 – 2015), are also investigated.
- (iv) Investigate the spatio-temporal evolutions and characteristics of different droughts (meteorological, agricultural, and hydrological) by analysing drought indices using a fourth order cumulant statistics. The study at this point examines a suitable method for assessing drought characterisation and variability over West Africa. Two major catchments (Lake Chad and Volta basins) located in different climatic and geographic zones of West Africa, where drought events are endemic and mostly unreported are identified as tentative test beds to demonstrate the potentials of this method.
- (v) Investigate the potential of GRACE-derived TWS as a suitable hydrologic control for surface vegetation dynamics. The utility of GRACE observations in this capacity, that is, as an eco-hydrological tool would be a significant progress in the latest of GRACE applications for data deficient region.

1.8 Thesis outline

This thesis is a combination of the authors peer reviewed journal papers during the period of candidature (2014 – 2017). As shown in this thesis, the published paper(s) adapted for each chapter is(are) presented in their original journal formats (except for the 2 revised and resubmitted papers). After the introduction, the other chapters of this thesis, which address the specific objectives of this thesis listed in Section 1.7 are summarised using these papers as indicated in Table 1.1. Also, in the respective chapters that follows (i.e., chapters 2-6), the major findings of all the paper(s) is(are) also provided as introductory remarks. The thesis synopsis and overall conclusion drawn from the various components of the research are indicated in Chapter 7.

Table 1.1: Published peer-reviewed journal papers (i.e., during the candidature) adapted for the thesis and the respective chapters and thesis objectives they cover. The full bibliographic details of all papers have been provided in the list of publications above.

Paper	Journal	Chapter	Thesis Objective	References
1. Paper 1	Adv. Water Resour	2	1	Ndehedehe et al. (2016a)
2. Paper 2	Int. J. Climatol.	2	1	Andam-Akorful et al. (2017)
3. Paper 3	J. Hydrol: Reg. stud.	3	2	Ndehedehe et al. (2017c)
4. Paper 4	Hydrol. Processes	4	3	Ndehedehe et al. (2017d)
5. Paper 5	Glob. Planet. Chang.	4	3	Ndehedehe et al. (2017e)^a
6. Paper 6	Sci. Total Environ.	5	4	Ndehedehe et al. (2016c)
7. Paper 7	J. Hydrol	5	4	Ndehedehe et al. (2016b)
8. Paper 8	J. Arid Environ	6	5	Ndehedehe et al. (2017b)^b

^aThe revised version of this manuscript is currently under revision in *Global and Planetary Change*

^bManuscript submitted to *Journal of Arid Environments*

2 Terrestrial water storage over West Africa

This chapter is covered by the following publications ([Ndehedehe et al., 2016a](#); [Andam-Akorful et al., 2017](#)):

1. **Christopher Ndehedehe**, Joseph Awange, Nathan Agutu, Michael Kuhn, and Bernhard Heck (2016). Understanding changes in terrestrial water storage over West Africa between 2002 and 2014. *Advances in Water Resources*, 88, 211–230, [dx.doi.org/10.1016/j.advwatres.2015.12.009](https://doi.org/10.1016/j.advwatres.2015.12.009).
2. S.A. Andam-Akorful, V.G. Ferreira **C.E. Ndehedehe** & J.A. Quaye-Ballard (2017). An investigation into the freshwater variability in West Africa during 1979–2010. *International Journal of Climatology*, 37(S1), 333–349, [dx.doi.org/10.1002/joc.5006](https://doi.org/10.1002/joc.5006).

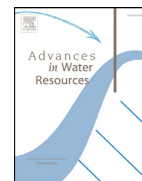
This chapter contributes significantly towards understanding the hydrological characteristics of West Africa by exploring the potentials of GRACE satellite gravimetry in large scale hydrological studies over the region. The chapter provides useful insight on the spatio-temporal variability of TWS and TRMM-based precipitation over West Africa. Specifically, for the first time, GRACE-derived TWS was analysed in relation to satellite precipitation (TRMM V7) changes using principal component analysis and multiple linear regression analysis (MLRA). This study was motivated by the facts that hydrological conditions and large scale TWS dynamics over West Africa are unknown due to the lack and scarcity of in-situ hydrological data. Since the impacts of hydrology and rainfall variability on economic growth (e.g., Gross Domestic Product) are significant (see, [Brown and Lall, 2006](#)), understanding hydrological variability in West Africa will strengthen infrastructure and management initiatives on water resources development. The various mechanisms of meteorological processes such as the role of West African Monsoon, mesoscale convective systems, transitions in the rainbelt, ocean perturbations, and land surface conditions, *inter alia*, as outlined in several communications are notable elements of West Africa’s climate. These prominent West African climate elements determine the magnitude and the trajectory of regional variations in precipitation. However, the mechanistic understanding of how these meteorological patterns drive GRACE-derived TWS (groundwater; surface water-lakes, rivers, wetlands; snow; soil moisture; and canopy) is unknown. Because of the profound challenges posed by extreme rainfall variability to the availability of freshwater for agriculture and ecosystem services in the region, large scale analysis of variations in

TWS is a logical step towards understanding not only the impact of climate variability on water resources systems, but other complex eco-hydrological systems of the region. The focus on hydrological processes, especially those resulting from precipitation-TWS relationship is the mainstay of this chapter. As the findings suggest, the use of a second order statistical method, PCA, is a helpful tool in analysing large scale surface mass variations and show that most parts of West Sahel and the Guinea Coast are the *water towers* of West Africa. Strong annual variability of GRACE-derived surface mass variations caused by considerable high rainfall amounts at seasonal and inter-annual time scales are observed in these areas. Precipitation is the principal driver of GRACE-derived TWS and is dominated by annual and semi-annual signals that are influenced by circulation features, ocean warming, physiographic features, and other processes of oceanic inter-annual variability (e.g., ENSO). Time variable gravity field observations provided by the GRACE mission remains an important tool that will benefit studies of mass transport in the region and also help to understand the impacts of climate variability on freshwater systems and ecosystem dynamics. In another related study, wavelet power transforms and coherence analysis were employed to analyse the variability of available freshwater expressed in terms of net-precipitation during the 1979 – 2010 period.



Contents lists available at ScienceDirect

Advances in Water Resources

journal homepage: www.elsevier.com/locate/advwatres

Understanding changes in terrestrial water storage over West Africa between 2002 and 2014



Christopher Ndehedehe^{a,c,*}, Joseph Awange^{a,b,e}, Nathan Agutu^{a,d}, Michael Kuhn^a, Bernhard Heck^b

^a Western Australian Centre for Geodesy and The Institute for Geoscience Research Curtin University, Perth, Australia

^b Geodetic Institute, Karlsruhe Institute of Technology, Karlsruhe 76131, Germany

^c Department of Geoinformatics and Surveying, University of Uyo P.M.B. 1017, Uyo, Nigeria

^d Department of Geomatic Engineering and Geospatial Information systems JKUAT, Nairobi, Kenya

^e Department of Geophysics, Kyoto University, Kyoto 606-8502, Japan

ARTICLE INFO

Article history:

Received 9 August 2015

Revised 6 November 2015

Accepted 9 December 2015

Available online 17 December 2015

Keywords:

GRACE

PCA

TRMM

GLDAS

Satellite altimetry

Multiple linear regression analysis

ABSTRACT

With the vast water resources of West Africa coming under threat due to the impacts of climate variability and human influence, the need to understand its terrestrial water storage (TWS) changes becomes very important. Due to the lack of consistent in-situ hydrological data to assist in the monitoring of changes in TWS, this study takes advantage of the Gravity Recovery and Climate Experiment (GRACE) monthly gravity fields to provide estimates of vertically integrated changes in TWS over the period 2002–2014, in addition to satellite altimetry data for the period 1993–2014. In order to understand TWS variability over West Africa, Principal Component Analysis (PCA), a second order statistical technique, and Multiple Linear Regression Analysis (MLRA) are employed. Results show that dominant patterns of GRACE-derived TWS changes are observed mostly in the West Sahel, Guinea Coast, and Middle Belt regions of West Africa. This is probably caused by high precipitation rates at seasonal and inter-annual time scales induced by ocean circulations, altitude and physiographic features. While the linear trend for the spatially averaged GRACE-derived TWS changes over West Africa for the study period shows an increase of 6.85 ± 1.67 mm/yr, the PCA result indicates a significant increase of 20.2 ± 5.78 mm/yr in Guinea, a region with large inter-annual variability in seasonal rainfall, heavy river discharge, and huge groundwater potentials. The increase in GRACE-derived TWS during this period in Guinea, though inconsistent with the lack of a significant positive linear trend in TRMM based precipitation, is attributed to a large water surplus from prolonged wet seasons and lower evapotranspiration rates, leading to an increase in storage and inundated areas over the Guinea region. This increase in storage, which is also the aftermath of cumulative increase in the volume of water not involved in surface runoff, forms the huge freshwater availability in this region. However, the relatively low maximum water levels of Kainji reservoir in recent times (i.e., 2004/2005, 2007/2008, and 2011/2012) as observed in the satellite altimetry-derived water levels might predispose the Kainji dam to changes that probably may have a negative impact on the socio-economic potentials of the region. GRACE-derived TWS is not well correlated with TRMM-based precipitation in some countries of West Africa and apparently indicates a lag of two months over much of the region. On the other hand, the regression fit between GLDAS-derived TWS and GRACE-derived TWS shows R^2 of 0.85, indicating that trends and variability have been well modeled.

© 2015 Elsevier Ltd. All rights reserved.

1. Introduction

With an estimated population of 300 million people whose livelihood depends on rain-fed agriculture [see, e.g., 1–3], West Africa is one of the regions in the world with highly variable and

extreme climatic conditions (i.e., droughts and floods), which impacts directly on the hydrological cycle and the human population. Despite its vast water resources, which includes lakes, rivers, wetlands, and groundwater systems, West Africa has a history of vulnerability to the impacts of climate change, which threatens these water resources and agriculture [e.g., 4,2,5–7].

More often than not, the region is subjected to food insecurity, famine, health issues, and social instability due to water related problems induced by the frequency and persistence of extreme

* Corresponding author at: Western Australian Centre for Geodesy and The Institute for Geoscience Research Curtin University, Perth, Australia. Tel.: +61470307034.
E-mail address: christopherndehehe@gmail.com (C. Ndehedehe).

25 hydrological/hydro-climatological conditions (e.g., droughts and floods) [see, e.g., 5,8–10]. Therefore, understanding the spatio-temporal variability of changes in terrestrial water storage (TWS) (i.e., the total of surface waters, soil moisture, canopy storage, and groundwater) in this region can support sustainable decisions and effective management of water resources. In addition, it can also provide information on the hydrological footprints, which probably can help reveal the impacts of climate variability on the region's TWS.

Furthermore, in West Africa, changes in any component of the TWS do have socio-economic and environmental implications [e.g., 11]. For example, as described in Moore and Williams [12] in a recent study in Africa, the surface waters are needed to maintain fisheries, which are a principal contributor to the food basket of the region. Consequently, changes to any component of these surface waters (i.e., lakes and rivers) or groundwater resources might jeopardize the livelihood and the economic viability of the region. Apparently, for a region such as West Africa that depends heavily on rain-fed agriculture; reduced rainfall and freshwater availability may lead to crop failure, and low agricultural productivity [13,10]. This ultimately will affect agricultural development and the economy of the region. Besides the reduced freshwater availability occasioned by changes in rainfall patterns of the region [14], the increasing irrigation development [13], ecosystem functioning and other various forms of anthropogenic influence puts water resources at risk [e.g., 4], hence the need to examine the changes in TWS and its variability over West Africa, which in the long term can support effective allocation, governance, and management.

Changes in TWS, be they groundwater, soil moisture, canopy storage, surface waters (i.e., lakes, wetlands, and rivers) remain one of the most critical components of the hydrological cycle. However, estimating these changes in TWS over West Africa remains a major challenge due to few in-situ monitoring stations, lack of large scale hydrological data, and unreliable field measurements amongst others. While Grippa et al. [11] specifically noted that the monitoring of water budget components in West Africa are hampered by scarcity of in-situ measurements, Anayah and Kaluarachchi [15] reported that the monitoring of groundwater in the upper east region of northern Ghana started in 2005 and continued until the end of 2008 (i.e., from 5 monitoring wells). Local measurements from dedicated networks such as the AMMA-CATCH¹ hydro-meteorological observing system have been used in validation studies [e.g., 17] and to characterize rainfall regime for the Gourma region located in Mali [e.g., 18]. However, hydrological studies over large spatially heterogeneous areas remain difficult as the AMMA-CATCH networks are highly insufficient and only available in few countries (i.e., Niger, Mali, and Benin). Besides the scarcity and the incomplete records of in-situ data in the sub-regions due to limited and degraded weather hydrological infrastructures precipitated by poor government funding, Nicholson et al. [19] reported that the acquisition of rainfall data despite its availability was largely hindered by political and economic instability, in addition to government policies. Due to these sparse in-situ meteorological and hydrological monitoring networks in West Africa, degraded hydrological infrastructures, data inaccessibility, and the gaps in routine measurements of relevant hydrological variables (e.g., river discharge, groundwater), our understanding of the spatio-temporal patterns of TWS changes is limited, hence the need for a large scale holistic assessment of water storage estimation. Due to the lack of in-situ hydrological data to assist in the accurate monitoring of TWS changes, indices such as effective drought index (EDI), standard precipitation index (SPI), and

palmer drought severity index (PDSI) have been used as proxies for monitoring water availability and hydrological conditions [see, e.g., 20–23]. However, these indices do not account for the changes in the state of other water storage components (e.g., groundwater) [24], which is an important resource for livelihood. While it has been reported that these indices are associated with uncertainties [see, e.g., 25], the use of hydrological models has shown relatively good performance [26] on the one hand, and inconsistent results on the other hand [13]. However, land water storage output from models underestimate changes in water storage, and might be restricted due to limited data for evaluation and calibration purposes [9,27]. In order to circumvent this problem, previous studies have combined remote sensing data and outputs from models to improve the estimation of changes in TWS [e.g., 28,29].

Since March 2002, the Gravity Recovery and Climate Experiment (GRACE) satellite mission under the auspices of National Aeronautic and Space Administration (NASA) in the United States and its German counterpart the Deutsches Zentrum für Luft- und Raumfahrt (DLR) has been collecting and archiving time variable monthly gravity fields [30]. These monthly gravity fields are provided as sets of spherical harmonic coefficients, which can be inverted to global and regional estimates of vertically integrated TWS at a spatial resolution of few hundred kilometers or more [31–33].

GRACE data has been used in the estimation of changes in TWS over West Africa in recent times. For instance, Grippa et al. [11] in a validation study, compared estimated TWS variations from different GRACE products with outputs from 9 land surface models operating within the framework of the African Monsoon Multidisciplinary Analysis Land Surface Inter-comparison Project (ALMIP). From the study, model outputs had a good agreement with GRACE-derived TWS changes. However, the analysis did not include the Western Sahel and some parts of Guinea coast, the region whose general rainfall pattern is highly influenced by ocean circulations and physiographic features. Ferreira et al. [34], [35] estimated mass changes and sink terms over the Volta basin in West Africa while Forootan et al. [14] proposed a prediction approach of TWS over West Africa for a duration of two years using a combination of past GRACE data, precipitation, and SST over the oceans. Still in West Africa, while Nahmani et al. [36] in a comparative study showed how the observed vertical deformation component from GPS data was fairly consistent with regional-scale estimates from GRACE satellite products and geophysical models, Hinderer et al. [37], had previously compared in-situ data from GPS with satellite observations such as GRACE in a project labeled Gravity and Hydrology in Africa. Furthermore, at continental and basin-wide scales, GRACE data have been used to investigate trends, and seasonal cycles of the various TWS components [see, e.g., 25,38–41]. For example, results of GRACE TWS solutions computed over Africa from 2003 to 2012 in Ramillien et al. [41] indicate a water loss from the North Saharan aquifers.

In order to improve our understanding of the land water storage over West Africa and to further extend the studies mentioned above, this study attempts to highlight the recent annual and seasonal variability of TWS changes for the period 2002–2014. Contrary to previous studies in the region, the approach here is to analyze the variability and the relationship between GRACE-derived TWS changes and rainfall patterns over West Africa using principal component analysis (PCA) [42,43] and multiple linear regression analysis (MLRA). The study looks into the inter-annual and seasonal variability of TWS changes, lake height variations of water reservoirs, and precipitation patterns. To evaluate GRACE-derived TWS changes over West Africa, total water storage content (TWSC) from the Global Land Data Assimilation System (GLDAS) [44] were also explored.

Therefore, this study explores hydrological fluxes such as precipitation and satellite altimetry data, alongside with TWS changes

¹ African Monsoon Multidisciplinary Analysis-Couplage Atmosphere Tropicale Cycle Hydrologique [16].

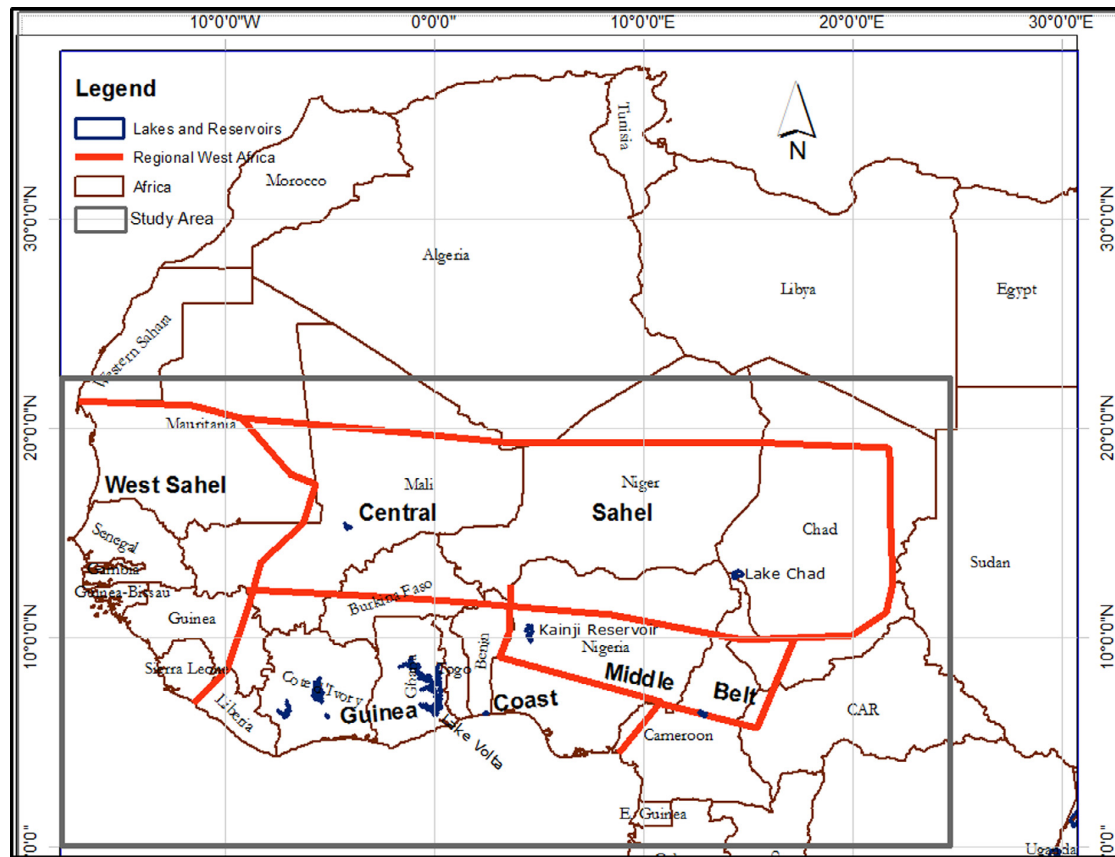


Fig. 1. Study area showing the definitions of sub-regions of West Sahel (WS), Central Sahel (CS), Guinea Coast (GC), and Middle Belt modified after Diatta and Fink [50].

from GRACE and GLDAS in order to understand the spatio-temporal dynamics of these hydrological variables and the available water resources that can support sustainable agriculture and ecosystem functioning. Specifically the study seeks to (i) identify trends and dominant patterns of TWS changes and its relation to precipitation over West Africa and (ii) understand the annual seasonal cycles of TWS and precipitation changes over West Africa and the response time between them.

The remainder of the study is segmented as follows; in Section 2, a brief introduction to the study area is provided while in Section 3, a discussion on the data and methodology is given. This is followed by analysis and discussion of the results in Section 4. The conclusion of the study is provided in Section 5.

2. West Africa

2.1. Location

West Africa is located between latitudes 0–20°N and longitudes 20°W–20°E (Fig. 1) and comprises a group of 16 countries covering an area of approximately 7.5 Million km². The two major geographical zones are the countries of the gulf of Guinea (i.e., the area between latitudes 4°N and 8°N), and the Sahelian countries [e.g., 3]. The southern boundary is the Atlantic ocean; on the north is the Sahara desert, while the eastern boundary is flanked by the Cameroon mountains.

2.2. Climate

The climate of West Africa is governed by the seasonal migration of the intertropical convergence zone (ITCZ) [e.g., 45]. The

location, position, and intensity (strength) of both the circulation features and ITCZ are responsible for the extreme wet and dry conditions, and intra-annual rainfall distribution in the Sahel and likewise the gulf of Guinea [46–49]. While rainfall ranges from less than 200 mm/yr in the Sahelian countries to over 2000 mm/yr in the gulf of Guinea, an increasing annual trend in temperature of 0.20°C/yr has been observed [e.g., 5,7]. Rain seasons in the gulf of Guinea occur between April–June and July–September, with the wettest months being June and September or sometimes October [19]. In the Sahel and fringe of the desert, the rain season takes place between June and September with maximum rainfall occurring in August.

3. Data and methodology

3.1. Data

3.1.1. Gravity Recovery and Climate Experiment (GRACE)

The GRACE satellite mission has been in space since March 2002, collecting monthly gravity fields used to estimate global changes in TWS [30]. GRACE time-variable gravity field products have been frequently used to study the Earth's water storage changes at basin, continental, and global scales [34,11,51]. The standard GRACE products, which are usually referred to as sets of spherical harmonic coefficients, were used in estimating TWS changes. These spherical harmonic coefficients do suffer from signal attenuation and satellite measurement errors causing noise in the higher degree coefficients [52,32]. Consequently, GRACE data undergo filtering in the form of spatial averaging and smoothing in order to reduce the effect of noise [see, e.g., 53,31]. Prior to

the smoothing of GRACE data, degree 2 coefficients were replaced with estimates from satellite laser ranging [54] while the degree 1 coefficients provided by Swenson et al. [55] were used. This is a conventional practice since GRACE does not provide changes in degree 1 coefficients (i.e., C_{10} , C_{11} , and S_{11}), and is also affected by large tide-like aliases in the degree 2 coefficients (i.e., C_{20}). The GRACE Release-05 (RL05) spherical harmonic coefficients truncated at degree and order 60 from Center for Space Research (CSR), covering the period 2002–2014 is used in this study to compute changes in TWS. The three well known processing centers such as the CSR, GeoForschungsZentrum (GFZ) and the Jet Propulsion Laboratory (JPL) use different algorithms to compute gravity field harmonic coefficients from the raw GRACE observations. Over West Africa, Grippa et al. [11] observed that seasonal water storage computed from the three GRACE products show significant differences, as opposed to their temporal evolutions, which were rather consistent. We use the CSR data set because of its wide application in continent-wide studies.

The fully normalized spherical harmonic coefficients were smoothed using the DDK2 de-correlation filter [56] before converting it to equivalent water heights (EWH) following the approach of Wahr et al. [33]. While taking notice of Landerer and Swenson [52] computed TWS solution, which uses an isotropic Gaussian averaging filter, the choice of the DDK2 filter used here is because it embodies both decorrelation and smoothing and also accommodates better the an-isotropic GRACE error structure [57]. The computed TWS was synthesized on a $1^\circ \times 1^\circ$ grid and then rescaled in order to restore the geophysical signal loss caused by the effect of spatial averaging using the de-correlation filter during the post-processing of the GRACE data [58,52]. Considering the progress made so far and the advances in the use of GRACE data, i.e., from validation to full utilization especially in hydrological studies, rescaling GRACE data in order to remedy signal loss caused by the filtering is critical. For instance, Landerer and Swenson [52], emphasized that if the effect of the filter is not accounted for in the transformed GRACE observations, the signal attenuation will become an error in the residual in the regional water balance or will serve as a constraint in water budget closure. In appendix A, we show the impact of filtering on CSR and JPL GRACE products and their relationship with model-generated water storage. In particular, the effect of the DDK2 filter on computed GRACE-derived TWS before and after restoring the geophysical signal loss was measured by comparing it with the GLDAS-TWS. The rescaled monthly TWS grids had a few random gaps of up to 12 months in between that were filled through interpolation, which is a common reconstruction method for hydrological time series [e.g., 59]. This is particularly important for principal component analysis, which requires continuous spatio-temporal data [60]. Though we have also computed GRACE derived TWS using coefficients from those of JPL, however, the desired objectives of this study are realized by using a single product, given the observed consistency in the temporal patterns of CSR and JPL (see Appendix A). Also, Ferreira et al. [34] showed similar consistency between the time series of GRACE-derived TWS changes using GFZ and CSR coefficients in the region.

3.1.2. Tropical rainfall measuring mission (TRMM)

The TRMM 3B43 [61,62] provides monthly precipitation estimates of high temporal (month) and spatial ($0.25^\circ \times 0.25^\circ$) resolution, with global coverage between the geographic latitudes 50°S and 50°N . For this study, monthly TRMMv7 3B43 precipitation rates from National Aerospace and Space Administration (NASA) Goddard Space Flight Center (GSFC) covering the period 1998–2013 was used to analyze the spatio-temporal variability of rainfall over West Africa. TRMM data has been validated (i.e., comparing satellite rainfall observations with gauge datasets) for the region [e.g., 63] and significantly improved [e.g., 64]. Also, especially

for West Africa, TRMM validation using in-situ data showed zero bias (i.e., the magnitude of TRMM was consistent with those of gauges), with a root mean square error (RMSE) of 0.7/0.9 mm/day for the seasonal and August rainfall [e.g., 48]. Unlike East Africa where the Global Precipitation Climatology Center (GPCC) gauge dataset is inconsistent with TRMM, over West Africa, the GPCC gauge data shows good agreement with TRMM [see, 65,63]. Further, the monthly TRMM precipitation were resampled into $1^\circ \times 1^\circ$ in order to maintain a common spatial resolution with other datasets such as GRACE-TWS solutions.

3.1.3. Global Land Data Assimilation System (GLDAS)

GLDAS [44] drives four land surface models (Mosaic, Community Land Model (CLM), Variable Infiltration Capacity (VIC), and Noah) to produce different fields of the land surface [e.g., 66]. In this study, GLDAS-derived monthly total water storage content (TWSC) at $1^\circ \times 1^\circ$ spatial resolution was used for a comparative analysis to evaluate GRACE data over the region. In addition, similar to Landerer and Swenson [52] and Long et al. [58], the derived TWSC from GLDAS was also used to rescale the GRACE-derived TWS in order to restore the signal loss due to filtering. Also, we highlight briefly that the relationship between the original and DDK2-filtered GLDAS data was used to obtain the scale factor. The data covering the years 2002–2013 was obtained from the Goddard Earth Sciences Data and Information Services Center (GESDICS)².

3.1.4. Satellite altimetry

Lake height variations computed from TOPEX/POSEIDON (T/P), Jason-1 and Jason-2/OSTM altimetry provided by the United States Department of Agriculture (USDA) was used in the study as auxiliary information to analyze water reservoirs in the study area. Time series of lake levels can be downloaded from www.pecad.fas.usda.gov/cropexplorer/globalreservoir and the hydroweb Laboratoire d'Etude en Géophysique et Oceanographie Spatiale (LEGOS) database. The data covering the period 1993–2013 was used in the study to analyze lake height variation. We rely on altimetry data for this study since the estimated errors of lake height variation with respect to the reference mean level for Lake Volta, Lake Chad, and Kainji dam are mostly in the sub-centimeter range. The USDA lake height variation time series used in this study were already smoothed with a median type filter to eliminate outliers and reduce high frequency noise.

3.2. Methodology

3.2.1. Principal component analysis (PCA)

Principal component analysis (PCA) is an extraction technique that is used to reduce the dimension of large multivariate data, and at the same time account for the most dominant variations in the original data set [e.g., 42,67,68,43]. Its mathematical simplicity and the ability to explain the optimized variance, using a small number of principal components, has probably made this method the most widely used statistical data analysis tool in climate science [68]. In addition to its simplicity, the choice of PCA in this study is also due to its capability to isolate both inter-annual signals, and long-term periodic variations [e.g., 60]. Fundamentally, PCA reduces the dimensions of multivariate data by creating new variables that are linear functions of the original variables. Given k variables at a given time period i , the linear combinations for k

² <http://grace.jpl.nasa.gov/data/gldas/>.

28 principal components (PCs) are

$$\begin{cases} y_{i,1} = p_{11}x_{i,1} + p_{12}x_{i,2} + p_{13}x_{i,3} + \dots + p_{1k}x_{i,k} \\ y_{i,2} = p_{21}x_{i,1} + p_{22}x_{i,2} + p_{23}x_{i,3} + \dots + p_{2k}x_{i,k} \\ \dots \\ y_{i,k} = p_{k1}x_{i,1} + p_{k2}x_{i,2} + p_{k3}x_{i,3} + \dots + p_{kk}x_{i,k} \end{cases} \quad i = 1, \dots, n \quad (1)$$

The data matrix $x_{i,k}$ contains rows representing the time i in months and k , the variables, i.e., the observations, which in our case is TWS or rainfall. In the linear combinations above (Eq. 1) the y values are orthogonal and also the new uncorrelated variables called the PCs such that y_{i1} explains the highest variability while y_{i2} up to y_{ik} explain the remaining variance. The coefficients of the linear combinations are called loadings (i.e., the eigenvectors) and they provide the weights of the original variables in the PCs. The eigenvalues (i.e., the amount of covariance in time explained by each eigenvector) and eigenvectors, which is also referred to as empirical orthogonal functions (EOFs) can be derived from the sample covariance matrix or correlation matrix of the centered data matrix $x_{i,k}$. The EOF is the spatial distribution or the spatial patterns of rainfall or TWS while the EOF/PC pair is called the PCA mode. In our case, the covariance PCA method was used since it is more ideal for climate analysis, in addition to extracting PCs that emphasize areas with very high temporal variability [e.g., [69,42]]. While the eigenvectors (e.g., $p_{11}, p_{12}, p_{13} \dots p_{kk}$), which have been normalized are the loadings, each eigenvalue (i.e., $\lambda_1 \geq \lambda_2 \geq \lambda_3 \dots \lambda_k$) explains the fraction of the total variance explained by the loadings [e.g., 59]. Further details on the choice of dimensions to reduce (i.e., dominant modes), geometric and statistical properties of PCA can be found e.g., in Jolliffe [42]. The use of a component extraction method such as PCA to decompose GRACE data, and satellite precipitation data into sets of principal components (PCs) and EOFs might probably help address some questions such as what are the trends and dominant spatio-temporal patterns of TWS variations in the region. Most importantly, using PCA in this study will provide a good knowledge of the spatio-temporal distribution of TWS and rainfall, which is important for water resources planning and understanding the impacts of climate on the hydrological system of West Africa. Hence, PCA was used in this study to analyze spatio-temporal patterns of changes in TWS and precipitation over West Africa.

3.2.2. Multiple linear regression analysis(MLRA)

The MLRA method is a statistical technique used to model the relationships between a dependent variable and one or more independent variables. It uses a least squares approach and has been widely applied in hydrology and climate science to explain the possible relationships between key variables [see, e.g., 50,70]. In order to understand the seasonal and inter-annual variations in the data series (i.e., TWS and rainfall) at a given grid point, the regression model of the form [e.g., 71]:

$$X(t) = \beta_0 + \beta_1 t + \beta_2 \sin(2\pi t) + \beta_3 \cos(2\pi t) + \beta_4 \sin(4\pi t) + \beta_5 \cos(4\pi t) + \varepsilon, \quad (2)$$

has been fitted to the time series of the data. $X(t)$ is TWS or rainfall at time t , β_0 is a constant offset, β_1 is the linear trend, β_2 and β_3 account for the annual signal while β_4 and β_5 represent the semi-annual signals. The model bias ε is taken as the deviation between model outputs and observations. Least squares fitting approach is used to estimate the regression coefficients, and the selected harmonic components (i.e., annual amplitude and semi-annual amplitude) are computed as:

$$\text{Annual Amplitude} = \sqrt{(\beta_2)^2 + (\beta_3)^2}, \quad (3)$$

$$\text{Semi Annual Amplitude} = \sqrt{(\beta_4)^2 + (\beta_5)^2}, \quad (4)$$

and the root-mean-square-error was computed as:

$$RMSE = \sqrt{\frac{1}{n} \sum_{i=1}^n (x_{obs} - x_{sim})^2}, \quad (5)$$

where x_{obs} and x_{sim} are observations and simulated values from the regression model respectively for n months. In order to assess the model's fitness in simulating TWS and rainfall, the coefficient of multiple determinations was computed for each grid point of the data. Besides the root mean square errors (RMSEs) and the coefficients of multiple determinations, the bias (i.e., difference between the true value being estimated and the expected value of an estimator) was also computed to further evaluate the performance of the MLRA over West Africa. Further, the use of MLRA will provide insight regarding the extent to which simulations of TWS and precipitation can be relied upon. This method was applied here to model the trend, annual and semi-annual components of TWS changes and precipitation over West Africa.

3.2.3. Variability index and trends

To examine the variation in trends, and further analyze the seasonal variations in the region for the period investigated, the variability index was computed for precipitation and TWS, from which annual and semi-annual components have been removed using MLRA. In essence, this study analyzed the monthly variability of trends and seasonal signals for the two products. The reason for this approach is to help classify the time series of changes in TWS and rainfall residuals, which consists of trends and seasonal components, into different climatic regimes such as wet, dry, normal, and extreme [72]. For precipitation, the variability index is computed as standardized precipitation departure while for TWS, it is computed as standardized TWS deviation:

$$\delta_{TWS/P} = (X_{TWS/P} - \mu) / \sigma, \quad (6)$$

where $\delta_{TWS/P}$ is the variability index for the TWS or rainfall (P), $X_{TWS/P}$ is the data (i.e., TWS or P) averaged over the region (i.e., over land), μ and σ are the mean and standard deviation for the data over the study period respectively, e.g., using all spatio-temporal data. Besides the computation of standardized deviation for TWS and precipitation, a trend was fitted into the monthly grids of rainfall for the period 2002–2013. In addition to this, rainfall was averaged over the region in order to understand the evolving annual amplitude of rainfall from the temporal patterns. In order to decrease the strong effect of the annual signal in the spatially averaged rainfall over the region, the monthly rainfall was smoothed using a moving average filter. Also, the least squares method was used to estimate the trends in (i) the time series of averaged TWS for the period between 2002–2014 and (ii) the temporal evolution of relevant PC modes derived from TWS decomposition using the PCA method.

3.2.4. Correlation analysis

Several approaches appropriated for modelling the relationships between multivariate data measured at different times include autocorrelation, coherence analysis, dynamic factor analysis, cross-correlation, etc., [73]. In this study, Pearson's correlation coefficient is used to examine the strength of agreement between two different hydrological variables (e.g., rainfall and TWS) while cross-correlation is used to determine the time lag between the hydrological signals (i.e., TRMM based precipitation and GRACE-derived TWS). Monthly grids of precipitation and GLDAS TWSC were correlated with that of GRACE-derived TWS at 95% confidence level in order to study the relations between them. In the cross-correlation approach, the position of the peak value indicates the time offset

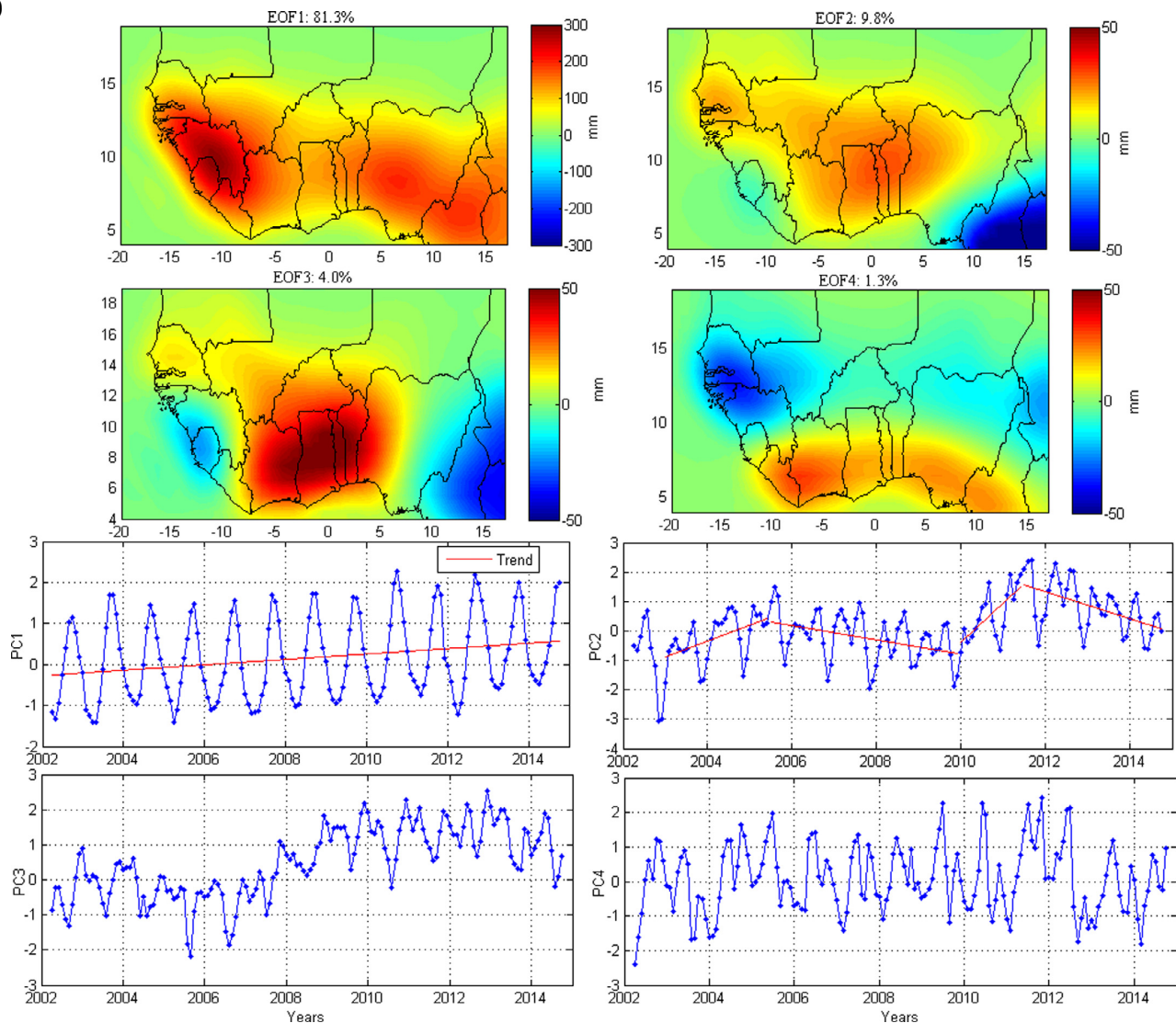


Fig. 2. PCA decomposition of TWS changes over West Africa. The EOFs are loadings showing spatial patterns of variations in TWS over West Africa while the corresponding PCs are temporal variations which are normalized using their standard deviation to be unitless.

when the peak association occurred (i.e., when the two signals are the most similar) in the hydrological time series. In order to understand the response time (i.e., the time lag with maximum correlation) of TWS to rainfall in the region, the cross-correlation method was used. Besides the cross correlation approach, the seasonal cycles of rainfall and TWS were also used to understand the lag relationship. A regression fit was also applied to understand the relationship and the variability between time series of GRACE-derived TWS and GLDAS TWSC for the common period (i.e., 2002–2014).

4. Results and discussions

4.1. Dominant patterns of total water storage (TWS) over West Africa

The PCA method has been used to identify the dominant spatio-temporal patterns of changes in TWS over West Africa within the period of 2002–2014. For statistical inference, the TWS grid is decomposed into sets of principal components (PCs, i.e., the temporal patterns), and their corresponding empirical orthogonal functions

(EOFs, i.e., the spatial patterns) using the PCA covariance method. While the EOFs (also referred to as the eigenvectors) are standardized using the standard deviation of their corresponding PCs, the standard deviation of the respective PCs were used to normalize the PCs in order to make them unit-less. From our scree plot analysis (not shown), i.e., a plot showing the statistically significant PC modes [see, e.g., 67], the first four PCA modes, which gave a cumulative variance of 96.4%, were adopted as meaningful signals representing over 95% of the total TWS variability over West Africa. The results of the principal component analysis indicate that the highest EOF loadings are observed in some parts of West Sahel and Middle Belt in the first orthogonal mode (Fig. 2).

This first PCA mode, which explains 81.3% of the variance, represents the annual variability of TWS changes in the region. The first PCA mode of the GRACE-derived TWS changes shows the strongest annual variability over Guinea and Sierra Leone and to a lesser extent over the Middle Belt region in Nigeria. Especially over Guinea, Sierra Leone, Guinea Bissau, and Liberia, the magnitude of rainfall make the regions exceptionally wet, with an

average monthly rainfall ranging from 150 mm to 350 mm (see Section 4.2). Furthermore, EOF1 and its corresponding PC (Fig. 2) show an increasing trend in TWS changes over West Africa for the study period. This trend, which points towards an overall wetness in the region is discussed further in Section 4.5. The second EOF and its corresponding PC, which explains 9.8% of the total TWS variability, represents multi-annual variation in TWS changes over some countries in West Africa for the study period (Fig. 2). As can be seen in the corresponding EOF (i.e., EOF 2 in Fig. 2), the multi-annual variation is relatively strong over Ghana, Togo, Benin and southern Burkina Faso, the riparian countries that constitute the Volta basin. Also, over the Guinea Coast and West Sahel, a considerable multi-annual variation can be seen in the second EOF. Multi-annual variations with strong amplitudes ranging from 45 mm to 62.5 mm are observed in the Volta basin between 2010 and 2012 compared to the negative TWS change of -60 mm observed in late 2006. These multi-annual variations for example between 2010 and 2012, if related to the size of the Volta basin of approximately $407,093 \text{ km}^2$, will translate to $\sim 18.3 \text{ km}^3$ and $\sim 25.4 \text{ km}^3$ of water volume respectively, a rather significant amount of water when compared to Lake Volta's storage capacity of 148 km^3 . These somewhat strong multi-annual changes in the TWS between 2010 and 2012 as indicated in PC2 of Fig. 2 can be attributed to increased rainfall within the period (i.e., between 2010 and 2012). This period also coincides with the period where most African lakes experienced severe flooding due to strong seasonal variations in rainfall [12]. Also, ponding of water behind the dam might also play a critical role in the observed TWS variation in the period (this is discussed further in Section 4.5). Further, we note a phase shift (i.e., an opposite phase) in EOF2 (i.e., Fig. 2), which is due to differences in rainfall patterns in the region. For instance, Cameroon experiences an equatorial climate pattern and receives about 400 mm monthly rainfall during the wet season and peaks in October/November while over much of the Volta basin, rainfall peaks occur in July/August. The stronger loadings (i.e., when compared to the one over the Volta basin) observed in this mode in southern Cameroon is attributed to a much stronger variability in the seasonal rainfall patterns, which are also driven by West African Monsoon winds.

Since the second PCA mode explains about 10% of the total TWS variability, we further analyze the trends in the multi-annual variations of its temporal evolutions (PC2, Fig. 2) in relation to the corresponding EOF loadings over the Volta basin (i.e., Ghana, Togo, Benin and southern Burkina Faso). Our attention is particularly drawn to the Volta basin because of the huge socio-economic potential of Lake Volta and the 20 million people who depend on the water resources of the basin. To this end, we used least squares method to analyze the multiple trends observed. Instead of fitting a direct simple line to PC2 in Fig. 2, its temporal evolution was splitted and least squares method was applied to each section. That way the strong multi-annual variation will not affect the trend estimation. A linear fit (i.e., using least squares) to the second PC (Fig. 2), which represents the trend in multi-annual changes in TWS for the period investigated indicate an overall increase of $13.5 \pm 4.25 \text{ mm/yr}$ between 2003 and mid 2005 while a decrease of $6.0 \pm 2.0 \text{ mm/yr}$ was observed between mid-2005 and 2009. The period between 2010 and 2012 was quite exceptional as it experienced an increase in TWS change of about $33.5 \pm 8.75 \text{ mm/yr}$ (see, e.g., PC2 of Fig. 2). Though this period of the observed trend is short, however, it stimulates a rather strong hydrological interest regarding the possible cause of such a dramatic increase in TWS during the period (i.e., 2010–2012). This increase in TWS could be due to the magnitude in June, July and August precipitation of that year (i.e., 2010), which made it extremely wet. After this period, a decreasing trend of about $11.5 \pm 3 \text{ mm/yr}$ is observed from 2012 up to 2014 as shown by the amplitudes of

PC2. This observed negative trend in PC2 (i.e., 2012–2014) indicates a decline in TWS change due to declining rainfall totals over the Volta basin and its riparian countries. Overall, as shown in the next section, the rainfall trend estimate shows a decline over the Volta basin and is consistent with Ahmed et al. [25] who also reported a decline in rainfall within this period. In a previous study, Owusu et al. [74] had specifically attributed the decline in rainfall totals over the Volta basin to the impact of El Niño Southern Oscillation Index (ENSO) event.

The third PCA mode represents about 4% of the total TWS variability and shows again a multi-annual variation. This variation is approximately centred over Lake Volta and extends over the complete Volta basin. The strong EOF loading observed in this mode is directly over the lake and indicates multi-annual variations over the lake area. The lake (i.e., Lake Volta, which nicely fits with EOF3 of Fig. 2) had low water levels between 2003 and 2007 (Lake Volta is discussed further in Section 4.8), and had increased since the early rain onset in 2007 (see PC3 in Fig. 2). The fourth PCA mode, which accounts for 1.3% total TWS variability represents mostly a semi-annual signal due to the strong rainfall patterns at the Guinea Coast where rainfall is bimodal (i.e., two periods of wet seasons), largely influenced by intensity, and regulated by the impact of sea surface temperature (SST) [e.g., 75,46]. For instance, concerning the bimodal nature of rainfall in this area (i.e., eastern Liberia up to western and southern Nigeria), low SST anomalies lead to reduced precipitation such that rainfall decreases from about 60 cm in eastern Liberia and Nigeria to about 20 cm in Côte d'Ivoire and western Ghana [76]. These low SST anomalies occur between July and August and generate a *temporal dry period* or Little Dry Season [see more details in 77,76] in the mid summer by supporting a condition of static stability, which hinders the development of convection, leading to low precipitation. The warm SST anomalies, on the other hand, occur in other months of the year, bringing higher precipitation before and after the *temporal dry period*, hence the bimodal rainfall in this region. Concerning rainfall intensity (i.e., strong magnitude of rainfall) over these areas, while Paeth et al. [65] reported an abundant rainfall of 467 mm in August 2007 at Gaya station in Nigeria (i.e., 11.53°N , 3.27°E), Nguyen et al. [75] observed that rainfall intensity between May and June in the areas near the coast varied largely between 5.1 mm/day and 11 mm/day. This kind of intensity, number of extreme rainy days, cumulative annual rainfall, and the strong bimodal character of rainfall in this coastal region (i.e., eastern Liberia, Côte d'Ivoire, Ghana, western and southern Nigeria) are the main triggers of the observed hydrological signal in the fourth orthogonal mode of Fig. 2.

4.2. Precipitation patterns over West Africa for the period 2002–2013

The discussion in this section focuses on the TRMM rainfall distribution over West Africa for a 12-year climatological window (i.e., 2002–2013). While mean monthly rainfall distribution within the time period investigated varied from less than 50 mm to more than 300 mm in West Sahel, the Central Sahel received less than 100 mm (Fig. 3a). Also, mean monthly rainfall distribution ranged from less than 80 mm to more than 300 mm at the Guinea Coast while rainfall in the Middle Belt region ranged from less than 100 mm to more than 200 mm (Fig. 3a). Besides the movement of the ITCZ, and the influence of atmospheric circulation features such as African Easterly Jets (AEJ), West African Westerly Jets (WAWJ), and Tropical Easterly Jet (TEJ) [see, e.g., 46,49], the influence of altitude and physiographic features plays a major role in the annual and monthly rainfall distribution in the region [see, e.g., 78]. For instance, the highland areas such as Sierra Leone, Guinea, and Cameroon receive more rainfall than the surrounding lowlands in the Central Sahel (Fig. 3a). In addition, trends in spatial precipitation patterns over the region indicate an increase

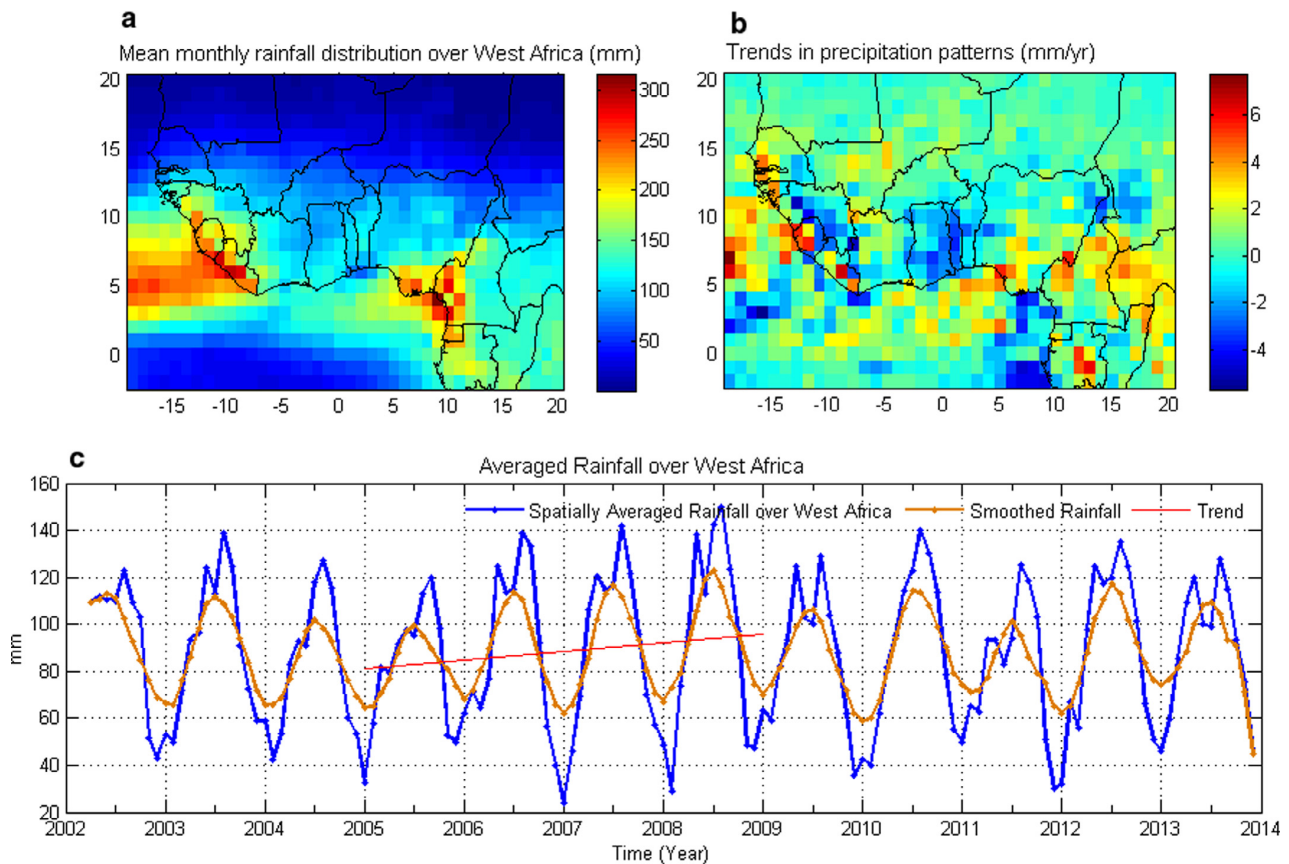


Fig. 3. Rainfall distribution and trends over West Africa, (a) Mean monthly rainfall distribution for the period 2002–2013, (b) Trends in rainfall, and (c) Temporal variations of rainfall (2002–2013).

between 1.5 mm/year and above 6 mm/year and a decrease of more than 4 mm/year in the sub-region (see Fig. 3b). This value, which is statistically insignificant at $\alpha = 5\%$ significance level, agrees with the findings of Marshall et al. [79] who also observed an insignificant decreasing trend in precipitation over the region. Also, visual analyses from the temporal variations of the smoothed rainfall over West Africa show an increased magnitude of the annual signal between 2005 and 2009 (Fig. 3c). While Paeth et al. [65] reported on flood events, which prevailed over some parts of the sub-region in 2007, this period also coincides with the period of upsurge in Lake Volta water levels (i.e., from 2006–2010), where an increase of more than 6 m was recorded. More discussion on this item will be provided in Section 4.8. Also, reports from the World Meteorological Organization in 2012 indicated that above normal rainfall resulted in flood events in south eastern Mauritania, Mali, Senegal, northern Burkina Faso, Lake Chad basin in Niger, Nigeria and Cameroon [80].

Despite this apparent rainfall intensity that culminates in serious flood events, the observed increase in linear trend of the spatially averaged rainfall over West Africa for the entire period (not shown) is statistically insignificant. This is consistent with Panthou et al. [81], who noted that, despite the intermittent torrential rains, and floods in the region, dry conditions still persist, since rainfall average in recent times is still lower than in the wet periods of the 1950's and 1970's. However, concerning the relative wetness and flood incidence that have been reported in the region, the strong variability in the intensity of the annual cycle of West African Monsoon rainfall might be responsible for the occasional floods and relative wetness seen in the region. For instance, while

findings in Paeth et al. [65] suggest that the above normal rainfall in August 2007 induced by ENSO event was responsible for the flood event in some parts of the river basins across the region, other studies have reported strong rain seasons near the Guinea coast around the June–September period [see, e.g., 50,75]. The seasonal variation of rainfall is discussed in subsequent sections.

4.3. Spatio-temporal variability of rainfall

From the PCA results, the cumulative variability explained by the first four most dominant modes is approximately 72.2%. Since the size of the spatial domain determines the performance of PCA [68], the variance explained by the first four most dominant modes can be improved if the analysis is limited to the sub-regions within the study area (i.e., if the oceans are masked). However, since the West African Monsoon (WAM) system conveys moisture from the surrounding ocean, understanding the spatio-temporal patterns of rainfall along the oceans as well will improve our knowledge of land-ocean dynamics in the region. In our analysis, the highest loadings from the first EOFs, representing 49.5% of the total variability, are concentrated around West Sahel, Central Sahel, and some parts of the Guinea Coast (Fig. 4). This orthogonal mode describes the sub-regions with considerably strong annual rainfall variability. The second PCA mode, which explains 12.2% of the total variability, represents semi-annual rainfall patterns mostly over the ocean but also extending to the Guinea coastal region. The third and fourth orthogonal modes and their corresponding PCs, which explain 6.2% and 4.3% of the total variability, respectively, represent a combination of multi-annual and seasonal variability of rainfall

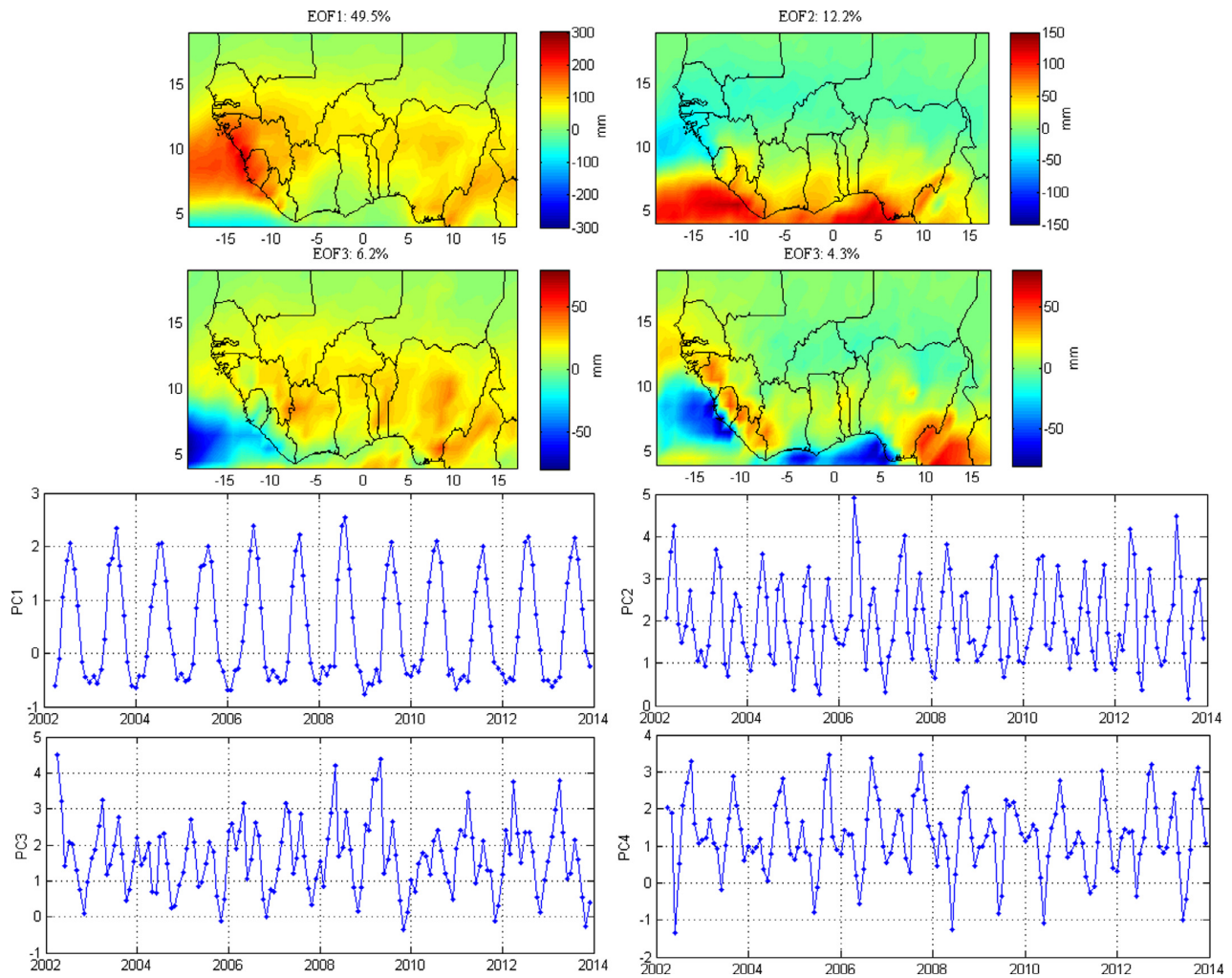


Fig. 4. PCA decomposition of TRMM precipitation over West Africa. The EOFs are loadings showing spatial patterns of variations in precipitation over West Africa while the corresponding PCs are temporal variations which are normalized using their standard deviation to be unitless.

in the region. These variations (i.e., PC1, PC2, and PC3 of Fig. 4) are largely due to annual rainfall cycles, circulation features, and influence of ocean warming and climate teleconnections in the Sahel and Guinea coast region [see, e.g., 50,65,47].

These rainfall structures and patterns over West Africa suggest the dominance of annual and semi-annual variability in West African Monsoon rainfall, and a progressive shift in the semi-annual cycles of rainfall from the Guinea Coast to the Central Sahel [see, e.g., 82,47,50]. This annual variability can be linked to changes in August and September rainfall [69]. Also, the sea surface temperature (SST) of the eastern Atlantic and the role of the Atlantic Cold Tongue (ACT), which regulates the intensity and timing of coastal rainfall in spring, have been largely associated with the dominance of inter-annual and seasonal variability of rainfall in these sub-regions [75].

In addition to the impact of SST on seasonal and inter-annual rainfall, other climate indices such as the Atlantic Multi-decadal Oscillation (AMO), Atlantic Meridional Mode (AMM), and Madden Julian Oscillation (MJO) have been identified to have positive correlation with rainfall patterns in the region [see, 50,48]. However, the PCA method could not represent any of such patterns in either of the EOF loadings or the corresponding principal components. This

weakness in the PCA method, which arises due to the orthogonality of its temporal and spatial components, will be addressed in future studies by investigating other higher order statistical methods such as Varimax rotation and independent component analysis (ICA), which maximises regional phenomena [e.g., 68,83].

Further, there were no significant linear trends in the principal components as determined by a least squares fit (not shown). Considering the observed increase in the annual TWS temporal patterns (PC1, Fig. 3), it is normal to assume a linear relationship between rainfall and change in storage over time. However, over Guinea and parts of West Sahel, such relationships might not be completely linear as annual variation in discharge for example can only be partly explained by the annual variation in precipitation [84]. This non-linear relationship can be attributed to variations in the type and morphology of rivers, geology, physiography, vegetation, soil type, ponding of water behind dams and reservoirs, and the catchment extent amongst others. We provide more discussion on this in Section 4.5. However, the lack of a significant positive trend in rainfall as observed in the temporal evolutions of PC1 in Fig. 4 suggests a fairly stable climatic regime for the whole study area (see also, Fig. 3b) regardless of occasional changes in intensity and increased inter-annual and seasonal variability in rainfall. This

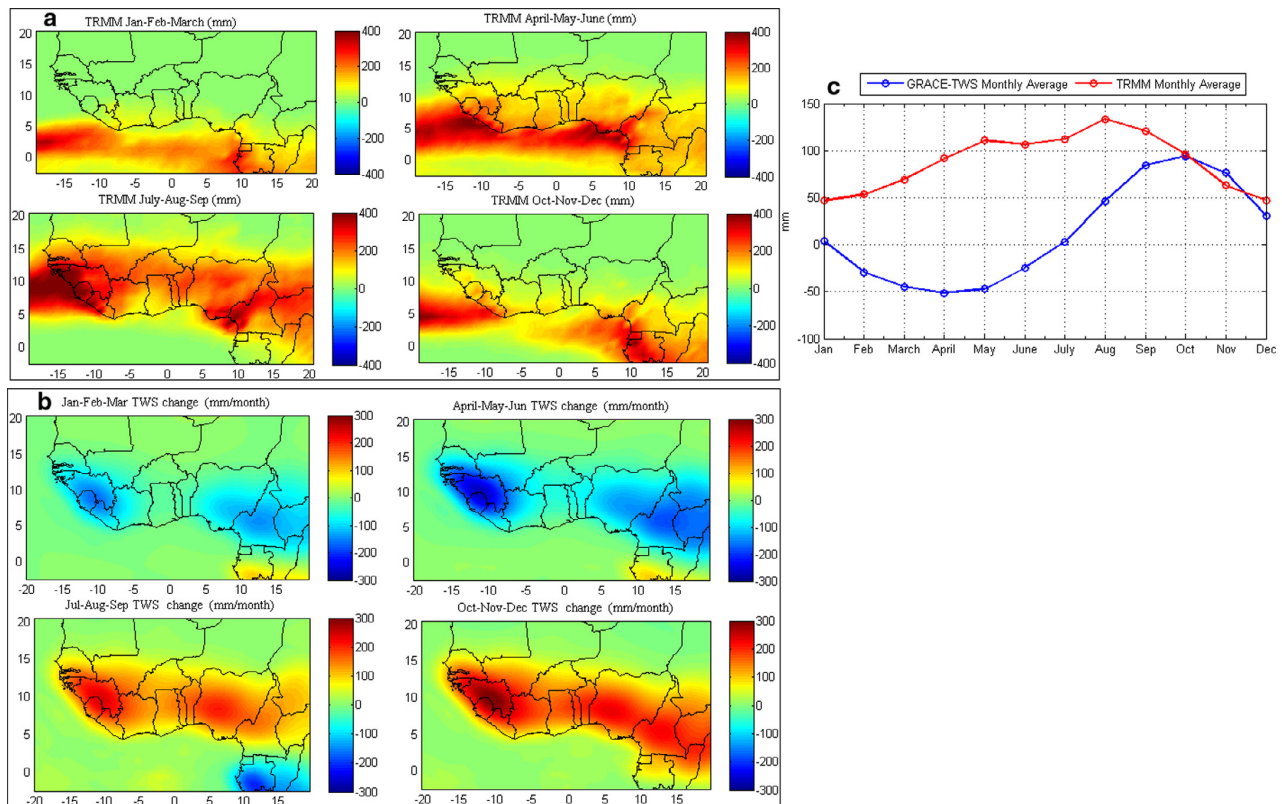


Fig. 5. Seasonal cycles of GRACE derived TWS changes and precipitation; (a) TRMM averaged values for the seasonal periods, (b) GRACE-TWS averaged values for the seasonal periods, and (c) mean monthly rainfall and TWS change over West Africa.

position is consistent with Giannini et al. [85] who reported that increased daily rainfall intensity is a contributing factor to the perceived rainfall recovery in the region. However, a decline in rainfall mostly over parts of the West/Central Sahel and Lake Volta basin is observed (Fig. 3a and b). There is a tendency towards aridity in those regions, particularly over the Volta basin where Owusu et al. [74] had previously reported that the declining rainfall totals, triggered by the warm phase of ENSO, are the main cause of the decline in Lake Volta water levels in the Volta basin. In view of this result, the region's susceptibility to drought conditions might increase as reported in Asefi-Najafabady and Saatchi [86].

4.4. Analysis of trend and seasonal variations of precipitation and TWS

The seasonal cycle of precipitation and changes in TWS were estimated by spatially averaging monthly values over the study period. While the averaged values for the rainfall seasonal windows shows maximum rainfall in the July–August–September period, the change in TWS shows maximum seasonal variations in the October–November–December period (Fig. 5a and b). On the other hand, the mean monthly rainfall shows a peak in August, while the mean monthly change in TWS for the study period shows a peak in October (Fig. 5c). Apparently, this shows that TWS lags behind rainfall in the region by approximately two months. To further ascertain the time response of TWS to rainfall, the temporal evolutions of the dominant TWS and rainfall orthogonal modes (i.e., PC1 Fig. 2 and PC1 Fig. 4) clearly indicate a two month lag between TWS and rainfall when their annual peaks are compared (i.e., while rainfall peaks in August, TWS peaks in October). On the whole, the analysis of our rainfall grouping (i.e., the differ-

ent seasonal periods) is consistent with the classification of major West African annual rainfall settings outlined in recent studies [see, e.g., 87,88]. That is, for instance, our Jan–Feb–March period describes the oceanic phase when the rainbelt is large with maximum precipitation values just north of the equator; April–May–June refers to the coastal phase with peak rainfall values around coastal regions within the gulf of Guinea, i.e., Guinea Coast; while the July–August–September period describes the Sahelian phase where maximum rainfall is established around latitude 10N (see Fig. 5a and b).

From the TWS variability index, the years 2002–2006, and early 2007 are indicative of dry years, while the year 2010 and beyond was quite wet (Fig. 6a). The rainfall shows dry conditions in 2004–2006, wet conditions in 2010, extreme conditions in 2011, and near normal conditions in 2009 and 2013 (Fig. 6b). One relevant observation made from the rainfall variability index is that the dry periods of 2004–2006 correspond to the dry periods observed in the TWS index of variability. This implies that rainfall is a major contributor to the hydrological flux in the region, and that change in precipitation patterns as observed in the region is likely to be the most significant driving factor for the surface mass variations, hence the dominant patterns observed in TWS changes. The PCA results (especially the dominant patterns) for both GRACE-TWS and rainfall confirms this hypothesis (see Sections 4.1 and 4.3). Further, our analysis of TWS variability index in terms of trends and seasonal variability shows that the region experienced water deficit between 2002 and mid-2007 (Fig. 6b). This perspective is very similar to results of Asefi-Najafabady and Saatchi [86], who reported that West Africa experienced strong negative water storage anomalies between 2005 and 2007. Though our analysis of rainfall variability commenced in 2002, we infer based on previous

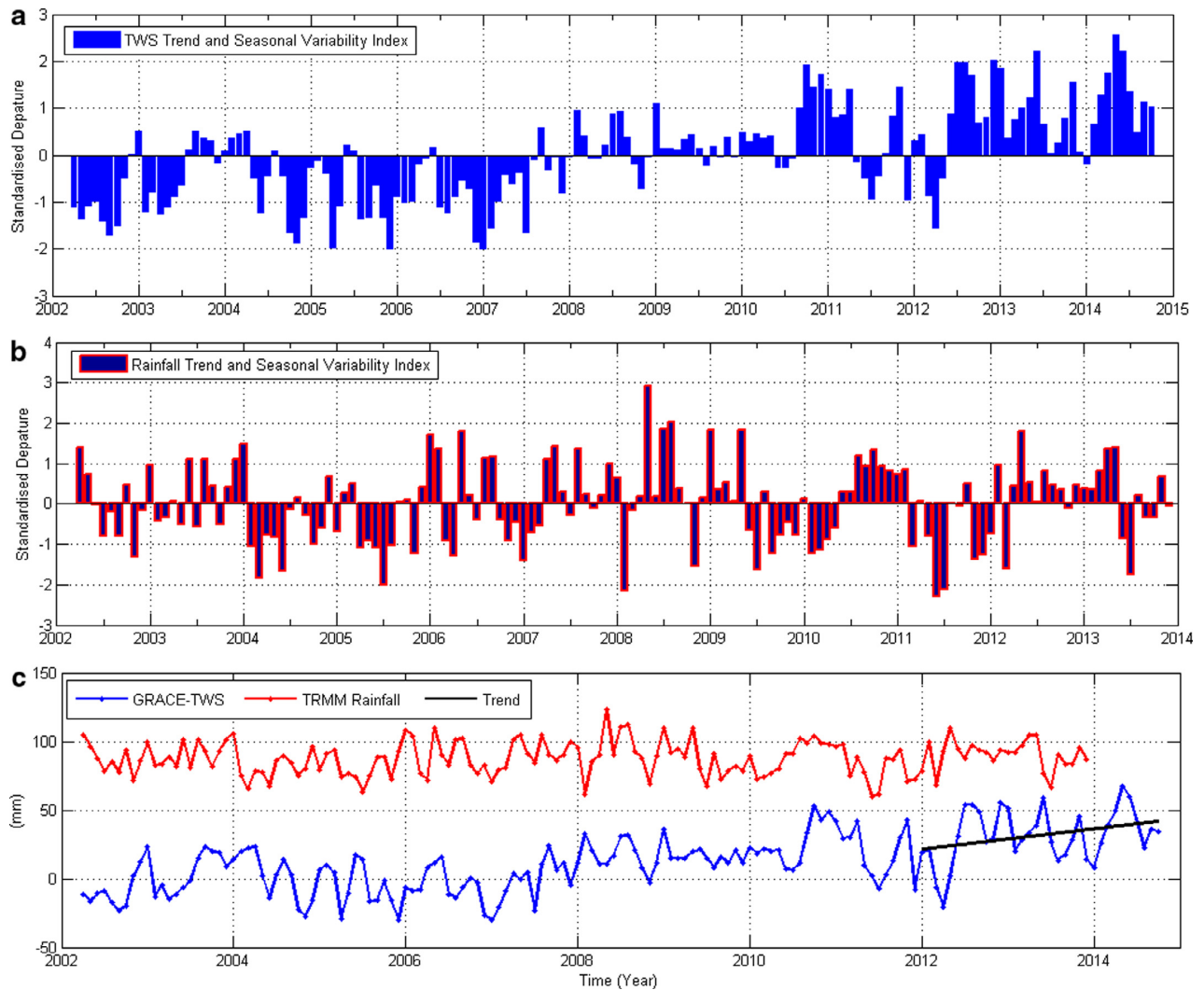


Fig. 6. Variability Index after removing annual and semi annual components. (a) GRACE-TWS variability index, (b) TRMM rainfall variability index, and (c) Least squares fit of TWS anomalies for the period 2012–2014 (i.e., not standardized).

studies [e.g., 48,81] that the observed water deficit between 2002 and 2007 is an extension of the drought period in the 90s, which continued unabated despite the perceived rainfall recovery. While the impact of the 1991 and 1997 El Niño events, which caused low rainfall in the region, are noted [e.g., 46,74], Nicholson [48], specifically pointed out that the relative recovery in rainfall over West Africa was not all encompassing, and that the mean annual rainfall within the period (i.e., 1990–2007) is significantly not different from the mean of the acknowledged drought period.

However, from our analysis of changes in TWS averaged over West Africa (i.e., after removing the harmonic components), there seems to be a relative increase in water availability in recent times (i.e., the period between 2012 and 2014). Since Fig. 6a shows wet conditions between 2012 and 2014, we fitted a linear trend to the GRACE-derived TWS for the same period in order to understand TWS trend in recent times, which is useful for planning and management. While the least squares fit for the period between 2012 and 2014 for the averaged GRACE TWS changes after removing annual and semi-annual components shows a significant increase of 7.47 ± 3.98 mm/yr in the linear trend (Fig. 6c), the averaged TWS anomalies over West Africa (i.e., over land) for the study period

show a linear increase of 6.85 ± 1.67 mm/yr (Fig. 7), which is statistically significant at 95% significance level. This increase in TWS trends over the region, could be attributed to a large water surplus from prolonged wet seasons and lower evaporation rates in coastal West Africa (i.e., Guinea Coast and some parts of West Sahel), which remarkably increases the water storage and inundated areas along the coastal catchments that sustain the dry season river flow [7]. In view of this recent trend in TWS change, it is expected that crop development, moisture conservation, and soil fertility for some parts of the region might be significantly improved. In Section 4.5, we provide further details to highlight the non-linear behavior observed in the temporal evolutions of the annual signals of our PCA results for TWS and rainfall as indicated in PC1 of Figs. 2 and 4, respectively.

4.5. The hydrology of the Fouta Djallon Highlands

The Fouta Djallon Highlands (FDH) comprises chains of mountainous landscapes mostly in Guinea and extend into countries such as Sierra Leone, Guinea-Bissau, Senegal, Mali, Côte d'Ivoire and Liberia [84]. The highlands, which are small watersheds and

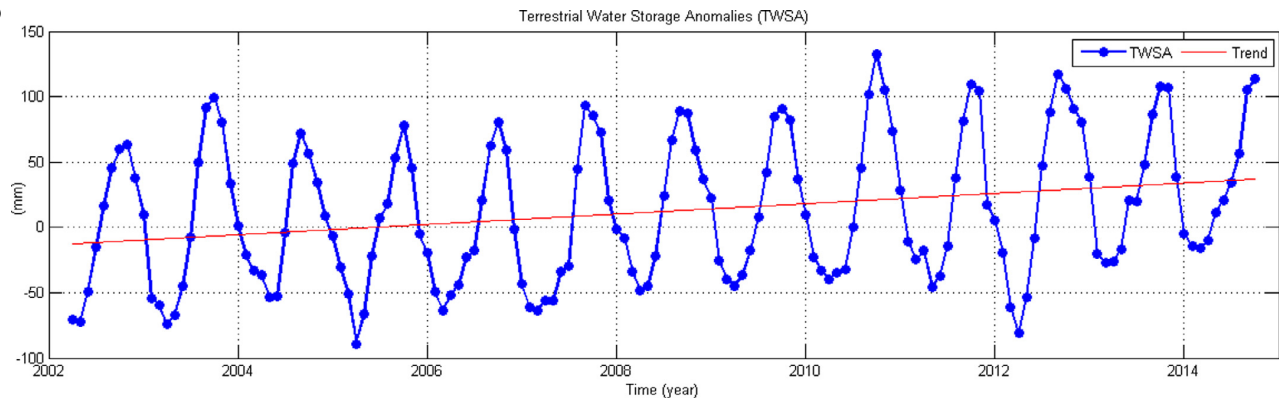


Fig. 7. Trend in TWS anomalies over West Africa for the period 2002–2014 (i.e., without removing the harmonic components). The trend is also clearly visible in PC1 of (Fig. 2).

sources to major West African rivers (e.g., River Niger, Senegal, Gambia, and Mano) have been labeled the *water towers* of West Africa. These rivers provide drinking water, irrigation and hydro-electric power to millions of people who make their homes in the catchment. Our interest in FDH is due to the strong dominant spatio-temporal behavior observed in our PCA results for TWS and precipitation. While the annual variability of TWS especially in Guinea (PC1 Fig. 2) shows a steady increase in water storage change, annual variability of precipitation shows no obvious significant increase in the same area (PC1 Fig. 4). The temporal evolution of PC1 in Fig. 2 indicates a significant rise of 20.2 ± 5.78 mm/yr in Guinea while no significant increase was observed in rainfall. The hydrology of these watersheds (i.e., FDH) is largely controlled by components of the hydrological cycle such as precipitation, runoff, and recharge. The water balance model can be written as

$$P = E + Q + \delta S, \quad (7)$$

where P , E , Q , and δS are precipitation, evapotranspiration, runoff, and change in storage respectively. The storage variable, that is the runoff deficit variable, R_D , can be defined as

$$R_D = P - Q, \quad (8)$$

where the runoff deficit R_D is the amount of water, which is stored in watershed, evaporated, or water lost through the process of transpiration (i.e., the yearly water availability). For the FDH, vegetation has not been modified and both temperature and evaporation are relatively low in these areas especially during rainy season [84]. Hence, it is reasonable to assume that no change has occurred in transpiration within the period. Increase in R_D implies increase in the volume of water not involved in surface runoff. This quantity, which is assumed to have increased over time, represents the aquifer storage. With precipitation spreading over 8–12 months of every year, lack of significant change in evapotranspiration, and huge groundwater potentials, in addition to very high aquifer productivity as shown in MacDonald et al. [89], the aquifer storage is likely to increase despite the lack of positive trend in rainfall within the studied time period. The apparent increase in temporal patterns of annual TWS signal (PC1 Fig. 2), which coincides with the somewhat limited alimentation due to lack of significant positive trend in rainfall, is consistent with the findings of Verschoren [84] who observed over the FDH a non-linear relationship where a higher increase in discharge was inconsistent with observed precipitation. Comparatively, the amplitudes of annual rainfall observed in PC1 of Fig. 4 indicate that the years 2003 and 2006–2008 have relatively stronger annual peaks. Recently, McSweeney et al. [45] reported that the variations in the latitudinal movements and intensity of the ITCZ

from year to year can cause large inter-annual variability in the wet season rainfall leading to 1000 mm of monthly rainfall at the east coast of Guinea. This kind of variability, besides increasing the inundated areas in the catchment, will largely increase the amount of water stored in the watersheds, given that evaporation is generally low during the wet seasons in Guinea. Further, besides the high precipitation amounts of more than 3000 mm annually, Guinea is a region with heavy discharge, huge base flow and abundant water resources. For instance, the quantity of water entering Mali from Guinea is estimated at $40 \text{ km}^3/\text{yr}$, greater than the quantity entering Nigeria from Niger, which is estimated at $36 \text{ km}^3/\text{yr}$ [90]. In south-west Guinea where the EOF loadings are relatively strong, the average annual peak rainfall in the wet season ranges from $\sim 687.5 \text{ mm/yr}$ between 2006 and 2008 to $\sim 550 \text{ mm/yr}$ between 2010 and 2013 when jointly derived from the PC/EOF (PC1/EOF1, Fig. 4). With sub-regions such as Boke, Boffa, and Forecariah (i.e., local areas in Guinea where these rainfall amounts are observed), which lie along the coast in Guinea and covers a total surface area of $\sim 40,500 \text{ km}^2$, these rainfall amounts will give average annual water volume (i.e., in the wet season) estimated at $27.8 \text{ km}^3/\text{yr}$ and $22.3 \text{ km}^3/\text{yr}$ for the 2006–2008 and 2010–2013 peak periods respectively. This estimated amount of water volume excludes that of the northern and extreme western regions of Guinea where our PC/EOF method estimates average annual peak rainfall of 375 mm/yr and 300 mm/yr for the two periods, respectively. Since about $40 \text{ km}^3/\text{yr}$ of water leaves the country (i.e., Guinea), R_D increases over time despite lack of positive trend in rainfall, hence the increase in TWS trend observed over Guinea in PC1/EOF1 of Fig. 4. Also, note that our rainfall estimate here is for the peak rainfall only, which is more like the average rainfall in August with respect to the mean of 2002–2013. Considering a minimum of eight months of significant precipitation in south-west of Guinea, the water balance will apparently indicate a surplus regardless of stability or lack of positive trend in rainfall.

Moreover, in a related study, a similar relationship of increased TWS not being consistent with precipitation trends was recently reported by Ahmed et al. [25] in a continent-wide study. The study observed an increase of $15.35 \pm 0.79 \text{ mm/yr}$ and $16.68 \pm 1.09 \text{ mm/yr}$ in Okavango and Zambezi basins, respectively with no obvious significant increase in precipitation. The increase in TWS was attributed to the increased size of inundated areas of the basins and the cyclical nature of recurrent floods amongst other factors. Further, human activities such as building of dams and reservoirs will impound surface water in man-made lakes from the dams upstreams, inducing infiltration and consequently leading to increase in recharge from the lakes to groundwater. This example

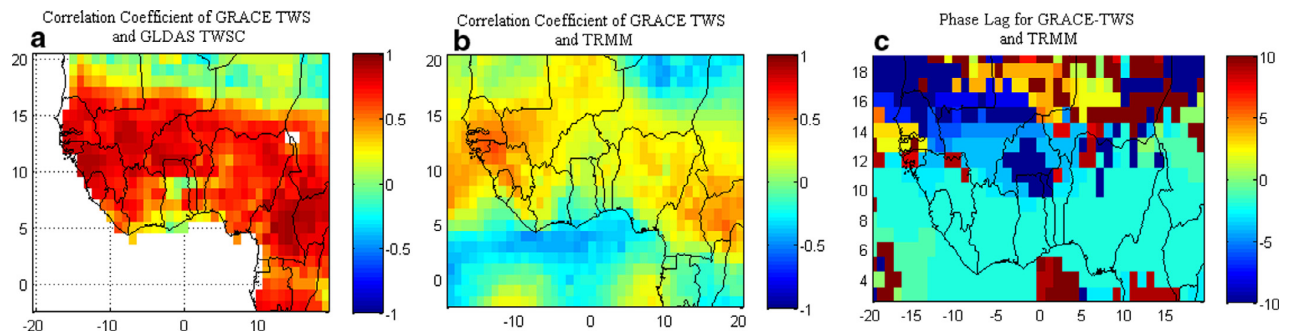


Fig. 8. Correlation analysis and time lag with maximum correlation using TRMM precipitation and GRACE-TWS. (a) Correlation between GRACE-TWS, and GLDAS TWSC (b) Correlation between GRACE-TWS, and Rainfall and (c) Time lag with maximum correlation for GRACE-TWS and TRMM precipitation in months.

was reported for the Lake Volta basin in the region where an increase of 14.41 ± 1.02 mm/yr was observed for the period between 2003 and 2012, despite lack of a significant trend in rainfall for more than a period of 10 years [see, 25]. The observed TWS over the basin (i.e., Lake Volta basin) was attributed to ponding of water behind the dam, which is also evident in the apparent increase of 7 m in Lake Volta water levels as shown in Section 4.8 (Fig. 12a). Also, over the Niger basin (which includes Guinea, Nigeria, Mali, and countries with dominant patterns in TWS as observed in the PCA result (i.e., PC1 Fig. 2), Ahmed et al. [25] also observed an increase of 6.31 ± 0.36 mm/yr in TWS for the period 2003–2012, which is somewhat consistent with the trend of 6.85 ± 1.67 mm/yr in observed TWS in our study. While a detailed study will be required to understand the role of land use in the hydrology of the FDH, Favreau et al. [91], had shown a rising water table of about 4 m between 1963 and 2007 in southwest Niger despite about 3% deficit in rainfall from 1970 to 2007. This paradoxical relationship, which is similar to the behavior of our hydrological time series (i.e., rainfall and TWS) as observed in Guinea and the surrounding areas, was attributed to a change in landuse pattern. Furthermore, since West Africa and the continent at large were worst hit by droughts in the 1980's (especially the Sahel), we also speculate that the recovery in the 1990's, which was not all-encompassing could account for the inconsistent trends between TRMM based precipitation and TWS, given that the huge aquifers of the Guinea region is still filling up. GRACE measures vertically integrated water storage from catchment stores (i.e., aquifer, soil moisture, etc.), any form of increase from these catchment stores will be apparent and captured by GRACE, unlike rainfall were transition periods from dry to wet might not be very obvious due to the impact of the previous extreme and frequent dry periods as in the case of the Sahel region. Generally, the water resources of West Africa are complex as seepages and evaporation are said to have triggered large reductions in runoff in the inner delta of Mali [90] in addition to the impact of land use change, human influence, and climate variability [see, e.g., 25,91,90]. Anthropogenic effect on changes in TWS over West Africa can be modelled from Water Gap Hydrological Model (WGHM) and this can be explored in future studies.

4.6. Relationship between GRACE-TWS, GLDAS-TWS, and TRMM

The cross-correlation result shows that TRMM rainfall leads GRACE-TWS changes in most parts of the region with a maximum phase lag of two to three months (Fig. 8c, see also Fig. 6c). This is consistent with the results in Section 4.4. Also in this study, the Pearson correlation coefficient was employed to examine the relationship between GRACE/TRMM and GRACE/GLDAS total water storage contents (TWSC) at 95% significance level. Prior to this analysis, the gridded TRMM rainfall product was resampled to a $1^\circ \times 1^\circ$ regular grid as the GRACE-derived TWS. The result from

TRMM rainfall product and GRACE-TWS comparison shows a high correlation in some parts of West Sahel and Middle Belt regions (e.g., Guinea) while weak correlation is observed in most sub-regions of West Africa (e.g., Niger, Burkina Faso, etc.) (Fig. 8b). The observed correlation in these regions is due to the presence of a strong annual signal as can be seen in the corresponding EOF1 of TWS (Fig. 2) and TRMM (Fig. 4). While the high correlation in West Sahel apparently defines the impact of rainfall on changes in TWS of the sub-region, the weak correlations could be the unexplained impact of water storage in the region's tropical forest. GLDAS-TWSC on the other hand, has a good correlation with GRACE-TWS for most parts of the region except for some locations in the upper Central Sahel and some parts of the Volta basin (Fig. 8a). The poor correlation of GLDAS-TWSC in those areas might be due to anthropogenic influence and probably intensified land surface processes, which the model could not account for [e.g., 92]. For example, water withdrawals and increased surface runoff due to change in land cover could possibly contribute to weak correlations in these areas.

Moreover, as mentioned earlier in this study, lack of in-situ data for calibration and parameterization of the GLDAS model outputs could largely be responsible for the poor correlation between GLDAS-TWSC and GRACE-TWS in these locations. Since GRACE TWS observations have been previously compared with GLDAS over the Volta basin and Southern Mali [see, e.g., 93,35], the poor correlation of GLDAS in some areas could not have emanated from GRACE TWS. This assumption follows the numerical results of Henry et al. [93], where observed monthly groundwater-storage variability in the region correlated strongly with monthly GRACE TWS changes whereas the timing of GLDAS-derived soil moisture was not well predicted. concerning the weak correlation between TRMM precipitation and GRACE-derived TWS, some anthropogenic contributions that impact on land surface conditions might play a major role.

For instance, the loss of 21,342 hectares of mangrove vegetation in the lower Niger Delta of the Middle Belt region between 1986 and 2003 due to urbanization, might introduce some imbalance in the hydrological routines of the region [92]. Future studies with focus on the land surface processes such as increased potential evaporation loss during the dry season, the contributions of land surface conditions, and historical land use/land cover activities in some parts of West Africa might provide some insight and clarity as to the cause of the weak correlations between GRACE-TWS and TRMM rainfall products in these sub-regions.

However, the high correlation between TWSC output from GLDAS and GRACE TWS in most parts of West Africa suggests that hydrological monitoring and climate research in these areas of West Africa can be reliable even with the use of hydrological models (i.e., outputs from GLDAS). Furthermore, the GRACE-derived TWS and the TWSC from GLDAS were averaged over land areas in the region. Their temporal variations both indicate

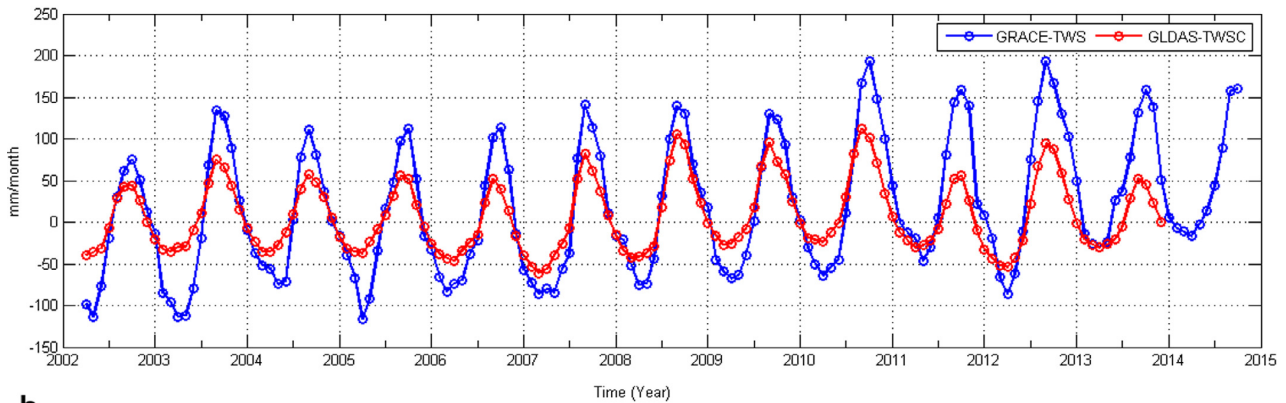
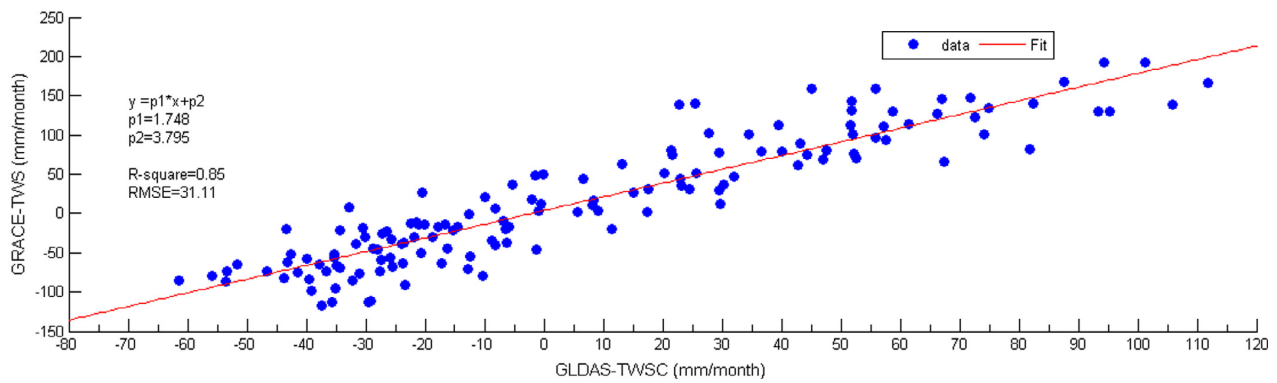
37 **a****b**

Fig. 9. (a) Temporal variations of GRACE-TWS and GLDAS TWSC and (b) Regression fit on GRACE TWS and GLDAS TWSC.

annual cycles with similar high and low peaks that correspond to rain and dry seasons in the region (Fig. 9a). While GRACE-TWS and the TWSC from GLDAS show peaks that correspond to the same time period, however, TWS output from GLDAS is underestimated for the region. Our conclusion here is similar to findings from a related study in southern Mali, where predicted soil moisture from GLDAS was poor (i.e., underestimated) [93]. The poor prediction of soil water storage using GLDAS in the region corroborates our account of GLDAS underestimation of simulated TWS in the present study. However, the regression fit between the two variables, which shows a coefficient of determination (R^2) of 0.85 indicates that most parts of the region have been well modelled in terms of trends and variability (Fig. 9b).

4.7. Modelling TWS anomalies and rainfall over West Africa

The MLR analysis was applied in order to further explore the relationship between TWS changes and precipitation patterns over West Africa. Comparatively, MLR allows the test of statistical significance on the spatio-temporal patterns as opposed to PCA that divulges the dominant spatio-temporal patterns [71]. Here, we compare the results of MLRA of TWS and rainfall, especially their annual amplitudes, semi-annual amplitudes, and trends. We point out briefly that since seasonality induces the largest signals in hydrological quantities, our intent here is also to examine the capability of MLRA in mimicking TWS and rainfall using linear trend, annual, and semi-annual signals. While their annual amplitudes are quite similar, the semi-annual signals show some disparity especially in rainfall patterns along the Central Sahel (Figs. 10 and 11). This probably suggests that the incoming rainfall

leaves the region through some intensified outgoing hydrological fluxes and processes such as evapotranspiration, and surface runoff from major rivers. For instance, Marshall et al. [79] showed how evapotranspiration correlates strongly with precipitation in the region. On the other hand, trends of both rainfall and GRACE-derived TWS are different. While higher positive trends in TWS are concentrated around the Volta basin and the Lake Volta area (Fig. 10), precipitation trends over the same area show both low/high negative and positive patterns (Fig. 11). The strong hydrological signals from the Volta basin as a result of the presence of Lake Volta largely accounts for the observed positive trends in TWS. From the coefficient of determination (Figs. 10 and 11), the multi-linear regression (MLR) model approximates TWS and rainfall quite well by using trend, annual, and semi-annual signals only. Considering the performance of MLR for rainfall in this study, similar conclusions to those of Diatta and Fink [50] can be reached. That study concluded that using MLRA, the West African Monsoon rainfall can be better predicted especially when combined with teleconnection indices. However, as indicated in their RMSEs and coefficients of determination, some parts of West and Central Sahel are poorly modelled in the two products (see Figs. 10 and 11). Furthermore, since the coefficient of determination for the TWS simulation in the West Sahel, Guinea Coast, Middle Belt and some parts of Central Sahel show a good fit, the change in TWS for these sub-regions can be predicted quite well.

4.8. Lake water levels in West Africa

In order to understand the seasonal fluctuations of surface waters (i.e., lakes), the annual and semi-annual components of

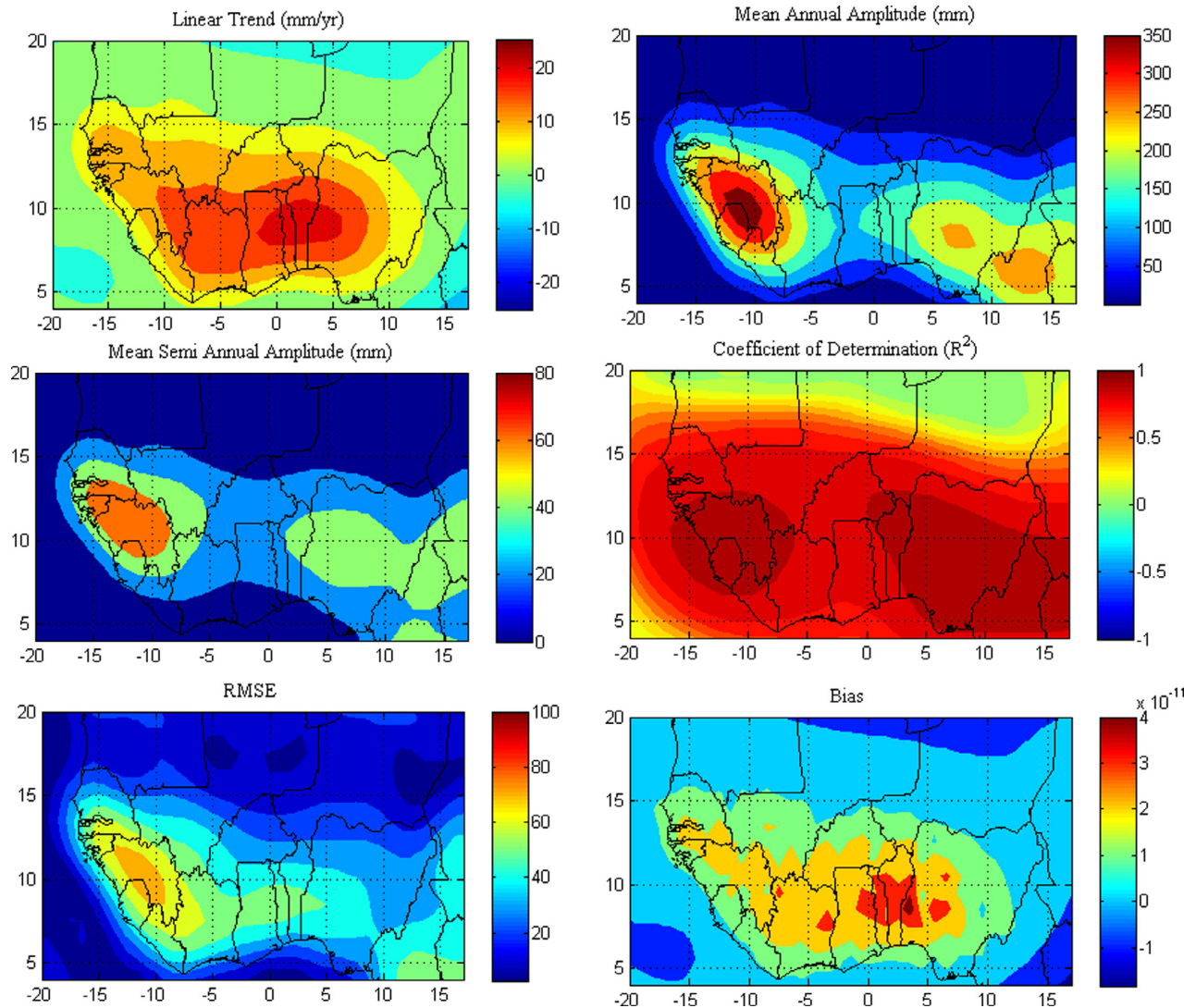


Fig. 10. MLR analysis of GRACE-TWS.

fluctuating water levels from Lake Volta, Lake Chad, and Kainji dam for the period 1993–2013 were removed using the least squares approach. The results show that Lake Chad and Kainji dam were dominated by annual and semi-annual variations while Lake Volta has a considerably strong annual signal (see Fig. 12a). The Lake Chad water level reduced by about 90% during the intense drought of 1968–1974, and its surface area had since shrunk from 24,000 km² in the 1950's to about 1800 km² in the 1980's [94,95]. Generally, the declining Lake Chad surface area has been attributed to agricultural activities (i.e., water use for irrigation) and the impact of climate variability [e.g., 4,96].

With strong annual variability, the minimum water level of Lake Chad is observed between May/June (see Fig. 12a). Wald [95], observed that the Lake Chad water level decreases in November and later rose to its maximum in January as a result of inflow from Logone - Chari - El Beid rivers. With a clearly marked annual fluctuation, observed minimum water levels and less pronounced annual signals of Lake Chad between the period 2004 and 2007 are indicative of dry periods induced by low summer rainfall in that sub-region while an increasing trend is also observed in maximum

water level in recent years (i.e., 2010–2013) (Fig. 12a), which is consistent with increased rainfall. For Lake Volta, its temporal variation (i.e., from 2006 to 2014) is similar to the third principal component from our GRACE-TWS PCA, which represents multi-annual variations over the lake area (see, e.g., Fig. 2). The lake's residuals show a decrease in the periods 1993–1995, 1996–1998, 2000–2002, 2005–2007, 2011–2013 and an increase in the period 2007–2011.

While it might be assumed that the decreasing phase is the impact of relatively strong inter-annual variations of rainfall, the increasing phase in Lake Volta water level is attributed to the impact of a moderate La Niña event in 2007 triggering increased rainfall in the region [65]. It is worth mentioning, that besides the impacts of La Niña on the water level, the ponding of water behind the dam as mentioned in Section 4.5 could be a factor in the observed increase in water levels. Further, Owusu et al. [74] attributed the lake level decline, which occurred between 2000 and 2002, and the relatively low maximum water levels between 2002 to late 2007, to a decline in rainfall totals influenced by the warm phase of ENSO. Although the Lake Volta water levels between 2011 and 2014 show

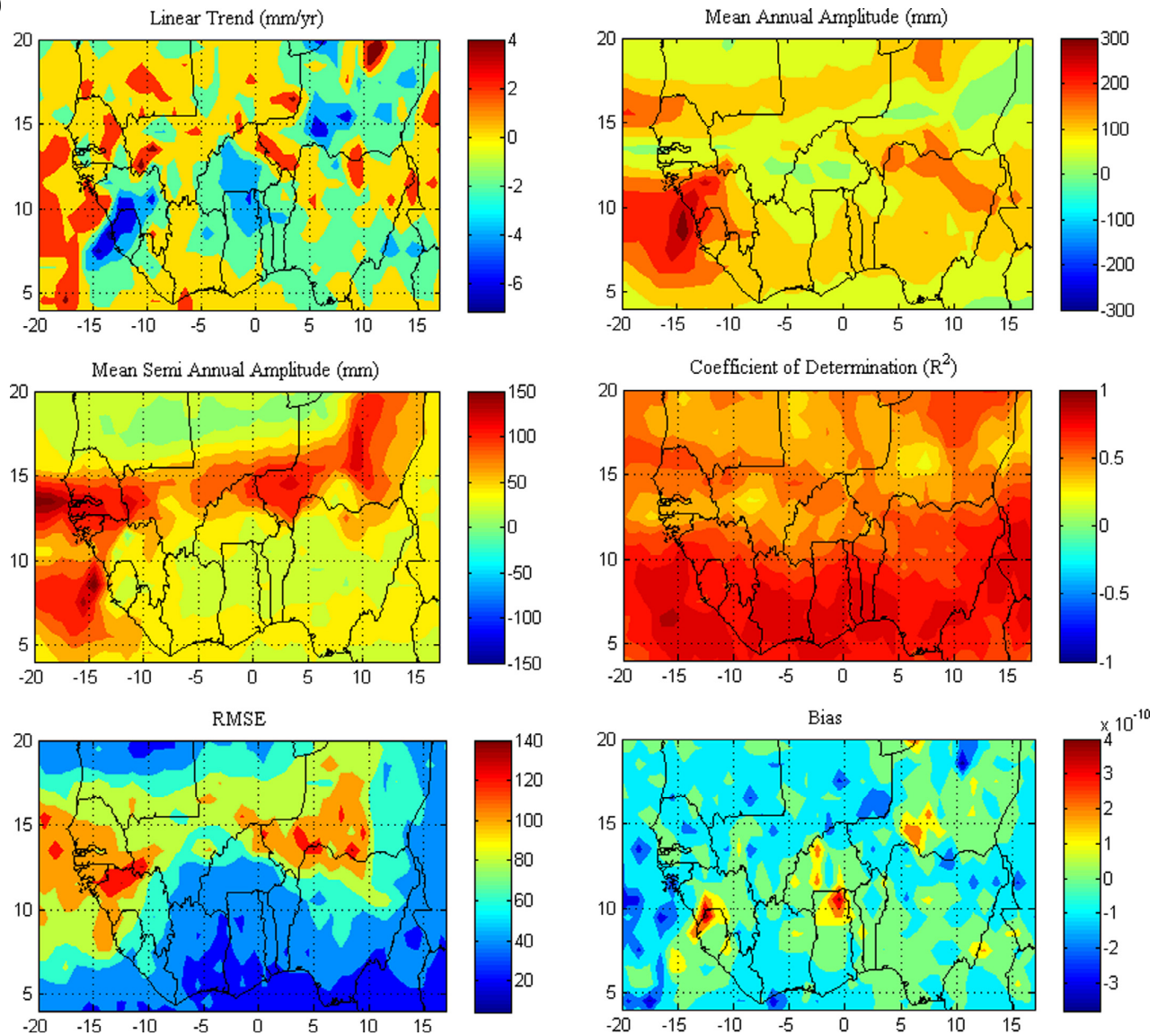


Fig. 11. MLR analysis of TRMM rainfall.

a gradual decline, however, the observed maximum water levels as captured in Fig. 12a and b still show a much higher maximum water level compared to the preceding decades, pointing towards water availability. Lake Volta, which has a total surface area of 8500 km² and stores approximately 150 km³, is equipped with a hydropower generation capacity of more than 900 MW [74]. In view of the observed low minimum water levels (e.g., 1998, 2002–2004 and 2007 of Fig. 12a), the hydropower capacity of Lake Volta might be limited, and as reported in [74] will lead to energy crises and conflicts amongst riparian countries who depend on this lake for energy production.

The Kainji dam is one of Nigeria's largest dam with a surface area of 130 hectares and primarily used for hydro-power generation [97]. The dam supplies most of the domestic and industrial power needs of Nigeria and fluctuates seasonally according to the variability of rainfall. According to Jimoh [98], semi-annual floods, which are separated by a period of 4–5 months and low water level between the months of March and May, occur at Kainji dam

every year. The first part of this flood session, which originates from the head waters, arrives at Kainji in November and reaches its maximum in February while the second, which emanates from local tributaries, reaches Kainji in August and peaks in September and October. This signal (i.e., semi-annual flood patterns) is part of the dominant multi-annual signals observed in our PCA results of GRACE-TWS (i.e., the second orthogonal mode), which is mostly visible over Guinea Coast and some parts of West Sahel (see Fig. 2). In addition, the observed maximum peaks reported in Jimoh [98] due to inflow from local tributaries, which occurs in February and November, are also consistent with our altimetry observations for Kainji dam (Fig. 12a). Despite lacking a notable trend, relatively strong seasonal amplitudes, which correspond to intra-annual rainfall variability and water use, are observed in the residuals (see Fig. 12b).

While the lowest maximum water levels of Kainji reservoir observed in 1996 and 2005 (Fig. 12a) correspond to the lowest residuals shown in Fig. 12b of the same period, the lowest minimum

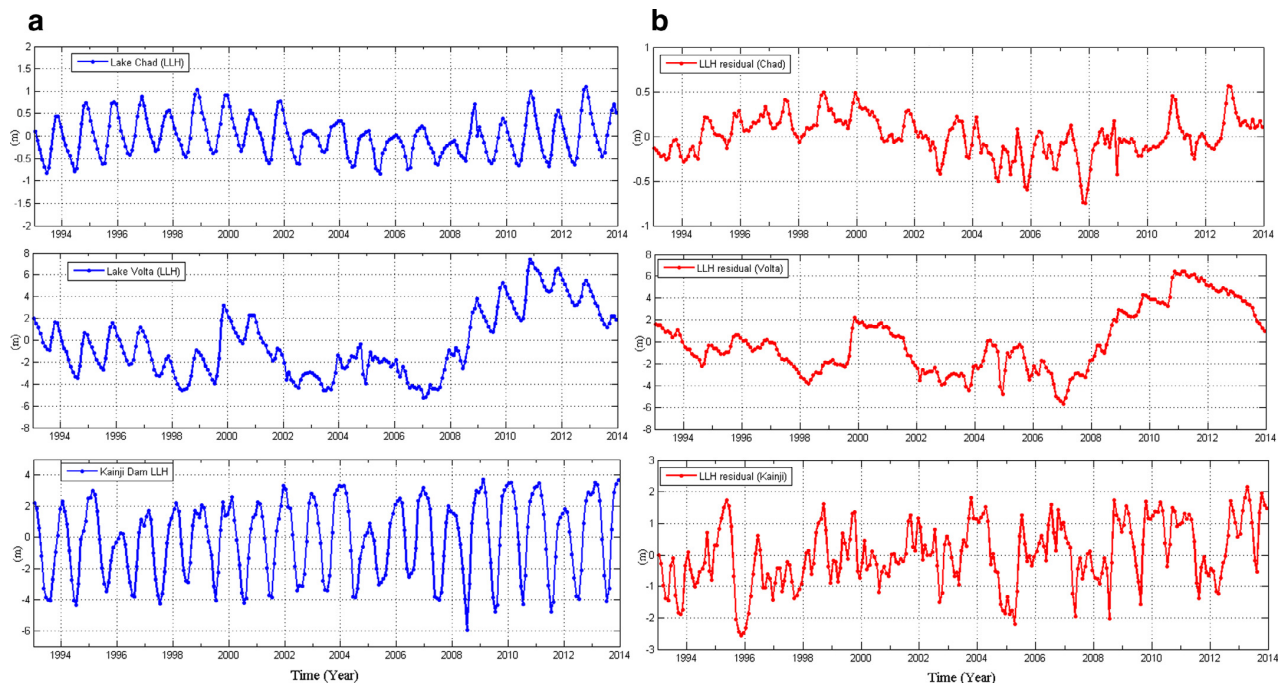


Fig. 12. Analysis of lake water levels (a) Lake water levels before removing annual and semi-annual signals and (b) Lake water levels after removing annual and semi-annual signals. * LLH-Lake Level Heights.

observed water level (i.e., 2008) is not clearly marked out from the corresponding residuals indicated in Fig. 12b as they are dominated with more random signals that might be due to miss-fit to annual and semi-annual signals. However, since the maximum water levels of 2007 and 2011/2012 are not as strong for example, as those of 2002–2004, 2009–2010, and 2013 (Fig. 12a), the low minimum observed residuals of 2007 and 2011/2012 (Fig. 12b) might be the aftermath of those less pronounced maximum water levels (or relatively low maximum water levels) of 2007 and 2011/2012, while the low minimum residuals of 2008 (Fig. 12b) could be the result of the observed lowest minimum water level of 2008 in Fig. 12a. These observed minimum and low maximum water levels and the multi-annual fluctuations of the Kainji reservoir (Fig. 12a and b) are consistent with recent studies [99,100] that have reported a decrease in the reservoir inflow due to the development of infrastructures at the upstream of Kainji reservoir and changes in hydrological fluxes such as precipitation, evaporation, and temperature of the river Niger sub-basin where the dam is located.

Lakes, reservoirs, etc., respond naturally to climate and environmental conditions and can be used as indicators of water availability and water loss [101]. Therefore, the observed low minimum water level residuals (i.e., 2005, 2007/2008, and 2011/2012) from our analyses and the decrease in the reservoir inflow at Kainji as reported by Salami et al. [100] might be indicators to a water deficit in the Middle Belt region. In retrospect to our observed increase in water availability from the spatially averaged changes in TWS over West Africa (see Section 4.4), our analysis of the Kainji reservoir has indicated a water deficit triggered by low reservoir inflow. With decreased precipitation due to climate variability, reduced reservoir inflow, and the low residuals in water levels as observed in recent times, the hydrology of the Kainji reservoir might undergo large changes that probably may impact negatively on the socio-economic prospects of the Middle Belt region.

5. Conclusions

In order to understand the changes in TWS over West Africa, this study used PCA and MLR to identify and analyze the dominant spatio-temporal variability of TWS and precipitation. Results from our analyses show that: (i) High annual variability of GRACE-derived surface mass variations are observed in Guinea, Sierra Leone, Guinea Bissau, Liberia and Nigeria due to a considerable high rainfall amounts at seasonal and inter-annual time scales. The Lake Volta signal, which is largely dominated by multi-annual signals was identified from the PCA result.

(ii) Increasing multi-annual changes in TWS over riparian countries that constitute the Volta basin is also observed. This increase is seen as a response to intensified rainfall events due to ocean warming, and possibly the influence of ENSO in the region around the basin.

(iii) Precipitation over the region is dominated by annual and semi-annual signals influenced by circulation features, ocean warming, and climate tele-connections. Also, the region's susceptibility to drought conditions is also consistent with recent studies [e.g., 86,81].

(iv) Analysis of TWS variability indicates a water deficit between 2002 and mid-2007 in the region. However, there is relative increase in water availability in recent times 2012–2014. Overall, the trend in TWS at Guinea between the period 2002 and 2014 is inconsistent with the linear trend in rainfall. This has been attributed to cumulative increase in the volume of water not involved in surface runoff, in addition to the water surplus from prolonged wet seasons, and lower evapotranspiration rates over the Guinea coast region. (v) Despite the poor correlation of GLDAS TWSC in some parts of the region, the regression fit between the two variables (i.e., GRACE and GLDAS), with a coefficient of determination (R^2) of 0.85, however, indicates that trends and variability have been well modelled in most parts of the region. Further,

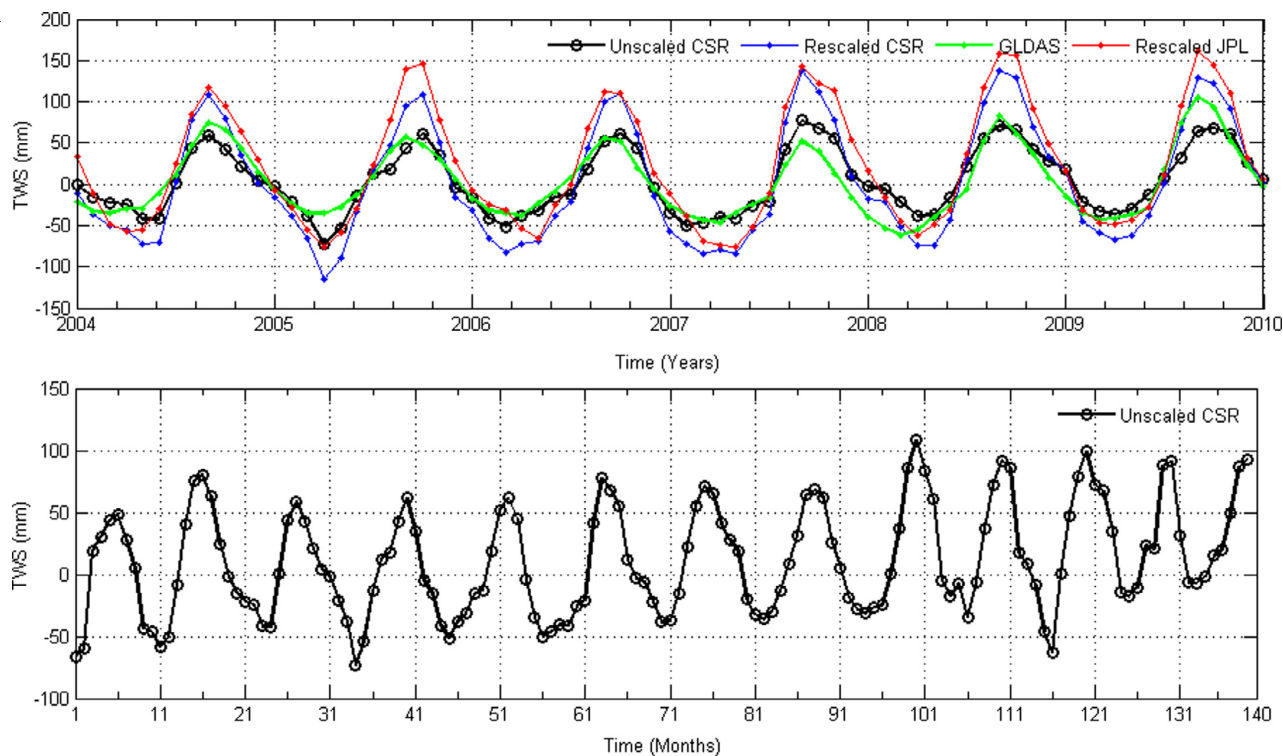


Fig. 13. Time series of TWS from CSR, JPL, and GLDAS. The effect of the DDK2 filter on computed GRACE-derived TWS before and after restoring the geophysical signal loss is compared with the GLDAS-TWS (top panel). This comparison is done for the common time period where there are no data gaps in GRACE-derived TWS (i.e., 2003–2010). The bottom panel is the time series of GRACE-derived TWS (i.e., without restoring the signal loss caused by the DDK2 filter) before interpolation.

the multi-linear regression (MLR) model simulates TWS and rainfall quite well using trend, annual, and semi-annual signals only, though some parts of the Central Sahel are poorly modelled. Considering the performance of the MLR model in TWS simulations for most parts of the region, changes in TWS can therefore be predicted quite well. (vi) Increased magnitude in recent annual signals of Kainji reservoir as seen in the higher maximum and lower minimum water levels would imply increased flood/dry events throughout the year. These fluctuations coupled with relatively low maximum water levels of 2005, 2007/2008 and 2011/2012, which is also reflected in the observed residuals, might probably impact negatively on the socio-economic potentials of the Middle Belt region.

Lake Volta and the Kainji reservoir are largely used for hydroelectric power generation. With relatively strong annual and seasonal variability observed in these surface waters, their hydropower capacity might be limited in years where water levels are low. Despite the observed gradual decline in Lake Volta water level between 2011 and 2014, the observed maximum water level, which remains higher than in the preceding decades, points towards water availability in the Lake.

Acknowledgments

Christopher Ndehedehe is grateful to Curtin University for his PhD funding through the CSIRS programme, and University of Uyo, Nigeria, for the study leave. The Authors are grateful to CSR and NASA for the data used in this study. Joseph is grateful for the financial support of the Alexander von Humboldt Foundation for supporting his stay at Institute of Technology (KIT, Germany) and Japan Society of Promotion of Science for supporting his stay at Kyoto University (Japan), the period during which part of this study

was undertaken. He is grateful to the warm welcome and conducive working atmosphere provided by his hosts Prof. Bernhard Heck (Geodetic Institute, KIT, Germany) and Prof Yoichi Fukuda (Department of Geophysics, Kyoto University, Japan).

Appendix A

Generally as mentioned previously in Section 3.1.1, the CSR and JPL data sets are somewhat consistent for the region. However, there are some uncertainties in terms of the magnitudes estimated by the two products (Fig. 13 top). The time series of CSR data for the entire period before interpolation is also shown in Fig. 13 (bottom).

References

- [1] USAID. 2013 World population data sheet. United States Agency International Development 2013. Retrieved from: www.prb.org. [Accessed 2.08.14].
- [2] Roudier P, Sultan B, Quirion P, Berg A. The impact of future climate change on West African crop yields: what does the recent literature say? *Global Environ Change* 2011;21:1073–83. <http://dx.doi.org/10.1016/j.gloenvcha.2011.04.007>.
- [3] Amani A, Thomas J, Abou MN. Climate change adaptation and water resources management in West Africa. Synthesis report WRITESHOP. UNESCO 2007. Retrieved from: www.nicap.net/032135.070920.NCAP. [Accessed 15.04.14].
- [4] Coe MT, Foley JA. Human and natural impacts on the water resources of the Lake Chad basin. *J Geophys Res* 2001;106(4):3349–56. doi: 0148-0227/01/2000JD900587509.00.
- [5] Okpara J, Tarhule AA, Perumal M. Study of climate change in niger river basin, west africa: reality not a myth. *INTECH Open science* 2013. <http://dx.doi.org/10.5772/55186>.
- [6] Oyebande L, Odunuga S. Climate change impact on water resources at the transboundary level in West Africa: the cases of the Senegal, Niger and Volta Basins. *Open Hydrol J* 2010;4:163–72. <http://dx.doi.org/10.2174/1874378101004010163>.
- [7] Ojo O, Gbuyiro SO, Okoloye CU. Implications of climate variability and climate change for water resources availability and management in West Africa. *GeoJournal* 2004;61(2):111–19. <http://dx.doi.org/10.1007/s10708-004-2863-8>.

- [8] Descroix L, Mahé G, Lebel T, Favreau G, Galle S, Gautier E, et al. Spatio-temporal variability of hydrological regimes around the boundaries between Sahelian and Sudanian areas of West Africa. *J Hydrol* 2009;375(12):90–102. <http://dx.doi.org/10.1016/j.jhydrol.2008.12.012>.
- [9] Boone A, Decharme B, Guichard F, Rosnay PD, Balsamo G, Belaars A, et al. The AMMA land surface model intercomparison project (ALMIP). *Bull Am Meteorol Soc* 2009;90(12):1865–80. <http://dx.doi.org/10.1175/2009BAMS2786.1>.
- [10] Vierich HID, Stoop WA. Changes in West African savanna agriculture in response to growing population and continuing low rainfall. *Ecosyst Environ* 1990;31(2):115–32. [http://dx.doi.org/10.1016/0167-8809\(90\)90214-X](http://dx.doi.org/10.1016/0167-8809(90)90214-X).
- [11] Grippa M, Kergoat L, Frappart F, Araud Q, Boone A, de Rosnay P, et al. Land water storage variability over West Africa estimated by gravity recovery and climate experiment (GRACE) and land surface models. *Water Resour Res* 2011;47(5):W05549. <http://dx.doi.org/10.1029/2009wr008856>.
- [12] Moore P, Williams SDP. Integration of altimetry lake levels and GRACE gravimetry over Africa: inferences for terrestrial water storage change 2003–2011. *Water Resour Res* 2014;50:6966–720. <http://dx.doi.org/10.1002/2014WR015506>.
- [13] Xie H, Longuevergne L, Ringler C, Scanlon BR. Calibration and evaluation of a semi-distributed watershed model of Sub-Saharan Africa using GRACE data. *Hydrol Earth Syst Sci* 2012;16(9):3083–99. <http://dx.doi.org/10.5194/hess-16-3083-2012>.
- [14] Forootan E, Kusche J, Loth I, Schuh WD, Eicker A, Awange J, et al. Multivariate prediction of total water storage changes over West Africa from multi-satellite data. *Surv Geophys* 2014;35(4):913–40. <http://dx.doi.org/10.1007/s10712-014-9292-0>.
- [15] Anayah F, Kaluarachchi J. Groundwater resources of northern Ghana: initial assessment of data availability. Unpublished Manuscript, Utah State University, USA 2009. Retrieved from: gw-africa.iwmi.org/Data/Sites/24/media/pdf/fieldreport-usu.pdf. [Accessed 25.05.14].
- [16] Lebel T, Cappelraere B, Galle S, Hanan N, Kergoat L, Levis S, et al. AMMA-CATCH studies in the Sahelian region of West-Africa: an overview. *J Hydrol* 2009;375(12):3–13. <http://dx.doi.org/10.1016/j.jhydrol.2009.03.020>.
- [17] Gosset M, Viarre J, Quantin G, Alcoba M. Evaluation of several rainfall products used for hydrological applications over West Africa using two high-resolution gauge networks. *Q J R Meteorol Soc* 2013;139:923–40. <http://dx.doi.org/10.1002/qj.2130>.
- [18] Frappart F, Hiernaux P, Guichard F, Mouglin E, Kergoat L, Arjounin M, et al. Rainfall regime across the Sahel band in the Gourma region, Mali. *J Hydrol* 2009;375(12):128–42. <http://dx.doi.org/10.1016/j.jhydrol.2009.03.007>.
- [19] Nicholson SE, Some B, Kone B. An analysis of recent rainfall conditions in West Africa, including the rainy seasons of the 1997 El Niño and the 1998 La Niña Years. *J Clim* 2000;13(14):2628–40. [http://dx.doi.org/10.1175/1520-0442\(2000\)013\(2628:AAORRC\)2.0.CO;2](http://dx.doi.org/10.1175/1520-0442(2000)013(2628:AAORRC)2.0.CO;2).
- [20] Laux P. Statistical modeling of precipitation for agricultural planning in the Volta Basin of West Africa. Doctoral dissertation, Mitteilungen/Institut für Wasserbau, Universität Stuttgart 2009;179(198). Retrieved from: elib.uni-stuttgart.de/opus/volltexte/2009/4016/pdf/Dissertation-Laux.pdf. Accessed 25 July, 2014.
- [21] Heim RR. A review of twentieth-century drought indices used in the United States. *Bull Am Meteorol Soc* 2002;83(8):1149–65.
- [22] McKee TB, Doeskin NJ, Kieist J. The relationship of drought frequency and duration to time scales. In: Conference on Applied Climatology. Boston, Massachusetts: American Meteorological Society; 1993. p. 179–84. Retrieved from: www.ccc.atmos.colostate.edu/relationshipofdroughtfrequency.pdf. [Accessed 27.06.14].
- [23] McKee TB, Doeskin NJ, Kieist J. Drought monitoring with multiple time scales. In: Conference on Applied Climatology. Boston, Massachusetts: American Meteorological Society; 1995. p. 233–6. Retrieved from: www.southwestclimatechange.org/node/911. [Accessed 13.07.14].
- [24] Long D, Scanlon BR, Longuevergne L, Sun AY, Fernando DN, Save H. GRACE satellite monitoring of large depletion in water storage in response to the 2011 drought in Texas. *Geophys Res Lett* 2013;40(13):3395–3401. <http://dx.doi.org/10.1002/GRL.50655>.
- [25] Ahmed M, Sultan M, Wahr J, Yan E. The use of GRACE data to monitor natural and anthropogenic induced variations in water availability across Africa. *Earth Sci Rev* 2014;136:289–300. <http://dx.doi.org/10.1016/j.earscirev.2014.05.009>.
- [26] Pedinotti V, Boone A, Decharme B, Crtaux JF, Mognard N, Panthou G, et al. Evaluation of the ISBA-TRIP continental hydrologic system over the Niger basin using in situ and satellite derived datasets. *Hydrol Earth Syst Sci* 2012;16(6):1745–73. <http://dx.doi.org/10.5194/hess-16-1745-2012>.
- [27] Schuol J, Abbaspour KC. Calibration and uncertainty issues of a hydrological model (SWAT) applied to West Africa. *Adv Geosci* 2006;9:137–43. doi: [advgeosci.9.137.2006](http://dx.doi.org/10.5194/advgeosci.9.137.2006).
- [28] Wagner S, Kunstmann H, Brdossy A, Conrad C, Colditz R. Water balance estimation of a poorly gauged catchment in West Africa using dynamically downscaled meteorological fields and remote sensing information. *Phys Chem Earth* 2009;34:225–235. <http://dx.doi.org/10.1016/j.pce.2008.04.002>.
- [29] Leblanc M, Favreau G, Tweed S, Leduc C, Razack M, Mofor L. Remote sensing for groundwater modelling in large semiarid areas: Lake Chad Basin, Africa. *Hydrogeol J* 2007;15:97–100. <http://dx.doi.org/10.1007/s10040-006-0126-0>.
- [30] Tapley B, Bettadpur S, Watkins M, Reigber C. The gravity recovery and climate experiment: mission overview and early results. *Geophys Res Lett* 2004;31:1–4. <http://dx.doi.org/10.1029/2004GL019920>.
- [31] Swenson S, Wahr J. Multi-sensor analysis of water storage variations of the Caspian Sea. *Geophys Res Lett* 2007;34(16). <http://dx.doi.org/10.1029/2007gl030733>.
- [32] Swenson S, Wahr J. Methods for inferring regional surface-mass anomalies from gravity recovery and climate experiment (GRACE) measurements of time-variable gravity. *J Geophys Res Solid Earth* 2002;107(B9). <http://dx.doi.org/10.1029/2001jb000576>.
- [33] Wahr J, Molenaar M, Bryan F. Time variability of the Earth's gravity field: hydrological and oceanic effects and their possible detection using GRACE. *J Geophys Res Solid Earth* 1998;103(B12):30205–29. <http://dx.doi.org/10.1029/98jb02844>.
- [34] Ferreira VG, Gong Z, Andam-Akorful SA. Monitoring mass changes in the volta river basin using GRACE satellite gravity and TRMM precipitation. *Boletim De Ciencias Geodesicas* 2012;18(4):549–63. doi: [/WOS:000313106300003](http://dx.doi.org/10.1003/13106300003).
- [35] Ferreira V, Andam-Akorful SA, He X, Xiao R. Estimating water storage changes and sink terms in Volta Basin from satellite missions. *Water Sci Eng* 2014;7(1):5–16. <http://dx.doi.org/10.3882/j.issn.1674-2370.2014.01.0028>.
- [36] Nahmani S, Bock O, Bouin M-N, Santamar-a-Gmez A, Boy J-P, Collilieux X, et al. Hydrological deformation induced by the West African monsoon: comparison of GPS, GRACE and loading models. *J Geophys Res-Solid Earth* 2012;117(B5). <http://dx.doi.org/10.1029/2011JB009102>.
- [37] Hinderer J, de Linage C, Boya J-P, Gegout P, Masson F, Rogister Y, et al. The GHYRAF (Gravity and Hydrology in Africa) experiment: description and first results. *J Geodyn* 2009;48:172–81. <http://dx.doi.org/10.1016/j.jog.2009.09.014>.
- [38] Awange J, Forootan E, Kusche J, Kiema J, Omond P, Heck B, et al. Understanding the decline of water storage across the Ramsar-Lake Naivasha using satellite-based methods. *Adv Water Resour* 2013;60(0):7–23. <http://dx.doi.org/10.1016/j.advwatres.2013.07.002>.
- [39] Awange J, Forootan E, Kuhn M, Kusche J, Heck B. Water storage changes and climate variability within the Nile Basin between 2002 and 2011. *Adv Water Resour* 2014;73(0):1–15. <http://dx.doi.org/10.1016/j.advwatres.2014.06.010>.
- [40] Awange J, Gebremichael M, Forootan E, Wakbulcho G, Anyah R, Ferreira V, et al. Characterization of Ethiopian mega hydrogeological regimes using GRACE, TRMM and GLDAS datasets. *Adv Water Resour* 2014;74(0):64–78. <http://dx.doi.org/10.1016/j.advwatres.2014.07.012>.
- [41] Ramillien G, Frappart F, Seoane L. Application of the regional water mass variations from GRACE satellite gravimetry to large-scale water management in Africa. *Remote Sens* 2014;6(8):7379–405.
- [42] Jolliffe IT. *Principal component analysis (second edition)*. In: Springer Series in Statistics. New York: Springer; 2002.
- [43] Preisendorfer R. *Principal component analysis in meteorology and oceanography*. Dev Atmos Sci 17 1988. Elsevier, Amsterdam.
- [44] Rodell M, Houser PR, Jambor U, Gottschalk J, Mitchell K, Meng K, et al. The global land data assimilation system. *Bull Am Meteorol Soc* 2004;85(3):381–94. <http://dx.doi.org/10.1175/BAMS-85-3-381R>.
- [45] McSweeney C, New M, Lizcano G, Lu X. The UNDP climate change country profiles improving the accessibility of observed and projected climate information for studies of climate change in developing countries. *Bull Am Meteorol Soc* 2010;91(2):157–66. <http://dx.doi.org/10.1175/2009BAMS2826.1>.
- [46] Nicholson SE, Webster PJ. A physical basis for the interannual variability of rainfall in the Sahel. *Q J R Meteorol Soc* 2007;133(629):2065–84. <http://dx.doi.org/10.1002/qj.104>.
- [47] Lebel T, Ali A. A physical basis for the interannual variability of rainfall in the Sahel. *Q J R Meteorol Soc* 2009;375(1-2):5264. <http://dx.doi.org/10.1016/j.jhydrol.2008.11.030>.
- [48] Nicholson S. The West African Sahel: a review of recent studies on the rainfall regime and its interannual variability. *ISRN Meteorol* 2013;2013(453521):1–32. <http://dx.doi.org/10.1155/2013/453521>.
- [49] Nicholson S, Grist J. A conceptual model for understanding rainfall variability in the West African Sahel on interannual and interdecadal timescales. *Int J Climatol* 2001;21:1733–57. <http://dx.doi.org/10.1002/joc.648>.
- [50] Diatta S, Fink AH. Statistical relationship between remote climate indices and West African monsoon variability. *Int J Climatol* 2014;34(12):3348–67. doi: [10.1002/joc.3912](http://dx.doi.org/10.1002/joc.3912).
- [51] Ramillien G, Bouhours S, Lombard A, Cazenave A, Flechtner FR, Schmidt. Land water storage contribution to sea level from GRACE geoid data over 2003–2006. *Glob Planet Change* 2008;60(3-4):381–92. <http://dx.doi.org/10.1016/j.gloplacha.2007.04.002>.
- [52] Landerer FW, Swenson SC. Accuracy of scaled GRACE terrestrial water storage estimates. *Water Resour Res* 2012;48(4):W04531. <http://dx.doi.org/10.1029/2011WR011453>.
- [53] Wouters B, Bonin JA, Chambers DP, Riva REM, Sasgen I, Wahr J. GRACE, time-varying gravity, Earth system dynamics and climate change. *Rep Progr Phys* 2014;77(11):116801. <http://dx.doi.org/10.1088/0034-4885/77/11/116801>.
- [54] Cheng MK, Tapley BD, Ries JC. Deceleration in the Earth's oblateness. *J Geophys Res* 2013;118:1–8. <http://dx.doi.org/10.1002/jgrb.50058>.
- [55] Swenson S, Chambers D, Wahr J. Estimating geocenter variations from a combination of GRACE and ocean model output. *Geophys Res Lett* 2008;31:1–4. <http://dx.doi.org/10.1029/2004GL019920>.
- [56] Kusche J, Schmidt R, Petrovic S, Rietbroek R. Decorrelated GRACE time-variable gravity solutions by GFZ, and their validation using a hydrological model. *J Geodesy* 2009;83(10):903–13. <http://dx.doi.org/10.1007/s00190-009-0308-3>.
- [57] Kusche J. Approximate decorrelation and non-isotropic smoothing of time-variable GRACE-type gravity field models. *J Geodesy* 2007;81(11):733–49. <http://dx.doi.org/10.1007/s00190-007-0143-3>.

- [58] Long D, Longuevergne L, Scanlon BR. Global analysis of approaches for deriving total water storage changes from GRACE satellites. *Water Resour Res* 2015;51(4):2574–94. <http://dx.doi.org/10.1002/2014WR016853>.
- [59] Santos Ja F, Pulido-Calvo I, Portela MM. Spatial and temporal variability of droughts in Portugal. *Water Resour Res* 2010;46(3):W03503. <http://dx.doi.org/10.1029/2009WR008071>.
- [60] Rangelova E, van der Wal W, Braun A, Sideris MG, Wu P. Analysis of gravity recovery and climate experiment time-variable mass redistribution signals over North America by means of principal component analysis. *J Geophys Res: Earth Surf* 2007;112(F3):2156–202. <http://dx.doi.org/10.1029/2006JF000615>.
- [61] Huffman GJ, Adler RF, Bolvin DT, Gu G, Nelkin EJ, Bowman KP, et al. The TRMM multisatellite precipitation analysis (TMPA): quasi-global, multi-year, combined-sensor precipitation estimates at fine scales. *J Hydrometeorol* 2007;8:38–55. <http://dx.doi.org/10.1175/JHM560.1>.
- [62] Kummerow C, Simpson J, Thiele O, Barnes W, Chang ATC, Stocker E, et al. The status of the tropical rainfall measuring mission (TRMM) after two years in orbit. *J Appl Meteorol* 2000;39(12):1965–82. [http://dx.doi.org/10.1175/1520-0450\(2001\)040\(1965:TSOTTR\)2.0.CO;2](http://dx.doi.org/10.1175/1520-0450(2001)040(1965:TSOTTR)2.0.CO;2).
- [63] Nicholson SE, Some B, Mccollum J, Nelkin E, Klotter D, Berte Y, et al. Validation of TRMM and other rainfall estimates with a high-density gauge datasets for West Africa. Part I: Validation of GPCP rainfall product and pre-TRMM satellite and blended products. *J Appl Meteorol* 2003;42:1337–54. [http://dx.doi.org/10.1175/1520-0450\(2003\)042C1337:VOTAOR3E2.0.CO;2](http://dx.doi.org/10.1175/1520-0450(2003)042C1337:VOTAOR3E2.0.CO;2).
- [64] Duan Z, Bastiaanssen WGM. First results from Version 7 TRMM 3B43 precipitation product in combination with a new downscaling calibration procedure. *Remote Sens Environ* 2013;131(0):1–13. <http://dx.doi.org/10.1016/j.rse.2012.12.002>.
- [65] Paeth H, Fink A, Pohle S, Keis F, Machel H, Samimi C. Meteorological characteristics and potential causes of the 2007 flood in sub-Saharan Africa. *Int J Climatol* 2012;31:1908–26. <http://dx.doi.org/10.1002/joc.2199>.
- [66] Hassan AA, Jin S. Water cycle and climate signals in Africa observed by satellite gravimetry. *IOP Conf Ser: Earth Environ Sci* 2014;17:1–6. <http://dx.doi.org/10.1088/1755-1315/17/1/012149>.
- [67] Martinez WL, Martinez AR. *Exploratory data analysis with MATLAB. In: Computer science and data analysis series. UK: Chapman and Hall/CRC Press LLC; 2005. ISBN 1-58488-366-9.*
- [68] Westra S, Brown C, Lall U, Koch I, Sharma A. Interpreting variability in global SST data using independent component analysis and principal component analysis. *Int J Climatol* 2010;30(3):333–46. <http://dx.doi.org/10.1002/joc.1888>.
- [69] Nicholson SE. Spatial teleconnections in African rainfall: a comparison of 19th and 20th century patterns. *Holocene* 2014;24(12):1840–8. <http://dx.doi.org/10.1177/0959683614551230>.
- [70] Seidou O, Asselin JJ, Ouarda TBMJ. Bayesian multivariate linear regression with application to change point models in hydrometeorological variables. *Water Resour Res* 2007;43:W08401. <http://dx.doi.org/10.1029/2001jw000576>.
- [71] Rieser D, Kuhn M, Pail R, Anjasmara IM, Awange J. Relation between GRACE-derived surface mass variations and precipitation over Australia. *Aust J Earth Sci* 2010;57(7):887–900. <http://dx.doi.org/10.1080/08120099.2010.512645>.
- [72] LHôte Y, Mahé G, Somé B, Triboulet JP. Analysis of a Sahelian annual rainfall index from 1896 to 2000; the drought continues. *Hydrol Sci J* 2002;47(4):563–72. <http://dx.doi.org/10.1080/02626660209492960>.
- [73] Boker SM, Xu M, Rotondo JL, King K. Windowed cross correlation and peak picking for the analysis of variability in the association between behavioral time series. *Psychol Methods* 2002;7(3):338–555. <http://dx.doi.org/10.1037/1082-989X.7.3.338>.
- [74] Owusu K, Waylen P, Qiu Y. Changing rainfall inputs in the Volta basin: implications for water sharing in Ghana. *Geojournal* 2008;71(4):201–10. <http://dx.doi.org/10.1007/s10708-008-9156-6>.
- [75] Nguyen H, Thorncroft CD, Zhang C. Guinean coastal rainfall of the West African monsoon. *Q J R Meteorol Soc* 2011;137(660):1828–40. <http://dx.doi.org/10.1002/qj.867>.
- [76] Odekunle TO, Eludoyin AO. Sea surface temperature patterns in the Gulf of Guinea: their implications for the spatio-temporal variability of precipitation in West Africa. *Int J Climatol* 2008;28:15071517. <http://dx.doi.org/10.1002/joc.1656>.
- [77] Adejuwon J. *Food security, climate variability and climate change in Sub-Saharan West Africa. The International START Secretariat USA 2006. Assessments of Impacts and Adaptations to Climate Change (AIACC) final reports.*
- [78] FAO. *Integrating crops and livestock in West Africa. Food and Agriculture Organization Of The United Nations; 1983. Retrieved from: www.fao.org/docrep/004/x6543e/X6543E00.* [Accessed 10.05.15].
- [79] Marshall M, Funk C, Michaelsen J. Examining evapotranspiration trends in Africa. *Clim Dyn* 2012;38(9–10):1849–65. <http://dx.doi.org/10.1007/s00382-012-1299-y>.
- [80] WMO. WMO statement on the status of the global climate in 2012, WMO No.1108. World Meteorological Organization; 2013. Retrieved from: www.wmo.int/pages/prog/wcp/wcdmp/documents/WMO1108.pdf. [Accessed 15.06.15].
- [81] Panthou G, Vischel T, Lebel T, Blanchet J, Quantin G, Ali A. Extreme rainfall in West Africa: a regional modeling. *Water Resour Res* 2012;48(8):W08501. <http://dx.doi.org/10.1029/2012wr012052>.
- [82] Barbe LL, Lebel T, Tapsoba D. Rainfall variability in West Africa during the years 1950–90. *J Clim* 2002;15(2):187–202. [http://dx.doi.org/10.1175/1520-0442\(2002\)015\(0187:Rviwad\)2.0.Co;2](http://dx.doi.org/10.1175/1520-0442(2002)015(0187:Rviwad)2.0.Co;2).
- [83] Common P. Independent component analysis, A new concept? *Signal Process* 1994;36:314–1994.
- [84] Verschoren V. Trends in the hydrology of small watersheds in the Fouta Djallon Highlands. Food Agric Org UN, Rome 2012. Retrieved from: <http://www.fao.org/forestry/35845-051437ea2d60e968ba2e8ce3fb3c3f95.pdf>. [Accessed 26.09.15].
- [85] Giannini A, Salack S, Lodoun T, Ali A, Gaye A, Ndiaye O. A unifying view of climate change in the Sahel linking intra-seasonal, interannual and longer time scales. *Environ Res Lett* 2013;8:1–8. <http://dx.doi.org/10.1088/1748-9326/8/2/024010>.
- [86] Asefi-Najafabady S, Saatchi S. Response of African humid tropical forests to recent rainfall anomalies. *Trans R Soc* 2013;368:20120306. <http://dx.doi.org/10.1098/rstb.2012.0306>.
- [87] Druyan LM, Fulakeza M. The impact of the Atlantic cold tongue on West African monsoon onset in regional model simulations for 1998–2002. *Int J Climatol* 2015;35(2):275–87. <http://dx.doi.org/10.1002/joc.3980>.
- [88] Thorncroft CD, Nguyen H, Zhang C, Peyrill P. Annual cycle of the West African monsoon: regional circulations and associated water vapour transport. *Q J R Meteorol Soc* 2011;137(654):129–47. <http://dx.doi.org/10.1002/qj.728>.
- [89] MacDonald AM, Bonsor HC, Dochartaigh BEO, Taylor RG. Quantitative maps of groundwater resources in Africa. *Environ Res Lett* 2012;7. <http://dx.doi.org/10.1088/1748-9326/7/2/024009>.
- [90] FAO. Irrigation potential in africa: a basin approach. FAO Land Water Bull 1997;4. Retrieved from: <https://books.google.com.au/books>. [Accessed 28.09.15].
- [91] Favreau G, Cappelaere B, Massuel S, Leblanc M, Boucher M, Boulain N, et al. Land clearing, climate variability, and water resources increase in semiarid southwest Niger: a review. *Water Resour Res* 2009;45:W00A16. <http://dx.doi.org/10.1029/2007WR006785>.
- [92] James GK, Adegoke JO, Saba E, Nwilo P, Akinyede J. Satellite-based assessment of the extent and changes in the mangrove ecosystem of the Niger Delta. *Mar Geodesy* 2007;30:249–67. <http://dx.doi.org/10.1080/01490410701438224>.
- [93] Henry C, Allen DM, Huang J. Groundwater storage variability and annual recharge using well-hydrograph and GRACE satellite data. *Hydrogeol J* 2011;19:741–55. <http://dx.doi.org/10.1007/s10040-011-0724-3>.
- [94] Okonkwo C, Demoz B, Gebremariam S. Characteristics of lake Chad level variability and links to ENSO, precipitate, and river discharge. *Sci World J* 2014;13(4):13. <http://dx.doi.org/10.1155/2014/145893>.
- [95] Wald L. Monitoring the decrease of lake Chad from space. *Geocarto Int* 1990;5(3):31–6. <http://dx.doi.org/10.1080/10106049009354266>.
- [96] Gbuyiro SO, Ojo O, Iso M, Okoloye C, Idowu O. Climate and water resources management. In: WEDC conference Zambia, 27; 2001. p. 383–6. Retrieved from: www.wedc.lboro.ac.uk/resources/conference/27/Gbuyiro.pdf. [Accessed 15.05.15].
- [97] Ita E, Sado E, Balogun JK, Pandogari A, Ibitoye B. A preliminary checklist of inland water bodies in Nigeria with special reference to lakes and reservoirs. Kainji Lake Research Institute; 1985. Retrieved from: www.fao.org/docrep/005/t0360e/t0360E09.htm#11. [Accessed on 10.05.15].
- [98] Jimoh OD. Optimised operation of Kainji reservoir. *AU JT* 2008;12(1):34–42.
- [99] Salami A, Sule BF, Okeola O. Assessment of climate variability on Kainji hydro-power reservoir. In: Annual conference of the national association of hydrological sciences; 2011. Hydrology for Sustainable Development and Management of Water Resources in the Tropic, Nigeria.
- [100] Salami AW, Mohammed AA, Adeyemo JA, Olanlokun OK. Assessment of impact of climate change on runoff in the Kainji lake basin using statistical methods. *Int J Water Resour Environ Eng* 2015;7(2):7–16. <http://dx.doi.org/10.5897/IJWREE2014.0513>.
- [101] Deus D, Gloaguen R, Krause P. Water balance modelling in a semi arid environment with limited in situ data using remote sensing in lake Manyara, East African rift, Tanzania. *Remote Sens* 2013;5:1651–80. <http://dx.doi.org/10.3390/rs5041651>.

An investigation into the freshwater variability in West Africa during 1979–2010

S. A. Andam-Akorful,^a V. G. Ferreira,^{b*} C. E. Ndehedehe^c and J. A. Quaye-Ballard^a

^a Department of Geomatic Engineering, Kwame Nkrumah University of Science and Technology, Kumasi, Ghana

^b School of Earth Sciences and Engineering, Hohai University, Nanjing, China

^c Western Australian Centre for Geodesy and the Institute for Geoscience Research, Curtin University, Perth, Australia

ABSTRACT: After the frequent and long drought episodes of the 1980s, a plethora of case studies have shown that West Africa remains a hot spot in the continent where despite its numerous water resources, extreme rainfall variability remains a profound challenge to the availability of freshwater for agriculture and ecosystem services. In this paper, we assess the recent flux in water availability over West Africa by investigating variations in net-precipitation (i.e. the maximum available freshwater flux) using wavelet analysis. Net-precipitation was obtained as a residual of the atmospheric water balance, and its variability compared to precipitation, temperature, evaporation, soil moisture and normalized difference vegetation index using wavelet power transforms and coherence analysis. Results from the study indicate that the variance in water flux over the region has been progressively reducing, suggesting a relative reduction in extreme hydrological conditions. Also, the wavelet coherence analysis revealed that the observed decreasing rate of available freshwater is highly coupled to a low frequency modulating El-Niño activity that induced lower changes in rainfall variance, as well as higher evaporation variance. Spatial trends in the annual-scaled average wavelet power indicated that the south-western parts of the region experienced the most reduction in rainfall flux. The highest deficit in net-precipitation flux was found in the dry sub-humid climatic zone, which is drained by major regional rivers, including the Niger and Volta. Considering the long-term variability in freshwater (i.e. from 1979 to 2010), we found the 1980s to be the driest decade and the 1990s being its recovery period, while the 2000s proved to be a considerably dry decade, suggesting a strong multi-decadal variability.

KEY WORDS freshwater; net-precipitation; rainfall; wavelet transforms; West Africa

Received 27 June 2016; Revised 27 December 2016; Accepted 30 December 2016

1. Introduction

In Africa, deficits in inter-annual changes in precipitation, widespread decline in vegetation greenness and droughts (see, e.g. Zhou *et al.*, 2014; Shiferaw *et al.*, 2014) are relevant indicators of climate change that contribute significantly to famine and food insecurity in the region. West Africa (WA) for instance, remains a hot spot in the continent where despite its numerous water resources (e.g. Conway *et al.*, 2009), extreme rainfall variability remains a profound challenge to the availability of freshwater for agriculture and ecosystem functioning. Consequently, the region sometimes suffers significant socio-economic losses due to its dependence on rain-fed agriculture (e.g. Shiferaw *et al.*, 2014).

The persistent drought episodes of the late 1960s and early 1980s, which resulted in considerable impacts on water resources, food security and livelihood, triggered numerous scientific discourse on the hydrology and climate of the region (see, e.g. Mahé and Olivry, 1999;

Nicholson *et al.*, 2000; Conway *et al.*, 2009; Lebel and Ali, 2009; Ndehedehe *et al.*, 2016a; Nicholson, 2013, and the references therein). While some studies have reported that rainfall amounts over WA have shown some degree of recovery as observed in the Sahel (e.g. Nicholson, 2005; Lebel and Ali, 2009) the question on the state of general moisture conditions remains unclear (cf., Nicholson, 2013). For instance, Mahé and Paturel (2009) reported that although the Sahelian rainfall amounts increased towards the late 1990s, mean annual rainfall remains well below the amounts in the pre-1970s-era. They further noted that the increase in temperature over WA during the end of the 20th century induced an increase in evaporation, and may lead to reduction in freshwater yields. Moreover, conflicting behaviour in rainfall and runoff exist in much of the region (e.g. Conway *et al.*, 2009) while despite the recent increase in rainfall amounts in the Sahel, dry conditions persists (e.g. Descroix *et al.*, 2009). These and other specific case studies (see, e.g. Kaspersen *et al.*, 2011; Anyamba and Tucker, 2005; Ndehedehe *et al.*, 2016b) in the region suggest complex eco-hydrological systems.

A plethora of case studies have reported that both climate and anthropogenic factors contribute considerably to freshwater variability in WA (e.g. Wittig *et al.*, 2007; Roudier *et al.*, 2014). For instance, some region-specific

*Correspondence to: V. G. Ferreira, School of Earth Sciences and Engineering, Hohai University, Jiangning Campus, 8th Focheng Xilu Road, 211100, Nanjing, China. E-mail: vagnergf@hhu.edu.cn

studies (see, e.g. Amogu *et al.*, 2010; Descroix *et al.*, 2009; Mahé *et al.*, 2005) have reported that despite the reduction of rainfall rates, runoff in some sub-basins within the Niger and Volta basins have been increasing since the 1970s, a phenomenon partly attributed to human-induced impacts (e.g. land cover change). Further, Huber *et al.* (2011) reported inconsistent trends in Normalized Difference Vegetation Index (NDVI) and soil moisture in the African Sahel. Although they did not link it to any human influence, the preponderance of evidence from related studies, mostly those that have examined rainfall as a driver of vegetation dynamics (see, e.g. Herrmann *et al.*, 2005; Anyamba and Tucker, 2005; Kaspersen *et al.*, 2011), suggest the impacts of human activities and large scale climatic influence in the region. This lack of clarity in water availability and how it drives the ecosystem necessitates a further investigation to provide a more general perspective of recent variability in available freshwater over the region, at least in the long term. Analysing freshwater variability in WA, however, is hampered by the fact that the region is data deficient (e.g. Oyebande, 2001; Conway *et al.*, 2009) due to the required hydroclimatic information not being readily available. This makes it difficult to provide a more reliable account of the state of freshwater in WA.

Despite the problem of limited hydroclimatic data, various studies have attempted to analyse and explain the variability of available freshwater in the context of runoffs, rainfall patterns and vegetation dynamics by combining available in situ and satellite data (see, e.g. Conway *et al.*, 2009; Descroix *et al.*, 2009; Roudier *et al.*, 2014; Herrmann *et al.*, 2005; Anyamba and Tucker, 2005; Kaspersen *et al.*, 2011). Nonetheless, most of these studies were region-specific focusing on the impacts of climate variability on vegetation production (see, e.g. Herrmann *et al.*, 2005; Kaspersen *et al.*, 2011), while others analysed the uncertainties in water budget quantities derived from reanalysis and model data (see, e.g. Meynadier *et al.*, 2010). Also, the African Monsoon Multidisciplinary Analysis (AMMA) project (e.g. Boone *et al.*, 2009; Lebel *et al.*, 2009) has made some progress in the region, with some observational networks now available in Niger, Mali and Benin. In addition to the AMMA project, significant efforts on water resources development in the region include the synergy between the German research program on the global water cycle (GLOWA) and the Integratives Management-Projekt für einen Effizienten und Tragfähigen Umgang mit Süßwasser in West Afrika (IMPETUS) initiative (Speth and Fink, 2010, p. 7).

However, the investigations of all aspects of the hydrological cycle under the framework of the IMPETUS project were carried out basically over two river basins namely Ouémé and Wadi Drâa in Benin and Morocco, respectively, due to the availability of data among other criteria (cf., Speth and Fink, 2010, p. 9). Further, hydrological studies over WA that employed Gravity Recovery and Climate Experiment (GRACE, Tapley *et al.*, 2004) have also been documented (see, e.g. Ndehedehe *et al.*, 2016a; Forootan *et al.*, 2014a; Grippa *et al.*, 2011). However, these studies are restricted to the last decade because

of the limited GRACE-observations. Since WA is one of the tropical regions of the world characterized by strong inter-annual variability in rainfall, with an increasing potential of drought vulnerability (e.g. Ndehedehe *et al.*, 2016b), a further investigation into the long term freshwater flux of WA is therefore warranted.

WA is a well known climatic hot spot, where the land–ocean–atmosphere coupling plays an important role, through the spatio-temporal changes in precipitation and evaporation, which frequently result in the modulation of rainfall gradients (Douville *et al.*, 2006). Some studies (see, e.g. Ndehedehe *et al.*, 2016c; Diatta and Fink, 2014; Nicholson *et al.*, 2000; Janicot *et al.*, 1996) have suggested a possible relationship between climate indices (e.g. Atlantic multi-decadal oscillation-AMO, Atlantic meridional mode-AMM, El-Niño Southern Oscillation-ENSO, Pacific Decadal Oscillations-PDO) and rainfall extremes over WA. As the hydrological cycle is accelerating due to global changes in climate (see, e.g. Malhi and Wright, 2004), the perceived influence of such changes underscores the need for a long-term quantitative assessment of freshwater flux in the region.

In this study, wavelet analysis is employed for the first time to provide a quantitative analysis of flux in freshwater (availability and variability) over WA at the sub-climatic scale using long-term multi-resolution data (soil moisture, rainfall, temperature, evaporation and NDVI) during the period of 1979 to 2010. The main objectives of this study are threefold, to (1) investigate the spatio-temporal variations of freshwater flux (referred henceforth as net-precipitation) over the entire WA region, (2) investigate the impacts of ENSO on WA's freshwater and, (3) analyse the co-variability between different parameters that influence variations in freshwater (i.e. net-precipitation, rainfall, temperature, evaporation and ENSO index) in order to determine the nonlinear relationships between available freshwater and climate variability. To achieve these objectives, the wavelet approach (e.g. Torrence and Compo, 1998; Grinsted *et al.*, 2004), which has shown some skills in identifying temporal variability and trends in hydrological signals (e.g. Beecham and Chowdhury, 2009; Szolgayová and Arlt, 2014) is employed to extract localized variations in the dominant modes of the assessed parameters.

The remainder of the study is organized as follows; following the introduction, the study area is presented in Section 2, followed by the data and method of analysis in Section 3. The results are presented in Section 4, and the study is concluded in Section 5.

2. Study area

2.1. Geography

The WA region spans an area of approximately 6 million km², roughly 20% of Africa's total land area (refer to Figure 1 for the location of WA) with a total population of about 290 million. The region lies between longitudes

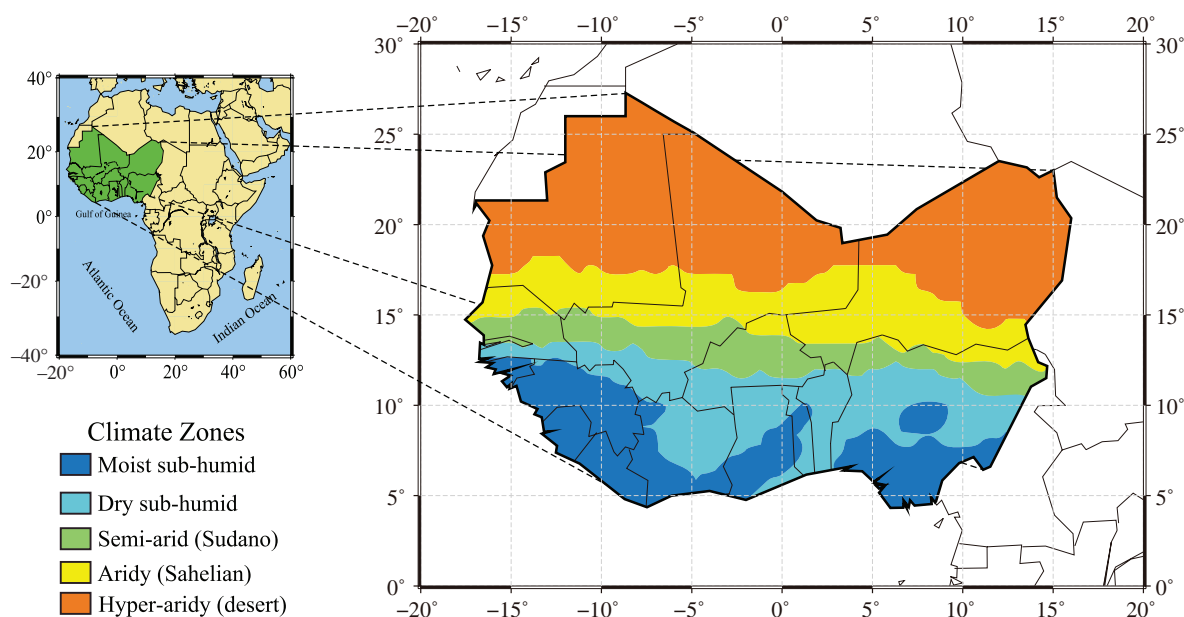


Figure 1. The study area domain in West Africa as well as its sub-climatic zones as proposed in Section 2.2.

18°W and 16°E and latitudes 3° and 28°N and it is bounded in the west and south by the Atlantic Ocean, the north by the Sahara desert, and the east by the Central African nations of Chad and Cameroon. The topography of the region is mainly flat; most parts lie less than 300 m above m.s.l. with several isolated high points along the coastal areas. The main river of the region is the Niger, which drains an area of 2 million km², and is shared by nine of the 17 countries in the region. Other important rivers are the Gambia, Senegal, Comoe and Volta, which are shared, respectively by three, four, four, and five riparian countries.

2.2. Climate

The region of WA is traditionally partitioned into three sub-climatic zones (Meynadier *et al.*, 2010), including: (1) the dry north, known as the Sahel, which lies just below the Sahara desert, (2) the Sudano transitional zone, and (3) the relatively wet Guinean zone located in the south. This wet and dry regions depends on the latitude and the distance from the Atlantic Ocean while the degree of aridity increases from south to north and to a lesser extent from west to east as reported by Menz (2010, p. 56). However, in order to gain a more localized perspective to variations in moisture conditions, the K-means clustering algorithm was used to reclassify the climatic zones by their annual rainfall amounts to maintain consistency with the general African sub-climatic classification (e.g. Wamukonya *et al.*, 2006) and it is presented in Figure 1. Consequently in this contribution, the climatic zones have been classified as hyper-arid (HyA) in the north, arid, semi-arid (SA), dry sub-humid (DSH) and moist sub-humid (MSH) in the south. Generally, the hyper-arid sub-region coincide with the desert area; arid, Sahel; semi-arid, Sudano; the

moist and dry sub-humid areas, Guinean (see Figure 1). Rainfall in the region is modulated by the northeast trade winds from the Sahara and the southwest monsoon winds from the Gulf of Guinea in a dipolar manner (see, e.g. Nicholson, 2013).

3. Methods and data

3.1. Datasets

3.1.1. ERA-interim

The European Centre for Medium-Range Weather Forecasts (ECMWF) Reanalysis dataset (ERA-Interim) provides a third generation ocean-land-atmosphere processes reanalysis data for estimating mass, moisture, and energy budget products (Dee *et al.*, 2011). Data fields of specific humidity, zonal (U) and meridional (V) components of wind at different pressure levels (i.e. from the Earth's surface to the top of the atmosphere) were used in this study to compute changes in atmospheric water storage and moisture flux divergence as described at Section 3.2.2. Additionally, temperature, evaporation, and soil moisture datasets from ERA-Interim were used in this study to understand the co-varying relationships with net-precipitation. The ERA-Interim datasets were obtained from http://apps.ecmwf.int/datasets/data/interim_full_moda/ for the period 1980 to 2010. The datasets were all retrieved at a gridded spatial resolution of 0.25° at a monthly temporal interval.

3.1.2. Global land data assimilation system

The Global Land Data Assimilation System (GLDAS) products combines satellite and ground-based observed

data to generate optimal fields of land surface states and fluxes using advanced land surface modelling and data assimilation techniques (Rodell *et al.*, 2004). It is driven by four land surface models (LSMs) namely the Variable Infiltration Capacity (VIC), Noah, Mosaic, and Community Land Model (CLM). The four LSMs output hydrological and meteorological fields at 1° and 0.25° resolutions, as well as a three-hourly and monthly temporal resolutions. The GLDAS model data are available from 1979 to the present. For this study, the monthly precipitation and evaporation fields at the 1° resolution for the period 1979 to 2010 were used. The GLDAS data were retrieved from <http://disc.sci.gsfc.nasa.gov/hydrology/data-holdings>.

3.1.3. Global precipitation climatology centre

The precipitation data used in this study were obtained from the Global precipitation Climatology Centre (GPCC) and covers the period of 1979 to 2010. This data is made available by Deutscher Wetterdienst (DWD, National Meteorological Service of Germany) and include rain gauge data collected from national meteorological agencies (e.g. Becker *et al.*, 2013). Other sources of inputs comprise of archives in the Global Telecommunication Systems (GTS), daily surface synoptic observations (SYNOP) messages, and monthly climatological data (CLIMAT messages). GPCC also utilizes published global datasets from the Food and Agriculture Organization (FAO) FAOCLIM 2.0, Climate Research Unit (CRU), Global Historical Network (GHCN), as well as several regional datasets, making it the most comprehensive quality controlled global gauge archive that is readily available (Becker *et al.*, 2013). The precipitation products are provided at different time and spatial resolutions for specific applications (see, e.g. Becker *et al.*, 2013; Schneider *et al.*, 2014). This study used the Full Data Product (i.e. GPCC-FD) at a spatial resolution of 0.5° and a monthly temporal resolution from 1980 to 2010. The GPCC rainfall fields were retrieved from ftp://ftp-anon.dwd.de/pub/data/gpcc/html/download_gate.html.

3.1.4. Multivariate ENSO index

The El-Niño Southern Oscillation (ENSO) is a major coupled ocean–atmosphere phenomenon that causes global climate variability on inter-annual time scales. In this study, the Multivariate ENSO Index (MEI) was obtained from the Physical Sciences and Physical Oceanography divisions of the National Oceanic & Atmospheric Administration (NOAA). MEI represents ENSO events based on six variables: sea-level pressure, zonal and meridional components of the surface wind, sea surface temperature, surface air temperature and total cloudiness fraction of the sky (Wolter and Timlin, 2011). By adopting a multivariate approach, MEI provides a more complete and exible description of the ENSO phenomenon (Wolter and Timlin, 2011). The cold (negative) phase (La Niña) results in wet period in WA, while the converse is true for the warm (positive) phase (El Niño) as observed by Nicholson (2013). The ENSO index time series (Figure 2) used in

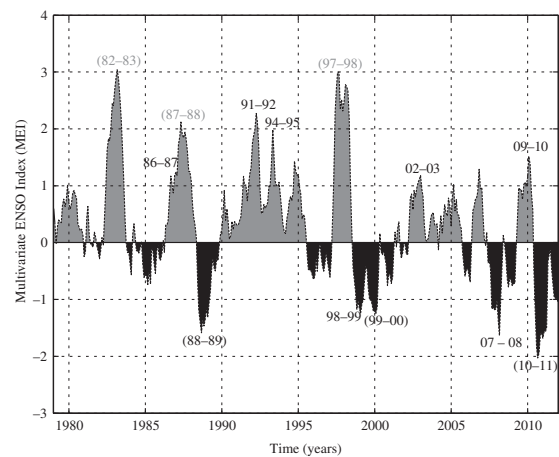


Figure 2. Multivariate ENSO Index (MEI) where El-Niño (positive phase) is presented in grey and La Niña (negative phase) in black. Numbers on the plot indicate El-Niño/La Niña event years. Grey and black digits between parentheses represent strong El-Niño and La Niña events, respectively, while black digits only show the moderate years for both events.

the study were retrieved from <http://www.esrl.noaa.gov/psd/enso/mei/>.

3.1.5. Normalized difference vegetation indexes

Since moisture changes over the region are also highly coupled to changes in vegetation (e.g. Huber *et al.*, 2011), variations in net-precipitation with respect to NDVI were assessed. NDVI time series covering the period of 1981 to 2006 were obtained from the Global Inventory Modeling and Mapping Studies (GIMMS). The GIMMS NDVI data is derived from satellite imagery generated from the Advanced Very High Resolution Radiometer (AVHRR) instrument on-board the NOAA satellite series 7, 9, 11, 14, 16, and 17 at a 15 day and approximately 0.0833° temporal and spatial resolutions, respectively (Tucker *et al.*, 2005). The vegetation index data was retrieved from <http://iridl.ldeo.columbia.edu/SOURCES/.UMD/.GLCF/.GIMMS/.NDVIg/.global/.ndvi/index.html?Set-Language=en> and the bi-monthly dataset was aggregated to monthly series.

3.2. Methodology

Maximum renewable freshwater availability fields were derived from the atmospheric water budget approach and compared to the net-precipitation from GLDAS model's rainfall and evaporation datasets. All the gridded datasets, with the exception of the GLDAS products, were up-scaled (i.e. filtered with a low pass filter and re-sampled with the bi-cubic interpolation technique) to a spatial resolution of 0.5° to ensure consistency with the GPCC rainfall data. In comparing the ERA-Interim and GLDAS products, the former was up-scaled to a coarser resolution of 1°. Next, continuous wavelet analyses (Section 3.2.3.) were then performed on the different data sets in order to investigate their wave power spectra patterns. Finally, cross coherencies between the datasets

were also investigated with the wavelet coherence method (Section 3.2.4.).

3.2.1. Net-precipitation

Net-precipitation can be obtained by the direct differencing of precipitation and evaporation (e.g. Meynadier *et al.*, 2010; Morrow *et al.*, 2011) or through the atmospheric water budget approach (e.g. Yirdaw *et al.*, 2008; Syed *et al.*, 2009; Munier *et al.*, 2012). Comparing global runoff anomalies from the coupled atmospheric-terrestrial water budget, Munier *et al.* (2012) indicated consistency between net-precipitation from observed P and modelled E. Meynadier *et al.* (2010), used modelled evaporation and Tropical Rainfall and Measuring Mission (TRMM) rainfall data and reported that the moisture flux divergence and precipitation minus evaporation are quite similar over WA.

Essentially, net-precipitation is a measure of the flux in the maximum available renewable freshwater resource (Oki and Kanae, 2006). Consequently, a system with a long-term deficit in net-precipitation tends to face dry conditions and vice-versa (Lee *et al.*, 2014). For this study, net-precipitation is computed as a residual of the atmospheric water balance using meteorological data from the ERA-Interim. Additionally, net-precipitation was estimated from the land-based approach using the GLDAS models and compared to the ERA-Interim estimate. Our motivation to select the ERA-Interim reanalysis data to perform the investigations was due to its long-term consistency as reported by Lorenz and Kunstmann (2012) and Forootan *et al.* (2014b). The evaporation estimates from GLDAS were used due to their acceptable uncertainty over WA as illustrated by Andam-Akorful *et al.* (2015).

3.2.2. Atmospheric water budget

From the atmospheric perspective, the instantaneous water balance equation is given as (e.g. Yirdaw *et al.*, 2008):

$$\frac{\partial W}{\partial t} + \nabla \cdot \mathbf{Q} = -(P - E), \quad (1)$$

where P and E are precipitation and evaporation respectively, and t represents time. W is the atmospheric water storage obtained as the total water column in a unit area of the atmosphere, calculated as (e.g. Yirdaw *et al.*, 2008):

$$W = \frac{1}{g\rho} \int_{p_s}^{p_t} q dp, \quad (2)$$

where the surface pressure, p_s and the pressure at the top of the atmosphere, p_t are the limits of the integral, q , which is the specific humidity; g , the gravity value and ρ , the density of water.

The moisture flux divergence (or convergence depending on its sign) or net outflow of water vapour across the atmosphere computed from specific humidity, the eastern and northern direction winds (e.g. Yirdaw *et al.*, 2008):

$$\nabla \cdot \mathbf{Q} = \frac{1}{R \cos \phi} \left(\frac{\partial Q_\lambda}{\partial \lambda} + \frac{\partial (Q_\phi \cos \phi)}{\partial \phi} \right), \quad (3)$$

where Q_λ and Q_ϕ represent the east–west and north–south components of vapour flux respectively. R is the mean radius of the Earth, λ and ϕ are the longitude and latitude, respectively.

3.2.3. Wavelet transform

Wavelet analysis allows the investigation of localized changes in sampled time series by decomposing them into time–frequency space (Jänicke *et al.*, 2009). The frequency and time domains of hydroclimatic time series are usually non-stationary. As a result, the amplitude and frequency of the dominant periodic components of fluxes evolve in both space and time domains, making their identification using techniques such as Fourier Transforms or Least Square Spectral Analysis, very difficult (e.g. Beecham and Chowdhury, 2009; Sharifi *et al.*, 2013). Wavelet transforms, in contrast, can be applied to identify localized changes from available observations by projecting them onto different resolutions (scales) base-functions that vary with respect to time and frequency (e.g. Torrence and Compo, 1998; Keller, 2004, p. 24). The continuous wavelet transform (CWT) was used, here, to compute the wave power spectrum (WPS) in order to quantify the distribution of variances in the available datasets such as net-precipitation and rainfall (Torrence and Compo, 1998). Mathematically, CWT is expressed as (Beecham and Chowdhury, 2009):

$$C(a, b) = \frac{1}{\sqrt{a}} \int s(t) \psi \left(\frac{t-b}{a} \right) dt, \quad (4)$$

where C is the wavelet coefficient, a and b are the scale and position functions respectively, $s(t)$ is the signal, and ψ is the wavelet function. Morlet wavelet was used as the mother-wavelet since it is well suited for feature extraction from oscillatory samples such as the hydroclimatic time series employed in this study (e.g. Domingues *et al.*, 2005; Jänicke *et al.*, 2009). Seasonal fluctuations and short-term biases were removed before application of the wavelet analysis by standardizing the time series, i.e. their temporal mean values were removed and the resulting series scaled by their corresponding standard deviations (Nakken, 1999). For detailed explanations of wavelet analysis using WPS, we refer to Keller (2004) and Torrence and Compo (1998).

3.2.4. Wavelet coherence

To identify co-varying relationships between net-precipitation and the other datasets, the wavelet squared coherency (WTC) algorithm was employed (Torrence and Webster, 1999; Grinsted *et al.*, 2004). WTC between two CWTs is useful to locate significant coherence against a background of red noise (Grinsted *et al.*, 2004). The WTC between two signals is given as (Grinsted *et al.*, 2004):

$$R_n^2(s) = \frac{|S(s^{-1} W_n^{XY}(s))|^2}{S(s^{-1} |W_n^X(s)|^2) \cdot S(s^{-1} |W_n^Y(s)|^2)}, \quad (5)$$

49

where S is a smoothing operator, W^{XY} , the cross wavelet transform between the two CWTs W^X and W^Y , and X and Y represent the two time series (e.g. net-precipitation and temperature). Following Grinsted *et al.* (2004), the WTC can be seen as a localized correlation coefficient in a time-frequency space.

3.2.5. Trend analysis

The Sens slope estimator (Sen, 1968) was used to determine trends in the power spectrum of each dataset. This method of robust linear regression estimation chooses the median slope among all lines through pairs of two dimensional points in a time series (Machiwal and Jha, 2012, p. 70). For an equally spaced time series, the slope estimator is defined as (Sen, 1968):

$$f(t) = Qt + B \quad (6)$$

where Q is the slope and B is a constant. The slope rate, – i.e. linear rate of change – Q , is obtained by finding the median of all the slopes of the data pairs as:

$$Q_i = \frac{x_j - x_k}{t_j - t_k}, \quad i = 1, 2, \dots, N, \quad N = \frac{n(n-1)}{2}, \quad (7)$$

for all $j > k$, $k = 1, 2, \dots, (n-1)$ and $j = 2, 3, \dots, n$, where n and N is the number of data and the number of slope estimations, respectively; and x_j and x_k are the measurements at times t_j and t_k , respectively. Using the median for computation of Q_i in Equation (7) makes the estimation more robust to the outliers or extreme observations. The significance of the estimated Q was tested using the Mann–Kendall test at a 95% confidence interval (see, e.g. Machiwal and Jha, 2012, p. 69).

3.2.6. Change point analysis

Hydro-climatic sequences, which are the results of certain natural processes remain the same as long as conditions are steady. However, if the processes undergo significant changes, the sequences exhibit jumps and present different statistical properties (Wong *et al.*, 2006). A change point analysis enables the estimation of the point at which the change(s) occur. We make use of the *change point* package by Killick and Eckley (2014) in the *R* statistical software to detect changes in the series studied in this paper.

4. Results and discussion

The net-precipitation estimations from the atmospheric and land-based water budgets are first compared. The results of the wave power spectrum (WPS) of each data set (i.e. net-precipitation, rainfall, temperature, evaporation, soil moisture and NDVI) and the analysis of mean changes of the data sets at the decadal scale, as well as their spatial trends in the wavelet transforms and signal coherency analysis are presented.

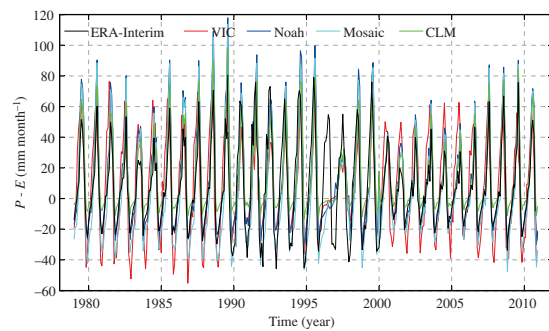


Figure 3. Spatially averaged time series of monthly net-precipitation estimates over West Africa, based on four GLDAS products (VIC, Noah, Mosaic and CLM) and ERA-Interim data from 1979 to 2010. While all datasets appear to be consistent, especially with regards to seasonal patterns, the GLDAS products present some inconsistencies around 1997.

4.1. Data comparisons

To compare different estimations of net-precipitation over WA, areal averages were computed from the GLDAS products (i.e. from the land-based water balance perspective) and ERA-Interim (atmospheric water balance approach). Although the five different datasets show some degree of consistency, there are significant differences in their estimates as can be seen in Figure 3. The CLM product for instance seems to overestimate net-precipitation, with most of its values being largely above zero. Similarly, Noah and Mosaic seem to overestimate the quantity while VIC's time series is the closest to that of ERA. For all the GLDAS products however, there seem to be a systematic error in the time series between 1996 and 1997 where the seasonal cycle was not adequately represented. This was also reported by Huang *et al.* (2013), who assessed the GLDAS-Noah and ERA-Interim time series over the Yangtze River Basin of China.

In light of the performed comparisons (see, Figure 3), the ERA-Interim estimates were used for the rest of the analysis. However, further investigation is needed in order to find the sources of these differences. For example, uncertainties in the GLDAS-estimated evaporation fields come from various sources such as meteorological and surface data as well as the algorithm used (e.g. Xue *et al.*, 2013).

4.2. Spatially averaged temporal analysis

Figure 4 shows the results of the wavelet analysis derived from the areal averages of rainfall over WA. Dominant modes of the signal occur at the annual (maximum occurs at the 1 year period) and the semi-annual scales (maximum occurs at the 0.5 year period) as shown by Figure 4(c). The variance of the seasonal cycle as presented in Figure 4(d) appears to be modulated by a low frequency oscillation, as its magnitude show peaks and troughs at a 2 to 8 year periodicity, which is consistent with the ENSO cycle (see Figure 2). Similarly, the annual variabilities follow this oscillation (Figures 4(b) and 4(d)). In the early 1980s, the spectral power at the annual scale were of relatively low

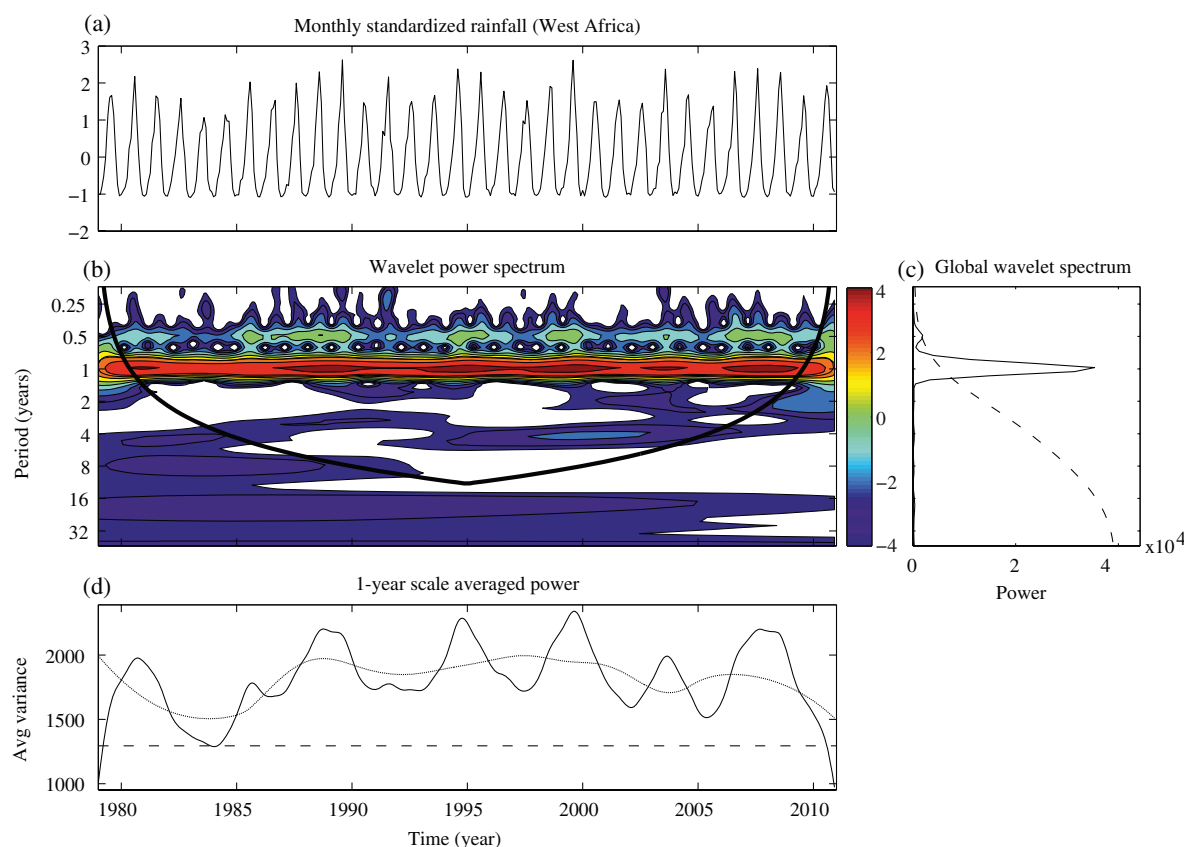


Figure 4. Wavelet transform of areal averaged standardized rainfall over West Africa. (a) Is the standardized time series of rainfall, (b) is the wavelet power transform, where the thick black arc defines the cone of influence which indicates the boundary beyond which the spectral information are vulnerable to distortions due to edge effects (Torrence and Compo, 1998; Grinsted *et al.*, 2004), (c) is the global wavelet spectrum for the WPS and (d) is the averaged power at the annual scale (solid line), where the dashed line represents the significance at a 95% confidence level; and dotted line, the long-term trend. The rainfall WPS show a modest recovery from the dry spells in the 1980s.

magnitudes, which corresponds to the 1982/83 drought in WA (Nicholson, 2013). Coincident with the comparatively wet period following the anomalously dry spell, higher annual amplitudes are observed for the second half of the decade, peaking around 1989. Weaker annual variances are then observed between 1990 to early 1993, rising to a peak in the third quarter of 1994 before dipping in 1997 and then again, rising to another peak in 1999 (see Figure 4(d)). Spectral signatures at the annual scale show a slight increasing linear trend as shown by Figure 4(d). This signifies an increase in annual rainfall rates between 1983 and 2010, which was confirmed with the Mann–Kendall significance test.

The wavelet transform results for net-precipitation over the entire region is presented in (Figure 5(d)). Similar to rainfall, most of the dominant spectral power is located at the annual and semi-annual time scales. Relatively weak sub-annual variances are observed before early 1984, followed by higher variances between the boreal summer of 1984 to early 1991. Relatively low amplitudes are observed between 1991 to early 1993 and 1994 to 1996. From late 1995 to 2010, however, it is observed that the

wavelet power within this period is significantly lower than the one between 1979 to 1995. Similarly for the annual signals, the mean power before 1996 is found to be higher than those after this period (cf., Figure 5(d)), which implies that, the variance of water flux over the region reduced significantly since 1995 afterwards. A Mann–Kendall significance test showed a significant decrease in the averaged power of the net-precipitation at the annual scale.

A change point analysis was performed to detect the changes in both the mean and variance in the extracted averaged power at the annual cycle (Figure 6). Both tests divided the series into groups respectively at a confidence level of 95%. The extracted rainfall flux returned a change point in April 1985, whereas that of net-precipitation was in April 1996.

In order to confirm this apparent significant decrease in water flux variance, wavelet analyses were performed on evaporation, soil moisture change, temperature and NDVI time series. Figure 7 shows the WPS and the averaged signal power at the annual scale of the respective datasets. Figure 7 (a and b) shows relatively high temperature signal power during the 1980s and a significant dip in 1991 before

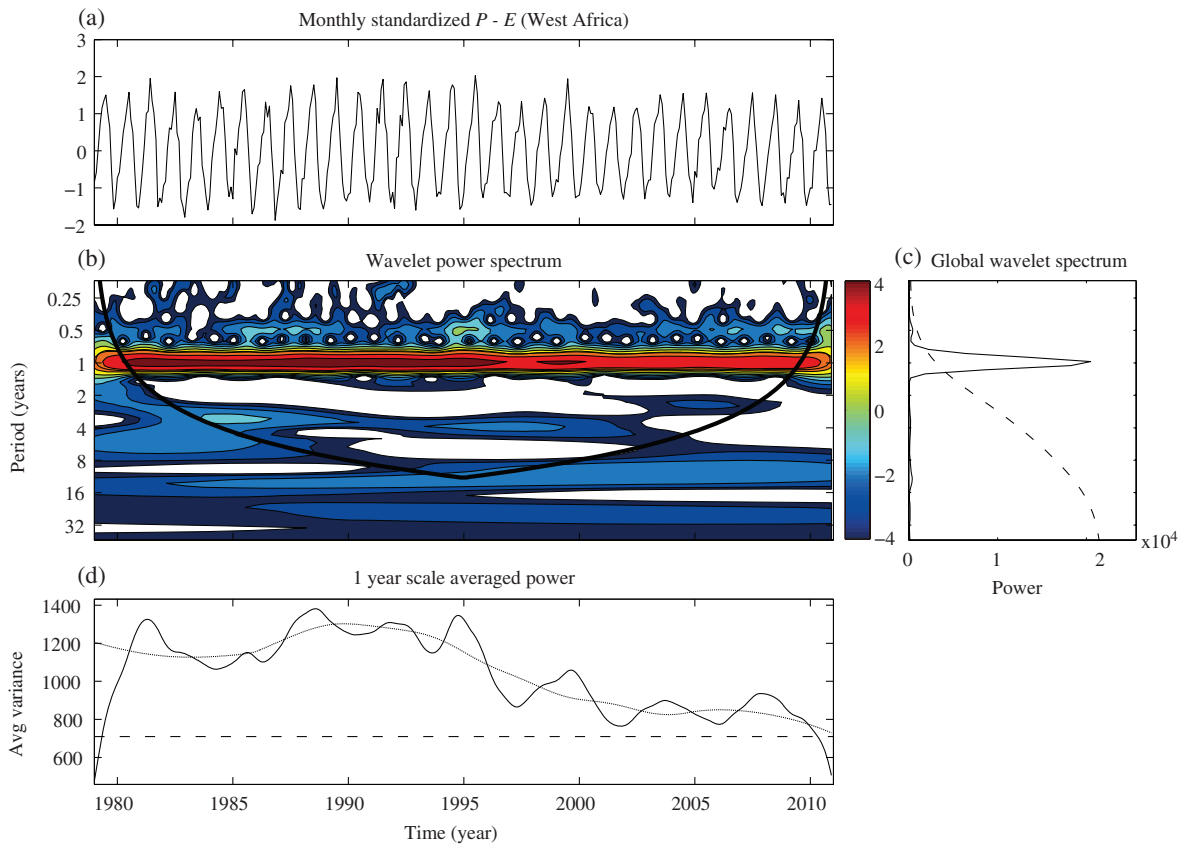


Figure 5. Wavelet transform of areal averaged standardized net-precipitation ($P-E$) over West Africa. (a) is the standardized time series of $P-E$, (b) is the wavelet power transform, which the thick black arc defines the cone of influence, (c) is the global wavelet spectrum for the WPS and (d) is the averaged power at the annual scale (solid line), which the dashed line shows the significance at a 95% confidence level, while the dotted line is the long-term trend. In contrast to rainfall, net-precipitation WPS show decreasing trend between 1979 to 2010.

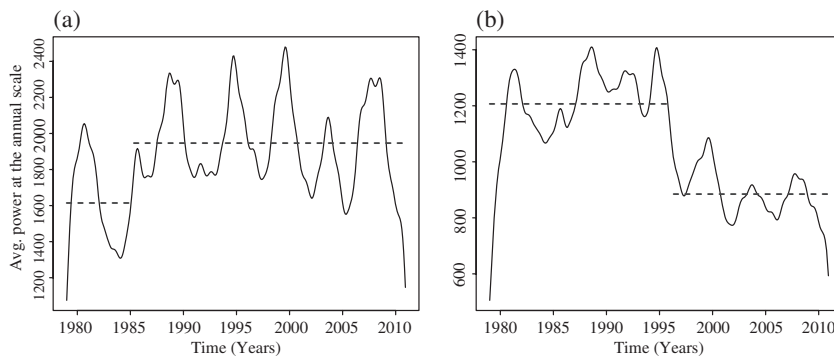


Figure 6. Step change analysis for the averaged power at the 1-year scale for rainfall (a) and $P-E$ (b). Rainfall over WA experienced a positive change in both mean and variance at epochs 1985.25 and 1996.25, respectively. Note that the dashed lines indicate the different means as indicated by the analysis.

experiencing a minimal positive trend. It is observed that the averaged annual-scaled power (Figure 7(b)) shows a repetitive pattern of approximately 5 to 8 years. This is in agreement with ENSO activity, which presents cycles between 2 to 8 years. Signal power of evaporation during the drought years of the early 1980s was relatively low

(Figure 7(d)), but experienced an increase in amplitude, which coincided with high rainfall power (see Figure 4). After a significant peak in 1988/1989, we found a progressively decreasing trend in the variance of evaporation for the next 20 years (Figure 7(d)). The reduction in the variance of the evaporation signal could account for the lower

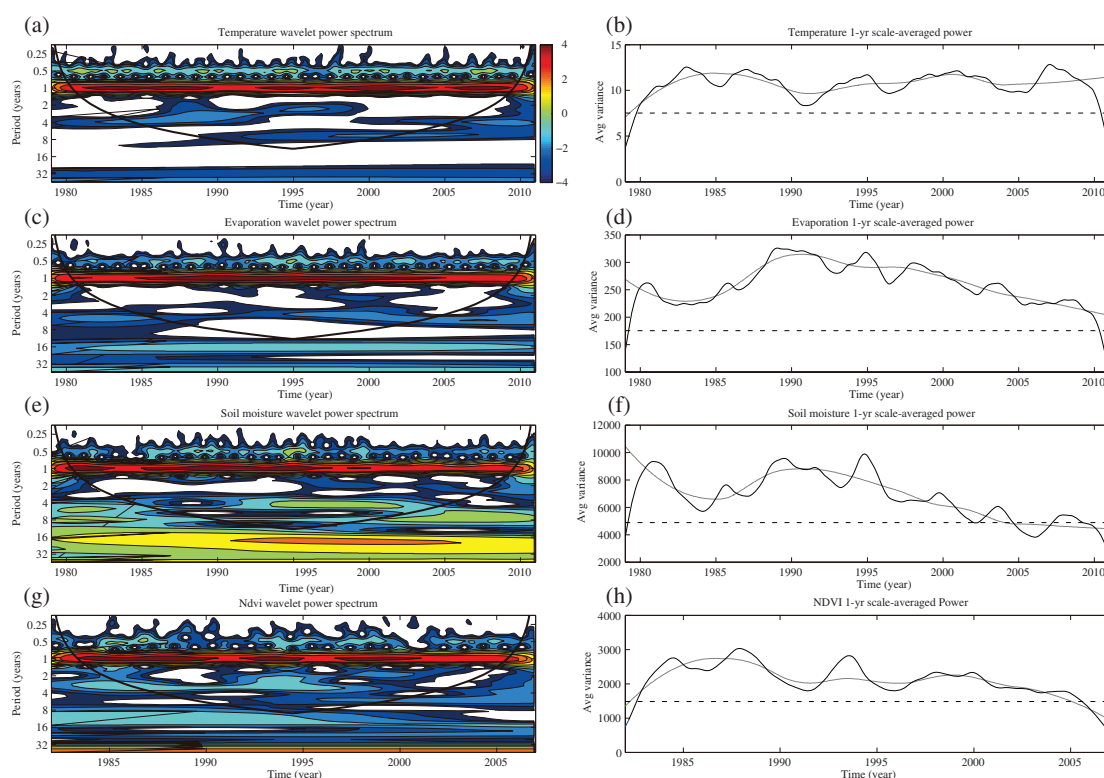


Figure 7. The WPS for (a) temperature, (c) evaporation, (e) soil moisture and (g) NDVI and their averaged power at the annual time scale in (b), (d), (f), and (h), respectively (at the panels b, d, f, and h the solid line is the averaged power at the annual scale, the dashed line shows the significance at a 95% confidence level, and the dotted line is the long-term trend). Evaporation, soil moisture and NDVI all present decreasing trends in WPS as shown in the average 1-year scaled power.

Table 1. Mean power changes between 1979–1995 and 1996–2010. dPow is the mean change in the signal’s power spectrum and pPow is the proportion of power contributed by the sub-climatic zone. The acronym MSH stands for moist sub-humid zone, DSH stands for dry sub-humid, SUD stands for Sudano, SAH stands for the Sahelian, HyA stands for Sahara desert and WA stands for the entire West African region.

Region	Precipitation		Temperature		Evaporation		P–E	
	dPow (%)	pPow (%)	dPow (%)	pPow (%)	dPow (%)	pPow (%)	dPow (%)	pPow (%)
MSH	–12.56	42.97	–11.38	0.19	–31.35	0.17	–0.55	21.75
DSH	+2.69	42.22	+10.26	0.92	+4.36	12.58	–33.60	63.34
SUD	+17.22	8.88	+2.65	2.67	–0.80	46.48	–50.11	10.51
SAH	+34.16	5.08	+2.95	22.44	–7.14	39.81	–42.25	3.75
HyA	+48.08	0.85	+0.08	73.78	–52.17	0.96	+223.97	0.65
WA	+4.05	100	+7.80	100	–8.09	100	–26.02	100

DSH, dry sub-humid; dPow, mean change in the signal’s power spectrum; HyA, Sahara desert; MSH, moist sub-humid zone; pPow, proportion of power contributed by the sub-climatic zone; SAH, Sahelian; SUD, Sudano; WA, entire West African region.

variance in water flux. Similar patterns from soil moisture change, and NDVI (see Figure 7 panels e-h) with respect to net-precipitation and evaporation were observed.

It can therefore be concluded here that, the increasing trend in rainfall variance is coherent with the decreasing trend in freshwater flux together with all other datasets (i.e. NDVI, evaporation and soil moisture changes). As variations in net-precipitation show two distinct regime periods (i.e. 1979 to 1995 and 1996 to 2010), an evaluation of the mean percentage changes in the four main parameters (i.e. net-precipitation, rainfall, temperature and evaporation)

with respect to those periods was undertaken. Altogether, the mean monthly precipitation power at the annual scale between 1979 to 1995 and 1996 to 2010 increased by 4% while temperature increased by 8%. The variances of evaporation, soil moisture change, and net-precipitation however decreased by 8, 30 and 26%, respectively (Table 1). Additionally, soil moisture flux from the different GLDAS models (not shown here) show a mean reduction in annual variance of 30%. NDVI annual signal power between 1982 to 1995 and 1996 to 2006 decreased by 22%. Thus, the decreased annual signal power of available freshwater in

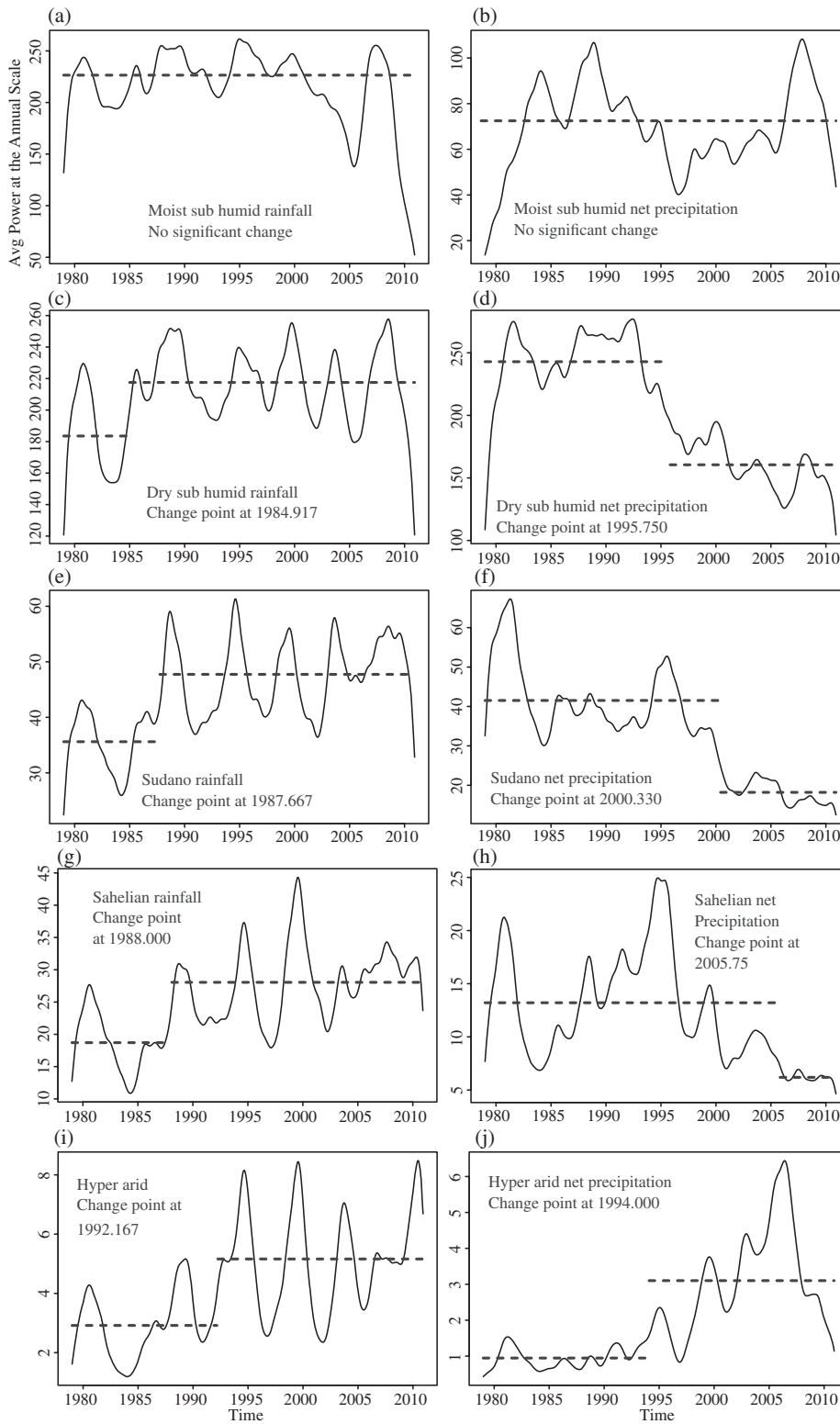


Figure 8. 1-year scale-averaged power of rainfall and net-precipitation for the different sub-climatic zones in WA (see Figure 1), i.e. (a) Moist sub-humid, (b) Dry sub-humid, (c) Sudano, (d) Sahelian and (e) Hyper-arid. Step change analysis showed that for (b) to (d), rainfall in the 1980s had lower means and higher means from the 1990s. On the other hand, mean power for net-precipitation was higher in the first half of the period of study and lower in the other. The moist sub-humid zone (a), however, shows a no significant change in mean.

the region is confirmed by the wavelet transforms analyses of the different datasets.

4.2.1. Sub-climatic zones

Since WA is a large region with different hydroclimatic regimes, wavelet analysis was performed on spatially averaged signals for each sub-climatic zone (see Figure 1) in order to identify the main source of variability in net-precipitation and rainfall. Figure 7 presents the 1-year scale-averaged wavelet spectral power in the respective zones. The power of rainfall in the moist sub-humid zone (including countries such as Guinea, Sierra Leone and Liberia) during the drought period of 1982/83, which coincided with a positive ENSO event, is expectedly low as compared to the period between 1984 to 2004 (Figure 8). Very low signal amplitudes are however observed between early 2004 and late 2005. The amplitude of rainfall then rose to a significant peak during 2007, coincident with the 2007's La Niña event (Paeth *et al.*, 2011). The nature of the WPS of net-precipitation before 1993 was found to be largely consistent with that of rainfall (Figure 8(b)). Afterwards the annual signal variance show an inverse pattern till early 2004, after which, the two series exhibit similar troughs and peaks. Step change analysis (shown as dashed lines on the figure) indicated that no significant change in mean or variance occurred within the period of consideration for both series.

For the dry sub-humid zone, whereas rainfall (Figure 8(c)) experienced a positive increase within the period of study, water availability (Figure 8(d)) decreased significantly. Rainfall in this zone experienced a positive change in mean power at epoch 1984.917 (i.e. December 1984), on the other hand, there was a negative change in net-precipitation at 1995.750 (October, 1995). Similarly, the Sudano zone experienced increased rainfall power with a positive change in mean at 1987.667 (September, 1987) while net-precipitation saw a negative step change at 2000.330 (May, 2000) as shown in Figures 8(e) and (f) respectively. Rainfall (Figure 8(g)) in the Sahelian zone had a positive step change at 1988.000 (January 1988), whereas a negative change in mean and variance for the net-precipitation series begun at 2005.750 (October, 2005), Figure 8(f). The hyper-arid zone however, experienced positive changes in rainfall (Figure 8(i)) and net-precipitation (Figure 8(j)) respectively at 1992.167 (March, 1992) and 1994.000 (January, 1994).

Overall, with the exception of the hyper-arid zone, the variances of rainfall at the annual scale show increasing trends, while those of net-precipitation show decreasing trends. This result is consistent with those from other data sets, presented in section 4.2. Furthermore, Figure 8 shows that, the rainfall deficits lasted for longer periods in the drier zones compared to the relatively moist ones. It is also important to note that, while rainfall and net-precipitation in the hyper-arid region both indicate increasing trends, their respective WPSs are negligible when the entire region is considered (refer to Table 1).

4.2.2. Mean decadal changes at the annual scale

Table 1 provides a summary of the changes in the annual scale signal variances of precipitation, temperature, evaporation and net-precipitation for the respective zones between 1979 to 1996 and 1997 to 2010. The moist sub-humid zone experienced deficits in all the four quantities. The total contribution of this region to temperature and evaporation changes over WA are, however, nearly negligible. In contrast, its total contribution to rainfall and net-precipitation (of approximately 43 and 22%, respectively) was found to be very significant despite the relatively small area it covers. This humid sub-climatic zone, which is located mostly in the southwestern highlands of WA is an important source for a number of rivers including the Niger, the Gambia and the Senegal (see, e.g. Simier *et al.*, 2006; Sall *et al.*, 2007; Oguntunde and Abiodun, 2012). Consequently, a reduction in rainfall signal power in this zone could have triggered the reduction of the variance of net-precipitation over WA. It is worth noting that, this sub-region was not significantly affected by the reduced rainfall rates as it only experienced a minimal change (−0.55%) in net-precipitation.

Meanwhile, the dry sub-humid zone experienced a 33.6% deficit in net-precipitation variance. Conversely, rainfall, temperature and evaporation, however, increased by 2.69, 10.26 and 4.36%, respectively. Although its total rainfall power contribution to the region is slightly lower than that of the moist sub-humid zone, it contributes 63.34% to the total net-precipitation signal power. This is likely due to the fact that its land area is drained by the main rivers of WA (e.g. the Niger, Gambia, Senegal and Volta). Accordingly, most of the observed reduction in available water over the region could be attributed to the net-precipitation deficit in this zone. The Sudano and Sahelian zones both exhibited positive changes in rainfall and temperature but negative for evaporation and net-precipitation. These two zones are mostly drained by rivers (e.g. Niger and Senegal) predominantly sourced from the more humid zones (moist and dry sub-humid zones). Consequently, it is concluded that a possible reduction in runoff from the humid areas likely led to a deficit in freshwater availability in WA.

4.3. Spatial trends in signal variances

Figure 9 presents the WPS spatial trends in rainfall, temperature, evaporation, net-precipitation, soil moisture and NDVI. Rainfall power mostly in the MSH and DSH zones along the coast (see Figure 9(a)) experienced decreasing trends, especially in the Guinean Highlands, which caused reduction in runoff into rivers that take their sources from this region. Conversely, most areas in the Sudano, Sahelian and desert regions experienced increased rainfall power. This observation agrees with the findings made in a number of studies, see, e.g. Nicholson (2005); Anyamba and Tucker (2005); Ali and Lebel (2008); Lebel and Ali (2009); Nicholson (2013). However, as observed in Section 4.2.2, rainfall in these zones represents a small portion of the total rainfall of the entire WA. Therefore, it did not

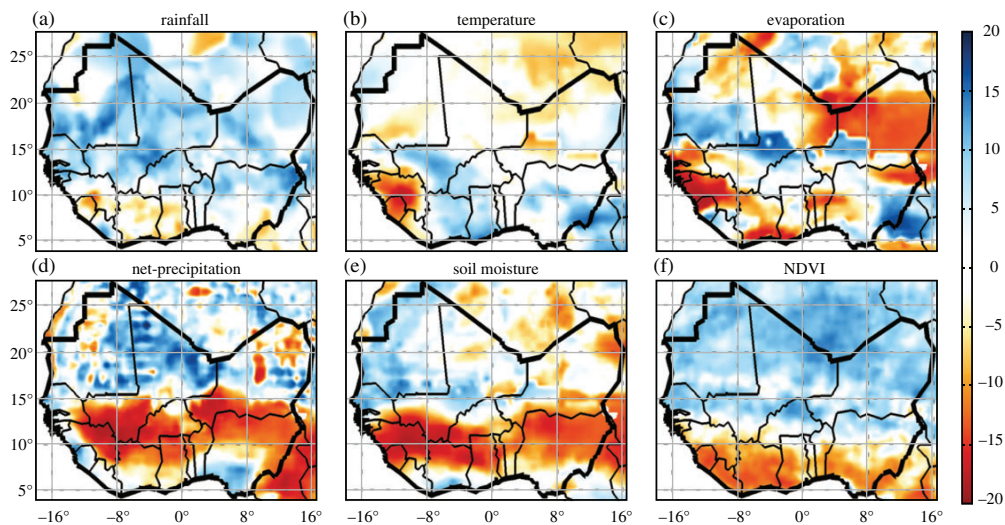


Figure 9. Spatial wave power spectrum trends at the annual timescale over West Africa, where (a) rainfall, (b) temperature, (c) evaporation, (d) $P-E$ (net-precipitation), (e) soil moisture and (f) NDVI.

significantly improve the water availability conditions in the region.

Temperature changes (Figure 9(b)) in the south-western part of WA indicated decreasing trends, whereas parts of Mali, Côte d'Ivoire, Burkina Faso, Ghana and Nigeria exhibited modest positive trends. The drier northern parts of the region largely had small negative or insignificant trends in terms of temperature. Evaporation (Figure 9(c)) rates experienced reduction in most parts of the region. Parts of the Sahel and desert areas experienced negative trends, consistent with our results from temperature changes. Although the dry north (specifically the Sahel and desert areas) largely experienced positive trends in net-precipitation, the north eastern and western areas both saw negative trends (Figure 9(d)). Areas lying along the western coast as well as the eastern coast indicated positive trends, while most of the MSH, DSH and Sudano zones exhibited negative trends. Most parts of the dry north experienced increasing trends, however, areas in the north eastern and north western parts exhibited decreasing trends in power.

A high consistency was found between the trends in the vegetation index and those of rainfall and net-precipitation (Figures 9(f), (a) and (d)). Generally, the drier parts of the region seem to have experienced some degree of greening (i.e. positive trends of 5 to 15 square units in NDVI variance), whereas the humid south presented negative trends. The trends in the NDVI data set is largely consistent with those in rainfall and net-precipitation. The increased wetness and cooler temperatures in the arid and semi-arid parts of the region and the converse in the Guinean sub-regions agree with the findings of Huber *et al.* (2011).

4.4. Decadal changes

In Figure 10, panels a to d, the deviations of rainfall, net-precipitation, evaporation and temperature from their

32-year means are plotted, respectively. It is evident from Figure 10(a) that, the amount of rainfall in the 1980s was less than the long-term mean (i.e. from 1979 to 2010), with relatively higher rainfall rates in the following two decades. Low evaporation rates were also observed in the first decade, indicating a deficit in soil moisture and surface water for evaporation, whereas the higher rates of the following decade were likely due to availability of more water (Figure 10(c)). Coincident with higher temperatures from 2000, evaporation rates since 2003 were found to be consistently above the mean value for the 32 year period, which coincided with relatively lower rainfall rates in the 2000s. Similarly, the mean annual net-precipitation in the 1980s was lower than that of the 1990s, while the last decade (i.e. the 2000s) also presented lower amounts (Figure 10 (b)).

With respect to Table 2, the mean annual rainfall in the first decade (i.e. 1979 to 1989) increased by 7%, and 3.7% in the second (i.e. 1990 to 1999) but fell by 3.3% in the third decade, whereas temperature had a cumulative rise of 0.14% in the last decade (i.e. 2000 to 2010). The mean annual evaporation increased by 3.59 and 0.82% leading to a cumulative rise of 4.41% by the third decade. It is, therefore, apparent that reducing rainfall rates coupled with rising temperatures, and consequently evaporation, led to 30.86% decrease in net-precipitation with respect to the second and third decades and a cumulative reduction of 10.54% since the 1980s. Taking into account observations made in Section 4.2.2. decreasing rainfall rates in the humid climatic zone and rising temperatures in the other zones resulted in increased evaporation rates and consequently reduced the amount of maximum available freshwater in WA.

4.5. Signal coherencies

Coherency between spatially averaged time series between four data sets (i.e. rainfall, net-precipitation, temperature

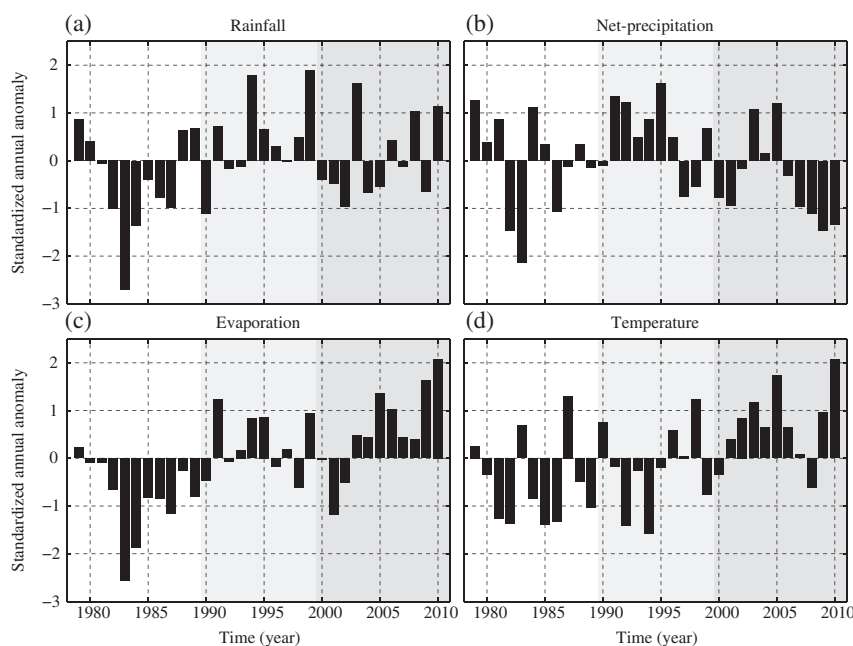


Figure 10. Deviations from mean annual: (a) rainfall; (b) net-precipitation; (c) evaporation; (d) temperature. The backgrounds in grey graduations show the different decades of interest.

Table 2. Mean annual changes of $P-E$, rainfall, evaporation, and temperature with respect to the three decades (1979–1989, 1990–1999 and 2000–2010, labelled as 1, 2 and 3, respectively) within the period of study. Note that $\Delta_{(i,j)}$, with $i = 2, 3$ and $j = 1, 2$, is the difference between the average quantity observed in decade i and decade j .

Differences	$P-E$ (%)	Rainfall (%)	E (%)	Temperature (%)
$\Delta_{(2,1)}$	+20.32	+7.03	+3.59	+0.04
$\Delta_{(3,1)}$	-10.54	+3.74	+4.41	+0.14
$\Delta_{(3,2)}$	-30.86	-3.29	+0.82	+0.10

and evaporation) as well as ENSO index are shown in Figure 11. Wavelet coherency (WTC) between rainfall and MEI (Figure 11(a)) shows limited coherency between the two parameters at the annual and seasonal scales (i.e. around periods 1 and 0.5 years, respectively). However, significant coherence at the annual scale can be observed between late 1988 and early 1991, coincident with the La Niña event between 1988 and 1989 (see Figure 2(b)). This is in agreement with the findings of Nicholson *et al.* (2000), who reported relatively high rainfall amounts during those years. High co-varying power is also observed between mid 1999 and early 2001, also coincident with the La Niña event between 1998/1999.

At the seasonal scale however, the region of high co-variability between 1992 and 1995 are found to be anti-correlated. This period coincides with the moderate ENSO events (see Figure 2). This implies that although the seasonal rainfall was significantly affected, the ENSO effect was not significant at the annual scale. Conversely, the moderate La Niña events between 2007 and 2008

seem to present positive impacts both on the seasonal and annual rainfall between overlapping periods in 2005 and 2009 (cf., Paeth *et al.*, 2011; Samimi *et al.*, 2012).

At the three to five year cycle, rainfall and MEI are approximately 6 months out of phase between 1979 and 1984 (although parts of the significant area is outside the COI due to the length of the time series), indicating the extreme dry conditions that coincided with the 1982/1983 ENSO event. Additionally, from 1995 to 2010 (note that 2005–2010 is outside the COI), ENSO is approximately 10 months out of phase with rainfall. This is consistent with low rainfall amounts in the last decade as found in Section 4.4. Consequently, it can be inferred that the warm phase of ENSO during the two different periods resulted in dry conditions in the 1980s, as well as the mid 1990s to the present decade. This period of low rainfall amplitudes coincides with the low net-precipitation signal power as reported in Section 4.2. It can be concluded therefore, that low frequency modulation of rainfall by ENSO activity from late 1995 played a major role in the observed reduction in available water within WA.

The WTC between net-precipitation and MEI at the annual and seasonal scales generally follow the same pattern as rainfall except over the years between 2004 and 2010 at the 2-year band, where it is estimated to be about 10 months out of phase. The characteristics of this coherency is similar to the one observed between 1979 and 1985 (the period before August 1983 is outside the COI), where a relatively low net-precipitation power was found. Thus, it can be deduced that this could be due to a low frequency oscillation, which is associated with dry conditions in WA. The coherency of evaporation and MEI at the annual scale largely resemble that of rainfall and MEI,

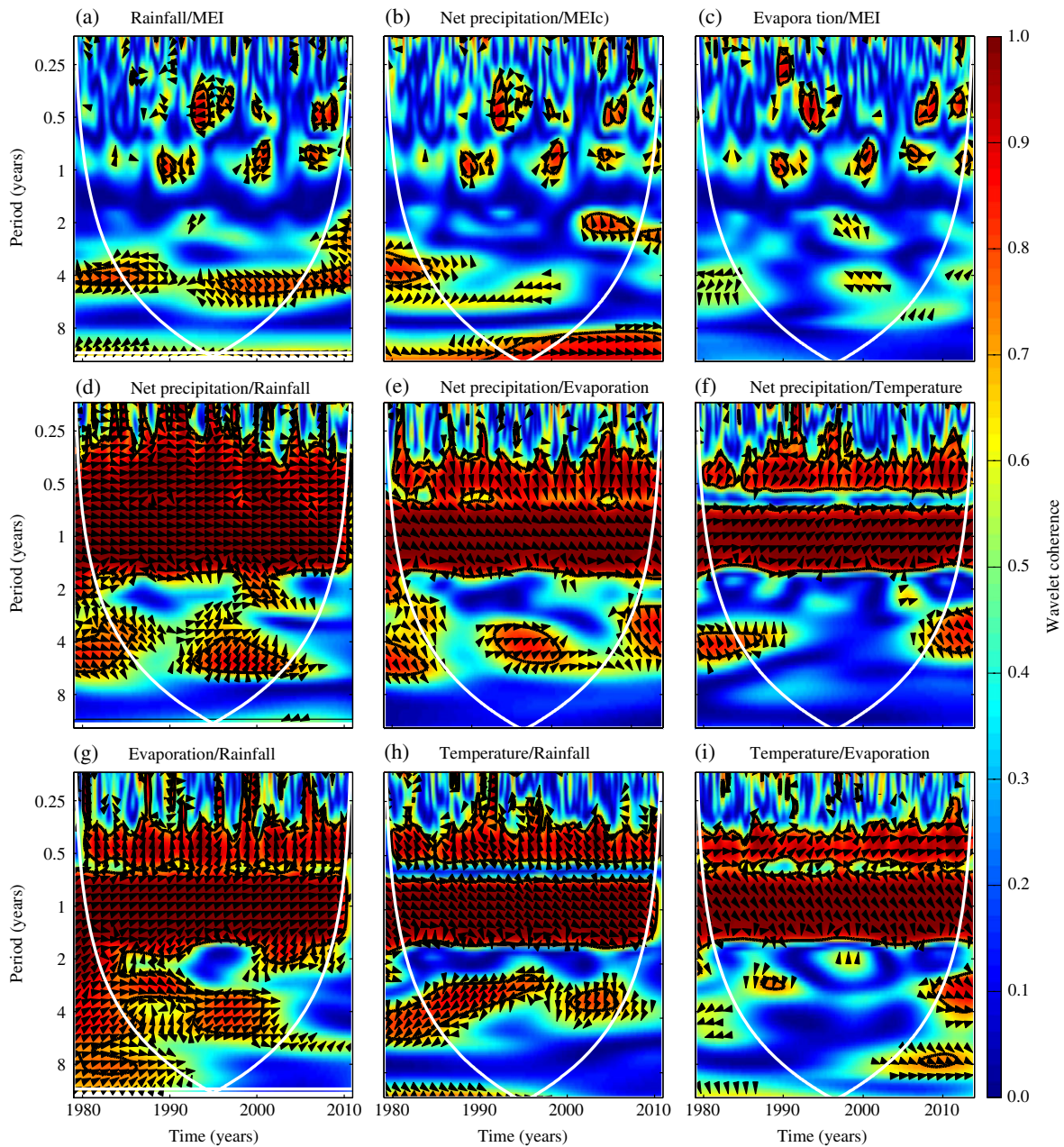


Figure 11. Wavelet coherence between: (a) rainfall and MEI; (b) net-precipitation ($P-E$) and MEI; (c) evaporation and MEI; (d) net-precipitation and rainfall; (e) net-precipitation and evaporation; (f) net-precipitation and temperature; (g) evaporation and rainfall; (h) temperature and rainfall; and (i) temperature and evaporation. The areas outside the COI (white solid line) show regions where edge effects might cause some distortion in the time-frequency spectrum while the thick black contours designate the 95% confidence level against red noise. The arrows show the phase difference between the signals, for two series, X and Y (Grinsted *et al.*, 2004): a right pointing arrow indicates an in-phase relationship; left, anti-phase; down, X leads Y by 90° and up, Y leads X by 90° . Net-precipitation exhibits a strong relationship with rainfall, evapotranspiration and NDVI but not so much with temperature.

which generally indicates that, evaporation rates increase with increasing rainfall in agreement with Meynadier *et al.* (2010). Consequently, evaporation rates may show positive correlation with respect to rainfall and by extension, net-precipitation. However, sustained high evaporation rates during periods of low rainfall may lead to rapid moisture depletion (Otkin *et al.*, 2013). The Lake Chad

basin, for example, is one of such areas in WA where high evaporation rates due to low humidity and high temperatures can sometimes result in soil moisture deficits even during periods of significant increase in rainfall (Ndehedehe *et al.*, 2016b).

Although the derived regions of high coherence are similar to rainfall/MEI WTC, the phase differences are

reversed at the intra-annual scale. This can be seen between the years 1992 and 1994, where low evaporation rates are observed after moderate ENSO events. Similar relationships can be observed at the seasonal level between 2007 and 2009. No significant coherency was, however, established between the two parameters at the 2 to 7 year band, meaning that ENSO did not introduce significant long term modulating effects on evaporation as it does on rainfall.

Figures 11(d)–(f) show the multi-resolution coherency between net-precipitation in relation to rainfall, temperature and evaporation, respectively. We found significant in-phase coherency between net-precipitation and rainfall at both the annual and sub-annual scale, whereas it precedes peak temperatures by approximately 80° and lags evaporation by approximately 60° at the intra-annual scale. The annual scale coherency with temperature indicates a phase difference of approximately 60° and a phase difference of approximately 120° with evaporation. At the 4 to 7 year band in Figure 11(d), rainfall and net-precipitation show a strong co-variance between 1992 and 2005, which is reflected in the evaporation/net-precipitation WTC (Figure 11(f)). Taking into account the adverse ENSO impact on rainfall in Figure 10(a), a joint reduction in the amplitude of net-precipitation and rainfall can be concluded. The observed co-variance between $P-E$ and evaporation around the 4 to 7 year band may be due to anthropogenic influences (such as human withdrawals and land use/land cover changes) since no obvious changes were found, as shown in either MEI/E or $temperature/E$ in Figures 11(c) and (i), respectively. This however, should be confirmed with a land cover change analysis, which is the subject of an ongoing study.

In Figure 11(g), evaporation and rainfall indicate strong coherence in the late 1980s to the early 1990s. The signal characteristics, however, change to reflect similar patterns observed for the 4 to 8 year band during the dry early 1980s (outside the COI) from around 1994 to 2001 (similar to observations made in Figures 11(d) and (f)). Consequently, it can be inferred that the low frequency oscillation, associated with reduced net-precipitation power was likely caused by a moderate and slowly evolving ENSO activity that resulted in lower rainfall coupled with high evaporation rates in the 3 to 7 year band. Temperature/rainfall coupling in Figure 11(h) show an inversed relationship especially around the 3 to 7 year cycle till the mid 1990s, followed by a brief period of low coherency between 1996 and 2001 (note that this was the period in which the lowest net-precipitation amplitudes were observed) and high coherence from 2001 till 2005. Hence, it can be deduced that, although temperature increased slightly in WA, its impact on water availability may not be as strong as lower rainfall induced by the ENSO activity. A recent study over WA during the 2012–2014 period confirms that high precipitation rates, induced by ocean circulations, remain principal drivers of the region's stored water (Ndehedehe *et al.*, 2016a). The extent to which anthropogenic activities contributed to the reduction of available water is however,

not covered in this study as it is the subject of further studies.

5. Conclusions

The purpose of this study was to provide a synoptic view of current trends and variabilities in freshwater availability in West Africa. Specifically, in this contribution, the variability of available water expressed in terms of net-precipitation over the region has been investigated using wavelet analysis. Continuous wavelet transforms at the annual scale indicated that, although rainfall rates marginally increased between 1979 and 2010, available water in the hydrological system of the region reduced considerably. The observed reduction in net-precipitation was confirmed with similar patterns in soil moisture and NDVI, which are two critical indicators of available water. Additionally, the wavelet power spectrum of spatially averaged temperature showed a slight positive trend while evaporation had a considerable negative trend. Spatially, the wavelet analysis at the annual scale showed that the dry northern part of the region largely experienced positive trends in freshwater availability whereas the relatively wet south experienced negative trends.

Mean standardized anomalies of the different data sets revealed that the 1990s experienced a recovery from the droughts of the 1980s, whereas the last decade was substantially dry. Wavelet coherency analysis, however, revealed that the reduction in net-precipitation power was highly coupled to lower rainfall rates induced by a moderate and slowly evolving ENSO activity that begun in 1995 as well as low frequency high evaporation rates. Since most major rivers (e.g. Comoe, Gambia, Niger, Senegal and Volta) in West Africa are fed from this area (i.e. south-western Guinean zone), the reduced rainfall rates translated to a reduction in available water over West Africa. To further clarify the influence from anthropogenic sources, consideration of land use/land cover changes on the hydrological dynamics at the sub-climatic scale as well as evaluation of variabilities in the various components of total water storage will be the subject of future studies.

Acknowledgements

V.G.F. acknowledges funding support from the National Natural Science Foundation of China (Grant Nos. 41574001 and 41204016) and from the Fundamental Research Funds for the Central Universities (Grant No. 2015B21014). S.A.A.-A. is grateful to Hohai University for his PhD funding. C.E.N. expresses his sincere gratitude to Curtin University for his PhD funding through the Curtin Strategic International Research Scholarship (CSIRS). We also extend our appreciations to the scientists and engineers at NASA, ECWMF, GPCC, NOAA, GIMMS for the GLDAS, meteorological, precipitation, MEI and NDVI datasets. Finally, we would like to thank the following people for their support on the early version of this work: Prof. Joseph L. Awange, Curtin University;

59 Prof. Richard Anyah, University of Connecticut; and Ehsan Forootan, Bonn University. We thank Prof. Ian G. McKendry (Associate Editor) and two anonymous reviewers for their constructive comments that helped us to improve the article. Without those help this work would never have been possible.

References

- Ali A, Lebel T. 2008. The Sahelian standardized rainfall index revisited. *Int. J. Climatol.* **29**(12): 1705–1714.
- Amogu O, Descroix L, Yéro KS, Le Breton E, Mamadou I, Ali A, Vischel T, Bader J-C, Moussa IB, Gautier E, Boukaraoui S, Belleudy P. 2010. Increasing river flows in the Sahel? *Water* **2**(2): 170–199.
- Andam-Akorful SA, Ferreira VG, Awange J, Forootan E, He XF. 2015. Multi-model and multi-sensor estimation of evapotranspiration over the Volta Basin, West Africa. *Int. J. Climatol.* **35**(10): 3132–3145.
- Anyamba A, Tucker CJ. 2005. Analysis of Sahelian vegetation dynamics using NOAA-AVHRR NDVI data from 1981–2003. *J. Arid Environ.* **63**: 596–614.
- Becker A, Finger P, Meyer-Christoffer A, Rudolf B, Schamm K, Schneider U, Ziese M. 2013. A description of the global land-surface precipitation data products of the Global Precipitation Climatology Centre with sample applications including centennial (trend) analysis from 1901–present. *Earth Syst. Sci. Data* **5**(1): 71–99.
- Beecham S, Chowdhury RK. 2009. Temporal characteristics and variability of point rainfall: a statistical and wavelet analysis. *Int. J. Climatol.* **30**(3): 458–473.
- Boone A, Decharme B, Guichard F, de Rosnay P, Balsamo G, Beljaars A, Chopin F, Orgeval T, Polcher J, Delire C, Ducharme A, Gascoïn S, Grippa M, Jarlan L, Kergoat L, Mougïn E, Gusev Y, Nasonova O, Harris P, Taylor C, Norgaard A, Sandholt I, Ottlé C, Pocard-Leclercq I, Saux-Picart S, Xue Y. 2009. The AMMA Land Surface Model Intercomparison Project (ALMIP). *Bull. Am. Meteorol. Soc.* **90**(12): 1865–1880.
- Conway D, Persechino A, Ardoin-Bardin S, Hamandawana H, Dieulin C, Mahé G. 2009. Rainfall and Water Resources Variability in Sub-Saharan Africa during the Twentieth Century. *J. Hydrometeorol.* **10**(1): 41–59.
- Dee DP, Uppala SM, Simmons AJ, Berrisford P, Poli P, Kobayashi S, Andrae U, Balmaseda MA, Balsamo G, Bauer P, Bechtold P, Beljaars ACM, van de Berg L, Bidlot J, Bormann N, Delsol C, Dragani R, Fuentes M, Geer AJ, Haimberger L, Healy SB, Hersbach H, Hólm EV, Isaksen L, Kållberg P, Köhler M, Matricardi M, McNally AP, Monge-Sanz BM, Morcrette J-J, Park B-K, Peubey C, de Rosnay P, Tavolato C, Thépaut J-N, Vitart F. 2011. The ERA-interim reanalysis: configuration and performance of the data assimilation system. *Q. J. Roy. Meteorol. Soc.* **137**(656): 553–597.
- Descroix L, Mahé G, Lebel T, Favreau G, Galle S, Gautier E, Olivry J-C, Albergel J, Amogu O, Cappelae B, Dessouassi R, Diedhiou A, Le Breton E, Mamadou I, Sighomnou D. 2009. Spatio-temporal variability of hydrological regimes around the boundaries between Sahelian and Sudanian areas of West Africa: a synthesis. *J. Hydrol.* **375**(1–2): 90–102.
- Diatta S, Fink AH. 2014. Statistical relationship between remote climate indices and West African monsoon variability. *Int. J. Climatol.* **34**(12): 3348–3367.
- Domingues MO, Mendes O, da Costa AM. 2005. On wavelet techniques in atmospheric sciences. *Adv. Space Res.* **35**: 831–842.
- Douville H, Conil S, Tyteca S, Voldoire A. 2006. Soil moisture memory and West African monsoon predictability: artefact or reality? *Climate Dyn.* **28**(7–8): 723–742.
- Forootan E, Kusche J, Loth I, Schuh W-D, Eicker A, Awange J, Longuevergne L, Diekkrüger B, Schmidt M, Shum C. 2014a. Multivariate prediction of total water storage changes over West Africa from multi-satellite data. *Surv. Geophys.* **35**: 913–940.
- Forootan E, Didova O, Schumacher M, Kusche J, Elsaaka B. 2014b. Comparisons of atmospheric mass variations derived from ECMWF reanalysis and operational fields, over 2003–2011. *J. Geodesy* **88**(5): 503–514.
- Grinsted A, Moore JC, Jevrejeva S. 2004. Application of the cross wavelet transform and wavelet coherence to geophysical time series. *Nonlinear Processes Geophys.* **11**(5/6): 561–566.
- Grippa M, Kergoat L, Frappart F, Araud Q, Boone A, de Rosnay P, Lemoine J-M, Gascoïn S, Balsamo G, Ottlé C, Decharme B, Saux-Picart S, Ramillien G. 2011. Land water storage variability over West Africa estimated by Gravity Recovery and Climate Experiment (GRACE) and land surface models. *Water Resour. Res.* **47**(5): W05549.
- Herrmann SM, Anyamba A, Tucker CJ. 2005. Recent trends in vegetation dynamics in the African Sahel and their relationship to climate. *Glob. Environ. Chang.* **15**(4): 394–404.
- Huang Y, Salama MS, Krol MS, van der Velde R, Hoekstra AY, Zhou Y, Su Z. 2013. Analysis of long-term terrestrial water storage variations in the Yangtze River basin. *Hydrol. Earth Syst. Sci.* **17**(5): 1985–2000.
- Huber S, Fensholt R, Rasmussen K. 2011. Water availability as the driver of vegetation dynamics in the African Sahel from 1982 to 2007. *Global Planet. Change* **76**(3–4): 186–195.
- Jänicke H, Böttinger M, Mikolajewicz U, Scheuermann G. 2009. Visual exploration of climate variability changes using wavelet analysis. *IEEE Trans. Vis. Comput. Graph.* **15**(6): 1375–1382.
- Janicot S, Moron V, Fontaine B. 1996. Sahel droughts and ENSO dynamics. *Geophys. Res. Lett.* **23**(5): 515–518.
- Kaspersen PS, Fensholt R, Huber S. 2011. A spatiotemporal analysis of climatic drivers for observed changes in Sahelian vegetation productivity (1982–2007). *Int. J. Geophys.* **2011**: 1–14.
- Keller W. 2004. *Wavelets in Geodesy and Geodynamics*. De Gruyter: Berlin, Germany.
- Killick R, Eckley IA. 2014. changepoint: An R Package for Changepoint Analysis. *J. Stat. Softw.* **58**(3): 1–19.
- Lebel T, Ali A. 2009. Recent trends in the Central and Western Sahel rainfall regime (1990–2007). *J. Hydrol.* **375**(1–2): 52–64, surface processes and water cycle in West Africa, studied from the AMMA-CATCH observing system.
- Lebel T, Cappelae B, Galle S, Hanan N, Kergoat L, Levis S, Vieux B, Descroix L, Gosset M, Mougïn E, Peugeot C, Seguis L. 2009. AMMA-CATCH studies in the Sahelian region of West-Africa: an overview. *Journal of Hydrology* **375**(12): 3–13.
- Lee TM, Sacks LA, Swancar A. 2014. Exploring the long-term balance between net-precipitation and net groundwater exchange in Florida seepage lakes. *J. Hydrol.* **519**: 3054–3068.
- Lorenz C, Kunstmann H. 2012. The hydrological cycle in three state-of-the-art reanalyses: intercomparison and performance analysis. *J. Hydrometeorol.* **13**(5): 1397–1420.
- Machwal D, Jha MK. 2012. *Methods for Time Series Analysis*. Springer: Dordrecht, Netherlands, 51–84.
- Mahé G, Olivry J-C. 1999. Assessment of freshwater yields to the ocean along the intertropical Atlantic coast of Africa (1951–1989). *Earth Planet. Sci.* **328**(9): 621–626.
- Mahé G, Paturol J-E. 2009. 1896–2006 Sahelian annual rainfall variability and runoff increase of Sahelian Rivers. *Comptes Rendus Geosci.* **341**(7): 538–546.
- Mahé G, Paturol J-E, Servat E, Conway D, Dezetter A. 2005. The impact of land use change on soil water holding capacity and river flow modelling in the Nakambe River, Burkina-Faso. *J. Hydrol.* **300**(1–4): 33–43.
- Malhi Y, Wright J. 2004. Spatial patterns and recent trends in the climate of tropical rainforest regions. *Philos. Trans. R. Soc. London* **359**: 311–329.
- Menz G. 2010. Regional geography of West and Northwest Africa: an introduction. In *Impacts of Global Change on the Hydrological Cycle in West and Northwest Africa*, Speth P, Christoph M, Diekkrüger B (eds), Springer: Heidelberg, Germany, 30–103.
- Meynadier R, Bock O, Guichard F, Boone A, Roucou P, Redelsperger J-L. 2010. West African Monsoon water cycle: 1. A hybrid water budget data set. *J. Geophys. Res.* **115**(D19): D19, 106.
- Morrow E, Mitrovica JX, Fotopoulos G. 2011. Water storage, net-precipitation, and evapotranspiration in the Mackenzie River Basin from October 2002 to September 2009 inferred from GRACE Satellite Gravity Data. *J. Hydrometeorol.* **12**(3): 467–473.
- Munier S, Palanisamy H, Maisongrande P, Cazenave A, Wood EF. 2012. Global runoff anomalies over 1993–2009 estimated from coupled land–ocean–atmosphere water budgets and its relation with climate variability. *Hydrol. Earth Syst. Sci.* **16**(10): 3647–3658.
- Nakken M. 1999. Wavelet analysis of rainfall–runoff variability isolating climatic from anthropogenic patterns. *Environ. Model. Software* **14**(4): 283–295.
- Ndehedehe C, Awange J, Agutu N, Kuhn M, Heck B. 2016a. Understanding changes in terrestrial water storage over West Africa between 2002 and 2014. *Adv. Water Resour.* **88**: 211–230.
- Ndehedehe CE, Agutu NO, Okwaashi OH, Ferreira VG. 2016b. Spatio-temporal variability of droughts and terrestrial water storage over Lake Chad Basin using independent component analysis. *J. Hydrol.* **540**: 106–128.

- Ndehedehe CE, Awange JL, Corner R, Kuhn M, Okwuashi O. 2016c. On the potentials of multiple climate variables in assessing the spatio-temporal characteristics of hydrological droughts over the Volta Basin. *Sci. Total Environ.* **557–558**: 819–837.
- Nicholson S. 2005. On the question of the “recovery” of the rains in the West African Sahel. *J. Arid Environ.* **63**(3): 615–641.
- Nicholson SE. 2013. The West African Sahel: A review of recent studies on the rainfall regime and its interannual variability. *ISRN Meteorol.* **2013**: 1–32.
- Nicholson SE, Some B, Kone B. 2000. An analysis of recent rainfall conditions in West Africa, including the rainy Seasons of the 1997 El-Niño and the 1998 La Niña Years. *J. Clim.* **13**(14): 2628–2640.
- Oguntunde PG, Abiodun BJ. 2012. The impact of climate change on the Niger River Basin hydroclimatology, West Africa. *Climate Dyn.* **40**(1–2): 81–94.
- Oki T, Kanae S. 2006. Global hydrological cycles and world water resources. *Science* **313**(5790): 1068–1072.
- Otkin JA, Anderson MC, Hain C, Mladenova IE, Basara JB, Svoboda M. 2013. Examining rapid onset drought development using the thermal infrared-based evaporative stress index. *J. Hydrometeorol.* **14**(4): 1057–1074.
- Oyebande L. 2001. Water problems in Africa – how can the sciences help? *Hydrol. Sci. J.* **46**(6): 947–962.
- Paeth H, Fink AH, Pohle S, Keis F, Mächel H, Samimi C. 2011. Meteorological characteristics and potential causes of the 2007 flood in sub-Saharan Africa. *Int. J. Climatol.* **31**(13): 1908–1926.
- Rodell M, Houser PR, Jambor U, Gottschalck J, Mitchell K, Meng C-J, Arsenault K, Cosgrove B, Radakovich J, Bosilovich M, Entin JK, Walker JP, Lohmann D, Toll D. 2004. The global land data assimilation system. *Bull. Am. Meteorol. Soc.* **85**(3): 381–394.
- Roudier P, Ducharne A, Feyen L. 2014. Climate change impacts on runoff in West Africa: a review. *Hydrol. Earth Syst. Sci.* **18**(7): 2789–2801.
- Sall SM, Viltard A, Sauvageot H. 2007. Rainfall distribution over the Fouta Djallon – Guinea. *Atmos. Res.* **86**(2): 149–161.
- Samimi C, Fink AH, Paeth H. 2012. The 2007 flood in the Sahel: causes, characteristics and its presentation in the media and FEWS NET. *Natural Hazards Earth Syst. Sci.* **12**(2): 313–325.
- Schneider U, Becker A, Finger P, Meyer-Christoffer A, Ziese M, Rudolf B. 2014. GPCC’s new land surface precipitation climatology based on quality-controlled in situ data and its role in quantifying the global water cycle. *Theor. Appl. Climatol.* **115**(1–2): 15–40.
- Sen P. 1968. Estimates of the regression co-efficient based on Kendall’s tau. *Am. Statist. Assoc.* **63**(324): 1379–1389.
- Sharifi M, Forootan E, Nikkhoo M, Awange J, Najafi-Alamdari M. 2013. A point-wise least squares spectral analysis (LSSA) of the Caspian Sea level fluctuations, using TOPEX/Poseidon and Jason-1 observations. *Adv. Space Res.* **51**(5): 858–873.
- Shiferaw B, Tesfaye K, Kassie M, Abate T, Prasanna B, Menkir A. 2014. Managing vulnerability to drought and enhancing livelihood resilience in sub-Saharan Africa: technological, institutional and policy options. *Weather Clim. Extremes* **3**: 67–79.
- Simier M, Laurent C, Ecoutin J-M, Albaret J-J. 2006. The Gambia River estuary: a reference point for estuarine fish assemblages studies in West Africa. *Estuar. Coast. Shelf Sci.* **69**: 615–628.
- Speth P, Fink AH. 2010. Introduction. In *Impacts of Global Change on the Hydrological Cycle in West and Northwest Africa*, Speth P, Christoph M, Diekkrüger B (eds). Springer: Heidelberg, Germany, 4–11.
- Syed TH, Famiglietti JS, Chambers DP. 2009. GRACE-based estimates of terrestrial freshwater discharge from basin to continental scales. *J. Hydrometeorol.* **10**(1): 22–40.
- Szolgayová E, Arlt J. 2014. Wavelet based deseasonalization for modelling and forecasting of daily discharge series considering long range dependence. *J. Hydrol. Hydromech.* **62**(1): 24–32.
- Tapley B, Bettadpur S, Watkins M, Reigber C. 2004. The gravity recovery and climate experiment: mission overview and early results. *Geophys. Res. Lett.* **31**: 1–4.
- Torrence C, Compo G. 1998. A practical guide to wavelet analysis. *Bull. Am. Meteorol. Soc.* **79**(1): 61–78.
- Torrence C, Webster PJ. 1999. Interdecadal changes in the ENSO–monsoon system. *J. Clim.* **12**(8): 2679–2690.
- Tucker C, Pinzon J, Brown M, Slayback D, Pak E, Mahoney R, Vermote E, El Saleous N. 2005. An extended AVHRR 8-km NDVI dataset compatible with MODIS and SPOT vegetation NDVI data. *Int. J. Remote Sens.* **26**: 4485–4498.
- Wamukonya N, Masumbuko B, Gowa E, Asamoah J. 2006. Environmental state-and-trends: 20-year retrospective. In *Africa Environment Outlook 2: Our Environment, Our Wealth*, Mohamed-Katerere JC, Sabet M (eds). DEWA/UNEP: Nairobi, Kenya, 48–50.
- Wittig R, König K, Schmidt M, Szarzynski J. 2007. A study of climate change and anthropogenic impacts in West Africa. *Environ. Sci. Pollut. Res. Int.* **14**(3): 182–189.
- Wolter K, Timlin MS. 2011. El-Niño/Southern Oscillation behaviour since 1871 as diagnosed in an extended multivariate ENSO index (MEI.ext). *Int. J. Climatol.* **31**(7): 1074–1087.
- Wong H, Hu B, Ip W, Xia J. 2006. Change–point analysis of hydrological time series using grey relational method. *J. Hydrol.* **324**(1–4): 323–338.
- Xue B-L, Wang L, Li X, Yang K, Chen D, Sun L. 2013. Evaluation of evapotranspiration estimates for two river basins on the tibetan plateau by a water balance method. *J. Hydrol.* **492**: 290–297.
- Yirdaw S, Snelgrove K, Agboma C. 2008. GRACE satellite observations of terrestrial moisture changes for drought characterization in the Canadian Prairie. *J. Hydrol.* **356**: 84–92.
- Zhou L, Tian Y, Myneni RB, Ciaï P, Saatchi S, Liu YY, Piao S, Chen H, Vermote EF, Song C, Hwang T. 2014. Widespread decline of congo rainforest greenness in the past decade. *Nature* **509**(7498): 86–90.

3 The impacts of reservoir systems on terrestrial water storage

This chapter is covered by the following publication ([Ndehedehe et al., 2017c](#)):

Christopher E. Ndehedehe, Joseph L. Awange, Michael Kuhn, Nathan O. Agutu, and Yoichi Fukuda (2017). Analysis of hydrological variability over the Volta river basin using in-situ data and satellite observations. *Journal of Hydrology: Regional Studies*, 12, 88-110, [dx.doi.org/10.1016/j.ejrh.2017.04.005](https://doi.org/10.1016/j.ejrh.2017.04.005).

This chapter is one of the novel contributions of the thesis that will benefit hydrological research and support meaningful decisions on water resources planning. The impact of large reservoir systems such as the Lake Volta on TWS dynamics is discussed. Previous studies identified in the literature (see, e.g., [Ndehedehe et al., 2016a](#); [Ahmed et al., 2014](#)) indicated that water ponding behind the Akosombo dam in Ghana affected observed trends in GRACE-derived TWS. Other reports showed that Ghana, the host country of the Volta reservoir, suffered power rationing in time past due to low water levels of Lake Volta resulting from the impacts of climate variability and the developments of small and medium surface water schemes along the upper Volta region of the basin. Whereas surface water development schemes will have direct implications in water budget assessment, quantifying the impact of natural climate variability on the Volta basin's hydrology would be challenging. This is because of the considerably strong gravimetric changes of the Lake Volta. To enhance the knowledge of hydrological variability, this chapter addresses that problem by exploring a novel approach based on a two-step procedure that incorporates a weighted least squares formulation of global spherical harmonic analysis and cumulant statistics. Significant reductions in rainfall, stream flows of the Volta river system, and the rising evapotranspiration in the upper Volta region of the basin are prominent signals of climate variability affecting the Lake Volta water level and TWS decline in the lower Volta. Apart from the Lake's hydropower potential being threatened, recent trends in the Lake's water storage, and the limited river flows into the Lake are critical indicators of dangerous hydrological thresholds. These unfavourable hydrological conditions, raise concerns on the Lake's vulnerability to the impact of climate change. Whereas the Lake's gradual desiccation could be a reality in the near future if these trends in water fluxes are not reversed, the impact of human interventions such as the development of small and medium surface water schemes in the Volta basin, on the Lake's survival, are more challenging and weightier issues that require an integration of science and policy.



Contents lists available at ScienceDirect

Journal of Hydrology: Regional Studies

journal homepage: www.elsevier.com/locate/ejrh

Analysis of hydrological variability over the Volta river basin using in-situ data and satellite observations



Christopher E. Ndehedehe^{a,*}, Joseph L. Awange^{a,b}, Michael Kuhn^a,
Nathan O. Agutu^{a,c}, Yoichi Fukuda^b

^a Department of Spatial Sciences, Curtin University, Perth, Australia

^b Department of Geophysics, Kyoto University, Japan

^c Department of Geomatic Engineering and Geospatial Information Systems, JKUAT, Nairobi, Kenya

ARTICLE INFO

Keywords:

Volta basin
Rainfall
Satellite altimetry
Freshwater
Lake Volta
Climate variability

ABSTRACT

By combining satellite altimetry with Gravity Recovery and Climate Experiment derived terrestrial water storage-TWS (2002–2014), this study used a two-step procedure based on spherical harmonic synthesis and statistical decomposition to support the understanding of the Volta basin's natural hydrology and its freshwater systems. Results indicate that Lake Volta contributed 41.6% to the observed increase in TWS over the basin during the 2002–2014 period. The statistical decomposition of TWS over the basin (after removing the Lake's water storage) resulted in a statistically significant ($\alpha = 0.05$) loss of 59.5 ± 8.5 mm/yr of TWS in the lower Volta region of the basin between 2007 and 2011. This trend is attributed to a base flow recession resulting from the negative trends in precipitation around the lower Volta (2002–2014) and limited river flows of the Volta river system. While it also coincides with observed decline in net precipitation (-15 mm/yr), the long dry periods in the basin (2001–2007) also contributed to this storage depletion. The Lake Volta shows sensitivity to incoming flows of the Volta river system with a lag spanning between less than one and up to two years. In addition to this, a 4–5 year cycle in the clustering of dry and wet periods resulting from the impact of climate variability on the basin was noticed.

1. Introduction

Lake Volta, one of the highly esteemed projects from the period of Africa's decolonisation, is the largest man-made reservoir by surface area in the world, covering a total area of approximately 8500 km². This Lake, which was built in 1964, has an estimated capacity of 150 km³ with an installed hydropower generation capacity of about 912 MW (e.g., Owusu et al., 2008; Gyau-Boakyee, 2001). Besides being one of the most important surface water in West Africa, the Lake, which is formed by the Akosombo dam in Ghana, is a symbol of high socio-economic importance and progress in the region, and remains a major source of livelihood and hydro-power to approximately 20 million people whose livelihood depends on the Volta river basin (hereafter the Volta basin, Fig. 1).

The impact of extreme climatic conditions on the Lake is a timely topical research issue of public-policy interest due to its implications on the people and local economy. For instance, Ghana suffered power rationing during the hydrological drought years of 1983, 1998, and 2006, leading to shortfalls in the production of goods, unemployment, and reduced gross domestic product (see, e.g., Bekoe and Logah, 2013). Apparently, in the wake of global climate change, the impacts of extreme climate conditions on Lake Volta

* Corresponding author.

E-mail address: c.ndehedehe@postgrad.curtin.edu.au (C.E. Ndehedehe).

<http://dx.doi.org/10.1016/j.ejrh.2017.04.005>

Received 6 December 2016; Received in revised form 13 April 2017; Accepted 18 April 2017

2214-5818/© 2017 The Authors. Published by Elsevier B.V. This is an open access article under the CC BY-NC-ND license (<http://creativecommons.org/licenses/by-nc-nd/4.0/>).

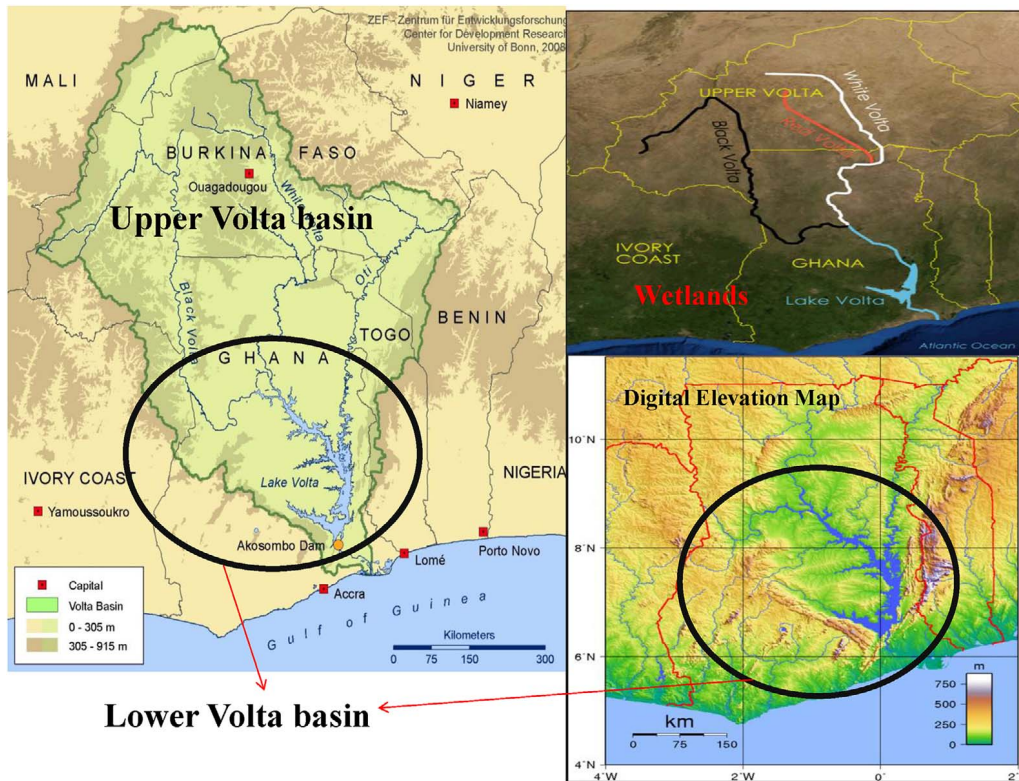


Fig. 1. Study area showing the Volta river basin. The riparian countries (Ghana, Togo, Benin, Burkina Faso, Mali, and Ivory Coast) of the basin are also indicated. The Lake Volta, the Volta river system (White Volta, Black Volta, and Oti rivers), and the location of the Akosombo dam have also been indicated. Original maps adapted from <http://www.21stcentech.com/wp-content/uploads/2013/12/Volta-River-basin.jpg> and <https://en.wikipedia.org/wiki/Geography-of-Ghana>.

could largely limit the generation of hydro-electric power in future, leading to untold hardship in the region. The low impoundment levels of Akosombo dam and the decline in Lake Volta's water level, owing to negative trends in rainfall (e.g., Owusu et al., 2008) are arguably indications of the region's vulnerability to the impacts of climate variability.

In the Volta basin, analysis of long term historical hydro-climatic conditions (1901–2002) have shown that large changes in water budget quantities (precipitation, river discharge, and evapotranspiration) have occurred (Oguntunde and Friesen, 2006). These changes, which impact on the local climate through feedback mechanisms and land atmosphere interactions, have the potentials of restricting the freshwater systems of the basin. As reported in earlier studies (e.g., Friesen et al., 2005; Andreini et al., 2000), the marked variability in rainfall and stream flow records in the pre and post construction periods of the Akosombo dam revealed the impact of damming on the basin. This inadvertently resulted in the non-linearity of hydrological processes, thereby complicating our understanding of the hydrological variability of the basin. One of such instance in the basin, is the observed decline in precipitation, which was inconsistent with observed increase in terrestrial water storage (TWS, i.e., the sum total of surface waters, soil moisture, and groundwater) derived from Gravity Recovery and Climate Experiment (GRACE, Tapley et al., 2004) during the 2003–2012 period (e.g., Ahmed et al., 2014; Moore and Williams, 2014). These observed trends in GRACE-derived TWS changes over the basin have been attributed to the impact of water ponding in the Akosombo dam (e.g., Ferreira and Asiah, 2015; Moore and Williams, 2014; Ahmed et al., 2014). Such impacts do have implications in water budget assessment and quantifying the impact of climate variability on the Volta basin's hydrology.

Although in some studies within the mainstream of water resources, droughts and GRACE-TWS have been reported in the Volta basin (e.g., Ndehedehe et al., 2016c; Bekoe and Logah, 2013; Ferreira et al., 2012; Owusu and Waylen, 2013; Kasei et al., 2010; Owusu et al., 2008; Oguntunde and Friesen, 2006; Friesen et al., 2005; Andreini et al., 2000, 2002; Giesen et al., 2001), the hydrological variability of the basin is largely unreported. In fact, the lack of clear perspectives regarding the impact of human activities on the hydrological changes of the basin have been partly and loosely attributed to increase in surface water storage in the reservoirs and decrease in soil moisture storage (e.g., Friesen et al., 2005). Although Giesen et al. (2010) argues that the causes of climate change in the basin remains unclear, however, the lack of in-situ data and existing data gaps in stream flow records of the region have particularly limited our understanding of the impacts of climate variability and the natural hydrology of the basin. The use of a non-physical based hydrological model to study the water balance of the basin as reported in Andreini et al. (2000) could be restricted as stream flow and rainfall could be affected by a number of factors, e.g., climate variability and human activities (e.g., water abstraction, land use change) amongst others (e.g., Bekoe and Logah, 2013; Owusu et al., 2008). Given the economic importance of the Lake Volta in hydropower generation for the southern catchment of the basin (Ghana) and the freshwater of the Volta river system for agricultural purposes in Burkina Faso, it is pertinent to understand the hydrological variability of the Volta

64 basin and the restrictions of climate variability on its water fluxes and freshwater systems (rivers, lakes, and TWS).

Consequently, the current study employs a multi-satellite approach to monitor and quantify recent inter-annual changes in GRACE-derived TWS over the Volta basin (also includes the Lake Volta). In Ndehedehe et al. (2016c), the potentials of multiple climate variables to assess hydrological droughts over the basin were considered, while GRACE-derived TWS variability over West Africa was analysed during the 2002–2014 period in Ndehedehe et al. (2016a). In contrast, here, we analyse for the first time the spatio-temporal variability of TWS over the Volta basin after removing the hydrological signal induced by Lake Volta water level changes (hereafter called Lake Volta induced TWS). In addition, the impact of climate variability on the basin's freshwater systems is considered. This is achieved using the Global Precipitation Climatology Centre based precipitation product (GPCC, Schneider et al., 2014), in-situ river discharge, evapotranspiration, and satellite altimetry data. Furthermore, use is made of a cumulant based statistical method, the independent component analysis (ICA, see, e.g., Common, 1994; Cardoso and Souloumiac, 1993; Cardoso, 1999) to support the localisation of hydrological signals that are masked by the dominant signals caused by the impact of large water projects such as the Akosombo dam.

Specifically, this study aims at (i) understanding the hydrological variability of the Volta basin, (ii) examining the contributions of Lake Volta to the overall trends in TWS over the Volta basin, and (iii) understanding the impact of climate variability on the freshwater systems of the Volta basin. As the Lake Volta provides hydropower and other multiple strings of ecosystem services to the region, this study is warranted essentially to support water resources planning and sustainability of the Lake and its catchment areas. Apart from investigating whether long term trends and changes in stream flow records and Lake levels in the basin are climate driven or human related (e.g., irrigation), the study employs a two-step procedure based on a weighted least squares formulation of global spherical harmonic analysis and statistical decomposition, to support the monitoring of spatio-temporal hydrological variability and trends resulting from natural climate variability in the basin.

The remainder of the study is structured as follows; in Section 2, a brief introduction to Lake Volta is provided while in Section 3, a description of the data is given. This is followed by the method used in Section 4 while the analysis and discussion of the results are provided in Section 5. The conclusion of the study is provided in Section 6.

2. Lake Volta

Lake Volta is located at the lower Volta basin, a low elevation area (cf. see digital elevation map, Fig. 1) that is naturally connected to the Volta river system (i.e., Oti, Black Volta, and White Volta rivers – Fig. 1) and other small freshwater tributaries. The aquifer system of the lower Volta seems to be rather confined with the Akosombo dam impounding surface water at the Lake. This natural connection of the Lake with the Volta river system leads to relatively strong inter-annual variability in TWS around the precinct of the lower Volta. During periods of extreme rainfall such as the 2007 La-Niña event (e.g., Paeth et al., 2012), the amplitudes of the Lake induced TWS become relatively strong due to heavy stream flows from the Volta river system creating a pseudo trend in TWS change over the basin that most times obscures other hydrological signals. Not only does the Lake induced TWS signal obscures other hydrological signals in the basin, it also complicates the natural hydrological setting of the lower Volta. For instance, in a recent study where the authors analysed hydrological drought over the basin (see, Ndehedehe et al., 2016c), it was noted that despite the significant fall in the amplitudes of annual rainfall (i.e., during the 2008–2013 period) and severe hydrological drought conditions in the Lake Volta area (i.e., 2010–2013 period), TWS over the basin increased significantly during these periods. While Ahmed et al. (2014) attributed the increasing trend in TWS over the basin (2003–2012) to water ponding by the Akosombo dam, Moore and Williams (2014) reported that the influence of major lakes such as the Lake Volta contributes significantly to the observed trend and seasonal changes in GRACE-derived TWS of the corresponding basin. Moreover, despite having a surface area (approximately 8500 km²) that corresponds to 2% of the basin, Lake Volta, because of its strong change in water levels (see, Fig. 2), has the strongest hydrological signal, when compared to other Lakes in Africa (e.g., Lake Victoria with approximately 68,800 km² in surface area) with larger surface areas (see, Moore and Williams, 2014). Beyond that, the Lake Volta show strong fluctuations in trends (Fig. 2) of water level variations in recent times (see more details in Appendix A2). These impacts of the Lake's fluctuation in water levels during the 2002–2015 period on the hydrology of the basin is largely unreported. Investigating the impact of this Lake on the spatio-temporal changes of TWS in the Volta basin provides useful indications and broad scale assessments of the overall change

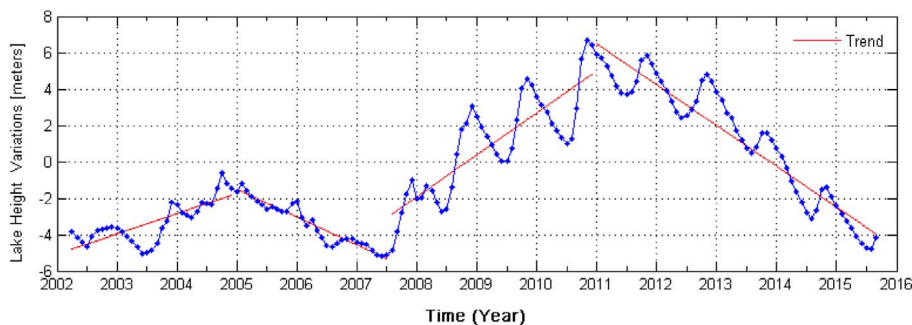


Fig. 2. Trends in lake height variations of Lake Volta after removing the temporal mean for the period (2002–2015). These trends and fluctuations in lake water level are discussed further in Appendix A2.

65 in hydro-climatic conditions. In addition to this, the opening of the spillways of the Akosombo dam, in order to allow excess water in the reservoir to flow down stream in November 2010 due to excess rainfall as reported by Owusu and Waylen (2013) is one of the isolated cases that may also impact on the changes in TWS over the basin, further complicating its hydrological variability. Consequently, the ICA technique has been employed to specifically support the localisation of obscured hydrological signals in the basin (i.e., after removing the lake induced TWS). The statistical decomposition of this residual water storage is shown and discussed in Section 5.2.

3. Data

3.1. Terrestrial water storage observed by Gravity Recovery and Climate Experiment (GRACE)

This study used GRACE (Tapley et al., 2004) Release-05 (RL05) spherical harmonic coefficients truncated at degree and order 60 from Center for Space Research (CSR), covering the period 2002–2014 (data files accessed at <http://icgem.gfz-potsdam.de/ICGEM/shms/monthly/csr-rl05/>). Continental water storage anomalies are one of the most important geophysical phenomena derived from these spherical harmonic coefficients and typically serves as the hydrological quantity of interest (see, e.g., Sneeuw et al., 2014; Wahr et al., 1998) in studies of terrestrial and ocean mass transport. Since GRACE satellites are insensitive to the degree 2 coefficients (i.e., C_{20}) of the gravity field due to orbit configuration (e.g., Seo et al., 2008; Schrama et al., 2007; Sneeuw et al., 2014), they were replaced by estimates from satellite laser ranging (Cheng et al., 2013). Also, since GRACE does not provide changes in degree 1 coefficients (i.e., C_{10} , C_{11} , and S_{11}), the degree 1 coefficients provided by Swenson et al. (2008) were used. Given that GRACE spherical harmonic coefficients are affected by noise in the higher degree coefficients (e.g., Belda et al., 2015; Landerer and Swenson, 2012; Swenson and Wahr, 2002), a regularization filter of Kusche (2007) was applied to reduce the effect of noise. This filter, which accommodates better the GRACE error structure when compared to the conventional isotropic Gaussian filter (see, e.g., Werth et al., 2009), reduces the north-south stripes in the GRACE monthly solutions. The filtered monthly solutions were then converted into equivalent water heights (EWH) on a $1^\circ \times 1^\circ$ grid using the approach of Wahr et al. (1998) as follows:

$$\Delta W(\psi, \lambda, t) = \frac{R\rho_{ave}}{3Q_w} \sum_{l=0}^{l_{max}} \frac{2l+1}{1+k_l} \sum_{m=-l}^l P_{lm}(\psi, \lambda) \Delta Y_{lm}(t), \quad (1)$$

where ΔW is the EWH for each month in time (t), and ψ, λ are the geodetic latitudes and longitudes respectively. R is the mean radius of the Earth (i.e., 6378.137 km), ρ_{ave} is the average density of the Earth (5515 kg/m^3), Q_w is the average density of water (1000 kg/m^3), k_l is the load Love numbers of degree l , P_{lm} are the normalized associated Legendre function of degree l and order m with $l_{max} = 60$ and ΔY_{lm} are the normalized complex spherical harmonic coefficients of temporal anomalies of the geoid after subtracting the long term mean. The regularisation filter leads to leakage and attenuation of the signal's amplitude (e.g., Wouters and Schrama, 2007; Baur et al., 2009), hence a scaling factor was computed following Landerer and Swenson (2012) in order to account for the geophysical signal loss, which occurred during the pre-processing of GRACE data. Specifically, the scale factor was empirically derived using GLDAS-derived total water storage content (see more details in Section 3.5). Accounting for the leakage effect in GRACE observations has become necessary as the signal attenuation can contribute to significant errors in regional water balance studies (see Landerer and Swenson, 2012). Since we are also interested in average TWS values (i.e., ΔW) over the basin, the estimated EWH (hereafter called TWS), were averaged over the basin using area weighted averaging (see, e.g., Sneeuw et al., 2014):

$$\Delta W(\chi; t) = \sum_{i=1}^n \Delta W(\psi_i, \lambda_i, t) \frac{A_i}{A_\chi}, \quad (2)$$

where χ is the basin index, n is the number of grid points in the basin, A_i is the area of the grid cell i in χ and A_χ is the total area of χ .

3.2. Satellite altimetry

Observed lake height variations computed from TOPEX/POSEIDON (T/P), Jason-1 and Jason-2/OSTM altimetry provided by the United States Department of Agriculture (USDA) were used in this study. The use of altimetry-based measurements for a data deficient region is beneficial since they are continuous and potentially available few days after measurement (Coe and Birkett, 2004). Besides the irregularities and inconsistencies of gauge measurements, acquiring gauge data can be difficult due to government policies and bureaucracies. Thus, time series of lake levels covering the period from 1993 to 2015 were downloaded from www.pecad.fas.usda.gov/cropeplorer/globalreservoir database and used in this study to recover water storage changes over Lake Volta during the 2002–2014 period. As reported in Swenson and Wahr (2009), satellite altimetry data has been successfully validated by comparing altimetric time series and in situ observations. Further, the hydrological condition of the Lake Volta was characterised by combining the annual lake variations (1993–2015) with the stream flows of the Volta river system and the Akosombo dam (Section 3.3).

3.3. In-situ river discharge

Monthly river discharge rates observed at the Senchi hydrological station, which is downstream of the Akosombo dam in Ghana were also used in the study. The data, covering the period from 1979 to 2012, was obtained from the Water Research Institute of

66

Table 1

Details of the stream flow records of the Volta river system (i.e., the White Volta, Black Volta, and Oti rivers) retrieved from the GRDC archives.

River	GRDC no	Latitude	Longitude	Area (km ³)	Station	Duration
White Volta	1531450	9.70	−1.08	92950	Nawuni	1986–2007/02
Oti	1531800	9.28	0.23	58670	Sabari	1996–2007/02
Black Volta	1531050	10.63	−2.92	93820	Lawra	1990/03–2007/02

Ghana. Here, the data, which has no missing record is used as an auxiliary information to investigate the impact of climate variability in the vicinity of the Lake Volta. Also, the river discharge data from the Global Runoff Data Centre (GRDC) (see, www.bafg.de/GRDC), for the three rivers (Black Volta, White Volta and Oti rivers) that drain into Lake Volta have been retrieved and used as a complementary data to support the analysis of hydrological variability of the basin. The White Volta and the Oti rivers are mostly referenced in the manuscript since they contribute more to Lake Volta compared to the Black Volta river. Although the data from these rivers have gaps and missing values, they have been used to support our analysis of the impact of climate variability on the Volta reservoir system. Further details on the GRDC stream flows of the three rivers, which are usually referred to as the Volta river system in the manuscript have been highlighted in [Table 1](#).

3.4. Global Precipitation Climatology Centre (GPCC)

GPCC (Schneider et al., 2014; Becker et al., 2013) product, which provides quality controlled monthly gridded data sets of global land-surface precipitation were used. The gridded precipitation products were accessed through the GPCP download site (www.ftp.dwd.de/pub/data/gpcp/html/downloadgate.html). The 0.5° × 0.5° GPCP data covering the period from 1979 to 2014 was applied in the study to analyse seasonal rainfall variability in the region. Also, the impacts of rainfall conditions on the observed lake level variations from satellite altimetry and in-situ river discharge (Volta river system and Akosombo dam) were investigated using the GPCP precipitation product. Specifically, the long term GPCP based precipitation was combined with river discharge data and satellite altimetry derived water levels to study the hydrological behaviour of the basin.

3.5. Global Land Data Assimilation System (GLDAS)

GLDAS (Rodell et al., 2004) data, which simulates various fields of land surface states and fluxes was obtained from the Goddard Earth Sciences Data and Information Services Center (GESDISC) (<http://grace.jpl.nasa.gov/data/gldas/>). The NOAA monthly total water storage content (TWS) of GLDAS, covering the years 2002 to 2013 at 1° × 1° spatial resolution was used in this study to account for the lost signals in GRACE-derived TWS caused by filtering, similar to previous studies (e.g., Landerer and Swenson, 2012). Since GRACE observations will have to be filtered before use in order to reduce noise in the high degree and order Stoke's coefficients (Belda et al., 2015), accounting for the signal damping resulting from the filtering is necessary to benefit hydrological applications. To account for signal attenuation in the filtered GRACE solution, the regularization filter of Kusche (2007) was applied to the gridded GLDAS TWS in order to derive a synthetic signal that reflects the inherent impact of the filter. This signal, which was thereafter compared with the unfiltered synthetic signal through a least square minimization procedure, resulted in a spatially distributed (grid-based) scale factor that was applied to the filtered GRACE solutions similar to previous studies (e.g., Landerer and Swenson, 2012). The derived scale factor is independent of the GRACE-derived TWS as it is based on simulated TWS changes and does not match the GRACE-derived TWS to those of GLDAS, rather it only restores the relative amplitude of the 'original' data (e.g., Andam-Akorful et al., 2015; Ferreira et al., 2013; Landerer and Swenson, 2012). Consequently, the resulting GRACE solutions can be averaged over arbitrary regions (e.g., the Volta basin) and compared to other gridded data (e.g., precipitation) without having to apply the regularization filter to that data in the spherical harmonic domain (see, Landerer and Swenson, 2012).

3.6. MODIS global terrestrial evapotranspiration project

The MODIS global terrestrial evapotranspiration (ET) products (Mu et al., 2011) was combined with precipitation in this study to estimate net precipitation, a measure of the maximum available renewable freshwater resource. The data, which has a spatial resolution of 0.5° × 0.5° covers the period 2000–2014 and is available for download at the Earth Observing System of NASA's website (<http://www.ntsg.umt.edu/project/mod16>). The MODIS-derived ET estimates indicated relatively lower magnitude of uncertainties over the Volta basin compared to estimates from GLDAS and terrestrial water budget (see, Andam-Akorful et al., 2015). Hence, the MODIS-derived ET was used to estimate net precipitation over the basin. In this study, trends in the monthly grids of MODIS-derived ET over the LVRB were estimated using a least square method.

4. Method

4.1. Lake Volta induced TWS changes

Observed trends in TWS in the Volta basin are dominated by TWS changes induced by Lake Volta water level changes and the

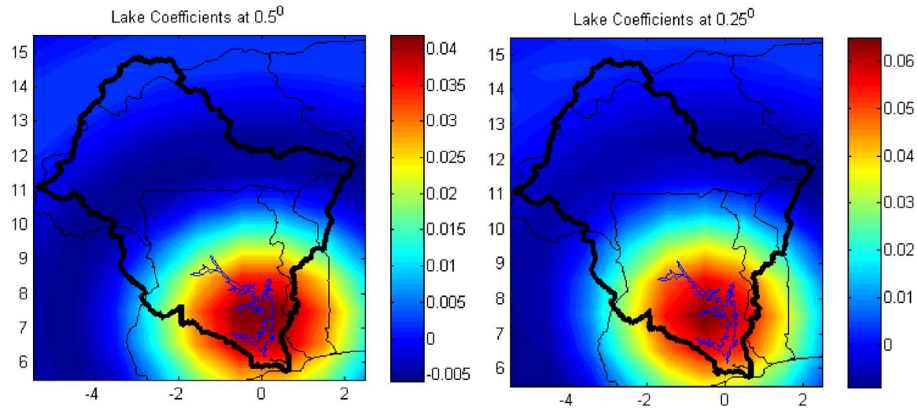


Fig. 3. Lake kernel functions for Lake Volta (blue polygon is the Lake's boundary) whose surface extent of 8500 km² was used for the synthesized mask. A grid mask constructed at grid intervals of 0.5° × 0.5° (left) was compared with a grid mask constructed at 0.25° × 0.25° (right). Although the spherical harmonic expansion which is restricted to degree and order 60, similar to GRACE monthly spherical harmonic coefficients, affects the representation of the Lake's extent, uncertainties in the residual water storage over the Lake is somewhat reduced using a grid mask of 0.25° × 0.25°. The solid black polygon is the basin boundary. (For interpretation of the references to color in this figure legend, the reader is referred to the web version of the article.)

lower Volta where the Volta river system converges. This signal (Lake Volta water level changes) could result in a biased assessment of water storage changes over the entire basin as observed trends in TWS changes of the basin are predominantly from the vicinity of Lake Volta due to water impoundment in the Akosombo dam (i.e., besides that of the lower Volta). In order to remove the Lake Volta signal (i.e., water storage changes due to variations in the Lake's surface) from the observed GRACE-derived TWS, the Lake Volta water level variations were converted to mass changes expressed in terms of TWS following similar approaches in recent studies (see, e.g., Ferreira and Asiah, 2015; Moore and Williams, 2014; Awange et al., 2014). Consistent with other case studies above, a constant surface is assumed over the Lake since the impact of the tidal gravitational force on it can be assumed to be negligible, even despite the shrinking and swelling of the Lake's surface during dry and wet seasons. Consequently, the derived surface water storage (i.e., altimetry water storage) over the Lake would be an approximation given its relatively small size, and the nature of its north-south orientation (cf. Fig. 1). To this end, a global grid mask was defined by a lake kernel function f_{Lake} (Fig. 3) using the geodetic coordinates of the Lake extent as

$$f_{Lake}(\varphi, \lambda) = \begin{cases} 1, & \text{Over Lake Volta} \\ 0, & \text{Outside Lake Volta,} \end{cases} \quad (3)$$

where φ is geodetic latitude and λ the geodetic longitude. This global grid mask is constructed at grid intervals of 0.25° × 0.25° to adequately capture the lake's shape. A value of 1 was assigned within the Lake surface and 0 outside the Lake. These values are assumed to correspond to 1 mm and 0 mm of EWH over the inland water and elsewhere, respectively. The spherical harmonic synthesis used in the study is based on the Neumann's method, which like the approximate quadrature method fits into the general framework of a weighted least-squares formulation of global spherical harmonic analysis (Sneeuw, 1994). Using the global spherical harmonic analysis, a grid integrable function $f(\varphi, \lambda)$ on a sphere can be synthesized into harmonic coefficients $C_{l,m}$ and $S_{l,m}$ as (e.g., Sneeuw, 1994)

$$\begin{cases} C_{l,m} \\ S_{l,m} \end{cases} = \frac{1}{4\pi} \int \int_{\sigma} f(\varphi, \lambda) P_{l,m}(\sin \varphi) \begin{cases} \cos m\lambda \\ \sin m\lambda \end{cases} d\sigma, \quad (4)$$

where $d\sigma = \sin \varphi d\varphi d\lambda$ and $P_{l,m}$ is the normalized associated Legendre function of degree l and order m . Since GRACE fields are snapshots of the static geoid given in terms of spherical harmonic coefficients, the Lake's function $f_{Lake}(\varphi, \lambda)$ (Eq. (3)) is reconstructed (Eq. (4)) and expressed through a spherical harmonic expansion as (e.g., Moore and Williams, 2014)

$$f_{Lake}(\varphi, \lambda) = \frac{1}{4\pi} \sum_{l=1}^{l_{\max}} \sum_{m=0}^l (C_{l,m}^{\text{Lake}} \cos m\lambda + S_{l,m}^{\text{Lake}} \sin m\lambda) P_{l,m}(\sin \varphi), \quad (5)$$

where $C_{l,m}^{\text{Lake}}$ and $S_{l,m}^{\text{Lake}}$ are the dimensionless lake spherical harmonic coefficients. The use of spherical harmonic representation in estimating water storage over lakes is a standard procedure evident in specific case studies listed above. The main essence of this approach as applied in the Volta basin is to help us recover the time series of TWS over the basin that is not associated with Lake Volta. For the Volta basin, these time series mostly would represent changes in groundwater, wetlands, and other small and medium scale reservoirs. The estimated spherical harmonic coefficients $C_{l,m}^{\text{Lake}}$ and $S_{l,m}^{\text{Lake}}$, which were derived by spherical harmonic synthesis up to degree and order 60, are used to recover the time series of the Lake induced TWS (altimetry water storage). The truncation of spherical harmonic coefficients at degree and order 60 is consistent with the CSR RL05 GRACE monthly fields used in this study. Thereafter, each field was scaled by using the time series of USDA altimetry-derived water level variations (previously converted to millimeters). This was achieved by multiplying the changes in the altimetry height with the synthesized kernel function (Fig. 3), which represents the relative sensitivity of GRACE to a unit of water over the lake (e.g., Moore and Williams, 2014). Thus, GRACE-

68 derived TWS over the Lake was simulated by converting lake level changes from altimetry to water storage changes. To remove the contribution of the Lake from the GRACE observed TWS over the basin, the Lake induced TWS changes (altimetry water storage) were subtracted from the observed TWS over the entire basin.

4.2. Statistical decomposition of TWS

For the statistical decomposition of GRACE-derived TWS into spatial and temporal components, we used the independent component analysis (ICA), a higher order statistical technique that decomposes multivariate data into statistically independent patterns (see, e.g., Cardoso and Souloumiac, 1993; Cardoso, 1999). The method, which has emerged as a complement to principal component analysis (PCA, e.g., Jolliffe, 2002; Preisendorfer, 1988), explores the unknown dynamics of a system through the rotation of the classical empirical orthogonal functions (Aires et al., 2002). ICA has shown great skills in geophysical signal separation (see, e.g., Boergens et al., 2014; Frappart et al., 2011) and spatio-temporal drought analysis (Ndehedehe et al., 2016b). As highlighted earlier, the strong GRACE hydrologic signals of Lake Volta dominates the observed trends in TWS changes over the Volta basin. The Lake's signal was removed and ICA was employed to localise the space-time hydrological signals over the basin. ICA was also applied on TWS changes over the basin before removing the Lake signal in order to examine the dominant patterns and the impact of removing the Lake induced TWS on the total variability of TWS over the basin. The ICA method is based on the JADE (Joint Approximate Diagonalisation of Eigen matrices) algorithm fully described in Cardoso and Souloumiac (1993). The JADE approach exploits the fourth order cumulants of the data matrix (Cardoso, 1999). These cumulants are formed through the process of empirical orthogonal function and diagonalised in order to find a rotation matrix that solves the optimization problem (Cardoso and Souloumiac, 1993). The regionalization (signal localization) process of JADE employs an optimization method to diagonalize the cumulant matrices based on a Jacobi technique (an iterative technique of optimization over the set of orthonormal matrices) (Cardoso, 1999). From the JADE approach (Cardoso and Souloumiac, 1993), the fourth-order cumulant tensor provides the suitable matrices to be diagonalized, which are non-Gaussian (e.g., Ziehe, 2005; Cardoso, 1999):

$$C_{i,j}(\mathbf{M}) = \sum M_{u,v} \text{cum}(x_i, x_j, x_u, x_v), \quad (6)$$

such that \mathbf{M} is an arbitrary matrix. After the eigen decomposition of the centered covariance data matrix (e.g., Ndehedehe et al., 2016b), the JADE algorithm performs an approximate joint diagonalisation of the set of eigen matrices of the cumulant tensor with an orthogonal transformation, which comprises a sequence of plane rotations (see, e.g., Ziehe, 2005; Cardoso and Souloumiac, 1993). Further mathematical details on the cumulant-based methods are provided in the pioneering works of Cardoso and Souloumiac (1993), Common (1994), Cardoso (1999). Also, applications of the JADE technique have been well documented (see, e.g., Ndehedehe et al., 2016b; Ziehe, 2005; Theis et al., 2005; Forootan and Kusche, 2012). In this study, use is made of the JADE technique (algorithm available at <http://perso.telecom-paristech.fr/cardoso/Algo/Jade/jadeR.m>) to decompose GRACE-derived TWS, \mathbf{X}_{TWS} into spatial maps \mathbf{S} , and temporal patterns \mathbf{T} (i.e., after removing the water storage contributions from Lake Volta) as:

$$\mathbf{X}_{TWS}(x, y, t) = \mathbf{TS}, \quad (7)$$

where (x, y) are grid locations (e.g. geographic coordinates) and t is the time in months. \mathbf{T} is unit-less since it has been normalised using its standard deviation while the corresponding spatial patterns \mathbf{S} , have also been scaled using the standard deviation of its independent components (i.e., \mathbf{T}). \mathbf{T} and \mathbf{S} are interpreted together and integrated to form what is traditionally called the ICA mode of variability.

4.3. Terrestrial stored water of the Volta basin

GRACE measures vertically integrated water storage that sums up to changes in total hydrological quantities. For the Volta basin, changes in these quantities are given as

$$\Delta TWS = \Delta SW + \Delta SM + \Delta GW + \Delta S_T, \quad (8)$$

where ΔSW is the change in total surface water storage (i.e., Lake Volta and the rivers), ΔSM is the change in soil moisture, ΔGW is the change in groundwater, and ΔS_T is the change in unquantified surface waters in wetlands and vegetation. After removing the contribution of $\Delta SW_{Lake\ Volta}$ (i.e., the Lake induced TWS signal), the residual water storage change component, ΔW_T is expressed as

$$\Delta W_T = \Delta TWS - \Delta SW_{Lake\ Volta}. \quad (9)$$

This quantity (i.e., ΔW_T), which is the summation of ΔGW , ΔSM , and ΔS_T was statistically decomposed using the ICA method (see Section 4.2) in order to understand its dominant spatio-temporal patterns over the basin.

4.4. Multiple Linear Regression Analysis (MLRA)

The strongest signals in rainfall variability over the Volta basin emanates from the annual and semi-annual signals of the data, hence the annual and semi annual components of GPCC based precipitation were removed in order to understand the impacts of climate variability on the basin. This was achieved by using a multiple linear regression analysis (MLRA) model that parameterizes the trends, cosine, and sine harmonic components. The dataset $\mathbf{Y}_{Rainfall}$, is parameterized as

$$69 \quad \mathbf{Y}(i, j, t) = \beta_0 + \beta_1 t + \beta_2 \sin(2\pi t) + \beta_3 \cos(2\pi t) + \beta_4 \sin(4\pi t) + \beta_5 \cos(4\pi t) + \varepsilon(t), \quad (10)$$

where (i, j) are the grid locations, t is the time in months, β_0 is the constant offset, β_1 is the linear trend, β_2 and β_3 accounts for the annual signals while β_4 and β_5 represents the semi-annual signals and ε the error term. The deseasonalized data $\mathbf{X}_{\text{Rainfall}}$, is characterised as

$$\mathbf{X}_{\text{Rainfall}} = \mathbf{Y} - [\beta_1 t + \beta_2 \sin(2\pi t) + \beta_3 \cos(2\pi t) + \beta_4 \sin(4\pi t) + \beta_5 \cos(4\pi t)]. \quad (11)$$

The deseasonalized GPCP data was then standardised using its standard deviation after removing the mean (see Section 4.6). This is done in order to investigate the relationship between extreme rainfall conditions and the behaviour of discharge at Akosombo and water level variations over the Lake. This should lead to improved understanding of the Lake's hydrology and the impacts of climate variability and human related influence.

4.5. Trend and extreme analysis

A least squares fit was employed to estimate the trends in (i) the time series of averaged residual TWS (after removing the Lake induced water storage) for the period during 2002–2014, (ii) the temporal evolution of independent modes derived from residual TWS decomposition using the ICA method, (iii) time series of the lake height variations after removing the long term mean, and (iv) the gridded precipitation, evapotranspiration and TWS (before and after removing the Lake induced water storage) data sets. The Students' t -statistic was used to determine whether the trend was statistically significant (i.e., at 95% confidence level). Furthermore, the trends in the time series of annual maximum and minimum of rainfall, river discharge, and Lake Volta water levels were explored as it is also possible that the impacts of rainfall and river discharges on the Lake (or the influence of rainfall on the Volta river system) may not always be reflected in the mean but instead through changes in the extremes.

4.6. Standardised anomalies

Monthly anomalies for GPCP-based precipitation, river discharge, and the lake height variations were calculated by subtracting the monthly time series of each of these hydrological quantities from their respective monthly mean climatology as

$$\Delta A_i = X_i - \frac{1}{n} \sum X_i, \quad (12)$$

where ΔA_i are the monthly anomalies, X_i is the monthly variable of hydrological quantity of interest, i is the month, and n is the total number of months considered. Furthermore, the monthly anomalies of rainfall, lake levels, and river discharge of Akosombo were aggregated to yearly values and then the cumulative rainfall departure (CRD) (Weber and Stewart, 2004) and cumulative river discharge departure (hereafter called CRDD) were computed. Besides its utility in a predictive capacity, that is, when combined with comprehensive water budget analysis, according to Weber and Stewart (2004), the CRD may be very helpful when employed as a general indicator of rainfall trends, with the upward and downward gradient indicating relatively a rise and decline in rainfall, respectively. Note that the CRDD is computed in a similar way to the CRD and is also employed to evaluate trends in river discharge against rainfall. To further understand the water fluxes and the hydrology of the Lake Volta area, lake levels, river discharge, and TWS with CRD were compared. The annual anomalies of the Lake Volta, Akosombo and the White Volta river stream flow records were standardised and used to study the hydrological condition of the Lake. The value of one standard deviation was used to set the limits for the groupings of the hydrological conditions (Table 2), which is similar to the range of variability approach (RVA) and standardised precipitation index (see, Genz and Luz, 2012; McKee et al., 1993).

5. Results and discussion

5.1. TWS changes induced by Lake Volta water level changes

The discussion in this section focuses on the results of satellite altimetry-derived water storage changes of Lake Volta and residual TWS changes over the Volta basin. The water impoundments at Lake Volta by the Akosombo dam impacts on GRACE-derived TWS changes (hydrological signal), leading to artifacts in the observed TWS trends over the Volta basin. This hydrological signal induced

Table 2
The classification system of hydrological conditions of the Lake Volta based on the annual anomalies of lake water level and stream flow records of the Akosombo station, White Volta and Oti rivers.

Description	Hydrologic condition class
Very wet	> 1.5
Wet	+ 0.5 to + 1.5
Average	– 0.5 to + 0.5
Dry	– 0.5 to – 1.5
Very dry	< – 1.5

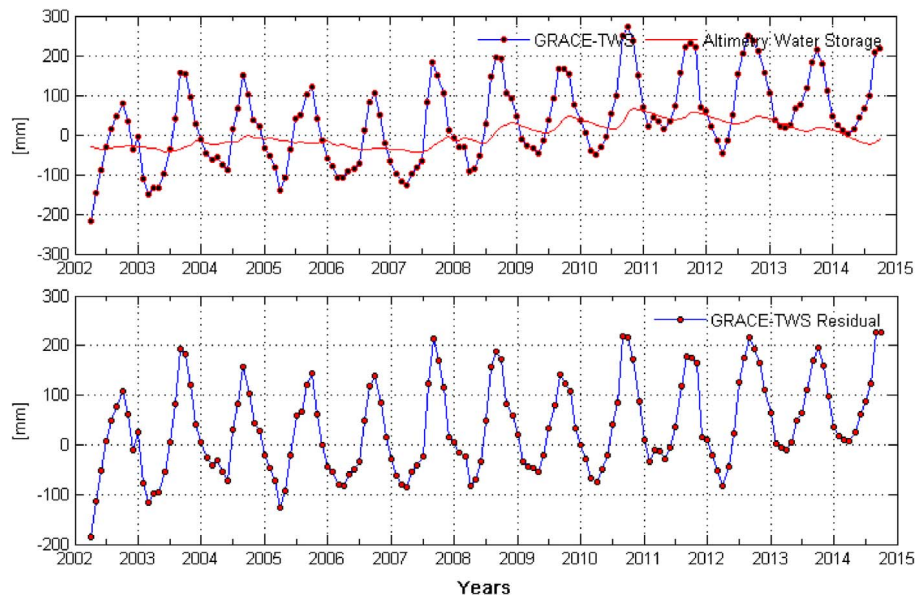


Fig. 4. GRACE-derived TWS changes and altimetry-derived water storage changes (i.e., surface water variability) induced by Lake Volta and the corresponding basin. Top panel: Time series of averaged GRACE-derived TWS over the Volta basin and altimetry-derived water storage changes over the Lake for the common period (2002–2014). Bottom panel: Time series of averaged GRACE-derived TWS over the Volta basin after removing the water storage contributions of Lake Volta.

by water level changes of the reservoir (i.e., Lake Volta), could be misleading and can adversely impact on our knowledge of the hydrological processes in the Volta basin. To understand the temporal hydrological changes in the Volta basin, the Lake Volta TWS change (derived from satellite altimetry water level changes via the method outlined in Section 4.1) is removed from the averaged TWS over the basin to obtain the residual TWS (i.e., ΔW_r in Eq. 9).

Over the basin, the linear trends over a common time period (i.e., between 2002 and 2014) for TWS (i.e., GRACE-TWS, Fig. 4, top) and residual water storage changes (i.e., GRACE-TWS residual, Fig. 4, bottom) were compared to understand the Lake's contribution to the overall trend in the basin. The water storage over the Volta basin (i.e., GRACE-TWS and GRACE-TWS residual) both indicate an increasing trend over the period investigated (see top and bottom panel, Fig. 4). Specifically, GRACE-TWS (i.e., ΔTWS) indicate a monthly trend of 13.96 ± 2.02 mm, which is about 5.83 km^3 of water over the basin during the 2002–2014 period, while GRACE-TWS residual (i.e., ΔW_r) show a monthly increase of 8.15 ± 1.3 mm (i.e., 3.40 km^3 of water). The difference between the two trends provides an indication on the contribution of the Lake, i.e., about 5.81 mm/month around the vicinity of the Lake. This contribution (i.e., the trend from the Lake's water storage) amounts to approximately 41.6% of the trend in water storage over the basin for the period between 2002 and 2014. It is fundamentally important to note that the observed trend in TWS over the Lake also depends on the amount of evaporation and rainfall over the Lake. Evaporation and rainfall amounts over the Lake also determine largely not only the Lake's contribution to the observed trend in TWS but also the net flow at the Akosombo dam. This in turn affect the overall trend and amplitudes of TWS change in the basin, as TWS is largely determined by the balance between precipitation and sink terms (river discharge and evapotranspiration). Also, in regard to the synthesized water storage over the lake, the study is also leery of the fact that the Lake's shape (i.e., arborescent with a north-south orientation) may somewhat contribute to uncertainties in the estimated water storage trend over the reservoir. Theoretically, the representation of the Lake's boundary in a spherical harmonics domain, affect significantly the amount of surface water storage recovered from the Lake, owing to the truncation at degree and order 60 similar to GRACE coefficients. Hence, the trend in altimetry water storage (Fig. 4, top) is interpreted with some caution. Nonetheless, our empirical approach to disengaging the Lake induced water storage, allows the understanding of the natural hydrological variability or behaviour of the Volta basin. In the view of increasing attention to the impacts of climate variability, this will be helpful and instructive.

Furthermore, the water storage changes over the Lake (i.e., altimetry water storage) during the 2002–2004 and 2006–2008 periods show deficit conditions (Fig. 4, top). These periods (especially 2002/2003 and 2006/2007) are generally consistent with droughts in the region (e.g., Ndehedehe et al., 2016c; Bekoe and Logah, 2013). More than that, the residual TWS over the basin is instructive of the non-linear hydrological response of the basin (Fig. 4, bottom). The peak amplitude of residual TWS in 2003 is somewhat similar to those of 2007, 2010, and 2012 in the basin, and does not suggest water deficit compared to the observed peak amplitude of TWS in 2002 (Fig. 4, bottom) that indicates the lowest during the 2002–2014 period. Rather, the precipitation deficits during the 2001–2002 period (Section 5.3), resulted in considerable low stream flows of the Oti and Volta rivers (White and Black Volta rivers), which affected the water level of the reservoir in 2003 (Fig. 2). As would be expected, the limited stream flows of the Volta rivers resulted in water deficit in the Lake (i.e., the altimetry water storage) between 2002 and 2004 (Fig. 4, top). Also, the impact of precipitation deficits on the Oti and Volta rivers largely accounts for the deficit conditions in altimetry water storage between 2006 and 2008 (Fig. 4, top). However, the improved rainfall condition of 2003 impacted on the Volta basin leading to a

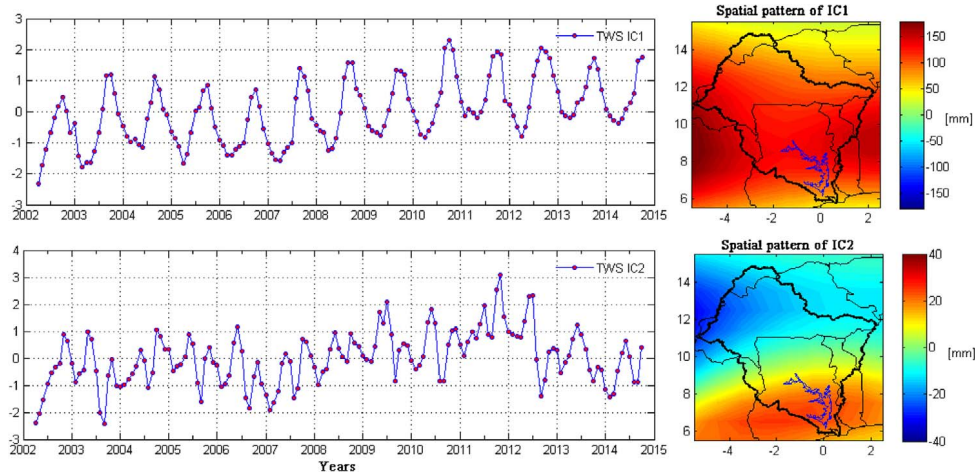


Fig. 5. Independent Components of TWS over the Volta basin (i.e., before removing the Lake Volta signal). These independent components are unitless since they have been standardised using their standard deviations. The spatial patterns (right) are scaled using the standard deviation of the computed independent components (left).

relatively strong peak amplitude of residual TWS (i.e., GRACE-TWS residual, Fig. 4, bottom). Interestingly, strong peaks in residual TWS over the basin are consistent with those of rainfall while strong peaks in altimetry water storage (i.e., Lake Volta) are largely related to strong peaks in stream flows of the Volta river system. This and other intricacies around the basin's hydrology are discussed further in the manuscript (Sections 5.3–5.5).

5.2. Hydrological characteristics based on TWS changes

Contrary to Section 5.1, this section provides further hydrological analysis of the Volta basin by employing the ICA technique to analyse residual GRACE-derived TWS changes (i.e., after removing the contributions of the Lake Volta). In this Section, results of statistical decomposition of TWS changes and residual TWS changes ΔW_T over the basin are discussed further, essentially to better understand the hydrology of the region and to also find a hydrological rationale and scientific justification for the behaviour of observed TWS changes during periods of reduced rainfall and hydrological drought.

Using the ICA method, GRACE-derived TWS was statistically decomposed into spatial and temporal patterns (before and after removing the Lake Volta induced TWS). Two statistically significant independent modes of TWS variability (i.e., without removing Lake Volta signal) were found. The first mode indicates a relatively strong spatial variability over the entire basin; Ivory Coast, Ghana, Togo, and western Burkina Faso (IC1, Fig. 5), which is the source of the Black Volta while the second mode showed spatial variability around the Lake area (IC2 Fig. 5). IC1 and IC2 of Fig. 5 explained 96.5% and 1.9% variances, respectively from the cumulated variance. While IC1 is driven by inter-annual rainfall variability over the entire basin, IC2 is dominated by hydrological signals around the Lake Volta area mostly emanating from wetlands and smaller rivers. The Lake induced TWS (see Section 5.1) showed a correlation of 0.51 with IC2 of Fig. 5, indicating that at least 50% of the variability in the observed TWS over the Lake is explained by IC2. Their temporal evolutions (IC1 and IC2 of Fig. 5) indicate an increase of 26.0 ± 4 mm/yr and 2.25 ± 0.5 mm/yr for IC1 and IC2, respectively when jointly derived from the spatial and temporal patterns. The observed trends in the temporal evolution of TWS (IC1 and IC2, Fig. 5) also include the unquantified water storage in wetlands and smaller coastal rivers, which include Chi-Nakwa, Ochi Amissah, Ayensu, Densu and the Tordzie (see details on the geomorphology of rivers in Barry et al., 2005).

After removing the contribution of Lake Volta, the results of the statistical decomposition also show two statistically significant modes of TWS change over the basin. Unlike Fig. 5, the first independent mode shows spatial and temporal patterns of TWS over Ivory Coast, upper Black Volta catchment and the Oti river catchment (explaining about 76.2% of the total variability), which includes Ghana and Burkina Faso while the second independent mode indicates TWS signal in the lower Volta catchment (explaining about 21.5% of the total variability), which is in Ghana (Fig. 6). The first ICA mode indicates an increase of 24 ± 4 mm/yr in TWS over the basin (IC1, Fig. 6) while a decline in water storage (59.5 ± 8.5 mm/yr) around the lower Volta between 2007 and 2011, which approximates to a loss of 14.19 km^3 of water in Ghana, is observed in the second ICA mode. This loss coincides with declines in the spatial patterns of precipitation in the lower Volta (Fig. 7a) during the same period (2002–2014). Although evapotranspiration does not indicate declines within the vicinity of the Lake (Fig. 7b) as would have been expected, suggesting the non-linearity of hydrological processes in the tropical transition zone of the basin, the estimated trends in the spatial patterns of TWS (Fig. 7c) over the basin (statistically significant at 95% confidence interval), is consistent with the observed trends in dominant patterns of TWS (IC1, Figs. 5 and 6). The spatial patterns of IC1 of Fig. 6 is a prototype of the estimated residual TWS trend shown in Fig. 7d. After removing the lake induced TWS, which explained about 20% of the TWS signal of the basin (i.e., by comparing the variabilities of the first ICA modes of Figs. 5 and 6), the obscured hydrological signal of the lower Volta basin where the White and Black Volta tributaries of the Volta River system converge (i.e., in Ghana) became obvious.

A careful look at IC2 of Fig. 6 shows that the TWS change over Lake Volta area revolves around latitudes 9° N and 6° N , where the Volta river system is mostly concentrated, in addition to other smaller reservoirs and lakes (e.g., Lake Bosomtwe), river tributaries,

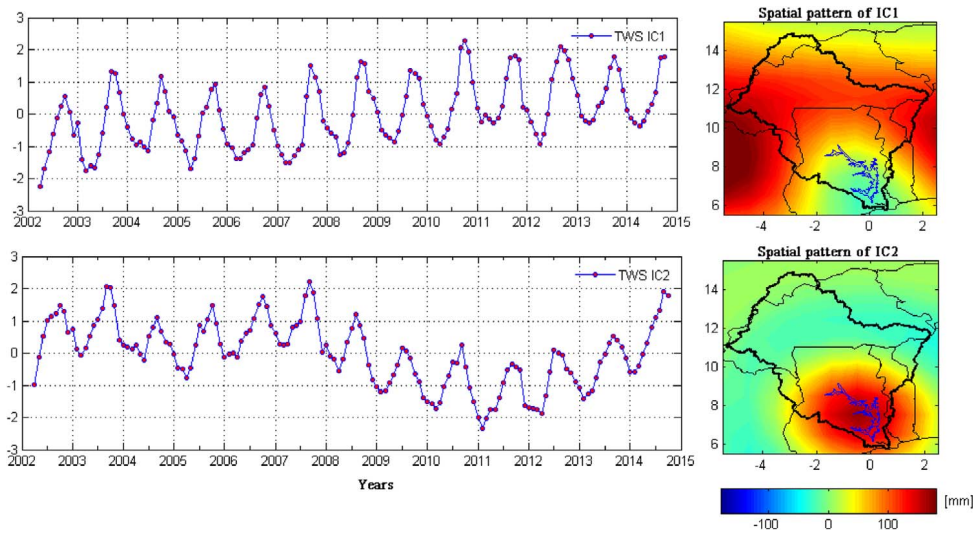


Fig. 6. Independent Components of TWS over the Volta basin (i.e., after removing the Lake Volta induce TWS signal). These independent components are unit-less since they have been standardised using their standard deviations. The spatial patterns (right) are scaled using the standard deviation of the computed independent components (left).

and wetlands. The changes in TWS in this Lake Volta area (IC2, Figs. 6) is largely driven not only by rainfall variability, but also by the annual variability of the three rivers (i.e., the Black Volta River on the west, White Volta river to the east, and the Oti river on northwestern Benin and Togo, see Fig. 1) in Ghana. These rivers, whose flows are high during heavy rainfall periods (e.g., June and July), leading to a high runoff, are the main river systems that drains into Ghana. The loss of stored water at the lower Volta basin in Ghana during the 2007 – 2011 period (IC2, Figs. 6) can also be attributed to the loss of freshwater from these main river systems due to low stream flows and base flow recessions, resulting from precipitation decline during the 2002–2014 period and perhaps human intervention as occasioned by the development and expansion of small and medium scale reservoirs in the basin (e.g., Leemhuis et al., 2009). Since GRACE integrates precipitation over time, base flow recessions resulting from the extended periods of precipitation

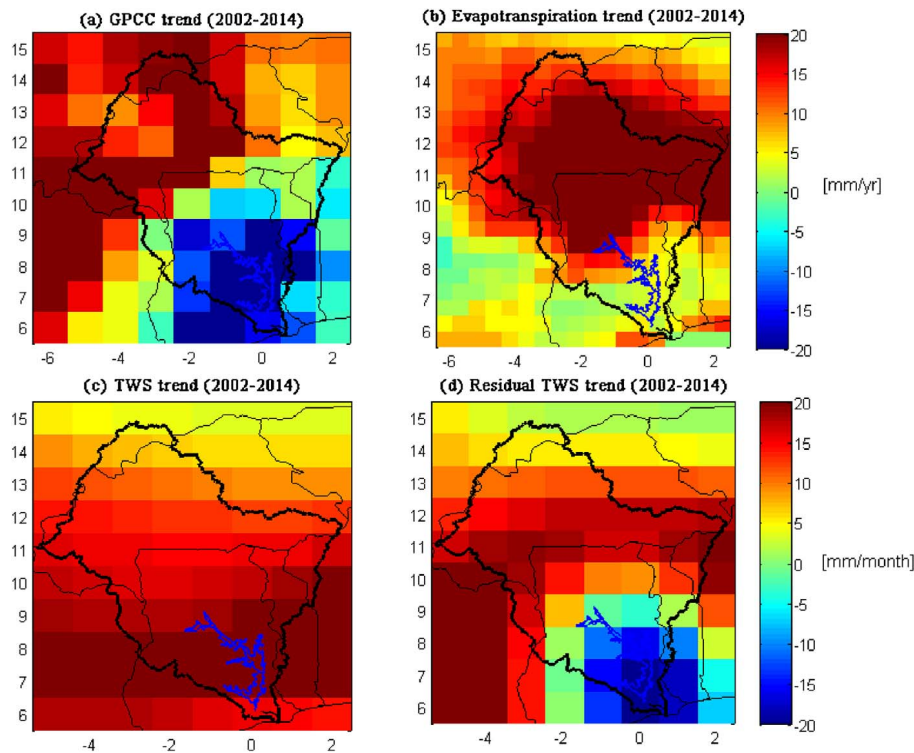


Fig. 7. Trends in water fluxes over the Volta basin during the 2002–2014 period. (a) GPCP based precipitation (b) evapotranspiration (c) GRACE-TWS (i.e., before removing the lake induced TWS) and (d) GRACE-TWS residual (i.e., after removing the lake induced TWS).

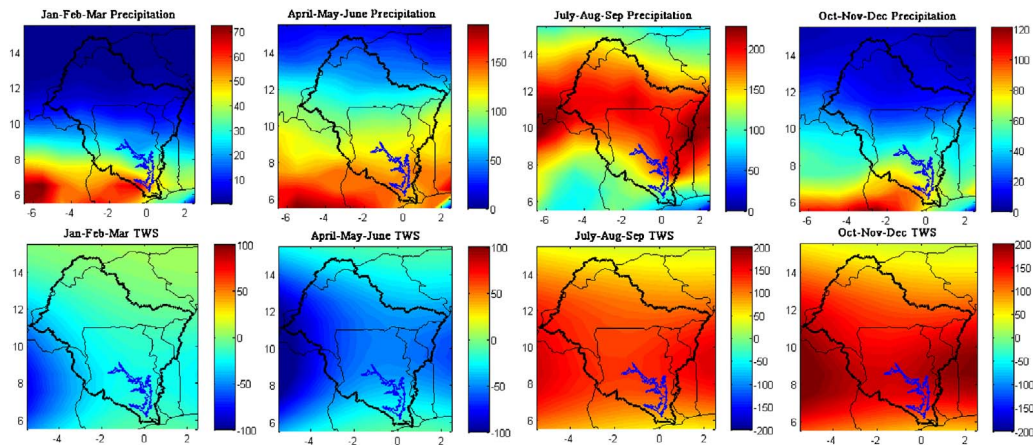


Fig. 8. Seasonal spatial rainfall and TWS patterns over the Volta basin and its surroundings. First row: Seasonal spatial variability of GPCP-based precipitation (2002–2014). Second row: Seasonal spatial variability of TWS (2002–2014).

decline (2002–2014) can cause an extensive temporary storage depletion that are volumetrically significant. However, such storage depletion emanating from an extensive water table decline can be recovered as weather cycles are reversed (see, [Alley and Konikow, 2015](#)).

Given the circumstances of increased irrigation schemes and the development of small and medium scale reservoirs within the basin (e.g., [Leemhuis et al., 2009](#); [Andreini et al., 2002](#)), one can also argue that the increase in the use of surface water resources in Burkina Faso must have limited the inflow into the lower Volta basin in Ghana, leading to a decline in the observed ΔW_T within that period. Add to this, [Leemhuis et al. \(2009\)](#) presented results that indicated that the expansion of small and medium scale reservoir storage capacity from 0.7 km³ to 0.79 km³ during the 1992–2000 period in northern Ghana was related to the storage loss of Lake Volta within the period. With the observed recent decline in Lake Volta water level heights since 2011 till date ([Fig. 2](#)), coupled with the observed loss of water storage over the lower Volta (IC2, [Fig. 6](#)), the impression is that the Volta basin may be tilting towards drier conditions. However, it is not completely clear if TWS decline (2007–2011) around the lower Volta (IC1, [Fig. 6](#)) is strongly linked to the negative trends in rainfall during the 2002–2014 period ([Fig. 7a](#)). The sensitivity of lakes, reservoirs, etc., to climate and extreme environmental conditions have been reported (e.g., [Ndehedehe et al., 2016a](#); [Deus et al., 2013](#)) and as demonstrated in Section 5.4, the water fluxes of the lower Volta respond to rainfall conditions in the basin with about 1 year lag. While our results in Section 5.3 show relatively drier conditions during the 2011–2013 period ([Fig. 9](#)), a recent analysis of spatio-temporal characteristics of hydrological droughts over the Volta basin indicated that the lower Volta area experienced severe drought conditions during the 2010–2013 period (see, [Ndehedehe et al., 2016c](#)) (i.e., with respect to the mean of the last four decades). Apparently, rainfall conditions in the western Burkina Faso and the surrounding areas have improved (i.e., showing positive trends – [Fig. 7a](#)). Although it is rather empirical than speculative, the negative trends in rainfall patterns around the lower Volta (cf. [Fig. 7a](#)) may account for the decline of TWS indicated in IC2, [Fig. 6](#).

However, while it is somewhat becoming drier in recent years around the lower Volta, that is, from the lake levels and the cumulative rainfall departure (see Section 5.4), the rise in TWS during 2011–2014 period in the lower Volta area may be a simple return to ‘normal’ conditions after the decline in inter-annual variations of TWS during the period between 2007 and 2011 (IC1, [Fig. 6](#)). Increased rainfall in 2014 may indicate a reversal of the decline and also a possible return to a normal hydrological state in the lower Volta and the basin at large. This would be consistent with the 4–5 year dry-wet cycle indicated in Sections 5.3.2 and 5.5. As will be highlighted further in Section 5.3.2, observed declines in net precipitation over the basin also coincides with the decline in residual water storage of the lower Volta (IC2, [Fig. 6](#)) during the 2002–2014 period. It should be noted that as the hydro-meteorological cycles of the region changes, the loss in water storage changes of the tropical lower Volta are usually recoverable as the hydrology naturally resets to reflect new conditions.

5.3. The response of Volta basin's hydrological system to precipitation

Given that rainfall in the Volta basin translates into a greater proportion of river discharge that feeds the Lake Volta, the stream flow records of the Volta river system (i.e., White, Black, and Oti rivers) were retrieved from the Global Runoff Data Centre (GRDC) archives and analysed. They were combined with flow records of Akosombo and Kpong dams to understand the response of the basin's freshwater systems to rainfall conditions and climate variability. Specifically, all river discharges, lake level variations and TWS were compared with GPCP-based rainfall. As described earlier in Section 4.4, the annual and semi-annual components of GPCP-based precipitation (1979–2014) were removed (deseasonalized) since rainfall in the region is dominated by these components. Removing these components in the time series of the data (e.g., rainfall) allows the examination of peaks and extremes that are perhaps associated with the impact of climate variability. The river discharge data and lake level variation were not deseasonalized but were standardised after removing their long term mean to enhance the evaluation of the sensitivity of the lake level variations and discharge to the vagaries of extreme rainfall conditions over the basin.

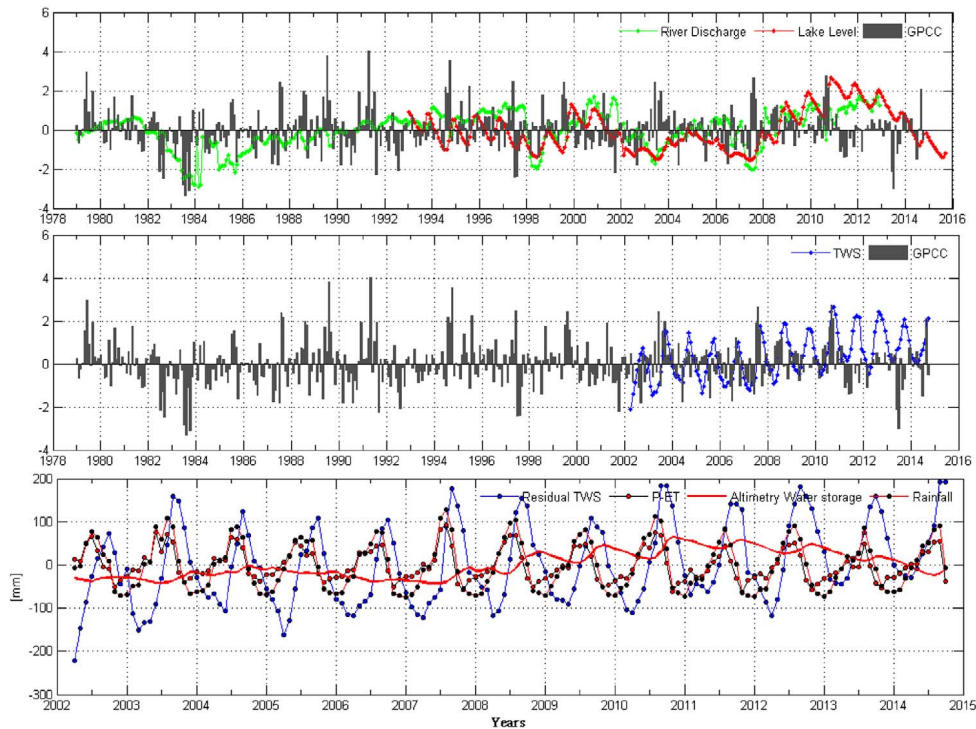


Fig. 9. Relationship between GPCC-based precipitation (extreme conditions) and observed in-situ river discharge and satellite altimetry. The annual and semi annual components of GPCC-based precipitation have been removed using Eq. (10) and then standardised using its standard deviation. Top: Relationship of deseasonalized GPCC (1979–2014) to standardised anomalies (i.e., using their standard deviation) of river discharge at Akosombo (1979–2012), and satellite altimetry-derived water level (1993–2016). Middle: Relationship of deseasonalized GPCC to standardised anomalies of averaged TWS over the Volta basin. Bottom: Time series of net precipitation, residual TWS, altimetry water storage (lake induced TWS) and rainfall anomalies during the GRACE period (2002–2014).

5.3.1. Spatial patterns of seasonal precipitation and stored water

The seasonal rainfall patterns indicate that rainfall is predominant in the July–September period (Fig. 8, row 1) towards the northern part of the basin (upper Volta), where mean rainfall in northern Ghana and Burkina Faso is about 200 mm while it is relatively higher in Ivory Coast/Mali and Benin (not shown). Mean rainfall distribution is more than 200 mm in the upper Volta only during the July–September period while around the lower Volta, mean rainfall distribution for all seasons (except January–March) reaches 120 mm. Areas with observed high seasonal rainfall especially during the July–September period (i.e., Fig. 8, row 1) coincides with relatively high elevation regions such as Ivory Coast and Benin (cf. Fig. 1). Typically, the presence of considerable rainfall can be seen in the southern catchment (lower Volta) all through the seasons unlike the northern catchment (upper Volta) where it is restricted to the April–June and July–September periods.

For TWS, their seasonal patterns show amplitudes of more than 200 mm outside/within the basin area (i.e., in Côte d’Ivoire or Ivory Coast) during the October–December period while the basin area indicates amplitudes of about 150 mm in the spatial patterns of July–August period (Fig. 8, row 2). Comparatively, this is about two months away from rainfall (i.e., indicating a lag of about two months), which shows peaks (strong spatial patterns) in the July–September and April–June periods. The observed strong seasonal TWS spatial patterns in Côte d’Ivoire (Fig. 8, row 2) in the July–September period is that of Lake Kossou, where the hydroelectric power plant is located 16 km upstream of the Bandama river and about 40 km away from Yamoussoukro the administrative capital. We do not dwell on this observed seasonal spatial pattern of TWS in Côte d’Ivoire, as it is outside the Volta basin area. Overall, due to the movement of freshwater from the upper Volta catchment, and the presence of rainfall (usually bimodal in nature) and reservoirs along the coast, large amplitudes of seasonal spatial patterns in TWS are mostly found within the tropical transition zone (i.e., lower Volta). In essence, the large volume of freshwater in the lower Volta is mostly furnished by the upper Volta region, which lies in the Sahel transition zone. This has prominent negative implications for the runoff hydrology of the Volta river system that nourishes the Lake Volta during periods of significant changes in climate. It has been reported that the effects of such periods, for example, rising temperatures and decline in rainfall, are normally felt in areas of hydropower and the negative impact on the morphology of the river estuary (e.g., Gyau-Boakye, 2001).

5.3.2. Precipitation impacts on stream flow at the Akosombo dam

Since the lack of consistent flow records of the Volta river system limits the overall hydrological assessment of the basin, the stream flow record of Akosombo is explored to assess the impacts of climate variability on the basin. This is possible as the topography and the confined aquifer system of the basin naturally links the Volta river system with the man-made reservoir (Lake Volta, cf. Fig. 1). Generally, relatively dry (e.g., 1983/1984, 1997/1998, and 2013) and wet (e.g., 1991, 1994, and 2010) years are

75 quite obvious (Fig. 9 top). Lake water level variations and river discharge anomalies responded to the trends of the wet and dry episodes quite well except for 2003 and 2007 (Fig. 9 top). Despite the relatively wet period of 2003 over the entire basin, observed river discharge at Akosombo and the altimetry water levels over Lake Volta indicate extreme negative anomalies, presupposing a dry condition. It seems the extreme dry years of 2001 and 2002 must have prevailed upon the wet period of 2003 leading to strong negative anomalies in river discharge and satellite altimetry water level variations. As there was a rather strong dry (i.e., the rainfall deficiency of 2001 and 2002) period (Fig. 9 top), it took some time for the Lake to respond and also to replenish the TWS in the basin. It can also be argued that, after a wet period, considerable stream flow from the Volta river system reaches the lake after significant proportion of precipitation has been absorbed by the dry areas around the lake's catchment, creating a non-linear response. For instance, the response of river discharge and the Lake to the wet period in 2003 can be seen at the end of 2004 while the wet period in late 2007 after a previous drought period in 2006 can be seen in 2008 and beyond (Fig. 9 top). This implies a time lag of about 12 months or more between an extreme dry period and the time for the Lake to transit into a wet condition.

A recent study over the Volta basin (Ndehedehe et al., 2016c) confirmed this late response of reservoirs and surface water to extreme rainfall conditions. The study showed that standardised precipitation index (SPI) and standardised runoff index (SRI) exhibited inconsistent behaviour in observed wet years over the Volta basin presupposing a non-linear relationship that demonstrates the lag between long term river discharge and precipitation especially after a previous extreme dry period. For instance, Ghana suffered electric power rationing during 1983–1984, 1997–1998, 2003, and 2006–2007 due to hydrological drought (Bekoe and Logah, 2013). However, the limited hydro-power capacity of the Akosombo dam in 2003 that resulted in electric power rationing was not caused by hydrological drought of the year, rather, it was attributed to the effects of previous drought years of 2001 and below average rainfalls in 2002 (Bekoe and Logah, 2013). This observation is consistent with our results that indicate drier conditions in 2001–2002 and relatively wet conditions in 2003 (Fig. 9, top). It should also be pointed out that while the decline in the lake levels between 2014 and September 2015 can be seen as a response to the dry condition in late 2013, the decline of the lake level between 2011 and 2013 could be due to precipitation deficits of 2011 (Fig. 9, top), that is assuming a 12-month lag between rainfall and the inflow of water from the upper Volta basin to the Lake. Of course, the spilling of the reservoir in November 2010 due to increase in annual rainfall totals in most parts of Ghana (see, Owusu and Waylen, 2013) is not left out. Although the amplitudes of TWS and residual TWS over the basin during wet periods of 2003, late 2007, and 2010 are somewhat consistent with those of rainfall anomalies (Fig. 9, middle and bottom panels), the observed peaks of net precipitation does not capture this unique hydrological periods occasioned by the impact of climate variability. Rather, a net precipitation (i.e., $P-ET$) decline of -15 mm/yr was observed during the period (Fig. 9, bottom), coinciding with the observed decline in residual water storage in the precinct of the lower Volta between 2007 and 2011 (IC2, Fig. 6), and the negative trends in precipitation patterns reported in Section 5.2.

Further, recall that as indicated earlier, Bekoe and Logah (2013) attributed the low hydro-power production of 2003 to the impacts of 2001 drought episode and the below average rainfall of 2002. Likewise, the observed extreme low anomalies of river discharge and altimetry water levels observed in late 2007 (Fig. 9, top) are inconsistent with rainfall in the same period. This behavior demonstrates the general physical hydrological phenomenon within the basin where wet periods are preceded by low water level in the Lake, due to limited rainfall. Generally, this behavior is observed in the wet years of 1994, 1999, 2003, 2007, and 2010, which are preceded by dry periods (Fig. 9, top).

Furthermore, from the standardised rainfall in Fig. 9, it seems there is a 4–5 year cycle between dry and wet periods (the classification of wet and dry periods are based on 1 standard deviation as mentioned in Section 4.6). Again, the consistent low rainfall amplitudes between 2004 and early 2007 and the acknowledged drier conditions of 2006 can possibly account for the pronounced negative anomalies of Akosombo river discharge and altimetry water levels in late 2007. As it will be shown later, it seems the White Volta and Oti rivers contributed to the low amplitudes of the Akosombo discharge. These rivers show a linear relationship with rainfall in the basin and are naturally linked to the tropical transition zone, the lower Volta. The flow regimes of these rivers are however not only affected by the hydraulic characteristics of the region, but may also be influenced by human activities in the basin such as infrastructure watershed development (e.g., Leemhuis et al., 2009). Moreover, observed relationship between TWS and the rainfall over the Volta basin appears to be consistent (Fig. 9, middle). However, the drier conditions of 2013 as shown in the extreme negative anomalies of rainfall in the mid-year is inconsistent with observed TWS change (Fig. 9, middle). We have not identified any potential cause regarding this inconsistency, further discussions on the cumulative annual rainfall anomalies and TWS have been provided in Section 5.4.

5.3.3. Freshwater systems

The major freshwater systems of the Volta basin are basically the White, Black, and Oti rivers (hereafter called the Volta river system) and Lake Volta. The natural variability of these rivers have been compared with flow records of Akosombo and Kpong dams (Fig. 10a), which are meant to manage the reservoir outflow for hydropower purposes. In addition, the relationship of the Volta river system with rainfall variability and the Lake Volta, that is, based on their monthly anomalies have been examined. From visual inspection, the White Volta and the Oti rivers are more related to the Akosombo and Kpong flows (hereafter called dam flows), that is in terms of their lowest minimum peaks (lowest minimum peaks of the White Volta and Oti rivers impact on dam flows). The well known periods of hydrological droughts and water shortage (1983/1984, 1997/1998, and 2006/2007) in the Lake, resulting in low flows (Fig. 10a) during the same periods are consistent with the observed precipitation anomalies (Fig. 10b). More importantly, antecedent conditions and the impact of water carried forward from previous storage is also observed. For instance, extreme low flows of the White Volta and Oti rivers (1997, 2002, and 2005/2006) consistently resulted in extreme low flows of the dams in the year that followed (approximately 12 months). Add to this, while the impacts of the 1997 El-Niño and 1999 La-Niña are reflected in the peak amplitudes of the two rivers, it is further confirmed that 2003 was not a dry year as the rainfall anomalies and the Volta river

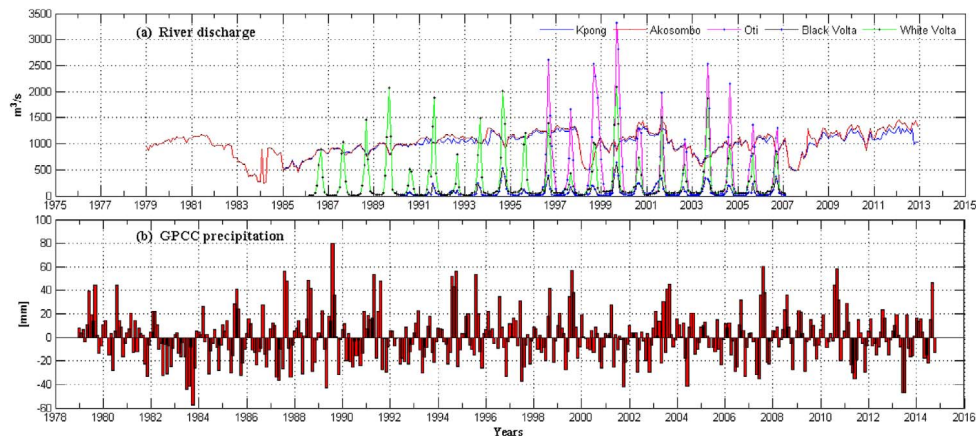


Fig. 10. Influence of precipitation on stream flow records of the Volta river system. (a) Time series of observed river discharge at the Kpong/Akosombo (1979–2012), Black Volta (1990/03–2007/02), White Volta (1986/03–2007/02) and Oti (1996/03–2007/02) rivers. (b) Time series of GPCP based precipitation anomalies over the Volta basin (1979–2014).

system show relatively strong amplitudes of discharge (with maximum Oti river discharge reaching $2500 \text{ m}^3/\text{s}$) and rainfall anomalies (Fig. 10a and b). Rather, the rainfall deficits of 2002 (Fig. 10b), which is consistent with the extreme low flows of the the Volta river system (Fig. 10a) caused the water shortage in the reservoir (cf. Fig. 9, top), resulting in limited dam flows.

The Volta river system generally shows a linear response to rainfall, with the White Volta and Black Volta rivers explaining higher variabilities in rainfall (31% and 34%, respectively) compared to the Oti river (Table 3). However, the Oti river is well correlated with rainfall over the basin at 2 months lag. Although the Black Volta is actually a far larger catchment nourishing Burkina Faso and other catchments outside Ghana, the White Volta and Oti rivers contribute more freshwater to the Lake Volta as can be seen in their annual amplitudes (Figs. 10a and 11a–c). According to Andreini et al. (2002), of all the water flowing into Lake Volta, about 67% comes from outside Ghana through the Volta river system, with Oti river contributing the largest share (about 32%) to the Lake. This perhaps explains the observed limited alimentation in the Lake during the 1996–2007 period (Section 5.5), consistent with the declines of $380 \text{ m}^3/\text{s}/\text{yr}$ and $6.96 \text{ m}^3/\text{s}/\text{yr}$ in the Oti and White Volta river flows (Table 3), respectively. Oti river explains about 14% of the changes in rainfall (i.e., $R^2 = 0.14$) compared to the White and Black Volta rivers with relatively higher variabilities (see Table 3 and Fig. 11d–f) while stronger extremes in Oti river flow (e.g., 2003) are also sometimes inconsistent with observed water levels in Lake Volta (Fig. 11c).

Furthermore, unlike the Volta river system, the dam flow records, which do not show natural variability (Fig. 10a) indicate a non-linear response to rainfall due to damming of the rivers. Although the flow records of the Volta river system are missing for the remaining periods studied (i.e., 2007/03–2014), the rising trend of the dam flows after the 2007 La-Niña up to 2010 is consistent with the increasing trend in observed water levels and water storage in the Lake (cf. Fig. 9). Our results confirm that the dam flow records are largely indicative of the Lake's water level, which in turn relies on the Volta river system. As the stream flow records of the Volta river system are incomplete, the dam flows can be combined with rainfall over the basin to provide hydrological information that will support our understanding of the impact of climate variability in the basin. This is further discussed in Section 5.4.

5.4. Cumulative rainfall departure and water fluxes in the Volta basin

Here, the observed relationship between GPCP-based precipitation and water fluxes (specifically the Akosombo river discharge and the satellite altimetry derived water levels) using annual cumulative departures is discussed further. The cumulative rainfall departure (CRD) and cumulative river discharge departure (CRDD) (i.e., annual) indicates a statistically significant correlation of 0.75, suggesting that there is a link between rainfall in the Volta basin and the river discharge at Akosombo (see Fig. 12). Evaluating the relative increase or decrease of river discharge in relation to rainfall, we found that the increase or decline in rainfall was not accompanied immediately by a similar rise/fall in river discharge, indicating that the current Akosombo discharge is influenced by the rainfall conditions of the previous year. For example, the decline of river discharge in 1981/1982 was a response to the rainfall

Table 3

The relationship between precipitation in the Volta basin and the Volta river system (i.e., White Volta, Black Volta, and Oti rivers). Correlations (r) are statistically significant at 95% confidence interval. Trends marked with * are not statistically significant at the 95% confidence interval. The maximum r is with respect to the lags indicated.

River	Correlation (r)	Maximum r	R^2	Lag	Period	Trends ($\text{m}^3/\text{s}/\text{yr}$)
White Volta	0.56	0.75	0.31	1 month	1986/03–2007/02	-6.96^*
Oti	0.38	0.80	0.14	2 months	1996/03–2007/02	-380.24
Black Volta	0.58	0.80	0.34	1 month	1990/03–2007/02	27.6^*

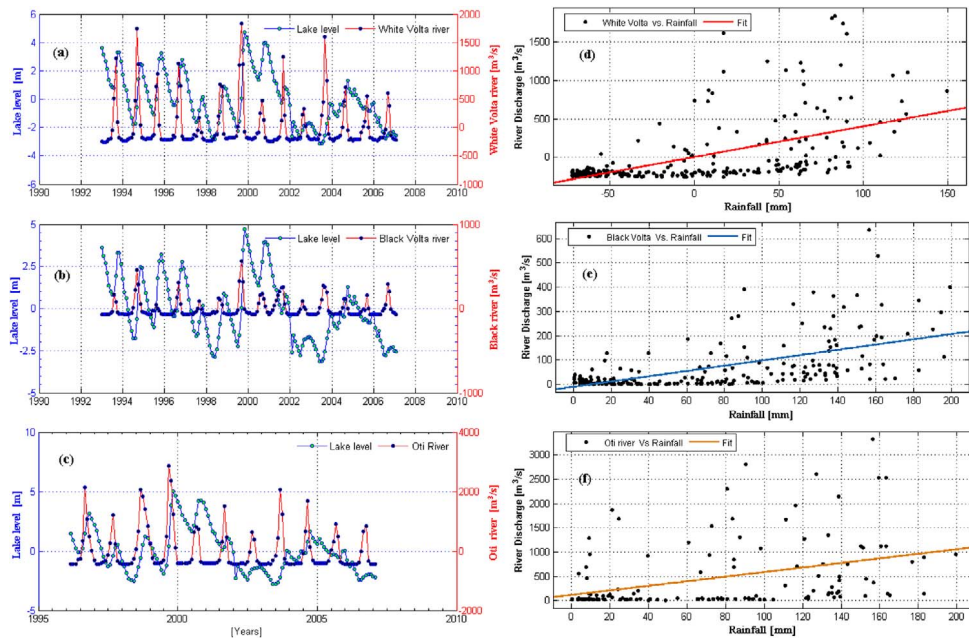


Fig. 11. Relationship between precipitation in the Volta basin and the Lake Volta/the Volta river system. (a)–(c) Time series of Lake Volta water level anomalies (i.e., after removing the mean) and anomalies of White Volta (1993–2007), Black Volta (1990/03–2007/02), and Oti (1996/03–2007/02) rivers. (d)–(f) Regression fits between rainfall and the stream flows of White Volta (1986–2007/02), Black Volta (1990/03–2007/02), and Oti (1996/03–2007/02) rivers. The R^2 values summarising the relationship between precipitation and the Volta river system are provided in Table 3.

decline of 1980 while the increase of rainfall, which started in 2006 was reflected in river discharge in 2007 (Fig. 12), presupposing a lag of 1–2 years or less (i.e., when other time windows are also analysed). This is also consistent with the results discussed previously in Section 5.3. This preceding circumstance (i.e., the time lag) in the observed relationship between rainfall and river discharge, which may not be unconnected with the diversions from the Volta basin watershed and the interconnected Volta river system with numerous tributaries, could be critical information useful for management decisions in water resources planning. The link between rainfall and river discharge (i.e., CRD and CRDD) was also found to be stronger at annual scales compared to monthly scales, which showed a correlation of 0.57 (See Appendix A1 Fig. 16).

Further comparison of lake levels, river discharge, and TWS (i.e., at annual scales) with CRD, generally show the apparent relationship of rainfall and these water fluxes (see Fig. 13). TWS show the strongest association with a correlation of 0.81 with CRD compared to river discharge and lake levels with correlations of 0.42 and 0.57 with CRD, respectively. Such relationship may be

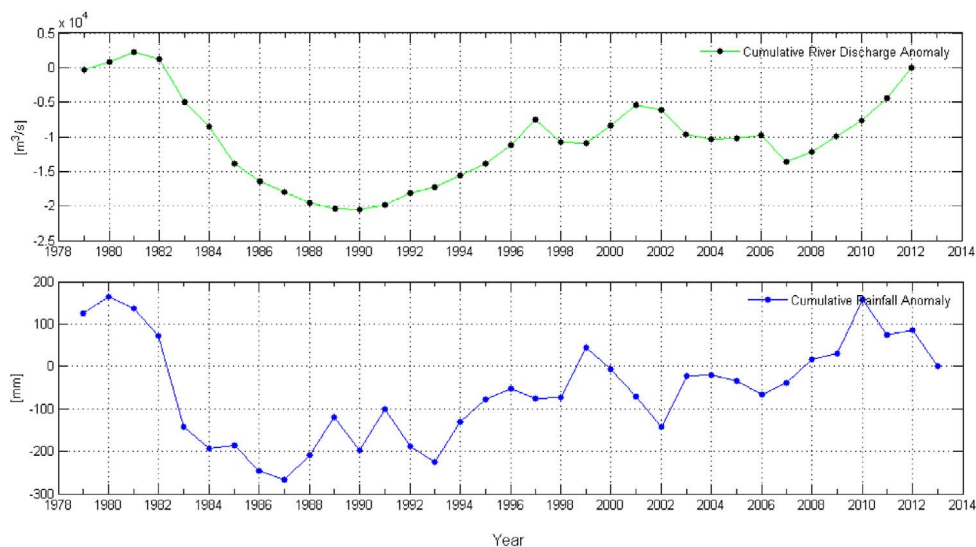


Fig. 12. Cumulative river discharge departure (CRDD) and cumulative rainfall departure (CRD) over Lake Volta basin using the GPCC based precipitation and river discharge at Akosombo station, respectively. Top: Annual cumulative river discharge anomaly over the basin during 1979–2012 period. Bottom: Annual cumulative rainfall anomaly over the basin during 1979–2013 period.

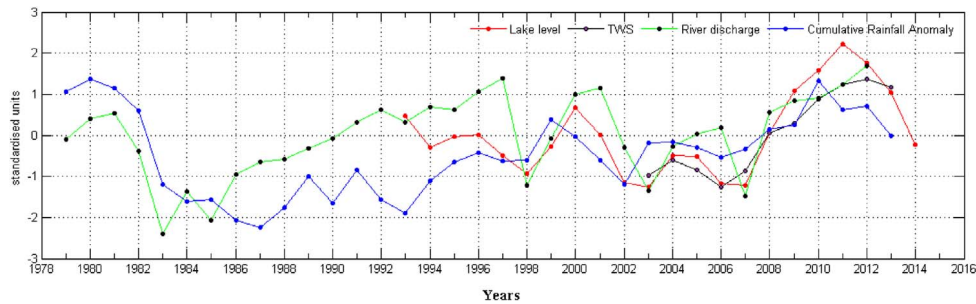


Fig. 13. Comparison of river discharge at Akosombo station, Lake Volta water levels, and change in TWS to cumulative rainfall departures (i.e., using GPCP based precipitation). The standardised annual cumulative quantities of river discharge (1979–2012), lake level variations (1993–2014), and TWS anomalies (2003–2013) over the Volta basin are compared to cumulative rainfall departures (1979–2013).

expected as TWS in the basin is driven mostly by precipitation changes. Although all water fluxes demonstrate a level of significant sensitivity to rainfall conditions in the basin, river discharge and lake levels in particular reveal some reservoir storage characteristics. For example, a close examination of Fig. 13 shows that a rise in river discharge preceded a rise in CRD during the 1984–1986 period while in the case of the Lake Volta water levels, we found that lake level declines prior to a decline in CRD mostly with an approximate time lag of one year (Fig. 13). Besides the diversion of water into other watersheds and tributaries in the Volta river system, which may partly account for this hydrological response, the influence of previous years rainfall largely controls the Lake's current behaviour and by extension the river discharge at Akosombo, which depends on the inflow from the Volta river system into the Lake. This, for example, was the case in 2003 when the lake level and river discharge were extremely low due to extreme dry conditions of the immediate previous years of 2000–2002 (see Fig. 9, top).

However, opening the spillways of the Akosombo dam to let out excess water in the reservoir as was the case in 2010 due to extreme wet conditions in the basin during late 2007 and 2010 periods (e.g., Ndehedehe et al., 2016c), may create an exception to this rule of thumb, given that a fall in CRD from 2010 up until 2013 was accompanied by a rise in river discharge during the same period (see Fig. 13). During low rainfall periods, low water table and diminished base flows are expected. As further explained by Weber and Stewart (2004), when decreased base flows are combined with reduced over-land runoff, it unarguably culminates in lower stream discharge. In our case, the river discharge showed a consistent rise since late 2007 up until 2012 (see top panels of Figs. 9 and 13) even when the CRD had indicated decline since 2010, confirming an excess discharge flow that was inconsistent with rainfall trends in the basin during the 2010–2012 period (see Fig. 9, top).

It has been argued that periods of unusual rainfall caused by climate teleconnection patterns (e.g., ENSO) create the probability of a reset of hydrological conditions through the provision of extensive recharge to aquifers and filling up of existing surface storage (Weber and Stewart, 2004). Consequently, such influence (i.e., extraordinary rainfall) leads to flood conditions in the region (e.g., Paeth et al., 2012) on the one hand, while on the other hand, the aftermath of such stupendous amount of rainfall increases aquifer storage and inundated areas leading to increased TWS changes (e.g., Ndehedehe et al., 2016a). This occurs specifically in regions with high soil infiltration capacity and hydraulic conductivity (e.g., Descroix et al., 2009). Since surface waters, soil moisture, groundwater, and wetlands are the major catchment stores that drives changes in TWS in the Lake Volta area (i.e., around the lower Volta basin), the water ponding and spilling of Akosombo is likely to create a provisional or spurious trend in TWS. This is one reason why the TWS (i.e., with the Lake induced TWS) over the basin also indicated a rise during the 2010–2012 period, consistent with river discharge during the same period despite the apparent fall in CRD since 2012 (Fig. 13). To buttress further on the impacts of the Lake on TWS over the basin, when it was separated (see Section 5.1), interestingly, a close inspection revealed that the Lake-induced TWS (see Fig. 4 top), which is usually triggered by annual and seasonal rainfall over the basin indicated a decline during 2010–2014 period, consistent with CRD and the lake level (Fig. 13). However, between 2012 and 2013, it seems there was a reset of hydrological conditions as both the CRD and TWS indicated a fall (Fig. 13), consistent with the lake level, which also indicates a fall during the same period (Fig. 13).

5.5. Hydropower reservoir system of the Lake Volta and the impact of climate variability

The concept of stationarity assumption in hydrological time series is said to have been compromised by human activities in river basins (Genz and Luz, 2012). The construction of dams and land use change, for example, apart from contributing to non-stationarity in hydrological time series (e.g., Ngom et al., 2016; Descroix et al., 2009; Leblanc et al., 2008), amplifies natural climate changes, environmental conditions (e.g., increase in Hortonian runoff due to changes in infiltration capacity), and the impacts of atmospheric circulations and low frequency internal variability. This is the case for the Volta basin, where the flow records (not shown) of the Volta river downstream Akosombo during the 1936–1966 period indicate natural variability consistent with precipitation changes in the pre dam construction era, unlike the post dam era, where the generation of flows at Akosombo are the results of water management strategy. After the damming of the river at Akosombo, not only has there been tremendous changes in the hydrological regimes of the river, the impact of small changes in precipitation leading to large changes in runoff has also been reported (Oguntunde and Friesen, 2006; Friesen et al., 2005). Apart from other known consequence of damming rivers in order to generate hydropower (for example, decline in annual sediment flux and discharge, reservoir aggradations, and water quality degradation) (see,

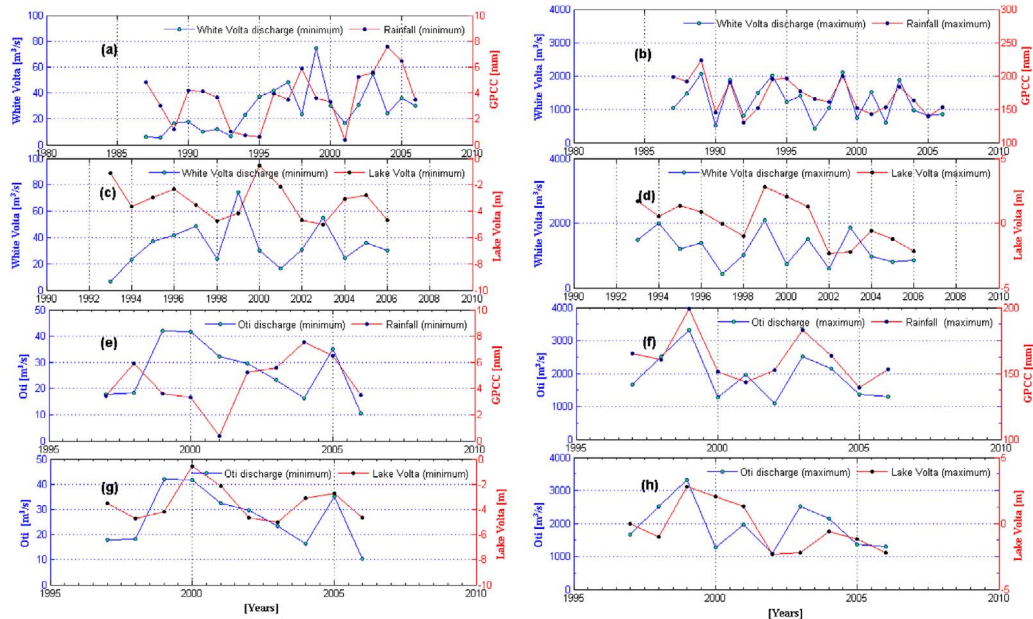


Fig. 14. Analysis of extreme annual rainfall (1986–2006), White Volta river discharge (1986–2006), Oti river discharge (1997–2006), and satellite altimetry derived water levels (1993–2006). (a)–(d) Maximum and minimum White Volta river discharge compared with those of Lake Volta water levels, and GPCC based precipitation over the Volta basin. (e)–(h) Maximum and minimum Oti river discharge compared with those of Lake Volta water levels, and GPCC based precipitation over the Volta basin.

e.g., Fan et al., 2015; Gyau-Boakye, 2001), the impacts of climate variability on water availability in the Lake and the corresponding basin is a critical issue for consideration. In the preceding sections, much about the associations of the Volta river system with rainfall have been discussed. Here, the mechanisms of extremes in rainfall and its link to stream flow (especially the Oti and White Volta rivers) and Lake levels are considered. Most importantly, the hydrological condition of Lake Volta is characterised using annual stream flow of Akosombo and the Lake levels.

5.5.1. Analysis of extremes on the Volta river system and Lake Volta

The statistically significant (i.e., $\alpha = 0.05$) rising trend of $1.66 \text{ m}^3/\text{s}/\text{yr}$ in minimum flow of the White Volta coincides with the increase in rainfall ($0.13 \text{ mm}/\text{yr}$) in the basin during 1986–2006 period (Fig. 14a). But the observed decline in maximum flow ($20.4 \text{ m}^3/\text{s}/\text{yr}$) of White Volta is not statistically significant unlike the decline in maximum rainfall ($1.92 \text{ mm}/\text{yr}$) during the period (Fig. 14b). Comparing the White Volta and Lake Volta water levels during a common period where both data are available (1992–2006), the trends in their minimum quantities ($0.56 \text{ m}^3/\text{s}/\text{yr}$ and $-0.1 \text{ m}/\text{yr}$, respectively) are not statistically significant (Fig. 14c) while only Lake Volta showed a statistically significant trend ($-0.25 \text{ m}/\text{yr}$) (Fig. 14d) when the trends of their maximum values were estimated. While rainfall is expected to impact on the generation of flows, their extremes in the Volta basin raises the question of whether observed trends have any connection with human influence. Since the White Volta river nourishes the Lake, the lack of a statistically significant trend in the maximum flow of the White Volta may suggest water loss through evaporation from the Lake's surface. In fact, there has been a unanimous position confirming the extensive loss of water through evaporation from the Lake's surface (see, e.g., Leemhuis et al., 2009; Gyau-Boakye, 2001; Giesen et al., 2001).

Although other existing smaller water infrastructures in the basin contribute to water loss, Leemhuis et al. (2009) emphasized that water losses through evaporation from Lake Volta are three times higher than losses emanating from small and medium scale reservoirs in the basin. Also, given the source of the White Volta (i.e., Burkina Faso) where larger withdrawals of surface water are mainly employed in agriculture as reported by Giesen et al. (2001), the coupled effect of a statistically significant decline in rainfall and human intervention, which restrict the rate of inflow into the Lake, when superimposed on the water loss through evaporation from the Lake's surface are possible reasons that may largely account for the statistically significant decline in maximum lake water levels observed during the period. Changes in evaporation of lakes impact significantly on the energy and water budgets. For instance, in the Lake Volta, Giesen et al. (2001) reported a net precipitation deficit resulting from water budget imbalance between precipitation and evaporation while Gyau-Boakye (2001) attributed the decline in the Lake's water level to observed rising temperatures and diminished runoff from the Volta river system, resulting from precipitation deficits. As shown earlier in Section 5.3.2, during the 2002–2014 period, the observed decline in net precipitation coincides with precipitation decline and loss of water storage in the Volta basin. However, irrespective of the period considered for the trend analysis, the negative trend in maximum rainfall, is consistent with those of White Volta ($-41.9 \text{ m}^3/\text{s}/\text{yr}$, though statistically insignificant) and Lake levels.

For the Oti river (Fig. 14, e–h), the trends in the maximum and minimum river discharge ($-88.1 \text{ m}^3/\text{s}/\text{yr}$ and $-0.82 \text{ m}/\text{yr}$, respectively) were negative, consistent with those of Lake Volta water levels ($-0.33 \text{ m}/\text{yr}$ and $-0.04 \text{ m}/\text{yr}$ for maximum and minimum estimates, respectively) and rainfall (only the maximum estimate indicated a decline of $-2.0 \text{ mm}/\text{yr}$ while the minimum

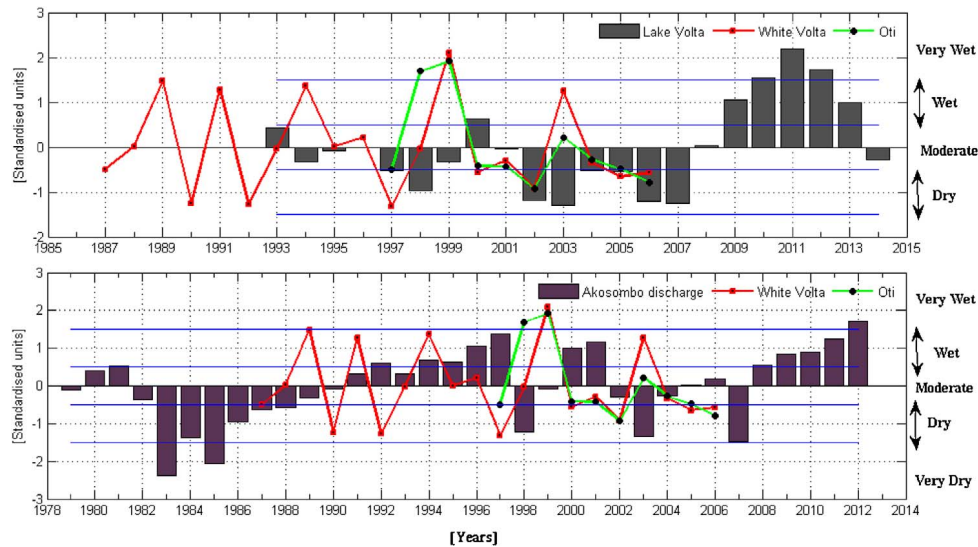


Fig. 15. Recent hydrologic condition of Lake Volta. Top: Time series of annual Lake Volta water level changes (1993–2014), the White Volta (1987–2006), and Oti (1997–2006) rivers. Bottom: Time series of annual Akosombo discharge (1979–2012), White Volta and Oti (1997–2006) rivers. The blue lines define the limits of each hydrological condition class. (For interpretation of the references to color in this figure legend, the reader is referred to the web version of the article.)

estimate was 0.22 mm/yr) during the common period (1997–2006). These trends were all statistically insignificant ($\alpha = 0.05$) for the different periods evaluated. The observed association between the extremes of the White Volta and Oti rivers with rainfall in the basin and the Lake Volta is however, instructive and revealing. For instance, a negative correlation of -0.42 was observed between minimum White Volta river and the Lake Volta water level (Fig. 14c) while the Oti river showed positive correlation of 0.53 with Lake Volta water level (Fig. 14g). Apart from the hydraulic characteristics of the catchment, this could imply that a large proportion of the minimum flow of the White Volta (possibly due to limited and declining rainfall) does not reach the Lake, as it is likely to be lost in transit or intercepted due to diversions in the watersheds outside Ghana. The maximum flows of these two rivers however indicated positive correlations (0.38/0.38) with the Lake (Fig. 14d and h), consistent with their strong positive correlations of 0.69 (White Volta river) and 0.81 (Oti river) with rainfall (Fig. 14b and f) during the periods considered. Generally, maximum correlations ranging from 0.79 to 0.94 between the two rivers and rainfall were obtained at 1 year lag and less (i.e., their minimum and maximum quantities), consistent with the results in previous sections. This relationship is useful in assessing the alterations in hydrological regime resulting from climate variations.

5.5.2. Recent hydrological conditions of the Lake Volta

To understand the hydrological regimes of the Lake Volta, the flow records of Akosombo and lake water levels were combined with the flow data of the two major rivers that nourish the Lake (i.e., White Volta and Oti rivers). Contrary to Section 5.3.2, the standardised annual anomalies of the Lake have been used to express the hydrological characteristics of the Lake. The standardised annual anomalies of the White Volta and Oti rivers for the available period have also been incorporated to support the discussion in this section. Between 2001 and 2007 it appears the Lake has been consistently dry (Fig. 15, top) compared to the 2009–2013 period that is wet. The dry condition of the 2002–2007 period is consistent with the water storage (i.e. altimetry derived water storage) deficit over the Lake during the same period (Fig. 4, top). After the 1999 La-Niña, which resulted in very wet conditions of the Volta river system and wet conditions in the Lake, the dry (2000 and 2002) and moderate (2001) conditions of the White Volta and Oti rivers have significantly impacted the Lake hydrological condition in 2002 and 2003, resulting in dry conditions (Fig. 15, top), despite the improved rainfall over the basin and the wet conditions of these rivers in 2003 (though the Oti river indicated a moderate condition in 2003 possibly due to the mean of the period analysed). Since mankind naturally responds to variations in climate, the periods of limited flows in the White Volta and Oti rivers must have been exacerbated by human intervention (e.g., irrigation development), owing to increased demand and use of surface water in the basin. This is marginally stated as the impact of climate variability in the basin, (e.g., the low flows of these rivers during 2000–2002 and 2004–2006 periods) appears to be more critical. However, as reported by Smakhtin (2001), human activities such as deforestation and irrigation development have lead to increased frequency of occurrence of low-flow discharges in hydrological regimes of rivers.

Under the global change in the hydrological cycle Volta Project (see, Andreini et al., 2002), the impact of water infrastructures in the Volta basin, such as the development of small and medium scale reservoirs in Burkina Faso and northern Ghana in the early 1970s is known to have initiated the loss of water storage in the Lake Volta (Leemhuis et al., 2009). While the White Volta and Oti rivers indicate moderate and dry conditions during 2004–2006 period, consistent with the Lake (Fig. 15, top), the Lake's water storage, which is also marginally affected by these small water infrastructures during long dry periods, naturally affects the generation of flows downstream Akosombo (Fig. 15, bottom). We note that the difference in the hydrological condition of the Lake (2002–2007) as characterised using the satellite altimetry data (Fig. 15, top) and that of the Akosombo river flow during the same period (Fig. 15,

81 bottom), could be due to the adopted mean of the Akosombo stream flow, which references the 1979 climatology. Apart from the response of the Lake to incoming flows, which is about 12 months or less, the hydrological rationale for a relationship between river discharge (i.e., the Volta river system) and the Lake's water level spanning a period of 1–2 years is true for the Volta basin. The probable impact of climate variability on the Lake's water level as indicated in the clustering of dry years 2002–2007 and wet years 2009–2013 (Fig. 15, top), appears to be a 4–5 year cycle (cf. Fig. 9, top), consistent with the long term Akosombo stream flow (Fig. 15, bottom). Continuous gauge measurements of the three rivers (White Volta, Black Volta, and Oti rivers) will allow this cycle to be further confirmed and also for the impacts of climate variability and human interventions in the basin to be quantified.

6. Conclusions

The impacts of large water projects such as the Akosombo dam in the Volta river basin and other human interventions have complicated the understanding of natural hydrological variability and the influence of climate variations on the basin's freshwater systems. In this contribution, we have investigated the hydrological variability of the Volta basin (including the Lake Volta) using GPCP based precipitation, river discharge, GRACE-derived TWS, evapotranspiration, and satellite altimetry water level variations. A two-step procedure based on a weighted least squares formulation of global spherical harmonic analysis and statistical decomposition was employed to support the understanding of the Volta basin's natural hydrology and its freshwater systems. The results from this study are summarised as follows:

- (1) Increased trends of TWS over the Volta basin and the Lake Volta were observed. The empirical approach adopted to disengage the Lake induced water storage enhanced the understanding of the natural hydrological variability of the Volta basin. In view of the increasing attention to the impacts of climate variability in the region, this information is helpful and instructive for regional water resources management and in addition, provides a basis for productive trans-boundary water sharing conversations.
- (2) The statistical decomposition of residual TWS (i.e., after removing Lake Volta induced TWS) resulted in a decline of water storage for the period between 2007 and 2011 at the lower Volta catchment. The loss of water storage during this period could be a base flow recession resulting from precipitation decline during the 2002–2014 period and the extended periods of dry conditions around the vicinity of the Lake between 2000 and late 2007.
- (3) Declining trends in recent altimetry-derived water level variations of Lake Volta (2011–2015) are consistent with the decline of rainfall and net precipitation during the 2002–2014 period. This decline is also attributed to the cumulative impact of limited stream flows from the Volta river system. The study also confirms the impact of critical hydrological periods (e.g., previous extreme dry periods) and human water management (e.g., spilling of the reservoir at downstream Akosombo in 2010) on the basin. During these periods, trends in rainfall are usually accompanied with inconsistent trends in lake water levels and discharge flow at Akosombo.
- (4) The results also show that extended dry periods as observed between 2001 and late 2007 diminishes the quantity of freshwater that is required to sufficiently satisfy water demand for agriculture (in Burkina Faso) and hydro-power (in Ghana) in the region, such that the extreme wet periods (e.g., 2003) made no hydrological difference in the dry condition of the Lake Volta during the period that followed (2003–2006). Although the amplitude of Oti river discharge was more than 2000 m³/s in 2004, the limited flows of the Volta river system in 2005 and 2006 created a water deficit condition that resulted in a long dry period in the basin.
- (5) The Lake Volta shows relatively strong sensitivity and lag to rainfall conditions and incoming flows from the Volta river system in the basin spanning between less than one year and up to two years. Nonetheless, the wet conditions of 2003 in the basin as indicated in (4) above, is inconsistent with the clustering of dry conditions in the Lake during 2003–late 2007 period. Since mankind naturally responds to changes in climate, this may suggest a possible water conservation and management strategy by the Volta river basin authority, to cushion the impact of the extended dry periods of the previous years caused by the influence of natural climate variations, on the Lake's hydropower potential. In addition, a 4–5 year cycle between dry and wet periods, resulting from the impact of climate variability in the basin was noticed.
- (6) As the reservoir system of the Lake Volta is naturally connected to the Volta river system, the effects of this change in flow regime of the Volta river system and rainfall is likely to impact negatively on the water resources of the basin, perhaps the beginning of the Lake's desiccation if the trends are not reversed. With the availability of consistent and up to date gauge measurements of the three rivers (White Volta, Black Volta, and Oti rivers), the probability of the Lake's desiccation and the impact of human interventions such as the development of small and medium scale reservoir systems in the basin can be quantified.

Acknowledgments

Christopher E. Ndehedehe and Nathan Agutu are grateful to Curtin University for the funding received through the CSIRS programme. Joseph is grateful for the financial support of the Japan Society of Promotion of Science for supporting his stay at Kyoto University (Japan) and the conducive working atmosphere provided by his host Prof Yoichi Fukuda (Department of Geophysics, Kyoto University, Japan). Also, we thank the USDA for the Satellite altimetry data and GPCP for the precipitation product used. The Authors are grateful to CSR, NASA, and Water Research Institute of Ghana and GRDC, for the river discharge data used in this study. The support and contributions of Tertiary Trust Fund (TETFUND) Nigeria towards this research is also acknowledged.

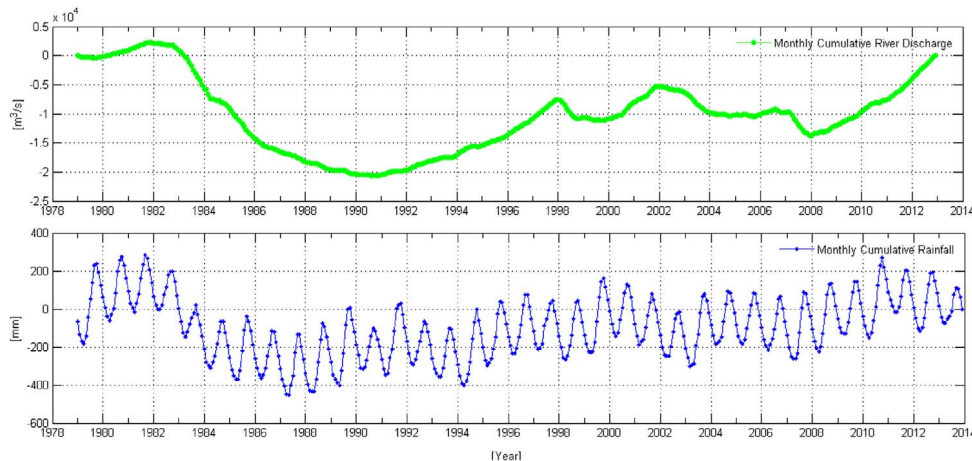


Fig. 16. Cumulative monthly rainfall and river discharge anomalies averaged over the Volta basin using the GPCP based precipitation and river discharge at Akosombo station, respectively. Top: Monthly cumulative river discharge anomaly over the basin during 1979–2012 period. Bottom: Monthly cumulative rainfall anomaly over the basin during 1979–2013 period.

Appendix A1. : Cumulative rainfall and river discharge departures

Appendix A2. : Recent trends in Lake Volta water levels (2002–2015)

The trends in Lake height variations (i.e., after removing the temporal mean of the period between 2002 and 2015) were further analysed using the method of least squares. The results indicate that 19.635 km^3 of water was gained between August 2007 and December 2010 while about 19.125 km^3 of water has been lost from January 2011 to date. Fig. 2 shows these periodic fluctuations and trends in lake level variations over Lake Volta during the GRACE period. The Lake Volta apparently shows a relatively strong rise and fall in lake heights during the 2007–2015 period compared to the 2002–late 2006 period. Specifically, between the periods 2002–2005 and 2005–2007, an estimated loss of 3.57 km^3 of water, compared with the gain of 0.51 km^3 of water for the periods between 2007–2011 and 2011–2015 largely indicates an approximate loss of 3.06 km^3 of water in the Lake for the entire period (i.e., 2002–2015). Since changes in surface water (i.e., Lakes, and reservoirs) in this region is largely driven by rainfall, the decline in the lake level is mostly attributed to the negative trends in precipitation (during the 2002–2014 period) around the vicinity of the Lake. The fall in the amplitude of the lake level in 2010/2011 may have been the fall-out of spilling the reservoir (Owusu and Waylen, 2013) due to heavy rainfall caused by a La-Niña event in 2010. Although this is rather implied than stated, the results of this study confirm that extreme rainfall in 2010 in the Volta basin is consistent with the strong rise of water level in the Lake Volta in the same year (Fig. 2). However, from a long term perspective of extreme rainfall conditions, emerging facts in a recent study by Ndehedehe et al. (2016c) indicate that Burkina Faso and the Lake Volta areas are predominantly drought zones with the possible influence of low frequency large scale oscillations. They specifically reported a hydrological drought condition at the Lake Volta area during the 2011–2013 period. This period falls within the most recent time window (2011–2015) of observed declines in lake level (Fig. 2). The results presented in Section 5.4 also confirm that besides 2003, 2007, and 2010, which were relatively wet years due to ENSO rainfall, the basin was generally characterised by precipitation deficits as extreme low standardised rainfall values were largely predominant.

The impact of rainfall on the Lake is well known. For instance, during the severe drought of 1983, the water level dropped drastically, reaching its lowest limit of 72 m (i.e., above mean sea level) in 1984 and rising again to maximum levels in 1989 and 1992, respectively during the periods of high rainfall (see, Zwiiten et al., 2011). Moreover, hydrological drought years such as 1983, 1998, 2006 culminated in power rationing for the successive years of 1983/1984, 1999, and 2006/2007, respectively (see, Ndehedehe et al., 2016c; Bekoe and Logah, 2013). Tributaries such as the Black Volta and White Volta (see Fig. 1), which flows into Lake Volta are largely rain-fed. The Lake, which benefits from these tributaries swells and shrinks during the rainy and dry seasons, respectively. Furthermore, between 1966 and 2006, Zwiiten et al. (2011) reported an average gradual decrease of 15 cm/yr in water levels. The observed decline of $2.25 \pm 0.10 \text{ m/yr}$ from January 2011 to date may impact negatively on the Lake as the lowest minimum water level of 2015 is approaching those of water deficit years of 2003 and early 2007 (Fig. 2). In addition to the influence of hydro-meteorological conditions, non-climatic factors such as the widespread construction of numerous hydraulic infrastructures (e.g., small-scale reservoirs and large scale irrigation systems) in Burkina Faso and Ghana for water mobilization to support agriculture in the basin, especially during the long dry season, have been reported (e.g., Amisigo et al., 2014). This and evaporation loss over the Lake may ultimately put the water resources of the lower Volta at risk.

83 References

- Ahmed, M., Sultan, M., Wahr, J., Yan, E., 2014. The use of GRACE data to monitor natural and anthropogenic induced variations in water availability across Africa. *Earth Sci. Rev.* 136, 289–300. <http://dx.doi.org/10.1016/j.earscirev.2014.05.009>.
- Aires, F., Rossow, W.B., Chédin, A., 2002. Rotation of EOFs by the independent component analysis: toward a solution of the mixing problem in the decomposition of geophysical time series. *J. Atmos. Sci.* 59, 111–123. [http://dx.doi.org/10.1175/1520-0469\(2002\)059<0111:ROEBTI>2.0.CO;2](http://dx.doi.org/10.1175/1520-0469(2002)059<0111:ROEBTI>2.0.CO;2).
- Alley, W.M., Konikow, L.F., 2015. Bringing GRACE down to earth. *Groundwater* 53 (6), 826–829. <http://dx.doi.org/10.1111/gwat.12379>.
- Amisigo, B.A., McCluskey, A., Swanson, R., 2014. Modeling impact of climate change on water resources and agriculture demand in the Volta Basin and other basin systems in Ghana. pp. 20. Retrieved from: <http://www.wider.unu.edu/publications/working-papers/2014/en-GB/wp2014-033> (accessed 10.11.15).
- Andam-Akorful, S.A., Ferreira, V.G., Awange, J.L., Forootan, E., He, X.F., 2015. Multi-model and multi-sensor estimations of evapotranspiration over the Volta Basin, West Africa. *Int. J. Climatol.* 35 (10), 3132–3145. <http://dx.doi.org/10.1002/joc.4198>.
- Andreini, M., van de Giesen, N., van Edig, A., Fosu, M., Andah, W., 2000. Volta Basin water balance. Zentrum für Entwicklungsforschung (ZEF)-Discussion Papers On Development Policy. pp. 29. Retrieved from: http://www.zef.de/uploads/tx_zefportal/Publications/zef-dp21-00.pdf (accessed 05.09.16).
- Andreini, M., Vlek, P., Giesen, N.V.D., 2002. Water sharing in the Volta basin. In: Proceedings of the Fourth International FRIEND Conference. South Africa FRIEND. pp. 329–335.
- Awange, J., Forootan, E., Kuhn, M., Kusche, J., Heck, B., 2014. Water storage changes and climate variability within the Nile Basin between 2002 and 2011. *Adv. Water Resour.* 73 (0), 1–15. <http://dx.doi.org/10.1016/j.advwatres.2014.06.010>.
- Barry, B., Obuobie, E., Andreini, M., Andah, W., Pluquet, M., 2005. Comprehensive assessment of water management in agriculture: comparative study of river basin development and management. *Int. Water Manag. Inst.* Retrieved from: www.iwmi.cgiar.org/assessment (accessed 11.11.15).
- Baur, O., Kuhn, M., Featherstone, W.E., 2009. GRACE-derived ice-mass variations over Greenland by accounting for leakage effects. *J. Geophys. Res.: Solid Earth* 114 (B6), B06407. <http://dx.doi.org/10.1029/2008JB006239>.
- Becker, A., Finger, P., Meyer-Christoffer, A., Rudolf, B., Schamm, K., Schneider, U., Ziese, M., 2013. A description of the global land-surface precipitation data products of the Global Precipitation Climatology Centre with sample applications including centennial (trend) analysis from 1901 to present. *Earth Syst. Sci. Data* 5 (1), 71–99. <http://dx.doi.org/10.5194/essd-5-71-2013>.
- Bekoe, E.O., Logah, F.Y., 2013. The impact of droughts and climate change on electricity generation in Ghana. *Environ. Sci.* 1 (1), 13–24.
- Belda, S., García-García, D., Ferrándiz, J.M., 2015. On the decorrelation filtering of RL05 GRACE data for global applications. *Geophys. J. Int.* 200, 173–184. <http://dx.doi.org/10.1093/gji/ggu386>.
- Boergens, E., Rangelova, E., Sideris, M.G., Kusche, J., 2014. Assessment of the capabilities of the temporal and spatiotemporal ICA method for geophysical signal separation in GRACE data. *J. Geophys. Res. Solid Earth* 119, 4429–4447. <http://dx.doi.org/10.1002/2013JB010452>.
- Cardoso, J.F., 1999. High-order contrasts for independent component analysis. *Neural Comput.* 11, 157–192.
- Cardoso, J.F., Souloumiac, A., 1993. Blind beamforming for non-Gaussian signals. *IEE Proc.* 140 (6), 362–370.
- Cheng, M.K., Tapley, B.D., Ries, J.C., 2013. Deceleration in the Earth's oblateness. *J. Geophys. Res.* 118, 1–8. <http://dx.doi.org/10.1002/jgrb.50058>.
- Coe, M.T., Birkett, C.M., 2004. Calculation of river discharge and prediction of lake height from satellite radar altimetry: example for the Lake Chad basin. *Water Resour. Res.* 40 (10), W10205. <http://dx.doi.org/10.1029/2003WR002543>.
- Common, P., 1994. Independent component analysis. A new concept? *Signal Process.* 36, 287–314.
- Descroix, L., Mahé, G., Lebel, T., Favreau, G., Galle, S., Gautier, E., Olivry, J.-C., Albergel, J., Amogu, O., Cappelaere, B., Dessouassi, R., Diedhiou, A., Breton, E.L., Mamadou, I., Sighomnou, D., 2009. Spatio-temporal variability of hydrological regimes around the boundaries between Sahelian and Sudanian areas of West Africa: a synthesis. *J. Hydrol.* 375 (1–2), 90–102. <http://dx.doi.org/10.1016/j.jhydrol.2008.12.012>.
- Deus, D., Gloaguen, R., Krause, P., 2013. Water balance modelling in a semi arid environment with limited in situ data using remote sensing in lake Manyara, East African rift, Tanzania. *Remote Sens.* 5, 1651–1680. <http://dx.doi.org/10.3390/rs5041651>.
- Fan, H., He, D., Wang, H., 2015. Environmental consequences of damming the mainstream Lancang-Mekong river: a review. *Earth-Sci. Rev.* 146, 77–91. <http://dx.doi.org/10.1016/j.earscirev.2015.03.007>.
- Ferreira, V., Asiah, Z., 2015. An investigation on the closure of the water budget methods over Volta Basin using multi-satellite data. *Int. Assoc. Geodesy Symposia.* <http://dx.doi.org/10.1007/1345-2015-137>.
- Ferreira, V.G., Gong, Z., Andam-Akorful, S.A., 2012. Monitoring mass changes in the Volta River Basin Using GRACE satellite gravity and TRMM precipitation. *Boletim De Ciencias Geodesicas* 18 (4), 549–563 /WOS:000313106300003.
- Ferreira, V.G., Gong, Z., He, X., Zhang, Y., Andam-Akorful, S.A., 2013. Estimating total discharge in the Yangtze River basin using satellite-based observations. *Remote Sens.* 5 (7), 3415–3430. <http://dx.doi.org/10.3390/rs5073415>.
- Forootan, E., Kusche, J., 2012. Separation of global time-variable gravity signals into maximally independent components. *J. Geodesy* 86 (7), 477–497. <http://dx.doi.org/10.1007/s00190-011-0532-5>.
- Frappart, F., Ramillien, G., Leblanc, M., Tweed, S.O., Bonnet, M.-P., Maisongrande, P., 2011. An independent component analysis filtering approach for estimating continental hydrology in the GRACE gravity data. *Remote Sens. Environ.* 115 (1), 187–204. <http://dx.doi.org/10.1016/j.rse.2010.08.017>.
- Friesen, J., Andreini, M., Andah, W., Amisigo, M.A., Giesen, N.V.D., 2005. Storage capacity and long-term water balance of the Volta Basin, West Africa. In: Proceedings of symposium S6 held during the Seventh IAHS Scientific Assembly. Brazil. Retrieved from: <http://iahs.info/uploads/dms/13203.2220138-14520Foz20S6-2-1420Friesen.pdf> (accessed 18.12.15).
- Genz, F., Luz, L., 2012. Distinguishing the effects of climate on discharge in a tropical river highly impacted by large dams. *Hydrol. Sci. J.* 57 (5), 1020–1034. <http://dx.doi.org/10.1080/02626667.2012.690880>.
- Giesen, N.V.D., Andreini, M., Edig, A.V., Vlek, P., 2001. Competition for water resources of the Volta basin. *Reg. Manag. Water Resour.* 268, 199–205. Retrieved from: <http://www.zef.de/fileadmin/template/Glowa/Downloads/> (accessed 12.11.14).
- Giesen, N.V.D., Liebe, J., Jung, G., 2010. Adapting to climate change in the Volta Basin, West Africa. *Curr. Sci.* 98 (8), 1033–1037.
- Gyau-Boakye, P., 2001. Environmental impacts of the Akosombo dam and effects of climate change on the lake levels. *Environ. Dev. Sustain.* 3 (1), 17–29. <http://dx.doi.org/10.1023/A:1011402116047>.
- Jolliffe, I.T., 2002. Principal component analysis. Springer Series in Statistics, second ed. Springer, New York.
- Kasei, R., Diekkrüger, B., Leemhuis, C., 2010. Drought frequency in the Volta Basin of West Africa. *Sustain. Sci.* 5 (1), 89–97.
- Kusche, J., 2007. Approximate decorrelation and non-isotropic smoothing of time-variable GRACE-type gravity field models. *J. Geodesy* 81 (11), 733–749. <http://dx.doi.org/10.1007/s00190-007-0143-3>.
- Landerer, F.W., Swenson, S.C., 2012. Accuracy of scaled GRACE terrestrial water storage estimates. *Water Resour. Res.* 48 (4), W04531. <http://dx.doi.org/10.1029/2011WR011453>.
- Leblanc, M.J., Favreau, G., Massuel, S., Tweed, S.O., Loireau, M., Cappelaere, B., 2008. Land clearance and hydrological change in the Sahel: SW Niger. *Global Planet. Change* 61, 135–150. <http://dx.doi.org/10.1016/j.gloplacha.2007.08.011>.
- Leemhuis, C., Jung, G., Kasei, R., Liebe, J., 2009. The Volta Basin water allocation system: assessing the impact of small-scale reservoir development on the water resources of the Volta basin, West Africa. *Adv. Geosci.* 21, 57–62. <http://dx.doi.org/10.5194/adgeo-21-57-2009>.
- McKee, T.B., Doeskin, N.J., Kieist, J., 1993. The relationship of drought frequency and duration to time scales. Conference on Applied Climatology. American Meteorological Society, Boston, MA, pp. 179–184. Retrieved from: www.ccc.atmos.colostate.edu/relationshipofdroughtfrequency.pdf (accessed 27.06.14).
- Moore, P., Williams, S.D.P., 2014. Integration of altimetry lake levels and GRACE gravimetry over Africa: inferences for terrestrial water storage change 2003–2011. *Water Resour. Res.* 50, 9696–9720. <http://dx.doi.org/10.1002/2014WR015506>.
- Mu, Q., Zhao, M., Running, S.W., 2011. Improvements to a MODIS global terrestrial evapotranspiration algorithm. *Remote Sens. Environ.* 115 (8), 1781–1800. <http://dx.doi.org/10.1016/j.rse.2011.02.019>.
- Ndehedehe, C., Awange, J., Agutu, N., Kuhn, M., Heck, B., 2016a. Understanding changes in terrestrial water storage over West Africa between 2002 and 2014. *Adv.*

- 84 Water Resour. 88, 211–230. <http://dx.doi.org/10.1016/j.advwatres.2015.12.009>.
- Ndehedehe, C.E., Agutu, N.O., Okwuashi, O.H., Ferreira, V.G., 2016b. Spatio-temporal variability of droughts and terrestrial water storage over Lake Chad Basin using independent component analysis. *J. Hydrol.* 540, 106–128. <http://dx.doi.org/10.1016/j.jhydrol.2016.05.068>.
- Ndehedehe, C.E., Awange, J.L., Corner, R., Kuhn, M., Okwuashi, O., 2016c. On the potentials of multiple climate variables in assessing the spatio-temporal characteristics of hydrological droughts over the Volta Basin. *Sci. Total Environ.* 557–558, 819–837. <http://dx.doi.org/10.1016/j.scitotenv.2016.03.004>.
- Ngom, F., Tweed, S., Bader, J.-C., Saos, J.-L., Malou, R., Leduc, C., Leblanc, M., 2016. Rapid evolution of water resources in the Senegal delta. *Global Planet. Change* 144, 34–47. <http://dx.doi.org/10.1016/j.gloplacha.2016.07.002>.
- Oguntunde, P.G., Friesen, J., van de Giesen, N., Savenije, H.H., 2006. Hydroclimatology of the Volta River Basin in West Africa: trends and variability from 1901 to 2002. *Phys. Chem. Earth Parts A/B/C* 31 (18), 1180–1188. <http://dx.doi.org/10.1016/j.pce.2006.02.062>.
- Owusu, K., Waylen, P., 2013. The changing rainy season climatology of mid-Ghana. *Theor. Appl. Climatol.* 112 (3), 419–430. <http://dx.doi.org/10.1007/s00704-012-0736-5>.
- Owusu, K., Waylen, P., Qiu, Y., 2008. Changing rainfall inputs in the Volta basin: implications for water sharing in Ghana. *GeoJournal* 71 (4), 201–210. <http://dx.doi.org/10.1007/s10708-008-9156-6>.
- Paeth, H., Fink, A., Pohle, S., Keis, F., Machel, H., Samimi, C., 2012. Meteorological characteristics and potential causes of the 2007 flood in sub-Saharan Africa. *Int. J. Climatol.* 31, 1908–1926. <http://dx.doi.org/10.1002/Joc.2199>.
- Preisendorfer, R., 1988. *Principal component analysis in meteorology and oceanography. Developments in Atmospheric Science 17.* Elsevier, Amsterdam.
- Rodell, M., Houser, P.R., Jambor, U., Gottschalk, J., Mitchell, K., Meng, K., Arsenault, C.J., Cosgrove, B., Radakovich, J., Bosilovich, M., Entin, J.K., Walker, J.P., Lohmann, D., Toll, D., 2004. The global land data assimilation system. *Bull. Am. Meteorol. Soc.* 85 (3), 381–394. <http://dx.doi.org/10.1175/BAMS-85-3-381.R>.
- Schneider, U., Becker, A., Finger, P., Meyer-Christoffer, A., Ziese, M., Rudolf, B., 2014. GPCC's new land surface precipitation climatology based on quality-controlled in situ data and its role in quantifying the global water cycle. *Theoret. Appl. Climatol.* 115 (1–2), 15–40. <http://dx.doi.org/10.1007/s00704-013-0860-x>.
- Schrama, E.J.O., Wouters, B., Lavallée, D.A., 2007. Signal and noise in Gravity Recovery and Climate Experiment (GRACE) observed surface mass variations. *J. Geophys. Res.: Solid Earth* 112 (B8), B08407. <http://dx.doi.org/10.1029/2006JB004882>.
- Seo, K.-W., Wilson, C.R., Chen, J., Waliser, D.E., 2008. GRACE's spatial aliasing error. *Geophys. J. Int.* 172 (1), 41–48.
- Smakhtin, V., 2001. Low flow hydrology: a review. *J. Hydrol.* 240 (34), 147–186. [http://dx.doi.org/10.1016/S0022-1694\(00\)00340-1](http://dx.doi.org/10.1016/S0022-1694(00)00340-1).
- Sneeuw, N., 1994. Global spherical harmonic analysis by least-squares and numerical quadrature methods in historical perspective. *Geophys. J. Int.* 118 (3), 707–716. <http://dx.doi.org/10.1111/j.1365-246X.1994.tb03995.x>.
- Sneeuw, N., Lorenz, C., Devaraju, B., Tourian, M., Riegger, J., Kunstmann, H., Bárdossy, A., 2014. Estimating runoff using hydro-geodetic approaches. *Surv. Geophys.* 35 (6), 1333–1359. <http://dx.doi.org/10.1007/s10712-014-9300-4>.
- Swenson, S., Chambers, D., Wahr, J., 2008. Estimating geocenter variations from a combination of GRACE and ocean model output. *Geophys. Res. Lett.* 31, 1–4. <http://dx.doi.org/10.1029/2004GL019920>.
- Swenson, S., Wahr, J., 2002. Methods for inferring regional surface-mass anomalies from Gravity Recovery and Climate Experiment (GRACE) measurements of time-variable gravity. *J. Geophys. Res. Solid Earth* 107 (B9). <http://dx.doi.org/10.1029/2001jb000576>.
- Swenson, S., Wahr, J., 2009. Monitoring the water balance of Lake Victoria, East Africa, from space. *J. Hydrol.* 370 (1–4), 163–176. <http://dx.doi.org/10.1016/j.jhydrol.2009.03.008>.
- Tapley, B., Bettadpur, S., Watkins, M., Reigber, C., 2004. The Gravity Recovery and Climate Experiment: mission overview and early results. *Geophys. Res. Lett.* 31, 1–4. <http://dx.doi.org/10.1029/2004GL019920>.
- Theis, F.J., Gruber, P., Keck, I.R., Meyer-bäse, A., Lang, E.W., 2005. Spatiotemporal blind source separation using double-sided approximate joint diagonalization. *Proc. EUSIPCO 2005*.
- Wahr, J., Molenaar, M., Bryan, F., 1998. Time variability of the Earth's gravity field: hydrological and oceanic effects and their possible detection using GRACE. *J. Geophys. Res. Solid Earth* 103 (B12), 30205–30229. <http://dx.doi.org/10.1029/98jb02844>.
- Weber, K., Stewart, M., 2004. Critical analysis of the cumulative rainfall departure concept. *Ground Water* 42 (6), 935–938. Retrieved from: <http://info.ngwa.org/gwol/pdf/042979908.pdf> (accessed 25.03.16).
- Werth, S., Günter, A., Schmidt, R., Kusche, J., 2009. Evaluation of GRACE filter tools from a hydrological perspective. *Geophys. J. Int.* 179 (3), 1499–1515.
- Wouters, B., Schrama, E.J.O., 2007. Improved accuracy of GRACE gravity solutions through empirical orthogonal function filtering of spherical harmonics. *Geophys. Res. Lett.* 34 (23), L23711. <http://dx.doi.org/10.1029/2007GL032098>.
- Ziehe, A., 2005. *Blind Source Separation Based on Joint Diagonalization of Matrices with Applications in Biomedical Signal Processing.* Universität Potsdam. (PhD thesis) Retrieved from: <http://en.youscribe.com/catalogue/reports-and-theses/knowledge/blind-source-separation-based-on-joint-diagonalization-of-matrices-1424347> (accessed 15.05.15).
- Zwieten, P., Béné, C., Kolding, J., Brummett, R., Valbo-Jørgensen, J., 2011. Review of African tropical reservoirs and their fisheries – The cases of Lake Nasser, Lake Volta and Indo-Gangetic Basin reservoirs. *FAO Fisheries and Aquaculture Technical Paper* 557. pp. 148. Retrieved from: <http://www.fao.org/docrep/015/i1969e/i1969e.pdf> (accessed 10.11.15).

4 The influence of climate variability on terrestrial water storage

This chapter is covered by the following publications ([Ndehedehe et al., 2017d,e](#)):

1. **Christopher E. Ndehedehe**, Joseph L. Awange, Michael Kuhn, Nathan Agutu, and Yoichi Fukuda (2017). Influence of climate teleconnections on West Africa's terrestrial water storage. *Hydrological Processes*, 31(18), 3206-3224, [dx.doi.org/10.1002/hyp.11237](https://doi.org/10.1002/hyp.11237).
2. **Christopher E. Ndehedehe**, Joseph L. Awange, Nathan O. Agutu, and Onuwa Okwuashi (2017). Changes in hydro-meteorological conditions over Sub-Saharan Africa (1980 – 2015) and links to global climate. *Revised and resubmitted to Global and Planetary Change*.

Considerable case studies in the past have investigated the impacts of perturbations of the nearby oceans, quasi-periodic phenomena (e.g., ENSO), and other low frequency climate oscillations on precipitation changes in Africa. While such impacts have been widely reported and less debated, the role of SST on changes in long term terrestrial water storage (TWS) has not been studied. This study presents the pioneer results of canonical correlation analyses (CCA) of long term TWS with global SST fields over Sub Sahara Africa-SSA (the region includes all the countries in West Africa and those of Equatorial Africa, which is interchangeably referred to as the Congo basin in this thesis). This study also takes advantage of the prominent gap in the knowledge of climate variability and its impacts on hydrological changes of the Congo basin or the Equatorial region of Africa. Climate modes that impact on TWS have also been identified by combining regression and cumulant statistics. Specifically, the first phase of this chapter discusses the homogenous SST fields from the surrounding oceans (Atlantic, Pacific, and Indian) that impacts on the spatial and temporal dynamics of TWS derived from reanalysis and GRACE data using canonical correlation analysis. Long term changes in rainfall, soil moisture, TWS, and model groundwater are also discussed. Finally (i.e., still in the first phase), in a detailed discussion of leading TWS modes over SSA obtained from a methodology that follows a previous effort discussed in Chapter 2, the driver of GRACE-derived TWS variability in the Congo basin and its link to global climate are also examined. The influence of three prominent climate teleconnection indices (ENSO, AMO, and IOD) on TWS derived from GRACE and global reanalysis data are discussed in the second phase. Although the title of the published paper (see, [Ndehedehe et al., 2017d](#)) suggests the study was limited to West Africa, the discussion

of results in the article covered SSA (i.e., West Africa and Equatorial Africa, which is interchangeably referred to as the Congo basin or Equatorial region in this thesis). Unlike West Africa (see Chapter 2), the Congo river discharge remains a prominent and principal driver of GRACE-derived TWS in the Congo basin and in addition, shows a considerable association with global SST anomalies. ENSO and other low frequency climate oscillations of the Atlantic Ocean (AMO) are also important drivers of long term variations in TWS over SSA, affecting its distributions and temporal changes. It is super interesting that these climate modes also play key roles in the characteristics of extreme climatic conditions in the region (Chapter 5). As the Congo basin is getting drier, it is likely that the huge biodiversity of the region could face a novel stress due to deforestation and climate change. GRACE gravimetry has recently shown agreement with other large scale satellite geodetic missions and the ability to resolve strong signals of water storage variations over surface waters in smaller basins (see, [Ndehedehe et al., 2017c,d](#)). This component of the thesis confirms it is gradually emerging as a stronger ‘tool in the box’ for studies of hydrological changes and monitoring the impacts of climate variability in the data deficient African region.

RESEARCH ARTICLE

Climate teleconnections influence on West Africa's terrestrial water storage

Christopher E. Ndehedehe^{1,3}  | Joseph L. Awange^{1,2} | Michael Kuhn¹ | Nathan O. Agutu^{1,4} | Yoichi Fukuda²

¹Department of Spatial Sciences, Curtin University, Perth, Western Australia, Australia

²Department of Geophysics, Kyoto University, Kyoto, Japan

³Department of Geoinformatics and Surveying, University of Uyo, Uyo, Nigeria

⁴Department of Geomatic Engineering and Geospatial Information Systems, Jomo Kenyatta University of Agriculture and Technology, Nairobi, Kenya

Correspondence

Christopher E. Ndehedehe, Department of Spatial Sciences, Curtin University, Perth, Western Australia, 6102, Australia.
Email: christopherndehe@gmail.com

Abstract

There is some evidence of rapid changes in the global atmosphere and hydrological cycle caused by the influence of climate variability. In West Africa, such changes impact directly on water resources leading to incessant extreme hydro-meteorological conditions. This study examines the association of three global climate teleconnections—El-Niño Southern Oscillation (ENSO), Indian Ocean Dipole (IOD), and Atlantic Multi-decadal Oscillation (AMO) with changes in terrestrial water storage (TWS) derived from both Modern-Era Retrospective Analysis for Research and Applications (MERRA, 1980–2015) and Gravity Recovery and Climate Experiment (GRACE, 2002–2014). In the Sahel region, positive phase of AMO coincided with above-normal rainfall (wet conditions) and the negative phase with drought conditions and confirms the observed statistically significant association ($r = 0.62$) between AMO and the temporal evolutions of standardised precipitation index. This relationship corroborates the observed presence of AMO-driven TWS in much of the Sahel region (though considerably weak in some areas). Although ENSO appears to be more associated with GRACE-derived TWS over the Volta basin ($r = -0.40$), this study also shows a strong presence of AMO- and ENSO-induced TWS derived from MERRA reanalysis data in the coastal West African countries and most of the regions below latitude 10°N. The observed presence of ENSO- and AMO-driven TWS is noticeable in tropical areas with relatively high annual/bimodal rainfall and strong inter-annual variations in surface water. The AMO has a wider footprint and sphere of influence on the region's TWS and suggests the important role of North Atlantic Ocean. IOD-related TWS also exists in West Africa and its influence on the region's hydrology maybe secondary and somewhat complementary. Nonetheless, presumptive evidence from the study indicates that ENSO and AMO are the two major climatic indices more likely to impact on West Africa's TWS.

KEYWORDS

climate variability, droughts, ENSO, rainfall, SPI, West Africa

1 | INTRODUCTION

Extreme climatic conditions (e.g., droughts and floods) in West African countries (Figure 1) caused by large-scale ocean–land–atmospheric interactions and global climate teleconnections, for example, El-Niño Southern Oscillation (ENSO), represent considerable impact on annual and seasonal variability in freshwater. Drying trends and deficits in precipitation, soil moisture, and net-precipitation flux, for instance, as observed in the region have been linked to warming of the tropical oceans, anthropogenic emissions of aerosols and greenhouse gases, and other processes of oceanic inter-annual variations (e.g., Andam-Akorful, Ferreira, Ndehedehe, & Quaye-Ballard, 2017;

Nicholson, 2013; Oguntunde and Abiodun, 2013; Sheffield and Wood, 2008; Giannini, Biasutti, Held, & Sobel, 2008). These trends, which are also driven and influenced by competing multiple physical mechanisms (Druryan, 2011), might impact substantially, either directly or indirectly on terrestrial water storage (TWS; total of surface waters [i.e., rivers, lakes, and wetlands], soil moisture, canopy storage, and groundwater) in the region.

The global atmosphere and hydrological cycle are undergoing rapid changes driven by the influence of climate variability and teleconnections (see, e.g., Phillips, Nerem, Fox-Kemper, Famiglietti, & Rajagopalan, 2012; Hurkmans, Troch, Uijlenhoet, Torfs, & Durcik, 2009; Malhi and Wright, 2004). Variability in ENSO amongst other factors

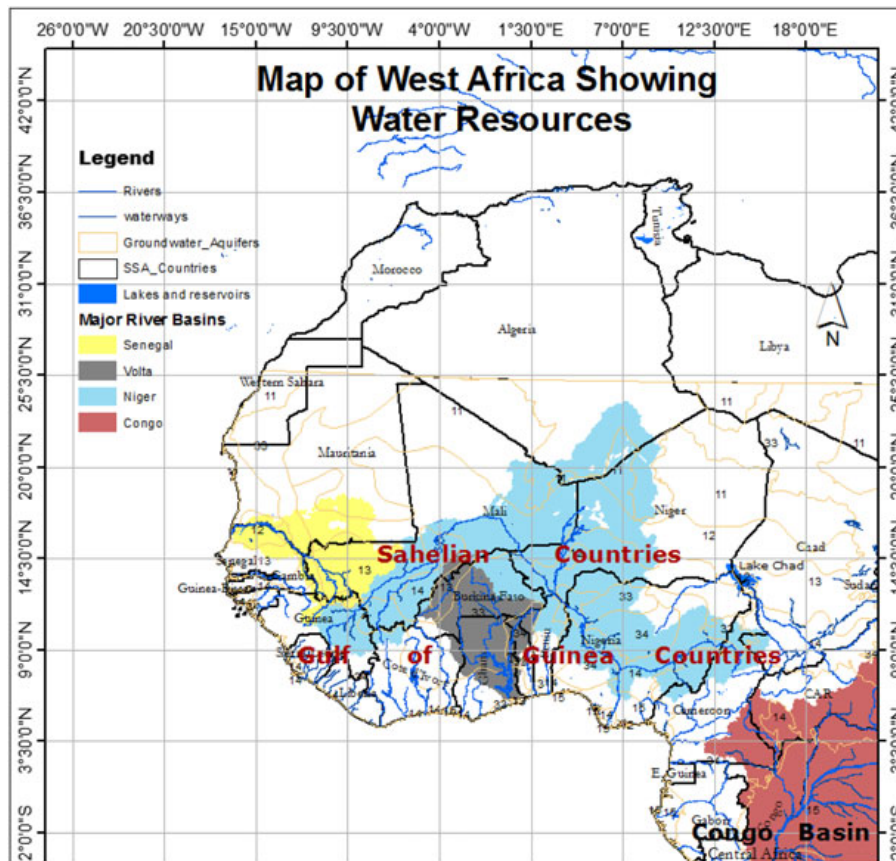


FIGURE 1 Study area showing countries in West Africa and some parts of Equatorial Africa (i.e., the Congo basin). Major river basins (e.g., Niger, Volta, Congo, and Senegal), rivers, lakes, and groundwater aquifers are also indicated. The Congo (tulip pink) and Niger (sky blue) river basins are considerably large and apparently the most significant and prominent basins in the region owing to the two major rivers (Niger and Congo) that provide numerous ecosystem services. The types of aquifers are described in terms of numbers; for example, the numbers ranging from 11 to 15 are found in major groundwater basins whereas the numbers 33 and 34 on the map are those found in local and shallow aquifers. Aquifer maps and some river distribution networks were adapted from the World-wide Hydrogeological Mapping and Assessment Programme (WHYMAP) (https://www.whymap.org/whymap/EN/Downloads/Global_maps/globalmaps_node_en.html)

(e.g., rainfall, temperature, barometric pressure, etc.), for example, was associated with changes in aquifer water levels in Japan (see Dong, Shimada, Kagabu, & Fu, 2015). In Africa, climate variability at decadal to century scales resulted in recharge rates of 30 mm/year (see Scanlon et al., 2006). Trans-Niño index showed strong association with stream flow during the warm phase of Pacific Decadal Oscillation (PDO) in the Upper Klamath Lake in the United States (see Kennedy, Garen & Koch, 2009) whereas more recently, a low frequency modulating El-Niño activity was found to have induced lower changes in rainfall variance over West Africa (see Andam-Akorful et al., 2017). Obviously, the observed extremes in West African rainfall (especially the Guinea Coast) is likely to increase owing to the strong impacts of climate variability, environmental changes, influence of tropical Atlantic sea surface temperature (SST) anomalies, and the nature of West African Monsoon, which is largely controlled by interactions between continental surfaces and the oceans (see, e.g., Rodríguez-Fonseca et al., 2011; Losada et al., 2010; Redelsperger and Lebel, 2009; Polo, Rodríguez-Fonseca, Losada & García-Serrano, 2008; Redelsperger et al., 2006). The overarching outcomes of a plethora of related studies in West Africa (see, e.g., Ndehedehe, Awange, Corner,

Kuhn & Okwuashi, 2016; Diatta and Fink, 2014; Nicholson, 2013; Paeth et al., 2012; Bader and Latif, 2011; Joly and Voltaire, 2010; Losada et al., 2010; Ali and Lebel, 2009; Giannini et al., 2008; Reason and Rouault, 2006), be it region-specific or basin scale, overwhelmingly agree on the roles of climatic variations through changes in the global oceans, mesoscale convective systems, and indices of climate variability (e.g., ENSO, Atlantic Multi-decadal Oscillation [AMO], PDO, etc.) on precipitation patterns and other water fluxes (e.g., stream flow). Thus, climate variability is expected to significantly impact on hydrological conditions, leading to considerable impacts on changes in TWS. Such impacts amongst other factors could restrict agriculture, ecosystem services, and the region's freshwater systems, warranting the study of climate teleconnections and its contributions to long term changes in TWS. Because climate teleconnections also provide significant influence on meteorological processes, and TWS being a hydrologic state variable that integrates hydrologic processes (e.g., recharge and infiltration), the knowledge of climate teleconnection's influence on TWS is critical and provides meaningful insights on drought events, wet conditions, and water resources management. Ultimately, identifying teleconnections that impact TWS in the region will be beneficial for forecasting.

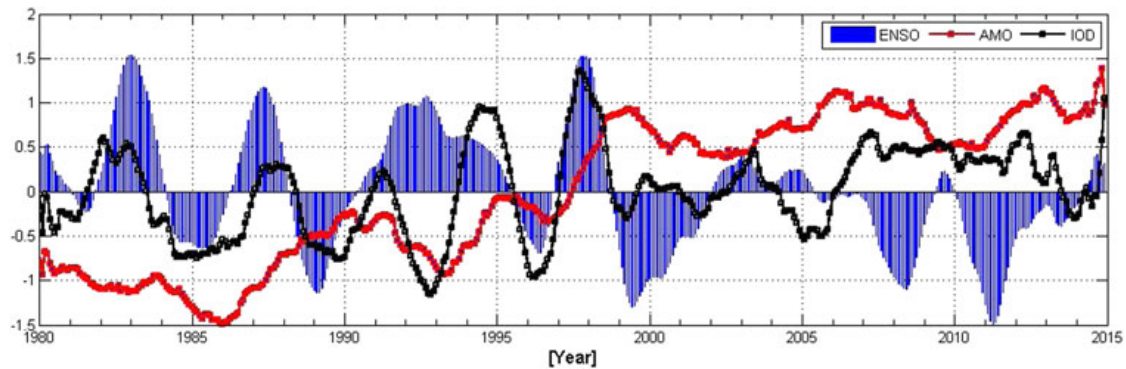


FIGURE 2 Time series of monthly climate indices—El-Niño Southern Oscillation (ENSO), Indian Ocean Dipole (IOD), and Atlantic Multi-decadal Oscillation (AMO)—for the period of 1980–2014 used in the study

The pioneering works of Phillips et al. (2012) and Boening, Willis, Landerer, Nerem, and Fasullo (2012) have shown how ENSO teleconnection patterns around the globe are associated with changes in global mean sea level and continental water storage derived from Gravity Recovery and Climate Experiment (GRACE; Tapley, Bettadpur, Watkins, & Reigber, 2004). Given that ENSO has large energy between 2–5 years, only a few cycles will occur in the 8-year GRACE data used by Phillips et al. (2012). On the other hand, Boening et al. (2012) did not dwell on the relationship between continental stored water and climate teleconnections but showed that the 5 mm decline in global mean sea level was tied to the 2010/2011 La-Niña. This significant decrease in global mean sea level according to the study caused an excess transport of freshwater from ocean to land areas. Because ENSO is mostly based on oceanic variability in the Pacific, the role of other climate indices that describes variability in the Atlantic and Indian Oceans on TWS also requires reckoning. An extended hydrological time series will provide more evidence on climate teleconnection-driven changes in TWS at the regional or global scale.

Globally, observed variations in precipitation, soil moisture, freshwater discharge, recharge, and drought characteristics have been attributed to variabilities in ENSO, AMO, and PDO (e.g., Andam-Akorful et al., 2017; Dai, Qian, Trenberth, & Milliman, 2009; Hurkmans et al., 2009; Sheffield and Wood, 2008; Scanlon et al., 2006). Like many other parts of the world, rainfall and hydro-climatic conditions in West Africa are influenced by ENSO and a number of other global climate teleconnections (AMO, Indian Ocean Dipole [IOD], etc.; see, e.g., Ndehedehe, Agutu, Okwuashi, & Ferreira, 2016; Ndehedehe, Awange, Corner, et al., 2016; Diatta & Fink, 2014; Molion & Lucio, 2013; Paeth et al., 2012; Bader & Latif, 2003, 2011; Giannini, Saravanan, & Chang, 2003; Nicholson, Some, & Kone, 2000; Nicholson, 2013, and the references therein). These climate teleconnections result in extreme hydrological conditions and intensification of the water cycle, all of which impact on TWS in the region. Although the influence of these climate teleconnections and other climate modes on West African rainfall has been widely studied as indicated, their influence on TWS in the region has, however, not been considered. Moreover, although rainfall is the main input of TWS, the influence of teleconnections on rainfall might not directly be the same as its influence on TWS, which is a vertical integration of surface water,

groundwater, soil moisture, ice/snow, and biomass, all of which might respond differently to climate variability. Despite this, the few studies available over West Africa that addressed TWS (see, e.g., Ndehedehe, Awange, Agutu, Kuhn, & Heck, 2016; Henry, Allen, & Huang, 2011; Grippa et al., 2011; Hinderer et al., 2009; Forootan et al., 2014) do not consider the influence of climate teleconnections on its TWS changes.

This manuscript investigates the association of three well-known global climate teleconnections (ENSO, IOD, and AMO) on the region's TWS and highlights the influence of climate teleconnection-induced rainfall on TWS. To this end, this study assumes that these teleconnection indices (Figure 2), which directly or remotely contribute to extreme hydro-meteorological conditions (i.e., extreme wetness and dryness) in the region (see, e.g., Diatta & Fink, 2014; Paeth et al., 2012; Nicholson et al., 2000), subsequently influences TWS changes over the region. Specifically, the two main objectives of this study are (a) to identify the spatio-temporal modes of precipitation anomalies (i.e., wet and dry conditions) over two different timescales (i.e., 6- and 12-month aggregations) that influence TWS variations over West Africa and (b) examine the relationship of TWS derived from GRACE (2002–2014) and Modern-Era Retrospective Analysis for Research and Applications (MERRA; Rienecker et al., (2011); 1980–2015) to climate teleconnections. In trying to achieve these objectives, the present study employs for the first time a methodological framework based on multivariate analysis that allows the assessment of hydrological processes, and extreme precipitation anomalies on TWS and its association with climate teleconnections over West Africa.

To comprehensively study teleconnections' influence on TWS over West Africa, multiple-linear regression analysis (MLRA) and independent component analysis (ICA; see, e.g., Westra, Brown, Lall, Koch, & Sharma, 2010; Aires, Rossow, & Chédin, 2002; Cardoso & Souloumiac, 1993; Cardoso, 1999) are combined to examine hydro-meteorological conditions and the association of climate indices with TWS derived from both GRACE (2002–2014) and global high-resolution MERRA data (1980–2015). The standardised precipitation index (SPI; McKee, Doeskin, & Kieist, 1993) and the ICA technique are employed to analyse the relationship of extreme hydro-meteorological conditions with these climate teleconnections.

The remainder of the study is organised as follows: In Section 2, a brief highlight on the study area is provided whereas Sections 3 and 4 provide, respectively, a discussion on the data and methodology used. This is followed by presentation and discussion of the results in Section 5. The conclusions of the study are summarised in Section 6.

2 | WEST AFRICA

2.1 | Location

West Africa covers an areal extent of 7.5 million km² and comprises two major geographical zones; the countries of the Gulf of Guinea and the Sahelian countries (e.g., Amani, Thomas, & Abou, 2007; Ndehedehe, Awange, Agutu, et al., 2016). The 16 member countries (Figure 1) of this region have an estimated population of 330 million people (USAID, 2013). The region is located between latitudes 0°N to 20°N and longitudes 20°W to 20°E excluding the highlands of Cape Verde. However, the analysis of the current study extends to the equatorial region, which includes the Congo basin (Figure 1).

2.2 | Climate and hydrology

The climate of the region consists of extreme wet and dry conditions, and the intra-annual rainfall distribution in the region is linked to seasonal migration of the intertropical convergence zone and circulation features (e.g., the African Easterly Jets, Tropical Easterly Jets, African Westerly Jet; Nicholson, 2013; Nicholson & Grist, 2001; FAO, 1983). Rainfall varies from less than 200 mm/year in the Sahelian countries to over 2,000 mm/year along the Gulf of Guinea. In the Gulf of Guinea region, the rainfall seasons occur between April–June and July–September, with the wettest months being June and September or sometimes October, whereas in the Sahel region, rainfall mostly occur between June and September, with maximum rainfall occurring in August (Nicholson et al., 2000). ENSO and AMO are well-known climate teleconnections that have been associated with extreme rainfall variability in the region (see, e.g., Diatta and Fink, 2014; Paeth et al., 2012; Nicholson et al., 2000). That said, the severe droughts of the 1980s were perceived as the combined effects of unusual warming in the Indian Ocean and the eastern equatorial Atlantic Ocean (see, e.g., Bader & Latif 2011; Giannini et al., 2003). Temperature varies with altitude, with lowland areas having a mean annual temperature above 18°C whereas in the Central Sahel, temperatures in July could

be as high as 58°C, differing from the the southern part of the Sahara where mean monthly temperatures could rise to 30°C (FAO, 1983).

Numerous rivers such as the Niger, Benue, Volta (Black and White Volta rivers), Senegal, Oti, Comoe, and Gambia amongst others drain the West African region (Figure 1) whereas the Congo river is the second largest river in Africa and drains one of the largest tropical forests of the world, that is, in the Congo basin (e.g., Shahin, 2008). The aforementioned rivers are mostly shared by four and up to eight riparian countries, which sometimes results in trans-boundary water conflicts. The Niger river in particular is the longest river in West Africa and is shared by several riparian countries in the region. The Fouta Djallon Highlands where the river Niger originates from is the water tower of West Africa and shows the strongest amplitudes of TWS and precipitation over the region (see Ndehedehe, Awange, Agutu, et al., 2016). TWS and stream flows are largely precipitation driven with time lags in some areas. However, diversity in local climates, soil infiltration characteristics, and multiple strings of anthropogenic factors, for example, land use change, dam constructions, and developments of small-scale reservoir systems for water mobilisation to support agriculture, have also contributed to changes in hydrological regimes of water fluxes in the region (e.g., Ndehedehe, Awange, Kuhn, Agutu, & Fukuda, 2017; Ndehedehe, Awange, Agutu, et al., 2016; Ahmed, Sultan, Wahr, & Yan, 2014; Descroix et al., 2009; Favreau et al., 2009; K. Li, Coe, Ramankutty, & Jong, 2007).

3 | DATA

All datasets used in this study are described below and key parameters are summarised in Table 1.

3.1 | Terrestrial water storage

1. Gravity Recovery and Climate Experiment (GRACE) TWS: Since the inception of GRACE (Tapley et al., 2004) in 2002, monthly estimates of Earth's gravity field have been used to infer changes in mass at and below the Earth's surface (e.g., Wahr, Molenaar, & Bryan, 1998). The Earth's water storage changes derived from GRACE observations both at basin and continental scales with global and regional applications in droughts, hydrology, climate, and validation of hydrological models have been widely studied (see, e.g., Wouters et al., 2014 and the references therein). The GRACE Release-05 (RL05) spherical harmonic coefficients

TABLE 1 Summary of precipitation, TWS products, and teleconnection indices used in this study

Data	Type	Period	Spatial res.	Temporal res.	Coverage
GPCP	Guage and satellite	1979–2014	2.5° × 2.5°	Monthly	Global
MERRA	Global reanalysis	1980–2015	0.625° × 0.5°	Monthly	Global
GRACE	Satellite gravity	2002–2014	1.0° × 1.0°	Monthly	Global
MEI	climate index	1980–2015	–	Monthly	
IOD	climate index	1980–2015	–	Monthly	
AMO	climate index	1980–2015	–	Monthly	

Note. AMO = Atlantic Multi-decadal Oscillation; GPCP = Global Precipitation Climatology Project; GRACE = Gravity Recovery and Climate Experiment; IOD = Indian Ocean Dipole; MERRA = Modern-Era Retrospective Analysis for Research and Applications; TWS = terrestrial water storage.

from the Center for Space Research for the period of 2002 to 2014 (<http://icgem.gfz-potsdam.de/ICGEM/shms/monthly/csr-r105/>) are used in this study to compute changes in TWS. Because GRACE does not provide changes in degree 1 coefficients (i.e., C_{10} , C_{11} , and S_{11}) coupled with the effect of large tide-like aliases (e.g., Seo, Wilson, Chen, & Waliser, 2008) in degree 2 coefficients, we replace degree 1 coefficients with estimates from satellite laser ranging (Swenson, Chambers, & Wahr, 2008), and following Chen and Wilson (2008), degree 2 coefficients are also replaced by those provided by Cheng, Tapley, and Ries (2013). DDK2 decorrelation filter (Kusche, Schmidt, Petrovic, & Rietbroek, (2009) is then applied on the spherical harmonic coefficients in order to reduce the effect of the correlated noise. The DDK2-filtered monthly GRACE solutions are then converted to equivalent water heights on a $1^\circ \times 1^\circ$ grid following the approach of Wahr et al. (1998). Monthly changes in TWS solutions $\mathbf{W}(\theta, \lambda, t)$, in time t (where θ and λ are the geographical latitudes and longitudes, respectively), after removing the long term mean $w(\lambda, \theta)$ over the investigated period are given as (Phillips et al., 2012):

$$\mathbf{X}_{TWS}(\theta, \lambda, t) = \mathbf{W}(\theta, \lambda, t) - w(\theta, \lambda). \quad (1)$$

2. Modern-Era Retrospective Analysis for Research and Applications (MERRA) TWS: One of the main purposes of the MERRA data was to improve upon the water cycle represented in previous generations of reanalyses (Rienecker et al., 2011). The data is a state-of-the-art reanalysis that provides atmospheric fields, water fluxes, and global estimates of soil moisture (Reichle et al., 2011). Also, it has been improved significantly when compared with previous reanalysis datasets (Rienecker et al., 2011). MERRA outputs have been used in the study of atmospheric circulations and assessing agricultural droughts in the African continent (see Agutu et al., 2017; Wu, Reale, & Schubert, 2013) and have been recommended for land surface hydrological studies (Reichle et al., 2011). The land TWS data component of MERRA used in this study covers the period of 1980–2015 and is available for download through the National Aeronautic and Space Administration data portal (<http://disc.sci.gsfc.nasa.gov/mdisc/>). The MERRA-TWS is employed to highlight the influence of climate teleconnections on long term terrestrial stored water, complementing the limited GRACE-TWS data record.

3.2 | Global precipitation climatology project

The global grids of monthly estimate of Global Precipitation Climatology Project (GPCP) data set from 1979 to 2014 (Huffman, Adler, Bolvin, & Gu, 2009; Adler et al., 2003) is used in this study. The GPCP data are a merged satellite-based product that is adjusted using rain gauge data and can be downloaded through the World Data Center website (see <http://lwf.ncdc.noaa.gov/oa/wmo/wdcamet-ncdc.html>). Previous studies (see, e.g., Ndehedehe, Agutu, Okwuashi, et al., 2016; Paeth et al., 2012; Yin, Gruber, & Arkin, 2004) have shown that the GPCP version 2 precipitation data have a relatively good correlation with rain gauge observations, Tropical Rainfall Measuring Mission-based precipitation, and Climate Prediction Center Merged Analysis data.

Because of its long-term record and availability, the GPCP data are used here to compute SPI over West Africa at 6- and 12-month aggregation. Our assumption is that 6- and 12-month SPI cumulations provide a reasonable lag for extreme rainfall conditions to be reflected in catchment stores.

3.3 | Climate modes

1. Multivariate ENSO index (MEI)

ENSO is a climate pattern that describes the presence of abnormally warm (El-Niño) and cold (La-Niña) SST anomalies in the eastern Pacific (e.g., Phillips et al., 2012). Although there are other ENSO indices such as Nino3.4 and Nino4, the Multivariate ENSO Index downloaded from NOAA (<http://www.esrl.noaa.gov/psd/enso/mei/>) is used here because it has been associated with inter-annual variability of water availability and comprises six other variables over the Pacific coupled with atmospheric anomalies (see, e.g., Phillips et al., 2012; Hurkmans et al., 2009).

2. Indian Ocean Dipole (IOD)

The IOD is a coupled ocean and atmosphere phenomenon in the equatorial Indian Ocean that mostly affects the climate of countries around the Indian Ocean (e.g., Saji, Goswami, Vinayachandran, & Yamagata, 1999). It is essentially mirrored in the the SST data over the Indian ocean (Cai et al., 2014). Indian Ocean SSTs have been associated with regional climate anomalies (Bader & Latif, 2003). Apart from ENSO, IOD is one of the relevant climate indices that has been identified as having a robust relationship with Sahel inter-annual rainfall variability (e.g., Okonkwo, 2014). The IOD time series can be accessed from European Climate Assessment & Data portal (<http://climexp.knmi.nl>).

3. Atlantic Multi-decadal Oscillation (AMO)

The AMO is a consistent pattern of variability in the North Atlantic SSTs with a period of about 60–80 years and conventionally computed from the average SST anomaly of the North Atlantic, that is, north of the equator (see Trenberth & Shea, 2006). Zhang and Delworth (2006) and Trenberth and Shea (2006) have linked multi-decadal variations of Sahel summer rainfall to AMO. More recently, Chylek, Klett, Dubey, and Hengartner (2016) showed that AMO contributed to the 1970–2005 global warming. In addition, its relative influence according to the study is expected to increase during the second half of the 21st century, further necessitating the need to examine its possible contribution to TWS. The AMO index used in this study was smoothed from the Kaplan SST V2, which is available for download at NOAA's website (<http://www.esrl.noaa.gov/psd/data/timeseries/AMO/>). The time series of all climate indices used in the study are indicated in Figure 2.

4 | METHODOLOGY

4.1 | Independent component analysis

The independent component analysis (ICA) is a higher order statistical method that uses statistical moments higher than second order. The method uses a statistically based identification technique to estimate directional vectors (i.e., independent patterns) from a data matrix (see,

e.g., Common, 1994; Cardoso & Souloumiac, 1993; Cardoso, 1999). The method explores the unknown dynamics of a system through the rotation of the classical empirical orthogonal functions (Aires et al., 2002). Fundamentally, ICA decomposes the time series of the data matrix $Z_p(t)$, into a mixing matrix A and a number of statistically independent source signals $s_j(t)$, where t is the time index. This can be expressed as (e.g., Ziehe, 2005)

$$Z_p(t) = \sum A_{ij}s_j(t), \quad (i = 1, \dots, n, \quad j = 1, \dots, m). \quad (2)$$

Further details on the computational routines, numerical steps of ICA implementation, algorithm development, and mathematical formulations have been documented (e.g., in Cardoso, 1991; Cardoso & Souloumiac, 1993; Common, 1994; Cardoso, 1999; Theis, Gruber, Keck, Meyer-bse, & Lang, 2005; Ziehe, 2005). The interest in regionalising hydro-climatic signals at global and basin scale is increasing and has resulted in several applications of ICA in geophysical signal separation and drought analysis (see, e.g., Ndehedehe, Agutu, Okwuashi, et al., 2016, Ndehedehe, et al., 2017; Boergens, Rangelova, Sideris, & Kusche, 2014; Forootan, Awange, Kusche, Heck, & Eicker, 2012, 2014; Frappart, Ramillien, Maisongrande, & Bonnet, 2010, 2011). Here, the ICA (algorithm available at <http://perso.telecom-paristech.fr/cardoso/Algo/Jade/jadeR.m>) is employed to decompose GRACE-derived TWS (after removing the annual and semi-annual parts) and gridded SPI values into statistically independent modes (spatial and temporal patterns). Note that MERRA-TWS was not statistically decomposed, as it does not contain groundwater component; however, because it is sensitive to climate, our focus is to examine and highlight the association of long term TWS changes with climate teleconnection indices. The temporal evolutions of residual TWS (section 4.2) were correlated with time series of ENSO, IOD, and AMO in order to assess their association with the observed TWS, which have been localised over West Africa using the ICA technique. ICA is employed to help the regionalisation (i.e., localisation) of GRACE-TWS values with the hope of studying their association with global climate teleconnections at large spatial scales. The advantage of using ICA for this region is that it improves the detection of regionally less dominant (i.e., obscured) signals (i.e., those of GRACE-derived TWS) and enables their spatial patterns to be localised making it possible for them to be examined concurrently with the association of climate modes, TWS, and SPI evolutions in different subregions. Furthermore, because rainfall in West Africa results in two homogeneous regions depending on the domain size and period investigated (e.g., Sanogo et al., 2015), the ICA technique was also employed to support the localisation of complex SPI signals and definition of regions with similar hydro-meteorological patterns in West Africa. It was pointed out in a recent study that regions in West Africa (especially the coastal areas) with large amplitudes of TWS are mostly areas that receive considerable rainfall, characterised by huge aquifers and endowed with surface waters such as lakes and reservoirs (see Ndehedehe, Awange, Agutu, et al., 2016). Because TWS variability over West Africa is largely precipitation driven, climate teleconnection-induced changes in precipitation such as the 2007 and 2010 La-Niñas may have caused larger changes in TWS in the region. In this study, our aim is to understand these modes of extreme precipitation anomalies in the region, as they can provide a clue regarding the mechanisms of larger changes in TWS. To this end, the ICA method was also applied to regionalise

(localize) SPI patterns (hereafter called drought and wet conditions) over West Africa, in order to help examine the impacts of regional fluctuations in rainfall on catchment storage.

4.2 | Multiple linear regression analysis

The strongest signals in TWS variability emanate from the harmonic components (i.e., annual and semi-annual signals) of the data, hence the trend, annual, and semi-annual components of the data were removed in order to allow for the estimation of the impact of climate indices. Essentially, our approach employs a MLRA model that parameterises the cosines' and sines' harmonic components of monthly GRACE and MERRA data. This is followed by the method of least squares, which is used to estimate the amplitude of a climate index (i.e., ENSO, IOD, and AMO) on the TWS whose trend and harmonic components have been removed (hereafter called deseasonalized TWS) over the region. Using the MLRA, the dataset Y_{TWS} is parameterised as

$$Y(l, k, t) = \beta_0 + \beta_1 t + \beta_2 \sin(2\pi t) + \beta_3 \cos(2\pi t) + \beta_4 \sin(4\pi t) + \beta_5 \cos(4\pi t) + \beta_6 E(t + \varphi_E) + \varepsilon(t), \quad (3)$$

where (l, k) is the grid location, t is the time in years, β_0 is the constant offset, β_1 is the linear trend, β_2 and β_3 account for the annual signal, and β_4 and β_5 represent the semi-annual signal. The variable β_6 is the amplitude of TWS changes or rainfall that is related to climate indices describing large-scale ocean-atmosphere phenomenon (e.g., ENSO, IOD, and AMO). E is the normalised time series (i.e., after removing long term mean) of each climate index (Figure 2), φ_E is the phase lag between the time series of TWS and each climate index, and $\varepsilon(t)$ is the random error term. The annual and semi-annual amplitudes of TWS (MERRA and GRACE) over the region are computed as

$$\text{Annual Amplitude} = \sqrt{(\beta_2)^2 + (\beta_3)^2} \quad (4)$$

and

$$\text{Semi Annual Amplitude} = \sqrt{(\beta_4)^2 + (\beta_5)^2}. \quad (5)$$

Removing these harmonic components and the trend in Equation 3 leaves the residual part, (i.e., deseasonalized TWS, X_{TWS}) which is here assumed to be associated with slow dynamic climate oscillations (e.g., AMO). This residual variability perhaps can also emanate from internal variability or regional forcings (though unclear for the region), but as indicated in Section 1, the impact of climate-related indices on rainfall are more likely to result in large amplitudes of TWS, dominating the time series of the deseasonalized TWS. This deseasonalized TWS is statistically decomposed into temporal and spatial patterns (i.e., using the ICA technique described in section 4.1). The deseasonalized X_{TWS} signal is characterised as

$$X_{TWS} = Y - [\beta_1 t + \beta_2 \sin(2\pi t) + \beta_3 \cos(2\pi t) + \beta_4 \sin(4\pi t) + \beta_5 \cos(4\pi t)]. \quad (6)$$

The coefficients of MLRA indicated in Equations 4–6 were estimated using the least square adjustment technique. The linear trend of TWS is removed in order to ensure that the pseudo trends (GRACE-TWS) emanating from the ponding of water behind large dams as is the case in Lake Volta (e.g., Ndehedehe et al., 2017; Moore & Williams, 2014) are not interpreted as contributions of climate modes to TWS changes. This deseasonalized TWS was statistically decomposed into spatial and temporal patterns using the ICA technique (see section 4.1).

The significant modes of variability of the deseasonalized TWS were selected for a further comparison with the normalised time series of each climate index. Doing this allows the evaluation of the quantitative estimates of climate-induced TWS in terms of the variability explained. Further, in order to estimate the contribution of each of the climate index (i.e., ENSO, IOD, and AMO) on the amplitudes of GRACE and MERRA-derived TWS, a least square fit on each grid location of X_{TWS} in Equation 6 was then performed as (e.g., Phillips et al., 2012)

$$X_{Indices}(x, y) = a(x, y) + b(x, y) * Indices + c(x, y) * imag(Hilbert(Indices)), \quad (7)$$

where coefficients b and c are used to estimate the climate-induced TWS change $X_{Indices}(x, y)$ at a grid location (x, y) , whereas the imaginary part of the Hilbert transform of the climate index represents the lag between TWS anomalies and a given climate index (see Phillips et al., 2012). The amplitude of TWS, A , given as

$$A_{ENSO/IOD/AMO} = \sqrt{b^2 + c^2}, \quad (8)$$

is the estimated magnitude of climate index on TWS (i.e., the estimated contribution of each of the climate index to TWS change).

4.3 | Standardised precipitation index

Prolonged rainfall deficit usually reduces the alimentation of a given hydrological system leading to agricultural and hydrological drought (see Ndehedehe, Awange, Corner, et al., 2016). It is reasonable therefore to assume that extreme rainfall conditions (i.e., wet and drought events) resulting from the influence of climate teleconnections on the region will have a direct impact on the amplitudes of TWS perhaps with some time lags of say 6–12 months. To this end, extreme rainfall conditions are analysed using standardised precipitation index (SPI) aggregated at 6 and 12 months. The choice of these aggregation scales is based on the hypothesis that SPI on longer time scales can provide the capability to monitor drought and wet conditions suitable for hydrological applications (see, e.g., Ndehedehe, Awange, Corner, et al., 2016; B. Li & Rodell, 2015; Lloyd-Hughes, 2012; Hayes, Svoboda, Wilhite, & Vanyarkho, 1999), which is what MERRA- and GRACE-derived TWS are mostly suited for (e.g., Awange, Khandu, Schumacher, Forootan, & Heck, 2016).

For example, Li and Rodell (2015) recently showed that averaged groundwater drought index had a strong correlation with SPI at 12- and 24-month cumulations. To understand the influence of climate-induced rainfall conditions on observed TWS over West Africa, SPI (McKee et al., 1993) was computed from the GPCP-based precipitation for the period of 1979–2014. Instead of the gamma distribution, log-normal, extreme value, and exponential distributions that have been widely used in the simulations of precipitation distributions (e.g., Mishra & Singh, 2010), this study uses a nonparametric approach to derive standardised index (see Farahmand & AghaKouchak, 2015; Hao & AghaKouchak, 2014). Although the gamma distribution, for instance, is efficient for low runoff values as noted by Shukla and Wood (2008), the sensitivity of the traditional SPI tails to distribution parameters (e.g., Farahmand & AghaKouchak, 2015), however, may lead to inconsistent results for different regions. The nonparametric approach on the other hand can be applied to different hydro-climatic data (e.g., precipitation) without having to assume representative parametric

TABLE 2 Standardised precipitation index thresholds based on McKee et al. (1993) classification system

Description	Threshold
Extreme wet	+2.0 and above
Very wet	+1.5 to +1.99
Moderately wet	+1.0 to +1.49
Near normal	−0.99 to +0.99
Moderate drought	−1.0 to −1.49
Severe drought	−1.5 to −1.99
Extreme drought	−2.0 or less

distributions (see Farahmand & AghaKouchak, 2015). This approach employs an empirical probability method as

$$\rho(x_j) = \frac{j - 0.44}{n + 0.12}, \quad (9)$$

where n is the sample size, j represents the rank of non-zero rainfall data starting from the smallest, and $\rho(x_j)$ is the corresponding empirical probability. Equation 9 is transformed to a SPI as (see Farahmand & AghaKouchak, 2015)

$$SPI = \phi^{-1}(\rho), \quad (10)$$

where ϕ is the standard normal distribution function and ρ is the probability obtained from Equation 9. The SPI values obtained from Equation 10 was subsequently decomposed into spatial and temporal patterns using the ICA technique (see section 4.1). The association of a climate index with the temporal SPI evolutions was examined through Pearson's correlation analysis. Dry and wet occurrence in this study is based on the McKee et al. (1993) classification system as highlighted in Table 2.

5 | RESULTS AND DISCUSSION

5.1 | Extreme hydro-meteorological conditions related to climate modes

This section relates extreme hydro-meteorological conditions (drought and wet conditions based on the description of Table 2) to climate modes using a spatio-temporal approach where the SPI values obtained over West Africa are statistically decomposed into spatial and temporal patterns.

For the 6-month SPI localised over the region, the spatio-temporal patterns show the spread of SPI patterns, its frequency, onset, and termination. The observed temporal SPI evolutions (i.e., IC1–IC4, Figure 3) are consistent with previous drought records of the region (e.g., Masih, Maskey, Mussá, & Trambauer, 2014). The wider spread of droughts in some parts of the Sahel as indicated in the SPI spatial and temporal patterns (IC1, Figure 3) confirms that the Sahel region was the worst hit by the droughts of 1982–1984, which affected West Africa and the continent at large. The AMO showed stronger association with SPI in some parts of the Sahel region and Central Africa Republic compared to ENSO and IOD (see IC1, Figure 3 and Table 3). Although this specific case study indicates that AMO is more associated with the temporal patterns of SPI in much of the Sahel region, extreme wet conditions related to ENSO have also been reported in the region (e.g., Paeth et al., 2012;

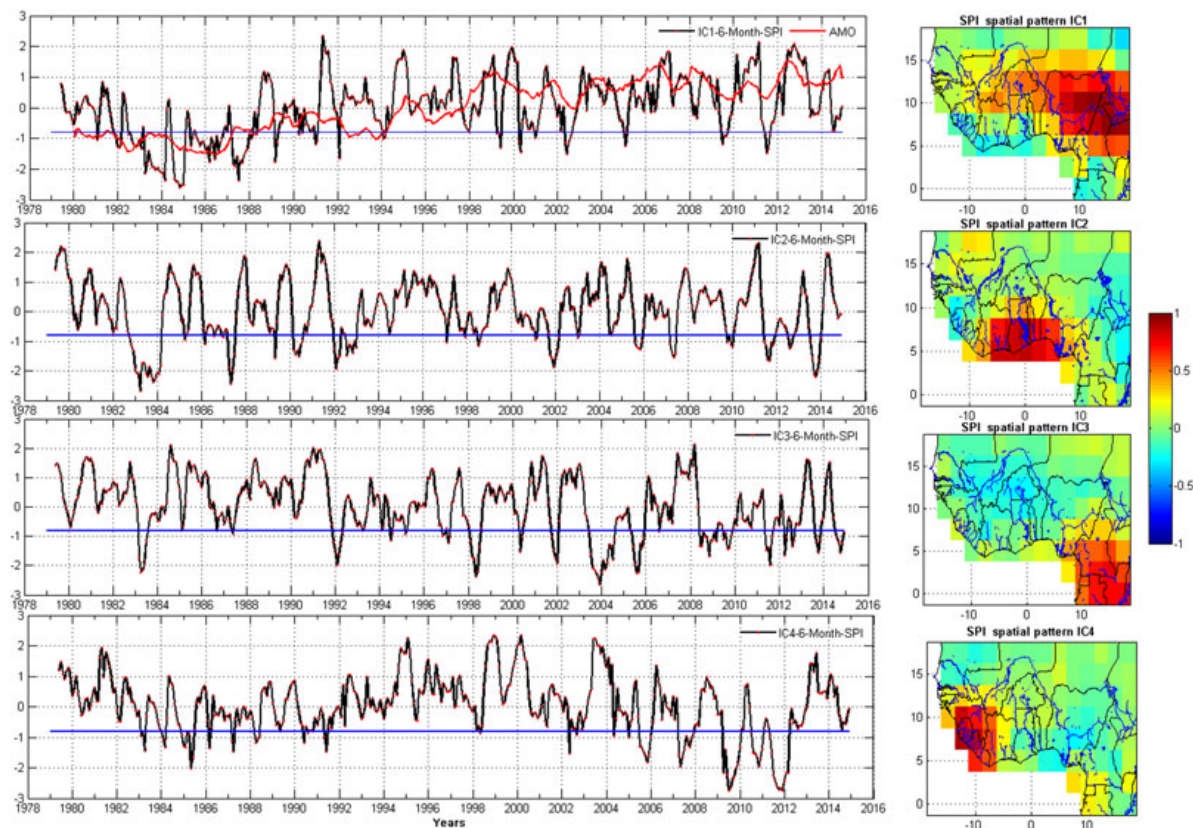


FIGURE 3 Spatio-temporal SPI patterns over West Africa using 6-month gridded SPI values. SPI values are computed using GPCP-based precipitation product over the period of 1979–2014. The variability of the statistically decomposed SPI values are 14.1%, 7.7%, 7.2%, and 4.6% for IC1, IC2, IC3, and IC4, respectively. Actual values for drought classification and categorisation with respect to McKee et al. (1993) description are jointly derived from the localised spatial patterns (right) and their corresponding temporal evolutions (left). The AMO showed relatively a better association with SPI over the Sahel region (IC1) compared to other climate indices (ENSO and IOD). The blue solid line (left) is the drought threshold. Hydrological units (rivers, lakes, and other water bodies) are also indicated on the spatial patterns of SPI (blue lines on the right)

Nicholson et al., 2000). As shown in the SPI temporal patterns (IC1, Figure 3), 1991, 1998/1999, 2007, and 2010 are instances of wet conditions that could be attributed to ENSO events because they coincide with the ENSO years. Over the Volta basin, 2010 was extremely wet (IC2, Figure 3) consistent with the strong amplitudes of TWS in the basin (see section 5.2.1 for more discussion). Although the observed trends in GRACE-derived TWS in the Volta basin have been attributed to the influence of Lake Volta due to water ponding behind the dam (e.g., Ndehedehe et al., 2017; Ahmed et al., 2014), the wet conditions of the late 2007/2008, and 2010 associated with ENSO event (IC2, Figure 3), resulted in water level rise of up to 7 m in 2010 over the lake (see Ndehedehe, Awange, Agutu, et al., 2016, Ndehedehe, et al., 2017). Strong fluctuations in SPI temporal patterns that coincided with ENSO events have also been highlighted in the Congo basin and some countries of the Guinea Coast (Liberia, Guinea, and Sierra Leone; IC3–IC4, Figure 3).

At the 12-month SPI, the Sahel seems to be extremely wet in 1994/1995, 1998/1999, 2003/2004, and recently during the 2012–2014 period (IC1, Figure 4). Nicholson et al. (2000) reported similar wet conditions for 1988 and 1994 emphasising a long term change in rainfall over the region. Depending on the structural stability, hydraulic conductivity, infiltration, and soil water holding capacity of

TABLE 3 Correlations between ICA-decomposed SPI-6-month/SPI-12-month temporal drought evolutions and climate indices

ICs/region	AMO	IOD	ENSO
IC1 (Sahel)	0.43/0.62	0.12/0.12	-0.22/-0.22
IC2 (Volta basin)	-0.01/-0.01	0.02/0.01	-0.30/-0.30
IC3 (Congo basin/Nigeria)	-0.33/0.30	-0.09/0.11	-0.21/-0.14
IC4 (Guinea Coast/Congo)	0.30/-0.17	0.15/0.0	0.18/-0.30
IC5 (Guinea Coast)	-0.01/-0.09	-0.01/-0.06	-0.03/0.03

Note. AMO = Atlantic Multi-decadal Oscillation; ENSO = El-Niño Southern Oscillation; IOD = Indian Ocean Dipole.

The correlation coefficient in bold are statistically significant at the 95% confidence level using the student t test.

the Sahel (see Desroix et al., 2009), extreme wet conditions such as the 2003/2004 and the 2012–2013 period (IC1, Figure 4) may translate to huge catchment storage and inundated areas, leading to increase in TWS (Ndehedehe, Awange, Agutu, et al., 2016). Apart from a wider SPI spatial distribution along the Sahel band, it is noticeable that the extreme droughts of the 1980s in the Sahel region (IC1, Figure 4) persisted a bit longer (1982–1985) at the 12-month aggregation when compared to 6-month SPI (IC1, Figure 3). Further, the Volta basin shows

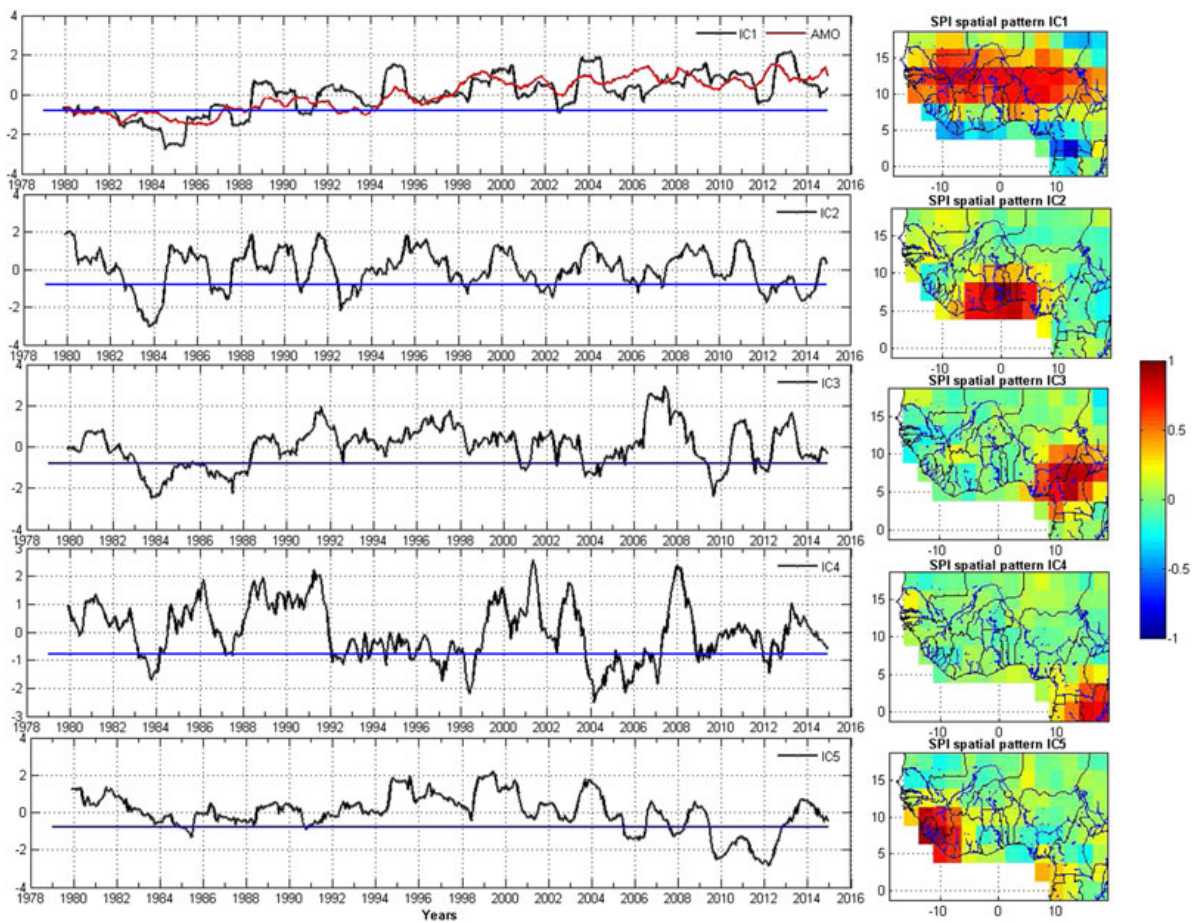


FIGURE 4 Spatio-temporal SPI patterns over West Africa using 12-month gridded SPI values. SPI values are computed using GPCP-based precipitation product for the period of 1979–2014. The variabilities of the statistically decomposed SPI values are 17.4%, 7.0%, 6.5%, 5.3%, and 5.1% for IC1, IC2, IC3, IC4, and IC5, respectively. Actual values for drought classification and categorisation with respect to McKee et al. (1993) description are jointly derived from the localised spatial patterns (right) and their corresponding temporal evolutions (left). The AMO showed stronger association with SPI over the Sahel region (IC1) compared to ENSO and IOD. The blue solid line (left) is drought threshold. Hydrological units (rivers, lakes, and other water bodies) are also indicated on the spatial patterns of SPI (blue lines on the right)

wet conditions, for example, in 2010 (IC2, Figure 4) similar to what is observed in the 6-month SPI aggregation (IC2, Figure 3). The wet conditions of 2007 in Cameroon/Nigeria and Congo maybe ENSO-related (IC3 and IC4, Figure 4), due to the fact that multiple strings of El-Niño and La-Niña episodes have been reported, for example, in Cameroon and the Congo basin (e.g., Molua & Lambi, 2006).

Lake Volta, a major physiographic feature seated in the southern part of the Volta basin derives its nourishment from the Volta river system (comprising the Black Volta, White Volta, and Oti Rivers). Besides the rainfall in Ghana and the Oti river that also contribute to the TWS around the Lake area, the Black and White Volta rivers have their sources in Burkina Faso and contribute about 30% of the total annual flow to Lake Volta (e.g., Barry, Obuobie, Andreini, Andah, & Pluquet, 2005). This implies that the magnitude of wet conditions in Burkina Faso, for example, during 2012–2013 (IC1, Figure 4), and Ghana for the 2008–2009 and 2010–2011 periods (IC2, Figure 4) may induce considerable changes in regional hydro-meteorological patterns leading to large amplitudes of TWS in the basin. Similarly, as the reservoir

system of the Lake Volta is naturally connected to the Volta river system (see Ndehedehe et al., 2017), climate teleconnection-induced reductions in rainfall may directly impact on the stream flows of the Volta river system, leading to deficits in stored water of the basin. Furthermore, the SPI spatial evolutions (i.e., without statistical decomposition) were sampled for the April–September months when considerable and significant rainfall occur in the region. This was done specifically for 2002, 2005, 2010, and 2013. The SPI spatial distribution for the year 2002 (Figure 5) confirms the severe wet and dry conditions previously observed in Ghana and countries in the Sahel (IC1–IC3, Figure 4). The Sahel also shows wet conditions in 2010 and 2013 (Figure 5) whereas Liberia and Sierra Leone indicate extreme drought condition (though 2013 was a moderate drought) during the same period consistent with IC1 and IC5 of Figure 4, respectively. Overall, the SPI spatial patterns (Figure 5) are consistent with the ICA-derived spatial evolutions of wet and dry conditions (Figures 3 and 4).

The association of SPI temporal evolutions (i.e., all the independent components of Figures 3 and 4) with climate teleconnections were

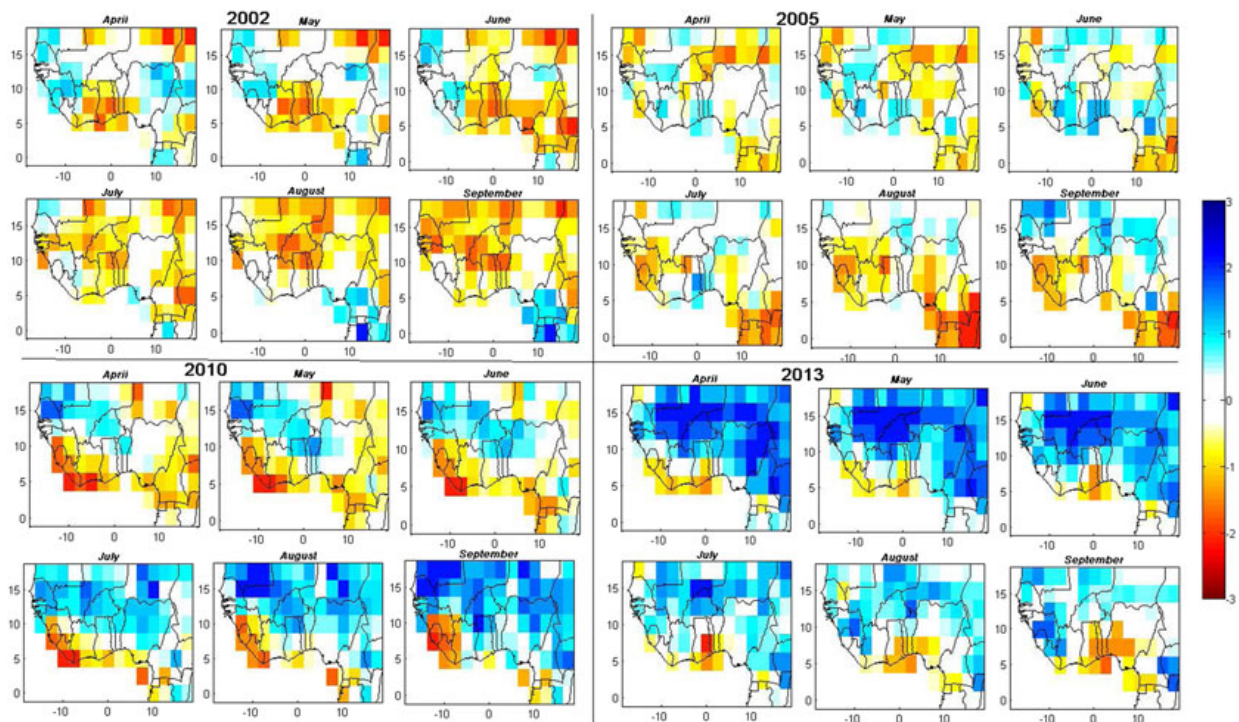


FIGURE 5 Space-time evolution of standardised precipitation index (SPI; i.e., 12-month aggregation) patterns for 2002, 2005, 2010, and 2013 over West Africa. Unlike Figures 3 and 4, these SPI patterns have not been localised

also evaluated. The temporal evolutions of SPI cumulated at 6 and 12 months (Figures 3 and 4) were correlated with ENSO, AMO, and IOD. The results show that AMO is associated with extreme dry and wet conditions in the Sahel (i.e., IC1, Figures 3 and 4), indicating statistically significant (at 95% confidence level) positive correlations of 0.43 and 0.62 with time series of SPI 6- and 12-month aggregations, respectively. The correlation results of these climate teleconnections with temporal evolutions of SPI over West Africa, which have been summarised in Table 3, also show negative correlations of $-0.30/0.30$ (ENSO), -0.33 (AMO), and positive correlation of 0.30 (AMO) with SPI temporal evolutions in the Volta and Congo basin areas (i.e., IC2 and IC3 of Figure 3 and IC2 and IC4 of Figure 4).

Whereas ENSO and AMO explain some of the variability in the observed rainfall conditions in West Africa, IOD does not show a statistically significant relationship as most correlations are relatively weak and statistically insignificant. However, as mentioned earlier, the droughts of the 1980s in the Sahel were attributed to the synergy between the abnormally warm Indian Ocean SST and that of the eastern Atlantic, which suppressed rainfall in the Sahel due to large-scale subsidence in the troposphere (see Bader & Latif, 2011). Given that IOD is a coupled ocean and atmosphere phenomenon mirrored in the the SST data over the Indian Ocean (see Cai et al., 2014; Saji et al., 1999), the impact of SST from the Indian Ocean, which is reported to have induced dryer conditions in the Sahel, is usually facilitated and induced by an occasionally warmer-than-average SST of the Atlantic Ocean (Giannini et al., 2003). Our hypothesis is that such impact, coupled with the association of ENSO and AMO on rainfall fluctuations as observed over the region, could be related to changes in TWS over West

Africa. In sections 5.2.1 and 5.2.2, such possibilities are further investigated using a combination of MLRA, Pearson correlation, and statistical decomposition method (i.e., the ICA).

5.2 | Terrestrial water storage variability and its association with climate teleconnections

5.2.1 | Relationship between climate modes and deseasonalized TWS changes

As a result of diversity in local climate in West Africa, which is mostly regulated by the movement of the rainbelt and other meteorological processes, similar to rainfall, TWS appears to be dominated by annual and semi-annual patterns. For example, considerable strong annual and semi-annual amplitudes of GRACE and MERRA-TWS are mostly found in Guinea and much of the Congo basin (i.e., in Gabon and Congo), respectively (Figure 6a-d), where rainfall is mostly annual and bimodal. Also, relatively strong TWS amplitudes of about 300 mm and more at the annual scale are found in Nigeria, Cameroon, and Central African Republic (Figure 6a), all of which are located in the humid parts of the study area. These humid parts of West Africa are mostly characterised by networks of rivers, lakes, and several groundwater aquifers (Figure 1). Essentially, as highlighted in a previous report (Ndehedehe, Awange, Agutu, et al., 2016), these TWS amplitudes are induced by a relatively strong annual and seasonal rainfall patterns, in addition to the presence of surface waters as is the case in the Congo basin and Nigeria. Moreover, the annual and semi-annual amplitudes of GRACE-TWS (Figure 6a,b) are stronger than those of MERRA-TWS (Figure 6c,d) probably due to

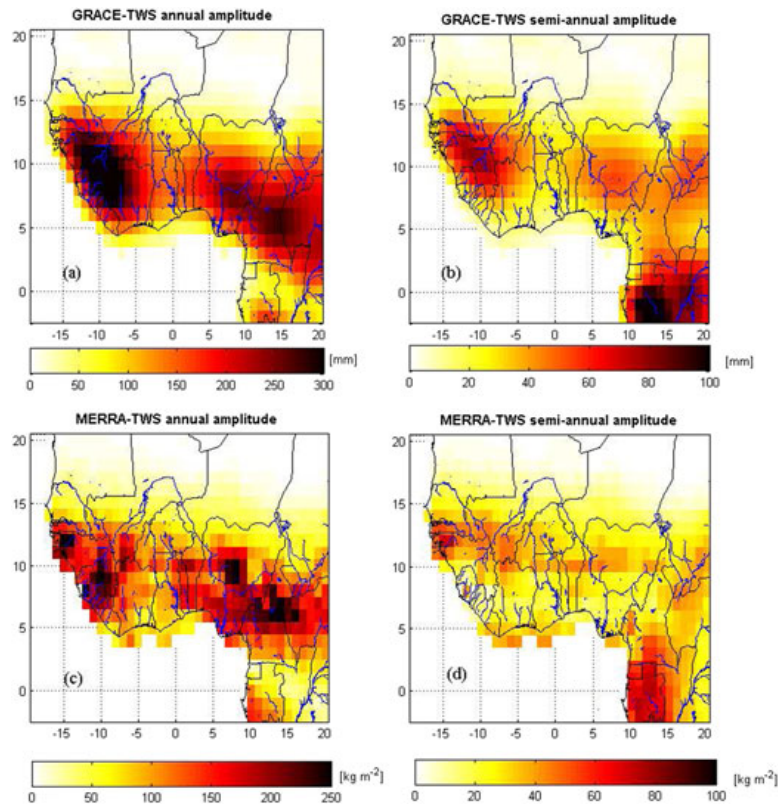


FIGURE 6 Spatial patterns of annual and semi-annual amplitudes of GRACE-derived TWS (2002–2014) and MERRA-TWS (1980–2015) over West Africa using the multiple linear regression analysis

the lack of groundwater and surface water component in the MERRA reanalysis data. Reanalysis data such as the MERRA-TWS may not be excellent representations of the real system; however, they are furnished with numerical weather predictions and observations and are extremely useful in circumstances where observations are lacking and insufficient. It is further observed that the semi-annual amplitudes of TWS dominates the equatorial regions (specifically Gabon and Congo) (Figure 6b,d) whereas Guinea is the only country with relatively strong annual and semi-annual amplitudes of TWS (Figure 6a–c) in West Africa.

As opposed to the Sahel region, the considerable strong annual and semi-annual patterns of TWS in the Guinea Coast countries and Congo basin (Figure 6a–d) confirm that these areas are the most favourable hydrological environments. Precipitation in these areas are largely seasonal and bimodal and are driven by numerous factors, such as atmospheric circulation features, mesoscale convective systems, ocean warming, physiographic features, and other processes of oceanic inter-annual variability (see, e.g., Hua et al., 2016; Mohino, Janicot, & Bader, 2011; Paeth et al., 2012; Bader & Latif, 2011; Boone et al., 2009; Giannini et al., 2008). In Guinea, for example, where GRACE-TWS annual amplitude is the strongest in the region (Figure 6a), topography also play key roles in rainfall variability. Generally, high-elevation areas in coastal West Africa tend to be characterised by stronger amplitudes of rainfall. Whereas the role of topography on hydrological conditions remains a subject for future considerations, these rainfall patterns provide significant con-

trols on inter-annual and inter-decadal variability in river flows and TWS in the region (see Ndehedehe, Awange, Agutu, et al., 2016; Conway et al., 2009). Interestingly, the groundwater maps of Africa developed by MacDonald, Bonsor, Dochartaigh, and Taylor (2012) also show that these coastal areas of West Africa have higher recharge and the shallowest groundwater levels (i.e., <7 mgbl) compared to the Central Sahel (50–250 mgbl). Whereas these groundwater maps also show that considerable amount of groundwater volumes exists in large sedimentary aquifers in North African countries, the distribution of freshwater and the huge water fluxes in coastal West Africa (e.g., Andam-Akorful et al., 2017; Ndehedehe, Awange, Agutu, et al., 2016) are generally consistent with the amplitudes of TWS indicated in Figure 6. Major rivers (e.g., the Niger, Congo, and the Volta river systems), which drain the region (cf. Figure 1), in addition to the numerous dams and reservoirs (e.g., Kainji, Akosombo, Kindia, Konkoure, etc.) serving hydropower purposes are indications of the active hydrological nature of the region. As will be highlighted later in the manuscript (section 5.2.2), the temporal and spatial distributions of TWS in these areas are also largely driven by teleconnections amongst other factors, similar to rainfall.

The relationship of climate modes with deseasonalized TWS (i.e., the localised TWS signals from the ICA procedure) was examined in the region. As indicated in Figure 7, the ICA technique localises the TWS changes, providing more meaningful space–time patterns that can be associated with physical phenomena. Similar to Ilin, Valpola, and Oja (2005) who identified the ENSO phenomenon in global climate

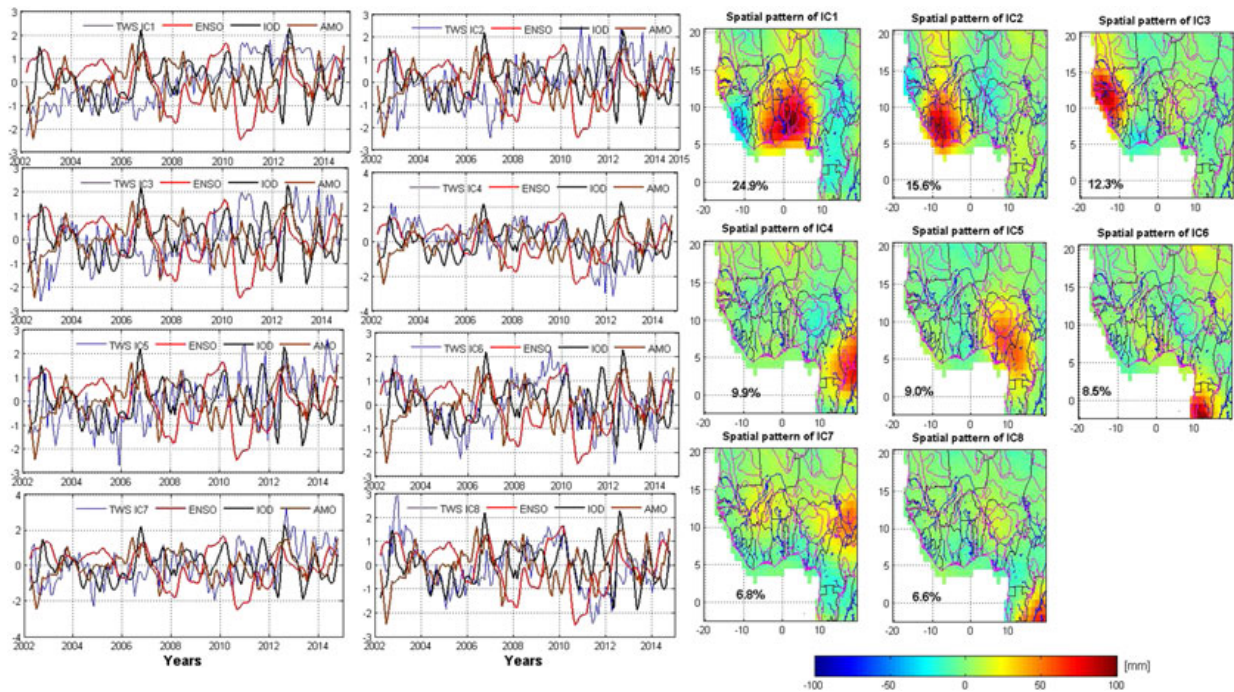


FIGURE 7 ICA decomposition of GRACE-derived TWS (2002–2014) over West Africa after separating the annual and semi-annual cycles (i.e., deseasonalized) using the multiple linear regression analysis. The independent components (left) are temporal patterns that are unitless and corresponds to the spatial patterns (right), which have been scaled using the standard deviation of the computed independent components of GRACE data. The total variabilities explained by each ICA mode are also indicated. Other hydrological units (rivers, lakes, and groundwater aquifers) have been indicated on the spatial patterns (blues and magenta lines on the right) associated with the temporal series of SPI (left)

TABLE 4 Correlations between ICA-derived temporal evolutions of TWS and climate teleconnections

ICs	ENSO	IOD	AMO	Region
IC1	-0.40	0.10	0.12	Volta basin/Nigeria
IC2	-0.30	0.08	0.20	Liberia/Ivory Coast/Guinea
IC3	-0.30	-0.02	0.23	Guinea/Senegal/Gambia
IC4	0.23	-0.01	0.01	Congo/Central African Republic
IC5	-0.14	0.14	0.19	Nigeria/Cameroon
IC6	0.16	0.20	-0.22	Gabon
IC7	-0.30	0.01	0.24	Chad
IC8	0.30	0.16	-0.14	Congo/Democratic Republic of Congo

Note. ICA = independent component analysis; TWS = terrestrial water storage.

The correlation coefficient in bold are statistically significant at the 95% significant level using the student *t* test.

The locations of the observed spatial patterns are also indicated.

data (surface temperature, sea level pressure, and precipitation) using signal separation techniques, the main target here is to identify physically meaningful oscillations of the climate system that disturbs the region’s hydrology and impacts on freshwater distribution and variability. In order to predict TWS changes in West Africa, Forootan et al. (2014) combined the ICA technique with an autoregressive model to statistically study the physical processes of the region (excluding countries of the Congo basin). Whereas they focused on developing a prediction model based on independent temporal series of TWS, SST, and rainfall, the approach in this study identifies independent

spatial elements of TWS over West Africa (including the Congo basin) with potential connections to climate modes. The ICA modes analysed in this study (Figure 7), however, show variability in TWS (spatial patterns) over the Guinea Coast countries and some Sahelian areas that compares well with the leading modes of TWS presented by Forootan et al. (2014). In addition to this, spatially independent patterns of TWS are also observed over the Congo basin area (Figure 7). ENSO shows a statistically significant negative correlation of -0.40 with TWS (IC1, Figure 7), suggesting that ENSO explains some of the observed variability in TWS over the Volta basin and some parts of Nigeria. A coupled association of ENSO and AMO in Guinea and Chad is also noticed as they both indicate negative correlations of -0.30 with ENSO, whereas AMO shows weak positive correlations of 0.23 and 0.24, respectively, with TWS (Table 4). Also, in Gabon, weak correlations of 0.20 and -0.22 for IOD and AMO, respectively, with TWS (IC6, Figure 7) are found. The correlation results of the climate teleconnections with the temporal evolutions of TWS over West Africa are summarised in Table 4. We do not claim any cause-effect relationship in the correlation results of TWS and climate indices. Considering that some of the strong peaks (wet or dry) observed in the SPI shown in Figures 3 and 4 (i.e., the SPI orthogonal modes) are climate indices related, the catchments within the Guinea Coast and Equatorial regions then become direct recipients of these extreme conditions. In the course of time (e.g., 1 year or more), probably owing to hydraulic characteristics of the region, the impact of these indices are likely to be reflected in storage conditions. We are cautious about this speculation, but Dong et al. (2015), in addition to observing an ENSO-induced variance in aquifer water levels in Japan,

found that the water level in recharge area mainly fluctuates between 1- and 2-year periods. Given that ENSO and AMO were associated with drought temporal evolutions in the region (see section 5.1), their association with TWS (Figure 7) might be expected, as rainfall is a major driver of TWS in the region (Ndehedehe, Awange, Agutu, et al., 2016). The AMO for instance, shows a correlation of 0.62 with SPI 12-month time series whereas ENSO indicates a statistically significant negative correlation of -0.30 with time series of SPI 6-month cumulation.

Observing more closely, one notes that unlike in the 2002–2007 period, Liberia and parts of Guinea/Ivory Coast/Seirra Leone indicated a considerable high pronounced amplitudes of TWS between 2010 and 2013 (IC2, Figure 7), inconsistent with extreme drought conditions during the same period when drought persisted during the 2009–2012 period (IC5, Figure 4). Although meteorological patterns in these countries (Guinea/Ivory Coast/Seirra Leone) are associated with El-Niño events amongst other factors, large inter-annual variability in annual and seasonal rainfall, huge catchment stores, and the cumulative increase in the volume of water not involved in surface runoff (Ndehedehe, Awange, Agutu, et al., 2016) are possible reasons for this inconsistency. There are indications, nonetheless, that these countries, which also indicate the strongest annual amplitude of TWS (Figure 6a), show the presence of climate-induced TWS (section 5.2.2).

Besides the observed association of ENSO with TWS in the region, our findings also confirm that the development of AMO can also be considered as a factor that could enhance more rainfall in the Sahel leading to significant contributions on TWS changes in the region. AMO in particular showed the strongest associations with rainfall condition (i.e., 0.43 and 0.62 for SPI at 6- and 12-month aggregations, respectively) in the Sahel region (IC1, Figures 3 and 4). Some studies (e.g., Ndehedehe, Agutu, Okwuashi, et al., 2016; Okonkwo, 2014; Mohino et al., 2011) have shown that the AMO index explains drought characteristics in the Sahel. Whereas Hodson et al. (2010) argued that the AMO played no role in the observed decline in Sahel rainfall, Rodríguez-Fonseca et al. (2011), however, attributed the decline in Sahel rainfall to the combined effects of AMO and global warming SST modes. They also speculated that a change in the AMO phase towards the end of the 20th century could have triggered the partial recovery in Sahel rainfall, consistent with Mohino et al. (2011) who had similar conclusions that the partial recovery was mainly driven by the AMO. The association of AMO with temporal evolutions of SPI over the Sahel region in this study is consistent with Diatta and Fink (2014) who found a positive correlation between Sahel rainfall and AMO. Rainfall over the Sahel is enhanced by the positive phase of the AMO whereas in the Gulf of Guinea AMO decreases it (Mohino et al., 2011). Consequently, this observed relationship between AMO and localised SPI time series (IC1, Figures 3 and 4) may have implications on TWS variations (especially the soil moisture components) and ecosystem performance, probably in complex and nonlinear ways that would perhaps require further analysis in the future.

5.2.2 | Spatial variability of climate-induced TWS

The spatial patterns of climate-induced TWS presented in Figure 8 are for areas where statistically significant ($\alpha = 0.05$) relationships (TWS vs. teleconnections) exist in the region. The amplitudes of the relative contributions (i.e., from the spatial patterns) of these climate telecon-

nections on TWS changes were estimated using Equation 8. The amplitudes of GRACE-TWS induced by all three climate modes in the equatorial regions (Gabon, Congo, and Democratic Republic of Congo-DRC) reached 30 mm for ENSO, AMO, and IOD, respectively, (Figure 8a–c). For the long term MERRA-derived TWS, the spatial patterns for all climate-induced TWS indicate an amount greater than 30 kg/m² in the Gulf of Guinea countries and equatorial regions (Figure 8d–f). The contributions of ENSO, AMO, and IOD are somewhat weak in much of the Sahel but strong along the coastal West African countries probably due to rainfall distribution patterns, which are modulated by intertropical convergence zone and transitions in the rain belt.

Overall, considerable strong contributions of climate teleconnections to TWS change in the region are found mostly in areas with a strong presence of surface water (rivers and lakes), subsurface storage changes (e.g., groundwater aquifers) and annual rainfall (cf. Figures 1 and 8d–f). For instance, high rainfall amounts at seasonal and annual scales are prominent drivers of TWS changes over West Africa as highlighted in, for example, Ndehedehe, Awange, Agutu et al. (2016). But the river discharge of the lower Congo basin, Lake Volta water level variations, and the Chari-Logone river system, which provide approximately 95% of the total input into Lake Chad basin, are also major triggers of observed trends and inter-annual variability in TWS.

The ENSO-induced amplitude of TWS indicated by GRACE and MERRA is relatively strong and has a wider spread over the Volta and Congo basins (Figure 8a,d) compared to the Sahel whereas the amplitude of AMO-induced TWS show strong presence in much of the Guinea Coast areas and the equatorial regions where rainfall is relatively high and bimodal (Figure 8b,e). Recall that in section 5.2.1, the temporal evolutions of TWS over the Volta basin (IC1, Figure 7) showed a statistically significant negative correlation of -0.40 with the normalised time series of ENSO. This observed relationship is moderate and also coincides with the negative correlation of ENSO (i.e., -0.30) with the temporal evolutions of SPI 6- and 12-month aggregation (see Table 3), indicating that ENSO has an association with rainfall conditions and TWS changes over the Volta basin. The ENSO phenomenon has been linked to increase in the variability and decline in rainfall totals, causing decline in Lake Volta water levels (Owusu, Waylen, & Qiu, 2008). Other regions such as the Congo basin also indicate similar association with ENSO, that is, positive correlations of 0.23 and 0.30 with TWS (IC4 and IC8, Figure 7, respectively) and a negative correlation of -0.30 with SPI temporal evolutions (IC7, Figure 7). Besides the associations of ENSO and AMO with rainfall conditions, we also found a somewhat weak correlation of IOD (0.20, Table 4) with temporal patterns of TWS in Gabon (IC6, Figure 7, respectively). In addition to the observed relationship of IOD with the temporal patterns of TWS in Gabon, the contributions of IOD-induced TWS (GRACE), which reached 30 mm (Figure 8c) may suggest a possible contribution of all three climate modes in this subregion. Coincidentally, the spatial patterns of IOD-induced TWS (GRACE) are in the same direction where increasing trend in GRACE-TWS was observed in previous studies (Ndehedehe, Awange, Agutu, et al., 2016; Ahmed et al., 2014). However, the magnitude and domain size of MERRA-TWS indicates that ENSO and AMO have had stronger impact on the TWS of the region during the 1980–2015 period (Figure 8d,e) compared to IOD (Figure 8f).

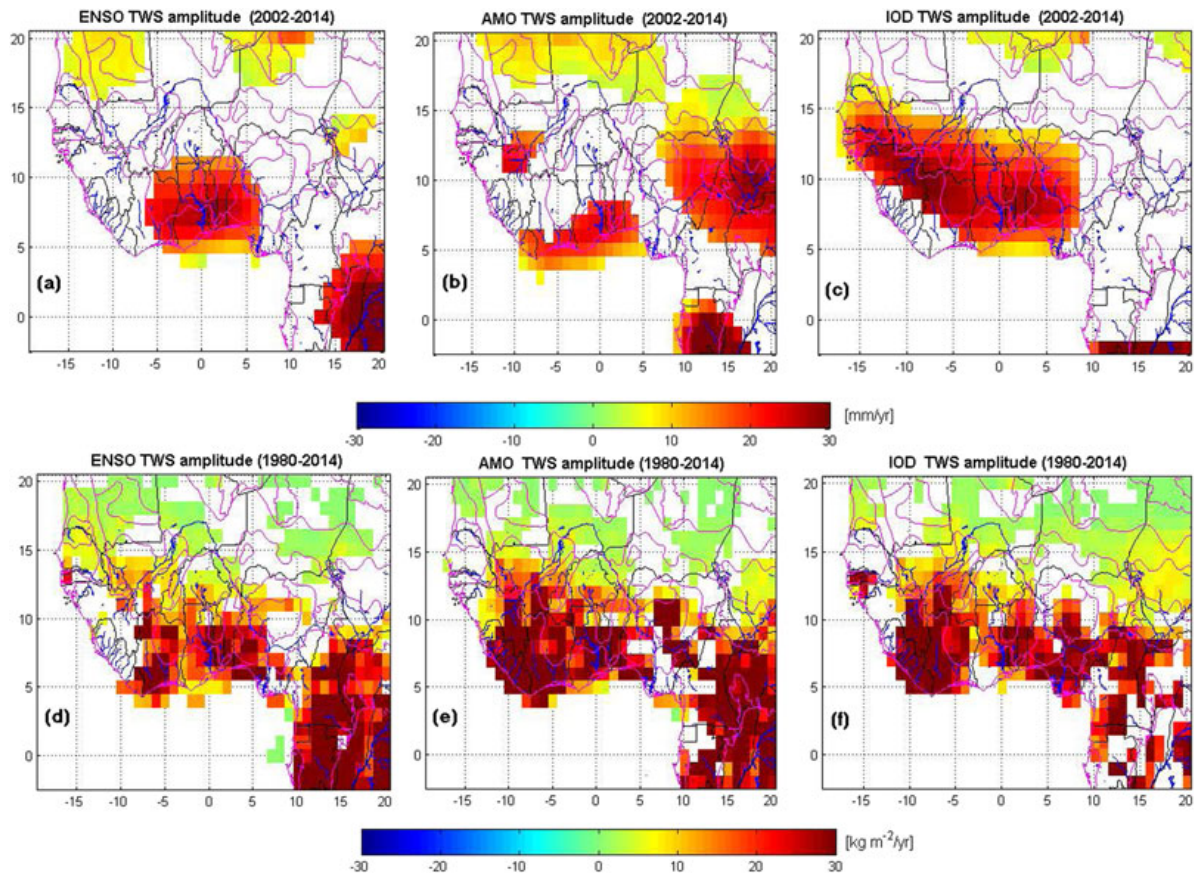


FIGURE 8 Spatial patterns of (a–c) climate-induced TWS derived from GRACE-TWS and (d–f) MERRA-TWS. These estimates (amplitudes of TWS) are derived using the multiple linear regression analysis technique. The regression coefficients indicated for both GRACE and MERRA data are those with statistically significant ($\alpha = 0.05$) association with climate indices (ENSO, AMO, and IOD). Groundwater aquifers (magenta), rivers, and lakes (blue) have also been shown on the spatial distribution of climate-induced TWS

The impact of the frequency and strength of IOD on West Africa's climate is still unclear. Bader and Latif (2011) and Giannini et al. (2003) have argued, however, that the warming in the Indian Ocean was a major forcing in the observed 1983 drought in the West Sahel. Whereas IOD indicates contributions of more than $30 \text{ kg}\cdot\text{m}^{-2}\cdot\text{year}$ in the long term MERRA-TWS in east Guinea (part of West Sahel), Côte d'Ivoire, Benin, Nigeria, Liberia, and the equatorial regions (mostly Cameroon), it shows weaker contributions in most Sahelian areas similar to ENSO and AMO (Figure 8f). Although possible uncertainties in the MERRA data over the region can also limit its capability in quantifying accurately the impacts of IOD on TWS, warranting future consideration of inherent uncertainties in the data, Diatta and Fink (2014) observed statistically significant negative correlations of IOD (-0.30 and -0.23) with rainfall indices at West and Central Sahel areas. Some studies based on model experiments and observations (see Nicholson, 2013, and the references therein) have argued that both Indian Ocean warming and SST gradients in the Indian Ocean have considerable influence on Sahel rainfall. Even though large-scale climatological shifts in the Indian Ocean SST are also the fallout of other processes of oceanic variability such as the ENSO (Farnsworth, White, Williams, Black, & Kniveton, 2011), the observed drying trend in the West Sahel from the 1950s to the 1990s was attributed to the warming trend in the

Indian Ocean (see Bader and Latif, (2003)). Put together, this may imply a possible signature of IOD in West Africa's rainfall, in addition to the well-known connection of AMO and ENSO with rainfall variability in the region (see, e.g., Martin & Thorncroft, 2014; Diatta & Fink, 2014; Nicholson, 2013; Paeth et al., 2012; Panthou et al., 2012; Nicholson et al., 2000). So far, this study speculates that the mechanism of influence of IOD on TWS in the region may be at best complementary. Based on the result shown in Figure 8 and our hypothesis that indices related rainfall impact on catchment storage (especially the Gulf of Guinea countries), it is our view that these indices of climate variability in the region collectively impact on the leading orthogonal modes of TWS (IC1, Figure 7) in the region, exacerbating its variability. Apparently, MERRA-TWS over the Guinea Coast countries show statistically significant associations with all climate modes probably due to its long-term records, which makes it possible to extract complete oscillations in each climate index unlike the GRACE data.

TWS over Gabon and some parts of the Congo basin have relatively strong semi-annual patterns (Figure 6). The presence of strong seasonal rainfall in Guinea Coast countries, Gabon, and much of the Congo basin also accounts for the observed TWS modes (Figure 7) and semi-annual amplitudes (Figure 6). Whereas nonsymmetric meteorological signals (e.g., a strong rise in summer rainfall anomalies) may also

create considerable peaks in the hydrological time series (TWS), much of the equatorial regions (e.g., Congo, Gabon, etc.) have huge water fluxes (e.g., surface runoff) and vegetative cover that show strong sensitivity to rainfall conditions, SST anomalies, and other perturbations of the nearby oceans. Given that the climate of Gabon is tropical in nature, with single wet season between October and May, leading to 200–250 mm of rainfall (see McSweeney, New, Lizcano, & Lu, 2010), the strong semi-annual amplitude of TWS (Figure 6b) in this area may also be associated with multiple climate modes as shown in Figure 8a–f. Such relationship, however, may require further clarification as the records of GRACE observation increases.

Furthermore, ENSO shows a stronger association (especially over the Volta basin, which explains the strongest variability in TWS –24.9%, IC1, Figure 7) with observed TWS changes (see Table 4). From all indications, apart from the observed amplitude of AMO TWS (i.e., using MERRA-TWS; Figure 8e), in much of the Guinea Coast countries, ENSO is more closely related to GRACE-TWS changes in the region. This is exemplified in the inter-annual fluctuations of TWS of the first three ICA modes, which jointly explained 52.8% of the total variability (i.e., IC1–IC3, Figure 7) and showed a much higher association with ENSO (–0.4 and –0.3) compared to other climate modes (IOD and AMO). Using GRACE-derived TWS during the 2003–2010 period, Phillips et al. (2012) observed that in tropical regions, ENSO was negatively correlated with TWS, consistent with our observed relationship of the leading TWS modes with ENSO (IC1, Figure 7). In a recent study over West Africa where available water expressed in terms of net-precipitation (1979–2010) was analysed using wavelet coherence analysis, decreasing rate in available water was highly coupled to a low frequency modulating El-Niño (see Andam-Akorful et al., 2017). Other remarkable footprints of these climate modes in the region are also documented. For example, in the Sahel, ENSO, AMO, and IOD were found to have strong association with precipitation at periodicity (Okonkwo, 2014). In a study analysing global trends and variability in soil moisture and drought characteristics, West Africa is one of the areas in the world where inter-annual and decadal variations in soil moisture are driven mainly by variabilities in ENSO and AMO (see Sheffield & Wood, 2008). Considering the results in preceding sections (Figures 3, 4, and 7), hydrological conditions of the Lake Volta arguably have some remote links with ENSO events and aligns with earlier reports (e.g., Owusu et al., 2008). Because TWS change over the Volta basin is also significantly driven by variations in Lake Volta water levels, the influence of ENSO in the basin presumably exists. For example, even after removing the annual and semi-annual components of TWS, the amplitudes of TWS in late 2010 and 2012 periods in the vicinity of the Volta basin reached ~200 mm (i.e., jointly derived from the temporal/spatial patterns), coinciding with the strong La-Niña events of 2010–2011 and 2011–2012 (IC1, Figure 7). Similarly, the hydrological drought of 2001/2002 in the Volta basin (e.g., Ndehedehe, Awange, Corner, et al., 2016; Bekoe & Logah, 2013) is also consistent with our observed spatio-temporal fluctuations of wet/dry conditions (IC2, Figures 4 and 5). The hydrological drought during this period (2001–2002) resulted in one of the lowest negative anomalies (i.e., approximately –200 mm when jointly derived from the first ICA mode of Figure 7) observed in GRACE-derived TWS in the Volta catchment since inception of GRACE observations. Although the observed

drought of 2001/2002 in the region remains the general signature of climate variability rather than the influence of these specific climatic indices, it nonetheless gives credence to our hypothesis that the impact of extreme rainfall fluctuations leads to increased or decreased catchment storage in the region.

Based on the premise that drought conditions are primarily the result of precipitation deficits and can lead to reduced recharge of the soil column (Sheffield & Wood, 2008), then this assumption holds. On the contrary, catchment characteristics, land use change, changes in temperature, and other meteorological and ecological processes can interact in complex ways that accentuates TWS variations in the region. For instance, during periods of precipitation deficits in Niger (Sahel region), an extensive network of well observations showed that groundwater levels and water table increased significantly due to land clearing and land-use change (see Favreau et al., 2009; Séguis et al., 2004; Leduc, Favreau, & Schroeter, 2001). Similar complex hydrological processes were reported for south-east Australia and south-west United States (see Scanlon, Reedy, Stonestrom, Prudic, & Dennehy, 2005; Allison et al., 1990). Although the influence of nonclimatic factors (e.g., shrub removal) on hydrological changes remains unclear in central Texas (see Wilcox, 2007), Cattle trampling and timber harvesting triggered an evolution of runoff regime in northern Mexico (see Viramontes & Descroix, 2003), confirming the influence of human activities on hydrological changes. The Sahel is a semiarid ecosystem, and one would naturally expect water availability through rainfall and soil moisture as major hydrological indicators of ecosystem performance. But Seghieri et al. (2012) found that a decrease in temperature was the strongest predictor of both leafing and reproductive phenophases in the Sahel. Collectively, these are some indications that the impact of nonclimate teleconnection factors on hydrological processes exists in the region, especially the Sahel and other semiarid regions.

From the foregoing, nonetheless, our presumptive evidence is that ENSO (i.e., depending on the phase) impacts more on TWS in West Africa and leads to strong changes in surface and subsurface storage (i.e., at seasonal scales). The analyses in this study also show a strong presence of AMO TWS in the coastal West African countries and much of the regions below latitude 10°N (Figure 8e). As noted over the Sahel, positive phase of AMO coincides with above-normal rainfall or wet conditions and the negative phase with drought conditions (IC1, Figures 3 and 4). This could be an evidence that corroborates the strong presence of AMO-driven TWS in the region as shown in Figure 8e. However, considering the rather weak correlations of these climate modes with the localised time series of the leading GRACE-TWS modes, there might be indication that other low-frequency climate oscillations combined with the influence of atmospheric circulations may be related to TWS over the region. The study is cautious in this regard but affirms that as the records of GRACE observation increases, this physical mechanisms and others can be investigated much more systematically with clarity and simplicity.

6 | CONCLUSIONS

The presence of climate teleconnection-induced (i.e., ENSO, AMO, and IOD) TWS changes derived from GRACE and MERRA over West

102 Africa was studied using a suite of statistical techniques. The leading spatio-temporal modes of TWS and extreme rainfall anomalies (wet and drought events) were identified and their possible relationship to climate teleconnections in the region were examined using correlation analysis. The results of the study are summarised as follows:

(a) The leading modes of SPI at 6- and 12-month aggregation indicating extreme drought/wet conditions coincided with extreme low/high amplitudes of TWS during the same period, giving credence to our hypothesis that the impact of extreme rainfall fluctuations leads to increased or decreased catchment storage in the region. Although it is generally expected that large anomalies in rainfall are likely to generate low/high values of SPI (drought or wet conditions), leading to large anomalies in TWS (extreme low/high amplitudes), it is sometimes not usually the case for areas where water availability is also driven by temperature and in ecosystems where human activities (e.g., land clearing) have modified the land surface and soil characteristics. These scenarios, which result in complex hydrological processes (e.g., increasing water table during periods of strong precipitation deficits), have been highlighted in previous reports in the Sahel region and are few exceptions to the above argument. AMO and ENSO noticeably explains some of the variability in the observed SPI over the Sahel and the equatorial regions, suggesting that these teleconnections also play key roles in the characteristics of extreme climatic conditions in the region.

(b) Whereas ENSO appears to be more associated with TWS in the region and shows a statistically significant correlation with the observed temporal patterns of TWS, our analysis here also shows a strong presence of AMO-induced TWS in the coastal West African countries and much of the regions below latitude 10°N. The AMO has a wider footprint and sphere of influence on the region's TWS and suggests the important role of North Atlantic temperature in the region. Its association with temporal evolutions of SPI may have implications on TWS, especially in the semiarid regions, though in complex ways, that requires further investigation. There are also statistically significant relationships between TWS and teleconnections (ENSO, AMO, and IOD) in much of the Sahel region. Nonetheless, the contribution of the latter to TWS in the Sahel is considerably weak and maybe related to the rainfall structure of the region.

(c) The impacts of IOD on the Western African hydrology appears to be unclear but shows statistically significant contribution to the long term MERRA-TWS for the countries along the coast and coincided with observed fluctuating drought conditions observed between 2005 and 2012 in eastern Guinea and Liberia. Global climate simulations in which IOD-like SST anomalies are imposed could help to clarify the role of IOD on the region's TWS and can be taken into consideration in future studies. Although this study confirmed the existence of IOD-induced TWS in the region, which at best may be complementary, TWS over much of West Africa and countries of the Congo basin is more likely to be influenced by ENSO and AMO events.

(d) As some areas in the Sahel show strong AMO contributions to GRACE-TWS compared to the observed weak AMO-related MERRA-TWS, there are possibilities of false associations of GRACE-TWS with teleconnections (especially AMO) probably due to the limited time span of GRACE observations. However, the rather weak correlations of these climate modes with localised time series of GRACE-TWS may also give the impression that other climate oscil-

lations and atmospheric circulations could be associated with TWS changes in the region. The study is rather cautious in this regard but optimistic that as the records of GRACE observation increases with time, these physical mechanisms and others can be investigated much more systematically with clarity, simplicity, and very limited uncertainties. A robust analysis to help examine specific zones of global SSTs that impacts on TWS amplitudes over West Africa could provide more insights into the relationship between TWS and climate teleconnections and will be the subject of future considerations.

ACKNOWLEDGMENTS

Christopher and Nathan are grateful to Curtin University for the funding through the CSIRS programme. Joseph is grateful for the financial support of the Japan Society of Promotion of Science for supporting his stay at Kyoto University (Japan) and the conducive working atmosphere provided by his host Prof. Yoichi Fukuda (Department of Geophysics, Kyoto University, Japan). We also thank the Editor and the two anonymous reviewers for their very useful comments, which helped improved the manuscript. The authors are grateful to the Center for Space Research, NOAA, and NASA for the various data used in this study.

ORCID

Christopher E. Ndehedehe  <http://orcid.org/0000-0003-1906-9764>

REFERENCES

- Adler, R. F., Huffman, G. J., Chang, A., Ferraro, R., Xie, P.-P., Janowiak, J., ... Nelkin, E. (2003). The version-2 Global Precipitation Climatology Project (GPCP) monthly precipitation analysis (1979-Present). *Journal of Hydro-meteorology*, 4(6), 1147–1167.
- Agutu, N., Awange, J., Zerihun, A., Ndehedehe, C., Kuhn, M., & Fukuda, Y. (2017). Assessing multi-satellite remote sensing, reanalysis, and land surface models' products in characterizing agricultural drought in East Africa. *Remote Sensing of Environment*, 194(0), 287–302.
- Ahmed, M., Sultan, M., Wahr, J., & Yan, E. (2014). The use of GRACE data to monitor natural and anthropogenic induced variations in water availability across Africa. *Earth Science Reviews*, 136, 289–300.
- Aires, F., Rossow, W. B., & ChéDin, A. (2002). Rotation of EOFs by the independent component analysis: Toward a solution of the mixing problem in the decomposition of geophysical time series. *Journal of the Atmospheric Sciences*, 59, 111–123.
- Ali, A., & Lebel, T. (2009). The Sahelian standardized rainfall index revisited. *International Journal Of Climatology*, 29, 1705–1714.
- Allison, G., Cook, P., Barnett, S., Walker, G., Jolly, I., & Hughes, M. (1990). Land clearance and river salinisation in the western Murray Basin, Australia. *Journal of Hydrology*, 119(1), 1–20.
- Amani, A., Thomas, J., & Abou, M. N. (2007). Climate change adaptation and water resources management in West Africa. Synthesis report WRITESHOP UNESCO. Retrieved from: www.nlcap.net/032135.070920.NCAP Accessed 15th April 2014.
- Andam-Akorful, S., Ferreira, V., Ndehedehe, C. E., & Quaye-Ballard, J. (2017). An investigation into the freshwater variability in West Africa during 1979 – 2010. *International Journal of Climatology*. <https://doi.org/10.1002/joc.5006>
- Awange, J., Khandu, Schumacher, M., Forootan, E., & Heck, B. (2016). Exploring hydro-meteorological drought patterns over the Greater Horn of Africa (1979-2014) using remote sensing and reanalysis products. *Advances in Water Resources*, 94, 45–59.

- Bader, J., & Latif, M. (2003). The impact of decadal-scale Indian Ocean sea surface temperature anomalies on Sahelian rainfall and the North Atlantic Oscillation. *Geophysical Research Letters*, 30(22), 2169.
- Bader, J., & Latif, M. (2011). The 1983 drought in the West Sahel: A case study. *Climate Dynamics*, 36(3-4), 463–472.
- Barry, B., Obuobie, E., Andreini, M., Andah, W., & Pluquet, M. (2005). Comprehensive assessment of water management in agriculture: Comparative study of river basin development and management. *International Water Management Institute*. Retrieved from: www.iwmi.cgiar.org/assessment, Accessed 11 November, 2015.
- Bekoe, E. O., & Logah, F. Y. (2013). The impact of droughts and climate change on electricity generation in Ghana. *Environmental Sciences*, 1(1), 13–24.
- Boening, C., Willis, J. K., Landerer, F. W., Nerem, R. S., & Fasullo, J. (2012). The 2011 La Nina: So strong, the oceans fell. *Geophysical Research Letters*, 39(19), L19602.
- Boergens, E., Rangelova, E., Sideris, M. G., & Kusche, J. (2014). Assessment of the capabilities of the temporal and spatiotemporal ICA method for geophysical signal separation in GRACE data. *Journal of Geophysical Research Solid Earth*, 119, 4429–4447.
- Boone, A., Decharme, B., Guichard, F., Rosnay, P. D., Balsamo, G., Belaars, A., ... Xue, Y. (2009). The AMMA land surface model intercomparison project (ALMIP). *Bulletin of American Meteorological Society*, 90(12), 1865–1880.
- Cai, W., Santoso, A., Wang, G., Weller, E., Wu, L., Ashok, K., ... Yamagata, T. (2014). Increased frequency of extreme indian ocean dipole events due to greenhouse warming. *Nature*, 510(7504), 254–258.
- Cardoso, J.-F. (1991). Super-symmetric decomposition of the fourth-order cumulant tensor, blind identification of more sources than sensors. Retrieved from: <http://perso.telecomparistech.fr/cardoso/Papers.PDF/icassp91.pdf> Accessed 15 January 2016.
- Cardoso, J. F. (1999). High-order contrasts for independent component analysis. *Neural Computation*, 11, 157–192.
- Cardoso, J. F., & Souloumiac, A. (1993). Blind beamforming for non-gaussian signals. *IEE Proceedings*, 140(6), 362–370.
- Chen, J. L., & Wilson, C. R. (2008). Low degree gravity changes from GRACE, Earth rotation, geophysical models, and satellite laser ranging. *Journal of Geophysical Research: Solid Earth*, 113, B06402.
- Cheng, M. K., Tapley, B. D., & Ries, J. C. (2013). Deceleration in the Earth's oblateness. *Journal of Geophysical Research*, 118, 1–8.
- Chylek, P., Klett, J. D., Dubey, M. K., & Hengartner, N. (2016). The role of Atlantic Multi-decadal Oscillation in the global mean temperature variability. *Climate Dynamics*, 47(9), 3271–3279.
- Common, P. (1994). Independent component analysis, a new concept?. *Signal Processing*, 36, 287–314.
- Conway, D., Persechino, A., Ardoin-Bardin, S., Hamandawana, H., Dieulin, C., & Mahé, G. (2009). Rainfall and water resources variability in sub-Saharan Africa during the twentieth century. *Journal of Hydrometeorology*, 10(1), 41–59.
- Dai, A., Qian, T., Trenberth, K. E., & Milliman, J. D. (2009). Changes in continental freshwater discharge from 1948 to 2004. *Journal of Climate*, 22(10), 2773–2792.
- Descroix, L., Mahé, G., Lebel, T., Favreau, G., Galle, S., Gautier, E., ... Sighomnou, D. (2009). Spatio-temporal variability of hydrological regimes around the boundaries between Sahelian and Sudanian areas of West Africa: A synthesis. *Journal of Hydrology*, 375(12), 90–102.
- Diatta, S., & Fink, A. H. (2014). Statistical relationship between remote climate indices and West African monsoon variability. *International Journal of Climatology*, 34(12), 3348–3367.
- Dong, L., Shimada, J., Kagabu, M., & Fu, C. (2015). Teleconnection and climatic oscillation in aquifer water level in Kumamoto plain, Japan. *Hydrological Processes*, 29(7), 1687–1703.
- Druyan, L. M. (2011). Studies of 21st-century precipitation trends over West Africa. *International Journal of Climatology*, 31(10), 1415–1424.
- FAO (1983). Integrating crops and livestock in West Africa. *Food and Agriculture Organization Of The United Nations*. Retrieved from: www.fao.org/docrep/004/x6543e/X6543E00 Accessed 10 May, 2015.
- Farahmand, A., & AghaKouchak, A. (2015). A generalized framework for deriving non parametric standardized drought indicators. *Advances in Water Resources*, 76, 140–145.
- Farnsworth, A., White, E., Williams, C. J., Black, E., & Kniveton, D. R. (2011). Understanding the Large Scale Driving Mechanisms of Rainfall Variability over Central Africa. In *African Climate and Climate Change: Physical, Social and Political Perspectives* (pp. 101–122). Netherlands, Dordrecht: Springer.
- Favreau, G., Cappelaeere, B., Massuel, S., Leblanc, M., Boucher, M., Boulain, N., & Leduc, C. (2009). Land clearing, climate variability, and water resources increase in semiarid southwest Niger: A review. *Water Resources Research*, 45, W00A16.
- Forootan, E., Awange, J., Kusche, J., Heck, B., & Eicker, A. (2012). Independent patterns of water mass anomalies over Australia from satellite data and models. *Remote Sensing of Environment*, 124, 427–443.
- Forootan, E., Kusche, J., Loth, I., Schuh, W. D., Eicker, A., Awange, J., ... Shum, M. S. C. K. (2014). Multivariate prediction of total water storage changes over West Africa from multi-satellite data. *Surveys in Geophysics*, 35(4), 913–940.
- Frappart, F., Ramillien, G., Leblanc, M., Tweed, S. O., Bonnet, M.-P., & Maisongrande, P. (2011). An independent component analysis filtering approach for estimating continental hydrology in the GRACE gravity data. *Remote Sensing of Environment*, 115(1), 187–204.
- Frappart, F., Ramillien, G., Maisongrande, P., & Bonnet, M.-P. (2010). Denoising satellite gravity signals by independent component analysis. *Geoscience and Remote Sensing Letters, IEEE*, 7(3), 421–425.
- Giannini, A., Biasutti, M., Held, I. M., & Sobel, A. H. (2008). A global perspective on African climate. *Climate Change*, 90(7), 359–383.
- Giannini, A., Saravanan, R., & Chang, P. (2003). Oceanic forcing of Sahel rainfall on interannual to decadal time scales. *Science*, 302(5647), 1027–1030.
- Grippa, M., Kergoat, L., Frappart, F., Araud, Q., Boone, A., de Rosnay, P., ... Ramillien, G. (2011). Land water storage variability over West Africa estimated by Gravity Recovery and Climate Experiment (GRACE) and land surface models. *Water Resources Research*, 47(5), W05549.
- Hao, Z., & AghaKouchak, A. (2014). A nonparametric multivariate multi-index drought monitoring framework. *Journal of Hydrometeorology*, 15(1), 89–101.
- Hayes, M. J., Svoboda, M. D., Wilhite, D. A., & Vanyarko, O. V. (1999). Monitoring the 1996 drought using the standardized precipitation index. *Bulletin of the American Meteorological Society*, 80, 429–438.
- Henry, C., Allen, D. M., & Huang, J. (2011). Groundwater storage variability and annual recharge using well-hydrograph and GRACE satellite data. *Hydrogeology Journal*, 19, 741–755.
- Hinderer, J., de Linage, C., Boya, J.-P., Gegout, P., Masson, F., Rogister, Y., ... Bouinck, M.-N. (2009). The GHYRAF (gravity and hydrology in Africa) experiment: Description and first results. *Journal of Geodynamics*, 48, 172–181.
- Hodson, D. L. R., Sutton, R. T., Cassou, C., Keenlyside, N., Okumura, Y., & Zhou, T. (2010). Climate impacts of recent multidecadal changes in atlantic ocean sea surface temperature: A multimodel comparison. *Climate Dynamics*, 34(7), 1041–1058.
- Hua, W., Zhou, L., Chen, H., Nicholson, S. E., Raghavendra, A., & Jiang, Y. (2016). Possible causes of the Central Equatorial African long-term drought. *Environmental Research Letters*, 11(12), 124002.
- Huffman, G. J., Adler, R. F., Bolvin, D. T., & Gu, G. (2009). Improving the global precipitation record: GPCP Version 2.1. *Geophysical Research Letters*, 36(17), L17808.
- Hurkmans, R., Troch, P. A., Uijlenhoet, R., Torfs, P., & Durcik, M. (2009). Effects of climate variability on water storage in the Colorado River Basin. *Journal Of Hydrometeorology*, 10, 1257–1270.
- Ilin, A., Valpola, H., & Oja, E. (2005). Semiblind source separation of climate

- data detects El Niño as the component with the highest interannual variability. In *Proceedings. 2005 IEEE International Joint Conference on Neural Networks*, 2005, 3, pp. 1722–1727.
- Joly, M., & Voldoire, A. (2010). Role of the Gulf of Guinea in the inter-annual variability of the West African monsoon: what do we learn from CMIP3 coupled simulations?. *International Journal of Climatology*, 30(12), 1843–1856.
- Kennedy, A. M., Garen, D. C., & Koch, R. W. (2009). The association between climate teleconnection indices and Upper Klamath seasonal streamflow: Trans-niño index. *Hydrological Processes*, 23(7), 973–984.
- Kusche, J., Schmidt, R., Petrovic, S., & Rietbroek, R. (2009). Decorrelated GRACE time-variable gravity solutions by GFZ, and their validation using a hydrological model. *Journal of Geodesy*, 83(10), 903–913.
- Leduc, C., Favreau, G., & Schroeter, P. (2001). Long-term rise in a Sahelian water-table: The continental terminal in south-west Niger. *Journal of Hydrology*, 243(1–2), 43–54.
- Li, B., & Rodell, M. (2015). Evaluation of a model-based groundwater drought indicator in the conterminous U.S. *Journal of Hydrology*, 526, 78–88.
- Li, K., Coe, M., Ramankutty, N., & Jong, R. D. (2007). Modeling the hydrological impact of land-use change in West Africa. *Journal of Hydrology*, 337(3–4), 258–268.
- Lloyd-Hughes, B. (2012). A spatio-temporal structure-based approach to drought characterisation. *International Journal of Climatology*, 32(3), 406–418.
- Losada, T., Rodríguez-Fonseca, B., Janicot, S., Gervois, S., Chauvin, F., & Ruti, P. (2010). A multi-model approach to the Atlantic Equatorial mode: Impact on the West African monsoon. *Climate Dynamics*, 35(1), 29–43.
- MacDonald, A. M., Bonsor, H. C., Dochartaigh, B. É. Ó., & Taylor, R. G. (2012). Quantitative maps of groundwater resources in Africa. *Environmental Research Letters*, 7(2), 024009.
- Malhi, Y., & Wright, J. (2004). Spatial patterns and recent trends in the climate of tropical rainforest regions. *Philosophical Transactions of the Royal Society of London*, 359(1443), 311–329.
- Martin, E. R., & Thorncroft, C. D. (2014). The impact of AMO on the West African monsoon annual cycle. *Quarterly Journal of the Royal Meteorological Society*, 140, 31–46.
- Masih, I., Maskey, S., Mussá, F. E. F., & Trambauer, P. (2014). A review of droughts on the African continent: A geospatial and long-term perspective. *Hydrology and Earth System Sciences*, 18(9), 3635–3649.
- McKee, T. B., Doeskin, N. J., & Kieist, J. (1993). The relationship of drought frequency and duration to time scales. In *Conference on Applied Climatology*, American Meteorological Society, Boston, Massachusetts, pp. 179–184.
- McSweeney, C., New, M., Lizcano, G., & Lu, X. (2010). The UNDP climate change country profiles improving the accessibility of observed and projected climate information for studies of climate change in developing countries. *Bulletin of the American Meteorological Society*, 91(2), 157–166.
- Mishra, A. K., & Singh, V. P. (2010). A review of drought concepts. *Journal of Hydrology*, 391, 202–216.
- Mohino, E., Janicot, S., & Bader, J. (2011). Sahel rainfall and decadal to multi-decadal sea surface temperature variability. *Climate Dynamics*, 37, 419–440.
- Molion, L. C. B., & Lucio, P. S. (2013). A note on Pacific Decadal Oscillation, El Niño Southern Oscillation, Atlantic Multidecadal Oscillation and the Intertropical Front in Sahel, Africa. *Atmospheric and Climate Sciences*, 3, 269–274.
- Molua, E. L., & Lambi, C. M. (2006). Climate, hydrology and water resources in Cameroon. CEEPA, Discussion Paper, (33). Retrieved from: <http://www.ceepa.co.za/uploads/files/CDP33.pdf> Accessed 6 August, 2014.
- Moore, P., & Williams, S. D. P. (2014). Integration of altimetry lake levels and GRACE gravimetry over Africa: Inferences for terrestrial water storage change 2003–2011. *Water Resources Research*, 50, 9696–9720.
- Ndehedehe, C., Awange, J., Agutu, N., Kuhn, M., & Heck, B. (2016). Understanding changes in terrestrial water storage over West Africa between 2002 and 2014. *Advances in Water Resources*, 88, 211–230.
- Ndehedehe, C. E., Agutu, N. O., Okwuashi, O. H., & Ferreira, V. G. (2016). Spatio-temporal variability of droughts and terrestrial water storage over Lake Chad Basin using independent component analysis. *Journal of Hydrology*, 540, 106–128.
- Ndehedehe, C. E., Awange, J., Kuhn, M., Agutu, N., & Fukuda, Y. (2017). Analysis of hydrological variability over the Volta river basin using in-situ data and satellite observations. *Journal of Hydrology: Regional studies*, 12, 88–110.
- Ndehedehe, C. E., Awange, J. L., Corner, R., Kuhn, M., & Okwuashi, O. (2016). On the potentials of multiple climate variables in assessing the spatio-temporal characteristics of hydrological droughts over the Volta Basin. *Science of the Total Environment*, 557–558, 819–837.
- Nicholson, S. E. (2013). The West African Sahel: A review of recent studies on the rainfall regime and its interannual variability. *ISRN Meteorology*, 2013(453521), 1–32.
- Nicholson, S. E., & Grist, J. P. (2001). A conceptual model for understanding rainfall variability in the West African Sahel on interannual and inter-decadal timescales. *International Journal of Climatology*, 21, 1733–1757.
- Nicholson, S. E., Some, B., & Kone, B. (2000). An analysis of recent rainfall conditions in West Africa, including the rainy seasons of the 1997 El Niño and the 1998 La Niña Years. *Journal of Climate*, 13(14), 2628–2640.
- Oguntunde, P. G., & Abiodun, B. J. (2013). The impact of climate change on the Niger River Basin hydroclimatology. *Climate Dynamics*, 40(1–2), 81–94.
- Okonkwo, C. (2014). An advanced review of the relationships between Sahel precipitation and climate indices: A wavelet approach. *International Journal of Atmospheric Sciences*, 2014, 11 pp.
- Owusu, K., Waylen, P., & Qiu, Y. (2008). Changing rainfall inputs in the Volta basin: Implications for water sharing in Ghana. *GeoJournal*, 71(4), 201–210.
- Paeth, H., Fink, A., Pohle, S., Keis, F., Machel, H., & Samimi, C. (2012). Meteorological characteristics and potential causes of the 2007 flood in sub-Saharan Africa. *International Journal of Climatology*, 31, 1908–1926.
- Panthou, G., Vischel, T., Lebel, T., Blanchet, J., Quantin, G., & Ali, A. (2012). Extreme rainfall in West Africa: A regional modeling. *Water Resources Research*, 48(8), W08501.
- Phillips, T., Nerem, R. S., Fox-Kemper, B., Famiglietti, J. S., & Rajagopalan, B. (2012). The influence of ENSO on global terrestrial water storage using GRACE. *Geophysical Research Letters*, 39, L16705.
- Polo, I., Rodríguez-Fonseca, B., Losada, T., & García-Serrano, J. (2008). Tropical atlantic variability modes (1979–2002). part i: Time-evolving SST modes related to West African rainfall. *Journal of Climate*, 21(24), 6457–6475.
- Reason, C. J. C., & Rouault, M. (2006). Sea surface temperature variability in the tropical southeast Atlantic Ocean and West African rainfall. *Geophysical Research Letters*, 33(21), L21705.
- Redelsperger, J.-L., & Lebel, T. (2009). Surface processes and water cycle in West Africa, studied from the AMMA-CATCH observing system. *Journal of Hydrology*, 375(1–2), 1–2.
- Redelsperger, J.-L., Thorncroft, C. D., Diedhiou, A., Lebel, T., Parker, D. J., & Polcher, J. (2006). African monsoon multidisciplinary analysis. An international research project and field campaign. *Bulletin of the American Meteorological Society*, 87(12), 1739–1746.
- Reichle, R. H., Koster, R. D., Lannoy, G. J. M. D., Forman, B. A., Liu, Q., Mahanama, S. P. P., & Tour, A. (2011). Assessment and enhancement of MERRA land surface hydrology estimates. *Journal of Climate*, 24(24), 6322–6338.
- Rienecker, M. M., Suarez, M. J., Gelaro, R., Todling, R., Bacmeister, J., Liu, E., ... Woollen, J. (2011). MERRA: NASA's modern-era retrospective analysis for research and applications. *Journal of Climate*, 24(14), 3624–3648.
- Rodríguez-Fonseca, B., Janicot, S., Mohino, E., Losada, T., Bader, J., Caminade, C., ... Voldoire, A. (2011). Interannual and decadal SST-forced

- responses of the West African monsoon. *Atmospheric Science Letters*, 12, 67–74.
- Saji, N. H., Goswami, B. N., Vinayachandran, P. N., & Yamagata, T. (1999). A dipole mode in the tropical Indian Ocean. *Nature*, 401, 360–363.
- Sanogo, S., Fink, A. H., Omotosho, J. A., Ba, A., Redl, R., & Ermert, V. (2015). Spatio temporal characteristics of the recent rainfall recovery in West Africa. *International Journal of Climatology*, 35(15), 4589–4605.
- Scanlon, B. R., Keese, K. E., Flint, A. L., Flint, L. E., Gaye, C. B., Edmunds, W. M., & Simmers, I. (2006). Global synthesis of groundwater recharge in semiarid and arid regions. *Hydrological Processes*, 20(15), 3335–3370.
- Scanlon, B. R., Reedy, R. C., Stonestrom, D. A., Prudic, D. E., & Dennehy, K. F. (2005). Impact of land use and land cover change on groundwater recharge and quality in the southwestern US. *Global Change Biology*, 11(10), 1577–1593.
- Séghier, J., Carreau, J., Boulain, N., De Rosnay, P., Arjounin, M., & Timouk, F. (2012). Is water availability really the main environmental factor controlling the phenology of woody vegetation in the central Sahel?. *Plant Ecology*, 213(5), 861–870.
- Séguis, L., Cappelaere, B., Mils, G., Peugeot, C., Massuel, S., & Favreau, G. (2004). Simulated impacts of climate change and land-clearing on runoff from a small Sahelian catchment. *Hydrological Processes*, 18(17), 3401–3413.
- Seo, K.-W., Wilson, C. R., Chen, J., & Waliser, D. E. (2008). GRACE's spatial aliasing error. *Geophysical Journal International*, 172(1), 41–48.
- Shahin, M. (2008). *Hydrology and Water Resources of Africa*. Water Science and Technology Library, Vol. 41. Dordrecht, the Netherlands: Kluwer Academic Publishers.
- Sheffield, J., & Wood, E. F. (2008). Global trends and variability in soil moisture and drought characteristics, 1950–2000, from observation-driven simulations of the terrestrial hydrologic cycle. *Journal of Climate*, 21(3), 432–458.
- Shukla, S., & Wood, A. W. (2008). Use of a standardized runoff index for characterizing hydrologic drought. *Geophysical Research Letters*, 35(2), L02405.
- Swenson, S., Chambers, D., & Wahr, J. (2008). Estimating geocenter variations from a combination of GRACE and ocean model output. *Geophysical Research Letters*, 31, 1–4.
- Tapley, B., Bettadpur, S., Watkins, M., & Reigber, C. (2004). The gravity recovery and climate experiment: Mission overview and early results. *Geophysical Research Letters*, 31, 1–4.
- Theis, F. J., Gruber, P., Keck, I. R., Meyer-bse, A., & Lang, E. W. (2005). Spatiotemporal blind source separation using double-sided approximate joint diagonalization. In *13th Proceeding of European Signal Processing Conference*, pp. 1–4.
- Trenberth, K. E., & Shea, D. J. (2006). Atlantic hurricanes and natural variability in 2005. *Geophysical Research Letters*, 33(12), L12704.
- USAID (2013). 2013 World population data sheet. *United States Agency International Development*. Retrieved from: www.prb.org Accessed 2nd August 2014.
- Viramontes, D., & Descroix, L. (2003). Changes in the surface water hydrologic characteristics of an endoreic basin of northern Mexico from 1970 to 1998. *Hydrological Processes*, 17(7), 1291–1306.
- Wahr, J., Molenaar, M., & Bryan, F. (1998). Time variability of the Earth's gravity field: Hydrological and oceanic effects and their possible detection using GRACE. *Journal of Geophysical Research-Solid Earth*, 103(B12), 30205–30229.
- Westra, S., Brown, C., Lall, U., Koch, I., & Sharma, A. (2010). Interpreting variability in global SST data using independent component analysis and principal component analysis. *International Journal of Climatology*, 30(3), 333–346.
- Wilcox, B. P. (2007). Does rangeland degradation have implications for global streamflow?. *Hydrological Processes*, 21(21), 2961–2964.
- Wouters, B., Bonin, J. A., Chambers, D. P., Riva, R. E. M., Sasgen, I., & Wahr, J. (2014). GRACE, time-varying gravity, Earth system dynamics and climate change. *Reports on Progress in Physics*, 77(11), 116801.
- Wu, M.-L. C., Reale, O., & Schubert, S. D. (2013). A characterization of Africaneasterly waves on 2.5 – 6-day and 6 – 9-day time scales. *Journal of Climate*, 26(18), 6750–6774.
- Yin, X., Gruber, A., & Arkin, P. (2004). Comparison of the GPCP and CMAP merged gaugesatellite monthly precipitation products for the period 1979–2001. *Journal of Hydrometeorology*, 5(6), 1207–1222.
- Zhang, R., & Delworth, T. L. (2006). Impact of Atlantic multidecadal oscillations on India/Sahel rainfall and Atlantic hurricanes. *Geophysical Research Letters*, 33(17), L17712.
- Ziehe, A. (2005). *Blind source separation based on joint diagonalization of matrices with applications in biomedical signal processing* (PhD thesis). Universitat Potsdam. Retrieved from: <http://en.youscribe.com/catalogue/reports-and-theses/knowledge/blind1167source-separation-based-on-joint-diagonalization-of-matrices-1424347> Accessed 15 May 2015.

How to cite this article: Ndehedehe CE, Awange JL, Kuhn M, Agutu NO, Fukuda Y. Climate teleconnections influence on West Africa's terrestrial water storage. *Hydrological Processes*. 2017;31:3206–3224. <https://doi.org/10.1002/hyp.11237>

1 Changes in hydro-meteorological conditions over Sub-Sahara Africa
2 (1980 – 2015) and links to global climate

3 Christopher E. Ndehedehe^{a,b}, Joseph L. Awange^a, Nathan O. Agutu^{a,c}, Onuwa Okwuashi^b

4 ^a*Department of Spatial Sciences, Curtin University, Perth, Western Australia, Australia.*

5 ^b*Department of Geoinformatics and Surveying, University of Uyo, P.M.B. 1017, Uyo, Nigeria.*

6 ^c*Department of Geomatic Engineering and Geospatial Information Systems JKUAT, Nairobi, Kenya.*

7 **Abstract**

8 The role of global sea surface temperature (SST) anomalies in modulating rainfall in the
9 African region has been widely studied and is now less debated. However, their impacts
10 and links to terrestrial water storage (TWS) in general, have not been studied. This study
11 presents the pioneer results of canonical correlation analysis (CCA) of TWS derived from both
12 global reanalysis data (1980 – 2015) and GRACE (Gravity Recovery and Climate Experiment)
13 (2002 – 2014) with SST fields. The major issues discussed include, (i) oceanic hot spots that
14 impact on TWS over Sub-Sahara Africa (SSA) based on CCA, (ii) long term changes in model
15 and global reanalysis data (soil moisture, TWS, and groundwater) and the influence of climate
16 variability on these water fluxes, and (iii) the principal driver of GRACE-derived TWS in the
17 Equatorial region of Africa (i.e., the Congo basin). Results of the CCA diagnostics show
18 that El-Niño Southern Oscillation related equatorial Pacific SST fluctuations is a major index
19 of climate variability identified in the main portion of the CCA procedure that indicates a
20 significant association with long term TWS reanalysis data over SSA ($r = 0.50$ at $\alpha = 0.05$).
21 Based on Man-Kendall's statistics, the study found fairly large long term declines ($\alpha = 0.05$)
22 in TWS and soil moisture (1982 – 2015), mostly over the Congo basin, which coincided with
23 warming of the land surface and the surrounding oceans. Meanwhile, some parts of the Sahel
24 show significant wetting (rainfall, soil moisture, and TWS) trends during the same period
25 (1982 – 2015) and aligns with the ongoing narratives of rainfall recovery in the region. Results
26 of singular spectral analysis and regression confirm that multi-annual changes in the Congo
27 river discharge provide the dominant control on observed inter-annual variations in GRACE-
28 TWS over the Congo basin, and show considerable association with global SST anomalies.

29 *Keywords:* Rainfall, sea surface temperature, canonical correlation analysis, Sub Sahara
30 Africa, Congo basin, climate variability

Email address: christopherndehedehe@gmail.com (Christopher E. Ndehedehe)

31 1. Introduction

32 Global interest in climate change is growing because of its anticipated impacts on agri-
33 culture, water security, and economic growth. As projected, impacts of climate change is
34 expected to have direct and profound negative effects on freshwater availability (see, e.g., Tall
35 et al., 2016; Prudhomme et al., 2014; Schewe et al., 2013). As a result, the focus on changes
36 in hydro-meteorological conditions and water resources is receiving increasing attention (e.g.,
37 Andam-Akorful et al., 2017; Ndehedehe et al., 2016a; Hall et al., 2014; Shiferaw et al., 2014;
38 Zhang et al., 2009; Conway et al., 2009; Descroix et al., 2009; Bekoe and Logah, 2013), espe-
39 cially with the perceived risk and vulnerability of future losses and socio-economic problems
40 (e.g., migration, famine, etc.) resulting from the acceleration of the water cycle.

41 Extreme hydro-meteorological conditions and strong hydrological variability are unpre-
42 dictable outcomes of changes in global climate that impacts on socio-economic systems of the
43 world. In Thailand, for example, about 59 billion dollars was lost to the 2011 flood while
44 economic growth was down by 38% due to hydrological variability in Ethiopia (see, Hall et al.,
45 2014). Whereas the productive seasons of the year are restricted in monsoonal and tropical
46 climates of the world due to strong seasonal and inter-annual rainfall variability (see, Hall
47 et al., 2014), the preponderance of evidence from considerable case studies in the African sub-
48 region (see, e.g., Ndehedehe et al., 2016b; Nicholson, 2013; Mohino et al., 2011a; Bader and
49 Latif, 2011; Losada et al., 2010; Giannini et al., 2008; Todd and Washington, 2004; Nicholson
50 et al., 2000) confirm that atmospheric circulation features, warming of the tropical oceans,
51 mesoscale convective systems, and climate teleconnections, amongst others have large impacts
52 on meteorological processes and induce extreme climatic conditions. Such impacts, teeming
53 up with other low-frequency variability that are connected to slow oceanic and climate sig-
54 nals from global sea surface temperature (SST) anomaly (e.g., Diaz et al., 2001; Enfield and
55 Mestas-Nuñez, 1999; Latif and Barnett, 1996), may have profound influence on hydrological
56 changes and water resources.

57 Studies of changes in global climate and how they impact on meteorological and hydro-
58 logical processes, are without doubt, emerging as active research. So far, our understanding
59 of global climate has improved due to significant progress and advances made in global and
60 regional climate models (i.e., GCMs and RCMs) (see, e.g., Tall et al., 2016; Erfanian et al.,
61 2016; Prudhomme et al., 2014; Dimri et al., 2013; Schewe et al., 2013; Mishra et al., 2012;
62 Li et al., 2004; Lebel et al., 2000). However, in regions where strong hydrological variability
63 have been linked to multiple environmental phenomena such as large scale ocean-atmosphere
64 phenomenon (e.g., Joly and Voldoire, 2010; Redelsperger and Lebel, 2009), land use changes

65 (e.g., Favreau et al., 2009; Descroix et al., 2009), and other human interventions (e.g., surface
66 water schemes) (e.g., Ngom et al., 2016; Ndehedehe et al., 2017a; Ahmed et al., 2014), the skills
67 of climate and hydrological models may be restricted. Primarily, this maybe due to a number
68 of factors that include, e.g., model dependence on computational estimates, model physics,
69 choice of parameterisations, bias, conceptual model and parameter uncertainties (e.g., Oettli
70 et al., 2011; Schuol and Abbaspour, 2006; Koster et al., 2004; Lebel et al., 2000). Despite
71 their potential useful applications in optimisation of water allocation schemes, early warning
72 systems, and estimation of water availability (e.g., Thiemig et al., 2013), the restrictions of
73 outputs from hydrological models, may affect meaningful management decisions related to
74 water resources.

75 The failure of GCMs to produce a realistic climatology in West Africa, for example, can be
76 damaging to hydrological applications (see, Lebel et al., 2000). All of the aforementioned issues
77 represent significant setbacks that have contributed to the poor understanding of hydrological
78 variability (e.g., Hall et al., 2014), especially in Africa, a region characterised by strong inter-
79 annual variability. The lack of sufficient in-situ and direct observations of land surface data
80 (e.g., Alsdorf and Lettenmaier, 2003; Lettenmaier, 2005; Robock et al., 2000) generally affects
81 regional configurations and adequate initialization of models (e.g., Jenkins et al., 2002) for the
82 purposes of hydrological studies. This problem can only be more intense in non-industrialised
83 regions such as Sub-Sahara Africa (SSA) (Fig. 1), where in-situ observations are either con-
84 siderably sparse or unavailable (see, Conway et al., 2009) due to lack of robust investments in
85 gauge measurements. Hence, more research using auxiliary data synthesized by forcing global
86 land surface models with historical meteorological data (e.g., Paolino et al., 2012; Sheffield
87 and Wood, 2008), are required to further assess the representation of the land surface and
88 atmospheric states in global reanalysis models.

89 SSA is indeed a strong climatic hot spot that play key roles in global climate. For instance,
90 the Congo basin's rainfall climatology dominates global tropical rainfall during transition sea-
91 sons (see, Washington et al., 2013). The long term decline in vegetation greenness in the
92 Central African rainforests, the second-largest on Earth (Zhou et al., 2014), are indications
93 that global biodiversity are under significant threat due to climatic disturbance. Sheffield and
94 Wood (2008) found large increase in drought extent over West Africa compared to other global
95 terrestrial areas. Furthermore, observed trends in the magnitude and frequency of flood events
96 in the Sahel and Sudano regions (Nka et al., 2015), strong water deficit anomalies in West and
97 Central Africa during the 2005 – 2007 period (see, Ndehedehe et al., 2016a; Asefi-Najafabady
98 and Saatchi, 2013), and the recent long term drying of Central African Republic (e.g., Hua

99 [et al., 2016](#)), are without doubt coherent impacts of climate variability and indicators of cli-
100 mate change in the region. Although it is now less debated that the global SST anomalies
101 regulate rainfall in SSA (see, e.g., [Odekunle and Eludoyin, 2008](#); [Nicholson and Webster, 2007](#);
102 [Fontaine and Bigot, 1993](#); [Semazzi et al., 1988](#); [Nicholson, 2013](#), and the references therein),
103 their impacts on and links to TWS and water fluxes (e.g., river discharge), in general, has not
104 been studied. As with rainfall, the annual amplitudes and leading modes of land water storage
105 (TWS) and river discharge in SSA is presumably expected to be influenced by ENSO-related
106 Pacific SST fluctuations and other triggers of ENSO, for example, SST anomalies of the north
107 tropical Atlantic (see, e.g., [Ham et al., 2013](#)). Identifying the association between TWS and
108 SST therefore, requires consideration and is significant to understanding global aspects of
109 ENSO effects, for example, on regional hydrology.

110 As opposed to all of these aforementioned studies and those highlighted earlier, this study
111 presents the first results of canonical correlation analysis (CCA, e.g., [Barnett and Preisendorfer, 1987](#);
112 [Graham et al., 1987](#); [Glahn, 1968](#)) of TWS derived from both reanalysis data and
113 GRACE (Gravity Recovery and Climate Experiment) with global SST fields over SSA. The
114 novel and underlying issues discussed include, (i) the linking of homogenous regions of TWS
115 amplitudes to specific zones of global SSTs based on CCA, (ii) analysing the long term changes
116 in water fluxes (rainfall, soil moisture, TWS, and groundwater), and (iii) examining the prin-
117 cipal driver of GRACE-derived TWS in the Equatorial region of Africa (i.e., the Congo basin),
118 which is prominently under-represented in hydrological research compared to other key global
119 basins (see, [Alsdorf et al., 2016](#)). Since the global climate is also affected by tropospherically
120 connected ENSO signals in other global oceans (see, e.g., [Enfield and Mestas-Nuñez, 1999](#);
121 [Latif and Barnett, 1996](#)), the link between long term changes in land water storage of the
122 region and SST anomalies of the Pacific, Indian, and Atlantic Oceans requires reckoning. This
123 is essential to (i) enhance the skills of hydrological models, (ii) close the gap of poorly under-
124 stood complex regional hydrology and water fluxes, and (iii) examine the potential indices of
125 climate variability that are associated with hydrological changes in SSA.

126 The three main objectives of this study are (i) to examine long term trends in water fluxes
127 (1980 – 2015) and the influence of climate variability on long term changes in these water
128 fluxes over SSA, (ii) to examine oceanic hot spots that impacts on TWS over SSA based on
129 CCA, and (iii) to assess the drivers of GRACE-TWS changes over the Congo basin.

130 2. Data

131 The data used in this study have been summarised in Table 1.

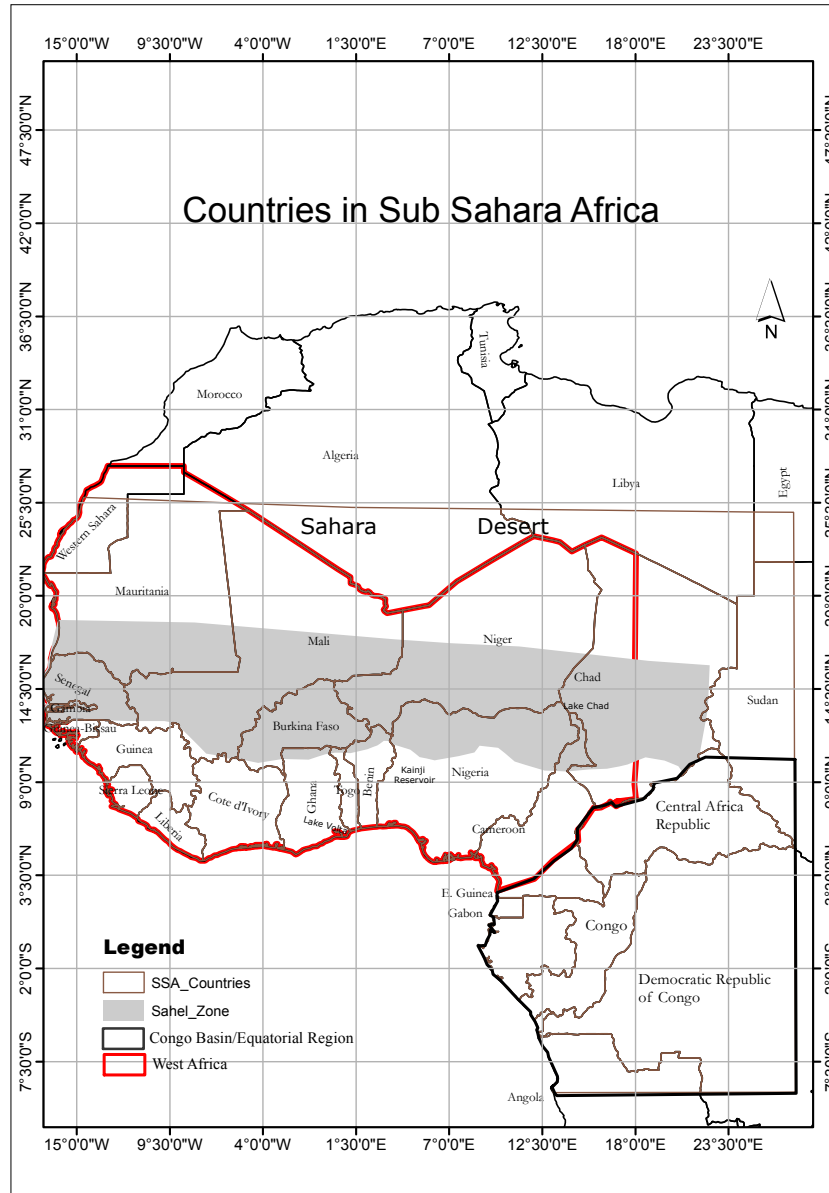


Figure 1: Study area showing some countries in the sub Sahara Africa (SSA) region. Other major sub-regions (i.e., Sahel, West Africa, Congo basin/Equatorial countries) in SSA have also been indicated.

132 *2.1. Terrestrial water storage (TWS)*

133 (1) Modern-Era Retrospective Analysis for Research and Applications (MERRA)

134 National Aeronautic and Space Administration (NASA) global high-resolution MERRA
 135 reanalysis data (see, [Rienecker et al., 2011](#)) was used to analyse the long term TWS and
 136 soil moisture trends. The data is a state-of-the-art reanalysis that provides atmospheric
 137 fields, water fluxes, and global estimates of soil moisture (e.g., [Rienecker et al., 2011](#);

138 [Reichle et al., 2011](#)). Also, it has been improved significantly compared to previous re-
139 analysis datasets ([Rienecker et al., 2011](#)). MERRA outputs have been used in the study
140 of atmospheric circulations and climate teleconnections over the African continent (e.g.,
141 [Wu et al., 2013](#)) and has been recommended for land surface hydrological studies (see, [Re-
142 ichle et al., 2011](#)). The land TWS data component of MERRA used in this study, covers
143 the period of 1980 – 2015 and is available for download through the National Aeronautic
144 and Space Administration (NASA) website (<http://disc.sci.gsfc.nasa.gov/mdisc/>). The
145 MERRA TWS (which are in kg m^{-2} similar to millimeters-mm) was employed to high-
146 light the influence of climate variability on long term terrestrial stored water over SSA,
147 complementing the limited GRACE-TWS data record.

148 (2) *WaterGap Global Hydrology Model (WGHM)*

149 A new version of the global hydrological model (WaterGAP 2.2a) (see, [Döll et al., 2014a](#))
150 was used to derive TWS and groundwater component over SSA. This model takes into
151 account groundwater recharge from surface water bodies in semi arid and arid regions
152 and groundwater depletion. The WaterGAP model data covering the period 1980 – 2009
153 with a spatial resolution of $1^\circ \times 1^\circ$ was downloaded from Center for Environment Systems
154 Research (CESR).

155 (3) *Gravity Recovery and Climate Experiment (GRACE)*

156 GRACE ([Tapley et al., 2004](#)) monthly Release-05 (RL05) spherical harmonic coeffi-
157 cients (degree and order 60 from Center for Space Research-CSR) (data files available
158 at <http://icgem.gfz-potsdam.de/ICGEM/shms/monthly/csr-rl05/>), covering the period
159 2002 – 2014 were processed following the approach of [Wahr et al. \(1998\)](#) as detailed in
160 previous studies (see, e.g., [Ndehedehe et al., 2016a](#); [Landerer and Swenson, 2012](#)). The
161 suitability of TWS outputs from reanalysis and model outputs were assessed by compar-
162 ing with GRACE-derived TWS using Pearson correlation. Since GRACE observations
163 provide an overall picture of the water budget, the principal driver of its variability over
164 the Congo basin was investigated using both rainfall data (Section 2.2) and the river
165 discharge from the Congo Kinshasa station (Section 2.4). Their links to SST anomalies,
166 on the other hand were examined to understand the vulnerability of the region’s stored
167 water to climate variability

168 2.2. *Precipitation data*

169 1. *Global Precipitation Climatology Centre (GPCC)*

170 GPCC ([Schneider et al., 2014](#); [Becker et al., 2013](#)) provides reliable monthly grid-

171 ded data sets of global land-surface precipitation, covering the period from 1901 to
172 present. The $1.0^\circ \times 1.0^\circ$ GPCC data was downloaded from the GPCC open access por-
173 tal (www.ftp.dwd.de/pub/data/gpcc/html/downloadgate.html) and used in the study to
174 analyse the spatial and temporal patterns of rainfall in the region during the 1980 – 2014
175 period.

176 2. Climate Hazards group Infrared Precipitation with Stations (CHIRPS)

177 Monthly CHIRPS (see, [Funk et al., 2015](#)) data (1981-2015) with a spatial resolution of
178 $0.05^\circ \times 0.05^\circ$ was also used in this study. The CHIRPS (data available at [ftp://ftp.chg.uc](ftp://ftp.chg.ucsb.edu/pub/org/chg/products/CHIRPS-2.0/)
179 [sb.edu/pub/org/chg/products/CHIRPS-2.0/](ftp://ftp.chg.ucsb.edu/pub/org/chg/products/CHIRPS-2.0/)) algorithm incorporates gauged locations
180 and infrared Cold Cloud Duration (CCD) precipitation estimates. Its validation results
181 at global and regional scales show that it is useful in the hydrological studies of regions
182 (e.g., Ethiopia) with complex topography, and deep convective precipitation systems.
183 To explore the potential of the higher spatial ($0.05^\circ \times 0.05^\circ$) and temporal (monthly)
184 resolutions of the data, it was employed to study long term spatial and temporal dynamics
185 of rainfall over SSA.

186 2.3. Soil moisture data

187 1. Climate Prediction Center (CPC) Soil Moisture

188 Soil moisture analysis is important in studies of land surface hydrological processes and
189 drought/flood monitoring applications (see, [Fan and Dool, 2004](#)). Monthly CPC soil
190 moisture data ([Fan and Dool, 2004](#)) with spatial resolution of $0.5^\circ \times 0.5^\circ$ for the pe-
191 riod between 1980 to 2014 was used in this study to investigate long term changes in soil
192 moisture. Though a one layer water balance model, the CPC soil moisture product is de-
193 rived from monthly global rainfall data that uses more than 17000 rain gauges worldwide
194 and monthly global temperature from reanalysis. The data is freely available at National
195 Oceanic & Atmospheric Administration (NOAA) ([http://www.esrl.noaa.gov/psd/data/gr](http://www.esrl.noaa.gov/psd/data/gridded/data.cpcsoil.html)
196 [idded/data.cpcsoil.html](http://www.esrl.noaa.gov/psd/data/gridded/data.cpcsoil.html)) for download.

197 2. MERRA Soil Moisture

198 The understanding of extreme hydro-meteorological conditions (e.g., drought) and the
199 climate system rely on the knowledge of soil moisture changes ([Robock et al., 2000](#)).
200 Hence, the soil moisture outputs of the MERRA product was also used in this study to
201 analyse the long term trends and spatio-temporal variability in soil moisture over SSA.
202 The data is in volumetric units ($m^3 m^{-3}$) and covers the period between 1980 and 2015.

Table 1: Summary of precipitation, soil moisture, TWS, and other data used in this study.

Data	Type	Period	Spatial Res.	Temporal Res.	Coverage	References
Precipitation products						
GPCC	Guage	1901 – 2014	1.0° x 1.0°	Monthly	Global	Schneider et al. (2014)
CHIRPS	Satellite & gauge	1981 – 2015	0.05° x 0.05°	Monthly	Global	Funk et al. (2015)
Soil moisture products						
CPC	Model	1948 – 2014	0.5° x 0.5°	Monthly	Global	Fan and Dool (2004)
MERRA	Reanalysis	1980 – 2015	0.625° x 0.5°	Monthly	Global	Rienecker et al. (2011)
Terrestrial water storage products						
WGHM	Model	1980 – 2009	1.0° x 1.0°	Monthly	Global	Döll et al. (2014b)
MERRA	Reanalysis	1980 – 2015	0.625° x 0.5°	Monthly	Global	Rienecker et al. (2011)
GRACE	Satellite	2002 – 2014	1.0° x 1.0°	Monthly	Global	Tapley et al. (2004)
Others						
GLDAS	Model	1982 – 2014	1.0° x 1.0°	Monthly	Global	Rodell et al. (2004)
SST	Satellite	1982 – 2014	1.0° x 1.0°	Monthly	Global	Reynolds et al. (2002)
GRDC	Gauge	1980 – 2010		Monthly	Congo	(www.bafg.de/GRDC)

203 2.4. Global Runoff Data Centre (GRDC)-river discharge data

204 GRDC (www.bafg.de/GRDC) provides river discharge data of nearly 9000 gauging stations
 205 from all over the world. In this study, river discharge data from 1980-2010 (see Table 1) at
 206 Congo Kinshasa station was used to analyse hydrological conditions over the Congo basin.

207 2.5. Sea Surface Temperature (SST)

208 SST ([Reynolds et al., 2002](#)) data (i.e., Atlantic, Indian, and Pacific Oceans) was downloaded
 209 from NOAA’s official earth system research laboratory portal (<http://www.esrl.noaa.gov/psd/d>
 210 [ata/gridded/data.noaa.oisst.v2.html](http://www.esrl.noaa.gov/psd/data/gridded/data.noaa.oisst.v2.html)) for the period covering 1982 to 2014 and used to inves-
 211 tigate the impacts of large scale ocean-atmosphere interactions on TWS over SSA.

212 2.6. Global Land Data Assimilation System (GLDAS)

213 The land surface temperature used in this study was derived from the CLM component of
 214 GLDAS. The data (Table 1) covering the years 1982 – 2014 was obtained from the Goddard
 215 Earth Sciences Data and Information Services Center (GESDICS) (<http://grace.jpl.nasa.gov/d>
 216 [ata/gldas/](http://grace.jpl.nasa.gov/data/gldas/)).

217 3. Method

218 3.1. Canonical correlation analysis

219 The canonical correlation analyses (CCA, see, [Graham et al., 1987](#); [Glahn, 1968](#); [Hotelling,](#)
 220 [1936](#)), a multivariate statistical method that determines a linear combination of two different

sets of variables such that the correlation between the two functions is a maximum, was employed in this study. Specifically, it is employed to examine the interrelationship between the leading modes of SST and inter-annual variations of TWS. Although the CCA technique bears some similarity to principal component analysis (PCA, e.g., Jolliffe, 2002; Preisendorfer, 1988) and multiple linear regression, it is usually viewed as a ‘double-barreled’ PCA (e.g., Wilks, 2011; Graham et al., 1987; Glahn, 1968), emphasizing its robustness over similar methods. Before applying the CCA technique, the SST (predictor) over the three oceans (Atlantic, Indian and Pacific) and TWS (predictand) were pre-orthogonalized and regularized (pre-filtering of the original data) using the PCA technique. This is a standard procedure when applying CCA on climate data (see, e.g., Singh et al., 2012a; Repelli and Nobre, 2004; Yu et al., 1997; Shabbar and Barnston, 1996), mostly because the large spatial fields causes difficulty in inverting the matrices and in the eigenvalue problem, leading to instabilities in the CCA solution. Because the CCA is a form of least squares regression, it is vulnerable to all the potential problems associated with that technique (see, Graham et al., 1987). The pre-filtering of the original data addresses these problems, which includes artificial skills and the uncertainties introduced by correlated predictors (see, Graham et al., 1987), by reducing the number of orthogonal predictors analysed in the primary portion of the CCA procedure.

The pre-orthogonalization process allowed an initial comparison of the dominant modes (the first and second modes were selected for the regression because of their physical interpretability) of the predictor with the predictand based on regression. The CCA procedure was made up of four dominant modes of TWS (GRACE and MERRA) variability and three modes of SST variability over the three Oceans (Atlantic, Indian, and Pacific). Consider that two matrices, $\mathbf{X}_{p,t}$ and $\mathbf{Y}_{q,t}$ represent the predictor (SST) and the predictand (TWS), respectively, where p and q are the spatial points (observations) and t represents the time (months) for each observation. After removing the mean of $\mathbf{X}_{p,t}$ and $\mathbf{Y}_{q,t}$, their statistical decomposition using the PCA technique results in

$$\mathbf{X}_{p,t} = B_{p,p} T_{p,t}, \quad (1)$$

$$\mathbf{Y}_{q,t} = B_{q,q} T_{q,t}, \quad (2)$$

where $B_{p,p}$ and $B_{q,q}$ are the empirical orthogonal functions-EOFs (spatial patterns or the EOF loadings) of the predictor and predictand matrices, respectively, and $T_{p,t}$ and $T_{q,t}$ represents their corresponding time coefficients (see, e.g., Singh et al., 2012b; Yu et al., 1997; Graham et al., 1987). Assuming that i, j are the retained PCA modes of the predictor and predictand time series, the canonical variables (u and v) and the linear combinations of

$$Z = u' T_{i,t} \text{ and } W = v' T_{j,t}, \quad (3)$$

253 can be determined using these retained modes as inputs to the CCA. The objective of CCA
 254 is to calculate two new paired sets of variables,

$$\mathbf{U} = [u', u'_2, \dots, u'_n]', \quad (4)$$

$$\mathbf{V} = [v', v'_2, \dots, v'_n]', \quad (5)$$

256 that are linear combinations of \mathbf{X} and \mathbf{Y} , respectively. The CCA is solved under the condition
 257 that u and v are maximally correlated (see, [Yu et al., 1997](#); [Graham et al., 1987](#); [Glahn, 1968](#)).

258 The correlation C is given as

$$\mathbf{C}_{n,n} = \begin{bmatrix} c_1 & & & 0 \\ & c_2 & & \\ & & \cdot & \\ 0 & & & c_n \end{bmatrix},$$

259 where c_1, \dots, c_n are the canonical correlations between Z and W , and $c_1 \geq c_2 \geq \dots, \geq c_n$
 260 and n are equivalent to i or j , depending on which is smaller. The reconstructed fields of
 261 the predictor and predictands from the PCA procedure (i.e., their EOFs) are projected into
 262 the temporal series (u and v) or canonical components to generate their corresponding spatial
 263 maps (i.e., for the predictands and predictors). These spatial maps are referred to as $g - map$
 264 (predictor map) and $h - map$ (predictand map) and are used to investigate the regions of
 265 variability in the the predictor fields that impacts on the variability of the predictand fields
 266 (see, [Repelli and Nobre, 2004](#)).

267 Compared to other prominent statistical tools (e.g., multiple regression and PCA), the
 268 CCA method is not very popular probably owing to its complex methodology. However, the
 269 method is robust and very useful in empirical climate forecast and diagnosing aspects of the
 270 coupled effect between oceans warming and meteorological patterns (see, e.g., [Singh et al.,](#)
 271 [2012a](#); [Repelli and Nobre, 2004](#); [Yu et al., 1997](#); [Shabbar and Barnston, 1996](#); [Graham et al.,](#)
 272 [1987](#)). Since CCA seeks to identify new sets of variables that optimizes the relationships
 273 between two data sets contrary to the PCA technique (e.g., [Wilks, 2011](#)), it was employed
 274 to investigate the indices of climate variability that impacts on TWS through a diagnostic of
 275 the interrelationships between global SST and inter-annual variations of TWS. It is worthy of
 276 note that the spatio-temporal characteristics of long term changes in rainfall, soil moisture,
 277 and TWS over SSA during the 1980 – 2015 period were also studied using the PCA method
 278 indicated in Eqns. 1 and 2. Apart from the more compact representation of variabilities in
 279 multivariate data, the method is an important tool for exploring large multivariate data (e.g.,
 280 [Jolliffe, 2002](#); [Wilks, 2011](#)). Studying the long term spatial and temporal dynamics of these

281 fluxes over SSA, where several mechanisms drive the climate system requires a multivariate
 282 statistics such as the PCA technique. PCA has the potential for yielding substantial insights
 283 into the spatial and temporal dynamics exhibited by these fluxes. The method has gain
 284 prominence in climate science and has been widely applied in meteorological (see, e.g., [Sanogo
 285 et al., 2015](#); [Fontaine and Bigot, 1993](#); [Janicot, 1992](#); [Janowiak, 1988](#); [Semazzi et al., 1988](#))
 286 and hydrological (see, [Ndehedehe et al., 2016a](#); [Rangelova et al., 2007](#)) studies.

287 3.2. Singular spectral analysis

288 Singular spectrum analysis (see, e.g., [Ghil et al., 2002](#), and the references therein) was
 289 employed to analyse river discharge (1980 – 2010) through a singular value decomposition
 290 (SVD) of the lagged covariance matrices. The method embeds a time series $\{X_{Discharge}(t) :$
 291 $t = 1, \dots, N\}$ in a vector space of dimension M . The embedding approach constructs a sequence
 292 of $\{\mathbf{X}(t)\}$ of M -dimensional vectors from the original time series by using lagged copies of the
 293 scalar data $\{X(t) : 1 \leq t \leq N\}$ (see, [Ghil et al., 2002](#)),

$$\mathbf{X}(t) = (X(t), X(t+1), \dots, X(t+M-1)), \quad (6)$$

294 the vectors $\mathbf{X}(t)$ are indexed by $t = 1, \dots, N'$, where $N' = N - M + 1$. The singular spectral
 295 analysis calculates the principal directions of extension of the sequence of augmented vector
 296 $\{\mathbf{X}(t) : t = 1, \dots, N'\}$ in phase space using an eigenvalue-eigenvector decomposition of the
 297 $M \times M$ covariance matrix or simply through a SVD of the trajectory matrix (see more details
 298 in [Ghil et al., 2002](#)). From the SVD decomposition, meaningful time series are reconstructed
 299 by means of diagonal averaging (see, e.g., [Unnikrishnan and Jothiprakash, 2015](#); [Ghil et al.,
 300 2002](#)). The method offers useful insights into understanding non-linear systems and is here
 301 employed to explore the relationship of river discharge oscillations of the Congo basin with
 302 GRACE-derived TWS.

303 3.3. Trends and annual amplitudes

304 The annual amplitudes of all fluxes (except river discharge) were estimated using the Multi-
 305 ple Linear Regression Analysis (MLRA). The harmonic components (e.g., annual, semi annual,
 306 etc.) of each data were formulated as detailed in [Ndehedehe et al. \(2016a\)](#). Furthermore, us-
 307 ing a non-parametric method, trends in rainfall, soil moisture, groundwater and TWS were
 308 estimated for each grid cell. Based on the least squares estimation of the regression coefficient,
 309 MLRA can also be used to estimate trends as parameterised in [Ndehedehe et al. \(2016a\)](#).
 310 However, the Sen's slope ([Sen, 1968](#)) estimator was used to estimate trends since it is robust

311 and resistant to outliers. Sen slope (S_i) is the median overall values of the whole data and is
 312 estimated as

$$S_k = \text{Median}\left(\frac{P_j - P_i}{j - i}\right), \text{ for } (1 \leq i < j \leq n), \quad (7)$$

313 where P_j and P_i represents data values at time j and i ($j > i$), respectively while n is the
 314 number of data. The slope can be positive indicating increasing trend or negative, indicating
 315 decreasing trend. The significance of observed trends was tested using the Man-Kendall's test
 316 (Mann, 1945; Kendall, 1970), a widely used non-parametric method in testing the significance
 317 of trends. Parametric trend tests (e.g., Student t test, turning point, regression, inversion
 318 tests, etc.) can also be used to examine the statistical significance of trends but sometimes
 319 they violate normality, hence the popularity and preference of non-parametric methods such
 320 as the Man-Kendall, Hotelling-Pabst test, and Sen test amongst others (see, Machiwal and
 321 Jha, 2012). The Mann-Kendall statistic (M) is a non-parametric method and is calculated as

$$M = \sum_{k=1}^{n-1} \sum_{j=k+1}^n \text{sgn}(P_j - P_i) \quad (8)$$

322 where n is the number of data locations. Machiwal and Jha (2012) suggests that even n values
 323 as low as 10 can be used in Man-Kendall 's test provided there are no too many tied values.
 324 Supposing that $x = P_j - P_i$, then $\text{sgn}(x)$ is estimated as

$$\text{sgn}(x) = \begin{cases} 1, & \text{if } x > 0 \\ 0, & \text{if } x = 0 \\ 1, & \text{if } x < 0 \end{cases} \quad (9)$$

325 The M statistic represents the positive and negative differences for all data samples under
 326 consideration. The mean of the statistics under the null hypothesis is zero and is given as
 327 $E[M]=0$ while its variance (σ) is given as

$$\sigma = \frac{n(n-1)(2n+5) - \sum_{k=1}^n (t_k-1)(2t_k+5)}{18}. \quad (10)$$

328 The Man-Kendall test statistics (M) is approximately normally distributed, subject to the
 329 following Z-transformation,

$$Z = \begin{cases} \frac{M-1}{[\sigma]^{1/2}}, & \text{if } M > 0 \\ 0, & \text{if } M = 0 \\ \frac{M+1}{[\sigma]^{1/2}}, & \text{if } M < 0 \end{cases} \quad (11)$$

330 The null hypothesis (no trend), H_0 , was tested at $\alpha = 0.05$ (95% confidence level). If the
 331 computed absolute value of the test statistics is greater than the critical value of the standard

332 normal distribution, the hypothesis of negative or positive trend cannot be rejected at the 95%
 333 confidence level.

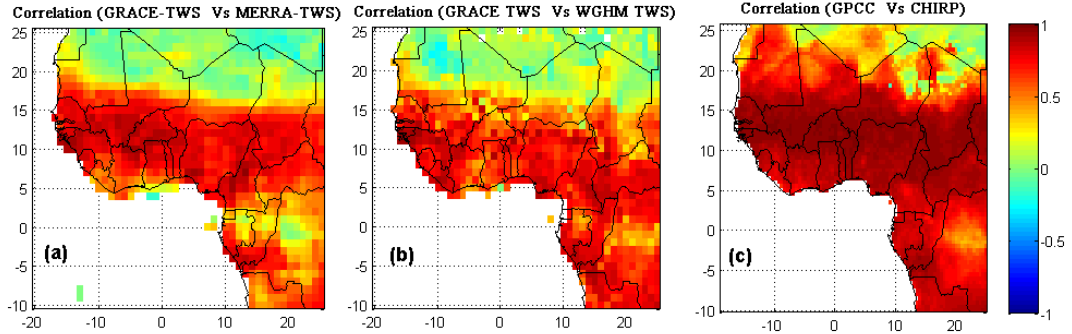


Figure 2: Correlation results for TWS products and the two precipitation products over SSA. (a) GRACE and MERRA TWS (2002 – 2014) (b) GRACE and WGHM TWS (2002 – 2009) and (c) GPCC and CHIRP (1980 – 2014).

334 3.4. Pre-validation of the reanalysis and model data

335 In order to examine the strength of agreement between two different hydrological variables
 336 (e.g., GRACE-derived TWS and MERRA-based TWS), the Pearson’s correlation coefficient
 337 was used while cross-correlation was employed to determine the time lag between the hydro-
 338 logical signals (e.g., precipitation and GRACE-derived TWS). Whereas these TWS products
 339 (MERRA and WGHM) were compared with GRACE-TWS, CHIRPS data was pre-validated
 340 by comparing it with GPCC gauge precipitation (Fig. 2). This is needful for data scarce re-
 341 gions such as SSA, particularly to help explore the increasing model and reanalysis data for
 342 hydrological applications. Also, this pre-validation effort is a milestone that provides insights
 343 as to the potential of these products for hydrological applications in SSA. The good correla-
 344 tion indicated in Fig. 2a-b, suggests that the spatial and temporal dynamics of MERRA and
 345 WGHM TWS products are consistent with GRACE-TWS. However, as will be shown later
 346 in the study, WGHM-TWS is underestimated in the region compared to MERRA-TWS. The
 347 CHIRPS precipitation data on the other hand shows a considerable strong consistency and
 348 agreement with GPCC-based precipitation in the region except in the extreme north-west Sa-
 349 hel (the Sahara Desert) (Fig. 2c). The GRACE-MERRA and GRACE-WGHM relationships
 350 in the Sahara Desert and the central Congo basin cuvette located in the upper Democratic
 351 Republic of Congo-DRC, are also considerably weak, and to some extent non-existent (Fig. 2a-
 352 b). Generally, the problem with these regions are considerable low density of gauge stations
 353 in the historical data used in forcing the model and global reanalysis products.

354 Controlled numerical experiments based on climate modelling have been performed as

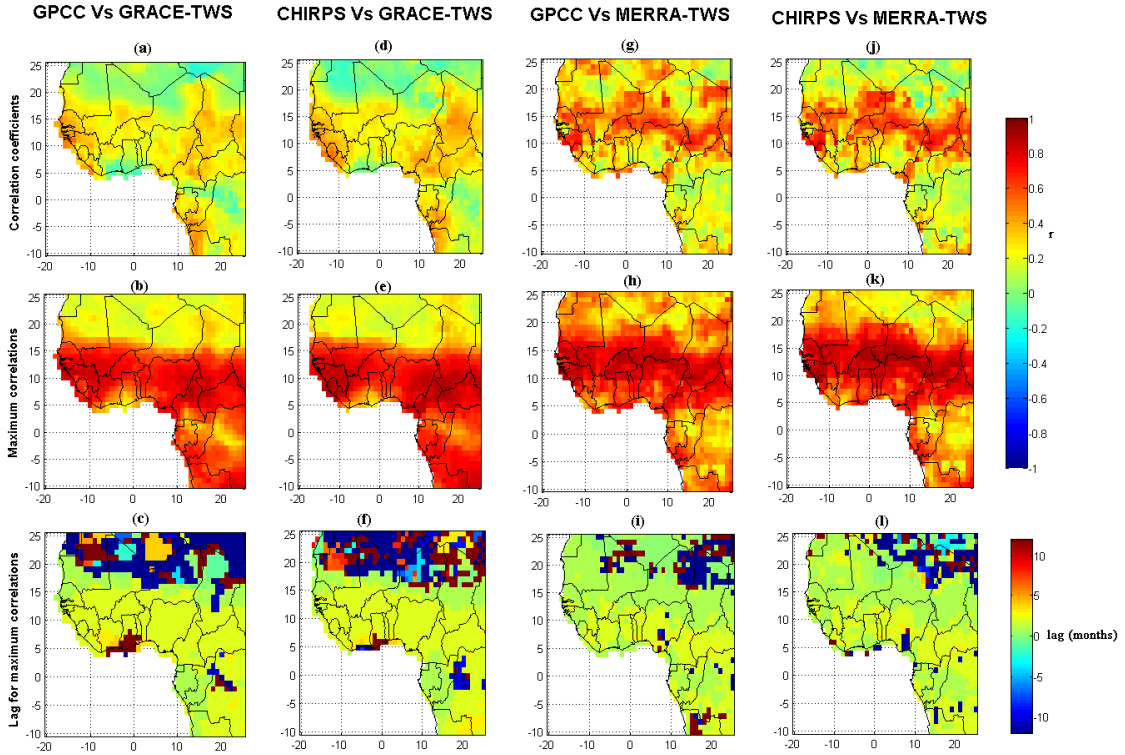


Figure 3: Spatial relations of rainfall (GPCC and CHIRPS) to stored water (MERRA and GRACE) over Sub-Saharan Africa based on correlation analysis during a common period. (a)-(c) GPCC Vs GRACE TWS (2002 – 2014), (d)-(f) CHIRPS Vs GRACE TWS (2002 – 2014), (g)-(i) GPCC Vs MERRA TWS (1981 – 2014), and (j)-(l) CHIRPS Vs MERRA TWS (1981 – 2014).

355 part of a coordinated effort to create proxy data (e.g., [Paolino et al., 2012](#); [Rienecker et al.,](#)
 356 [2011](#); [Koster et al., 2004](#); [Robock et al., 2000](#)) that are true representations of land surface
 357 conditions and can be used to study hydrological processes. Therefore, the relationship of
 358 GPCC and CHIRPS based precipitation with MERRA and GRACE TWS over the region is
 359 also examined to understand how GPCC and CHIRPS are associated with TWS (MERRA
 360 and GRACE) in the region both in the long term (1980 – 2014) and short term (2002 – 2014).
 361 This relationship is useful in optimising and initializing not only weather or climate models but
 362 also in the representation of physical phenomena in hydrological models. The precipitation-
 363 GRACE-derived TWS relationship are consistent and shows that GPCC and CHIRPS products
 364 leads TWS by two month in much of the region that excludes the northern Sahel (Fig. 3a-f).
 365 Towards the extreme north of Sahel where the Sahara Desert is located, precipitation lags TWS
 366 due to arid conditions (Fig. 3c/f/i/l). The precipitation-MERRA-derived TWS relationship
 367 shows stronger correlation coefficients in the Sahel, in addition to indicating a two month lag
 368 over much of the region (Fig. 3g-l). Unlike the maximum correlations of GRACE-TWS with

369 GPCP and CHIRPS (Fig. 3b and e), maximum correlations of MERRA-TWS with GPCP and
 370 CHIRPS (Fig. 3h and k) are poor in the central Congo basin (i.e., the Democratic Republic of
 371 Congo-DRC) possibly due to the absence of groundwater in the MERRA TWS data. Despite
 372 the uncertainty in reanalysis data (e.g., [Rienecker et al., 2011](#)), the association of GPCP and
 373 CHIRPS with MERRA TWS in the Sahel (Fig. 3g and j) are indications of the suitability of
 374 MERRA-TWS in semi-arid regions for hydrological applications.

375 4. Results and Discussion

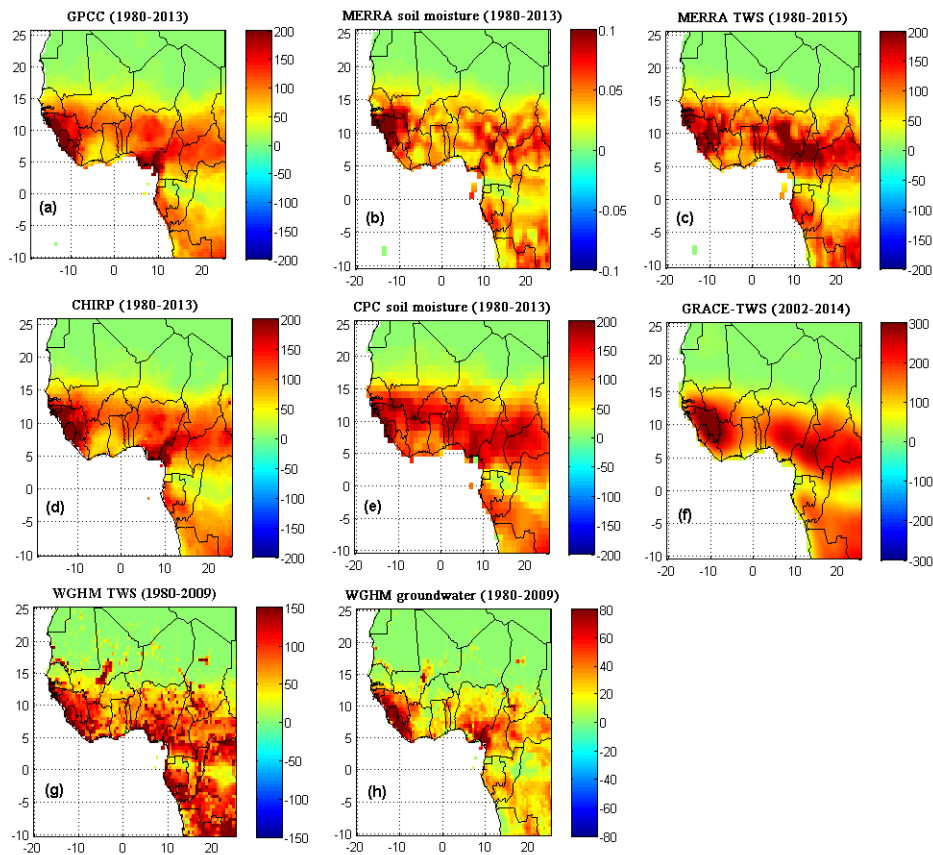


Figure 4: Annual Amplitudes of precipitation (a and d), soil moisture (b and e), TWS (c, f, and g), and groundwater (h) over Sub-Saharan Africa. All estimated amplitudes are in mm except MERRA soil moisture ($m^3 m^{-3}$).

376 4.1. Annual amplitudes of rainfall and land water storage

377 The annual amplitudes of all water fluxes (precipitation, TWS, soil moisture, and ground-
 378 water) show considerable strong patterns in Guinea, Sierra Leone, and Nigeria (Fig. 4a-h). In
 379 the southern Equatorial countries (cf. Fig. 1), relatively strong annual amplitudes in all water

380 fluxes (except WGHM-model groundwater) are also observed (Fig. 4a-g). The strongest an-
 381 nual amplitudes of WGHM-model groundwater in SSA (Fig. 4h) during the 1980 – 2009 period
 382 emanates from the Guinea coast countries (Guinea, Liberia, Sierra Leone, southern Nigeria,
 383 and south-east Cameroon) that receive the highest rainfall at annual time scales (Fig. 4a and
 384 d). Generally, as indicated in Fig. 4a-h, the strong amplitudes of observed water fluxes (rain-
 385 fall and land water storage) are predominant in West Africa (region bounded by latitudes
 386 2.5°N – 25°N and longitudes 20°W – 20°E). West Africa is typically active hydrologically be-
 387 cause of a plethora of physical phenomena that modulates its climate system. The West African
 388 monsoon (WAM) circulation, for instance, modulates the seasonal northward displacement of
 389 the intertropical convergence zone (ITCZ) and remains the principal source of precipitation
 390 over a large part of West Africa (Boone et al., 2009). In addition to this, the La-Niña and El-
 391 Niño cycles play important roles in the variability of rainfall in West Africa (e.g., Paeth et al.,
 392 2012; Nicholson et al., 2000), triggering considerable large amplitudes of water fluxes. Appar-
 393 ently, the observed annual amplitudes of land water storage (TWS, soil moisture, groundwater)
 394 in Fig. 4b-h, especially in Guinea, Liberia, Sierra Leone, and southern Nigeria, are driven by
 395 rainfall (Fig. 4a/d), which have strong seasonal and inter-annual variability (Fig. 5). Apart
 396 from the JFM period (Fig. 5a) that indicates the presence of rainfall only in the Equatorial
 397 countries (i.e., Congo, Gabon, Equatorial Guinea, and DRC), the presence of considerable
 398 rainfall can be seen all through the year (i.e., MAM, AMJ, JAS, SON, and OND-Fig. 5b-f) in
 399 some West African countries (Guinea, Liberia, Sierra Leone, southern Nigeria, and south-east
 400 Cameroon), and is largely consistent with the observed annual amplitudes in rainfall and land
 401 water storage (Fig. 4a-h).

402 4.2. Long-term spatio-temporal variability of precipitation and land water storage (1980-2015)

403 In this section, the spatio-temporal evolutions of leading precipitation and land water
 404 storage (soil moisture, groundwater, and TWS) modes for the 1980 – 2015 period over SSA
 405 are discussed. This is done to understand both the characteristics and homogeneous regions
 406 with strong dominant patterns of variability in SSA.

407 4.2.1. Changes in precipitation

408 The two leading modes of GPCC and CHIRPS-based precipitation over SSA accounts for
 409 about 70.4% and 80.3% of the total variability, respectively (Fig. 6). These leading EOF modes
 410 of rainfall variability from both data in SSA creates two homogeneous regions defined by similar
 411 temporal and spatial patterns. The strong magnitudes of variability (i.e., large amplitudes) in
 412 these leading modes show maximum loadings in regions with strong annual amplitudes in soil

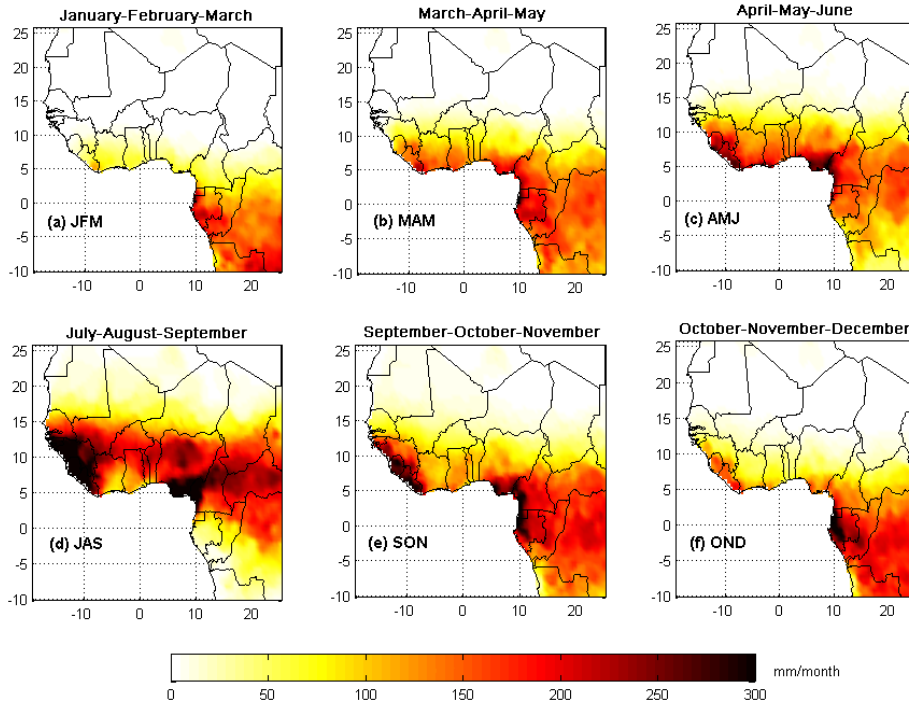


Figure 5: Seasonal mean variability of precipitation (GPCC version 7) during 1980–2013 period in Sub-Saharan Africa.

413 moisture, groundwater, and TWS as indicated in Fig. 4. Whereas the leading EOF (spatial
 414 patterns) shows rainfall anomalies with opposite signs to the north and south of 0°N , the
 415 second EOF mode indicates a contrast of rainfall anomalies with opposite signs to the north
 416 and south of 10°N . Specifically, the first mode highlights the annual variability of rainfall (PC1,
 417 Fig. 6) for the West African region (i.e., Sahel and Guinea coast countries) and a dipole pattern
 418 in the Equatorial region (e.g., Gabon, Cameroon, Congo, and Democratic Republic of Congo-
 419 DRC, see Fig. 1 for the respective countries). The second rainfall mode on the other hand,
 420 highlights multi-annual variations of rainfall in the Guinea coast countries and the Equatorial
 421 region (PC2, Fig. 6). Observed EOF loadings of this mode in southern Cameroon, Gabon,
 422 and Equatorial Guinea are the strongest in SSA. The temporal patterns of this second mode
 423 indicates a bimodal structure in rainfall (receiving annual rainfall twice in a year) of the coastal
 424 areas of SSA that may be linked to the latitudinal movement of the tropical rainbelt, and the
 425 influence of SST amongst other factors (e.g., [Mohino et al., 2011b](#); [Nicholson, 2008](#); [Odekunle
 426 and Eludoyin, 2008](#)). The spatial variability of rainfall as observed in these dominant patterns
 427 are much similar to the annual amplitudes and seasonal distribution of rainfall (Figs. 4a/d
 428 and 5d, respectively). Furthermore, the strong EOF loadings (GPCC and CHIRPS EOF1,
 429 Fig. 6) observed between latitudes 8°N and 12°N (the Sahel) are largely indicative of the

430 considerable changes in annual precipitation of West Africa during the July-September period.
 431 The temporal evolutions (GPCC and CHIRPS PC1, Fig. 6) of the corresponding leading EOF
 432 loadings show that the maximum peaks of precipitation are observed in August and sometimes
 433 in September. This is also largely consistent with the seasonal distribution of rainfall indicated
 434 in Fig. 5d, where strong spatial patterns of rainfall are observed between July and September.

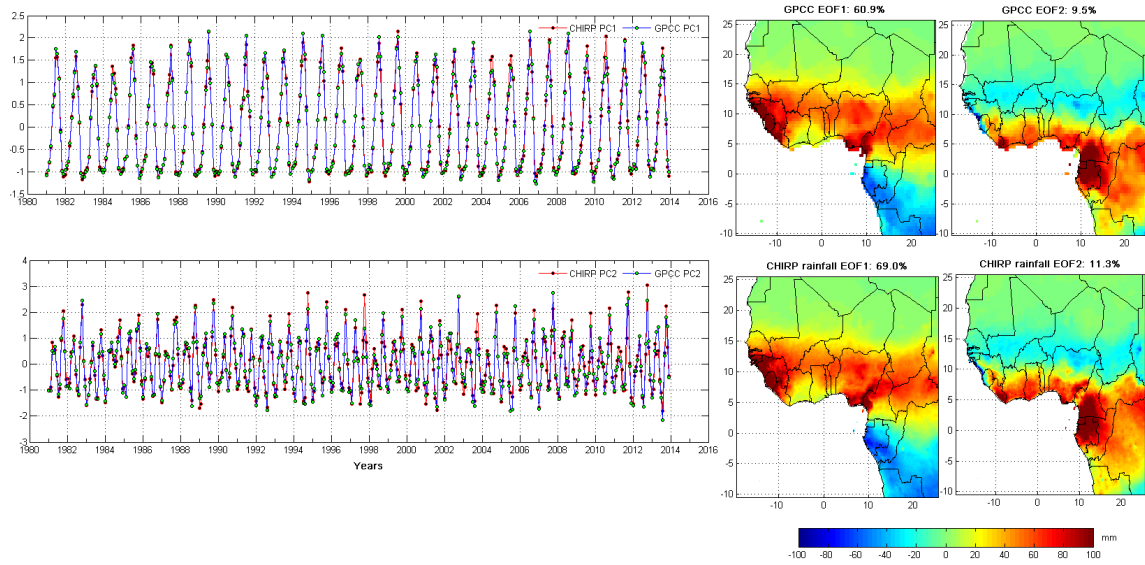


Figure 6: PCA decomposition of CHIRP and GPCC-based precipitation (1980 – 2014) over Sub-Sahara Africa. The EOFs (right) are loadings showing spatial patterns of variations in precipitation over Sub-Sahara Africa while the corresponding PCs (left) are temporal variations, which are normalised using their standard deviation to be unitless.

435

436 Some studies have indicated that this rainfall mode (PC1/EOF1, Fig. 6) dominates the
 437 summer West African rainfall variability and is highly coupled to Equatorial Atlantic SST (e.g.,
 438 [Losada et al., 2010](#); [Janowiak, 1988](#)). Whereas this same rainfall mode has been acknowledged
 439 to be representative of the entire Sahel-Sudan region by [Fall et al. \(2006\)](#), [Nicholson and](#)
 440 [Palao \(1993\)](#) identified three spatial modes of rainfall variability that describes the regional
 441 climate of West Africa, arguing that the Sahel cannot be treated as a homogeneous rainfall
 442 sector with other regions in West Africa. However, [Sanogo et al. \(2015\)](#) recently found no
 443 justification for further subdivision of the Sahel rainfall as their EOF analysis yielded two
 444 homogeneous rainfall zones (i.e., Sahel and Guinea Coast). Such contrast, primarily could
 445 emanate from the size of the spatial domain sampled and the climatological period examined.
 446 For instance, [Mohino et al. \(2011b\)](#) explored the characteristics of the inter-annual variability
 447 of West African rainfall (i.e, June-September rainfall only). Their observational EOF analysis

448 for the 1957 – 1978 period showed that the leading EOF mode (11% of the total variance)
449 had its maximum loadings concentrated over the Sahel whereas the second EOF mode (7%
450 of the total variance) exhibited inter-annual signals in the temporal patterns with maximum
451 loadings over the Guinea Coast. This analysis included all monthly precipitation because of
452 the diversity in local climates and the fact that precipitation is highly variable with strong
453 presence in all seasonal time scales in coastal and humid SSA (Fig. 5a-f). Over West Africa
454 (i.e., Lat 0°N-20°N and Lon 20°W-20°E) and the surrounding ocean, the two leading modes
455 of TRMM-based precipitation (2002 – 2014) as shown in [Ndehedehe et al. \(2016a\)](#), accounted
456 for 61.7% of the total variability. But when the surrounding ocean has been masked out and
457 the domain analysis extended to include Equatorial countries of the Congo basin (i.e., between
458 Lat 25°N and 10°S), the cumulative variance for the two leading modes increase to 70.4% and
459 80.3% for GPCC and CHIRPS based precipitation (1980 – 2014), respectively, confirming the
460 influence of domain size and probably the length of data record on the explained variance.

461 Essentially, the leading rainfall mode observed in SSA (GPCC and CHIRPS EOF1/PC1,
462 Fig. 6), which has strong EOF loadings over West Africa adequately describes the inter-annual
463 variability of rainfall in the region, consistent with previous studies (e.g., [Fontaine and Bigot,](#)
464 [1993](#); [Janicot, 1992](#); [Janowiak, 1988](#)), and is generally appropriated by decision makers for
465 planning purposes as reported by [Fall et al. \(2006\)](#). This is because the dominant rainfall
466 mode represents the main climatological properties and changes in the region. For instance,
467 the well known droughts of 1983/1984, which were continental in scale are marked out in the
468 amplitudes of the temporal evolutions (PC1, Fig. 6). Based on the observed peak amplitudes
469 (PC1, Fig. 6), extreme wet and dry years (e.g., 1982/1983, 1997/1998, 1988/1989, 1994/1995,
470 etc.) caused by the strong impacts of El-Niño (e.g., 1982/1983) and La-Niña (e.g., 1998/1999)
471 cycles can also be identified in the temporal evolutions of the first rainfall mode. The second
472 rainfall mode also show hydro-climatological events in SSA that are similar to the first rainfall
473 mode. For example, the amplitudes of PC2 in 1983 (Fig. 6) confirms the prominent drought
474 event over the continent that was forced by high Indian Ocean SST ([Bader and Latif, 2011](#)), and
475 in addition identifies years with the lowest summer rainfall (e.g., 1987). Years with relatively
476 low rainfall (e.g., 1991, 2001 and 2008) in this mode are characterised with less pronounced
477 amplitudes (i.e., for both the first and second rain) while extreme wet years (1994, 1997, 2007,
478 2011/2012) show strong pronounced maximum amplitudes (PC2, Fig. 6). These two modes of
479 rainfall variability are the major drivers of land water storage in SSA.

480 *4.2.2. Changes in soil moisture*

481 Soil moisture is a critical and highly variable component of the hydrological cycle. Because
482 of its strong influence on hydro-meteorological processes within the atmospheric boundary
483 layer (Petropoulos et al., 2015), and role in land-atmosphere coupling (e.g., Koster et al.,
484 2004), soil moisture is a major land state variable that can be used to study changes in
485 global climate and weather systems. In this section, the temporal and spatial dynamics of
486 CPC model and MERRA-reanalysis long term soil moisture data over SSA are discussed.
487 These spatio-temporal patterns of soil moisture are based on the PCA technique (Section
488 3) and is more robust compared to analysing regional averages of soil moisture as done in
489 Douville et al. (2007). The two dominant modes of variability in CPC and MERRA soil
490 moisture resulted in homogenous regions that describe the spatio-temporal variability of soil
491 moisture over SSA. These leading modes accounted for a total variability of 70.8% and 81.9%
492 for CPC and MERRA products, respectively (Fig. 7). Similar to rainfall, the first orthogonal
493 modes represent annual signals (PC1/EOF1, Fig. 7) while the second orthogonal modes show
494 multi-annual variations in the Equatorial region (PC2/EOF2, Fig. 7). Inter-annual variability
495 appears to be a prominent feature characterising the dominant temporal evolutions of both
496 soil moisture products (PC1, Fig. 7). The significantly less pronounced amplitudes of both soil
497 moisture products in 1983/1984, 1991, 1997, and during the 2000 – 2006 period over SSA are
498 consistent (PC1, Fig. 7). Some regions in West and Central Africa experienced relatively low
499 precipitation, water deficits, and drought conditions during this periods (see, e.g., Ndehedehe
500 et al., 2016b,c; Asefi-Najafabady and Saatchi, 2013), confirming the strong land-atmosphere
501 interaction of the region (Koster et al., 2004).

502 From the temporal evolutions of the CPC and MERRA soil moisture products, a long
503 term decline is observed between 1986 and 2008 in the second mode (PC2/EOF2, Fig. 7). The
504 observed sharp decline between 1995 and 2005, (about 16 mm/month estimated from the CPC
505 model soil moisture) represents about two decades of consistent shift in regional soil moisture
506 of the Equatorial countries (PC2/EOF2, Fig. 7). Although rainfall indicated no decline during
507 the same period (PC2/EOF2, Fig. 6), observed decline in evapotranspiration (ET) during the
508 2000 – 2014 period (not shown) over much of the Congo basin confirms the limited moisture
509 supply in the region. Interestingly, a study on global evapotranspiration trends (see, Jung
510 et al., 2010) showed that the decline in global land evapotranspiration (1998 – 2008) was
511 largely consistent with decline in soil moisture. As discussed further in Section 4.2.4, analysis
512 of long term trends in TWS and soil moisture (1982 – 2014) at the pixel scale over SSA confirms
513 this decline in the temporal series of soil moisture over the Congo basin and is consistent with

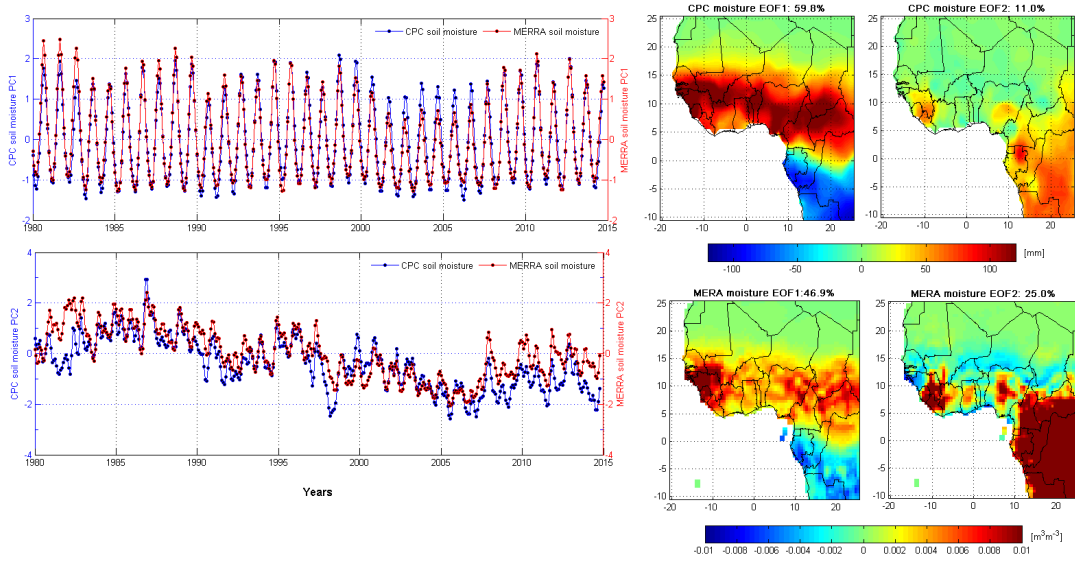


Figure 7: PCA decomposition of CPC model (mm) and MERRA reanalysis ($m^3 m^{-3}$) based soil moisture products over Sub-Sahara Africa for the 1980 – 2014 period. The EOFs (right) are loadings showing spatial patterns of variations in soil moisture over Sub-Sahara Africa while the corresponding PCs (left) are temporal variations, which are normalised using their standard deviation to be unitless.

514 decline in land surface temperature over the Congo basin. Focusing on the evolving trends
 515 of soil moisture in the last decade (2003 – 2014), short term trends are here reported for the
 516 temporal patterns of CPC soil moisture (trends are in normalised units for simplicity but can
 517 be adjusted to original units through multiplication with the EOFs). This choice was made
 518 to help relate soil moisture changes to those of GRACE-TWS in the Congo basin as it is one
 519 of the focus region in this study. A decline of 0.51 ± 0.09 during the 2003 – 2006 period and
 520 an increase of 0.09 ± 0.06 between 2006 and 2009 for soil moisture are observed (PC2, Fig. 7).
 521 Furthermore, declines of 0.28 ± 0.17 and 0.37 ± 0.11 were observed in the periods of 2010 – 2011
 522 and 2013 – 2014, respectively (PC2, Fig. 7). Interestingly, the observed trend for PC2 of Fig. 7
 523 (i.e., a decline of 0.51 ± 0.09) coincides with the second orthogonal mode of GRACE-derived
 524 TWS (PC2, Fig. 8) in Section 4.2.3, which indicates a decline of 0.58 ± 0.15 during the same
 525 period (i.e., 2003 and 2006). Except for the period between 2012 and 2014, the positive and
 526 negative trends indicated for the periods during 2006 – 2009 and 2010 – 2011, respectively
 527 for CPC model soil moisture (PC2, Fig. 7), are consistent with those of GRACE-TWS (PC2,
 528 Fig. 8). The actual values of the observed declining trends during the 2003 – 2006 period
 529 for GRACE-derived TWS and soil moisture second PCA modes (PC2, Figs. 7 and 8), when
 530 jointly derived from their corresponding EOFs are estimated as $\sim -78.4 \pm 20.3$ mm/yr and
 531 $\sim -45.9 \pm 8.1$ mm/yr, respectively. This loss of soil moisture during the period 2003 – 2006

532 (PC2, Fig. 7) points toward the significant role and contribution of soil moisture to observed
533 GRACE-derived TWS in the Equatorial countries of SSA. Although the MERRA TWS is in
534 volumetric units, it indicates similar trends in the observed temporal patterns as the CPC
535 model soil moisture (PC2, Fig. 7).

536 The long term decline in multi-annual variation of soil moisture (i.e., from 1986 to 2008)
537 observed in these Equatorial countries (PC2, Fig. 7) could be the cause of the observed decline
538 in vegetation greenness of the Congolese forest (Zhou et al., 2014). The spatial variations of
539 soil moisture, TWS, and rainfall trends over SSA (see Section 4.2.4) confirm a long term drying
540 in these Equatorial countries, consistent with the observed soil moisture modes of variability
541 in this section. In the cuvette central of the Congo basin, Zhou et al. (2014), in a bid to
542 justify the weak correlations between rainfall and GRACE-TWS, reported that GRACE-TWS
543 changes in tropical regions represents changes mainly in surface water and groundwater and
544 that the response of GRACE-TWS to rainfall could not have emanated from the small scale
545 and short-term rainfall anomalies. However, the PCA analysis of CPC model soil moisture
546 indicates total variability of 11.0% (PC2, Fig. 7), which to a very large extent is consistent
547 with GRACE-TWS total variability of 10.5% (see Section 4.2.3, as well as PC2, Fig. 8) in the
548 Congo basin (countries in Equatorial Africa). Hence, this study argues that GRACE-TWS
549 changes in the Congo basin also represents significant changes in soil moisture, in addition to
550 surface water and groundwater as earlier reported (e.g., Lee et al., 2011).

551 4.2.3. Terrestrial stored water

552 As an update to the analysis of GRACE-derived TWS over West Africa during the 2002 –
553 2014 period (see, Ndehedehe et al., 2016a), the spatio-temporal evolutions of long term reanal-
554 ysis and model derived TWS over SSA in the last 3.5 decades are discussed in this section.
555 Before then, the variability of these TWS products in space and time have been compared
556 with that of GRACE-derived TWS based on their PCA results over SSA (Fig. 8). The PCA
557 results for the GRACE-derived TWS indicate strong dominant patterns (i.e., annual signal)
558 in the first EOF, which represents total variability of 76% mainly from the countries between
559 latitudes 8°N and 15°N (PC1, Fig. 8). Be it West Africa or the entire SSA (cf. Fig. 1), this
560 mode of GRACE-TWS is the dominant and shows the strongest EOF loadings in Guinea with
561 an increasing trend in the corresponding temporal evolution (PC1, Fig. 8). Also interesting is
562 the dipole pattern in the EOF loadings of GRACE-TWS (EOF1, Fig. 8), which is consistent
563 with those of rainfall and soil moisture (Sections 4.2.1 and 4.2.2).

564 The presence of surface waters (e.g., lakes, reservoirs, and rivers), soil moisture, and
565 groundwater in West Africa (especially the Guinea Coast countries) are major components

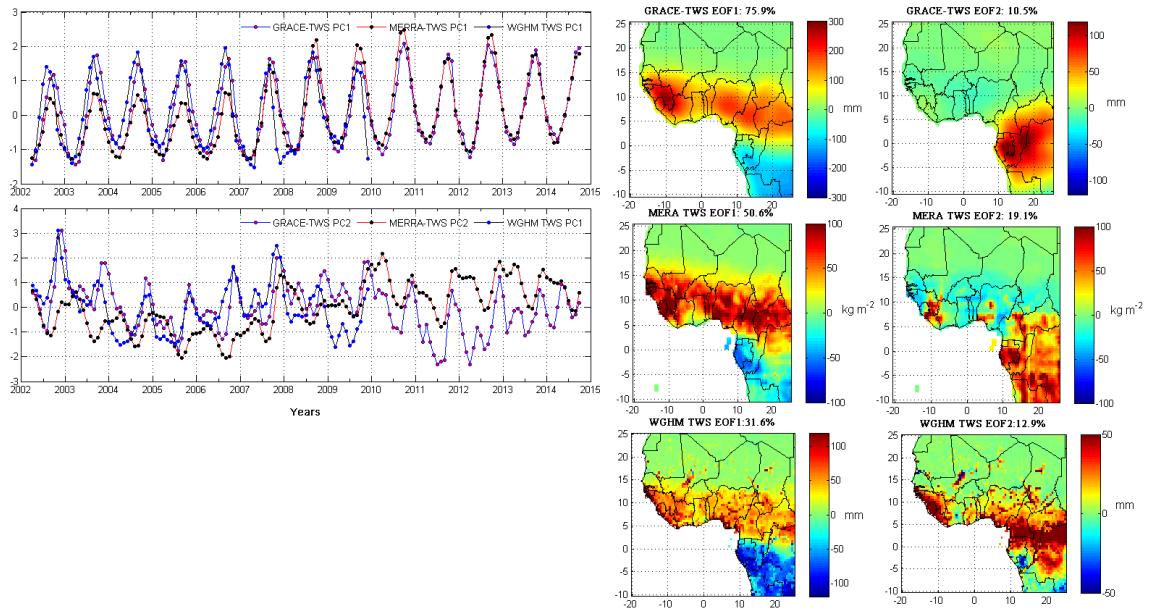


Figure 8: Comparing the space-time evolutions of MERRA (2002 – 2014) and WGHM-based TWS (2002 – 2009) products over Sub-Saharan Africa with GRACE-derived TWS (2002 – 2014). The EOFs (right) and the corresponding temporal patterns or PCs (left) are constructed similar to Fig. 7. The space-time evolutions of GRACE-TWS covers SSA (including Central African countries and the Congo basin) and is updated from a previous report (Ndehedehe et al., 2016a), which focused on West Africa.

566 of GRACE-TWS, which unarguably are driven by rainfall. In particular, reservoir systems
 567 (surface water schemes) and lakes have shown strong and considerable impacts on hydrologi-
 568 cal changes of river basins in Africa (e.g., Ndehedehe et al., 2017a; Moore and Williams, 2014).
 569 In the Volta basin, for example, increasing trends in GRACE-TWS changes were found to be
 570 inconsistent with rainfall due to the impacts of a large water project-the Akosombo dam (e.g.,
 571 Ndehedehe et al., 2017a; Ahmed et al., 2014). But the observed increase in GRACE-TWS,
 572 which is relatively stronger in Guinea because of the EOF loadings (PC1, Fig. 8), emanates
 573 mostly from extended wet seasons and strong seasonal precipitation changes (cf. Fig. 5c-e).
 574 With lower evapotranspiration rates in such region (not shown) and strong annual amplitudes
 575 in precipitation (Figs. 4a and d), increased water storage and inundated areas are more likely
 576 to occur. The second mode of GRACE-TWS observed over the Congo basin, which was not
 577 part of the earlier report in Ndehedehe et al. (2016a), accounts for 10.5% of the total variabil-
 578 ity over SSA. Whereas this variance explained is somewhat consistent with the second modes
 579 of rainfall (GPCC) and soil moisture (CPC model) variability over SSA (Sections 4.2.1 and
 580 4.2.2), this does not imply that rainfall is a prominent driver of GRACE-TWS in this region
 581 as river discharge at the Congo Kinshasa station shows stronger association with the observed

582 temporal evolutions in this mode. This will be discussed in detail in Section 4.2.5.

583 Meanwhile, the first mode of MERRA-TWS (PC1, Fig. 8) agrees strongly with GRACE-
 584 TWS, indicating a correlation of 0.91 compared to WGHM-TWS (0.81). But in the second
 585 mode (PC2, Fig. 8), WGHM-TWS is more associated with GRACE-TWS ($r = 0.57$) compared
 586 to MERRA-TWS ($r = 0.22$). Combining the total variability explained (Fig. 8) and the pre-
 587 validation results (Fig. 2a-b), MERRA-TWS is somewhat more suitable in West Africa than
 588 WGHM-TWS. This conclusion cannot be made for the Equatorial countries (especially for
 589 MERRA) as uncertainties exist in both data for this sub-region, given their weak associations
 590 with GRACE-TWS in the Congo basin cuvette. Specifically, the WGHM-TWS for the region
 591 show some underestimation while the absence of groundwater in the MERRA-TWS reanalysis
 592 data may constrain its performance in the Equatorial countries. It is noted that the spatial
 593 patterns of MERRA-TWS in the second mode compares well with that of GRACE-TWS
 594 (EOF2, Fig. 8) while the temporal patterns of WGHM-TWS in this same mode is more
 595 associated ($r = 0.57$) with that of GRACE-TWS (PC2, Fig. 8). Because of its longer duration
 596 (i.e., it extends to 2015), MERRA-TWS data was adopted for long term analysis of evolving
 597 temporal and spatial dynamics in TWS over SSA during the last 3.5 decades. In parallel, the
 WGHM groundwater changes over SSA are also analysed.

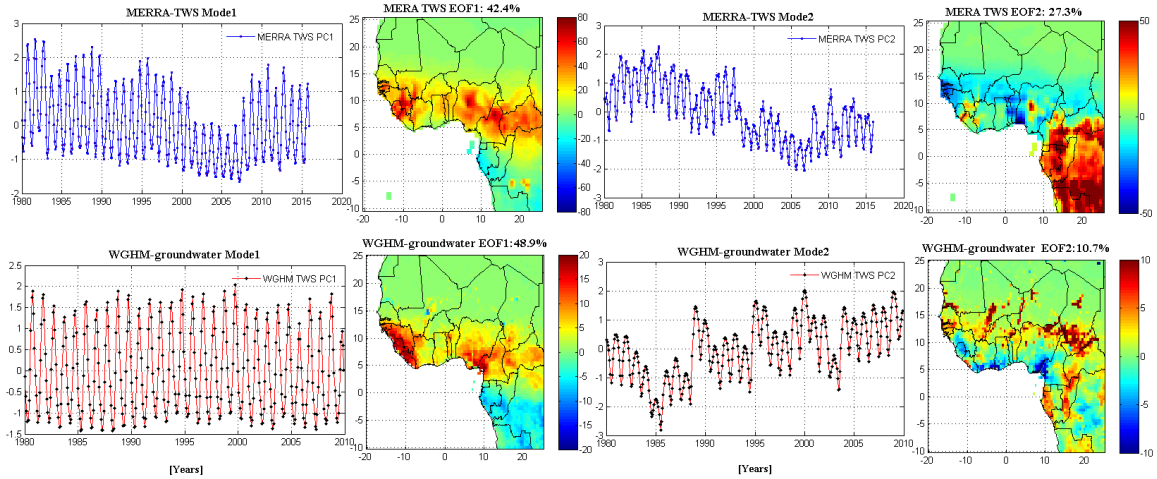


Figure 9: PCA decomposition of MERRA (1980–2015) and WGHM-based groundwater (1980–2009) over Sub-Saharan Africa. The EOFs are loadings showing spatial patterns of variations in TWS (kg m^{-2}) and WGHM-groundwater (mm) over Sub-Saharan Africa while the corresponding PCs are temporal variations, which are normalised using their standard deviation to be unitless. Row 1 shows the first and second modes of MERRA-TWS (temporal evolutions and their corresponding spatial patterns) while row 2 indicates the first and second modes of WGHM groundwater (temporal evolutions and their corresponding spatial patterns).

598

599 The MERRA-TWS show relatively strong spatial patterns in West Africa and the Equato-

600 rial countries for the first mode (42.4% variance) and second mode (27.3% variance), respec-
 601 tively (Row1, Fig. 9). The first mode of WGHM groundwater changes over SSA on the other
 602 hand, accounts for 48.9% of the total variability, with relatively strong spatial patterns in West
 603 Africa (Guinea, Liberia, Sierra Leone, and Nigeria) while the second mode accounts for 10.7%
 604 of the total variability (Row2, Fig. 9). The time series of MERRA-TWS associated with the
 605 band of EOF loadings over West Africa (Row1, PC1, Fig. 9) show strong inter-annual fluctu-
 606 ations with the lowest peak amplitudes (deficit conditions) observed during the 2001 – 2006
 607 period. The overall picture of this temporal evolutions (MERRA-TWS PC1, Fig. 9) somewhat
 608 suggests a multi-decadal variability, but apparently indicates the 2001 – 2006 period as the
 609 driest and hydrological drought years in West Africa and is consistent with previous stud-
 610 ies in West and Central Africa (e.g., Ndehedehe et al., 2016a; Asefi-Najafabady and Saatchi,
 611 2013). For the second MERRA-TWS mode (Row1, PC2, Fig. 9), considerable EOF loadings
 612 are observed over the Equatorial countries while its corresponding temporal patterns indicate
 613 a strong decline (about 26 kg m^{-2} / month) during the 1985 – 2005 period that is consistent
 614 with observed soil moisture declines (PC2, Fig. 7). The estimated trends in MERRA-TWS
 615 temporal patterns (Row1, PC2, Fig. 9) as compared with GRACE-TWS (PC2, Fig. 8) during
 616 the 2003 – 2006 period are somewhat close (0.58 ± 0.15 and 0.50 ± 0.10 , for MERRA-TWS and
 617 GRACE-TWS normalised units, respectively). The observed trends in MERRA-TWS over
 618 the Congo basin should, however, be interpreted with caution because of the slight restriction
 619 of MERRA data noted in the region (cf. Fig. 2a-c).

620 In the long term WGHM groundwater statistical decomposition, the leading patterns of
 621 WGHM groundwater indicate annual and multi-annual variations in their temporal series, i.e.,
 622 PC1 and PC2, respectively (Row2, Fig. 9). It is rather interesting that regions of observed
 623 spatial variability (EOF loadings) in groundwater are consistent with areas in West Africa that
 624 receive the highest rainfall (cf. Figs. 5d and 6). The lowest maximum peaks in the amplitudes
 625 of the time series associated with the EOFs of WGHM groundwater model (Row2, PC1,
 626 Fig. 9) are observed in 1983, 2005, and 2009. These years are significant hydrological periods
 627 known for extreme drought conditions and matches some meteorological records and reports for
 628 case-specific studies in West Africa (e.g., Ndehedehe et al., 2016b,c; Kasei et al., 2010). Unlike
 629 rainfall, soil moisture, and TWS, relatively strong spatial patterns of WGHM groundwater over
 630 SSA in the second mode are mostly observed in the Sahel region of West Africa. (Row2, PC2,
 631 Fig. 9). Countries in the Lake Chad basin-LCB (e.g., southern Chad and north-east Nigeria)
 632 show relatively strong spatial variability with their associated temporal patterns indicating
 633 trends in groundwater (Row2, PC2, Fig. 9). Except for the 1980 – 1985 period where the

634 strong decline in groundwater is a response to the extreme drought of 1983/1984, substantial
635 increase in groundwater during the 1985 – 2000 and 2003 – 2009 periods are pointers to
636 potential groundwater resources of the LCB. In Mali, Congo, and Equatorial Guinea, increase
637 in groundwater are also observed (further details on trends are provided in the next section).
638 The lowest minimum groundwater amplitude over SSA is observed in 1984/1985 (Row2, PC2,
639 Fig. 9), notably the impact of the extreme drought of 1983/1984 in the region.

640 4.2.4. Long term trends (1982-2014)

641 The long term trends in precipitation, TWS, soil moisture, and model groundwater were
642 estimated for each grid points over SSA for the common period (1982 – 2014), consistent
643 with SST (1982 – 2014) except for the WGHM outputs (1982 – 2009). The GPCP-based
644 precipitation shows some pockets of positive trends in the Sahel, Liberia, and Equatorial
645 Guinea (Fig. 10a). The trends in GPCP-based precipitation over the Sahel are somewhat
646 consistent with observed positive trends in soil moisture, TWS, and groundwater (Fig. 10b-
647 f). This would align with the two schools of thoughts on the hydro-climatic conditions of the
648 Sahel: the ‘Sahel greening’ (e.g., Dardel et al., 2014; Boschetti et al., 2013; Olsson et al., 2005;
649 Herrmann et al., 2005) and the recognised rainfall recovery in some parts of the Sahel (e.g.,
650 Nicholson, 2005; Lebel and Ali, 2009). Still within the context of previous studies, observed
651 positive trends in soil moisture (though dry conditions still persist in some parts) (Fig. 10b-c)
652 in some parts of West Africa (i.e., the Sahel) would be a reversal of the drying trend reported
653 by Sheffield and Wood (2008) during the 1950 – 2000 period.

654 Whereas the trends in the two soil moisture products (CPC and MERRA) and TWS
655 (WGHM and MERRA) observed over West Africa are somewhat inconsistent, they tend to
656 agree in the Equatorial countries (though WGHM shows negative trends mostly in DRC),
657 indicating negative patterns during the period (Fig. 10b-e). The gross similarity in the spatial
658 patterns of linear trends in soil moisture and TWS (between 40–60 mm/yr) over the Equatorial
659 countries reveal the long term drying in the region. As rainfall is a principal component of
660 the hydrological cycle, it is expected that long term changes in soil moisture should closely
661 follow rainfall. But over the Equatorial regions, trends in rainfall (except in some parts of
662 DRC and southern Gabon) are statistically insignificant (Fig. 10a) different from those of soil
663 moisture products (Fig. 10b-c). Such disagreement may result from land surface conditions
664 (e.g., temperature) or other meteorological processes. The former appears to be more critical
665 in this case as statistically significant trends in temperature (1982 – 2014) have been observed,
666 see, e.g., Fig. 10g. The Equatorial countries show considerable warming unlike the Sahel that
667 shows significant cooling during the period. The synergy between precipitation deficits or lack

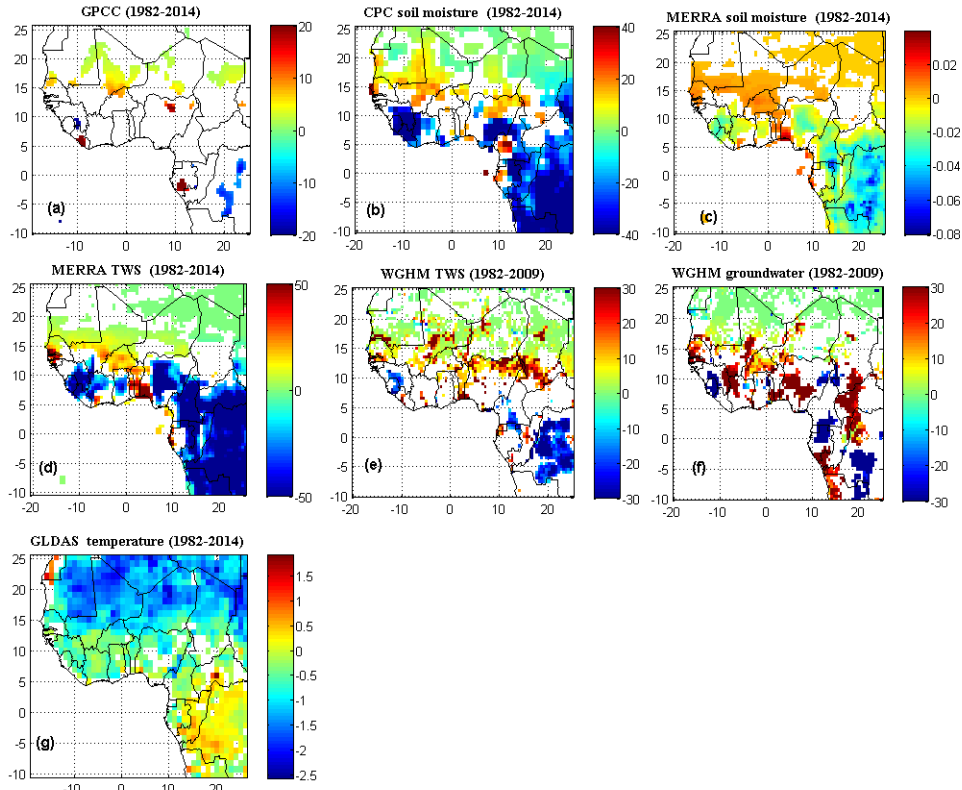


Figure 10: Spatial patterns of long term linear trends in (a) rainfall (1982 – 2014), (b)-(c) soil moisture (1982 – 2014), (d)-(e) TWS (1982 – 2014), (f) groundwater (1982 – 2009) and (g) land surface temperature (1982–2014) over SSA. The WGHM derived TWS covers the (1982–2009) period. Only statistically significant trends ($\alpha = 0.05$) are presented and they are estimated in mm/yr . The MERRA soil moisture product is in $\text{m}^3 \text{m}^{-3}/\text{yr}$ while temperature is estimated in DegC/yr .

668 of a statistically significant positive trend in precipitation and long term warming of the land
 669 surface can restrict recharge of the soil column leading to strong deficits in TWS/soil moisture
 670 as observed in the countries of the Congo basin. As [Jung et al. \(2010\)](#) noted, the 1998 El-Niño
 671 event coincided with decrease in global land ET, which was largely caused by soil moisture
 672 deficits during the 1998 – 2008 period. Climate change is expected to restrict the availability
 673 of freshwater and impact on the water resources sector. With the warming of the global oceans
 674 during the 1982 – 2014 period ([Fig. 11](#)), the concern on how such changes will impact on the
 675 region’s land water storage is amplified. The interaction of the global ocean with TWS over
 676 SSA is discussed further in [Section 4.3](#).

677 For obvious reasons such as the sensitivity of modeled land surface hydrology to forcing
 678 dataset that drives it (e.g., [Sheffield and Wood, 2008](#)), it is important to note that trends in
 679 these model and reanalysis soil moisture products would only be as strong as the historical

680 meteorological data used in their forcing. In most cases, they are however, more reliable than
681 satellite products (except GRACE data). Since uncertainties in the model and reanalysis data
682 are likely, here, we focus more on the consistency of hydrological outcomes in each data to
683 describe the observed changes during the period rather than an absolute value. Apparently,
684 combining the result in Section 4.2.2 with this section, there is a strong evidence of a consid-
685 erable loss in soil moisture in the Equatorial countries of SSA, which also aligns with some
686 site-specific reports in the region. These trends in soil moisture, for example, coincide with the
687 reported decline in vegetation greenness in the upper Congo basin (Zhou et al., 2014). Even
688 more recently, long term drying (1950–2014) in Central Equatorial Africa has been reported by
689 Hua et al. (2016). They identified SST variations over Indo-Pacific, and large scale circulation
690 changes related to a weaker West African monsoon as major causes. Hydrological conditions
691 of the Congo basin have shown some marked variability in recent times. Between 2002 and
692 2006, the Congo basin lost about 280 km^3 of stored water as estimated from GRACE-TWS
693 by Crowley et al. (2006) while observed declines in GRACE-TWS in three sub basins of the
694 Congo river basin (2003–2012) where attributed to deforestation by Ahmed et al. (2014). The
695 strong spatial distribution of negative trends in soil moisture and TWS over the Equatorial
696 countries (Fig. 10b-e), which are consistent with the aforementioned case studies above are
697 glaring evidence of acceleration and shifts in the hydrology of the region. On the other hand,
698 WGHM groundwater increased substantially in most parts of SSA (Fig. 10f). Of note is the
699 spread in positive distribution of groundwater trends in some areas (Congo basin and some
700 parts of West Africa) where GPCP precipitation and the soil moisture products indicated
701 negative trends and in some cases no statistically significant trends. Non-linear relationship
702 of rainfall to catchment stores (e.g., groundwater, soil moisture, aquifer, etc.) in some areas
703 of the Sahel exist (see, e.g., Descroix et al., 2009; Séguis et al., 2004). In spite of decreasing
704 rainfall in western Niger, Favreau et al. (2009), for example, reported a tremendous increase in
705 water table, which they attributed to changes in land use pattern. These are some complicated
706 and non-linear hydrological processes that characterise the region, which can possibly result
707 from some other factors that may include: vegetation cover, soil type, depth to water table,
708 greater infiltration, topography, amongst other factors. But in the key upstream and down-
709 stream areas of the Equatorial countries (e.g., DRC, Cameroon, and Gabon, etc.) that have
710 strong seasonal rainfall (cf. Figs. 5b and e-f), there are locations with considerable declines in
711 WGHM groundwater, suggesting long term hydrological droughts in the region (Fig. 10f).

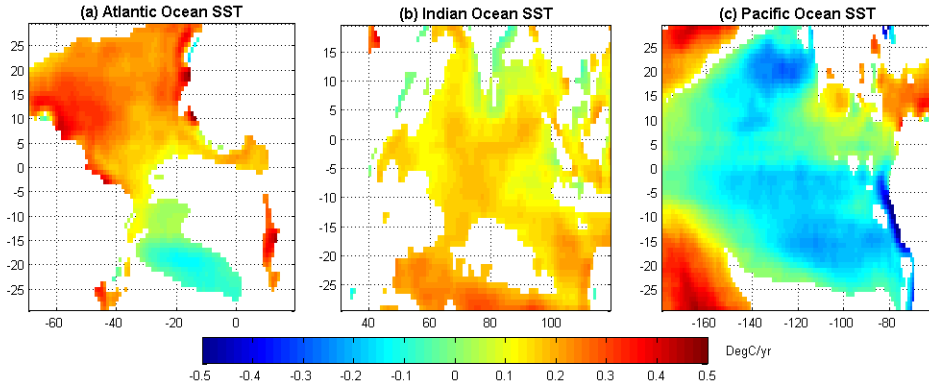


Figure 11: Spatial patterns of long term linear trends in SST (1982 – 2014), over the (a) Atlantic, (b) Indian, and (c) Pacific Oceans. Only areas with statistically significant trends ($\alpha = 0.05$) in the three Oceans are presented.

712 4.2.5. Impact of the Congo river on water storage dynamics of the Congo basin

713 Apart from being under-represented in the literature on African climate variability (e.g.,
 714 [Todd and Washington, 2004](#)), there is a prominent gap in our understanding of hydrological
 715 conditions in the Congo basin compared to other tropical continental river basins in SSA (e.g.,
 716 Volta and Lake Chad basins). Few GRACE studies, e.g., the pioneering work of [Crowley et al.](#)
 717 (2006) over the Congo basin and that of [Lee et al. \(2011\)](#) in the Congo basin cuvette have,
 718 nonetheless, been reported. As the aforementioned studies did not study the impact of Congo
 719 river on GRACE-derived TWS, this section discusses the role of the Congo river on the water
 720 storage dynamics of the basin. The Congo river (has an approximate length of 4700 – 5100
 721 km) is the second largest river in Africa and drains one of the largest tropical forests of the
 722 world ([Shahin, 2008](#)). Given that low discharge values are observed between July and August,
 723 a period corresponding to low annual rainfall and SST, the impact of climate variability on
 724 the flow regime of the Congo river is presumably expected to have significant influence on the
 725 hydrological system of the Cong basin. To further investigate the contribution of Congo river to
 726 TWS, the temporal evolutions of GPCC-based precipitation, soil moisture (CPC and MERRA
 727 products), and TWS (GRACE, WGHM, and MERRA) over the Equatorial countries (PC2,
 728 Figs. 6, 7, and 8, respectively), obtained from PCA in the preceding sections are compared
 729 with standardised river discharge anomalies for the common period (2002 – 2010). River
 730 discharge anomalies showed the strongest association with the time series associated with the
 731 second EOF of GRACE-TWS (PC2, Fig. 8), indicating a statistically significant correlation
 732 of 0.86 ($\alpha = 5\%$) compared to those of WGHM-TWS ($r = 0.61$), MERRA-TWS ($r = 0.37$),
 733 and GPCC-precipitation ($r = 0.02$) (Fig. 12a-d). But GPCC-precipitation (PC2, Fig. 6) is

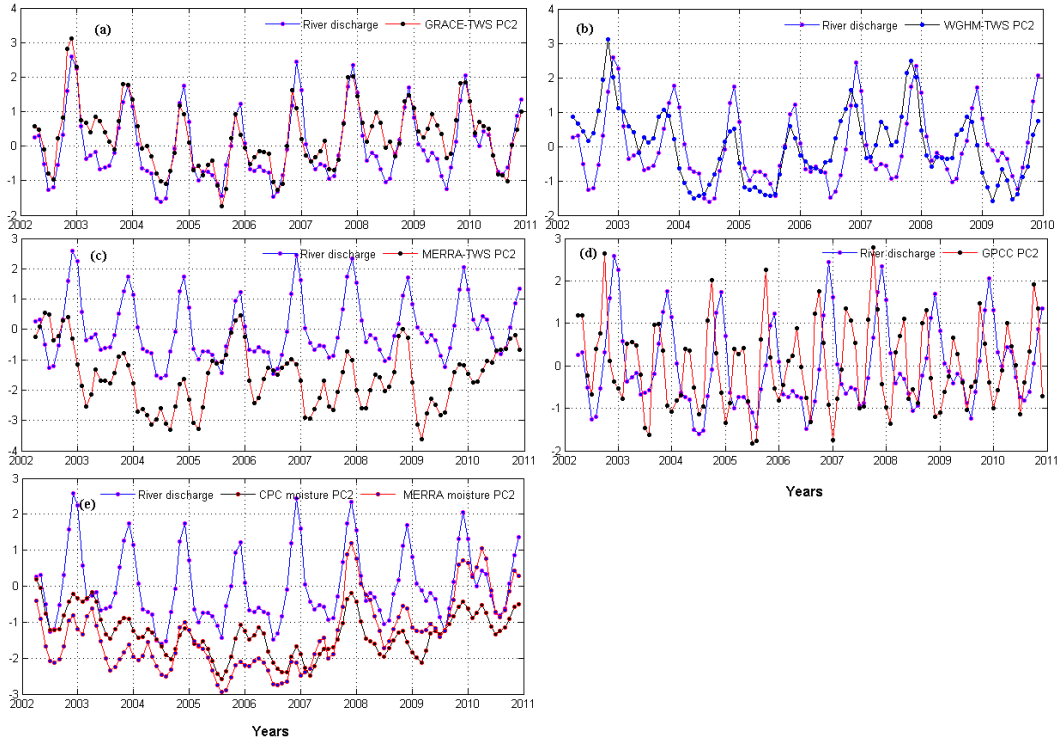


Figure 12: The relationship between the Congo river and TWS. The temporal patterns (PC2, Figs. 6, 7, and 8) of (a) GRACE-derived TWS, (b) WGHM-TWS, (c) MERRA-TWS, (d) GPCC-based precipitation, and (e) soil moisture (i.e., CPC and MERRA products) are compared with the standardised anomalies of river discharge at the Congo Kinshasa station for the common time period (2002 – 2010). All correlations are statistically significant at 95% confidence level.

734 associated with river discharge anomalies during the same period at 2 months lag ($r = 0.50$)
 735 (Fig. 12d). The temporal patterns of soil moisture over the Congo basin (CPC and MERRA
 736 PC2, Fig. 7) showed moderate associations ($r = 0.51$ and $r = 0.50$ for CPC and MERRA
 737 products, respectively) with river discharge (Fig. 12e).

738 The singular spectral analysis of two leading components of river discharge, which were
 739 based on SVD decomposition of the lagged covariance matrices were also compared with
 740 GPCC-precipitation (PC2, Fig. 6), soil moisture (PC2, Fig. 7), and GRACE TWS (PC2,
 741 Fig. 8) modes over the Congo basin using regression. The annual (first spectral mode indicat-
 742 ing $R^2 = 0.70$ with TWS) and the multi-annual (second spectral mode indicating $R^2 = 0.50$
 743 with TWS) variations of river discharge, which accounted for total variabilities of 75% and
 744 23%, respectively, explained 70% and 50% of the variability in GRACE-TWS (Fig. 13a-b).
 745 These river discharge modes, however, showed no relationship with GPCC-rainfall (Fig. 13c-
 746 d), but rather interestingly, similar to the earlier analysis, at two months lag time, maximum
 747 correlations were found ($r = 0.33$ and $r = 0.64$, respectively). The association of soil moisture

748 with the first spectral mode of river discharge (annual variations) are consistent as indicated
 749 earlier ($r = 0.50$ and $R^2 = 0.25$ for both CPC and MERRA soil moisture products) while the
 750 second spectral mode of river discharge (multi-annual variations) indicated correlations of 0.41
 751 ($R^2 = 0.17$) and 0.34 ($R^2 = 0.12$) with CPC and MERRA soil moisture products, respectively
 (Fig. 13e-f). Hence, this evidence suggests that the multi-annual changes in land water storage

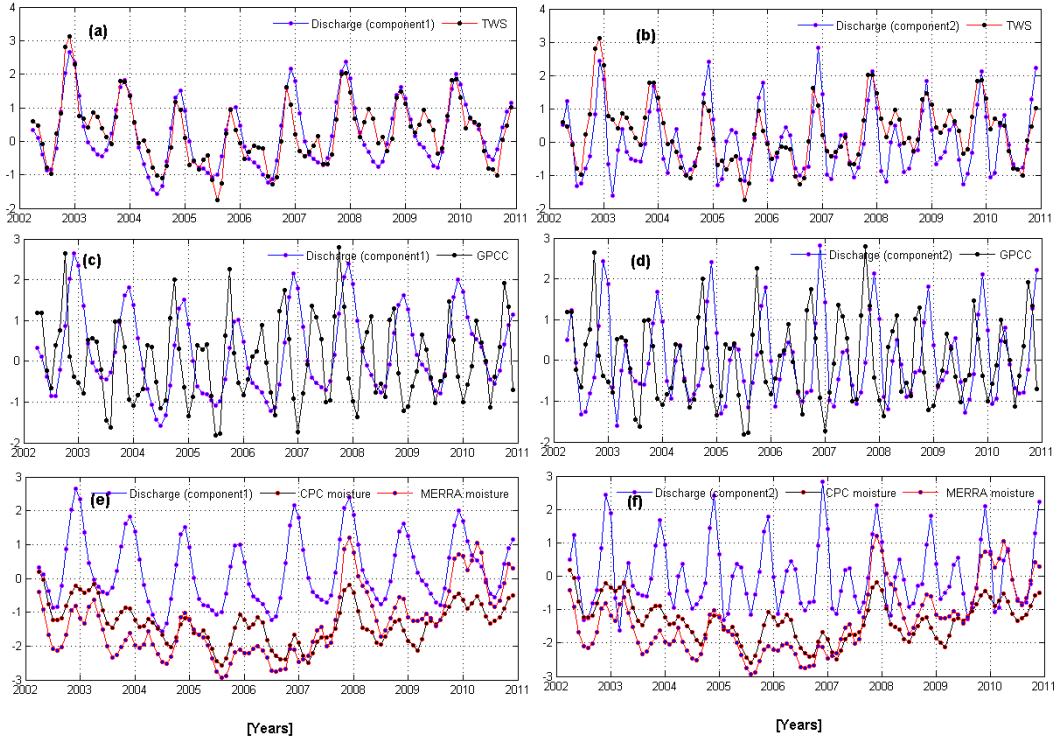


Figure 13: Singular spectral analysis of river discharge time series of the Congo basin. (a/c/e) The annual variations and (b/d/f) multi-annual variations of river discharge in the Congo basin are compared with GPCP-based precipitation (PC2, Fig. 6), soil moisture (i.e., CPC and MERRA PC2, Fig. 7), and GRACE-derived TWS (PC2, Fig. 8) over the Congo basin. The time series of river discharge are the reconstructed expansion coefficients.

752

753 (GRACE-derived TWS, PC2, 8) over the Congo basin is largely and prominently induced by
 754 its surface waters (river discharge), that is, in addition to the soil moisture variation previ-
 755 ously discussed. WGHM-TWS also shows a better association with river discharge (Fig. 12b)
 756 compared to MERRA-TWS (Fig. 12c) perhaps due to the presence of groundwater and dis-
 757 charge in the WGHM data. The hydrological significance of rainfall in the land water storage
 758 dynamics is not ruled out as the central Congo receives high tropical rainfall of 1800 – 2400
 759 mm annually with almost no dry season (Gupta, 2007). For example, between the early 2003
 760 and 2005, Crowley et al. (2006) noted that precipitation contributed roughly three times the
 761 peak water storage after an unusual rainy season in the Congo basin. On the analysis of

762 temporal variability in the water resources of SSA using historical stream flow data, [Conway](#)
763 [et al. \(2009\)](#) argues that rainfall amongst other factors (e.g., human interventions) provides the
764 dominant control on inter-annual and decadal variability in river flows. The aerial averaged
765 GPCP precipitation over the Congo basin indicates a strong association ($r = 0.70$) with river
766 discharge at one month lag. This simply reinforces the role of rainfall as a principal component
767 in the variations of river discharge of the Congo basin, though this relationship (rainfall-river
768 discharge) varies on decadal time scales as observed in West Africa by [Conway et al. \(2009\)](#).

769 But the flow regime of the Congo river is however, somewhat complex. Mostly because
770 of its catchment characteristics, equatorial climate and the multiple sources of discharge from
771 tributaries originating from the highlands and mountains of the East Africa Rift, Lake Tan-
772 ganyika, Lake Mweru, even up to the Lualaba river, and the central Congo (see details in
773 [Shahin, 2008](#)). Due to physiographic features, some of these rivers have complex drainage
774 systems that affect their temporal stability and relationship with rainfall. Whereas this is true
775 for the Congo basin as reported by [Conway et al. \(2009\)](#), they further reported a case study of
776 weak relationship between outflows from Lake Victoria and basin rainfall, even during periods
777 of stationary conditions. Such non-stationary behaviour between river discharge and rainfall
778 evolutions exists in the Congo basin. Because of its climatological diversity and the impacts of
779 physical mechanisms such as the Walker circulations, ENSO, and SST on rainfall variability
780 (e.g., [Farnsworth et al., 2011](#); [Nicholson and Selato, 2000](#)), the river discharge-rainfall relation-
781 ship in the basin can only be more complicated. However, since technically, GRACE measures
782 changes in the Earth's total water column, the combined effect of multiple discharge sources
783 (surface water) and heavy rainy seasons are major fluxes that will primarily drive the GRACE
784 water column in the Congo basin.

785 Furthermore, [Gupta \(2007\)](#) reported on the seasonal flow regime, indicating that observed
786 increase in river discharge at the Kinshasa station, occurs between April and June due to
787 increased flow from the southern basin, thereby triggering a second discharge peak, different
788 from the major first peaks that occurs between November and January. These two flow regimes
789 in the basin, coincides with the semi-annual patterns in the temporal evolutions of our PCA
790 results for TWS, soil moisture, and rainfall (see Sections [4.2.1](#), [4.2.2](#), and [4.2.3](#)). Considering
791 all of the above, and the fact that the Congo river has an average annual flow that represents
792 about 40% of the Continent's discharge, justify's the river discharge of the Congo basin (i.e.,
793 from the upstream and downstream areas) as a principal and direct driver of GRACE-TWS
794 in the region. In summary, while the TWS of most countries in West Africa (e.g., Guinea,
795 Nigeria, Mali, Liberia, Cameroon, etc.) are triggered by annual precipitation cycles induced

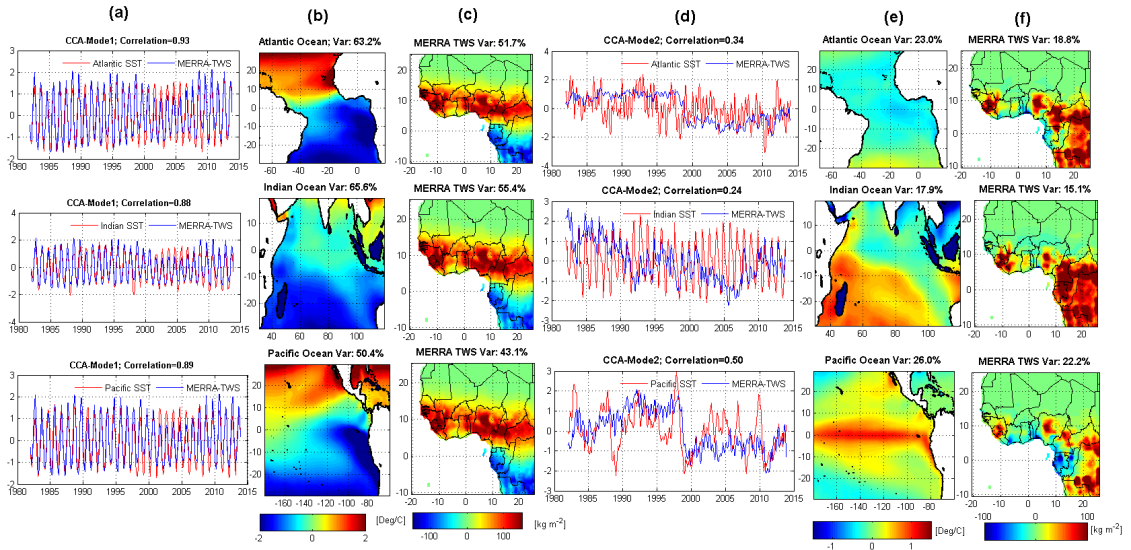


Figure 14: Leading canonical modes of SST (Atlantic, Indian and Pacific Oceans) and MERRA TWS (1982 – 2014). The canonical component time series of SST (predictors) and MERRA TWS (predictands) are in normalised units (a and d). The SST (b and e) and MERRA TWS (c and f) loadings have been adjusted to their original units (i.e., DegC and mm, respectively). Their variances (Var) explained in percentages are also indicated.

796 by ocean circulations, altitude and physiographic features as reported previously (Ndehedehe
 797 et al., 2016a), the analyses in this study show that GRACE-derived TWS over the Congo
 798 basin is however, largely determined and driven by changes in the river discharge of the Congo
 799 basin. In the next section, the impact of climate variability on the basin’s water fluxes (TWS
 800 and river discharge) is discussed.

801 4.3. TWS and links to sea surface temperature (SST)

802 4.3.1. Influence of global SST on long term MERRA-TWS (1982–2015)

803 Large scale SST anomalies have been identified as significant components of observed
 804 variabilities in rainfall over SSA (e.g., Odekunle and Eludoyin, 2008; Farnsworth et al., 2011;
 805 Semazzi et al., 1988; Nicholson, 2013, and the references therein). Establishing the association
 806 between SST and TWS forms the physical basis of understanding the response of land water
 807 storage to inter-annual changes in global climate. The focus in this section is to examine the
 808 links between TWS over SSA and global climates based on CCA. Prior to the implementation
 809 of canonical correlation analysis (CCA), the pre-orthogonalisation results (i.e., the first and the
 810 second modes of SST and TWS) were compared using regression. From the regression results
 811 summarised in Table 2, the leading temporal variations of TWS (PC1), especially GRACE
 812 show strong relationship with those of SST anomalies in the three Oceans. The temporal

Table 2: Regression results (R^2) of temporal evolutions of SST (PC1 and PC2) over the three oceans (Atlantic, Indian, and Pacific) with those of TWS MERRA (1982 – 2014) and GRACE (2002 – 2014). Relationships are significant at the 95% significant level for R^2 in bold.

Data	PCs	Atlantic Ocean		Indian Ocean		Pacific Ocean	
	Temporal	PC1	PC2	PC1	PC2	PC1	PC2
Merra TWS	PC1/PC2	0.56	0.03	0.44	0.008	0.53	0.006
GRACE-TWS	PC1/PC2	0.72	0.21	0.48	0.00	0.66	0.05

813 components of Atlantic and Pacific SST in these leading modes show strong association with
814 MERRA TWS compared to the Indian Ocean (Table 2). These relationships are reliable
815 indicators of SST anomalies as prominent drivers of TWS in the region. But in the CCA
816 results, significant associations are found in the two retained canonical modes. The CCA
817 maps (g -map or the predictor map and h -map or the predictand map) and their temporal
818 series, i.e., the canonical variables for the first and second modes of MERRA-TWS/SST and
819 GRACE-TWS/SST are indicated in Figs. 14 and 15, respectively. The principal loading
820 patterns (CCA spatial patterns or maps) associated with the temporal series (i.e., u and v) in
821 the first canonical modes (Figs. 14a-c) show that strong negative and positive SST anomalies in
822 the three oceans represent strong potential predictors for the dominant mode of MERRA-TWS
823 over SSA. Their temporal series (Fig. 14a) are highly correlated (Table 3) and indicate the
824 inter-annual variations in the observed amplitudes of the predictor loading patterns (Fig. 14b).
825 Two well known features are observed in the heterogenous patterns (except for the Indian
826 Ocean) of the first CCA modes of the predictor maps. Firstly, the warming of the northern
827 ocean indicated by strong positive canonical loadings and cooling of the south-eastern Oceans
828 (Fig. 14b). Secondly, these patterns are analogous to strong positive canonical loadings in
829 West Africa and strong negative loadings in Equatorial countries (Figs. 14b). These predictor
830 loadings, which essentially show an inter-hemispheric dipole configurations (except for the
831 Indian Ocean), strongly influences the variability of the predictand (Fig. 14c). Meanwhile, the
832 large scale coherent negative canonical loadings over the southern Indian Ocean exhibited by
833 the first CCA mode of SST field (Fig. 14b) suggests the predominant control of this Ocean on
834 the annual variability of TWS in the region. When instigated by other physical mechanisms
835 (e.g., ENSO), or sometimes in conjunction with the Atlantic Ocean, the Indian Ocean plays
836 a complementary role on inter-annual rainfall variability in SSA. For example, teeming up
837 with an anomalously warm eastern tropical Atlantic SST, an unusually warm Indian Ocean
838 SST is known to affect moisture transports, causing reduced rainfall and drought in the Sahel
839 region of SSA (Bader and Latif, 2011; Giannini et al., 2003). In Africa, some studies (e.g.,

Table 3: Results of canonical correlations of SST (CCA-1 and CCA-2) over the three oceans (Atlantic, Indian, and Pacific) with those of MERRA TWS (1982 – 2014) and GRACE-TWS (2002 – 2014). Relationships are significant at the 95% significant level for all canonical correlation values.

Data	Vectors	Atlantic Ocean		Indian Ocean		Pacific Ocean	
		CCA-1	CCA-2	CCA-1	CCA-2	CCA-1	CCA-2
Merra TWS	CCA-1/CCA-2	0.93	0.34	0.88	0.24	0.89	0.50
GRACE-TWS	CCA-1/CCA-2	0.96	0.61	0.96	0.63	0.95	0.65

840 [Farnsworth et al., 2011](#); [Nicholson and Selato, 2000](#)) have further confirmed that SSTs in the
 841 Indian and Atlantic Oceans influence rainfall variability. Whereas the impact of SST anomalies
 842 of these two Oceans is an important consideration for an ENSO event, their actual connection is
 843 undetermined and inconclusive ([Farnsworth et al., 2011](#)). However, strong changes in regional
 844 precipitation resulting from the perturbations of these Oceans have direct impacts on the
 845 variations in land water storage over SSA. Considering the total variabilities explained by the
 846 first and second canonical modes (65% and 17.9%, respectively) of SST over the Indian Ocean
 847 and their corresponding correlations (Table 3), this study confirms that the Indian Ocean are
 848 also predictors of variabilities in TWS over the region.

849 In the second canonical modes of SST and MERRA-TWS, the temporal components of
 850 pacific SST and MERRA-TWS are relatively better correlated, indicating a correlation of
 851 0.50 (Table 3 for Pacific Ocean) compared to other canonical vectors (Figs. 14d). Given the
 852 significance of the Pacific Ocean as a very popular oceanic *hot spot* that plays key roles in El-
 853 Niño and La-Niña cycles (e.g., [Koster et al., 2004](#); [Trenberth, 1997](#)), the temporal component
 854 of the second CCA mode of Pacific SST anomalies, accounting for 26.0% of the total variability
 855 (Fig. 14e) is an ENSO-related mode. This is because the temporal component (Pacific SST) of
 856 this CCA mode indicated a correlation of 0.90 with the ENSO index, suggesting the prominent
 857 role of ENSO in the inter-annual variations of MERRA-TWS in the tropical areas of SSA
 858 (Fig. 14f), especially the upstream and downstream areas of the Congo basin. Since rainfall
 859 patterns over Africa are strongly affected by a number of global climate modes as is the case
 860 in many parts of the world, the coupled effect of the ENSO phenomenon on a large part of the
 861 variability in MERRA TWS over SSA as shown in Fig. 14d-f (Pacific SST) would be expected.
 862 When this is juxtaposed with the significant correlation between rainfall anomalies in SSA
 863 and tropical Pacific SST reported e.g., by [Semazzi et al. \(1988\)](#), it is here argued that the
 864 equatorial Pacific represents a significant and probably one of the most relevant oceanic *hot*
 865 *spot* that play key roles in strong hydrological changes in SSA.

866 The second CCA modes of Atlantic and Indian SST anomalies (Figs. 14d-f), however, are

867 weakly associated with MERRA-TWS (0.34 and 0.24, respectively). Furthermore, Atlantic
 868 Multi Decadal Oscillation (AMO) is modestly associated with the Atlantic SST in the second
 869 CCA mode ($r = -0.50$ at $\alpha = 5\%$) (Fig. 14d), and may also represent a significant climate
 870 mode from the Atlantic Ocean that somewhat influences TWS in SSA. A study on global
 871 trends and variability in soil moisture and drought characteristics by [Sheffield and Wood \(2008\)](#)
 872 suggests that apart from ENSO, the variability in AMO accounts for some of the inter-annual
 873 and decadal variabilities in soil moisture and drought characteristics in West Africa and many
 874 other regions of the world. Although such influence may be different when TWS is considered,
 875 the CCA results show that the long term MERRA-TWS is able to detect prominent indices of
 876 climate variability (e.g., ENSO, AMO, etc.) that impacts on the climate system of SSA. This
 877 would be consistent with some pioneering studies (e.g., [Ndehedehe et al., 2017b](#); [Boening et al.,](#)
 878 [2012](#); [Phillips et al., 2012](#)) that have shown how teleconnection patterns around the globe are
 associated with changes in global mean sea level and continental water storage. Figure 11a-c

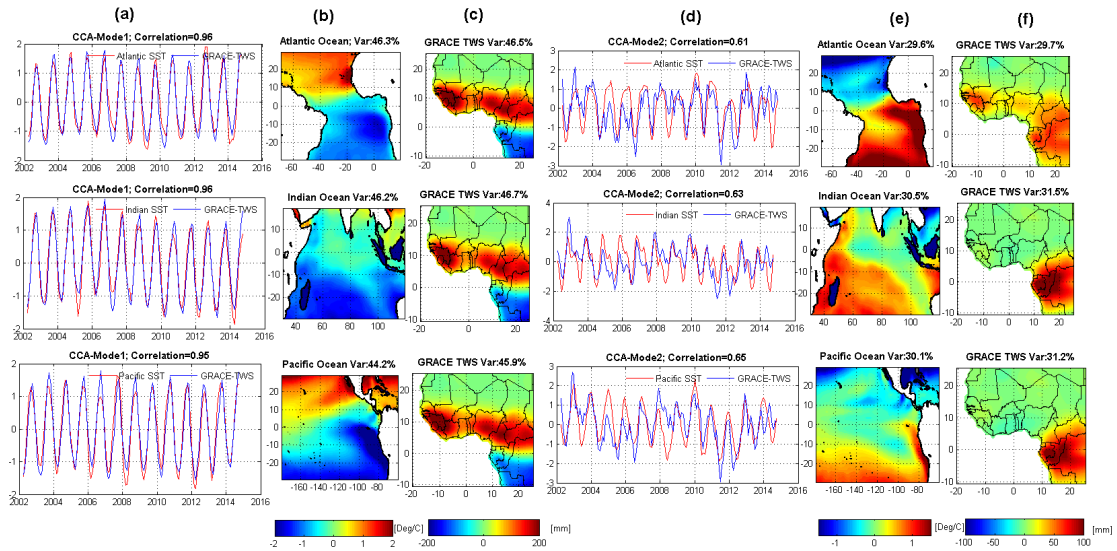


Figure 15: Leading canonical modes of SST (Atlantic, Indian and Pacific Oceans) and GRACE TWS (2002 – 2014). The canonical component time series of SST (predictors) and GRACE TWS (predictands) are in normalised units (a and d). The SST (b and e) and GRACE TWS (c and f) loadings have been adjusted to their original units (i.e., DegC and mm, respectively). Their variances (Var) explained in percentages are also indicated.

879

880 show strong warming in most parts of the Oceans except in the Pacific where some areas
 881 indicate both cooling and a considerable warming. Whereas this warming of the global oceans
 882 coincides with observed negative trends in TWS and soil moisture in much of SSA (Fig. 10b-e),
 883 it also suggests the interplay of the three Oceans in modulating moisture transports across the

884 region. For example, the weight of evidence have shown that changes in SST anomalies in the
885 north tropical Atlantic, apart from modulating the Pacific climate variability, can influence
886 the predictability and variability of ENSO and trigger its events (see, [Ham et al., 2013](#), and
887 the references therein). Consequently, the warming of the tropical Atlantic Ocean during the
888 1982 – 2014 period (Fig. 11a) maybe very significant to the observed relationships of ENSO
889 and AMO with TWS, confirming their roles in the region.

890 4.3.2. Relationship of SST with GRACE-TWS during the 2002–2014 period

891 The CCA diagnostics also show that the dominant modes of SST evolutions of the three
892 Oceans (Atlantic, Indian, and Pacific) have strong influence on annual GRACE-TWS varia-
893 tions (Figs. 15a-c) as the canonical correlations (Table 3) for the first and second CCA modes
894 are relatively high and statistically significant ($\alpha = 0.05$). The temporal components of SST
895 from all Oceans in the second CCA modes are reasonably or well correlated with GRACE-
896 TWS (Fig. 15d), indicating that all oceans play significant roles in the observed GRACE-
897 TWS changes of the Congo basin (Figs. 15e-f). Apart from the Congo basin, GRACE-TWS in
898 Guinea is potentially predictable from the inter-hemispheric dipole configurations of the strong
899 SST patterns in the Atlantic Ocean as can be seen in the second CCA mode (Fig. 15d-f). The
900 annual and bimodal features reflected in the inter-annual variations of rainfall (cf. Fig. 6) over
901 SSA are propagated in the CCA of the two fields-SST and GRACE-TWS (Fig. 15a and d)
902 and implies a strong coupling between the two. Large coherent positive loadings observed in
903 the predictor maps (i.e., g) of the southern and eastern parts of all Oceans in the CCA modes
904 (Fig. 15e) are in association with strong positive canonical loadings in the predictand maps
905 (i.e., h) observed over the Congo basin (Fig. 15f). These are useful CCA diagnostics, which
906 may provide some important explanations on observed physical mechanisms that help relates
907 the SST fields to those of GRACE-TWS. For instance, in the last half of the 20th century,
908 the warming of the South and North Atlantic Oceans have contributed to drying conditions
909 in the region (e.g., [Nicholson, 2013](#); [Giannini et al., 2013](#)). Although changes in the Indian
910 Ocean SST have also been identified as inducing dry conditions in the Sahel region as high-
911 lighted earlier, such impacts as reported by [Giannini et al. \(2003\)](#), are usually facilitated by
912 an occasionally warmer-than-average SST of the eastern Atlantic Ocean (cf. Fig. 11a and b).

913 Whereas it is agreed that SST in the equatorial Atlantic favour convection in the Guinea
914 Coast countries (see, e.g., [Odekunle and Eludoyin, 2008](#); [Nicholson and Webster, 2007](#)), [Aguilar
915 et al. \(2009\)](#) observed over Central Africa (much of the Congo basin) a decrease in heavy (total)
916 precipitation over the last half century. A similar change in the climate patterns of the region
917 has again emerged in a more recent study by [Hua et al. \(2016\)](#). They observed drying trends in

Table 4: Correlations results of SST canonical components (CCA-1 and CCA-2) over the Atlantic, Indian, and Pacific Oceans (Fig. 15) with observed river discharge anomalies during the same period (2002 – 2010). Correlations are statistically significant ($\alpha = 0.05$) for all values in bold. Those marked with asterisks (*) are not statistically significant.

Data	Vectors	Atlantic Ocean		Indian Ocean		Pacific Ocean	
		CCA-1	CCA-2	CCA-1	CCA-2	CCA-1	CCA-2
River discharge		*0.09	0.76	*0.07	0.77	*0.13	0.74
GPCC-rainfall		0.22	0.60	0.20	0.63	0.20	0.42

918 equatorial Africa and suggests that it is essentially modulated by SSTs and the regional/global
 919 atmospheric circulation pattern. As one of the major convective regions of the world, which
 920 during the transition seasons, dominates global tropical rainfall (Washington et al., 2013),
 921 the Congo basin’s rainfall climatology is strongly influenced by SST teleconnection patterns
 922 (notably ENSO and the Indian Ocean dipole oscillation) and provides more challenges in the
 923 set up of attribution studies (see, Otto et al., 2013). Considering that SST, atmospheric
 924 circulation features, synoptic and mesoscale convective systems regulate rainfall conditions in
 925 the Congo basin (Equatorial Africa), such influence play key role on hydrological processes
 926 (considerable changes in TWS) of the region at seasonal and annual time scales. It is suggested
 927 here that the relational stability (the somewhat consistent association between the canonical
 928 variate) observed in the temporal series (Fig. 15d) of the second CCA mode (Table 3) and the
 929 evolutionary developments of their corresponding predictor and predictand maps (Fig. 15e-f)
 930 would be logical indications that these parts of the Oceans have considerable influence on the
 931 regional variability of TWS in SSA. Specifically, the SST of all southern Oceans modulate
 932 GRACE-TWS changes in the Congo basin by directly influencing the tropical rain belt and
 933 the inter-tropical convergence zone (ITCZ). A plethora of case studies in Farnsworth et al.
 934 (2011) have reported on the observed relationships between large scale SST anomalies and
 935 rainfall variability in the region (including the Congo basin), confirming that SST variations
 936 and land-surface gradients modulate rainfall in the Congo basin area by directly influencing
 937 the strength and loci of the tropospheric jets. It is also noted that the temporal component of
 938 Atlantic SST in the second CCA mode (Fig. 15d) associated with the heterogenous patterns
 939 of the predictor map (Fig. 15e) covaries well with the Atlantic Meridional Mode-AMM index
 940 ($r = 0.50$ at $\alpha = 5\%$), re-emphasising the Atlantic SST as a driver of GRACE-TWS variability.

941 Unlike MERRA TWS, the short time series of GRACE-TWS makes its difficult to iden-
 942 tify any low frequency climate oscillation in the main portion of the CCA procedure that is
 943 associated with it changes. The AMO, for instance, is a ‘multi-decadal’ oscillation with a

944 large spectral energy density at periods spanning more than two decades compared to ENSO,
945 which has a large energy between 2-5 years, with positive and negative phases having large
946 asymmetric amplitude variations. Although the ENSO oscillations were not isolated in the
947 main portion of the CCA procedure (GRACE Vs SST), considerable strong and significant
948 relationship exist between the SST of the three Oceans and GRACE-TWS (Table 3) and could
949 be helpful to forecast the development of several types of ENSO episodes (Ham et al., 2013)
950 and other indices of climate variability that are known to have broad impacts on rainfall vari-
951 ance in the region. The coherent relationship of SST anomalies in the second CCA mode with
952 GRACE-TWS index in the Congo basin area (Fig. 15d-f) is sufficient to suggest that the scale
953 of oceanic influence in the basin is global. It is interesting that the temporal components of
954 SST in the CCA output presented in Fig. 15 are also related to inter-annual variability of
955 river discharge and precipitation in the Congo basin. Their correlation results summarised in
956 Table 4 suggest that river discharge of the Congo basin is more dynamically coupled to the
957 second CCA mode of SST over the three oceans (Fig. 15d-f). Although rainfall also show a
958 direct association as would be expected, river discharge indicated relatively stronger corre-
959 lation with the temporal series of SST from all oceans in the second CCA mode (Table 4).
960 This would be consistent with the discussion in Section 4.2.5, where river discharge is said
961 to provide the dominant control on GRACE-TWS in the Congo basin. The Congo basin's
962 river discharge indicates consistent and strong positive relationship with the SST anomalies
963 of the three oceans and is consistent with other studies that reported similar positive associ-
964 ation between rainfall in the Congo basin and SST of the Atlantic and Indian Oceans (e.g.,
965 Farnsworth et al., 2011; Todd and Washington, 2004). Considering that SST from the three
966 oceans explain large parts of the variability in the Congo river discharge (Table 4), which
967 is a principal driver of GRACE-TWS, then changes in SST will impact on the hydrological
968 variability of the Congo basin. With GRACE data being able to identify multi-annual changes
969 in the river discharge of the Congo basin (Figs. 12a and 13a), essentially, it is emerging as a
970 stronger tool for studies of hydrological processes, especially in the light of its recent agreement
971 with altimeter observations over the Caspian Sea (see, Chen et al., 2017).

972 5. Conclusion

973 Long term hydrological changes (1980 – 2015) based on model and global reanalysis data
974 over SSA and their links to SST anomalies were studied using canonical correlation analysis
975 (CCA), singular spectral analysis, and Man-Kendall's statistics. Short term analysis based on
976 GRACE data are also undertaken. The results are summarised as follows.

- 977 (1) The broad agreement across models and reanalysis data on declines in land water stor-
978 age (TWS, soil moisture, and groundwater) in the Congo basin confirms a statistically
979 significant ($\alpha = 0.05$) long term drying in the region and coincides with warming of the
980 land surface and the surrounding oceans. Some areas in West Africa and the Congo basin
981 however, show statistically significant positive trends in the model groundwater. Some
982 of these positive trends (model groundwater) are somewhat inconsistent with those of
983 rainfall, soil moisture, and TWS in some areas, probably due to land surface conditions
984 and complex hydrological processes. Meanwhile, the Sahel show some wetting trends
985 in rainfall, soil moisture, and TWS during the period. This generally aligns with the
986 ongoing narratives of rainfall recovery in the Sahel region. The observed trends in these
987 dataset should be interpreted with caution given that the output of these models maybe
988 sensitive to the forcing dataset that drives it and due to potential uncertainties that
989 maybe associated with them.
- 990 (2) GRACE hydrological signal over the Congo basin is strongly associated with the multi-
991 annual changes in the Congo river discharge ($r = 0.86$). The relationship between the two
992 leading components of river discharge obtained from singular spectral analysis and the
993 temporal evolutions of GRACE-derived TWS over the Congo basin (i.e., $R^2 = 0.70$ and
994 0.50 for the first and second spectral components, respectively), confirm that the Congo
995 river discharge remains a prominent and principal driver of GRACE-derived TWS. In ad-
996 dition, it shows a considerable association with SST anomalies of all the southern Oceans
997 (Atlantic, Indian, and Pacific). The declines in soil moisture ($\sim -45.9 \pm 8.1$ mm/yr)
998 in the basin coincided with those of GRACE-TWS ($\sim -78.4 \pm 20.3$ mm/yr) during the
999 2003 – 2006 period, also confirming the significant role of inter-annual changes in soil
1000 moisture to observed variations in GRACE-TWS. In the light of its recent agreement
1001 with other large scale satellite geodetic missions, and the ability to resolve strong sig-
1002 nals of water storage variations over surface waters in smaller basins, GRACE gravimetry
1003 emerges as a stronger ‘tool in the box’ for studies of hydrological changes and monitoring
1004 the impacts of climate variability in the data deficient African region.
- 1005 (3) The CCA diagnostics showed that the scale of oceanic influence on MERRA and GRACE
1006 TWS over SSA is global. ENSO related equatorial Pacific SST fluctuations was a ma-
1007 jor index of climate variability identified in the main portion of the CCA procedure
1008 that shows a considerable association with long term MERRA data over SSA. Vari-
1009 abilities in Atlantic Meridional Mode and Atlantic Multi-decadal Oscillation were also
1010 found to be modestly associated with the canonical components of Atlantic SST. These

1011 climate oscillations indicated statistically significant ($\alpha = 0.05$) association with TWS,
1012 re-emphasising the role of Atlantic SST variability in the region.

1013 (4) Over SSA, the leading modes (annual amplitudes) of long term variations in rainfall,
1014 soil moisture, and TWS data were found in West African countries (located between
1015 latitudes 5°N and 15°N) and some countries of the Congo basin while Guinea, Liberia,
1016 Sierra Leone, and southern Nigeria have the strongest variability in model groundwater.
1017 These annual amplitudes generally show linear and considerable relationship with SST
1018 anomalies from the surrounding oceans.

Acknowledgments

1019 Christopher E. Ndehedehe and Nathan O. Agutu are grateful to Curtin University for the
1020 funding that supported this project. The Authors are grateful to CSR, NASA, NOAA, and
1021 GRDC for the data used in this study. They are also grateful to Center for Environment
1022 Systems Research for the WaterGap model data.
1023

1024 **References**

- 1025 Aguilar, E., Aziz Barry, A., Brunet, M., Ekan, L., Fernandes, A., Massoukina, M., Mbah,
1026 J., Mhanda, A., do Nascimento, D. J., Peterson, T. C., Thamba Umba, O., Tomou, M.,
1027 and Zhang, X. (2009). Changes in temperature and precipitation extremes in western cen-
1028 tral Africa, Guinea Conakry, and Zimbabwe, 1955-2006. *Journal of Geophysical Research:*
1029 *Atmospheres*, 114(D2):D02115. doi:10.1029/2008JD011010.
- 1030 Ahmed, M., Sultan, M., J.Wahr, and Yan, E. (2014). The use of GRACE data to monitor
1031 natural and anthropogenic induced variations in water availability across Africa. *Earth*
1032 *Science Reviews*, 136:289–300. doi:10.1016/j.earscirev.2014.05.009.
- 1033 Alsdorf, D., Beighley, E., Laraque, A., Lee, H., Tshimanga, R., O’Loughlin, F.,
1034 Mah, G., Dinga, B., Moukandi, G., and Spencer, R. G. M. (2016). Opportuni-
1035 ties for hydrologic research in the congo basin. *Reviews of Geophysics*, 54(2):378–409.
1036 doi:10.1002/2016RG000517.
- 1037 Alsdorf, D. E. and Lettenmaier, D. P. (2003). Tracking fresh water from space. *Science*,
1038 301(5639):1491–1494. doi:10.1126/science.1089802.
- 1039 Andam-Akorful, S., Ferreira, V., Ndehedehe, C. E., and Quaye-Ballard, J. (2017). An inves-
1040 tigation into the freshwater variability in West Africa during 1979 – 2010. *International*
1041 *Journal of Climatology*. doi:10.1002/joc.5006.
- 1042 Asefi-Najafabady, S. and Saatchi, S. (2013). Response of African humid tropical
1043 forests to recent rainfall anomalies. *Transactions of the Royal Society*, 368:20120306.
1044 doi:10.1098/rstb.2012.0306.
- 1045 Bader, J. and Latif, M. (2011). The 1983 drought in the West Sahel: A case study. *Climate*
1046 *Dynamics*, 36(3-4):463–472. doi:10.1007/s00382-009-0700-y.
- 1047 Barnett, T. P. and Preisendorfer, R. (1987). Origins and levels of monthly and sea-
1048 sonal forecast skill for United States surface air temperatures determined by canoni-
1049 cal correlation analysis. *Monthly Weather Review*, 115(9):1825–1850. doi:10.1175/1520-
1050 0493(1987)115<1825:OALOMA>2.0.CO;2.
- 1051 Becker, A., Finger, P., Meyer-Christoffer, A., Rudolf, B., Schamm, K., Schneider, U., and
1052 Ziese, M. (2013). A description of the global land-surface precipitation data products

- 1053 of the Global Precipitation Climatology Centre with sample applications including cen-
 1054 tennial (trend) analysis from 1901 to present. *Earth System Science Data*, 5(1):71–99.
 1055 doi:10.5194/essd-5-71-2013.
- 1056 Bekoe, E. O. and Logah, F. Y. (2013). The impact of droughts and climate change on electricity
 1057 generation in Ghana. *Environmental Sciences*, 1(1):13–24.
- 1058 Boening, C., Willis, J. K., Landerer, F. W., Nerem, R. S., and Fasullo, J. (2012). The
 1059 2011 La Nia: So strong, the oceans fell. *Geophysical Research Letters*, 39(19):L19602.
 1060 doi:10.1029/2012GL053055.
- 1061 Boone, A., Decharme, B., Guichard, F., Rosnay, P. D., Balsamo, G., Belaars, A., Chopin,
 1062 F., Orgeval, T., Polcher, J., Delire, C., Ducharne, A., Gascoin, S., Grippa, M., Jarlan, L.,
 1063 Kergoat, L., Mougin, E., Gusev, Y., Nasonova, O., Harris, P., Taylor, C., Norgaard, A.,
 1064 Sandholt, I., Oettle, C., Pocard-Leclercq, I., Saux-Picart, S., and Xue, Y. (2009). The
 1065 AMMA Land Surface Model Intercomparison Project (ALMIP). *Bulletin of American Me-*
 1066 *teorological Society*, 90(12):1865–1880. doi:10.1175/2009BAMS27/86.1.
- 1067 Boschetti, M., Nutini, F., Brivio, P. A., Bartholom, E., Stroppiana, D., and Hoscilo, A.
 1068 (2013). Identification of environmental anomaly hot spots in West Africa from time series
 1069 of NDVI and rainfall. *ISPRS Journal of Photogrammetry and Remote Sensing*, 78:26 – 40.
 1070 doi:10.1016/j.isprsjprs.2013.01.003.
- 1071 Chen, J. L., Wilson, C. R., Tapley, B. D., Save, H., and Cretaux, J.-F. (2017). Long-term and
 1072 seasonal Caspian Sea level change from satellite gravity and altimeter measurements. *Journal*
 1073 *of Geophysical Research: Solid Earth*, 122(3):2274–2290. doi:10.1002/2016JB013595.
- 1074 Conway, D., Persechino, A., Ardoin-Bardin, S., Hamandawana, H., Dieulin, C., and Mahé, G.
 1075 (2009). Rainfall and water resources variability in Sub-Saharan Africa during the twentieth
 1076 century. *Journal of Hydrometeorology*, 10(1):41–59. doi:10.1175/2008JHM1004.1.
- 1077 Crowley, J. W., Mitrovica, J. X., Bailey, R. C., Tamisiea, M. E., and Davis, J. L. (2006).
 1078 Land water storage within the Congo Basin inferred from GRACE satellite gravity data.
 1079 *Geophysical Research Letters*, 33(19):L19402. doi:10.1029/2006GL027070.
- 1080 Dardel, C., Kergoat, L., Hiernaux, P., Mougin, E., Grippa, M., and Tucker, C. (2014). Re-
 1081 greening Sahel: 30 years of remote sensing data and field observations (Mali, Niger). *Remote*
 1082 *Sensing of Environment*, 140:350 – 364. doi:10.1016/j.rse.2013.09.011.

- 1083 Descroix, L., Mahé, G., Lebel, T., Favreau, G., Galle, S., Gautier, E., Olivry, J.-C., Albergel,
 1084 J., Amogu, O., Cappelaere, B., Dessouassi, R., Diedhiou, A., Breton, E. L., Mamadou, I.,
 1085 and Sighomnou, D. (2009). Spatio-temporal variability of hydrological regimes around the
 1086 boundaries between Sahelian and Sudanian areas of West Africa: A synthesis. *Journal of*
 1087 *Hydrology*, 375(12):90–102. doi:10.1016/j.jhydrol.2008.12.012.
- 1088 Diaz, H. F., Hoerling, M. P., and Eischeid, J. K. (2001). Enso variability, telecon-
 1089 nections and climate change. *International Journal of Climatology*, 21(15):1845–1862.
 1090 doi:10.1002/joc.631.
- 1091 Dimri, A., Yasunari, T., Wiltshire, A., Kumar, P., Mathison, C., Ridley, J., and Jacob, D.
 1092 (2013). Application of regional climate models to the Indian winter monsoon over the
 1093 western Himalayas. *Science of The Total Environment*, 468–469, Supplement:S36 – S47.
 1094 doi:10.1016/j.scitotenv.2013.01.040.
- 1095 Döll, P., Müller Schmied, H., Schuh, C., Portmann, F. T., and Eicker, A. (2014a). Global-
 1096 scale assessment of groundwater depletion and related groundwater abstractions: Combining
 1097 hydrological modeling with information from well observations and GRACE satellites. *Water*
 1098 *Resources Research*, 50(7):5698–5720.
- 1099 Döll, P., Müller Schmied, H., Schuh, C., Portmann, F. T., and Eicker, A. (2014b). Global-
 1100 scale assessment of groundwater depletion and related groundwater abstractions: Combining
 1101 hydrological modeling with information from well observations and GRACE satellites. *Water*
 1102 *Resources Research*, 50(7):5698–5720.
- 1103 Douville, H., Conil, S., Tyteca, S., and Voltaire, A. (2007). Soil moisture memory and West
 1104 African monsoon predictability: artefact or reality? *Climate Dynamics*, 28(7):723–742.
 1105 doi:10.1007/s00382-006-0207-8.
- 1106 Enfield, D. and Mestas-Núñez, A. (1999). Multiscale variabilities in global sea surface tem-
 1107 peratures and their relationships with tropospheric climate patterns. *Journal of Climate*,
 1108 12(9):2719–2733. doi:10.1175/1520-0442(1999)012<2719:MVIGSS;2.0.CO;2.
- 1109 Erfanian, A., Wang, G., Yu, M., and Anyah, R. (2016). Multimodel ensemble simulations of
 1110 present and future climates over West Africa: impacts of vegetation dynamics. *Journal of*
 1111 *Advances in Modeling Earth Systems*, 8. doi:10.1002/2016MS000660.
- 1112 Fall, S., Semazzi, F. H. M., Niyogi, D. D. S., Anyah, R. O., and Bowden, J. (2006). The
 1113 spatiotemporal climate variability over Senegal and its relationship to global climate. *Inter-*
 1114 *national Journal of Climatology*, 26(14):2057–2076. doi:10.1002/joc.1355.

- 1115 Fan, Y. and Dool, H. V. (2004). Climate prediction center global monthly soil moisture data
1116 set at 0.5° resolution for 1948 to present. *Journal Of Geophysical Research*, 109:D10102.
1117 doi:10.1029/2003JD004345.
- 1118 Farnsworth, A., White, E., Williams, C. J., Black, E., and Kniveton, D. R. (2011). *Under-*
1119 *standing the Large Scale Driving Mechanisms of Rainfall Variability over Central Africa,*
1120 *In African Climate and Climate Change: Physical, Social and Political Perspectives*, pages
1121 101–122. Springer Netherlands, Dordrecht. doi:10.1007/978-90-481-3842-5_5.
- 1122 Favreau, G., Cappelaere, B., Massuel, S., Leblanc, M., Boucher, M., Boulain, N., and Leduc, C.
1123 (2009). Land clearing, climate variability, and water resources increase in semiarid southwest
1124 Niger: a review. *Water Resources Research*, 45:W00A16. doi:10.1029/2007WR006785.
- 1125 Fontaine, B. and Bigot, S. (1993). West African rainfall deficits and sea surface temperatures.
1126 *International Journal Of Climatology*, 13:271–285.
- 1127 Funk, C., Peterson, P., Landsfeld, M., Pedreros, D., Verdin, J., Shukla, S., Husak, G., Row-
1128 land, J., Harrison, L., Hoell, A., and Michaelsen, J. (2015). The climate hazards infrared
1129 precipitation with stations a new environmental record for monitoring extremes. *Scientific*
1130 *Data*, 2:150066. doi:10.1038/sdata.2015.66.
- 1131 Ghil, M., Allen, M. R., Dettinger, M. D., Ide, K., Kondrashov, D., Mann, M. E., Robertson,
1132 A. W., Saunders, A., Tian, Y., Varadi, F., and Yiou, P. (2002). Advanced spectral methods
1133 for climatic time series. *Reviews of Geophysics*, 40(1):3–1–3–41. doi:10.1029/2000RG000092.
- 1134 Giannini, A., Biasutti, M., Held, I. M., and Sobel, A. H. (2008). A global perspective on
1135 African climate. *Climate Change*, 90(7):359–383. doi:10.1007/s10584-008-9396-y.
- 1136 Giannini, A., Salack, S., Lodoun, T., Ali, A., Gaye, A., and Ndiaye, O. (2013). A unifying
1137 view of climate change in the Sahel linking intra-seasonal, interannual and longer time scales.
1138 *Environmental Research Letters*, 8:1–8. doi:10.1088/1748-9326/8/2/024010.
- 1139 Giannini, A., Saravanan, R., and Chang, P. (2003). Oceanic forcing of Sahel rainfall on inter-
1140 annual to decadal time scales. *Science*, 302(5647):1027–1030. doi:10.1126/science.1089357.
- 1141 Glahn, H. R. (1968). Canonical correlation and its relationship to discriminant analysis and
1142 multiple regression. *Journal of the Atmospheric Sciences*, 25(1):23–31. doi:10.1175/1520-
1143 0469(1968)025<0023:CCAIRT>2.0.CO;2.

- 1144 Graham, N. E., Michaelsen, J., and Barnett, T. P. (1987). An investigation of the el nio
 1145 southern oscillation cycle with statistical models: 1. predictor field characteristics. *Journal*
 1146 *of Geophysical Research: Oceans*, 92(C13):14251–14270. doi:10.1029/JC092iC13p14251.
- 1147 Gupta, A. (2007). Large rivers; geomorphology and management. *John Wiley & Sons*. Re-
 1148 trieved from:https://books.google.com.au/books. Accessed 11 September, 2015.
- 1149 Hall, J. W., Grey, D., Garrick, D., Fung, F., Brown, C., Dadson, S. J., and Sadoff, C. W.
 1150 (2014). Coping with the curse of freshwater variability. *Science*, 346(6208):429–430.
 1151 doi:10.1126/science.1257890.
- 1152 Ham, Y.-G., Kug, J.-S., Park, J.-Y., and Jin, F.-F. (2013). Sea surface temperature in the
 1153 north tropical atlantic as a trigger for el nino/southern oscillation events. *Nature Geoscience*,
 1154 6(2):112–116. doi:10.1038/ngeo1686.
- 1155 Herrmann, S. M., Anyamba, A., and Tucker, C. J. (2005). Recent trends in vegetation dynam-
 1156 ics in the African Sahel and their relationship to climate. *Global Environmental Change*,
 1157 15(4):394 – 404. doi:10.1016/j.gloenvcha.2005.08.004.
- 1158 Hotelling, H. (1936). Relations between two sets of variates. *Biometrika*, 28(3-4):321–377.
 1159 doi: 10.2307/2333955.
- 1160 Hua, W., Zhou, L., Chen, H., Nicholson, S. E., Raghavendra, A., and Jiang, Y. (2016). Possible
 1161 causes of the Central Equatorial African long-term drought. *Environmental Research Letters*,
 1162 11(12):124002. doi:10.1088/1748-9326/11/12/124002.
- 1163 Janicot, S. (1992). Spatiotemporal variability of West African rainfall. part i: Re-
 1164 gionalizations and typings. *Journal of Climate*, 5(5):489–497. doi:10.1175/1520-
 1165 0442(1992)005;0489:SVOWAR;2.0.CO;2.
- 1166 Janowiak, J. E. (1988). An investigation of interannual rainfall variability in Africa. *Journal*
 1167 *of Climate*, 1(3):240–255. doi:10.1175/1520-0442(1988)001;0240:AIOIRV;2.0.CO;2.
- 1168 Jenkins, G. S., Adamou, G., and Fongang, S. (2002). The challenges of model-
 1169 ing climate variability and change in West Africa. *Climatic Change*, 52(3):263–286.
 1170 doi:10.1023/A:1013741803144.
- 1171 Jolliffe, I. T. (2002). Principal component analysis (second edition). *Springer Series in Statis-*
 1172 *tics*. Springer, New York.

- 1173 Joly, M. and Voldoire, A. (2010). Role of the Gulf of Guinea in the inter-annual variability of the
 1174 West African monsoon: what do we learn from CMIP3 coupled simulations? *International*
 1175 *Journal of Climatology*, 30(12):1843–1856. doi:10.1002/joc.2026.
- 1176 Jung, M., Reichstein, M., Ciais, P., Seneviratne, S. I., Sheffield, J., Goulden, M. L., Bonan,
 1177 G., Cescatti, A., Chen, J., Jeu, R. d., Dolman, A. J., Eugster, W., Gerten, D., Gianelle,
 1178 D., Gobron, N., Heinke, J., Kimball, J., Law, B. E., Montagnani, L., Mu, Q., Mueller,
 1179 B., Oleson, K., Papale, D., Richardson, A. D., Rouspard, O., Running, S., Tomelleri, E.,
 1180 Viovy, N., Weber, U., Williams, C., Wood, E., Zaehle, S., and Zhang, K. (2010). Recent
 1181 decline in the global land evapotranspiration trend due to limited moisture supply. *Nature*,
 1182 467(7318):951–954.
- 1183 Kasei, R., Diekkrüger, B., and Leemhuis, C. (2010). Drought frequency in the Volta Basin of
 1184 West Africa. *Sustainability Science*, 5(1):89–97.
- 1185 Kendall, M. G. (1970). Rank correlation methods. *Griffin, London*, (4th edition). UK.
- 1186 Koster, R. D., Dirmeyer, P. A., Guo, Z., Bonan, G., Chan, E., Cox, P., Gordon, C. T., Kanae,
 1187 S., Kowalczyk, E., Lawrence, D., Liu, P., Lu, C.-H., Malyshev, S., McAvaney, B., Mitchell,
 1188 K., Mocko, D., Oki, T., Oleson, K., Pitman, A., Sud, Y. C., Taylor, C. M., Verseghy, D.,
 1189 Vasic, R., Xue, Y., and Yamada, T. (2004). Regions of strong coupling between soil moisture
 1190 and precipitation. *Science*, 305(5687):1138–1140. doi:10.1126/science.1100217.
- 1191 Landerer, F. W. and Swenson, S. C. (2012). Accuracy of scaled GRACE terrestrial water
 1192 storage estimates. *Water Resources Research*, 48(4):W04531. doi:10.1029/2011WR011453.
- 1193 Latif, M. and Barnett, T. (1996). Decadal climate variability over the North Pacific
 1194 and North America: Dynamics and predictability. *Journal of Climate*, 9(10):2407–2423.
 1195 doi:10.1175/1520-0442(1996)009<2407:DCVOTN>2.0.CO;2.
- 1196 Lebel, T. and Ali, A. (2009). Recent trends in the Central and Western Sahel rainfall regime
 1197 (1990-2007). *Journal of Hydrology*, 375(12):52 – 64. doi:10.1016/j.jhydrol.2008.11.030.
- 1198 Lebel, T., Delclaux, F., Le Barbé, L., and Polcher, J. (2000). From GCM scales to hydrological
 1199 scales: rainfall variability in West Africa. *Stochastic Environmental Research and Risk*
 1200 *Assessment*, 14(4):275–295. doi:10.1007/s004770000050.
- 1201 Lee, H., Beighley, R. E., Alsdorf, D., Jung, H. C., Shum, C., Duan, J., Guo, J., Yamazaki, D.,
 1202 and Andreadis, K. (2011). Characterization of terrestrial water dynamics in the Congo Basin

- 1203 using GRACE and satellite radar altimetry. *Remote Sensing of Environment*, 115(12):3530
 1204 – 3538. doi:10.1016/j.rse.2011.08.015.
- 1205 Lettenmaier, D. P. (2005). Observations of the global water cycle global monitoring networks.
 1206 *in Encyclopedia of Hydrological Sciences*, 5, edited by M G Anderson.:2719–2732. John
 1207 Wiley & Sons, Ltd.
- 1208 Li, J., Lewis, J., Rowland, J., Tappan, G., and Tieszen, L. (2004). Evaluation of land perfor-
 1209 mance in Senegal using multi-temporal NDVI and rainfall series. *Journal of Arid Environ-*
 1210 *ments*, 59(3):463 – 480. doi:10.1016/j.jaridenv.2004.03.019.
- 1211 Losada, T., Rodríguez-Fonseca, B., Janicot, S., Gervois, S., Chauvin, F., and Ruti, P. (2010).
 1212 A multi-model approach to the Atlantic Equatorial mode: impact on the West African
 1213 monsoon. *Climate Dynamics*, 35(1):29–43. doi:10.1007/s00382-009-0625-5.
- 1214 Machiwal, D. and Jha, M. K. (2012). Hydrological time series: theory and practice. *Springer*.
 1215 India.
- 1216 Mann, H. B. (1945). Nonparametric tests against trend. *Econometrica*, 13(3):245–259.
 1217 doi:10.2307/1907187.
- 1218 Mishra, V., Dominguez, F., and Lettenmaier, D. P. (2012). Urban precipitation extremes:
 1219 How reliable are regional climate models? *Geophysical Research Letters*, 39(3):L03407.
 1220 doi:10.1029/2011GL050658.
- 1221 Mohino, E., Janicot, S., and Bader, J. (2011a). Sahel rainfall and decadal to multi-decadal sea
 1222 surface temperature variability. *Climate Dynamics*, 37:419–440. doi:10.1007/s00382-010-
 1223 0867-2.
- 1224 Mohino, E., Rodriguez-Fonseca, B., Losada, T., Gervois, S., Janicot, S., Bader, J., Ruti, P., and
 1225 Chauvin, F. (2011b). Changes in the interannual SST-forced signals on West African rainfall.
 1226 AGCM intercomparison. *Climate Dynamics*, 37(9-10):1707–1725. doi:10.1007/s00382-011-
 1227 1093-2.
- 1228 Moore, P. and Williams, S. D. P. (2014). Integration of altimetry lake levels and GRACE
 1229 gravimetry over Africa: Inferences for terrestrial water storage change 2003-2011. *Water*
 1230 *Resources Research*, 50:9696–9720. doi:10.1002/2014WR015506.
- 1231 Ndehedehe, C., Awange, J., Agutu, N., Kuhn, M., and Heck, B. (2016a). Understanding
 1232 changes in terrestrial water storage over West Africa between 2002 and 2014. *Advances in*
 1233 *Water Resources*, 88:211–230. doi:10.1016/j.advwatres.2015.12.009.

- 1234 Ndehedehe, C. E., Agutu, N. O., Okwuashi, O. H., and Ferreira, V. G. (2016b).
1235 Spatio-temporal variability of droughts and terrestrial water storage over Lake Chad
1236 Basin using independent component analysis. *Journal of Hydrology*, 540:106– 128.
1237 doi:10.1016/j.jhydrol.2016.05.068.
- 1238 Ndehedehe, C. E., Awange, J., Kuhn, M., Agutu, N., and Fukuda, Y. (2017a). Analysis of hy-
1239 drological variability over the Volta river basin using in-situ data and satellite observations.
1240 *Journal of Hydrology: Regional studies*, 12:88–110. doi:10.1016/j.ejrh.2017.04.005.
- 1241 Ndehedehe, C. E., Awange, J., Kuhn, M., Agutu, N., and Fukuda, Y. (2017b). Climate
1242 teleconnections influence on West Africa’s terrestrial water storage. *Hydrological Processes*.
1243 doi: 10.1002/hyp.11237.
- 1244 Ndehedehe, C. E., Awange, J. L., Corner, R., Kuhn, M., and Okwuashi, O. (2016c). On the
1245 potentials of multiple climate variables in assessing the spatio-temporal characteristics of
1246 hydrological droughts over the Volta Basin. *Science of the Total Environment*, 557-558:819–
1247 837. doi:10.1016/j.scitotenv.2016.03.004.
- 1248 Ngom, F., Tweed, S., Bader, J.-C., Saos, J.-L., Malou, R., Leduc, C., and Leblanc, M. (2016).
1249 Rapid evolution of water resources in the Senegal delta. *Global and Planetary Change*,
1250 144:34 – 47. doi:10.1016/j.gloplacha.2016.07.002.
- 1251 Nicholson, S. (2005). On the question of the recovery of the rains in the West African Sahel.
1252 *Journal of Arid Environments*, 63(3):615–641. doi:10.1016/j.jaridenv.2005.03.004.
- 1253 Nicholson, S. (2013). The West African Sahel: a review of recent studies on the
1254 rainfall regime and its interannual variability. *ISRN Meteorology*, 2013(453521):1–32.
1255 doi:10.1155/2013/453521.
- 1256 Nicholson, S. and Selato, J. (2000). The influence of La Nina on African rain-
1257 fall. *International Journal of Climatology*, 20(14):1761–1776. doi:10.1002/1097-
1258 0088(20001130)20:14<1761::AID-JOC580>3.0.CO;2-W.
- 1259 Nicholson, S. E. (2008). The intensity, location and structure of the tropical rainbelt over
1260 West Africa as factors in interannual variability. *International Journal Of Climatology*,
1261 28:1775-1785. doi:10.1002/joc.1507.
- 1262 Nicholson, S. E. and Palao, I. M. (1993). A re-evaluation of rainfall variability in the Sahel. part
1263 i. characteristics of rainfall fluctuations. *International Journal of Climatology*, 13(4):371–
1264 389. doi:10.1002/joc.3370130403.

- 1265 Nicholson, S. E., Some, B., and Kone, B. (2000). An Analysis of Recent Rainfall
 1266 Conditions in West Africa, Including the Rainy Seasons of the 1997 El Niño and
 1267 the 1998 La Nia Years. *Journal of Climate*, 13(14):2628–2640. doi:10.1175/1520-
 1268 0442(2000)013;2628:AAORRC;2.0.CO;2.
- 1269 Nicholson, S. E. and Webster, P. J. (2007). A physical basis for the interannual variability of
 1270 rainfall in the Sahel. *Quarterly Journal Of The Royal Meteorological Society*, 133(629):2065–
 1271 2084. doi:10.1002/qj.104.
- 1272 Nka, B. N., Oudin, L., Karambiri, H., Paturel, J. E., and Ribstein, P. (2015). Trends in floods
 1273 in West Africa: analysis based on 11 catchments in the region. *Hydrology and Earth System
 1274 Sciences*, 19(11):4707–4719. doi:10.5194/hess-19-4707-2015.
- 1275 Odekunle, T. O. and Eludoyin, A. O. (2008). Sea surface temperature patterns in the Gulf
 1276 of Guinea: their implications for the spatio-temporal variability of precipitation in West
 1277 Africa. *International Journal Of Climatology*, 28:15071517. doi:10.1002/joc.1656.
- 1278 Oettli, P., Sultan, B., Baron, C., and Vrac, M. (2011). Are regional climate models relevant
 1279 for crop yield prediction in West Africa? *Environmental Research Letters*, 6(1):014008.
 1280 doi:10.1088/1748-9326/6/1/014008.
- 1281 Olsson, L., Eklundh, L., and Ard, J. (2005). A recent greening of the Saheltrends,
 1282 patterns and potential causes. *Journal of Arid Environments*, 63(3):556 – 566.
 1283 doi:0.1016/j.jaridenv.2005.03.008.
- 1284 Otto, F. E. L., Jones, R. G., Halladay, K., and Allen, M. R. (2013). Attribution of changes in
 1285 precipitation patterns in african rainforests. *Philosophical Transactions of the Royal Society
 1286 of London B: Biological Sciences*, 368(1625). doi:10.1098/rstb.2012.0299.
- 1287 Paeth, H., Fink, A., Pohle, S., Keis, F., Machel, H., and Samimi, C. (2012). Meteorological
 1288 characteristics and potential causes of the 2007 flood in sub-Saharan Africa. *International
 1289 Journal of Climatology*, 31:1908–1926. doi:10.1002/Joc.2199.
- 1290 Paolino, D. A., III, J. L. K., Kirtman, B. P., Min, D., and Straus, D. M. (2012). The impact
 1291 of land surface and atmospheric initialization on seasonal forecasts with ccsn. *Journal of
 1292 Climate*, 25(3):1007–1021. doi:10.1175/2011JCLI3934.1.
- 1293 Petropoulos, G. P., Ireland, G., and Barrett, B. (2015). Surface soil moisture retrievals from
 1294 remote sensing: Current status, products, and future trends. *Physics and Chemistry of the
 1295 Earth, Parts A/B/C*, 83–84:36 – 56. doi:10.1016/j.pce.2015.02.009.

- 1296 Phillips, T., Nerem, R. S., Fox-Kemper, B., Famiglietti, J. S., and Rajagopalan, B. (2012). The
 1297 influence of ENSO on global terrestrial water storage using GRACE. *Geophysical Research*
 1298 *Letters*, 39:L16705. doi:10.1029/2012GL052495, 2012.
- 1299 Preisendorfer, R. (1988). Principal component analysis in meteorology and oceanography.
 1300 *Developments in Atmospheric Science 17*. Elsevier, Amsterdam.
- 1301 Prudhomme, C., Giuntoli, I., Robinson, E. L., Clark, D. B., Arnell, N. W., Dankers, R.,
 1302 Fekete, B. M., Franssen, W., Gerten, D., Gosling, S. N., Hagemann, S., Hannah, D. M.,
 1303 Kim, H., Masaki, Y., Satoh, Y., Stacke, T., Wada, Y., and Wisser, D. (2014). Hydro-
 1304 logical droughts in the 21st century, hotspots and uncertainties from a global multimodel
 1305 ensemble experiment. *Proceedings of the National Academy of Sciences*, 111(9):3262–3267.
 1306 doi:10.1073/pnas.1222473110.
- 1307 Rangelova, E., van der Wal, W., Braun, A., Sideris, M. G., and Wu, P. (2007). Analysis of
 1308 Gravity Recovery and Climate Experiment time-variable mass redistribution signals over
 1309 North America by means of principal component analysis. *Journal of Geophysical Research:*
 1310 *Earth Surface*, 112(F3):2156–2202. doi:10.1029/2006JF000615.
- 1311 Redelsperger, J.-L. and Lebel, T. (2009). Surface processes and water cycle in West Africa,
 1312 studied from the AMMA-CATCH observing system. *Journal of Hydrology*, 375(1-2):1–2.
 1313 doi:10.1016/j.jhydrol.2009.08.017.
- 1314 Reichle, R. H., Koster, R. D., Lannoy, G. J. M. D., Forman, B. A., Liu, Q., Mahanama, S.
 1315 P. P., and Tour, A. (2011). Assessment and enhancement of MERRA land surface hydrology
 1316 estimates. *Journal of Climate*, 24(24):6322–6338. doi:10.1175/JCLI-D-10-05033.1.
- 1317 Repelli, C. A. and Nobre, P. (2004). Statistical prediction of sea-surface temperature over the
 1318 tropical Atlantic. *International Journal of Climatology*, 24(1):45–55. doi:10.1002/joc.982.
- 1319 Reynolds, R. W., Rayne, N. A., Smith, T. M., Stokes, D. C., and Wang, W. (2002). An
 1320 improved in situ and satellite SST analysis for climate. *Journal of Climate*, 15(3):1609–
 1321 1625. doi:10.1175/1520-0442(2002)0153C1609:AIISAS3E2.0.CO;2.
- 1322 Rienecker, M. M., Suarez, M. J., Gelaro, R., Todling, R., Bacmeister, J., Liu, E., Bosilovich,
 1323 M. G., Schubert, S. D., Takacs, L., Kim, G.-K., Bloom, S., Chen, J., Collins, D., Conaty, A.,
 1324 da Silva, A., Gu, W., Joiner, J., Koster, R. D., Lucchesi, R., Molod, A., Owens, T., Pawson,
 1325 S., Pegion, P., Redder, C. R., Reichle, R., Robertson, F. R., Ruddick, A. G., Sienkiewicz, M.,
 1326 and Woollen, J. (2011). MERRA: NASA’s modern-era retrospective analysis for research
 1327 and applications. *Journal of Climate*, 24(14):3624–3648. doi:10.1175/JCLI-D-11-00015.1.

- 1328 Robock, A., Vinnikov, K. Y., Srinivasan, G., Entin, J. K., Hollinger, S. E., Speran-
 1329 skaya, N. A., Liu, S., and Namkhai, A. (2000). The global soil moisture data bank.
 1330 *Bulletin of the American Meteorological Society*, 81(6):1281–1299. doi:10.1175/1520-
 1331 0477(2000)081;1281:TGSMDB;2.3.CO;2.
- 1332 Rodell, M., Houser, P. R., Jambor, U., Gottschalck, J., Mitchell, K., Meng, K., Arsenault,
 1333 C. J., Cosgrove, B., Radakovich, J., Bosilovich, M., Entin, J. K., Walker, J. P., Lohmann,
 1334 D., and Toll, D. (2004). The global land data assimilation system. *Bulletin of American*
 1335 *Meteorological Society*, 85(3):381–394. doi:10.1175/BAMS-85-3-381.R.
- 1336 Sanogo, S., Fink, A. H., Omotosho, J. A., Ba, A., Redl, R., and Ermert, V. (2015). Spatio-
 1337 temporal characteristics of the recent rainfall recovery in West Africa. *International Journal*
 1338 *of Climatology*, 35(15):4589–4605. doi:10.1002/joc.4309.
- 1339 Schewe, J., Heinke, J., Gerten, D., Haddeland, I., Arnell, N. W., Clark, D. B., Dankers, R.,
 1340 Eisner, S., Fekete, B. M., Colón-Gonzlez, F. J., Gosling, S. N., Kim, H., Liu, X., Masaki, Y.,
 1341 Portmann, F. T., Satoh, Y., Stacke, T., Tang, Q., Wada, Y., Wisser, D., Albrecht, T., Frieler,
 1342 K., Piontek, F., Warszawski, L., and Kabat, P. (2013). Multimodel assessment of water
 1343 scarcity under climate change. *PNAS*, 111(9):3245–3250,. doi:10.1073/pnas.1222460110.
- 1344 Schneider, U., Becker, A., Finger, P., Meyer-Christoffer, A., Ziese, M., and Rudolf, B. (2014).
 1345 GPCP’s new land surface precipitation climatology based on quality-controlled in situ data
 1346 and its role in quantifying the global water cycle. *Theoretical and Applied Climatology*,
 1347 115(1-2):15–40. doi:10.1007/s00704-013-0860-x.
- 1348 Schuol, J. and Abbaspour, K. C. (2006). Calibration and uncertainty issues of a hydrological
 1349 model (SWAT) applied to West Africa. *Advances in Geosciences*, 9:137–143. doi:adv-
 1350 geosci.net/9/137/2006/.
- 1351 Séguis, L., Cappelaere, B., Milsì, G., Peugeot, C., Massuel, S., and Favreau, G. (2004). Simu-
 1352 lated impacts of climate change and land-clearing on runoff from a small Sahelian catchment.
 1353 *Hydrological Processes*, 18(17):3401–3413. doi:10.1002/hyp.1503.
- 1354 Semazzi, F. H. M., Mehta, V., and Sud, Y. (1988). An investigation of the relationship between
 1355 subSaharan rainfall and global sea surface temperatures. *Atmosphere-Ocean*, 26(1):118–138.
 1356 doi:10.1080/07055900.1988.9649293.
- 1357 Sen, P. K. (1968). Estimates of the regression coefficient based on Kendall’s Tau. *Journal of the*
 1358 *American Statistical Association*, 63(324):1379–1389. doi:10.1080/01621459.1968.10480934.

- 1359 Shabbar, A. and Barnston, A. G. (1996). Skill of seasonal climate forecasts in Canada
1360 using canonical correlation analysis. *Monthly Weather Review*, 124(10):2370–2385.
1361 doi:10.1175/1520-0493(1996)124;2370:SOSCFI;2.0.CO;2.
- 1362 Shahin, M. (2008). Hydrology and water resources of Africa. *Water Science and Technology*
1363 *Library*, (41). Kluwer Academic Publishers, Dordrecht, The Netherlands.
- 1364 Sheffield, J. and Wood, E. F. (2008). Global trends and variability in soil moisture and drought
1365 characteristics, 1950–2000, from observation-driven simulations of the terrestrial hydrologic
1366 cycle. *Journal of Climate*, 21(3):432–458. doi:10.1175/2007JCLI1822.1.
- 1367 Shiferaw, B., Tesfaye, K., Kassie, M., Abate, T., Prasanna, B., and Menkir, A. (2014).
1368 Managing vulnerability to drought and enhancing livelihood resilience in sub-Saharan
1369 Africa: technological, institutional and policy options. *Weather and Climate Extremes*,
1370 3(0):67 – 79. doi:10.1016/j.wace.2014.04.004.
- 1371 Singh, A., Kulkarni, M. A., Mohanty, U. C., Kar, S. C., Robertson, A. W., and Mishra, G.
1372 (2012a). Prediction of Indian summer monsoon rainfall (ISMR) using canonical correlation
1373 analysis of global circulation model products. *Meteorological Applications*, 19(2):179–188.
1374 doi:10.1002/met.1333.
- 1375 Singh, A., Seitz, F., and Schwatke, C. (2012b). Inter-annual water storage changes in the Aral
1376 Sea from multi-mission satellite altimetry, optical remote sensing, and GRACE satellite
1377 gravimetry. *Remote Sensing of Environment*, 123:187 – 195.
- 1378 Tall, M., Sylla, M. B., Diallo, I., Pal, J. S., Faye, A., Mbaye, M. L., and Gaye, A. T. (2016).
1379 Projected impact of climate change in the hydroclimatology of Senegal with a focus over
1380 the Lake of Guiers for the twenty-first century. *Theoretical and Applied Climatology*, pages
1381 1–11. doi:10.1007/s00704-016-1805-y.
- 1382 Tapley, B., Bettadpur, S., Watkins, M., and Reigber, C. (2004). The Gravity Recovery and
1383 Climate Experiment: Mission overview and early results. *Geophysical Research Letters*,
1384 31:1–4. doi:10.1029/2004GL019920.
- 1385 Thiemig, V., Rojas, R., Zambrano-Bigiarini, M., and Roo, A. D. (2013). Hydrological evalu-
1386 ation of satellite-based rainfall estimates over the Volta and Baro-Akobo Basin. *Journal of*
1387 *Hydrology*, 499:324 – 338. doi:10.1016/j.jhydrol.2013.07.012.
- 1388 Todd, M. C. and Washington, R. (2004). Climate variability in central equatorial

- 1389 Africa: Influence from the Atlantic sector. *Geophysical Research Letters*, 31(23):L23202.
1390 doi:10.1029/2004GL020975.
- 1391 Trenberth, K. E. (1997). The definition of El Niño. *Bulletin of the American Meteorological*
1392 *Society*, 78(12):2771–2777.
- 1393 Unnikrishnan, P. and Jothiprakash, V. (2015). Extraction of nonlinear rainfall trends
1394 using singular spectrum analysis. *Journal of Hydrologic Engineering*, 20(12):1–14.
1395 doi:10.1061/(ASCE)HE.1943-5584.0001237.
- 1396 Wahr, J., Molenaar, M., and Bryan, F. (1998). Time variability of the Earth's gravity field:
1397 Hydrological and oceanic effects and their possible detection using GRACE. *Journal of*
1398 *Geophysical Research-Solid Earth*, 103(B12):30205–30229. doi:10.1029/98jb02844.
- 1399 Washington, R., James, R., Pearce, H., Pokam, W. M., and Moufouma-Okia, W. (2013). Congo
1400 Basin rainfall climatology: can we believe the climate models? *Philosophical Transactions of*
1401 *the Royal Society of London B: Biological Sciences*, 368(1625). doi:10.1098/rstb.2012.0296.
- 1402 Wilks, D. (2011). Statistical methods in the atmospheric sciences. *Academic press*, (3rd
1403 Edition). USA.
- 1404 Wu, M.-L. C., Reale, O., and Schubert, S. D. (2013). A characterization of Africaneasterly
1405 waves on 2.5 – 6-day and 6 – 9-day time scales. *Journal of Climate*, 26(18):6750–6774.
1406 doi:10.1175/JCLI-D-12-00336.1.
- 1407 Yu, Z.-P., Chu, P.-S., and Schroeder, T. (1997). Predictive skills of seasonal to annual rainfall
1408 variations in the U.S. affiliated pacific islands: Canonical correlation analysis and multi-
1409 variate principal component regression approaches. *Journal of Climate*, 10(10):2586–2599.
1410 doi:10.1175/1520-0442(1997)010<2586:PSOSTA>2.0.CO;2.
- 1411 Zhang, Q., Xu, C.-Y., Becker, S., Zhang, Z. X., Chen, Y. D., and Coulibaly, M. (2009). Trends
1412 and abrupt changes of precipitation maxima in the pearl river basin, china. *Atmospheric*
1413 *Science Letters*, 10(2):132–144. doi:10.1002/asl.221.
- 1414 Zhou, L., Tian, Y., Myneni, R. B., Ciais, P., Saatchi, S., Liu, Y. Y., Piao, S., Chen, H.,
1415 Vermote, E. F., Song, C., and Hwang, T. (2014). Widespread decline of congo rainforest
1416 greenness in the past decade. *Nature*, 509(7498):86–90. doi:10.1038/nature13265.

5 A new method for spatio-temporal drought analysis

This chapter is covered by the following publications ([Ndehedehe et al., 2016b,c](#)):

1. **Christopher E. Ndehedehe**, Nathan Agutu, Onuwa Okwuashi, Vagner G. Ferreira (2016). Spatio-temporal variability of droughts and terrestrial water storage over Lake Chad Basin using independent component analysis. *Journal of Hydrology*, 540, 106 – 128, [dx.doi.org/10.1016/j.jhydrol.2016.05.068](https://doi.org/10.1016/j.jhydrol.2016.05.068).
2. **Christopher E. Ndehedehe**, Joseph L. Awange, Robert J. Corner, Michael Kuhn and Onuwa Okwuashi (2016). On the potentials of multiple climate variables in assessing the spatio-temporal characteristics of hydrological droughts over the Volta Basin. *Science of the Total Environment*, 557 – 558, 819 – 837, [dx.doi.org/10.1016/j.scitotenv.2016.03.004](https://doi.org/10.1016/j.scitotenv.2016.03.004).

This chapter is one of the significant and novel contributions of the thesis. Here, the suitability of a new method based on cumulant statistics, was explored to analyse different drought characteristics and metrics. The proposed method is a more objective approach to regionalization of extreme hydro-climatic conditions (above-normal conditions or deficits in precipitation and soil moisture). The method was applied to analyse the spatio-temporal characteristics of different droughts in Lake Chad basin, a semi-arid Sahelian environment where extreme weather events are not only endemic and unreported, but resulted in significant contractions of the Lake Chad's surface area. This basin consist of several riparian countries, which lie in different geographic zones within West Africa, and was chosen primarily as a tentative test bed to demonstrate the potential of the technique. Further, in another comprehensive study that employs a somewhat similar methodology to analyse multiple climate variables, the hydrological drought characteristics of the Volta basin were also studied. Unmitigated changes in climate will have significant effects on hydrological conditions of sub-humid regions such as the Volta basin where the availability of freshwater for agriculture, hydro-power, and other multiple strings of ecosystem services can be restricted due to extreme rainfall variability. In this basin, little is known about its response to extreme climatic conditions, and the strong spatial variability in rainfall, which has shown considerable impacts on the national income of some of its riparian countries. Consequently, the hydrological drought assessment of the Volta basin was also undertaken to examine the sensitivity of Lakes and reservoirs to natural climate variations. As reported in the publications above, cumulant-based approach to the analysis of extreme hydro-climatic

conditions has shown great skills in studying space-time developments of droughts compared to previous approaches (e.g., principal component analysis) of regionalizations and can be applied in other regions of the world. The use of a regionalization method as reported in this chapter enables the localization of drought signals in terms of its spatial variability and temporal evolutions at basin and region scales. As drought is also spatially distinct, climate oscillations and other quasi-periodic phenomena (e.g., ENSO) associated with the temporal series of extreme weather events in specific regions (or countries) can be identified. This arguably reduces the polarizations surrounding the debates on extreme rainfall conditions and the roles of climate modes that induces its variability. This new approach in spatio-temporal drought analysis, and the use of multiple climate variables in drought assessment of the region, are more comprehensive and robust, and contributes to a large framework for drought (meteorological, agricultural, and hydrological) assessment that will complement existing methods.



Contents lists available at ScienceDirect

Journal of Hydrology

journal homepage: www.elsevier.com/locate/jhydrol

Spatio-temporal variability of droughts and terrestrial water storage over Lake Chad Basin using independent component analysis



Christopher E. Ndehedehe^{a,*}, Nathan O. Agutu^{a,b}, Onuwa Okwuashi^c, Vagner G. Ferreira^d

^a Western Australian Centre for Geodesy and The Institute for Geoscience Research, Curtin University, Perth, Australia

^b Department of Geomatic Engineering and Geospatial Information Systems, JKUAT, Nairobi, Kenya

^c Department of Geoinformatics and Surveying, University of Uyo, P.M.B. 1017, Uyo, Nigeria

^d School of Earth Sciences and Engineering, Hohai University, Nanjing, China

ARTICLE INFO

Article history:

Received 17 February 2016

Received in revised form 25 May 2016

Accepted 28 May 2016

Available online 4 June 2016

This manuscript was handled by Andras Bardossy, Editor-in-Chief, with the assistance of Alon Rimmer, Associate Editor

Keywords:

TWS
Soil moisture
ICA
SPI
Drought
Rainfall

SUMMARY

Lake Chad has recently been perceived to be completely desiccated and almost extinct due to insufficient published ground observations. Given the high spatial variability of rainfall in the region, and the fact that extreme climatic conditions (for example, droughts) could be intensifying in the Lake Chad basin (LCB) due to human activities, a spatio-temporal approach to drought analysis becomes essential. This study employed independent component analysis (ICA), a fourth-order cumulant statistics, to decompose standardised precipitation index (SPI), standardised soil moisture index (SSI), and terrestrial water storage (TWS) derived from Gravity Recovery and Climate Experiment (GRACE) into spatial and temporal patterns over the LCB. In addition, this study uses satellite altimetry data to estimate variations in the Lake Chad water levels, and further employs relevant climate teleconnection indices (El-Niño Southern Oscillation-ENSO, Atlantic Multi-decadal Oscillation-AMO, and Atlantic Meridional Mode-AMM) to examine their links to the observed drought temporal patterns over the basin. From the spatio-temporal drought analysis, temporal evolutions of SPI at 12 month aggregation show relatively wet conditions in the last two decades (although with marked alterations) with the 2012–2014 period being the wettest. In addition to the improved rainfall conditions during this period, there was a statistically significant increase of 0.04 m/yr in altimetry water levels observed over Lake Chad between 2008 and 2014, which confirms a shift in the hydrological conditions of the basin. Observed trend in TWS changes during the 2002–2014 period shows a statistically insignificant increase of 3.0 mm/yr at the centre of the basin, coinciding with soil moisture deficit indicated by the temporal evolutions of SSI at all monthly accumulations during the 2002–2003 and 2009–2012 periods. Further, SPI at 3 and 6 month scales indicated fluctuating drought conditions at the extreme south of the basin, coinciding with a statistically insignificant decline in TWS of about 4.5 mm/yr at the southern catchment of the basin. Finally, correlation analyses indicate that ENSO, AMO, and AMM are associated with extreme rainfall conditions in the basin, with AMO showing the strongest association (statistically significant correlation of 0.55) with SPI 12 month aggregation. Therefore, this study provides a framework that will support drought monitoring in the LCB.

© 2016 Elsevier B.V. All rights reserved.

1. Introduction

Lake Chad Basin (LCB), the world's largest interior drainage basin, covers an approximate area of 2,500,000 km² and supports an estimated 37 million people who depend on its water resources for agriculture, fishing, and other domestic applications (e.g., Coe and Birkett, 2004; Leblanc et al., 2003). The basin is geographically bounded by latitudes 6°N and 24°N and longitudes 7°W and 24°E (Fig. 1) and is occupied by Lake Chad at the centre, a prominent

freshwater body, which largely forms the live wire of the basin's hydrology. The historic and dramatic decline in the spatial extent of the Lake from 24,000 km² in the 1950s to segmented open water pool of approximately 1700 km² (i.e., about 90% decline) in recent times, has been reported (see, e.g., Wald, 1990; Birkett, 2000; Coe and Foley, 2001; Leblanc et al., 2003; Lemoalle et al., 2012). Lake Chad receives its water supply primarily from the Chari–Logone river, which provides approximately 95% of the total inflows into the southern pool, and also the Komadugu–Yobe River (see Fig. 2), which provides less than 2.5% of water that flows into the northern pool of the Lake (Birkett, 2000; Coe and Birkett, 2004). In relation to other Lakes in Africa, recent illustration of Lake Chad

* Corresponding author.

E-mail address: christopherndehedehe@gmail.com (C.E. Ndehedehe).

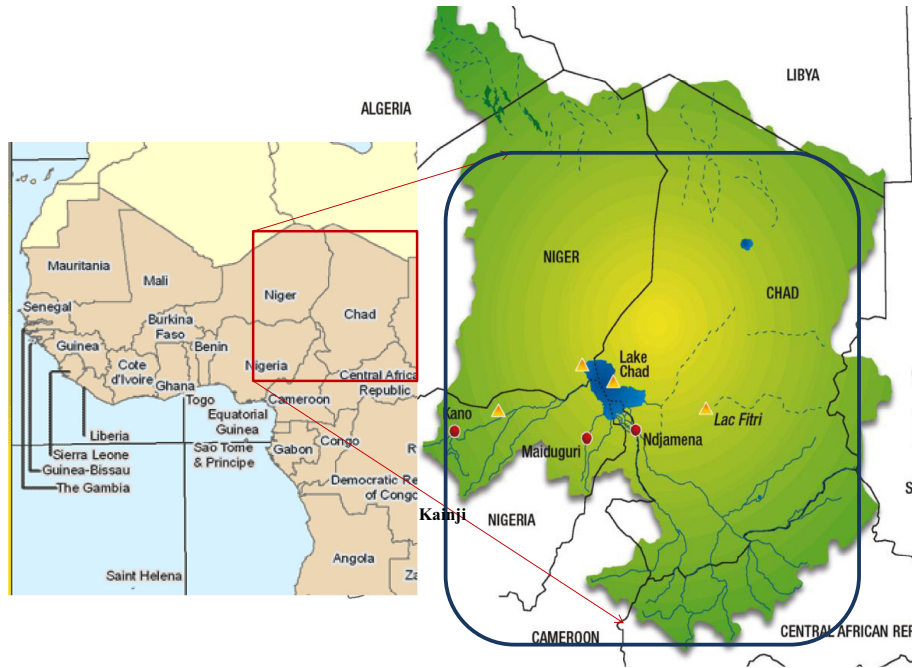


Fig. 1. Study area showing Lake Chad, the riparian countries that constitute the Lake Chad Basin, and important river networks (blue line) within the basin. Our analysis focuses on the conventional basin area (a subset of the blue polygon), which includes mostly southern and north eastern sections of Niger, Chad, north-eastern Nigeria, northern Cameroon, and most parts of Central African Republic. Maps are adapted from www.worldmap.org and <http://assets.panda.org/img/original/chadmap.gif>. The LCB lies at the south western crossroads of the Sahel and forest savanna, a transition zone between the Sahara Desert and the tropical savanna of West Africa (Okonkwo et al., 2013). (For interpretation of the references to colour in this figure legend, the reader is referred to the web version of this article.)

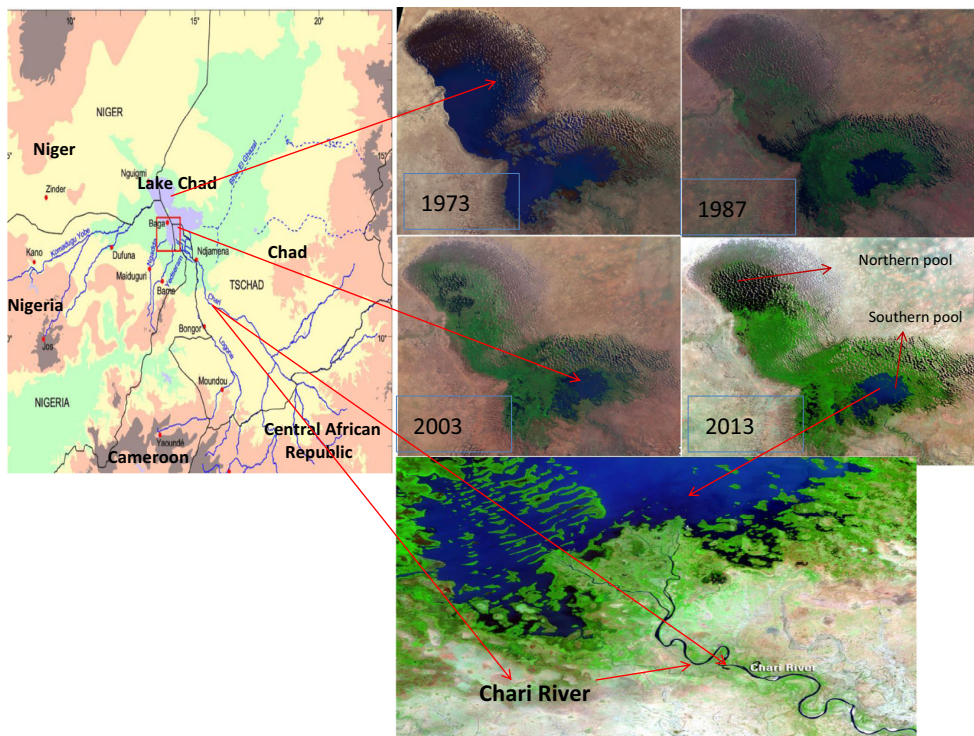


Fig. 2. The spatial and temporal changes in Lake Chad surface area as shown by Landsat imageries for 1973, 1987, 2003, and 2013. The Chari river, which provides about 95% of the inflow to the Lake is indicated. The blue lines on the map (left) show the river networks within the basin most of which constitute the Chari river system. The present Lake Chad show two segmented pools with the northern pool completely dried up during drought periods (right). Maps and imageries are adapted from (i) www-stud.informatik.uni-frankfurt.de/sfb268/d6/pics/misc/franke2000gr-abb1-gross.gif and (ii) United States geological surveys (<http://earthshots.usgs.gov/earthshots/Lake-Chad-West-Africa>). (For interpretation of the references to colour in this figure legend, the reader is referred to the web version of this article.)

presupposes a completely desiccated and almost extinct Lake (e.g., Moore and Williams, 2014; Coe and Foley, 2001; Birkett, 2000). This perception may be partly associated with lack of documented analyses of satellite-based observations (Lemoalle et al., 2012). Consequently, the drought narrative of the Lake and the entire LCB has been a subject of much less scientific discussion.

A number of studies on Lake Chad's hydrology and the corresponding basin have been carried out. For example, Coe and Birkett (2004) used satellite radar altimetric measurements of water height to estimate river discharge at the Chari/Ouham confluence while Lemoalle et al. (2012) used a hydrological model to reconstruct the past water levels of the Lake and inundated areas from 1973 to 2011 in order to compensate for the lack of hydrological data. Birkett (2000) and Coe and Foley (2001) had earlier reported the combined effects of regional precipitation patterns and the impact of human activities on the desiccation of the Lake while Okonkwo et al. (2014) examined the relationship of El-Niño Southern Oscillation (ENSO) with rainfall, river discharge at Chari river, and Lake Chad water level at Kalomand Kindjeria. Leblanc et al. (2003) used Advanced Very High Resolution Radiometer (AVHRR) and Meteosat data in a Geographic Information System (GIS) framework to map the fluctuations of the spatial extent of Lake Chad. But recently, Lopez et al. (2016) studied the quaternary phreatic aquifer of the basin, indicating that there is an association between piezometric levels and sedimentary thickness.

However, from the studies highlighted so far, we find a relatively strong research lacuna in the knowledge of water availability, drought patterns, and spatio-temporal variability of water storage over the LCB. Apart from the effort of Okonkwo et al. (2013), which provided a location-specific information regarding the probability distribution of rainfall and drought in the LCB during the 2002–2011 period, drought studies in the LCB are generally lacking and largely undocumented. Also, with increased human activities (e.g., irrigation schemes) in LCB (e.g., Lemoalle et al., 2012; Coe and Foley, 2001), especially within the precinct of the Lake, one may assume that the water resources of the basin could be more vulnerable, given the significant global drying trends observed in water availability and hydrological regimes in the Sahel region of West Africa (Greve et al., 2014). Furthermore, in the wake of global climate change and perturbations of ocean warming, it is likely that the limited alimentation occasioned by lack of or deficit in precipitation and human activities in the basin might get worse in the future. This may have significant impact on the local economy and the freshwater tributaries (that is, Chari and Logone rivers) that nourishes Lake Chad.

Furthermore, despite the recognised recovery of rainfall in some parts of the Sahel region (see, Nicholson, 2013, and the references therein), the impact of this recovery on the hydrology of Lake Chad and TWS changes over the entire basin are still rather unclear, largely unknown, and undocumented. For instance, in addition to the inconsistent trends between increased rainfall and lake level, Okonkwo et al. (2014) showed that the variability in ENSO could explain only 31% and 13% of variations in Lake Chad water level at Kindjeria and precipitation in the northern LCB, respectively. Notably, the LCB has been ravaged by frequent droughts leading to limited freshwater availability. The reduced alimentation of the basin in terms of freshwater shortage can be seen in the yearly water balance as reported by Odada et al. (2005). They reported that there was an inflow and outflow of 24.68 km³/yr and 24.5 km³/yr, respectively, with evapotranspiration being a major component of the outflow (approximately 23.1 km³/yr) in the basin between 1971 and 1990. Added to this is the drought narrative for the region, which may be highly generalised (that is, in terms of its spatial variability, characteristics, etc.) due to lack of an optimised framework to determine its space–time occurrence.

Considering the high spatial variability of rainfall in the region, and the fact that extreme climatic conditions could be intensifying in the basin possibly due to anthropogenic factors (for example, water abstractions for irrigation), a spatio-temporal approach to drought analysis becomes vital.

Numerous studies, mostly in the mainstream of satellite hydrology, have shown how multi-satellite data from altimetry, gravimetry, and optical remote sensing platforms can be used to estimate terrestrial water storage (TWS)¹ variations in drainage basins and poorly gauged regions, in addition to estimating water volume variations from surface waters such as lakes and reservoirs (see, e.g., Tourian et al., 2015; Baup et al., 2014; Duan and Bastiaansen, 2013a). In particular, the launch of Gravity Recovery and Climate Experiment (GRACE) satellite mission (Tapley et al., 2004) has enabled hydrologists to validate water storage outputs from hydrological models and also to fully utilise GRACE observations for the inter-annual variations of TWS and water balance studies (see, Wouters et al., 2014, and the references therein). While few hydrological studies that utilised GRACE data in West Africa (see, e.g., Ndehedehe et al., 2016a; Grippa et al., 2011; Hinderer et al., 2009) have been reported, some drought studies and extreme rainfall conditions have also been documented in other sub-regions of West Africa (see, e.g., Ali and Lebel, 2009; Ndehedehe et al., 2016b; Masih et al., 2014; Bader and Latif, 2011; Nicholson et al., 2000; Nicholson, 2013, and the references therein). Despite the progress made so far in the use of GRACE data in hydrological studies, for instance, applications in drought and flood estimation (e.g., Reager et al., 2014; Yirdaw et al., 2008), the potential of GRACE data in monitoring the space–time development of TWS changes and droughts in the LCB are yet to be fully explored.

In this study, we capitalise on GRACE observations to estimate the TWS over the LCB, in addition to satellite altimetry-derived water levels and other hydrological variables such as rainfall, and soil moisture to monitor water storage changes and the spatio-temporal characteristics of droughts. Contrary to previous studies that have analysed spatio-temporal drought events in other regions of the world (see, e.g., Bazrafshan et al., 2014; Santos et al., 2010; Bonaccorso et al., 2003) using principal component analysis (e.g., Jolliffe, 2002), we employ independent component analysis (ICA, see, e.g., Cardoso, 1999; Common, 1994; Cardoso and Souloumiac, 1993), a higher order statistical method to localise drought patterns and time-variable hydrological signals (i.e., TWS). Unlike in the Volta basin where the influence of low frequency climate oscillations on hydrological drought was reported by Ndehedehe et al. (2016b), here, the Lake Chad Basin (a semi-arid Sahelian environment) is adopted as a tentative test bed, primarily to demonstrate the use of a fourth-order cumulant statistics such as the ICA to analyse spatio-temporal evolutions of drought indices at different time scales (3, 6, and 12 months aggregation), and to examine the relationship of other climate modes (i.e., ENSO, AMO, and AMM), which were not considered with drought temporal evolutions in the Volta basin. Such analysis is essential not only in understanding drought variability, but also the causes of rainfall variability, which though unclear has been somewhat associated with sea surface temperature anomalies of the nearby Oceans (e.g., Bader and Latif, 2011). For the drought analysis, we used the recently introduced standardised non-parametric univariate and multivariate drought indices (see, Hao and AghaKouchak, 2013; Hao and AghaKouchak, 2014; Farahmand and AghaKouchak, 2015) for the characterisation of different droughts (e.g., meteorological, agricultural, and hydrological) over the LCB. The ICA technique was employed to statistically decompose SPI

¹ The sum total of surface waters (i.e., rivers, lakes, and wetlands), soil moisture, canopy, and groundwater.

and standardised soil moisture index (SSI) values into spatial and temporal patterns while the multivariate standardised index (MSDI), was used to evaluate the effectiveness of two climate variables (rainfall and soil moisture) in capturing drought properties such as frequency, persistence, and termination. This study specifically aims at (i) localising and characterising spatio-temporal evolutions of drought patterns over the LCB and (ii) identifying spatial variability of TWS changes and the estimation of trends in lake height variations over the LCB.

While we provide background information on the spatio-temporal variability of drought patterns in Section 2, further details on the method and the results of the study are presented in Sections 3 and 4, respectively.

2. Spatio-temporal variability of drought

The lack of in-situ measurements to assist in hydrological monitoring limits the prospects of a robust, large scale monitoring of major hydrological variables (i.e., rainfall, water levels, groundwater, and river discharge) in the LCB. Standard routine measurements of these hydrological quantities are lacking due to limited gauge stations and deterioration of existing hydrological facilities. Although local measurements from dedicated regional networks such as the African Monsoon Multidisciplinary Analysis-Couplage de l'Atmosphère Tropicale et du Cycle Hydrologique (AMMA-CATCH, Lebel et al., 2009) hydro-meteorological observing system have been used in some studies (e.g., Gosset et al., 2013), the AMMA-CATCH networks are highly insufficient for a regional study as they are only available in few countries (i.e., Niger, Mali, and Benin). Further, while most available data cannot be accessed by the public and relevant research institutions as a result of government policies and bureaucracies, political instability in the sub-regions complicates efforts to acquire such data. In addition, incomplete data records and gaps in available data tend to affect proper assessment and monitoring of hydrological conditions in the region.

However, with the plethora of available climate data either in the form of satellite observations or model-generated products, monitoring hydro-climatic conditions is somewhat not difficult. The critical issues have often revolved around the understanding and localisation of these multiple and growing climate signals. For instance, the use of mean standardised precipitation index (SPI, McKee et al., 1993) time series in estimating drought conditions over the Sahel has not been very effective. This is because of the influence of strong spatial variability of rainfall at annual scale and the mean inter-annual climatological gradients across the region (Ali and Lebel, 2009). Schewe et al. (2013) described the signal problem more succinctly, indicating that at regional scales, the projections of climate models for instance, in terms of precipitation patterns and magnitudes, are inconsistent when compared to global average changes. This unavoidably leads to uncertainties in the attempt to understand the effect of climate change on water resources at regional scales. In West Africa, Ali and Lebel (2009) reported that despite the significantly dry season of 2006, working with a rainfall product with spatial resolution of $0.5^\circ \times 0.5^\circ$ resulted in only 28% of the area being significantly dried while 15% of the Sahel region was significantly wet. They also observed that SPI on a $1^\circ \times 1^\circ$ grid in the Sahel was not representative of the whole region. Irrespective of the spatial resolution of the data and differences in climatic zones, drought analysis from a spatio-temporal point of view can improve our understanding of drought occurrence. One approach to spatio-temporal drought analysis would be the use of a component extraction technique, in particular, principal component analysis (PCA, Jolliffe, 2002). For example, Bazrafshan et al. (2014) in a recent study reported

on the multivariate approach, which uses the PCA of the SPI time series in capturing the temporal variability of drought patterns at different time scales (i.e., 3, 6, and 12 month scale) while Bonaccorso et al. (2003) studied long-term drought variability in Sicily during 1926–1996 period using the PCA technique. Further, using PCA and K-means clustering, Santos et al. (2010) was able to show that the south of Portugal had more frequent cycles of dry events (every 3.6 years) than the northern part where severe to extreme droughts occurred approximately every 13.4 years. Following the strong spatial variability of rainfall in the Sahel region where LCB is located, our approach uses a regionalisation process where the decomposed SPI time series from PCA are rotated towards statistical independence, a process referred to as independent component analysis (e.g., Aires et al., 2002; Cardoso, 1999; Cardoso and Souloumiac, 1993). Our approach differs from the aforementioned studies in that the derived SPI time series, which are based on a non-parametric approach derived from the empirical probability method (see Farahmand and AghaKouchak, 2015; Hao and AghaKouchak, 2014) are decomposed through a classical rotation of the PCA modes. This is done in a way to enable the localisation and extraction of physically meaningful drought signals that are statistically significant. The use of a regionalization method such as the ICA enables the localisation of SPI and standardised soil moisture index (SSI) signals in terms of its spatial variability and temporal evolutions in the basin. This approach is useful in understanding the space–time evolution of extreme rainfall and soil moisture conditions in the basin. For an endorheic basin such as the LCB, which lacks a suitable framework to monitor space–time occurrence of drought, this approach to drought monitoring, when integrated with the analysis of changes in TWS and altimetry derived water levels of Lake Chad, largely supports the assessment of available water resources. We provide more details on the ICA technique in Section 3.

Moreover, in this study, we hypothesised that following the dramatic decline and desiccation of Lake Chad surface area due to strong precipitation deficit of the 1980s (see cumulative rainfall anomalies, Fig. 3), meteorological drought propagates into both agricultural and hydrological droughts with strong impact on the catchment stores (i.e., lakes, rivers, soil water, and aquifers). Several drought studies have associated hydrological drought with precipitation deficit on a longer time scale such as 6, 12, and 24 months (see, e.g., Li and Rodell, 2015; Santos et al., 2010; Vicente-Serrano, 2006; Rouault and Richard, 2003; Hayes et al., 1999; Komuscu, 1999). In sum, we used precipitation and soil moisture data, covering a 35-year period to quantify drought frequency (how often a drought event occurs) and severity (the intensity or strength of a drought event) for all drought categories (meteorological, agricultural, and hydrological).

3. Data and method

3.1. Data

3.1.1. GRACE-derived Terrestrial Water Storage (TWS) changes

Gravity Recovery and Climate Experiment (GRACE, Tapley et al., 2004) Release-05 (RL05) spherical harmonic coefficients from Center for Space Research (CSR) for the period of April 2002 to October 2014 were used in this study to compute changes in TWS. The CSR RL05 gravity field solutions, which are truncated at degree and order 60 were retrieved from the open access files available at <http://icgem.gfz-potsdam.de/ICGEM/shms/monthly/csr-rl05/>. These spherical harmonic coefficients suffer from signal attenuation and satellite measurement errors leading to noise in the higher degree coefficients (Landerer and Swenson, 2012; Swenson and Wahr, 2002). As a first step in the processing, the degree 2

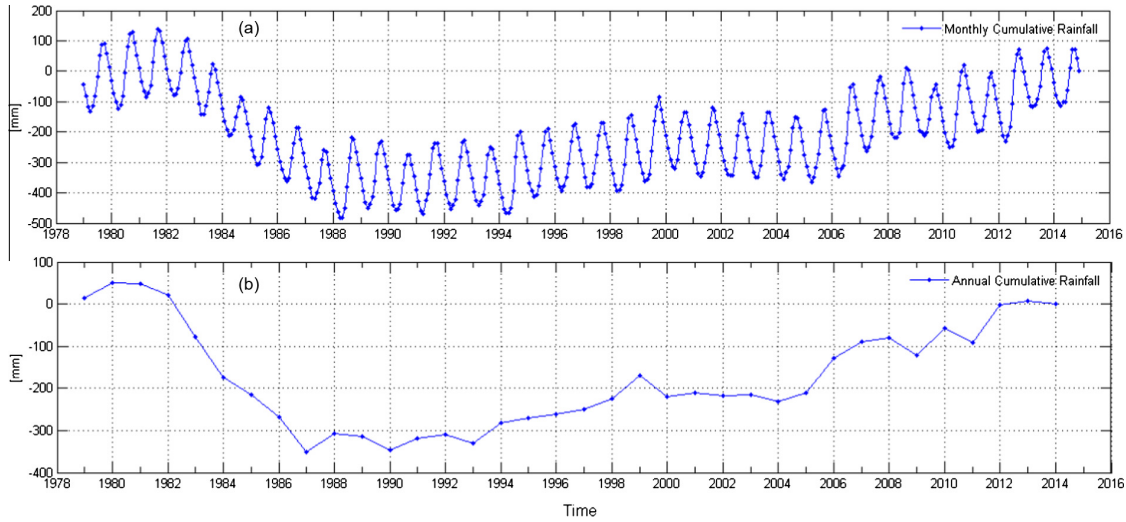


Fig. 3. Cumulative rainfall anomalies averaged over LCB using the GPCP based precipitation. (a) Monthly cumulative rainfall anomaly over the basin during 1979–2014 period. (b) Annual cumulative rainfall anomaly over the basin during 1979–2014 period.

coefficients were replaced with estimates from satellite laser ranging (Cheng et al., 2013) while the degree 1 coefficients provided by Swenson et al. (2008) were used. This was necessary since GRACE does not provide changes in degree 1 coefficients (i.e., C_{10} , C_{11} , and S_{11}), and is also affected by large tide-like aliases in the degree 2 coefficients (i.e., C_{20}). Secondly, after removing the long term mean, DDK2 de-correlation filter (Kusche, 2007) was applied on the GRACE monthly solutions in order to reduce the effect of correlated noise. Practically, non-isotropic filters such as the DDK2 (Kusche, 2007) accommodate better the GRACE error structure when compared to the conventional isotropic Gaussian filter (see, e.g., Werth et al., 2009). We point out briefly that there are no standard filtering procedures as most GRACE users would largely prefer the most convenient and easy-to-implement approaches. However, the filtering process can be significantly improved by using decorrelation filters, which unlike the Gaussian filter, fits better the noise in the data (e.g., Belda et al., 2015). The filtered monthly solutions were then converted to equivalent water heights on a $1^\circ \times 1^\circ$ grid using the approach of Wahr et al. (1998):

$$\Delta W(\phi, \lambda, \xi) = \frac{R\rho_{ave}}{3Q_w} \sum_{l=0}^{l_{max}} \frac{2l+1}{1+k_l} \sum_{m=-l}^l P_{lm}(\phi, \lambda) \Delta Y_{lm}(\xi) \quad (1)$$

where ΔW is equivalent water height (hereafter TWS) for each month in time (ξ), and where ϕ and λ are the latitudes and longitudes, respectively. R is the mean radius of the Earth (i.e., 6378.137 km), ρ_{ave} is the average density of the Earth (5515 kg/m³), Q_w is the average density of water (1000 kg/m³), k_l is the load Love numbers of degree l , P_{lm} are the normalised spherical harmonic functions of degree l and order m with $l_{max} = 60$ and ΔY_{lm} are the normalised complex spherical harmonic coefficients after subtracting the long term mean. Since the effect of the DDK2 filter whose radius coincides with 340 km of the Gaussian filter leads to attenuation of the signal amplitude (e.g., Wouters and Schrama, 2007; Baur et al., 2009), a scaling factor obtained from Global Land Data Assimilation System (GLDAS, Rodell et al., 2004) derived terrestrial water storage content (see details in Section 3.1.7) was computed in a manner similar to Landerer and Swenson (2012). This scaling factor was applied to the GRACE-derived TWS values in order to restore the geophysical signal loss caused by the impact of the DDK2 decorrelation filter. Apparently, the use of GRACE data has progressed in the direction of full scale hydrological applications

and water resources monitoring (see Wouters et al., 2014). Thus, accounting for the effect of the filter in the transformed GRACE observations becomes essential as the signal attenuation will become an error in the residual in regional water balance or might serve as a constraint in water budget closure (see Landerer and Swenson, 2012). The rescaled monthly TWS grids had a few random gaps of up to 12 months in between that were filled through interpolation. This is particularly important for the regionalisation process, which requires continuous spatio-temporal data.

3.1.2. Tropical Rainfall Measuring Mission (TRMM) data

Rainfall observations from TRMM 3B43 (Huffman et al., 2007; Kummerow et al., 2000) provide good estimates of rainfall magnitude not detected by other satellite precipitation products. In West Africa for example, Nicholson (2013) had reported that TRMM validation using in-situ data showed zero bias, having a root mean square error (RMSE) of 0.7 and 0.9 mm/day for the seasonal and August rainfall, respectively. Specifically, TRMM 3B43 version 7, which has a global coverage (i.e., 50°S and 50°N) provides monthly precipitation estimates at a spatial resolution of $0.25^\circ \times 0.25^\circ$ and has been significantly improved (e.g., Duan and Bastiaanssen, 2013b). Due to its spatial resolution and bias with in-situ observations, we used TRMM 3B43 to estimate monthly and seasonal rainfall in the LCB. The data covering the period 1998–2013 was used and is available at the National Aerospace and Space Administration (NASA) Goddard Space Flight Center (GSFC) website (<http://disc.gsfc.nasa.gov/datacollection/TRMM3B43-V7.shtml>).

3.1.3. Global Precipitation Climatology Project (GPCP)

The $2.5^\circ \times 2.5^\circ$ global grids of monthly estimate from GPCP version 2.2 precipitation data set (e.g., Huffman et al., 2009; Adler et al., 2003) is a merged satellite-based product (includes satellite microwave and infrared data) that is adjusted by the use of rain gauge analysis. Unlike Ethiopia and some other countries in East Africa where TRMM is completely inconsistent with GPCP (Paeth et al., 2012), the GPCP rainfall product is highly correlated and consistent with TRMM in the region and is used here for the spatio-temporal analysis of drought in the LCB. The GPCP version 2.2 data, covering the period of 1979–2015, was used since drought analysis using SPI requires data record of at least 30 years. The archived data is distributed through the World Data Center and is available

for download at <http://lwf.ncdc.noaa.gov/oa/wmo/wdcamet-ncdc.html>.

3.1.4. Satellite altimetry water level variations

Lake level height variations computed from TOPEX/POSEIDON (T/P), Jason-1 and Jason-2/OSTM altimetry provided by the United States Department of Agriculture (USDA) was used to study Lake Chad surface water. The data covering the period 1993 to 2015 was downloaded from www.pecad.fas.usda.gov/cropexplorer/globalreservoir and used to analyse water level variations. The time series of USDA monthly lake height variation used for the study have been smoothed with a median type filter in order to eliminate outliers and reduce high frequency noise. The use of altimetry-based measurements for a data deficient region such as the LCB, as stated by [Coe and Birkett \(2004\)](#), is beneficial since they are continuous and potentially available few days after measurement. That is quite unlike gauge data that are irregular and difficult to acquire due to government policies and bureaucracies.

3.1.5. Climate Prediction Center (CPC) soil moisture

The monthly CPC soil moisture data version 2 ([Fan and Dool, 2004](#)) with spatial resolution of $0.5^\circ \times 0.5^\circ$ for the period between 1979 and 2014 was used in this study to investigate water availability through standardised soil moisture index (SSI). The data, which is model-based is derived from monthly global rainfall data that uses more than 17,000 rain gauges worldwide and monthly global temperature from reanalysis. In addition, the data has been used to extract climate teleconnection patterns such as the El-Niño Southern Oscillation and long term trends ([Fan and Dool, 2004](#)). The data is freely available at NOAA (<http://www.esrl.noaa.gov/psd/data/gridded/data.cpcsoil.html>) for download.

3.1.6. Climate indices

Relevant and well known global climate teleconnections indices such as El-Niño Southern Oscillation (ENSO), Atlantic Multi-decadal Oscillation (AMO), and Atlantic Meridional Mode (AMM) have been associated with precipitation patterns (see, e.g., [Giannini et al., 2003, 2013](#); [Nicholson, 2013](#); [Paeth et al., 2012](#)), important factors that regulate the formation and persistence of drought events in the Sahel and some countries of West Africa. These indices, covering the period 1979–2014, were used to examine the relationship and possible links of observed temporal evolutions of droughts in LCB with coupled atmosphere–ocean system and perturbations of nearby oceans. We point out briefly that other ENSO indices such as Nino3.4 and Nino4.0 exist but we used Multivariate Enso Index-MEI (hereafter called ENSO) since it comprises six other variables over the Pacific coupled with atmospheric anomalies. The climate indices used in this study can be downloaded from National Oceanic & Atmospheric Administration (NOAA) websites (e.g., <http://www.cpc.ncep.noaa.gov>).

3.1.7. Global Land Data Assimilation System (GLDAS)

GLDAS ([Rodell et al., 2004](#)) derived monthly total water storage content (TWSC) at $1^\circ \times 1^\circ$ spatial resolution was used to rescale the GRACE-derived TWS change in order to remedy the signal loss due to filtering. GLDAS is unique because it integrates both satellite and in-situ data to produce optimal fields of land surface states and fluxes ([Rodell et al., 2004](#)). The TWSC was derived from summing all the layers from Noah 2.7.1 land surface model of GLDAS (i.e., all the soil moisture layers including the canopy water storage). This land surface model (i.e., the Noah component of GLDAS) showed a good agreement with GRACE-derived TWS in West Africa, indicating a coefficient of determination (R^2) of 0.85 ([Ndehedehe et al., 2016a](#)). However, the averaged TWSC and GRACE-derived TWS in the LCB showed a relatively stronger agree-

ment (i.e., R^2 of 0.88) with a root mean square error of 19.83 (see [Appendix A3, Fig. 17](#)). While it is important to acknowledge that the GLDAS model incorporates soil moisture and plant canopy surface water storage, it does not include surface and groundwater components. However, previous studies have reported a good agreement between GLDAS-TWSC and GRACE-derived TWS at basin scale (e.g., [Moore and Williams, 2014](#)). To derive the scale factor, TWSC was filtered using the DDK2 filter similar to GRACE observations. Thereafter, the ratio of the DDK2 filtered TWSC to the unfiltered and synthesised TWSC was used to derive a scale factor. This scale factor, which measures the impact of DDK2 filter on GRACE-observations, was then applied to the gridded TWS values similar to previous studies (see, e.g., [Long et al., 2015](#); [Landerer and Swenson, 2012](#)). GLDAS-derived TWSC covering the years 2001–2014 was obtained from the open access file available at <http://grace.jpl.nasa.gov/data/get-data/land-water-content/>.

3.1.8. Sea Surface Temperature (SST)

SST version 2 ([Reynolds et al., 2002](#)) data was downloaded from the website (<http://www.esrl.noaa.gov/psd/data/gridded/data.noaa.oisst.v2.html>) of the National Oceanic and Atmospheric Administration (NOAA). The period covered is from 2002 to 2014. The SST averaged of the Atlantic Ocean (30°S – 30°N and 70°W – 20°E) was used in this study to investigate its relationship with annual cycles of rainfall over the basin.

3.1.9. Satellite image analysis

Landsat 7 Enhanced Thematic Mapper plus (ETM+) and Landsat 8 imageries were downloaded from the United States geological surveys website (<http://glovis.usgs.gov/>). The imageries for 2000, 2003, and 2015 in the Lake Chad area were clipped and classified using Iterative Self-Organizing Data Analysis Technique Algorithm (IsoData) technique proposed by [Ball and Hall \(1965\)](#). The method is an unsupervised classification method that uses an iterative clustering algorithm and allows the number of clusters to be dynamically determined. The surface area of the Lake at different epoch was estimated using the classified pixels representing water bodies. Estimating the recent surface area is critical to understanding the desiccation story of the basin in recent times. It is also important to evaluate the wet/dry regimes of the basin in the last decade.

3.2. Method

3.2.1. Standardised drought indices

Drought phenomenon is usually expressed using standardised indices for example, standardised precipitation index (SPI, [McKee et al., 1993](#)) and standardised runoff index ([Shukla and Wood, 2008](#)) amongst others. The SPI is a very popular drought index. It is normalised so that wetter and drier climates can be represented in a similar way and can be calculated for other water variables and hydrological quantities such as snowpack, reservoir, streamflow, soil moisture, and ground water ([McKee et al., 1993](#)). In this study, we utilised two variables (rainfall and CPC model soil moisture) to implement a non-parametric standardised multivariate drought index in order to compensate for the weakness of single drought index as argued by [Hao and AghaKouchak \(2014\)](#). The mathematical framework of this non-parametric multivariate standardised drought index (MSDI) and other single drought indicators (e.g., SPI and SSI) is fully documented by [Farahmand and AghaKouchak \(2015\)](#). These drought indicators adopt empirical method to determine the marginal probability of precipitation and other variables such as soil moisture, evapotranspiration, and runoff. The MSDI combines two hydrological quantities to derive a composite drought index, which can be described as a multivariate prototype

of the popular SPI (AghaKouchak, 2015). Recently, the MSDI has been shown to be a statistically consistent drought index (Huang et al., 2015) and is employed here for the first time in the region. The joint distribution of two variables X and Y expressed as (Hao and AghaKouchak, 2013)

$$P(X \leq x, Y \leq y) = p, \quad (2)$$

where p represents the joint probability of any two variable (e.g., rainfall and soil moisture). The joint probability is then used to define the MSDI as

$$MSDI = \phi^{-1}(p) \quad (3)$$

where ϕ^{-1} is the standard normal distribution function. For the bivariate case, the Gringorten plotting position formula (see Farahmand and AghaKouchak, 2015; Hao and AghaKouchak, 2014) is used to estimate the empirical joint probability. The empirical Gringorten plotting position is expressed as:

$$p(x_k, y_k) = \frac{m_k - 0.44}{n + 0.12}, \quad (4)$$

where n is the number of the observation and m_k is the number of times which the pair (x_i, y_i) occur for $x_i \leq x_k$ and $y_i \leq y_k$ ($1 \leq i \leq n$). Eq. (4) is used in Eq. (3) to compute the MSDI while the standardised precipitation index (SPI) and standardised soil moisture index (SSI) are also estimated using the univariate form of Eq. (4). Thus, we combined averaged GPCP rainfall and soil moisture to derive time series of MSDI, in addition to the single drought indicators across different time scales (i.e., 1, 3, 6, and 12 months). The drought classification and extreme rainfall events used in this study are based on the description of McKee et al. (1993) (Table 1).

As discussed earlier in Section 2, localising drought signals has been a major limitation in drought studies. Hence, the ICA method (see details in Section 3.2.2) was used to decompose the gridded time series of computed SPI and SSI at 3, 6, and 12 month scales into independent modes (i.e., temporal and spatial patterns) where drought/wet signals are localised in terms of their spatial and temporal variations. The statistically significant modes of variability identified in the LCB were analysed further. Essentially, this statistical decomposition of meteorological and land surface state variables (i.e., rainfall and soil moisture) into spatial and temporal patterns allow the extraction of climate teleconnection patterns and other relevant coupled ocean atmosphere patterns that are related to the observed wet and dry periods in the basin. Prior to decomposing gridded rainfall and soil moisture drought indicators into spatial and temporal patterns, the spatially averaged time series of each of the two datasets were used to compute time series of SPI and SSI. That provides the opportunity to compare the results of the two approaches (i.e., the decomposed gridded drought indicators and time series of averaged indicators over the basin). To understand the relationship of climate teleconnection indices with ICA-derived temporal variability of drought patterns, Pearson correlation analysis was applied. The SPI values at 3, 6, and 12 month scales for all first and second ICA modes, were selected for this cor-

relation with global climate teleconnection indices (i.e., AMO, AMM, and MEI). This choice is based on the theoretical assumption that the first and second ICA modes have relatively stronger dominant modes of variability. The Student's t-test was then used to calculate the significance of the correlation at 95% confidence level.

3.2.2. Independent Component Analysis (ICA)

The ICA (see, e.g., Ziehe, 2005; Cardoso and Souloumiac, 1993; Cardoso, 1991, 1999; Common, 1994) technique (see further details in Appendix A2) was used to decompose a data matrix \mathbf{X} , into spatial maps \mathbf{M} , and temporal patterns \mathbf{T} , as:

$$\mathbf{X}_{SPI/SSI/TWS}(x, y, t) = \mathbf{TM}, \quad (5)$$

where (x, y) are grid locations, t is the time in months. \mathbf{T} is unit-less since it has been normalised using its standard deviation while the corresponding spatial patterns \mathbf{M} , have been scaled using the standard deviation of its independent components (i.e., \mathbf{T}). In this study, we used the JADE (see further details in Appendix A2) algorithm (available at <http://perso.telecom-paristech.fr/cardoso/Algo/Jade/jadeR.m>) to decompose standardised drought indicators (i.e., the gridded SPI and SSI data) and GRACE-derived TWS into spatial maps and temporal patterns. Each ICA mode (a pair of the independent components and spatial patterns) of variability is a combination of the temporal and spatial patterns and are usually interpreted together (i.e., the unit-less temporal evolution is multiplied with the spatial pattern in order to obtain the actual values of SPI, SSI, and TWS).

3.2.3. Trends and correlation analysis

The trends in observed temporal evolutions of TWS and Lake Chad water level variations were estimated using the least squares method. Further, we examined the relationship of climate teleconnections with observed temporal SPI patterns (i.e., at 3, 6, and 12 months aggregation) using the linear correlation coefficient (r). The significance of observed correlations were tested at 95% confidence level using the Student-t distribution test as

$$t = r \sqrt{\frac{n-2}{1-r^2}}, \quad (6)$$

where n is the total number of given observations for the data.

4. Results and discussions

4.1. Seasonal rainfall patterns over the Lake Chad Basin (LCB)

TRMM 3B43 version 7 precipitation product was used for the seasonal analysis and long term annual cycle while the GPCP version 2.2 precipitation data was used for the drought analysis because of its duration (35 years). A 35-year data meets the criteria for SPI since a 30-year data or less shortens the sample size and undermines the confidence in its usage (e.g., Svoboda et al., 2012). Comparing the TRMM and GPCP based precipitation products, the spatially averaged GPCP product was consistent (indicated a linear correlation of 0.99) with the spatially averaged TRMM product. This near-perfect correlation is expected since TRMM is adjusted by rain gauge observations, most of which are included in the GPCP datasets. Despite the differences in the spatial resolutions of these two precipitation products, their strong agreement over the LCB can be useful in future studies to characterise uncertainties in water budget analysis. Although no notable trend is observed in the spatially averaged rainfall over the basin, we observe a recent pronounced maximum peak in 2012 that is similar to other extreme wet years, for example, 1988, 1994, 1999, 2003, and 2006 (Fig. 4a). The lowest annual rainfall peak observed in 1984 (Fig. 4a) is consistent with the well known drought that

Table 1
Drought classification and extreme rainfall/soil moisture events based on McKee et al. (1993) classification system.

Description	Threshold
Extreme wet	+2.0 and above
Very wet	+1.5 to +1.99
Moderately wet	+1.0 to +1.49
Near normal	-0.99 to +0.99
Moderate drought	-1.0 to -1.49
Severe drought	-1.5 to -1.99
Extreme drought	-2.0 or less

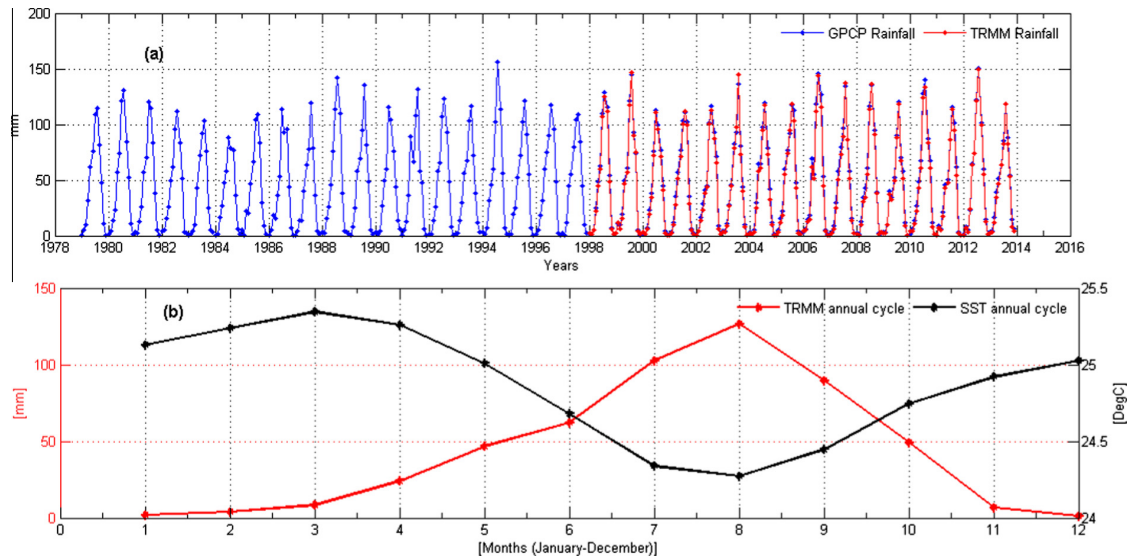


Fig. 4. Averaged monthly rainfall over Lake Chad Basin and annual cycles of TRMM-based precipitation and sea surface temperature (SST). (a) Time series of spatially averaged rainfall over Lake Chad Basin using GPCP version 2.2 (1979–2013) and TRMM 3B43 based precipitation (1998–2013). (b) Long term mean annual cycle of rainfall over Lake Chad Basin using TRMM 3B43 based precipitation and annual cycle of SST data averaged over the Atlantic Ocean (30°S–30°N and 70°W–20°E).

ravaged the African continent during the 1982–1984 period (e.g., Masih et al., 2014). The annual cycle of precipitation over LCB indicates a peak in August while the seasonality of SST shows an opposite phase with rainfall (Fig. 4b). Most parts of the LCB lies in the Sahel region, and the impact of SST variability on rainfall has been reported (Mohino et al., 2011; Paeth et al., 2012; Lebel and Ali, 2009). Rainfall decline in the coastal West African countries has been associated with cold SST along the Atlantic and warm SST in the eastern tropical Pacific while decadal rainfall trends in the Sahel is assumed to be influenced by a combination of multiple low-frequency SST signals (e.g., Rodriguez-Fonseca et al., 2011).

Moreover, the seasonal analysis show that maximum rainfall (temporal variations) comes between July and September with a maximum average rainfall of about 150 mm while other seasons have less than a 100 mm of rainfall (Fig. 5, right). The spatial distribution of rainfall indicates a maximum of about 250 mm of rainfall towards the southern part of the basin and more than 300 mm outside the conventional basin area (Fig. 5, left). Comparatively, the GPCP version 2 seasonal rainfall patterns over the basin also show similar temporal and spatial patterns with the July–September period indicating relatively low pronounced amplitudes of rainfall (e.g., 1983–1984, 1987, etc.) in the temporal variations due to extreme drought conditions (see Appendix A1, Fig. 16). Generally, the July–September rainfall (i.e., using the GPCP data) in the basin is the dominant rainfall as the most pronounced maximum peaks correspond to those of Fig. 5. Overall, the seasonal rainfall patterns over the basin, clearly show the dichotomy between the northern section (having low rainfall) and the southern band (which receives more rainfall especially between July and September) (Fig. 5). This seasonal picture of rainfall in the basin is crucial as it has the capacity to enhance the assessment of the basin's hydrology. The knowledge of the basin's climatology, in terms of seasonal rainfall can enhance our interpretation of the standardised drought indices.

4.2. Drought characteristics over the Lake Chad Basin (LCB)

4.2.1. Time series of standardised drought indicators

The standardised drought indicators (i.e., SPI, SSI, and MSDI) for the LCB were computed at 1, 3, 6, and 12 month cumulations using

spatially averaged GPCP and CPC soil moisture data over the basin. Results show that shorter time scales (e.g., 1 and 3 month cumulations) have high drought frequencies (Fig. 6a and b). The frequency reduces with increase of time scales (e.g., 6 and 12 month cumulations) (Fig. 6c and d). According to Komuscu (1999), this kind of relationship implies that the index responds more slowly as the time scales increases. Consistent decrease in SPI and MSDI values were observed from 1979 to 1985 (Fig. 6) but with recovery in 1984 at 3 and 6 months scale. The strong decline of SPI and MSDI within this period coincides with the hydrological drought record of the basin, which showed a dramatic loss of 15138 km² in the surface area of Lake Chad (see, Alfa et al., 2008). The MSDI and SSI show drought persistence in 1990/1991 at all scales (Fig. 6a–d); 1998 at 3 and 6 months (Fig. 6b and c); and 2009 at 6 and 12 months (Fig. 6c and d). The drought years as indicated in the standardised drought indicators are generally consistent with observed decline in the northern pool of the Lake as previously reported by Lemoalle et al. (2012). In addition, the observed wet (e.g., 1988 and 1994) and dry (e.g., 1983–1985) years (Fig. 6) are consistent with the records of observed water levels at Kindjeria (i.e., at the northern section of LCB) as reported in a previous study by Lemoalle et al. (2012). They noted that the northern pool gets flooded during extreme wet periods and completely dry for several years due to incessant drought conditions. Similar patterns in the behaviour of surface waters (e.g., Lakes) vis-à-vis drought and wet periods in the region have been reported (e.g., Bekoe and Logah, 2013; Lemoalle et al., 2012). Also, previous studies have associated the decline in the surface area of the lake to human activities (e.g., water use for irrigation) and the impact of climate variability (see, e.g., Coe and Foley, 2001; Gbuiyiro et al., 2001). Some of the drought cases identified in the study (i.e., using averaged SPI) are somewhat generalised and appear not to be very massive (i.e., in terms of severity). But the cases are significant enough to impact negatively on the agrarian system and food security conditions of the basin where agriculture is predominantly rain-fed.

Furthermore, extreme wet conditions in 1987/1988 (all through the year), and 1994/1995 show strong persistence in wetness by SSI (Fig. 6a–d). On the contrary, SPI and MSDI showed drought

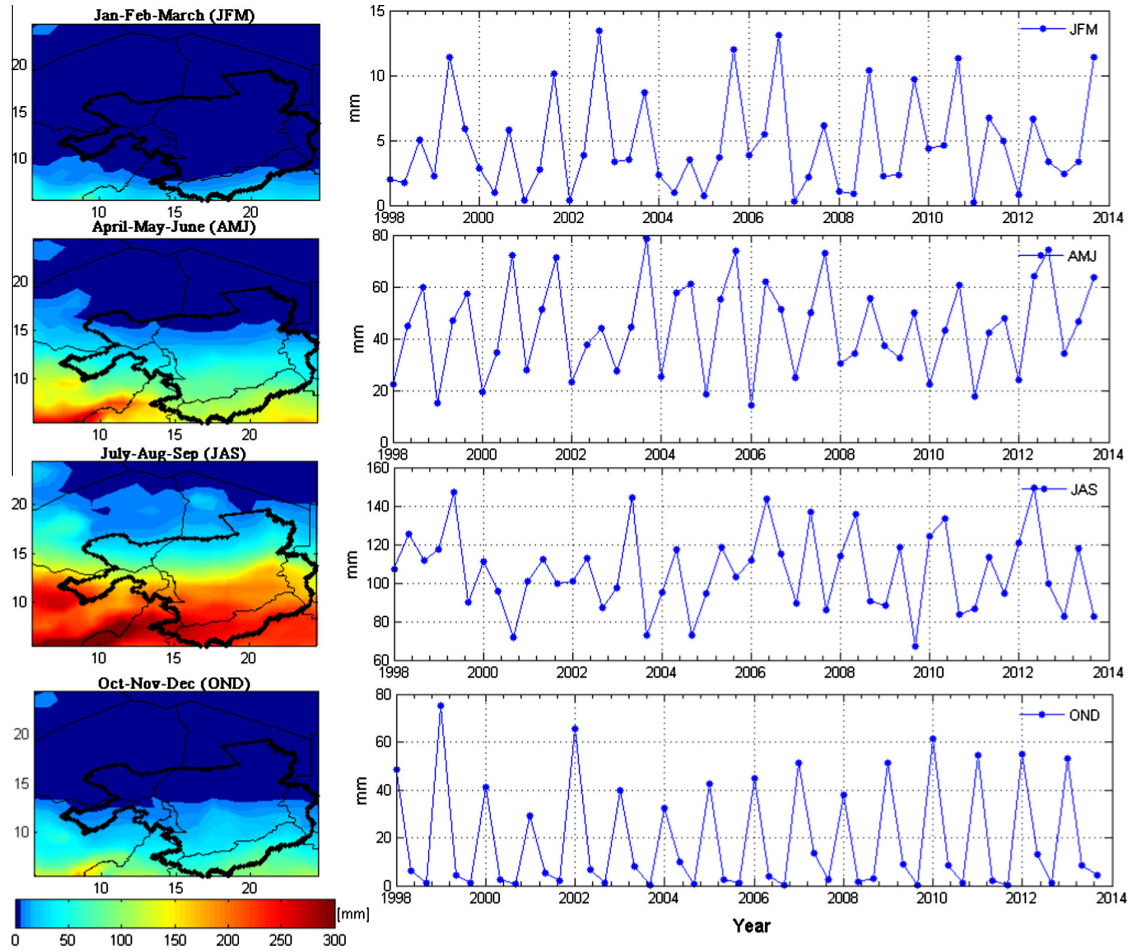


Fig. 5. Seasonal rainfall analysis for Lake Chad Basin (5.5°N–24.5°N and 5.5°E–24.5°E) using TRMM satellite data for the period 1998–2013. Spatial patterns (left) and temporal patterns (right) are averaged over the geographical boundary describing the spatial extent of Lake Chad Basin used in this study. The inset (i.e., the solid black line) is the conventional basin boundary.

conditions in 1987 while in 1995 they indicated that the wet conditions actually ended, unlike SSI, which indicated that the severe wet conditions that started in late 1994 persisted even till 1996 (Fig. 6b–d). This inconsistency is probably caused by intense rainfall occurring within few months while the remaining months of the year are consistently dry. The SPI values (i.e., at 1 and 3 months cumulation) tend to be very high during the 2003–2013 period (Fig. 6a and b), and are consistent with the findings of Okonkwo et al. (2013) whose report showed increase in SPI values between 2002 and 2011 in the basin. However, the SSI and MSDI show longer drought durations in late 2004 (Fig. 6) and 2005 (Fig. 6c and d). In the drought assessment done so far using the three standardised indicators over the LCB, recent conditions of wetness in late 2010 and 2012/2013 captured by SPI, SSI, and MSDI (Fig. 6a–d) appear to be a dramatic deviation from the long string of frequent drought conditions observed in the basin (note that at 12 month cumulation period, only SPI indicated wet condition in 2010 while SSI and MSDI showed a recovery from drought condition). This period (i.e., between 2010 and 2013), which also coincides with increased water level in Lake Chad as shown in Section 4, is largely consistent with the spatially averaged rainfall over the basin within the same period (Fig. 4a). Further, as the accumulation period increases (i.e., for SPI), soil moisture conditions tend to respond slowly to extreme wet conditions of

SPI. It seems that the extreme wet condition was not sufficient enough to cushion the deficit conditions of soil moisture in the basin. For instance, when we evaluate SPI (i.e., 12 month scale) values of 1991, 2006–2007 and 2012–2013 periods against SSI and MSDI (i.e., 12 month scale) values during the same period, the inconsistencies are rather obvious. SPI indicates extreme wet conditions during those periods (1991/1992 and 2006–2007) while MSDI and SSI show extreme drought (1991 and 2006–2007) and normal conditions (2011–2013 period) as against the extreme wet condition indicated by the SPI (2012–2013 period) (Fig. 6). Soil moisture deficits have been related to antecedent conditions, evaporation, seepage to groundwater, evapotranspiration, and runoff (e.g., Loon, 2015). According to Birkett (2000), Lake Chad loses about 80% of water through evaporation due to low humidity and high temperatures. Considering the fact that the basin is located in a semi-arid Sahelian environment, these factors and others (e.g., soil characteristics) may account for the observed inconsistencies between SPI and SSI. In subsequent sections we show results of the statistical decomposition of SPI and SSI signals into spatial and temporal patterns using the ICA technique.

4.2.2. Spatio-temporal analysis of drought patterns for SPI

Unlike Section 4.2.1, where the spatially averaged values of rainfall and soil moisture over LCB were used to compute the

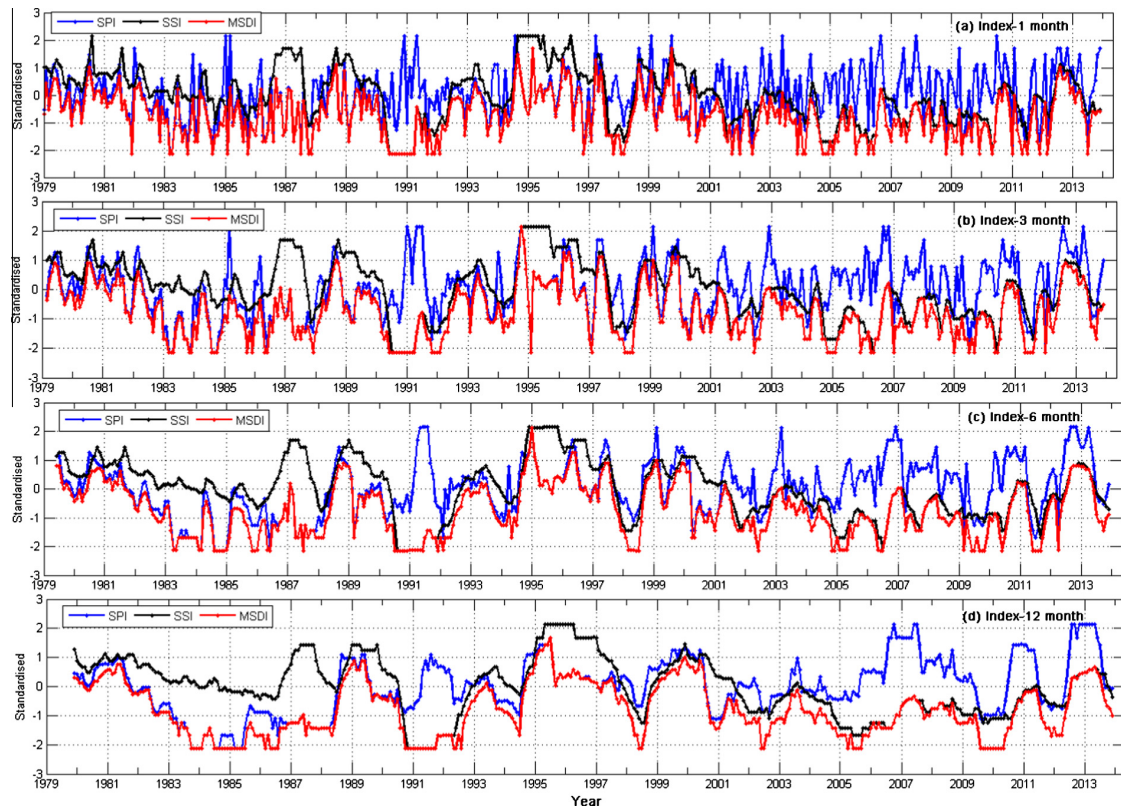


Fig. 6. Time series of standardised drought indicators (i.e., SPI, SSI, and MSDI) for Lake Chad Basin using averaged GPCP and CPC soil moisture data covering the period 1979–2013 (i.e., over the basin). The MSDI is derived through the combination of GPCP based precipitation and CPC based soil moisture data. These standardised drought indicators are based on empirical probability, different from the gamma distribution function used in the SPI case of [McKee et al. \(1993\)](#).

standardised indicators (e.g., SPI and MSDI), here, we use, the gridded values of rainfall and soil moisture to compute standardised indicators, which were subsequently decomposed into temporal and spatial patterns using the ICA technique. The spatial patterns are localised signals (i.e., spatial maps indicating the direction of wet/drought conditions) that show spatial variability of rainfall conditions corresponding to the temporal evolutions. The classification scales (e.g., extremely wet, moderately dry, severely dry, extremely dry) for the SPI values (see, e.g., [Hayes et al., 1999](#); [McKee et al., 1993](#)) are jointly derived from each ICA mode (i.e., a combination of the spatial and temporal patterns). The spatio-temporal SPI patterns were computed for three different time scales (3, 6, and 12 months). In Section 4.2.1, we showed drought index at 1 month scale (i.e., in the temporal drought patterns), however, in this section we choose these intermediate and long term scales (3, 6, and 12 months) for the spatio-temporal drought variability since they fit in well with agricultural and hydrological drought monitoring as indicated earlier in Section 2.

When comparing the temporal evolutions of SPI for 3 and 6 month time scales, a number of similar characteristics are observed. Declining SPI values from 1980 up to 1984 and extreme drought in 1984 are observed ([Figs. 7 and 8](#)) in the central part of the conventional basin. Also, there is a change in drought frequency as the time scale changes. In [Fig. 9](#), drought frequency is reduced when compared to [Figs. 7 and 8](#) where drought frequencies are high. However, drought persistence is higher on longer time scales than short aggregation windows (see, [Figs. 7–9](#)). This is not to suggest that all cases of longer drought duration are usually related to the aggregation window. SPI aggregated over longer time scales (e.g., 12 and 24 months) are sometimes used

in monitoring hydrological droughts (see e.g., [Ndehedehe et al., 2016b](#); [Li and Rodell, 2015](#); [Lloyd-Hughes, 2012](#); [Santos et al., 2010](#)). But the propagation processes from meteorological to hydrological drought conditions may take some time depending on the soil surface conditions, which creates a lagged response (see IC1, [Figs. 7–9](#)). At all monthly SPI scales, we observed relatively strong drought spatial patterns towards the north and centre of the conventional basin area and the entire basin at large. Even though we do not observe strong spatial drought patterns directly over Lake Chad, the southern part of the basin where the lake receives ~95% of its alimentation via the Chari-Logone river experienced drought at 3 and 6 month scales (IC2 and IC4 of [Figs. 7 and 8](#), respectively), that is, when the SPI values are jointly considered or interpreted together from the spatial and temporal patterns. From their temporal evolutions (i.e., IC2 and IC4 of [Figs. 7 and 8](#) respectively), specific years such as 1984, 1990, 1992/1993, 1996, 2000, 2002, and 2010 indicate similar drought characteristics, which we attribute to strong deficit in rainfall in those years. Still on the conventional basin area, the corresponding temporal evolution of drought spatial patterns at 12-month scale (i.e., hydrological drought) indicates extreme drought conditions, which began in 1983 and persisted till 1985 (IC1, [Fig. 9](#)). Similar temporal pattern is also observed in the section of the basin that belongs to Niger (IC4, [Fig. 9](#)). IC2 and IC3 of [Fig. 9](#) show SPI signals in Libya and northern Chad respectively. Apart from the extreme wet conditions of 1988, 1994, and 1998–1999 in some parts of the LCB (IC1 and IC4, [Fig. 9](#)), which was also reported by [Nicholson et al. \(2000\)](#), the period between late 1995 and 1997 indicates drought persistence with extreme dry conditions in 1996/1997 at northern Chad (IC3, [Fig. 9](#)). We point out briefly that while IC1 of [Fig. 9](#)

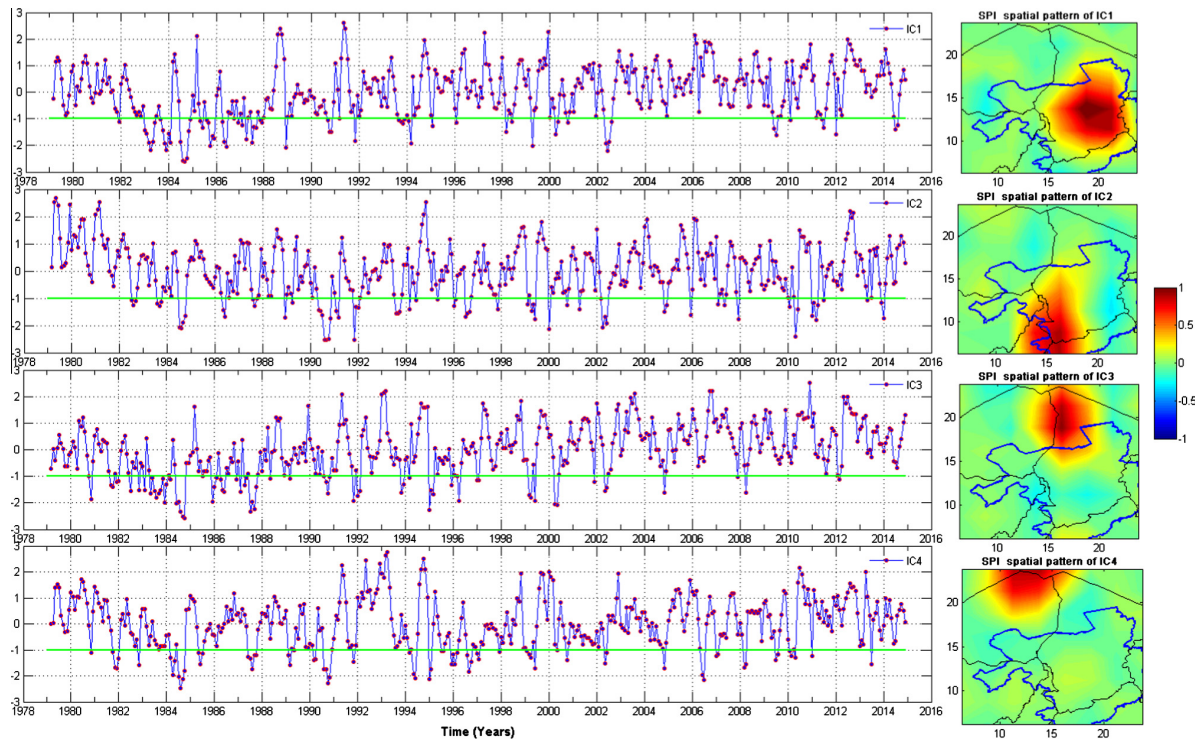


Fig. 7. ICA-derived spatio-temporal SPI patterns of LCB using 3-month gridded SPI values. The SPI values are computed using GPCP rainfall product for the period 1979–2014. Localised spatial SPI patterns (right) corresponds to the temporal evolutions (left). The actual SPI values to be used for drought classification are jointly derived from the spatial and temporal SPI patterns. The green solid line is drought threshold.

(i.e., Central Chad) showed extreme wet conditions in the 1988/1989 period, IC2 of Fig. 9 (i.e., Libya) indicated a drought condition in 1998 with recovery in 1999. As a result, Libya was more or less climatically stable (i.e., when compared to 1994, 2006, and 2012). While the conventional basin area was relatively wet during 2001–2014 period (though with fluctuating SPI values) (IC1 of Fig. 9), drought conditions in the last decade (2001, 2009, and late 2013–2014) in Libya (IC2, Fig. 9) and southern Niger (IC4, Fig. 9) demonstrate the importance of a spatio-temporal approach to drought analyses. Apart from the SPI signal in Libya, recent wet conditions in 2010–2013 seems to be prevalent in the basin (IC1, IC3–IC4, Fig. 9) with the conventional basin area indicating mostly wet conditions since 1999 (IC1, Fig. 9). The observed wet and dry periods from our localised drought signals, which we attribute partly to the impacts of La-Niña and El-Niño, respectively in the region are consistent with the findings of Nicholson et al. (2000) on the trends of rainfall conditions in West Africa. They identified 1988, 1994, and 1998 as the wettest years since the late 1960s (i.e., besides the pre-1980 period) while drier conditions prevailed in other areas of West Africa. In addition to these wet periods of 1988, 1994, and late 1998–2000 (IC1, Fig. 9), which are usually referred to as the rainfall recovery period in the Sahel (see, e.g., Nicholson, 2013; Nicholson et al., 2000), strong positive deviations in normal rainfall in 2012, which may be the combined influence of climate teleconnections (i.e., ENSO, AMM, and AMO as discussed further in the later part of the study) in the region are observed at all scales (see IC1–IC4, Figs. 7–9). Specifically, the 1998 and 1999 wet periods as observed in this study are consistent with the periods of high Chari flows, which led to flooding and loss of agricultural land within the southern basin (see Birkett, 2000). Moreover, for all monthly cumulations, we observed a relatively strong declining SPI values between 1980 and 1984 over the region

(IC1–IC4, Figs. 7–9), which are consistent with well known and acknowledged extreme drought conditions of 1983–1984 in Africa (e.g., Masih et al., 2014). Likewise, a relatively stronger decline of SPI values are observed between 1980 and 1991/1992 mostly at Niger (i.e. IC3, Fig. 8) and Chad (i.e. IC3, Fig. 9). These extreme drought periods especially those occurring during 1982–1984 period (see e.g., IC1 and IC4 of Fig. 9) have been attributed to the synergy between the abnormally warm Indian Ocean SST and that of the eastern Atlantic, which suppressed rainfall in the Sahel due to large scale subsidence in the troposphere (see, e.g., Bader and Latif, 2011; Giannini et al., 2003). The Lake Chad Basin had experienced prominent alterations in hydro-meteorological conditions in the past decades, which eventually led to widespread drought and sometimes flood in the region. From the analysis of other ICA-derived modes of drought variability in this study (not shown), either for rainfall or soil moisture (Section 4.2.3), extreme wet and drought conditions were also observed in the extreme southern and northern part of the basin.

Furthermore, we explored the relationship between SPI and global climate teleconnection indices that have been associated with rainfall variability and drought conditions in the Sahel. Results (Table 2) show that at 12 month SPI scale, AMO has a significant positive correlation of 0.55 with the first ICA mode of Fig. 9. In Fig. 10, we show the relationship of ICA-decomposed 12-month gridded SPI (i.e. IC1) with climate indices (i.e., AMO, ENSO, and AMM). We observe that the hydrological character vis-a-vis extreme rainfall conditions (e.g., droughts) of LCB could also be as a result of the influence of AMO. Our linear correlation result (Table 2) agrees with the findings of Diatta and Fink (2014), that pointed out the influence of AMO on rainfall conditions in the Sahel. They reported positive linear correlations (0.28 and 0.29) of AMO with West African Monsoon rainfall variability in two

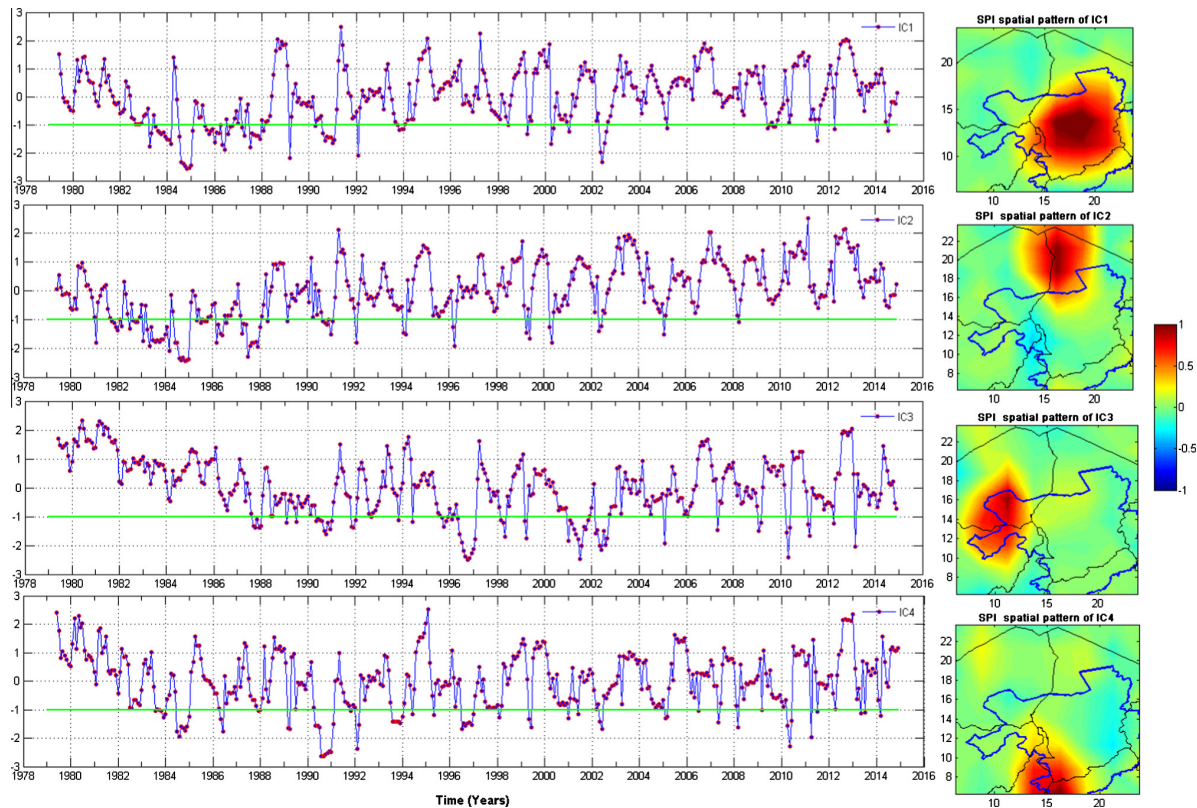


Fig. 8. ICA-derived spatio-temporal SPI patterns of LCB using 6-month gridded SPI values. The SPI values are computed using GPCP rainfall product for the period 1979–2014. Localised spatial SPI patterns (right) corresponds to the temporal evolutions (left). The actual SPI values to be used for drought classification are jointly derived from the spatial and temporal SPI patterns. The green solid line is drought threshold.

Sahel regions. Aligning with our perceived influence of AMO, Rodriguez-Fonseca et al. (2011) also reported on the impact of AMO on rainfall variability in the region. Still on the first independent mode of SPI 12 month scale (i.e., IC1 of Fig. 9), AMM showed positive correlations of 0.30, 0.38, and 0.38 with SPI at 3, 6, and 12 month cumulations, respectively (Table 2). The observed positive linear correlation of AMM with temporal evolutions of wet/dry periods in the first mode (i.e., IC1 of Fig. 9), which is along the Sahel strip, is also consistent with the results reported by Diatta and Fink (2014). The study reported a similar relationship of AMM with Sahel rainfall variability. On the other hand, ENSO showed negative correlations of -0.22 and -0.34 with 6 and 12 month SPI cumulations, respectively (Table 2). For ENSO, a similar negative relationship with Lake Chad water level variability was reported by Okonkwo et al. (2014). Overall, the observed relationships between these climate teleconnections and SPI temporal evolutions are statistically significant at 95% confidence level. The associations of AMM at 6 and 12 month scales and the relationship of ENSO and AMO with SPI temporal evolutions, gives us the impression that the observed wet and dry periods in this study are probably also influenced by multiple forcing mechanisms.

4.2.3. Spatio-temporal analysis of drought patterns for SSI

Apart from precipitation, society usually depends upon usable water from various sources, such as soil moisture, streamflow, lakes, and reservoir storage for agriculture, ecosystem functioning, domestic, and industrial purposes. Consequently, most drought impacts can also be related to soil water drought (i.e., agricultural drought) and hydrological drought (abnormally low water levels, in lakes, reservoir levels, and groundwater). Previous drought

studies have related hydrological and agricultural droughts with precipitation deficits on shorter and longer time scales such as 3, 6, 12, and 24 months cumulations (see, e.g., Li and Rodell, 2015; Lloyd-Hughes, 2012; Hayes et al., 1999; Komuscu, 1999). But the use of soil moisture in quantifying drought episodes that may be useful in hydrological applications and in understanding the propagation process of rainfall deficit to hydrological drought (i.e., through soil moisture deficit) are not known in the LCB. Hence, in order to investigate the spatio-temporal variability of agricultural and hydrological droughts, similar to the SPI concept of McKee et al. (1993), the CPC soil moisture product was used to derive the SSI. Results indicate that similar to the SPI (see Section 4.2.2), the 1983/1984 drought is captured here at all monthly scales in the basin (Figs. 11–13). Generally, while there seem not to be differences in drought frequency and persistence at all monthly scales, extreme wet years of 1988, 1994, 1998, and 2012 are consistent with results in Section 4.2.1. Apparently, at all monthly SSI accumulation scales, the central part of the conventional basin where the Lake is located (i.e., Lake Chad, Njamena and environs), show declining SSI values between 2008 and 2012, with extreme and severe drought conditions in 2011 and the early part of 2012, respectively (see IC3, Fig. 11 and IC2 of Figs. 12 and 13). Although the later part of 2012 in the central part of the conventional basin area shows drought recovery (e.g., IC2, Fig. 12), the inconsistency between the temporal evolutions of SSI and SPI in 2012 in this part of the basin is a contrasting hydrological situation that needs to be considered. This hydrological situation is attributed to a number of factors. First, in the previous years, drought persisted between 2010 and early 2012 with extreme drought condition observed in 2011 (see IC3, Fig. 11 and IC2 of Figs. 12

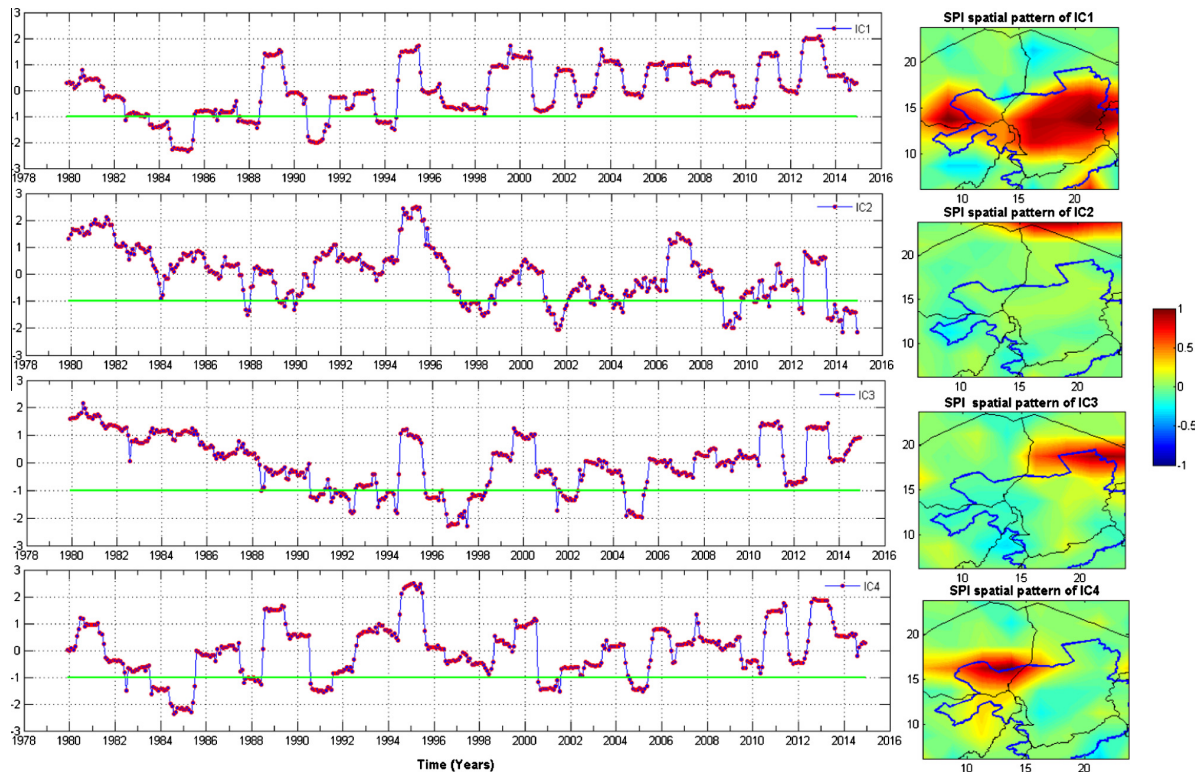


Fig. 9. ICA-derived spatio-temporal SPI patterns of LCB using 12-month gridded SPI values. The SPI values are computed using GPCP rainfall product for the period 1979–2014. Localised spatial SPI patterns (right) corresponds to the temporal evolutions (left). The actual SPI values to be used for drought classification are jointly derived from the spatial and temporal SPI patterns. The green solid line is drought threshold. (For interpretation of the references to colour in this figure legend, the reader is referred to the web version of this article.)

Table 2

Correlation coefficients between temporal evolutions of SPI (i.e., 3, 6, and 12 months SPI scales) derived from the ICA process and global climate teleconnection indices. Correlation values in bold are significant at $\alpha = 5\%$ confidence level.

SPI scale	Independent components	AMO	AMM	ENSO
3 month	1	0.31	0.30	-0.18
	2	-0.13	-0.21	0.07
6 month	1	0.38	0.38	-0.22
	2	-0.45	-0.33	0.18
12 month	1	0.55	0.38	-0.34
	2	0.36	0.08	-0.07

and 13), hence, the apparent soil moisture deficit even during periods of improved rainfall. Second, the rainfall must have been hyped-up due to its intensity in few months (e.g., July and August) while the remaining months of the year remained dry leading to observed drought condition. Third, it could be that the strong amplitude of rainfall in 2012 (see Fig. 4) and the wet conditions observed from the spatio-temporal analysis of SPI (Figs. 7–9) was not significant enough to be reflected in soil water storage. Another argument in this regard could be that the previous drought condition (e.g., 2009 and 2011) of the basin was quite overwhelming (IC1, Figs. 7 and 8). While Birkett (2000) had previously reported that about 80% of the lake's water is lost through evaporation, the tremendous loss of water in the basin through evapotranspiration process as further reiterated by Odada et al. (2005) could play a major role in the hydrological situation observed. In addition to all of these considerations, the surface characteristics of the soil (e.g., geological patterns) and local hydrodynamic behaviour (e.g.,

Descroix et al., 2009) of the region can create temporary soil water shortage conditions leading to observed inconsistencies between SPI and SSI signals. Moreover, model soil moisture products driven by observed meteorological forcing may show some limitations. They are inconsistent during extreme wet and dry conditions and tend to show limited skills in regions with strong annual rainfall cycle (Dirmeyer et al., 2004). Nevertheless, consistent with our arguments, Dirmeyer et al. (2004) indicated that the variability in model soil moisture products may not completely follow the variability in rainfall as a result of the surface characteristics of the soil.

In other drought events of the basin, extreme drought condition is observed on the southeast part of the conventional basin during the periods of 1984–1985, 1996–1997, and 2000–2003 (IC4, Figs. 11–13). Also, this period (2000–2003) shows one of the period with the longest drought duration (i.e., soil moisture deficit, IC4 of Figs. 11–13) in the study and is consistent with the observed well pronounced negative water levels shown in Section 4.3. Note that this southeastern part of the conventional basin is also made up of tributaries that flows into the Chari–Logone river system. Hence, the observed extreme drought for the periods of 1984–1985, 1996–1997, and 2000–2003 as indicated in IC4 of Figs. 11 and 12, are specific examples of severe water shortage with grave agricultural and domestic consequence in the Lake and the conventional basin. Further, longer drought duration in recent times, is observed in the part of the basin that belongs to Niger between 2008 and early part of 2010 (see IC1, Figs. 11–13). This generally leads us to the understanding that the hydrological footprint of LCB in recent times (e.g., 2008–2012), indicates reduced alimentation and water deficit. It is likely that the loss of soil water storage

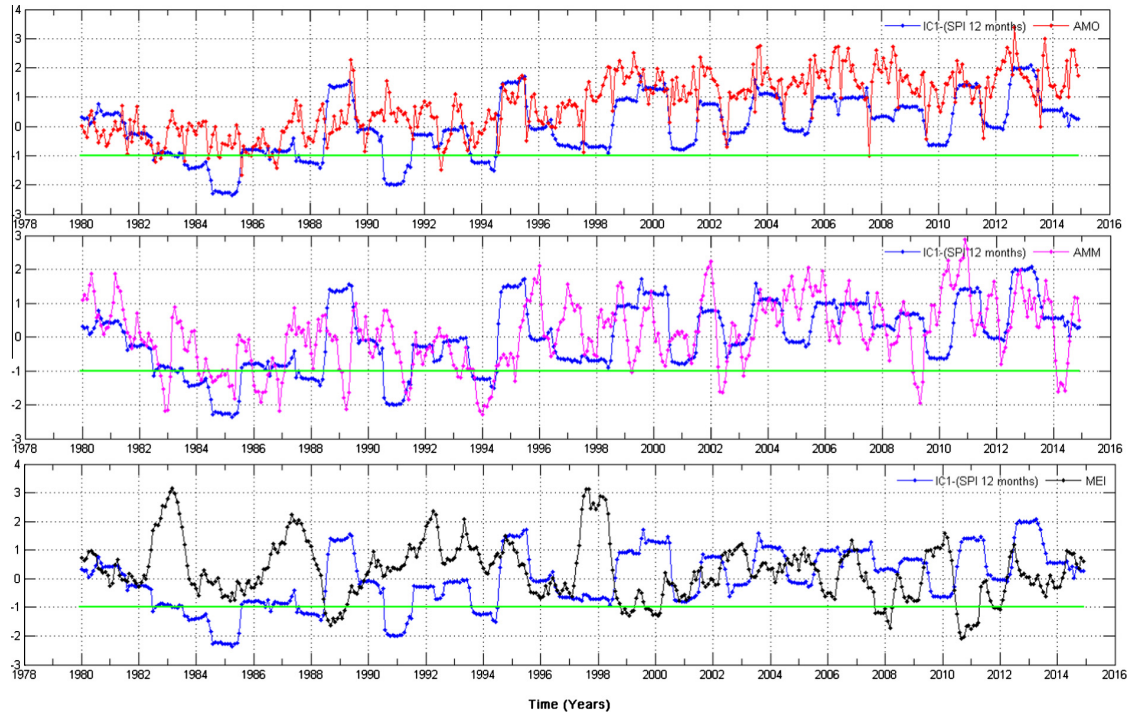


Fig. 10. Influence of global climate teleconnection indices (i.e., 1979–2014) on temporal evolutions of hydrological droughts (i.e., 12 month SPI). The temporal drought pattern of ICA mode 1 shown in Fig. 9 are correlated with AMO (top), AMM (middle), and MEI (bottom).

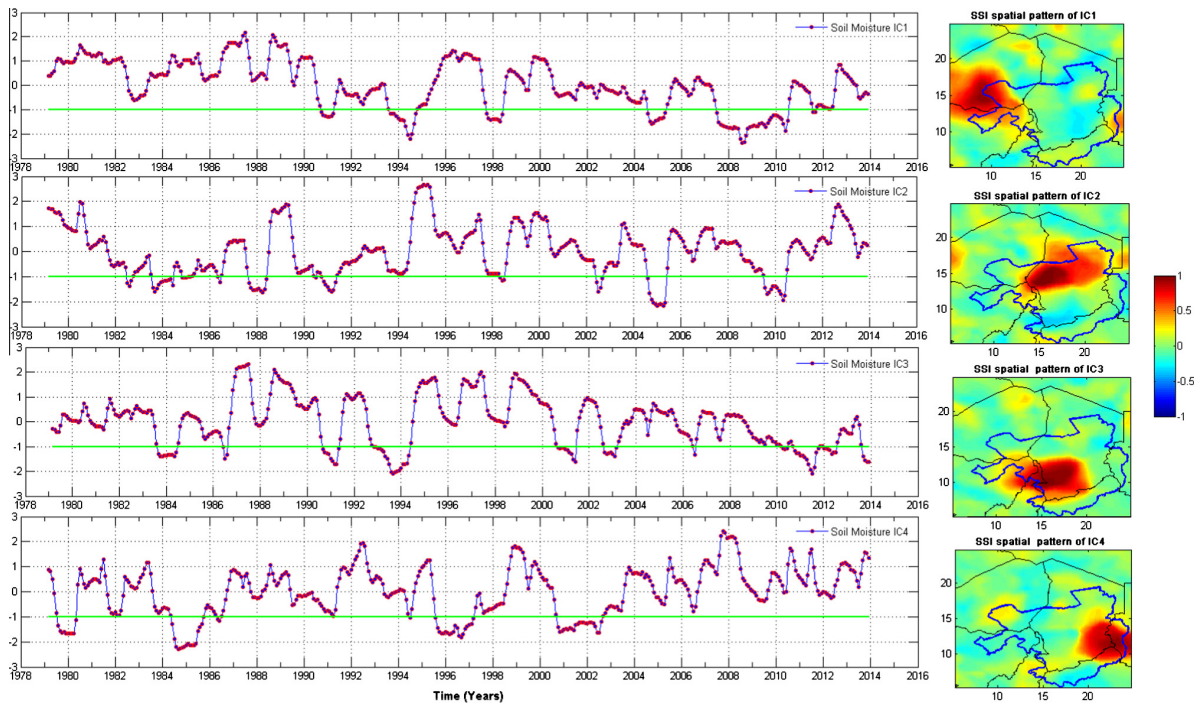


Fig. 11. ICA-derived spatio-temporal SSI patterns of LCB using 3-month gridded SSI values. SSI values are computed using CPC model soil moisture product for the period 1979–2013. Localised spatial SSI patterns (right) corresponds to the temporal evolutions (left). The actual SSI values to be used for drought classification are jointly derived from the spatial and temporal SSI patterns. The green solid line is drought threshold. (For interpretation of the references to colour in this figure legend, the reader is referred to the web version of this article.)

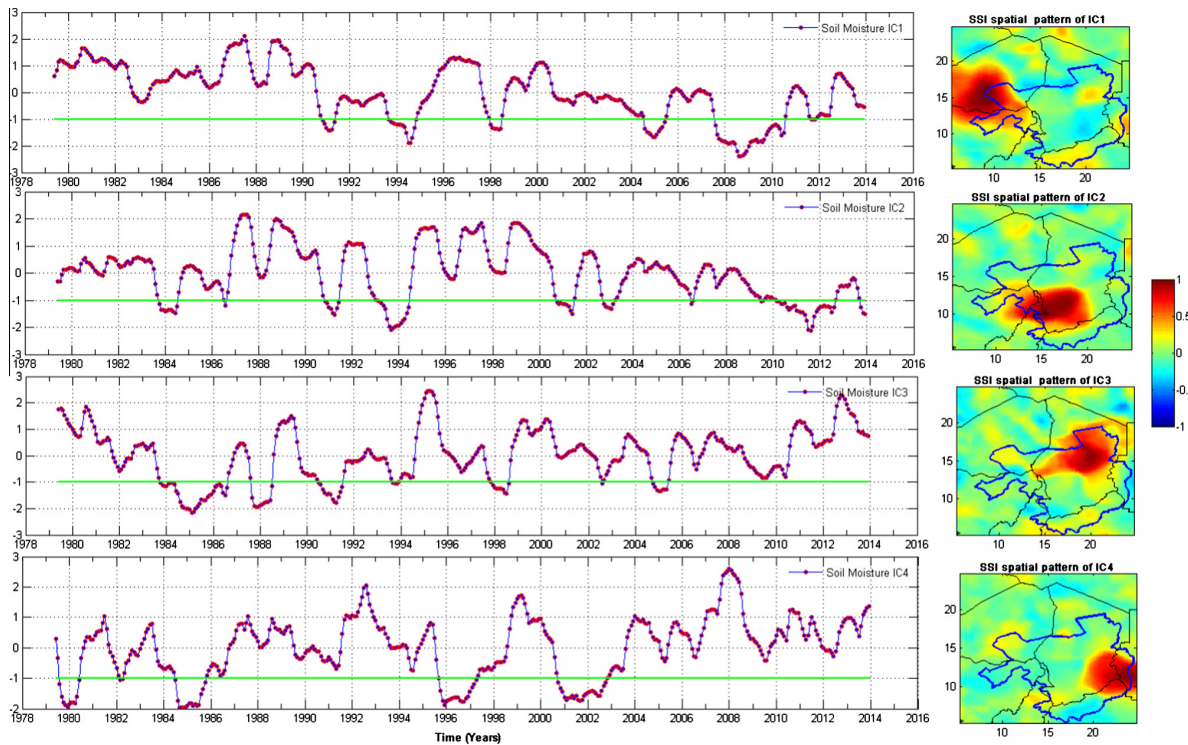


Fig. 12. ICA-derived spatio-temporal SSI patterns of LCB using 6-month gridded SSI values. SSI values are computed using CPC model soil moisture product for the period 1979–2013. Localised spatial SSI patterns (right) corresponds to the temporal evolutions (left). The actual SSI values to be used for drought classification are jointly derived from the spatial and temporal SSI patterns. The green solid line is drought threshold. (For interpretation of the references to colour in this figure legend, the reader is referred to the web version of this article.)

in the basin could be the result of huge evapotranspiration and insufficient rainfall during the previous years. Although other environmental conditions such as increased surface temperature in the basin may intensify the soil moisture deficit conditions, SPI temporal evolutions (i.e., at 3 and 6 months aggregation) showed drought conditions in 2009, 2011, and early 2012 (IC1 of Figs. 7 and 8), coinciding with the soil moisture deficits during 2009–2012 period (IC3 of Fig. 11 and IC2 of Figs. 12 and 13). To further consolidate on these findings, the results of TWS regionalisation is presented in the next section.

4.3. Dynamics in land water storage over the Lake Chad Basin

From the statistical decomposition of TWS changes over the LCB, four significant modes of variability were identified. The ICA approach generally, shows a relatively better performance in exploring the spatial dynamics of variability in GRACE-derived TWS changes compared to PCA, which was recently employed in analysing TWS and rainfall over West Africa by Ndehedehe et al. (2016a). The four modes of TWS variability (IC1–IC4, Fig. 14) analysed indicate a total variability of 67.6% with the first mode explaining 27.6% variability while IC2, IC3, and IC4 explained 16.2%, 13.6%, and 10.2%, respectively. IC1 (Fig. 14) is a strong hydrological signal emanating from the Benue river drainage basin (i.e., north-east Nigeria, as can be seen in the corresponding spatial pattern), which is made up of freshwater tributaries that also flows into LCB (cf. Fig. 1, left). This signal is mostly outside the conventional basin area but surface waters (i.e., rivers) from north-east Nigeria also provides nourishment to the LCB. From the temporal patterns (IC1, Fig. 14), a statistically significant increase of 12 ± 4.0 mm/yr between 2002 and 2014, which is attributed to

rainfall is observed. IC2 (Fig. 14) is TWS variability in the southern sector of the basin where ~95% of LCB's nourishment takes its origin. It is basically the TWS change in the southern catchment of the basin where average monthly rainfall between July and September could be up to 300 mm (cf. Fig. 5, left). TWS in this southern catchment indicates a statistically insignificant decline of 4.5 mm/yr (IC2, Fig. 14). This decline may be the result of marked fluctuations in precipitation patterns as the SPI indicates frequent drought conditions with relatively short durations during the 2002–2014 period (IC2 and IC4 of Figs. 7 and 8). IC3 (Fig. 14) is the hydrological signal from Nigeria, the Kainji reservoir area to be specific. The statistically significant increase of 22 ± 4.0 mm/yr can be attributed to water ponding in the Kainji reservoir and probably increase in rainfall within the period. Lastly, the statistically insignificant increase of 3.0 mm/yr in the central part of the conventional basin area, as observed in IC4 (Fig. 14), coincides with the water deficit conditions discussed in Section 4.2.3.

The hydrological condition of the LCB has not been a one-sided narrative of desiccation and decline in surface water extent as two inter-decadal wet/dry cycles have been observed in the altimetry time series (Fig. 15). Essentially, the cumulative rainfall anomalies in Fig. 3 and the increase of 0.04 ± 0.03 m/yr (statistically significant at 95% confidence level) in the satellite altimetry derived water levels of Lake Chad during the 2008–2014 period (see, Fig. 15) suggest wetter conditions given the endemic droughts that ravaged the basin in the past. Such circumstance (increased altimetry water levels of Lake Chad or wet conditions around the Lake area), which occasionally leads to flood in the basin can also be attributed to high flows from the Chari river catchment, a major source of the Lake's nourishment. During such periods (i.e., high flow) as noted by Coe and Birkett (2004), the marshlands and areas

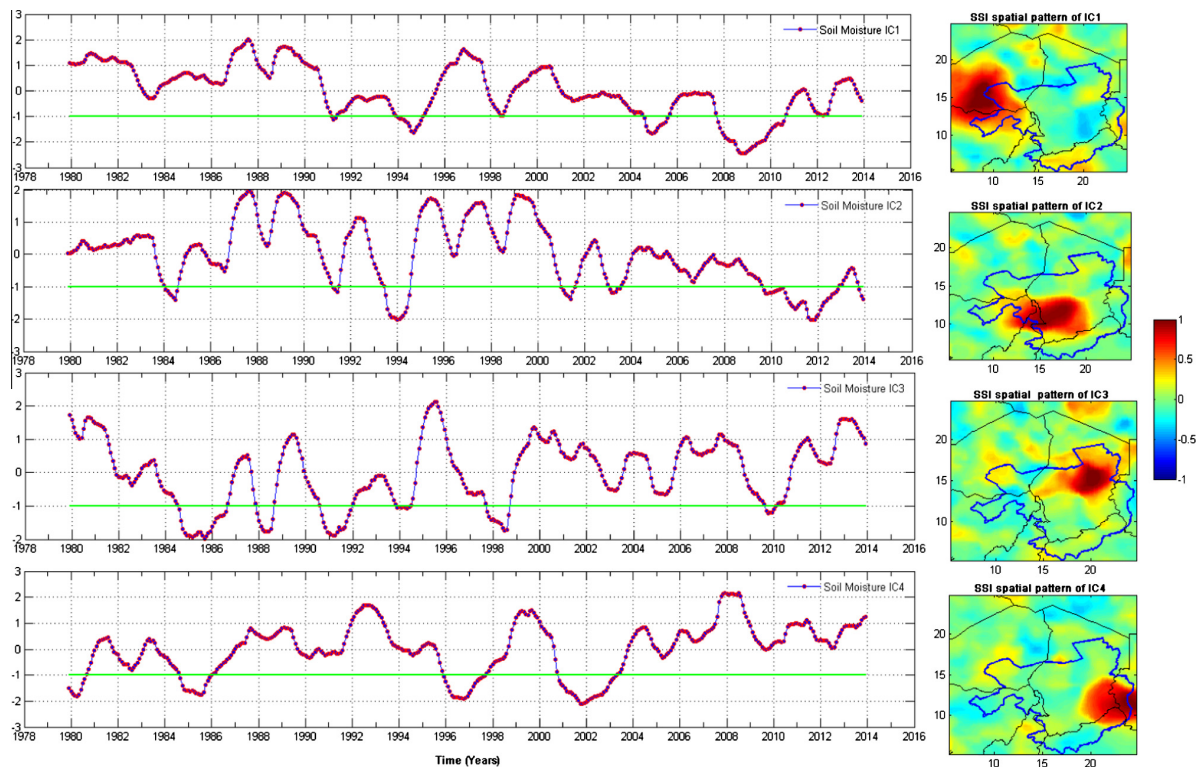


Fig. 13. ICA-derived spatio-temporal SSI patterns of LCB using 12-month gridded SSI values. SSI values are computed using CPC model soil moisture product for the period 1979–2013. Localised spatial SSI patterns (right) corresponds to the temporal evolutions (left). The actual SSI values to be used for drought classification are jointly derived from the spatial and temporal SSI patterns. The green solid line is drought threshold. (For interpretation of the references to colour in this figure legend, the reader is referred to the web version of this article.)

around the shores of Lake Chad get flooded and may lead to crop damage while the dry years lead to reduced yields in both fishing and farming. Such fluctuating hydrological conditions are largely caused by extreme rainfall conditions and can be seen in the Lake's temporal and spatial patterns (see Fig. 2). For instance, in 1987 when the SPI time series over the basin all indicated severe and extreme drought conditions at all monthly aggregations (see Fig. 6a–d and Figs. 7–9), the northern pool completely disappeared leaving behind debris and dunes (Fig. 2, right). Further, Lemoalle et al. (2012) reported the occasional flooding and drying of the Lake (mostly the northern pool) and associated them with inter-annual rainfall conditions in the basin (especially the southern part of the basin). The satellite image analysis of Lake Chad in recent decade indicates a loss of about 573 km² in surface area between 2000 and 2015 while an estimated loss of 249 km² between 2000 and 2003 was observed. Using NOAA's Advanced Very High Resolution Radiometer (AVHRR) images, Birkett (2000) estimated the Lake's areal extent as 1385 ± 25 km² in 2000 while Coe and Foley (2001) reported an area less than 1350 km² in 2001 as the active area of the Lake. This further emphasizes the continuous shrinking of the Lake even during a relatively short period of time. Our surface area estimation of the Lake in those years (i.e., 2000 (~1576 km²), 2003 (~1326 km²), and 2015 (~1003 km²)) was treated cautiously as they only followed the outline of the southern pool (cf. Fig. 2). There are indications that the lake is still receding though with possibilities of reverting back to the *Small Lake Chad* during increased rainfall, a period when the northern pool is partially inundated with Chari river discharge falling between 470 and 1080 m³/s (see, Lemoalle et al., 2012). Given the rising trend in cumulative rainfall anomalies during the 2012–2014 period

(Fig. 2) and trends in lake water level (Fig. 15), the likelihood of such possibilities in recent times (2008–2014) is apparent. However, the observed insignificant trends in TWS of the Lake Chad area (IC2 and IC4 of Fig. 14) and the soil moisture deficit conditions (see Section 4.2.3) make us to be cautiously optimistic about such tendencies. This is because soil moisture deficit decreases recharge to groundwater, leading to groundwater deficit and severe hydrological drought (Loon, 2015). But given that the Lake surface extent and inundation areas are related to wet periods in the basin, the rising trend in cumulative annual rainfall anomalies (Fig. 3b) and the wet periods observed in the conventional basin area (see Section 4.2) may be deviations in the hydro-meteorological patterns of the region that could improve agriculture and strengthen socio-economic activities within the basin. Notably, the slow desiccation of the Lake has been largely perceived as the combined effect of changes in regional precipitation patterns and anthropogenic influence (e.g., Birkett, 2000; Coe and Foley, 2001). The improved rainfall conditions in recent times as observed in the SPI and cumulative rainfall anomalies, could be a simple return to near-normal hydrological conditions in the Lake Chad area. As indicated in Fig. 3, the recent rainfall trends over the basin, which is also apparent in the recent (2008–2014) altimetry time series (Fig. 15) over the Lake, may reverse the drought narrative of the basin. This assumption may imply a possible resurgence of the normal Lake in the absence of any further severe marked alteration of the current hydro-meteorological patterns of the basin. This position contrasts with the perceptions of Moore and Williams (2014) regarding the present Lake Chad, who based on an earlier report (i.e., Coe and Foley, 2001) concluded that the Lake had completely disappeared.

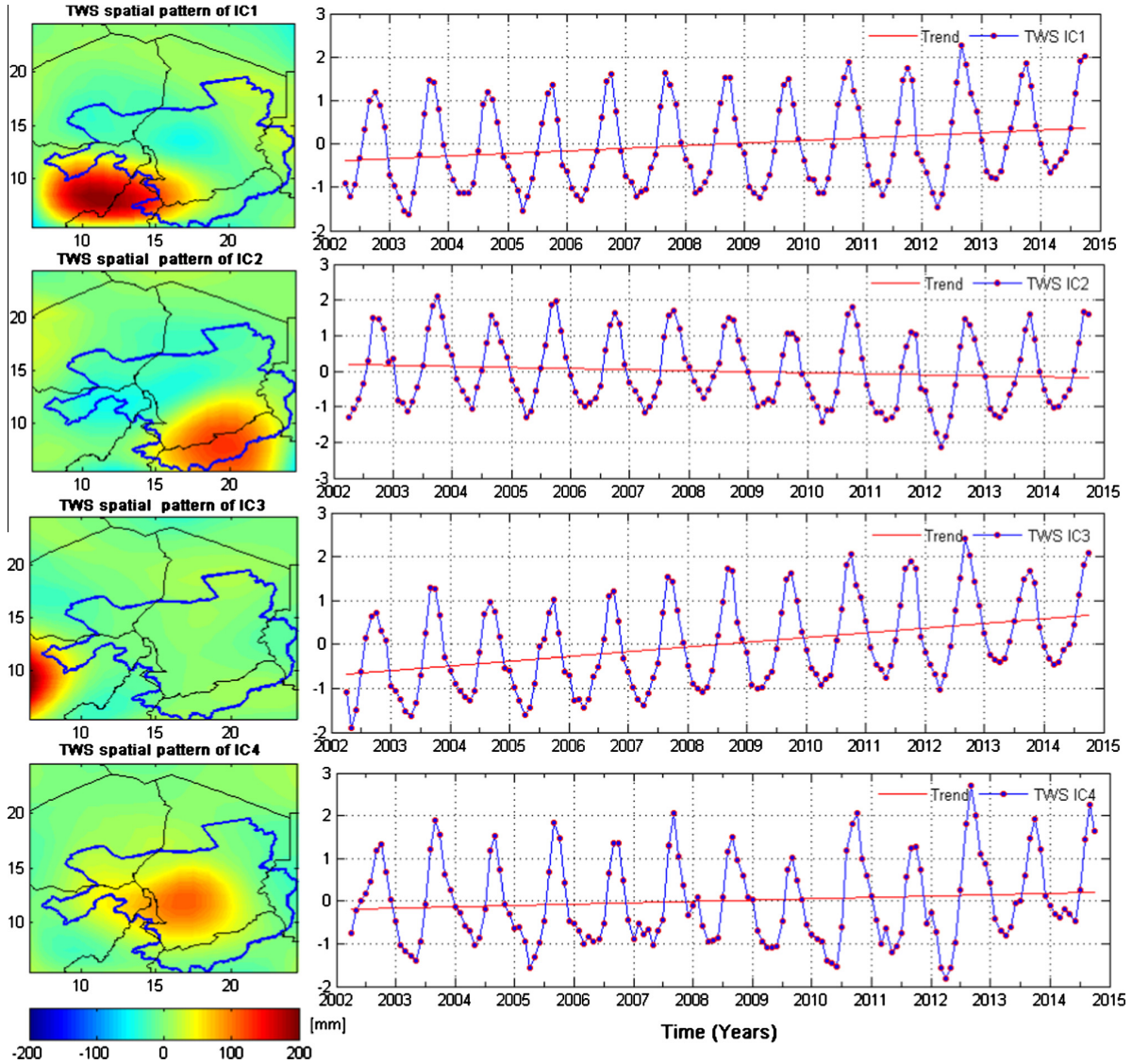


Fig. 14. The independent components (right) of GRACE-derived TWS (2002–2014) over LCB corresponding to spatial patterns (left), which are scaled using the standard deviation of the computed independent components. These independent components are unitless since they have been standardised using their standard deviations.

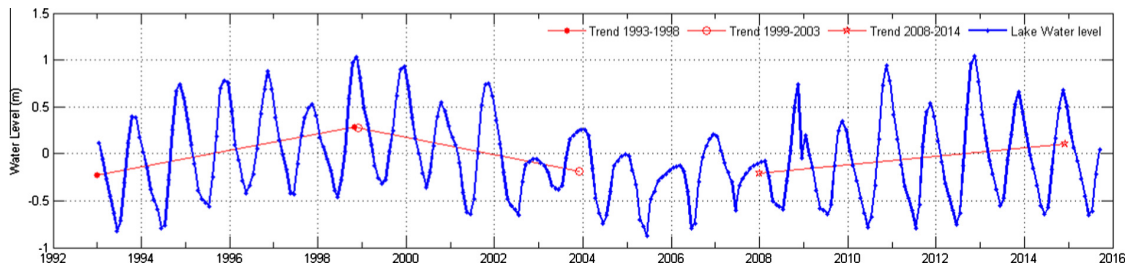


Fig. 15. Trends in Lake Chad water level variation derived from satellite altimetry data for the period 1993–2015.

4.4. Lake Chad water resources: synopsis and policy options

The desiccation and decline in the surface area of Lake Chad has been largely attributed to impacts of climate variability and human

activities (see, e.g., Coe and Foley, 2001; Birkett, 2000). As highlighted previously in Section 1, Lake Chad receives its nourishment from ~95% of discharge from the Chari/Logone river network in the southern part of the basin and ~2.5% of discharge from the

Komadougou-Yobe river system in Nigeria. According to [Coe and Birkett \(2004\)](#), the Chari/Logone river discharge, which is measured at N'Djamena (see [Fig. 1](#)) and the discharge from Komadougou-Yobe river system and precipitation over the lake surface are balanced by seepage to groundwater, evaporation, and inter-annual storage. Considering the importance of the two river systems that nourishes Lake Chad, the inter-annual variations of water storage from these two drainage systems can be used to predict and determine water storage changes in the Lake. Let us recall that IC2 and IC4 of [Fig. 14](#) are TWS signals from the Chari/Logone river system. Observed TWS trend in the Chari/Logone drainage system indicates a decline of 4.5 ± 3.0 mm/yr and an increase of 3.0 ± 2.0 mm/yr for IC2 and IC4 of [Fig. 14](#), respectively. Also within the Chari/Logone drainage system (see IC3, [Fig. 11](#) and IC2, [Figs. 12 and 13](#)), soil moisture deficit and hydrological drought (i.e., at 3, 6, 12 month scales) have been observed between 2010 and 2012. Given these hydrological situations in the LCB, one may assume that the potential for further desiccation and reduced alimentation are likely in the years to come. In a recent study, [Greve et al. \(2014\)](#) observed that the Sahel region (i.e., region where the basin is located) is actually leaning towards aridity. The dry gets dryer paradigm as observed in the study ([Greve et al., 2014](#)), was largely attributed to significant drying trends in water availability and changes in large-scale circulation patterns.

Further, when trends in the variations of Lake Chad water levels are considered, the increase of 0.09 ± 0.03 m/yr and 0.04 ± 0.03 m/yr in 1993–1998 and 2008–2014, respectively might be insignificant when compared to the decline of 0.09 ± 0.03 m/yr in 1999–2003 ([Fig. 15](#)). This is because the hibernation period in the Lake (2002–2007, [Fig. 15](#)) where a great deal of less pronounced annual amplitudes in water levels are observed may rescind the effect of the previous increase in the Lake's height (1993–1998), leading to a hypothetical water deficit (especially with the human disturbance of the Lake). We make this assumption because the impact of extreme drought conditions of previous years are known to have negative effects on surface waters even after an improved rainfall condition in the present (see, e.g., [Bekoe and Logah, 2013](#)). For example, the relatively strong and consistent negative anomalies, observed in water levels all through the period between 2004 and 2005 coincides with observed extreme drought conditions in the conventional basin area within the same period (see, IC4 of [Fig. 9](#); IC1–IC2 of [Fig. 11](#); IC1 and IC3 of [Fig. 12](#) and; IC1 of [Fig. 13](#)). In the same vein, the increase of ~ 0.04 m/yr between 2008 and 2014, when related to the current surface extent of the Lake, which stands at ~ 1002 km² gives an increase of ~ 0.04 km³/yr of water in the Lake. This amount of water is relatively small when compared to 33 km³/yr of water that flowed from the Central African Republic to the LCB in the 1970s and ~ 17 km³/yr in the 1980s ([FAO, 1997](#)). This comparison could be useful in assessing lake water level trends and the impact of climate variability and human influence on the Lake. Moreover, dam construction and increasing irrigation activities in the 1980s contributed a great deal to the desiccation of Lake Chad, putting the water requirements of the basin at 12.525 km³/yr ([FAO, 1997](#)). If human activities in the basin intensify, the resurgence of the Lake may be far away than expected, given that about 21 km³/yr of water is expected to permanently maintain the Normal Lake Chad as it was in the 1960s ([Lemoalle et al., 2012](#)). Going by the observed trends in TWS changes (see [Section 4.3](#)), much of the conventional basin, which is under the mandate of Lake Chad Basin commission, is somewhat stable in terms of freshwater availability. Although soil moisture indicated deficit (see [Section 4.2.3](#)) during 2009–2013 period, in the event that the observed improved rainfall conditions ([Section 4.2.2](#)) of the basin persist, the hydrological condition may be altered significantly, leading to freshwater availability. We acknowledged the limitation

of our study owing to the lack of in-situ river discharge data, especially for the Chari river system. However, the observed trends in TWS changes and altimetry-derived water levels, which depends largely on the river flow from the Chari river system, provides us with a clue regarding recent hydrologic conditions of the Chari river system. This is particularly true because, [Coe and Birkett \(2004\)](#) demonstrated the possibility of using radar altimetry to predict discharge at N'Djamena and the Lake stage within the permanent waters of the Lake bed (i.e., the Lake Chad).

Lake Chad, which is shared by four riparian countries (Nigeria, Chad, Cameroon, and Central African Republic) has suffered huge desiccation and decline in the last three decades due to decrease in rainfall and extreme hydrological drought conditions. But the corresponding basin has been a hub of huge loss of bio-diversity and extreme climate conditions with severe consequences on freshwater availability. In addition, large irrigation schemes and other forms of human activities (e.g., [Lemoalle et al., 2012](#); [Coe and Foley, 2001](#)) also profoundly contributed to the much pressure on the basin's water resources, leading to freshwater deficit. These resulted in the hypothetical decision of transferring water from the Congo basin to support the LCB (see, e.g., [Lemoalle et al., 2012](#); [Inogwabini et al., 2006](#)). While the use of legislation to ensure sustainable practices and long-term conservation of the basin's water resources is essential, we suggest that the ground water resources and aquifer storage be investigated. This can be achieved in future studies by using scientific methods such as the combination of GRACE observations, in-situ data, and outputs from hydrological models. Seepages, infiltration, evapotranspiration, and the effect of the Lake on local recycling of precipitation will have to be fully understood in order to address the challenging physical, and hydrological conditions of the basin. Our approach in drought monitoring and TWS analysis can be employed in inter-basin water transfer projects. For instance, understanding the space-time evolutions of extreme rainfall conditions and changes in TWS of the Congo basin could be useful in managing a hypothetical water transfer to the LCB. This will complement technological, institutional, and other policy solutions in water resources planning. While it is important to investigate the ground water resources of the basin using robust scientific methods as proposed, our contribution provides a general framework for drought monitoring and the understanding of changes in TWS of the region and other parts of the world. For the LCB, the findings of this study can assist and support improved legislation and policies tailored towards the regulation of unsustainable practices. Furthermore, as outlined in [Vassolo \(2012\)](#), few steps have been taken by the Lake Chad Basin commission to strengthen the trans-boundary water resources of the region. They include (i) the adoption of United Nations draft resolutions for trans-boundary aquifers as a basic document that will support groundwater management and (ii) the planned adoption of a Water Charter for the basin to enable the regulation of shared management of water resources and ecosystems. As indicated in the groundwater need assessment of [Vassolo \(2012\)](#), trans-boundary surface water has not been extensively studied since the establishment of the Lake Chad Basin Commission, leading to poor understanding of the trans-boundary groundwater resources. Hence, multi-satellites, especially satellite gravimetric approaches using GRACE observations and outputs from hydrological models can be adopted to monitor the groundwater resources of the basin in future studies.

5. Conclusions

In this study, we used independent component analysis (ICA), a fourth-order cumulant statistics to characterise and localise space-time evolutions of drought patterns over the LCB. Satellite

altimetry data was employed to analyse Lake Chad water level variations while normalised time series of climate teleconnection indices were used to examine the association of SPI temporal evolutions with coupled atmosphere–ocean system. In addition to the drought signature that have been identified, the LCB has also been used primarily as a tentative test bed to demonstrate the spatio-temporal variability of drought. Also, trends and spatial variability of TWS changes in LCB were investigated. The results in this study are summarised as follows:

1. We observed some unusual deviation from the long string of drought conditions observed in the basin as the time series of SPI values between late 2010 and early 2013 are indicative of wet conditions. These wet conditions are attributed to recent increase in rainfall over the basin and is also consistent with recent increase in Lake Chad water levels. However, from the spatio-temporal drought analysis and trends in TWS changes the southern part of the basin, which provides ~95% of the total input to the basin's surface water indicates a deficit, as the SSI between late 2009 and 2012 shows drought conditions at 6 and 12 month cumulations.
2. The time series of SSI and MSDI are inconsistent with extreme positive SPI values (wet conditions) at 12 month aggregation as they both indicate extreme drought conditions and in some cases near-normal conditions. For the SSI, this may be the effect of previous drought conditions, high evaporation due to low humidity and high temperatures, and seepage to groundwater amongst others.
3. Drought analysis with SPI shows that drought persistence is higher on a longer time scale while on short time scales drought becomes more frequent. Generally, while there seem not to be differences in drought frequency and persistence at all monthly scales for SSI spatio-temporal analysis, extreme wet years as identified in the study (e.g., 1988, 1994, and 1998) are consistent with results of spatio-temporal drought analysis for SPI.
4. Apart from the droughts of the 1980s, the spatio-temporal analysis of SPI at 3 and 6 month scales indicated fluctuating drought conditions with relatively short duration in the last two decades in the extreme southern part of the basin. These drought conditions coincide with the observed decline in TWS (though statistically insignificant at 95% confidence level) around the precinct of the southern part of the basin. On the contrary, the trend in TWS changes during the 2002–2014 period shows an insignificant increase at the centre of the basin, coinciding with soil moisture deficit indicated by the temporal evolutions of SSI at all monthly accumulations during the 2002–2003 and 2009–2012 periods. It is unclear if this could be a temporary soil water shortage condition due to surface and hydraulic characteristics of the soil, seepages or increased evapotranspiration and surface temperature over the basin. This can be clarified further in future studies by integrating GRACE-derived TWS and other soil moisture data to investigate the groundwater resources of the basin. Overall, the ICA approach to drought analysis demonstrates the spatio-temporal variability of drought, which largely may depend on the local climatic or meteorological conditions.
5. Also, while the ICA method shows a common hydrological drought period, which lasted for about two years (i.e., 1982–1984) in the basin, other areas within the conventional basin have been affected by both agricultural and hydrological droughts at different time periods.
6. Apart from the negative correlation of ENSO with 12 month SPI, our results show that at 12 month SPI scale, AMO and AMM have statistically significant positive correlations of 0.55 and 0.38, respectively with the first ICA mode of Fig. 9. This

indicates that the hydrological character in relation to extreme rainfall conditions (e.g., droughts) in LCB could also be influenced by these climate teleconnection modes.

7. In addition to improved rainfall conditions during 2010 and early 2013 period, two inter-decadal wet/dry cycles have been observed in the altimetry time series. Generally, our SPI, satellite altimetry, and TWS results within the precincts of the conventional basin indicate relatively wet conditions in the last decade as opposed to soil moisture deficits around the vicinity of the Lake. Our contribution provides a framework for drought monitoring that can assist and support management decisions, legislation, and policies tailored towards water resources and agriculture.

Acknowledgments

Christopher E. Ndehedehe and Nathan O. Agutu are grateful to Curtin University for the Curtin Strategic International Research Scholarship (CSIRS) programme. We thank the Editor and Journal of Hydrology's anonymous reviewers for their useful comments, which helped improved the manuscript. The authors are grateful to Center for Space Research, United States Department of Agriculture, National Oceanic and Atmospheric Administration, and National Aeronautics and Space Administration for all the data used in this study. The support and contributions of Tertiary Trust Fund (TETFUND) Nigeria towards this research is also gratefully acknowledged.

Appendix A

A.1. Seasonal rainfall variability using the GPCP-based precipitation

See Fig. 16.

A.2. Further description of the ICA technique

ICA is a higher order statistical technique that decomposes multivariate data into statistically independent signals (see, e.g., Cardoso and Souloumiac, 1993; Cardoso, 1999). The method, which is usually referred to as blind source separation in signal processing (e.g., Cardoso, 1999), explores the unknown dynamics of a system through the rotation of the classical empirical orthogonal functions (Aires et al., 2002). ICA has emerged as a better alternative to principal component analysis (PCA, e.g., Jolliffe, 2002), an extraction method that is used to reduce the dimension of large multivariate data. Though mathematically simple and a useful tool in terms of information compression, however, the capability of PCA to extract individual modes of variability that are physically meaningful is limited, hence the quest for higher order statistical method such as the ICA. In our case, the strong spatial variability of rainfall in the Sahel region at annual scale constrains the effectiveness of SPI in drought analysis. Hence, decomposing SPI time series using ICA will localise the space–time drought patterns in the region. Localising SPI and SSI signals in LCB will provide a better understanding as to the drivers of hydro-climatic variability in the region. To this end, as a first step in our analysis, the PCA method, was employed to identify statistically significant dominant modes of variability in the data (i.e. the computed gridded SPI and SSI values and GRACE-derived TWS). The significant PCA modes (i.e., a combination of the principal components and empirical orthogonal functions) were identified as

$$\mathbf{P}_i = \mathbf{e}_{ij} \mathbf{x}_j, \quad (7)$$

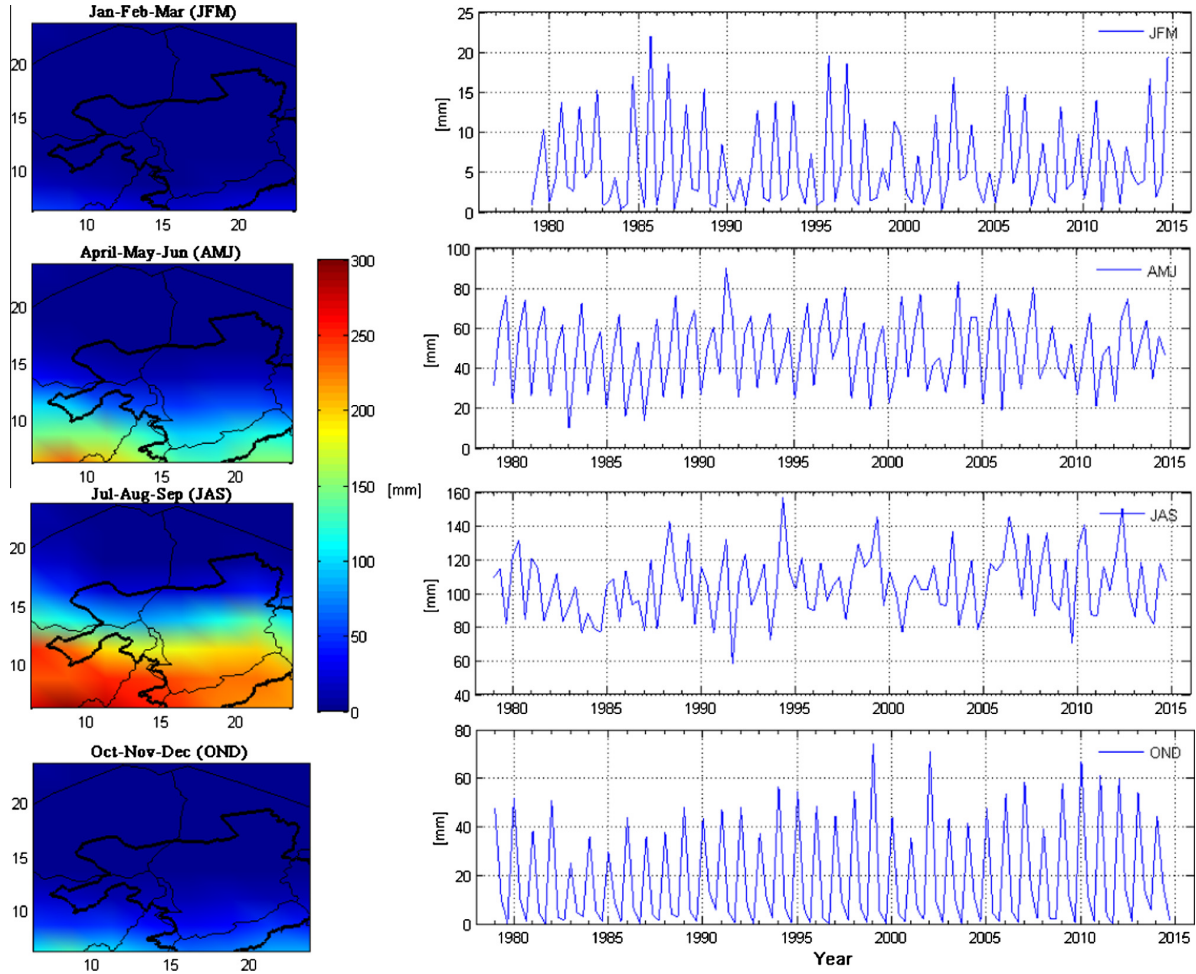


Fig. 16. Seasonal rainfall analysis for Lake Chad Basin (5.5°N–24.5°N and 5.5°E–24.5°E) using GPCP based precipitation for the period 1979–2014. Spatial patterns (left) and temporal patterns (right) are averaged over the geographical boundary describing the spatial extent of Lake Chad Basin used in this study. The insert (i.e., the solid black line) is the conventional basin boundary.

where P_i are linear combinations of \mathbf{x} and \mathbf{e}_{ij} are the set of empirical orthogonal functions (EOFs). Projecting the data \mathbf{x} onto the EOFs we obtain the principal components (PCs) P_i , which can be expressed as

$$\begin{aligned}
 P_{i,1} &= e_{11}\mathbf{x}_1 + e_{12}\mathbf{x}_2 + e_{13}\mathbf{x}_3 + \dots + e_{1k}\mathbf{x}_{i,k} \\
 P_{i,2} &= e_{21}\mathbf{x}_1 + e_{22}\mathbf{x}_2 + e_{23}\mathbf{x}_3 + \dots + e_{2k}\mathbf{x}_{i,k} \\
 &\vdots \\
 P_{i,k} &= e_{k1}\mathbf{x}_1 + e_{k2}\mathbf{x}_2 + e_{k3}\mathbf{x}_3 + \dots + e_{kk}\mathbf{x}_{i,k} \quad i = 1, \dots, n
 \end{aligned}
 \tag{8}$$

\mathbf{e}_{ij} is determined such that $P_{i,1}$ are the new uncorrelated variables and the expression of the original data in the new coordinate system. $P_{i,1}$ explains the highest variance of the multivariate data \mathbf{x} while $P_{i,2}$ up to $P_{i,k}$ explain the possible amount of the remaining variance. The EOF's are spatially orthonormal while the PC's are orthogonal and linearly independent. The next step was to rotate these dominant patterns (i.e., the statistically significant modes), which are uncorrelated towards statistical independence using the Joint Approximate Diagonalisation of Eigen matrices (JADE) algorithm described in Cardoso and Souloumiac (1993). The JADE approach exploits the fourth order cumulants of the data matrix rather than the moments (Cardoso, 1999). The cumulants are formed through the PCA process and diagonalised in order to find

a rotation matrix that solves the optimisation problem (Cardoso and Souloumiac, 1993). ICA decomposes the time series of data matrix $x_i(t)$, which consist of a mixing matrix A and a number of statistically independent source signals $s_j(t)$ where t is the time index. This can be expressed as (Ziehe, 2005)

$$x_i(t) = \sum A_{ij}s_j(t), \quad (i = 1, \dots, n, j = 1, \dots, m)
 \tag{9}$$

x_i in Eq. (9) is the mixing model and can be represented as a matrix as

$$\mathbf{X} = \mathbf{A}\mathbf{S},
 \tag{10}$$

where the entries of the data matrix \mathbf{X} are samples of the $x_i(t)$ given in Eq. (9), the $n \times m$ matrix \mathbf{A} has elements A_{ij} and \mathbf{S} , the source signals. Essentially, ICA aims at recovering the set of source signals \mathbf{S} completely from the observed data matrix or the mixed signal \mathbf{X} , by estimating either the mixing matrix \mathbf{A} or its inverse \mathbf{A}^{-1} . Overall, the ICA problem consist in factoring (i.e solving the optimisation problem) the observed signals in data matrix \mathbf{X} into the mixing matrix \mathbf{A} and the source signals matrix \mathbf{S} . The factoring problem is not uniquely determined and as such many solutions exist that solves the problem (see Ziehe, 2005). Most ICA methods are based on maximum-likelihood estimation, maximisation of the output

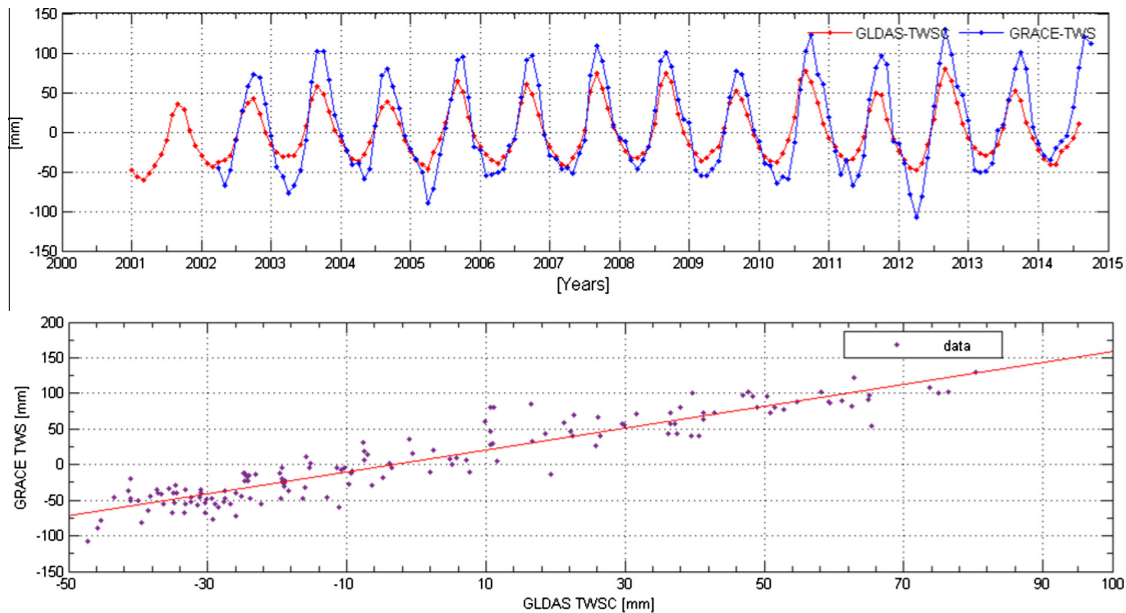


Fig. 17. Comparison between GRACE-derived TWS and GLDAS-derived terrestrial water storage content (TWSC). Top: Time series of GRACE-derived TWS (2002–2014) and GLDAS-TWSC for the period during 2001–2014 averaged over the Lake Chad Basin. Bottom: Regression fit on GRACE TWS and GLDAS TWSC over Lake Chad Basin for the common time period (i.e., 2002–2014).

entropy or minimisation of mutual information between the outputs, which is equivalent to the minimisation of the *Kullback–Leibler* divergence between the joint and the product of the marginal distributions of the outputs (see more details in Ziehe, 2005). However, on grounds of numerical and computational efficiency, our approach uses the joint diagonalisation of the fourth order cumulant matrices (see, Cardoso and Souloumiac, 1993). The cumulant-based method exploits the remote properties of the signals, which include non-Gaussianity, non-stationarity, and spectral non-Flatness (e.g., Ziehe, 2005). Cumulants are empirically computed from higher-order moments, which are estimated from the data. From the Joint Approximate Diagonalisation of Eigen matrices (JADE) approach (Cardoso, 1999; Cardoso and Souloumiac, 1993), this fourth-order cumulant tensor provides the suitable matrices to be diagonalized, which are non-gaussian (see, e.g., Cardoso, 1999; Ziehe, 2005):

$$\mathbf{C}_{ij}(\mathbf{M}) = \sum cum(x_i, x_j, x_u, x_v) \mathbf{M}_{u,v}, \quad (11)$$

such that \mathbf{M} is an arbitrary matrix. After the eigen decomposition of the centred covariance matrix \mathbf{x} , which is aimed at reducing the dimension of the original data, the JADE algorithm performs an approximate joint diagonalisation of the set of eigen matrices of the cumulant tensor with an orthogonal transformation, which comprises a sequence of plane rotations (see, e.g., Ziehe, 2005; Cardoso and Souloumiac, 1993). This cumulant-based methods have been exhaustively described in the pioneering works of Cardoso and Souloumiac (1993), Common (1994), and Cardoso (1999). For further details on numerical steps and mathematical formulations, we refer interested readers to relevant literatures on the subject (see, e.g., Forootan and Kusche, 2012; Theis et al., 2005; Ziehe, 2005; Cardoso and Souloumiac, 1993; Cardoso, 1991; Common, 1994; Cardoso, 1999). While ICA has been previously used to filter and analyse the hydrological signals in GRACE data (see, e.g., Boergens et al., 2014; Forootan and Kusche, 2012; Frappart et al., 2010, 2011), the current study employed ICA for the statistical decomposition of SPI, SSI, and TWS signals over the Lake Chad Basin.

A.3. Comparison of GLDAS TWSC and GRACE-derived TWS over Lake Chad Basin

See Fig. 17.

References

- Adler, R.F., Huffman, G.J., Chang, A., Ferraro, R., Xie, P.-P., Janowiak, J., Rudolf, B., Schneider, U., Curtis, S., Bolvin, D., Gruber, A., Susskind, J., Arkin, P., Nelkin, E., 2003. The version-2 Global Precipitation Climatology Project (GPCP) monthly precipitation analysis (1979Present). *J. Hydrometeorol.* 4 (6), 1147–1167. [http://dx.doi.org/10.1175/1525-7541\(2003\)004<1147:TVGPCP>2.0.CO;2](http://dx.doi.org/10.1175/1525-7541(2003)004<1147:TVGPCP>2.0.CO;2).
- AghaKouchak, A., 2015. A multivariate approach for persistence-based drought prediction: application to the 2010–2011 East Africa drought. *J. Hydrol.* 526, 127–135. <http://dx.doi.org/10.1016/j.jhydrol.2014.09.063>.
- Aires, F., Rossow, W.B., ChéDin, A., 2002. Rotation of EOFs by the independent component analysis: toward a solution of the mixing problem in the decomposition of geophysical time series. *J. Atmos. Sci.* 59, 111–123. [http://dx.doi.org/10.1175/1520-0469\(2002\)059<0111:ROEBT>2.0.CO;2](http://dx.doi.org/10.1175/1520-0469(2002)059<0111:ROEBT>2.0.CO;2).
- Alfa, N.I., Adeofun, C.O., Ologunorisa, E.T., 2008. Assessment of changes in aerial extent of Lake Chad using satellite remote sensing data. *J. Appl. Sci. Environ. Manage.* 12 (1), 101–107.
- Ali, A., Lebel, T., 2009. The Sahelian standardized rainfall index revisited. *Int. J. Climatol.* 29, 1705–1714. <http://dx.doi.org/10.1002/joc.1832>.
- Bader, J., Latif, M., 2011. The 1983 drought in the West Sahel: a case study. *Clim. Dyn.* 36 (3–4), 463–472. <http://dx.doi.org/10.1007/s00382-009-0700-y>.
- Ball, G.H., Hall, D.J., 1965. Isodata, a novel method of data analysis and pattern classification. Technical Report. Stanford Research Institute, Menlo Park, California. Retrieved from: <<http://oai.dtic.mil/oai/oai?verb=getRecord&metadataPrefix=html&identifier=AD0699616>> (accessed 25 March, 2016).
- Baup, F., Frappart, F., Maubant, J., 2014. Combining high-resolution satellite images and altimetry to estimate the volume of small lakes. *Hydrol. Earth Syst. Sci.* 18 (5), 2007–2020. <http://dx.doi.org/10.5194/hess-18-2007-2014>.
- Baur, O., Kuhn, M., Featherstone, W.E., 2009. GRACE-derived ice-mass variations over Greenland by accounting for leakage effects. *J. Geophys. Res.: Solid Earth* 114 (B6), B06407. <http://dx.doi.org/10.1029/2008JB006239>.
- Bazrafshan, J., Hejabi, S., Rahimi, J., 2014. Drought monitoring using the multivariate standardized precipitation index (MSPI). *Water Resour. Manage.* 28, 1045–1060. <http://dx.doi.org/10.1007/s11269-014-0533-2>.
- Bekoe, E.O., Logah, F.Y., 2013. The impact of droughts and climate change on electricity generation in Ghana. *Environ. Sci.* 1 (1), 13–24.
- Belda, S., García-García, D., Ferrándiz, J.M., 2015. On the decorrelation filtering of RL05 GRACE data for global applications. *Geophys. J. Int.* 200, 173–184. <http://dx.doi.org/10.1093/gji/ggu386>.
- Birkett, C.M., 2000. Synergistic remote sensing of Lake Chad: variability of basin inundation. *Remote Sens. Environ.* 72 (218236).

- Boergens, E., Rangelova, E., Sideris, M.G., Kusche, J., 2014. Assessment of the capabilities of the temporal and spatiotemporal ICA method for geophysical signal separation in GRACE data. *J. Geophys. Res. Solid Earth* 119, 4429–4447. <http://dx.doi.org/10.1002/2013JB010452>.
- Bonaccorso, B., Bordi, I., Cancelliere, A., Rossi, G., Sutera, A., 2003. Spatial variability of drought: an analysis of the SPI in Sicily. *Water Resour. Manage.* 17 (4), 273–296. <http://dx.doi.org/10.1023/A:1024716530289>.
- Cardoso, J.-F., 1991. Super-symmetric decomposition of the fourth-order cumulant tensor, blind identification of more sources than sensors. Retrieved from: <<http://perso.telecom-paristech.fr/cardoso/Papers/PDF/jicassp91.pdf>> (accessed 15.01.16).
- Cardoso, J.F., 1999. High-order contrasts for independent component analysis. *Neural Comput.* 11, 157–192.
- Cardoso, J.F., Souloumiac, A., 1993. Blind beamforming for non-gaussian signals. *IEE Proc.* 140 (6), 362–370.
- Cheng, M.K., Tapley, B.D., Ries, J.C., 2013. Deceleration in the Earth's oblateness. *J. Geophys. Res.* 118, 1–8. <http://dx.doi.org/10.1002/jgrb.50058>.
- Coe, M.T., Birkett, C.M., 2004. Calculation of river discharge and prediction of lake height from satellite radar altimetry: example for the Lake Chad basin. *Water Resour. Res.* 40 (10), W10205. <http://dx.doi.org/10.1029/2003WR002543>.
- Coe, M.T., Foley, J.A., 2001. Human and natural impacts on the water resources of the Lake Chad basin. *J. Geophys. Res.* 106 (4), 3349–3356. <http://dx.doi.org/10.1029/2000JD900587>.
- Common, P., 1994. Independent component analysis, a new concept? *Signal Process.* 36, 287–314.
- Descroix, L., Mahé, G., Lebel, T., Favreau, G., Galle, S., Gautier, E., Olivry, J.-C., Albergel, J., Amogu, O., Cappelaeere, B., Dessouassi, R., Diedhiou, A., Bregon, E.L., Mamadou, I., Sighomnou, D., 2009. Spatio-temporal variability of hydrological regimes around the boundaries between Sahelian and Sudanian areas of West Africa: a synthesis. *J. Hydrol.* 375 (12), 90–102. <http://dx.doi.org/10.1016/j.jhydrol.2008.12.012>.
- Diatta, S., Fink, A.H., 2014. Statistical relationship between remote climate indices and West African monsoon variability. *Int. J. Climatol.* 34 (12), 3348–3367. <http://dx.doi.org/10.1002/joc.3912>.
- Dirmeyer, P.A., Guo, Z., Gao, X., 2004. Comparison, validation, and transferability of eight multiyear global soil wetness products. *J. Hydrometeorol.* 5, 1011–1033. <http://dx.doi.org/10.1175/JHM-388.1>.
- Duan, Z., Bastiaanssen, W.G.M., 2013a. Estimating water volume variations in lakes and reservoirs from four operational satellite altimetry databases and satellite imagery data. *Remote Sens. Environ.* 134, 403–416. <http://dx.doi.org/10.1016/j.rse.2013.03.010>.
- Duan, Z., Bastiaanssen, W.G.M., 2013b. First results from version 7 TRMM 3B43 precipitation product in combination with a new downscaling calibration procedure. *Remote Sens. Environ.* 131, 1–13. <http://dx.doi.org/10.1016/j.rse.2012.12.002>.
- Fan, Y., Dool, H.V., 2004. Climate prediction center global monthly soil moisture data set at 0.5° resolution for 1948 to present. *J. Geophys. Res.* 109, D10102. <http://dx.doi.org/10.1029/2003JD004345>.
- FAO, 1997. Irrigation potential in Africa: a basin approach. *FAO Land and Water Bulletin*, 4. Retrieved from: <<https://books.google.com.au/books>> (accessed 28.09.15).
- Farahmand, A., AghaKouchak, A., 2015. A generalized framework for deriving nonparametric standardized drought indicators. *Adv. Water Resour.* (76), 140–145. <http://dx.doi.org/10.1016/j.advwatres.2014.11.012>.
- Forootan, E., Kusche, J., 2012. Separation of global time-variable gravity signals into maximally independent components. *J. Geodesy* 86 (7), 477–497. <http://dx.doi.org/10.1007/s00190-011-0532-5>.
- Frappart, F., Ramillien, G., Leblanc, M., Tweed, S.O., Bonnet, M.-P., Maisongrande, P., 2011. An independent component analysis filtering approach for estimating continental hydrology in the GRACE gravity data. *Remote Sens. Environ.* 115 (1), 187–204. <http://dx.doi.org/10.1016/j.rse.2010.08.017>.
- Frappart, F., Ramillien, G., Maisongrande, P., Bonnet, M.-P., 2010. Denoising satellite gravity signals by independent component analysis. *IEEE Geosci. Remote Sens. Lett.* 7 (3), 421–425. <http://dx.doi.org/10.1109/LGRS.2009.2037837>.
- Gbuyiro, S.O., Ojo, O., Iso, M., Okoloye, C., Idowu, O., 2001. Climate and water resources management. In: *WEDC Conference Zambia*, vol. 27, pp. 383–386. Retrieved from: <www.wedc.lboro.ac.uk/resources/conference/27/Gbuyiro.pdf> (accessed 15.05.15).
- Giannini, A., Salack, S., Lodoun, T., Ali, A., Gaye, A., Ndiaye, O., 2013. A unifying view of climate change in the Sahel linking intra-seasonal, interannual and longer time scales. *Environ. Res. Lett.* 8, 1–8. <http://dx.doi.org/10.1088/1748-9326/8/2/024010>.
- Giannini, A., Saravanan, R., Chang, P., 2003. Oceanic forcing of Sahel rainfall on interannual to decadal time scales. *Science* 302 (5647), 1027–1030. <http://dx.doi.org/10.1126/science.1089357>.
- Gosset, M., Viarre, J., Quantin, G., Alcobá, M., 2013. Evaluation of several rainfall products used for hydrological applications over West Africa using two high-resolution gauge networks. *Quart. J. Roy. Meteorol. Soc.* 139, 923–940. <http://dx.doi.org/10.1002/qj.2130>.
- Greve, P., Orlovsky, B., Mueller, B., Sheffield, J., Reichstein, M., Seneviratne, S.L., 2014. Global assessment of trends in wetting and drying over land. *Nat. Geosci.* 7, 716–721. <http://dx.doi.org/10.1038/NGE02247>.
- Grippa, M., Kergoat, L., Frappart, F., Araud, G., Boone, A., de Rosnay, P., Lemoine, J.M., Gascoin, S., Balsamo, G., Ottl, C., Decharme, B., Saux-Picart, S., Ramillien, G., 2011. Land water storage variability over West Africa estimated by Gravity Recovery and Climate Experiment (GRACE) and land surface models. *Water Resour. Res.* 47 (5), W05549. <http://dx.doi.org/10.1029/2009WR008856>.
- Hao, Z., AghaKouchak, A., 2013. Multivariate standardized drought index: a parametric multi-index model. *Adv. Water Resour.* (57), 12–18. <http://dx.doi.org/10.1016/j.advwatres.2013.03.009>.
- Hao, Z., AghaKouchak, A., 2014. A nonparametric multivariate multi-index drought monitoring framework. *J. Hydrometeorol.* 15 (1), 89–101. <http://dx.doi.org/10.1175/JHM-D-12-0160.1>.
- Hayes, M.J., Svoboda, M.D., Wilhite, D.A., Vanyarko, O.V., 1999. Monitoring the 1996 drought using the standardized precipitation index. *Bull. Am. Meteorol. Soc.* 80, 429–438. [http://dx.doi.org/10.1175/1520-0477\(1999\)080<0429:MTDUTS>2.0.CO;2](http://dx.doi.org/10.1175/1520-0477(1999)080<0429:MTDUTS>2.0.CO;2).
- Hinderer, J., de Linage, C., Boya, J.-P., Gegout, P., Masson, F., Register, Y., Amalvict, M., Pfeffer, J., Littel, F., Luck, B., Bayer, R., Champollion, C., Collard, P., Moigne, N.L., Diament, M., Deroussi, S., de Viron, O., Biancale, R., Lemoine, J.-M., Bonvalot, S., Gabalda, G., Bock, O., Genthon, P., Boucher, M., Favreau, G., Sguis, L., Delclaux, F., Cappelaeere, B., Oi, M., Desclotresh, M., Galleh, S., Laurent, J.-P., Legchenko, A., Bouink, M.-N., 2009. The GHYRAF (Gravity and Hydrology in Africa) experiment: description and first results. *J. Geodyn.* 48, 172–181. <http://dx.doi.org/10.1016/j.jog.2009.09.014>.
- Huang, S., Huang, Q., Chang, J., Zhu, Y., Leng, G., Xing, L., 2015. Drought structure based on a nonparametric multivariate standardized drought index across the Yellow River basin, China. *J. Hydrol.* 530, 127–136. <http://dx.doi.org/10.1016/j.jhydrol.2015.09.042>.
- Huffman, G.J., Adler, R.F., Bolvin, D.T., Gu, G., 2009. Improving the global precipitation record: GPCP version 2.1. *Geophys. Res. Lett.* 36 (17), L17808. <http://dx.doi.org/10.1029/2009GL040000>.
- Huffman, G.J., Adler, R.F., Bolvin, D.T., Gu, G., Nelkin, E.J., Bowman, K.P., Hong, Y., Stocker, E.F., Wolff, D.B., 2007. The TRMM Multisatellite Precipitation Analysis (TMPA): quasi-global, multiyear, combined-sensor precipitation estimates at fine scales. *J. Hydrometeorol.* 8, 38–55. <http://dx.doi.org/10.1175/JHM560.1>.
- Inogwabini, B.-I., Sandokan, B.M., Ndunda, M., 2006. A dramatic decline in rainfall regime in the Congo Basin: evidence from a thirty four-year data set from the Mabali scientific research centre, Democratic Republic Of Congo. *Int. J. Meteorol.* 31 (312), 278–285.
- Jolliffe, I.T., 2002. *Principal component analysis*, .. Springer Series in Statistics, second ed. Springer, New York.
- Komuscu, A.U., 1999. Using the SPI to analyze spatial and temporal patterns of drought in Turkey. *Drought Network News* 11 (1), 7–13.
- Kummerow, C., Simpson, J., Thiele, O., Barnes, W., Chang, A.T.C., Stocker, E., Adler, R. F., Hou, A., Kakar, R., Wentz, F., Ashcroft, P., Kozu, T., Hong, Y., Okamoto, K., Iguchi, T., Kuroiwa, H., Im, E., Haddad, Z., Huffman, G., Ferrier, B., Olson, W.S., Zipser, E., Smith, E.A., Wilhelm, T.T., North, G., Krishnamurti, T., Nakamura, K., 2000. The status of the Tropical Rainfall Measuring Mission (TRMM) after two years in orbit. *J. Appl. Meteorol.* 39 (12), 1965–1982. [http://dx.doi.org/10.1175/1520-0450\(2001\)040<1965:TSOTTR>2.0.CO;2](http://dx.doi.org/10.1175/1520-0450(2001)040<1965:TSOTTR>2.0.CO;2).
- Kusche, J., 2007. Approximate decorrelation and non-isotropic smoothing of time-variable GRACE-type gravity field models. *J. Geodesy* 81 (11), 733–749. <http://dx.doi.org/10.1007/s00190-007-0143-3>.
- Landerer, F.W., Swenson, S.C., 2012. Accuracy of scaled GRACE terrestrial water storage estimates. *Water Resour. Res.* 48 (4), W04531. <http://dx.doi.org/10.1029/2011WR011453>.
- Lebel, T., Ali, A., 2009. A physical basis for the interannual variability of rainfall in the Sahel. *Quart. J. Roy. Meteorol. Soc.* 375 (1–2), 5264. <http://dx.doi.org/10.1016/j.jhydrol.2008.11.030>.
- Lebel, T., Cappelaeere, B., Galle, S., Hanan, N., Kergoat, L., Levis, S., Vieux, B., Descroix, L., Gosset, M., Mougin, E., Peugeot, C., Seguis, L., 2009. AMMA-CATCH studies in the Sahelian region of West-Africa: an overview. *J. Hydrol.* 375 (12), 3–13.
- Leblanc, M., Leduc, C., Razack, M., Lemoalle, J., Dagorne, D., Mofor, L., 2003. Applications of remote sensing and GIS for groundwater modelling of large semiarid areas: example of the Lake Chad Basin, Africa. *Hydrol. Mediterr. Semiarid Regions* (278), 186–191, proceedings of the international symposium held at Montpellier, April 2003.
- Lemoalle, J., Bader, J.-C., Leblanc, M., Sedick, A., 2012. Recent changes in Lake Chad: observations, simulations and management options (19732011). *Global Planet. Change* 8081, 247–254. <http://dx.doi.org/10.1016/j.gloplacha.2011.07.004>.
- Li, B., Rodell, M., 2015. Evaluation of a model-based groundwater drought indicator in the conterminous U.S. *J. Hydrol.* 526, 78–88. <http://dx.doi.org/10.1016/j.jhydrol.2014.09.027>.
- Lloyd-Hughes, B., 2012. A spatio-temporal structure-based approach to drought characterisation. *Int. J. Climatol.* 32 (3), 406–418. <http://dx.doi.org/10.1002/joc.2280>.
- Long, D., Longuevergne, L., Scanlon, B.R., 2015. Global analysis of approaches for deriving total water storage changes from GRACE satellites. *Water Resour. Res.* 51 (4), 2574–2594. <http://dx.doi.org/10.1002/2014WR016853>.
- Loon, A.F.V., 2015. Hydrological drought explained. *WIRES Water* 2, 359–392. <http://dx.doi.org/10.1002/wat2.1085>.
- Lopez, T., Antoine, R., Kerr, Y., Darrozes, J., Rabinowicz, M., Ramillien, G., Cazenave, A., Genthon, P., 2016. Subsurface hydrology of the Lake Chad Basin from convection modelling and observations. *Surv. Geophys.* 37 (2), 471–502. <http://dx.doi.org/10.1007/s10712-016-9363-3>.
- Masih, I., Maskey, S., Mussá, F.E.F., Trambauer, P., 2014. A review of droughts on the African continent: a geospatial and long-term perspective. *Hydrol. Earth Syst. Sci.* 18 (9), 3635–3649. <http://dx.doi.org/10.5194/hess-18-3635-2014>.
- McKee, T.B., Doeskin, N.J., Kieist, J., 1993. The relationship of drought frequency and duration to time scales. In: *Conference on Applied Climatology*, American

- Meteorological Society, Boston, Massachusetts, pp. 179–184. Retrieved from: <www.ccc.atmos.colostate.edu/relationshipofpofdroughtfrequency.pdf> (accessed 27.06.14).
- Mohino, E., Rodriguez-Fonseca, B., Losada, T., Gervois, S., Janicot, S., Bader, J., Ruti, P., Chauvin, F., 2011. Changes in the interannual SST-forced signals on West African rainfall. AGCM intercomparison. *Clim. Dyn.* 37 (9–10), 1707–1725. <http://dx.doi.org/10.1007/s00382-011-1093-2>.
- Moore, P., Williams, S.D.P., 2014. Integration of altimetry lake levels and GRACE gravimetry over Africa: Inferences for terrestrial water storage change 2003–2011. *Water Resour. Res.* 50, 9696–9720. <http://dx.doi.org/10.1002/2014WR015506>.
- Ndehedehe, C.E., Awange, J., Agutu, N., Kuhn, M., Heck, B., 2016a. Understanding changes in terrestrial water storage over West Africa between 2002 and 2014. *Adv. Water Resour.* 88, 211–230. <http://dx.doi.org/10.1016/j.advwatres.2015.12.009>.
- Ndehedehe, C.E., Awange, J.L., Corner, R., Kuhn, M., Okwuashi, O., 2016b. On the potentials of multiple climate variables in assessing the spatio-temporal characteristics of hydrological droughts over the Volta Basin. *Sci. Total Environ.*, 819–837 <http://dx.doi.org/10.1016/j.scitotenv.2016.03.004>.
- Nicholson, S., 2013. The West African Sahel: a review of recent studies on the rainfall regime and its interannual variability. *ISRN Meteorol.* 2013 (453521), 1–32. <http://dx.doi.org/10.1155/2013/453521>.
- Nicholson, S.E., Some, B., Kone, B., 2000. An analysis of recent rainfall conditions in West Africa, including the rainy seasons of the 1997 El Niño and the 1998 La Niña Years. *J. Clim.* 13 (14), 2628–2640. [http://dx.doi.org/10.1175/1520-0442\(2000\)013<2628:AAORRC>2.0.CO;2](http://dx.doi.org/10.1175/1520-0442(2000)013<2628:AAORRC>2.0.CO;2).
- Odada, E.O., Oyebande, L., Oguntola, J.A., 2005. Lake Chad. Experience and Lessons Learned Briefed, pp. 75–91. Retrieved from: <www.worldlakes.org/uploads/06-Lake-Chad-27February2006.pdf> (accessed 05.10.15).
- Okonkwo, C., Demoz, B., Gebremariam, S., 2014. Characteristics of Lake Chad level variability and links to ENSO, precipitate, and river discharge. *Sci. World J.* 13 (4), 13. <http://dx.doi.org/10.1155/2014/145893>.
- Okonkwo, C., Demoz, B., Onyeukwu, K., 2013. Characteristics of drought indices and rainfall in Lake Chad Basin. *Int. J. Remote Sens.* 34 (22), 7945–7961. <http://dx.doi.org/10.1080/01431161.2013.827813>.
- Paeth, H., Fink, A., Pöhle, S., Keis, F., Machel, H., Samimi, C., 2012. Meteorological characteristics and potential causes of the 2007 flood in sub-Saharan Africa. *Int. J. Climatol.* 31, 1908–1926. <http://dx.doi.org/10.1002/joc.2199>.
- Reager, J.T., Thomas, B.F., Famiglietti, J.S., 2014. River basin flood potential inferred using GRACE gravity observations at several months lead time. *Nat. Geosci.* 7 (8), 588–592. <http://dx.doi.org/10.1038/ngeo2203>.
- Reynolds, R.W., Rayne, N.A., Smith, T.M., Stokes, D.C., Wang, W., 2002. An improved in situ and satellite SST analysis for climate. *J. Clim.* 15 (3), 1609–1625. [http://dx.doi.org/10.1175/1520-0442\(2002\)0153C1609:AIISAS3E2.0.CO;2](http://dx.doi.org/10.1175/1520-0442(2002)0153C1609:AIISAS3E2.0.CO;2).
- Rodell, M., Houser, P.R., Jambor, U., Gottschalk, J., Mitchell, K., Meng, K., Arsenault, C.J., Cosgrove, B., Radakovich, J., Bosilovich, M., Entin, J.K., Walker, J.P., Lohmann, D., Toll, D., 2004. The global land data assimilation system. *Bull. Am. Meteorol. Soc.* 85 (3), 381–394. <http://dx.doi.org/10.1175/BAMS-85-3-381.R>.
- Rodriguez-Fonseca, B., Janicot, S., Mohino, E., Losada, T., Bader, J., Caminade, C., Chauvin, F., Fontaine, B., Garca-Serrano, J., Gervois, S., Joly, M., Polo, I., Ruti, P., Roucou, P., Voldoire, A., 2011. Interannual and decadal SST-forced responses of the West African monsoon. *Atmos. Sci. Lett.* 12, 67–74. <http://dx.doi.org/10.1002/asl.308>.
- Rouault, M., Richard, Y., 2003. Intensity and spatial extension of drought in South Africa at different time scales. *Water SA* 29 (4), 489–500.
- Santos, J.A.F., Pulido-Calvo, I., Portela, M.M., 2010. Spatial and temporal variability of droughts in Portugal. *Water Resour. Res.* 46 (3), W03503. <http://dx.doi.org/10.1029/2009WR008071>.
- Schewe, J., Heinke, J., Gerten, D., Haddeland, I., Arnell, N.W., Clark, D.B., Dankers, R., Eisner, S., Fekete, B.M., Colón-González, F.J., Gosling, S.N., Kim, H., Liu, X., Masaki, Y., Portmann, F.T., Satoh, Y., Stacke, T., Tang, Q., Wada, Y., Wisser, D., Albrecht, T., Frieler, K., Piontek, F., Warszawski, L., Kabat, P., 2013. Multimodel assessment of water scarcity under climate change. *PNAS* 111 (9), 3245–3250. <http://dx.doi.org/10.1073/pnas.1222460110>.
- Shukla, S., Wood, A.W., 2008. Use of a standardized runoff index for characterizing hydrologic drought. *Geophys. Res. Lett.* 35 (2), L02405. <http://dx.doi.org/10.1029/2007GL032487>.
- Svoboda, M., Hayes, M., Wood, D., 2012. Standardized precipitation index user guide. World Meteorological Organization, WMO-No 1090, Geneva. Retrieved from: <<http://www.wamis.org/agm/pubs/SPI/WMO-1090-EN.pdf>> (accessed 13.04.16).
- Swenson, S., Chambers, D., Wahr, J., 2008. Estimating geocenter variations from a combination of GRACE and ocean model output. *Geophys. Res. Lett.* 31, 1–4. <http://dx.doi.org/10.1029/2004GL019920>.
- Swenson, S., Wahr, J., 2002. Methods for inferring regional surface-mass anomalies from Gravity Recovery and Climate Experiment (GRACE) measurements of time-variable gravity. *J. Geophys. Res.-Solid Earth* 107 (B9). <http://dx.doi.org/10.1029/2001jb000576>.
- Tapley, B., Bettadpur, S., Watkins, M., Reigber, C., 2004. The gravity recovery and climate experiment: mission overview and early results. *Geophys. Res. Lett.* 31, 1–4. <http://dx.doi.org/10.1029/2004GL019920>.
- Theis, F.J., Gruber, P., Keck, I.R., Meyer-bse, A., Lang, E.W., 2005. Spatiotemporal blind source separation using double-sided approximate joint diagonalization. In: *Proc. EUSIPCO 2005*.
- Tourian, M., Elmi, O., Chen, Q., Devaraju, B., Roohi, S., Sneeuw, N., 2015. A spaceborne multisensor approach to monitor the desiccation of Lake Urmia in Iran. *Remote Sens. Environ.* 156, 349–360. <http://dx.doi.org/10.1016/j.rse.2014.10.006>.
- Vassolo, S., 2012. Groundwater need assessment Lake Chad Basin. Institute for Geosciences and Natural Resources. Retrieved from: <http://splash-era.net/downloads/groundwater/9_LCBC_final_report.pdf> (accessed 03.11.15).
- Vicente-Serrano, S.M., 2006. Spatial and temporal analysis of droughts in the Iberian Peninsula (19102000). *Hydrol. Sci. J.* 51 (1), 83–97. <http://dx.doi.org/10.1623/hysj.51.1.83>.
- Wahr, J., Molenaar, M., Bryan, F., 1998. Time variability of the Earth's gravity field: hydrological and oceanic effects and their possible detection using GRACE. *J. Geophys. Res.-Solid Earth* 103 (B12), 30205–30229. <http://dx.doi.org/10.1029/98jb02844>.
- Wald, L., 1990. Monitoring the decrease of Lake Chad from space. *Geocart Int.* 5 (3), 31–36. <http://dx.doi.org/10.1080/10106049009354266>.
- Werth, S., Gntner, A., Schmidt, R., Kusche, J., 2009. Evaluation of GRACE filter tools from a hydrological perspective. *Geophys. J. Int.* 179 (3), 1499–1515.
- Wouters, B., Bonin, J.A., Chambers, D.P., Riva, R.E.M., Sasgen, I., Wahr, J., 2014. GRACE, time-varying gravity, earth system dynamics and climate change. *Rep. Prog. Phys.* 77 (11), 116801. <http://dx.doi.org/10.1088/0034-4885/77/11/116801>.
- Wouters, B., Schrama, E.J.O., 2007. Improved accuracy of GRACE gravity solutions through empirical orthogonal function filtering of spherical harmonics. *Geophys. Res. Lett.* 34 (23), L23711. <http://dx.doi.org/10.1029/2007GL032098>.
- Yirdaw, S.Z., Snelgrove, K., Agboma, C., 2008. GRACE satellite observations of terrestrial moisture changes for drought characterization in the Canadian Prairie. *J. Hydrol.* 356, 84–92.
- Ziehe, A., 2005. Blind Source Separation based on Joint Diagonalization of Matrices with Applications in Biomedical Signal Processing (Ph.D. thesis). Universität Potsdam. Retrieved from: <<http://en.youscribe.com/catalogue/reports-and-theses/knowledge/blind-source-separation-based-on-joint-diagonalization-of-matrices-1424347>> (accessed 15.05.15).



Contents lists available at ScienceDirect

Science of the Total Environment

journal homepage: www.elsevier.com/locate/scitotenv

On the potentials of multiple climate variables in assessing the spatio-temporal characteristics of hydrological droughts over the Volta Basin



Christopher E. Ndehedehe^{a,*}, Joseph L. Awange^{a,b}, Robert J. Corner^a, Michael Kuhn^a, Onuwa Okwuashi^c

^a Western Australian Centre for Geodesy, The Institute for Geoscience Research Curtin University, Perth, Australia

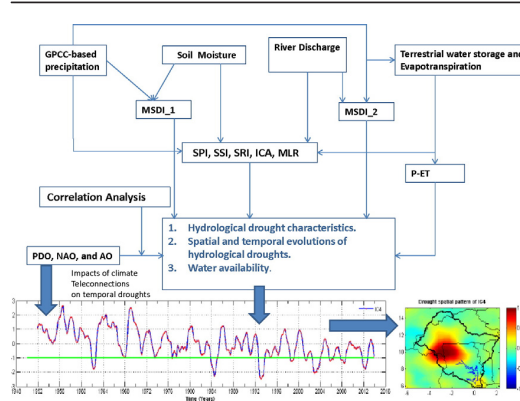
^b Department of Cartographic Engineering, UFPE Federal University of Pernambuco, Brazil

^c Department of Geoinformatics & Surveying, University of Uyo, P.M.B. 1017, Uyo, Nigeria

HIGHLIGHTS

- A new method for spatio-temporal hydrological drought analysis.
- Multiple drought indicators used in assessing drought characteristics.
- The MSDI shows an improved skill in hydrological drought monitoring.
- Burkina Faso and the Lake Volta areas are frequent drought zones.
- Possible influence of Pacific Decadal Oscillations in the wet and dry regimes.

GRAPHICAL ABSTRACT



ARTICLE INFO

Article history:

Received 28 January 2016

Received in revised form 2 March 2016

Accepted 2 March 2016

Available online xxxx

Editor: D. Barcelo

Keywords:

Soil moisture
River discharge
Drought
Volta basin
SPI
Rainfall

ABSTRACT

Multiple drought episodes over the Volta basin in recent reports may lead to food insecurity and loss of revenue. However, drought studies over the Volta basin are rather generalised and largely undocumented due to sparse ground observations and unsuitable framework to determine their space-time occurrence. In this study, we examined the utility of standardised indicators (standardised precipitation index (SPI), standardised runoff index (SRI), standardised soil moisture index (SSI), and multivariate standardised drought index (MSDI)) and Gravity Recovery and Climate Experiment (GRACE) derived terrestrial water storage to assess hydrological drought characteristics over the basin. In order to determine the space-time patterns of hydrological drought in the basin, Independent Component Analysis (ICA), a higher order statistical technique was employed. The results show that SPI and SRI exhibit inconsistent behaviour in observed wet years presupposing a non-linear relationship that reflects the slow response of river discharge to precipitation especially after a previous extreme dry period. While the SPI and SSI show a linear relationship with a correlation of 0.63, the correlation between the MSDIs derived from combining precipitation/river discharge and precipitation/soil moisture indicates a significant value of 0.70 and shows an improved skill in hydrological drought monitoring over the Volta basin during the study period. The ICA-derived spatio-temporal hydrological drought patterns show Burkina Faso and the Lake Volta areas as

* Corresponding author. Tel.: +61470307034.

E-mail address: christopherndehedehe@gmail.com (C.E. Ndehedehe).

predominantly drought zones. Further, the statistically significant negative correlations of pacific decadal oscillations (0.39 and 0.25) with temporal evolutions of drought in Burkina Faso and Ghana suggest the possible influence of low frequency large scale oscillations in the observed wet and dry regimes over the basin. Finally, our approach in drought assessment over the Volta basin contributes to a broad framework for hydrological drought monitoring that will complement existing methods while looking forward to a longer record of GRACE observations.

© 2016 Elsevier B.V. All rights reserved.

1. Introduction

As a catchment shared by six riparian countries (i.e., Ghana, Burkina Faso, Togo, Ivory Coast, Benin, and Mali), the Volta basin (Fig. 1), which lies between latitudes 5°N to 14°N and longitudes 2°E to 5°W with an approximate area of 400,000 km², is one of the poorest regions in Africa (Kasei et al., 2010). The region depends highly on rain-fed agriculture for its livelihood. Consequently, food security, the agrarian system, and economic development are threatened and highly vulnerable to the unreliable rainfall in the region (e.g., Lacombe et al., 2012). Kasei et al. (2010), specifically reported that the high variability in spatio-temporal rainfall distribution pattern was the major cause of fluctuation in food production while Bekoe and Logah (2013) showed that the hydrological drought years of 1983, 1998, 2003, and 2006 in the basin, which were evident from the strong decline of Lake Volta (a major physiographic feature in the basin) water levels, owing to rainfall decline, triggered limited production of electricity. Besides the seldom or rather infrequent scientific discussion probably due to limited and incomplete hydrological records, the drought story for the Volta basin is highly generalised due to lack of a suitable method to determine its spatio-temporal patterns.

Apparently, frequent extreme hydro-meteorological conditions (e.g., droughts and floods) may increase in the region due to the impacts of climate variability and coupled atmosphere-ocean phenomenon on rainfall variability. Climate phenomena is expected to exacerbate extreme drought tendencies and delayed rainfall in the Volta basin, where historical evidence from farmers suggests a seasonal forward shift in the onset of rain season (see, e.g., Giesen et al., 2010). This is probably true as global drying trends due to climate warming will ultimately impact on changes in hydrological conditions of the land surface. Also, the multiple strings of drought episodes in recent times, besides their negative impacts on water and energy balance (Owusu and Waylen, 2009), may have significant impacts on the economy and the agrarian system of the basin. For example, while food production was below normal in Ghana during the 1983 drought, food shortages of more than 50% in Burkina Faso were recorded (Kasei et al., 2010). Further, given that approximately 27% of Ghana's 238,540 km² land surface area is actually being cultivated, under a predominantly rain-fed agricultural system such as the Volta basin, the limited alimentation due to reduced rainfall in the northern boundary of mid-Ghana as reported by Owusu and Waylen (2013), is likely to prevent the cultivation of crops leading to food insecurity.

Away from Ghana, Burkina Faso which occupies 46.4% of the Volta basin (i.e., two-thirds of Burkina Faso is within the Volta basin) is one of the least urbanized countries in the world with about 90% of its population actively involved in the agricultural sector (see, Giesen et al., 2002). This level of active participation in rain-fed agriculture implies that if the observed drying trends in the Sahel (Greve et al., 2014), the shift in the onset of rainy season, and the 4th Assessment Report of the Intergovernmental Panel on Climate Change (IPCC), which re-emphasizes the dry gets drier paradigm (see, Giesen et al., 2010), are projections to go by, the region may be worst hit by food insecurity and poverty. In fact, in a recent study of local scale assessment and drought prediction (see, Nichol and Abbas, 2015), West Africa has been mentioned as one of the regions of the world that will be more susceptible to droughts due to climate change, leading to greater loss of

livelihoods. From studies of precipitation sheds, it has been reported that even a small decline in rainfall could have tremendous impacts on agricultural yields in societies that rely on rain-fed agriculture (see, Keys et al., 2014, 2012). In view of the foregoing, understanding the space-time evolution of drought occurrence in the region will only be a logical step that unarguably can support comprehensive regional adaptation strategies, such as growing rain-fed crop cultivars (Giesen et al., 2010) and building water infrastructures that can increase water storage for future use, especially during extreme dry periods.

Unlike the Sahel region of West Africa, studies on drought in the Volta basin are relatively few and largely undocumented. This lack of regional studies on drought can partly be attributed to lack of ground-based information, as traditional gauge measurements are inconsistent, incomplete, and difficult to retrieve, owing to government bureaucracies, logistics, and the high cost of managing reliable in-situ stations over large heterogeneous landscapes. Considering the regional nature of drought, understanding their regional context in terms of their space-time development is critical. Furthermore, drought studies in the Volta basin, besides being less regional in nature, have only employed precipitation as a major climate variable. The problem with this, is that drought analyses based on a single climate variable (e.g., rainfall) for a region with high spatio-temporal variability, may not sufficiently describe drought phenomena in terms of its propagation and characteristics such as onset, duration, severity, frequency and intensity (e.g., Hao and AghaKouchak, 2014).

Further, Hao and AghaKouchak (2013, 2014) argued that for tropical regions, deficit in precipitation may not lead to a deficit in soil moisture, given the fact that agricultural drought (i.e., deficit in soil moisture) responds rather slowly to a meteorological drought (i.e., precipitation deficit) condition with some time lag. Following recent recommendation of using multiple climate variables (e.g., rainfall, river discharge, lake levels, groundwater, etc.) in studying hydrological drought characteristics (Long et al., 2015), a composite drought indicator, therefore, may significantly improve our understanding of hydrological drought (deficit in water availability usually in the form of low river discharge, abnormally low water levels in lakes, stream flow records, and groundwater level) characteristics (e.g., onset, duration, severity, frequency and intensity) over the basin.

However, few studies on the hydro-climatological conditions of the basin have been reported in recent times. Oguntunde et al. (2006) investigated hydrological variability and trends in the Volta River Basin during the period 1901–2002. They reported a higher runoff of 87.5 mm/yr with coefficient of variation of 41.5% before dam construction compared to the post-dam period, when average runoff was 73.5 mm/yr and less varied (i.e., with coefficient of variation of 23.9%). Increased variability and declining rainfall totals associated with El-Niño Southern Oscillation (ENSO) phenomenon was reported by Owusu et al. (2008) as one of the devastating hydro-climatological changes in the basin. Furthermore, analysing long term precipitation data over Ghana for the period between 1951 and 2000, Owusu and Waylen (2009) reported large scale rainfall deficit with potential impacts on vegetation cover, water balance, and surface albedo that can trigger long-term below-normal rainfall. Using standardised precipitation index (SPI), Kasei et al. (2010) showed that the frequency of droughts in the Volta basin has increased since the 1970s. Also, trends in rainfall series were investigated at 16 stations in Ghana during the

188

period of 1960–2005 using a resampling-based Mann-Kendall test statistics (Lacombe et al., 2012). Analysing daily rainfall data for the period between 1951 and 2000, Owusu and Waylen (2013) observed a widespread decline of mean rainfall totals and number of rain days during the minor rainy seasons. These aforementioned studies, though topical on the general drying trends and the hydrological conditions in the region, are highly generalised and less regional in nature. The implication of drought and hydrological studies that are less regional in nature is that observed trends and patterns that may be misconstrued as insignificant in a particular location (i.e., at a local or less regional scale), might be significant when evaluated at a regional scale (e.g., Lacombe et al., 2012).

Further, the influence of local relief and the general southward shift in the seasonal movement of the Inter-Tropical Convergence Zone (ITCZ) are largely responsible for the rainfall variability in the basin (Lacombe et al., 2012; Owusu and Waylen, 2009). While rainfall in the Sahel region has a single peak mostly in summer, rainfall in the Guinea region, where the southern basin is located has a bimodal (i.e., two periods of wet seasons) seasonal distribution with two peaks occurring between May/October, with a short dry period (e.g., Ndehedehe et al., 2016; Odekunle and Eludoyin, 2008) in July/August separating the two peaks in rainfall (see, e.g., Lacombe et al., 2012; Owusu and Waylen, 2009). Hence, as argued by Owusu and Waylen (2009), the failure in the rainfall regime of a particular region does not necessarily mean the same for the other regions. Considering that different ocean circulation patterns and competing multiple physical mechanisms (Druyan, 2011) drive the variability of rainfall in the region, most drought related studies that have been reported in the region (see, e.g., Bekoe and Logah, 2013; Lacombe et al., 2012; Kasei et al., 2010)

are rather generalised and not fully representative of the prevailing hydro-climatological condition of the basin at the time. Such generalisations may not be very useful for effective and robust planning of water resources and regional adaptation strategies in the event of extreme hydro-meteorological conditions (e.g., droughts and floods). With the north-south dichotomy in the rainfall mechanisms of the dry Sahel and wet Guinea regions of the Volta basin, a suitable methodology to monitor the space-time occurrence of drought episodes becomes essential.

In this contribution, we combine multiple hydrological quantities such as in-situ river discharge, Global Precipitation Climatology Centre (GPCC) based precipitation, soil moisture, evapotranspiration, and terrestrial water storage (TWS) derived from Gravity Recovery and Climate Experiment (GRACE, Tapley et al., 2004) in order to investigate the spatio-temporal characteristics of hydrological droughts and water storage changes over the Volta basin. GRACE-derived TWS has been widely used in the field of hydrology and studies of mass transport (see, e.g., Fukuda et al., 2009; Ramillien et al., 2008; Swenson and Wahr, 2007; Crowley et al., 2006) and represents the total sum of integrated water storage from catchment stores (i.e., groundwater, aquifer, soil moisture, and biomass water). We capitalize on GRACE observations to estimate the spatio-temporal trends in TWS over the basin, which like previous studies in the basin (see, e.g., Ferreira and Asiah, 2015; Ferreira et al., 2014), will be useful in understanding the basin's TWS and its water footprint, a measure of human's use of freshwater resources (e.g., Hoekstra and Mekonnen, 2012). In order to understand the space-time patterns and development of hydrological droughts over the basin, we used a higher order statistical decomposition method of independent component analysis (ICA, see, e.g., Cardoso, 1999;

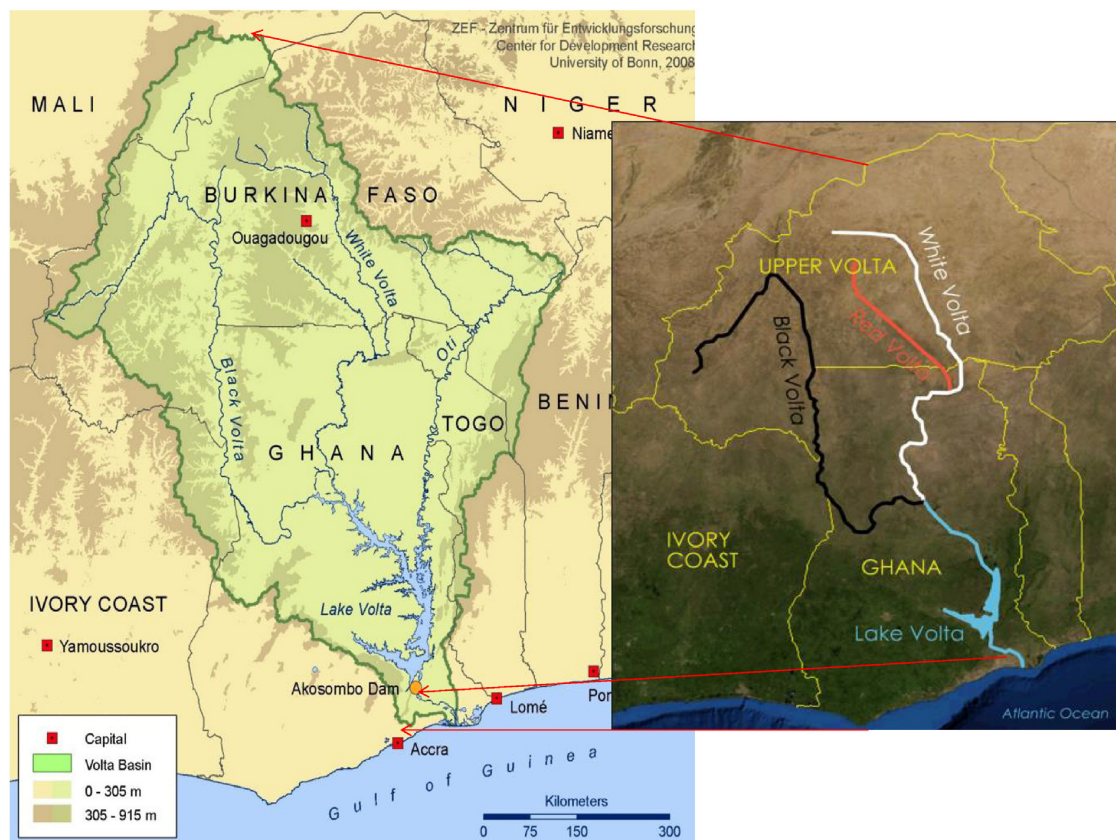


Fig. 1. Study area showing the riparian countries of the Volta Basin and the Lake Volta area in Ghana. The Volta river system comprising the Black Volta, White Volta, and the Oti river is also indicated. Original Map adapted from <http://www.21stcentech.com/wp-content/uploads/2013/12/Volta-River-basin.jpg>.

189 Common, 1994; Cardoso and Souloumiac, 1993) to localise the drought signals over the entire basin. The ICA approach, which enables the extraction of localised drought signals is different from previous studies (see, e.g., Bazrafshan et al., 2014; Santos et al., 2010) that have analysed spatio-temporal drought events in other regions of the world using principal component analysis (PCA, see, e.g., Jolliffe, 2002; Preisendorfer, 1988). The use of a statistical decomposition method such as the ICA is very helpful in understanding drought spatial variations and its temporal evolutions over the Volta basin, where a suitable framework for drought monitoring is lacking.

In addition, besides the use of standardised precipitation index (SPI, McKee et al., 1995; McKee et al., 1993), standardised soil moisture index (SSI, e.g., Mishra and Singh, 2010), and standardised runoff index (SRI, Shukla and Wood, 2008) to monitor hydrological drought of the Volta basin, we also used multivariate standardised index (MSDI, Hao and AghaKouchak, 2014; Farahmand and AghaKouchak, 2015) to evaluate the effectiveness of rainfall, soil moisture, and river discharge in capturing hydrological drought characteristics such as frequency (how often a drought event occurs), persistence, severity (the intensity of a drought event), and cessation. Specifically, this study aims at (i) characterising hydrological droughts over the Volta basin using multiple drought indicators such as SPI, SRI, SSI, and MSDI and (ii) characterising and localising space-time evolutions of hydrological drought patterns and TWS over the Volta basin.

While we provide a background information on the generalisations of drought patterns in Section 2, further details on the formulations of ICA and the results of the study are presented in Sections 3 and 4, respectively.

2. On the generalisations of drought patterns

Owing to the influence of strong spatial variability of rainfall at annual scale coupled with the mean inter-annual climatological gradients across the region, the use of a single mean SPI computed from averaged rainfall data in estimating drought conditions over the Sahel hides the underlying spatial variability of the index (see, e.g., Ali and Lebel, 2009). As pointed out in Section 1, this may lead to generalisations of wet/dry regimes and might not be very helpful for modelling and planning purposes. Also, differences in the spatial resolutions of hydrological data, seasonal patterns, and influence of multiple ocean-atmosphere systems through the so-called climate teleconnections may complicate our understanding of drought evolutions and the water footprints of the region. Regardless of differences in the spatial resolution of the data and climatic zones and the influence of ocean-atmosphere systems, drought analysis from a spatio-temporal point of view can improve our understanding of drought occurrences and persistence.

The PCA method has been employed in spatio-temporal drought analysis thereby addressing some of these problems (see, e.g., Bazrafshan et al., 2014; Santos et al., 2010; Bonaccorso et al., 2003). To optimise on the performance of the PCA method, our approach employs a higher order statistical method, ICA, to localise the decomposed drought signals (SPI and SSI) obtained from the PCA process, by rotating them towards statistical independence. Further discussions on the proposed method and the standardised indicators are detailed in Section 3. The space-time evolutions of SPI and SSI through ICA then enables us to understand hydrological drought processes, their impacts and characteristics such as the onset, duration, intensity and spatial extent (Loon, 2015).

Furthermore, previous drought studies have associated hydrological drought with precipitation deficit on longer time scales such as 6, 9, 12, and 24 months cumulations (see, e.g., Li and Rodell, 2015; Lloyd-Hughes, 2012; Santos et al., 2010; Nalbantis and Tsakiris, 2009; Hayes, 2007; Vicente-Serrano, 2006; Rouault and Richard, 2003; Hayes et al., 1999; Komuscu, 1999). More recently, it has been shown that region averaged groundwater drought index from the Princeton forced catchment land surface model (CLSM) and in-situ groundwater

observations, exhibited stronger correlation with SPI at 12 and 24 month cumulation, reflecting the lagged response of groundwater to rainfall anomalies (Li and Rodell, 2015). To this end, in our spatio-temporal drought analysis, we used long term precipitation and soil moisture data, covering a 63-year period (1950–2013) to characterise and quantify hydrological drought frequency and severity in the basin. Also, similar to Li and Rodell (2015), Santos et al. (2010) and Hayes et al. (1999) we used 12 and 24 month's cumulations of SPI and SSI, hypothesizing that this longer time scales for the rainfall and soil moisture drought indices will provide the capability to monitor drought and wet conditions suitable for hydrological applications in the Volta basin.

3. Data and method

3.1. Data

3.1.1. Gravity Recovery and Climate Experiment (GRACE)

The GRACE (Tapley et al., 2004) satellite mission, which has been in operation since March 2002, provides an integrated sum of changes in catchment stores (e.g., groundwater, soil moisture, etc.) based on observations of the Earth's time variable gravity fields. The GRACE Release-05 (RL05) spherical harmonic coefficients from Center for Space Research (CSR), truncated at degree and order 60 and covering the period from April 2002 to October 2014 was used in the study to estimate TWS. Since GRACE does not provide changes in degree 1 gravity coefficients (i.e., C_{10} , C_{11} , and S_{11}), and is also affected by large tide-like aliases in the degree 2 coefficients (i.e., C_{20}), we followed conventional procedures of using degree 1 gravity coefficients that are determined from ocean and atmospheric models (Swenson et al., 2008) and substituting degree 2 coefficients with estimates from satellite laser ranging (Cheng et al., 2013). The spherical harmonic coefficients are thereafter filtered using the DDK2 decorrelation filter of Kusche et al. (2009) in order to reduce the effect of correlated noise. Equivalent water heights (hereafter called TWS) are then derived on a $1^\circ \times 1^\circ$ grid from the filtered monthly solutions following the method of Wahr et al. (1998):

$$\Delta S(\phi, \lambda, t) = \frac{R\rho_{ave}}{3Q_w} \sum_{l=0}^{l_{max}} \frac{2l+1}{1+k_l} \sum_{m=-l}^l P_{lm}(\phi, \lambda) \Delta Y_{lm}(t), \quad (1)$$

where ΔS is the change in TWS for each month in time (t), and where ϕ, λ are latitudes and longitudes respectively. R is the radius of the Earth taken to be 6378.137 km, ρ_{ave} is the average density of the Earth (5515 kg/m^3), ρ_w is the average density of water (1000 kg/m^3), k_l is the load Love numbers of degree l , P_{lm} are the normalized associated Legendre functions of degree l and order m with $l_{max} = 60$ and ΔY_{lm} are the normalized complex spherical harmonic coefficients after subtracting the long term mean. The DDK2 decorrelation filter with a degree of smoothing corresponding to that of a Gaussian filter with a 340 km radius (Kusche et al., 2009) causes a reduction in the amplitude of observed GRACE signal (e.g., Wouters and Schrama, 2007; Baur et al., 2009). This was remedied by following approaches in previous studies (see, e.g., Long et al., 2015; Landerer and Swenson, 2012; Fenoglio-Marc et al., 2012), where a scale factor derived from hydrological models was used to account for the impact of the filtering on GRACE observations. The data gaps for the 12 missing months in the GRACE-TWS solutions were filled through an interpolation method that uses values at neighboring data points. Further, averaged TWS values over the basin, were computed using the area weighted average (see, e.g., Tourian et al., 2015; Sneeuw et al., 2014):

$$\Delta W(\chi; t) = \sum_{i=1}^n \Delta W(\phi_i, \lambda_i, t) \frac{A_i}{A_\chi}, \quad (2)$$

where χ is the basin index, n is the number of pixels in the basin, A_i is the area of the grid cell i in χ and A_χ is the total area of χ .

3.1.2. Global Precipitation Climatology Centre (GPCC)

The monthly gridded GPCC (Schneider et al., 2014; Becker et al., 2013) based precipitation product covering the period 1950 to 2014 is used in the study for the construction of SPI and long-term rainfall analysis over the Volta basin. The $0.5^\circ \times 0.5^\circ$ GPCC data, which is accessible through the GPCC download site (<http://www.ftp.dwd.de/pub/data/gpcc/html/down/loadgate.html>) was also combined with in-situ river discharge to estimate MSDI over the basin. The GPCC based precipitation uses about 67,200 rain gauge stations over global land areas and has been compared with other in-situ based precipitation such as the Global Precipitation Climatology Project (GPCP) (see Schneider et al., 2014). Specifically, over West Africa the GPCC based precipitation shows good agreement with Tropical Rainfall Measuring Mission (TRMM), which has been validated over the region [e.g., Awange et al., 2016; Ndehedehe et al., 2016; Paeth et al., 2012; Nicholson et al., 2003].

3.1.3. Climate Prediction Center (CPC) soil moisture

Monthly CPC soil moisture data (Fan and Dool, 2004), at spatial resolution of $0.5^\circ \times 0.5^\circ$ was used for spatio-temporal drought analysis through the construction of SSI over the basin. Also, averaged time series of soil moisture over the basin was combined with GPCC-based precipitation to construct MSDI, in addition to deriving SSI. The CPC soil moisture data is estimated using more than 17,000 rain gauges worldwide and monthly global temperature from reanalysis. The data used in this study covers the period between 1950 and 2014 and is freely available at National Oceanic and Atmospheric Administration's (NOAA) website for download (<http://www.esrl.noaa.gov/psd/data/gridded/data.cpcsoil.html>).

3.1.4. MODIS global terrestrial evapotranspiration project

The improved version of MODIS global terrestrial evapotranspiration products by Mu et al. (2011) was combined with precipitation in this study to estimate net precipitation, a measure of the maximum available renewable freshwater resource. The data, which has a spatial resolution of $0.5^\circ \times 0.5^\circ$ covers the period 2000–2014 and is available for download at the Earth Observing System of NASA's website (<http://www.nts.gov/umt.edu/project/mod16>).

3.1.5. In-situ river discharge data

Observed monthly discharge rates at Akosombo Dam, in Ghana were used to construct SRI. It was also combined with the GPCC-based precipitation to construct MSDI in order to analyse hydrological drought over the basin. The data covering the period 1979–2012 was obtained from the Water Research Institute of Ghana.

3.1.6. Climate teleconnection indices

In order to examine the possible connections of observed temporal evolutions of the statistically decomposed drought signals over the Volta basin with coupled atmosphere-ocean system, relevant global climate teleconnection indices such as the North Atlantic Oscillation (NAO), Pacific Decadal Oscillation (PDO) and Arctic Oscillation (AO) were investigated through correlation analysis. In particular, PDO has been linked to the decadal variability of Sahel rainfall (e.g., Rodriguez-Fonseca et al., 2011) while the influence of NAO on the local climate of the region has been reported (e.g., Okonkwo, 2014). Time series of these data sets covering the period 1950–2013 were downloaded from NOAA's website (<http://www.ncdc.noaa.gov/teleconnections>).

3.2. Method

3.2.1. Multiple linear regression analysis (MLRA)

This study used a multiple linear regression model to parameterize the cosine and sine harmonic components (i.e., the annual and semi-annual signals) of monthly GRACE-derived TWS changes. This is

obtained as

$$\mathbf{D} = \mathbf{X} - (\beta_0 + \beta_2 \sin(2\pi t) + \beta_3 \cos(2\pi t) + \beta_4 \sin(4\pi t) + \beta_5 \cos(4\pi t)), \quad (3)$$

where \mathbf{D} is the deseasonalized GRACE-derived TWS with harmonic components removed, \mathbf{X} is the data, β_0 is the constant offset, β_2 and β_3 accounts for the annual signals while β_4 and β_5 represents the semi-annual signals. The annual signals of TWS were separated from the GRACE-TWS and the residual, which comprises the semi-annual signals and trends were further analysed using the ICA method (see Section 3.2.2).

3.2.2. Statistical decomposition methods

ICA (see, e.g., Cardoso and Souloumiac, 1993; Cardoso, 1999), a higher order statistical technique usually referred to as blind source separation in signal processing (e.g., Cardoso, 1999) has emerged as a more suitable alternative in the decomposition of multivariate data into statistically independent signals. Recently, it has been used to separate relevant geophysical signals into their statistically independent components (see, e.g., Boergens et al., 2014; Awange et al., 2014; Forootan et al., 2012; Frappart et al., 2011). We have used it as an improvement to the PCA method, which has been applied to analyse drought signals and spatio-temporal variability of TWS in previous studies (e.g., Ndehedehe et al., 2016; Santos et al., 2010; Bonaccorso et al., 2003). In this study, it is used to localise drought signals over the Volta basin in order to provide a better understanding of the space-time patterns of droughts. Prior to implementing ICA, the PCA method is used to identify statistically significant modes of variability in the computed gridded SPI, SSI values and GRACE-derived TWS. Subsequently, the derived statistically significant patterns are further explored through a classical rotation of the principle components, using the Joint Approximate Diagonalisation of Eigen matrices (JADE) algorithm fully described in Cardoso and Souloumiac (1993) and Cardoso (1999). The JADE algorithm is statistical based and follows a Jacobi technique (so called because they seek to maximize measures of independence by a technique similar to the Jacobi method of diagonalization) in the process of orthogonal contrast optimization, different from other ICA online solutions that uses the gradient techniques (Cardoso, 1999). Fundamentally, ICA decomposes a data matrix $x_i(t)$, which consist of a number of statistically independent source signals $s_j(t)$ where t is the time index. This can be expressed as (e.g., (Ziehe, 2005))

$$x_i(t) = \sum A_{ij} s_j(t), \quad (i = 1, \dots, n, j = 1, \dots, m), \quad (4)$$

x_i in Eq. (4) is the mixing model or the linear mixture and can be represented as a matrix for notational convenience as

$$\mathbf{X} = \mathbf{A}\mathbf{S}, \quad (5)$$

where the entries of the data matrix \mathbf{X} are samples of the $x_i(t)$ given in Eq. (4) leading to column vectors $x[t] = [x_1[t], \dots, x_n[t]]^T$, the $n \times m$ matrix \mathbf{A} has elements $A_{i,j}$ and the source signals i.e., matrix \mathbf{S} , similar to the construction of \mathbf{X} , has column vectors $s[t] = [s_1[t], \dots, s_m[t]]^T$. Two major challenges of ICA lies in the definition of a measure of independence and the choice of algorithms to find the change of basis (or separating matrix) that fully optimizes this measure (Cardoso, 1999). These measures of independence are based on cumulant-based blind identification of the separation matrix. The fourth-order cumulant matrix is expressed as

$$C_{i,j}(\mathbf{M}) = \sum \mathbf{M}_{u,v} cum(x_i, x_j, x_u, x_v), \quad (6)$$

where \mathbf{M} is an arbitrary matrix (see, e.g., Ziehe, 2005). The plane rotations are applied to these Cumulant-based matrices to estimate the independent components through a multiplicative update of an

191 estimate of the separation matrix. Further theoretical details of these cumulant-based methods and ICA in general are provided in the works of Cardoso (1991); Cardoso and Souloumiac (1993); Common (1994); Cardoso (1999); Ziehe (2005); Theis et al. (2005) and Forootan and Kusche (2012). The ICA algorithm available at <http://perso.telecom-paristech.fr/cardoso/Algo/Jade/jadeR.m> was used to decompose standardised drought indicators (SPI and SSI data) and GRACE-derived TWS into spatial and temporal patterns. After the decomposition, the independent components were normalized using their standard deviations to be unitless. Each ICA mode is a combination of the temporal and spatial patterns and are usually interpreted together (i.e., the unit-less temporal evolution is multiplied with the spatial pattern in order to obtain the actual values).

3.2.3. Standardised drought indices

A drought index is a significant variable used for the assessment of the impacts of droughts and defining several drought properties such as duration, severity, intensity, and spatial extent (Mishra and Singh, 2010). In this study, four different drought indices (SPI, SSI, SRI, and MSDI) were used to quantify and analyse a drought event. Our standardised drought indices follow the non-parametric approaches of Hao and AghaKouchak (2014) and Farahmand and AghaKouchak (2015) where instead of gamma distribution function, an empirical approach was used to derive the marginal probability using the univariate form of the Gringorten plotting position (Gringorten, 1963). The joint

distribution of two variables X and Y expressed as

$$P(X \leq x, Y \leq y) = \rho, \quad (7)$$

where ρ represents the joint probability of any two variables (e.g., rainfall and soil moisture). The joint probability is used to define the MSDI (Hao and AghaKouchak, 2013) as

$$MSDI = \phi^{-1}(\rho), \quad (8)$$

where ϕ^{-1} is the standard normal distribution function. For the bivariate case, the Gringorten plotting position formula (Gringorten, 1963) reported by Farahmand and AghaKouchak (2015) is used to estimate the empirical joint probability. The empirical Gringorten plotting position is expressed as

$$p(x_k, y_k) = \frac{m_k - 0.44}{n + 12}, \quad (9)$$

where n is the number of the observation and m_k is the number of times which the pair (x_i, y_i) occurs for $x_i \leq x_k$ and $y_i \leq y_k$ ($1 \leq i \leq n$). Eq. (9) is applied in Eq. (8) to estimate the MSDI while the SPI, SSI, and SRI are also estimated using the univariate form of Eq. (9). Since it has been argued that a single drought index may not satisfactorily describe different aspects of drought onset, duration and termination (see Farahmand and AghaKouchak, 2015; Hao and AghaKouchak, 2014, 2013), we combined

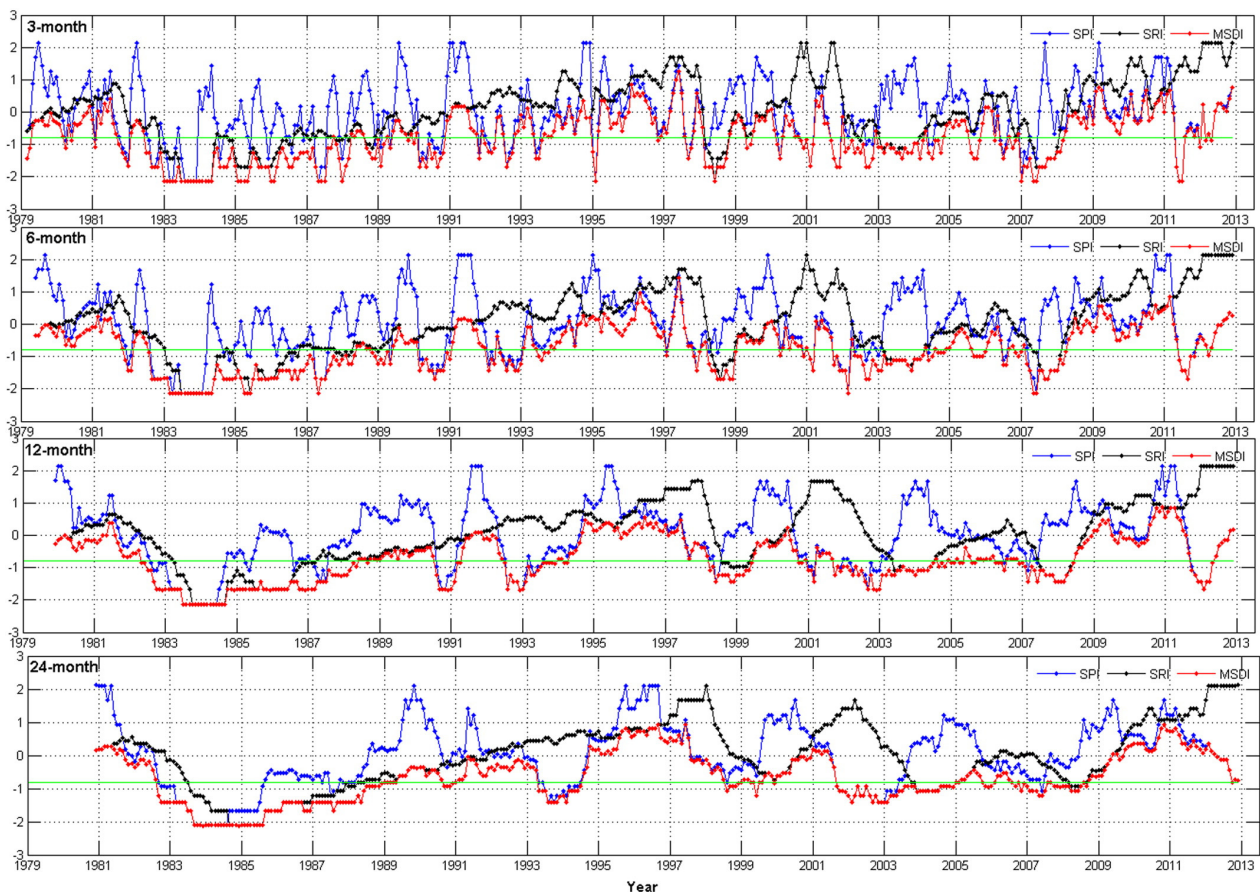


Fig. 2. Time series of standardised drought indicators (SPI, SRI, and MSDI) for the Volta basin based on GPCP-based precipitation and in-situ river discharge data at Akosombo station covering the period 1979–2013. MSDI is derived through the combination of GPCP-based precipitation and in-situ river discharge. These standardised drought indicators are based on empirical probability. The green solid line is drought threshold based on the description of McKee et al. (1993). (For interpretation of the references to color in this figure legend, the reader is referred to the web version of this article.)

192

on one hand, rainfall and river discharge data and on the other hand, rainfall and soil moisture data to estimate two different sets of MSDI over the basin, in addition to the single indicators (i.e., SPI, SSI, and SRI). Add to this, the gridded drought indicators (i.e., SPI and SSI) at 12 and 24 month time scales were also estimated and statistically decomposed using the ICA method (see Section 3.2.2) in order to understand their spatio-temporal variability for hydrological applications. The relationship between the two categories of MSDIs was obtained through Pearson correlation analysis while the relationship between the pairs SPI/SSI, and SRI/SPI was also examined through the same process.

4. Results and discussions

4.1. The potential of standardised indicators in characterising hydrological drought

Hydrological droughts refer to the period with insufficient water in the hydrological system. This is usually evident in shortages of surface and sub-surface water resources for established use and relevant applications in a given water resources management system (Mishra and Singh, 2010). The lack of comprehensive in-situ observations at local

or regional scales has encouraged the use of proxies and indices to quantify hydrological droughts (Kumar et al., 2015). To this end, we assessed the capability of three different standardised indicators (SPI, SRI, SSI) and their corresponding multi-index (MSDI), constructed using a non-parametric approach (Hao and AghaKouchak, 2014). The drought threshold level was defined similar to the SPI values of McKee et al. (1993) in order to support a better understanding of drought severity, duration, and intensity.

Results for the computed drought indices for 3, 6, 12, and 24 months cumulation over the Volta basin using a 34-year data record are indicated in Figs. 2 and 3. Two MSDIs were derived by combining rainfall and river discharge (Fig. 2) and rainfall and soil moisture (Fig. 3). Despite the poor correlation between SPI and SRI (0.11), the acknowledged hydrological drought years of 1983/1984, 1997/1998, 2003 and 2006/2007 that resulted in electricity power rationing in Ghana (Bekoe and Logah, 2013) have been captured by the two indices in all monthly cumulations (Fig. 2). Extreme wet periods tend to exhibit some lagged relationships, reflecting some significantly slow response of discharge (SRI) to extreme wet condition (SPI), especially after a previous extreme dry period. For instance, over longer time scales (i.e., 6, 12 and 24 months), the SRI responded to the extreme wet conditions of

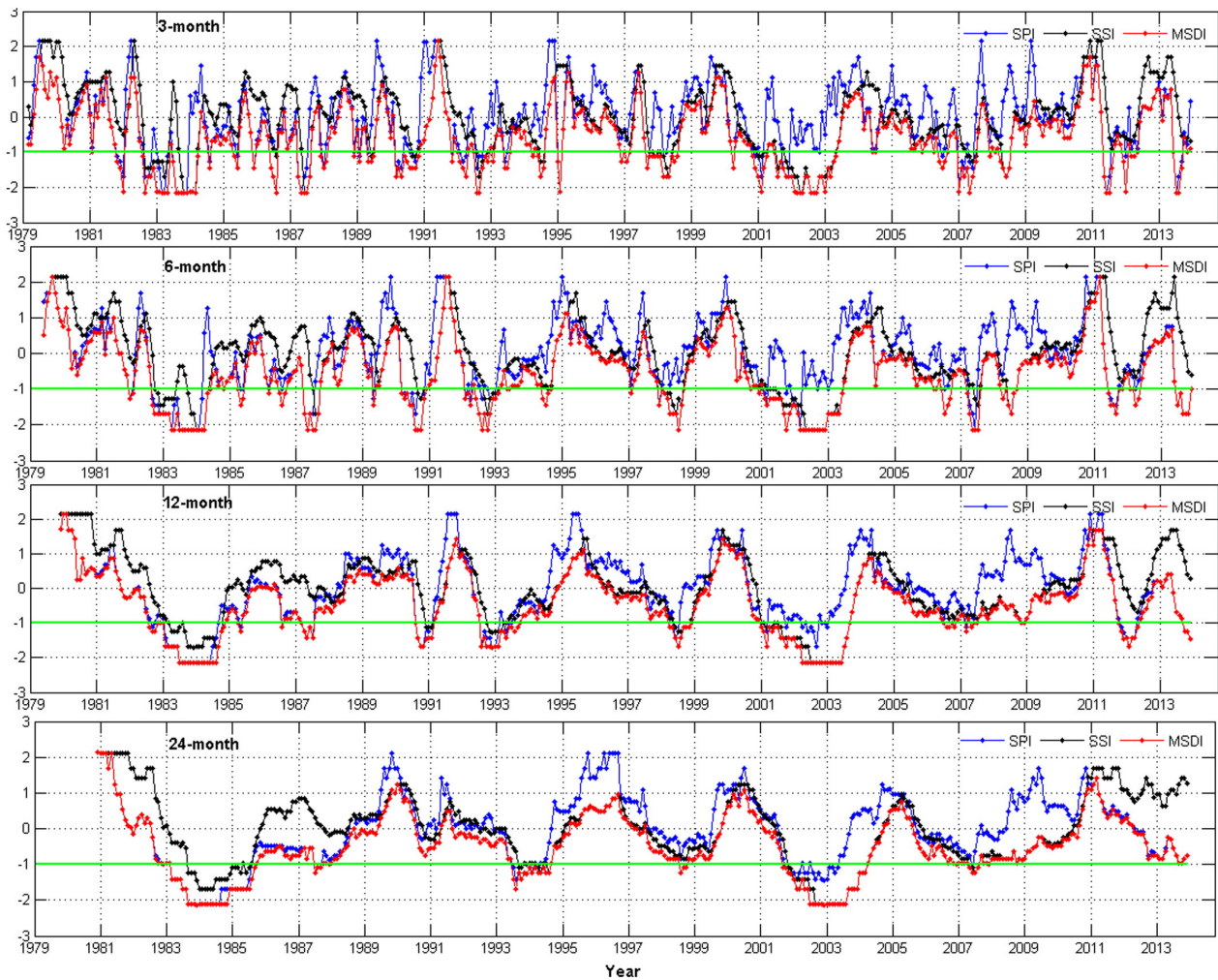


Fig. 3. Time series of standardised drought indicators (SPI, SSI, and MSDI) for the Volta basin based on GPCP-based precipitation and CPC soil moisture data covering the period 1979–2013. MSDI is derived through the combination of GPCP-based precipitation and CPC soil moisture. These standardised drought indicators are based on empirical probability. The green solid line is drought threshold based on McKee et al. (1993) description. (For interpretation of the references to color in this figure legend, the reader is referred to the web version of this article.)

1989, 1991, 1995 as a gradual rise starting from 1989 and peaking at 1997 (Fig. 2), a known hydrological drought year in the basin. Still on the relationship of rainfall and river discharge in the Volta basin, Friesen et al. (2005), observed that runoff had a much higher coefficient of variation (CV) (0.38) for the period between 1931 and 2005 while rainfall had a CV of 0.08 during the same period, leading to a non-linear response that amplified small changes in rainfall to large changes in runoff. Generally, the hydrological behaviour of the basin indicates some time lag (about 1–2 years) between the response of discharge to wet and dry conditions, in addition to a non-linear behaviour that could be amplified by the impacts of ocean circulations and perturbations on annual and seasonal rainfall. From our SPI result (Figs. 2 and 3), 2003 was a rather wet year consistent with the findings of Bekoe and Logah (2013). However, the SRI and the corresponding MSDI both indicated severe drought conditions in 2003 and 2004 in all time scales. This can be attributed to the impact of the previous drought years (2001/2002), indicating the filtering effect of the catchment storage conditions. Also, this kind of out-of-phase relationship or rather inconsistent behaviour, which was also reported by Hao and AghaKouchak (2013) for a different study, can also result from abnormally high precipitation lasting for a short period of time, while several other months within the same year remain dry (e.g., the 2007 period in the basin shows the same behaviour due to an ENSO event).

By and large, the MSDI derived from the combination of SPI and SRI demonstrates substantially a level of consistency and reliability in that the true representation of the hydrological drought situation is highlighted as the low water level of Lake Volta in 2003 (see, Fig. 2) actually resulted in limited hydro-power generation. It seems that profound and extreme drought conditions over the basin do have a rather strong signature that makes these hydrological quantities (e.g., rainfall, river discharge, and soil moisture) respond to its onset, persistence and termination. For example, despite the rather weak correlation of 0.11 at 95% confidence level between SPI and SRI, the acknowledged extreme hydrological drought years of 1983–1985, 1998, and early 2007 are all captured by the two indices. Further, it can be argued that due to increased irrigation schemes in the basin (e.g., Andreini et al., 2002) leading to increased use of surface waters in Burkina Faso, the inflow into the lower Volta basin in Ghana (i.e., the Lake Volta) where the river discharge at Akosombo station is observed will be largely reduced. Consequently, this may limit the potential of river discharge in assessing a hydrological drought condition in the basin.

However, as observed in Fig. 2, an estimated lead time of 1–2 years can be applied to accumulation periods of 6, 12, and 24 month SPI in order to forecast a hydrological drought condition over the basin. For instance, the hydrological drought condition of 2011/2012 from the SPI 6 and 12 month accumulation period (Fig. 2) will be evident in the discharge rate in 2013/2014 period. This was confirmed in the satellite

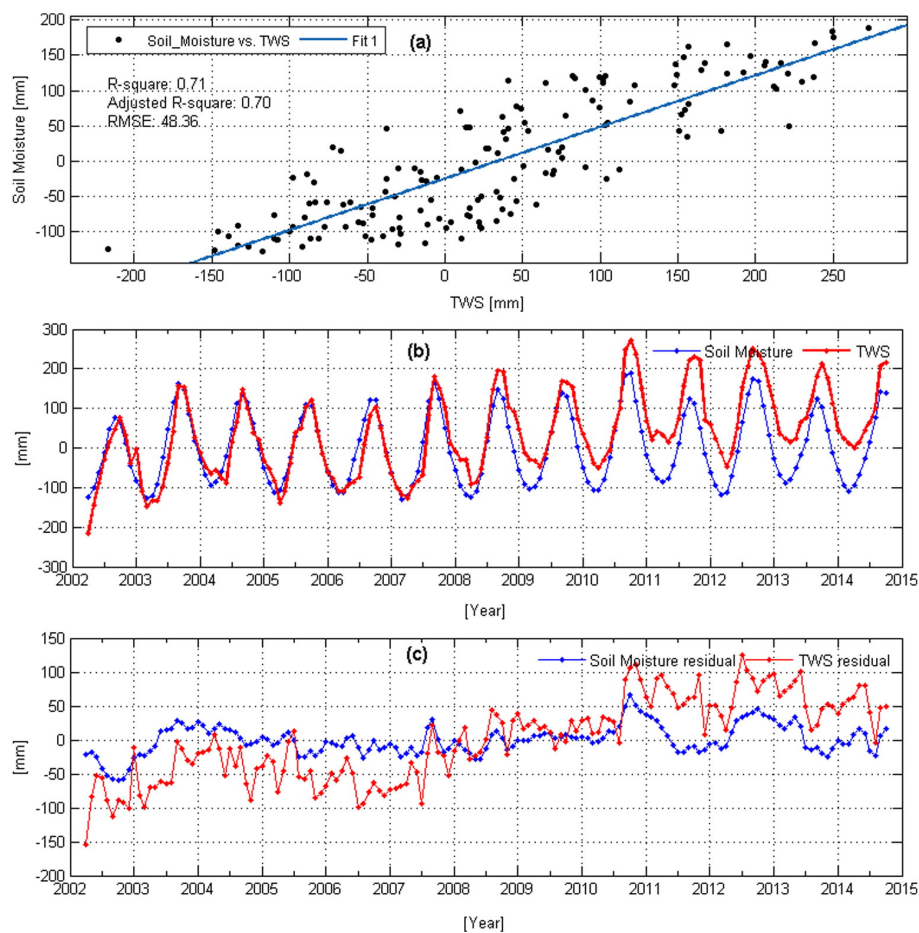


Fig. 4. Relationship of TWS anomalies and soil moisture over the Volta basin covering the period 2002–2014. (a) Regression fit on GRACE-derived TWS changes and soil moisture change. (b) Temporal variations of averaged TWS changes and soil moisture over the Volta basin. (c) Time series of deseasonalized averaged TWS changes and soil moisture (i.e. after removing the annual and semiannual components).

194 altimetry data (not shown) where Lake Volta, which is formed by the Akosombo Dam in Ghana is already showing a relatively strong negative anomaly in water levels similar to the 2003 and 2007 period observed in this study (see, Fig. 2).

On the other hand, SPI and SSI showed a significant correlation of 0.63 (i.e., at 12 month scale) at 95% confidence level indicating consistency in observed wet and dry periods (Fig. 3). At longer time scales, the SPI/SSI-derived MSDI has shown that the drought conditions of 2001/2002 persisted till 2003, in addition to indicating well known hydrological drought years of 1983/1984, 1997/1998, 2002/2003, 2006/2007 mentioned previously (Fig. 3). Also, SPI and SSI have shown some consistent behaviour that indicates a linear relationship with almost no time lag over the basin. In some studies (Kumar et al., 2015), the effectiveness of SPI as a meteorological drought index in translating precipitation deficits to a hydrological drought condition has been questioned probably due to its non-linear relationship with other hydrological variables, e.g., groundwater and river discharge, which is also observed in the current study. However, at longer time scales, (Li and Rodell (2015) recently showed that changes in groundwater are tightly coupled to precipitation variability, which could be in the short term (i.e., SPI 6 month cumulation) or long term (i.e., SPI 12 and 24 month cumulation). Apparently, this relationship between rainfall and groundwater and other catchment stores (e.g., aquifer, sub-surface and runoff) can be influenced by the depth to the water table and precipitation rates as the land surface part of the hydrological

cycle acts as a low-pass filter to the meteorological forcings (e.g., Loon, 2015; Li and Rodell, 2015).

Further, Bonsor and MacDonald (2011) and MacDonald et al. (2012) demonstrated the importance of rainfall and geomorphology/ weathering parameters as input for developing and estimating groundwater maps showing depth over Africa.

Much of the Volta basin, especially the seasonally wet areas (e.g., Ghana and Togo) as shown in the developed groundwater map of Africa (MacDonald et al., 2012) are regions with the shallowest groundwater-levels (i.e., <7 mgl) compared to the Central Sahel (i.e., the region North of the basin) where depth to groundwater ranges from 50 to 250 mgl. Given the relationship between rainfall and other hydrological quantities such as recharge, runoff, groundwater and discharge, the propagation of a meteorological drought (SPI) in the Volta basin to a hydrological drought condition is inferred, consistent with Bloomfield and Marchant (2013) who observed a good correlation and a site-specific relationship between standardised groundwater level index and SPI in a similar study in the UK.

In view of this, we align with the fact that observed precipitation and soil moisture deficits at 12 and 24 month accumulations over the Volta basin are typical of hydrological droughts as indicated in recent studies (Li and Rodell, 2015; Joetzjer et al., 2013; Lloyd-Hughes, 2012; Santos et al., 2010; Nalbantis and Tsakiris, 2009; Hayes, 2007). While it is true that prolonged precipitation deficit fundamentally reduces alimentionation of a given hydrologic system, Loon (2015) remarked that the

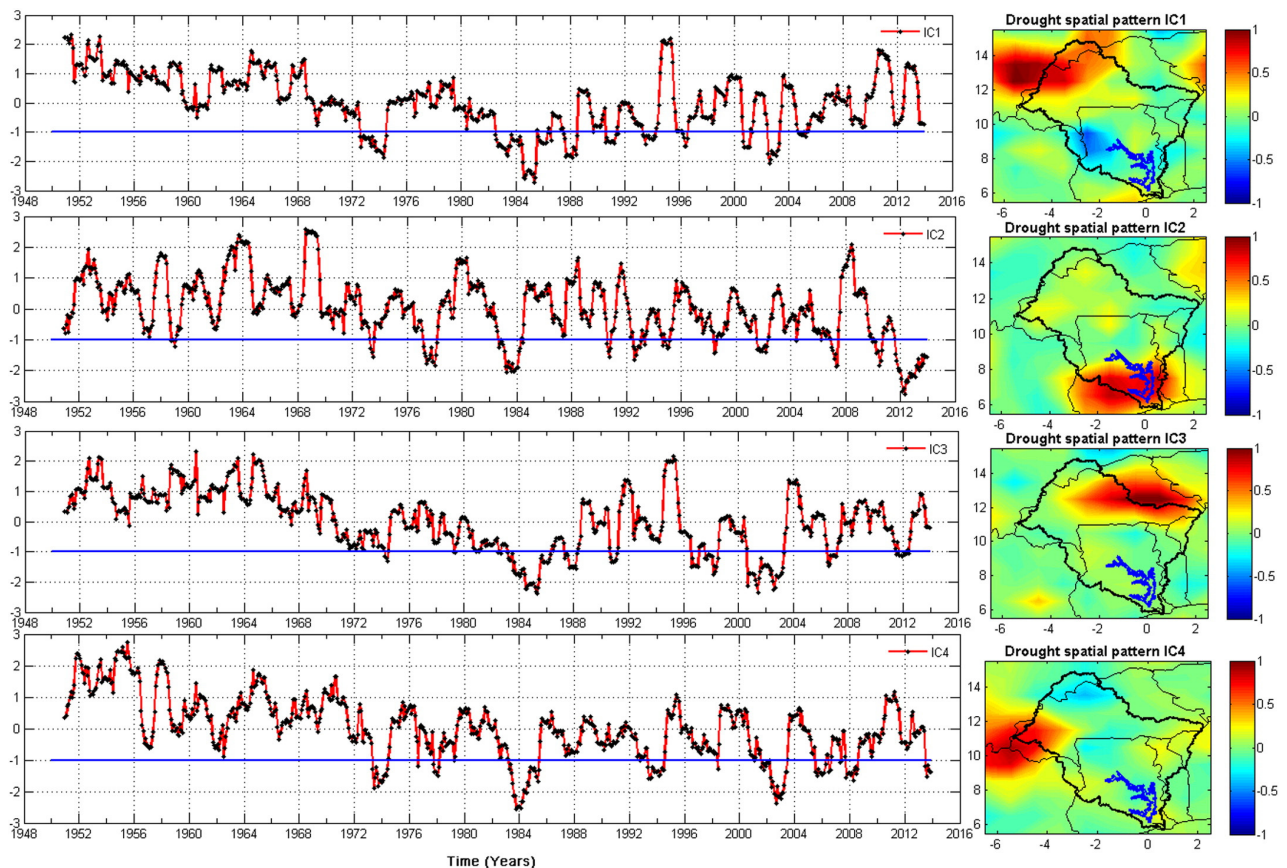


Fig. 5. ICA-derived spatio-temporal hydrological drought patterns over the Volta basin using 12-month gridded SPI values. SPI values are computed using GPCC-based precipitation for the period 1950–2013. The variability of the ICA modes (i.e., the spatial and temporal drought patterns) for the decomposed SPI values within the basin are 10.7%, 6.7%, 6.6%, and 6.3% for IC1, IC2, IC3, and IC4, respectively. Actual SPI values for drought classification and categorisation are jointly derived from the localised spatial drought pattern (right) and their corresponding temporal evolutions (left). The blue solid line shows the drought threshold based on McKee et al. (1993) description. (For interpretation of the references to color in this figure legend, the reader is referred to the web version of this article.)

195 depletion of soil moisture storage leads to decreased recharge and decline in groundwater levels.

Interestingly, the correlation between the two MSDIs computed using rainfall/river discharge and rainfall/soil moisture show a good correlation of 0.70 at 95% confidence level, indicating consistency in drought and wet periods captured (see, Figs. 2 and 3). The multi-index approach (i.e., the MSDI), which assesses drought based on multiple variables links individual drought indicators (i.e., SPI, SRI, and SSI) into a composite model (Farahmand and Aghakouchak, 2015), thereby providing a more robust assessment of droughts. Due to its improved skill and the capability to feature drought onset and persistence, the use of MSDI (in longer aggregation time scales such as 12 and 24 month) to analyse hydrological drought over the Volta basin is recommended.

4.2. Spatio-temporal variability of hydrological drought over the Volta basin

The spatio-temporal variability of hydrological drought was investigated using long term GPCP-based precipitation and CPC soil moisture data. While the use of SPI at longer time scales as hydrological drought proxies have been reported (e.g., Li and Rodell, 2015; Loon, 2015; Bloomfield and Marchant, 2013; Santos et al., 2010), the use of SSI in similar context is largely undocumented. To this end, we examined the potential of soil moisture as a surrogate for TWS over the Volta

basin, in order to effectively quantify drought events significant to hydrological applications. This has been achieved through a least squares fit. The regression fit between rainfall and soil moisture over the basin showed adjusted R^2 of 0.7 indicating that most parts of the basin are consistent with observed trends and variability in TWS (see, Fig. 4a and b). Besides the significant correlation of 0.84 at 95% confidence level observed between the two variables (i.e., TWS and soil moisture), the period between 2002 and 2007 as indicated in Fig. 4b appears to have temporal variations with similar strong peaks (i.e., maximum and minimum).

However, after removing the annual and semi-annual signals from the time series of the two variables using the MLRA (see Section 3.2.1), the correlation between the residual TWS and soil moisture (this include the trends and other signals) show a significant correlation value of 0.61 at 95% confidence level (Fig. 4c). However, the observed regression fit (Fig. 4a) makes it reasonable to employ soil moisture for a quantitative hydrological drought assessment over the Volta basin, especially with the limited availability of GRACE observations. The observed temporal variability between averaged TWS and soil moisture (Fig. 4b) leads us to the assumption that there were probably no significant subsurface storage changes in GRACE-derived TWS over the basin during 2002–2007 as this period was largely characterised by hydrological droughts (see, MSDI of Fig. 2 at all monthly cumulations) and pronounced low lake level changes, in addition to the lack of significant positive trend in rainfall in the last decade

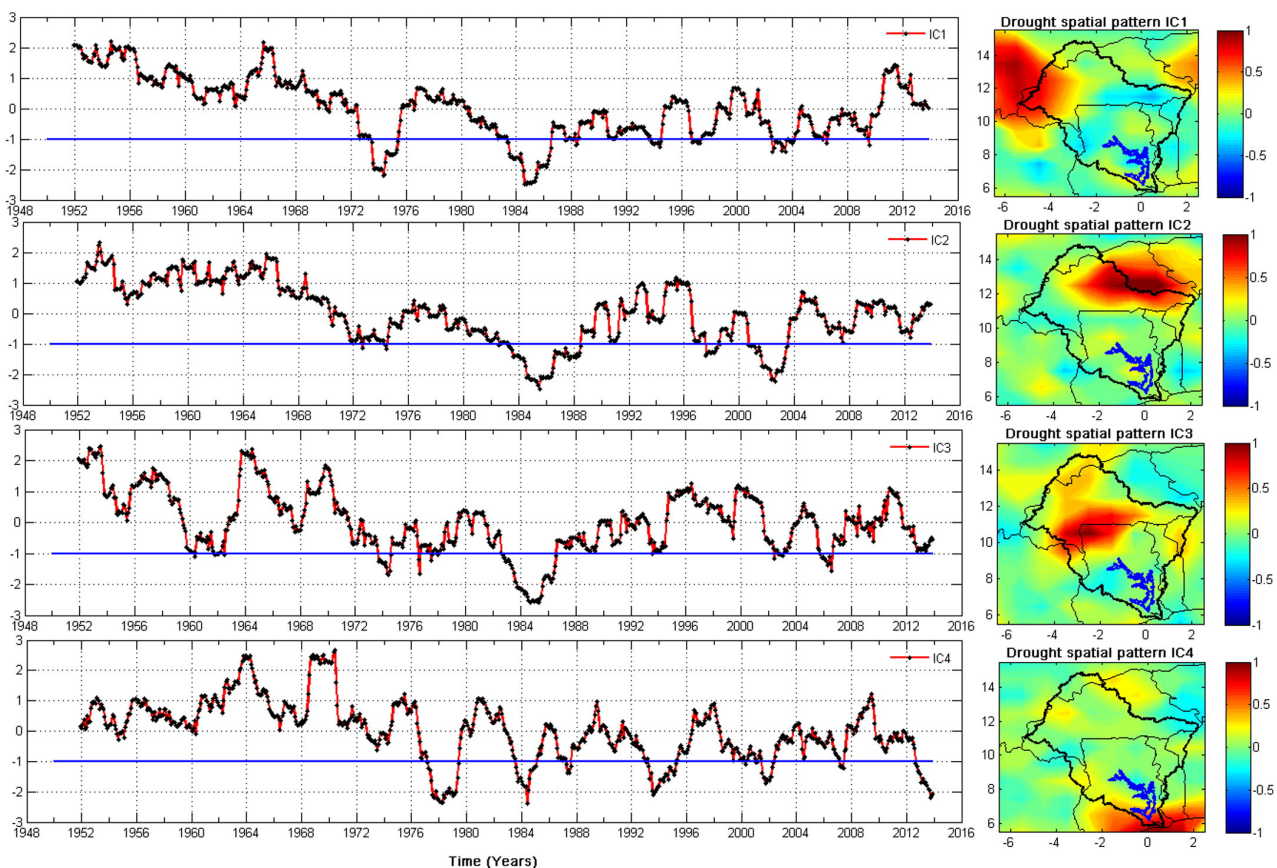


Fig. 6. ICA-derived spatio-temporal hydrological drought patterns over the Volta basin using 24-month gridded SPI values. SPI values are computed using GPCP-based precipitation for the period 1950–2013. The variability of the ICA modes (i.e., the spatial and temporal drought patterns) for the decomposed SPI values within the basin are 10.9%, 9.0%, 6.6%, and 6.5% for IC1, IC2, IC3, and IC4, respectively. Actual SPI values for drought classification and categorisation are jointly derived from the localised spatial drought pattern (right) and their corresponding temporal evolutions (left). The blue solid line shows the drought threshold based on McKee et al. (1993) description. (For interpretation of the references to color in this figure legend, the reader is referred to the web version of this article.)

(e.g., Ndehedehe et al., 2016). Hence, we speculate that strong deficits of soil moisture are somewhat analogous to TWS deficits over the Volta basin.

Results of the spatio-temporal drought analysis using GPCP-based precipitation for SPI 12 month indicate that the period during 1950–1968 was generally wet over the entire basin (Fig. 5) and is consistent with previous studies (Nicholson et al., 2000).

Unlike the hydrological drought analysis discussed in Section 4.1 above, here, the temporal variations of drought events and their corresponding spatial patterns are indicated. For instance, while the period between 2010 and 2013 show relatively moderate wet conditions (IC1, Fig. 5) in the north-western part of the basin (i.e., in Burkina Faso), the region in the lower Volta basin around the Lake Volta area in Ghana indicated an extreme dry condition during the same period though with a slight recovery in 2011 (IC2, Fig. 5). In fact, between late 2011 and 2013, the Lake area shows an extreme dry condition, consistent with a recent decline of about 2.25 ± 1.40 m/yr in Lake Volta water levels between 2011 and 2015 (not shown).

The results of statistical decomposition of SPI drought signals at 12 and 24 months cumulations are generally consistent except that drought frequency reduces at the SPI 24 month cumulation (Fig. 6) compared to the SPI drought signals at 12 months cumulations where drought frequencies are high (Fig. 5). More importantly, while the Lake Volta area still indicates an extreme drought condition even at the 24 month scale in the 2012/2013 period (IC4, Fig. 6), except for Ghana, observed drought episodes over the entire period (1950–2013) appear to be predominant in Burkina Faso (e.g., IC1 and IC3–IC4 Fig. 5). The spatial patterns of the observed drought signals are less patchy and more meaningful (i.e., Figs. 5 and 6) as they are well

localised while their corresponding temporal evolutions are consistent with previous drought records of the basin (see, e.g., Masih et al., 2014; Bekoe and Logah, 2013; Owusu and Waylen, 2013; Kasei et al., 2010).

Similar to the SPI, SSI was constructed at 12 and 24 month scales and decomposed statistically using the ICA technique. The spatio-temporal patterns of hydrological drought for the SSI are rather consistent with those of SPI (i.e., Figs. 5 and 6) except for IC3 that indicates extreme drought conditions in 2000–2003 and 2006–2007 at the south-eastern part of the basin, i.e., in Ghana, Togo, and Benin republic (Figs. 7 and 8). For the lower Volta basin and the Lake area, which happen to be a center of high socio-economic activities, the strong fluctuating drought signals between 2008 and 2013 (Figs. 7 and 8) had serious hydrological implications for the basin, culminating in relatively strong decline of the Lake Volta water level. In fact, the southern part of the basin shows the apparent distinction between the wet periods of the 1950s and 1970s with those of recent times especially 2008–2013 (see IC2 and IC3 Figs. 7 and 8) probably due to a decline in the decadal mean precipitation. Further discussion on this (i.e., decadal precipitation patterns) is provided in Section 4.2.2.

4.2.1. SPI and influence of teleconnections

Further, we attempt to explore the relationship between the ICA-derived SPI temporal evolutions with relevant global climate teleconnection indices that have been associated with rainfall variability in the region. This will help to examine the capability of ICA to highlight the impacts of teleconnections (see Section 3.1.6) on the observed drought signal (SPI). To this end, we correlated temporal evolutions of SPI for 12 and 24 months (i.e., IC1–IC4 of Figs. 5 and 6) with Pacific

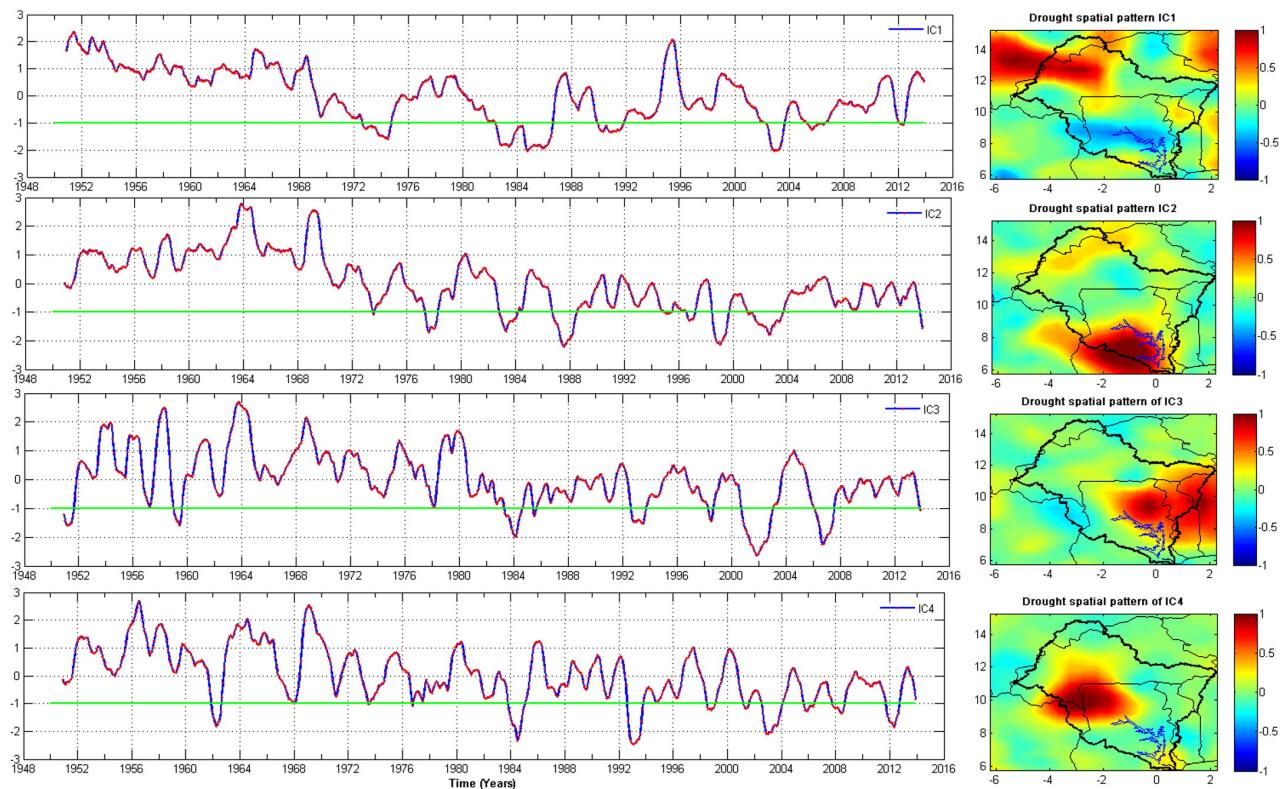


Fig. 7. ICA-derived spatio-temporal hydrological drought patterns over the Volta basin using 12-month gridded SSI values. SSI values are computed using CPC-based soil moisture for the period 1950–2013. The variability of the ICA modes (i.e., the spatial and temporal drought patterns) for the decomposed SSI values within the basin are 11.6%, 9.7%, 8.7%, and 6.9% for IC1, IC2, IC3, and IC4, respectively. Actual SSI values for drought classification and categorisation are jointly derived from the localised spatial drought pattern (right) and their corresponding temporal evolutions (left). The green solid line shows the drought threshold based on McKee et al. (1993) description. (For interpretation of the references to color in this figure legend, the reader is referred to the web version of this article.)

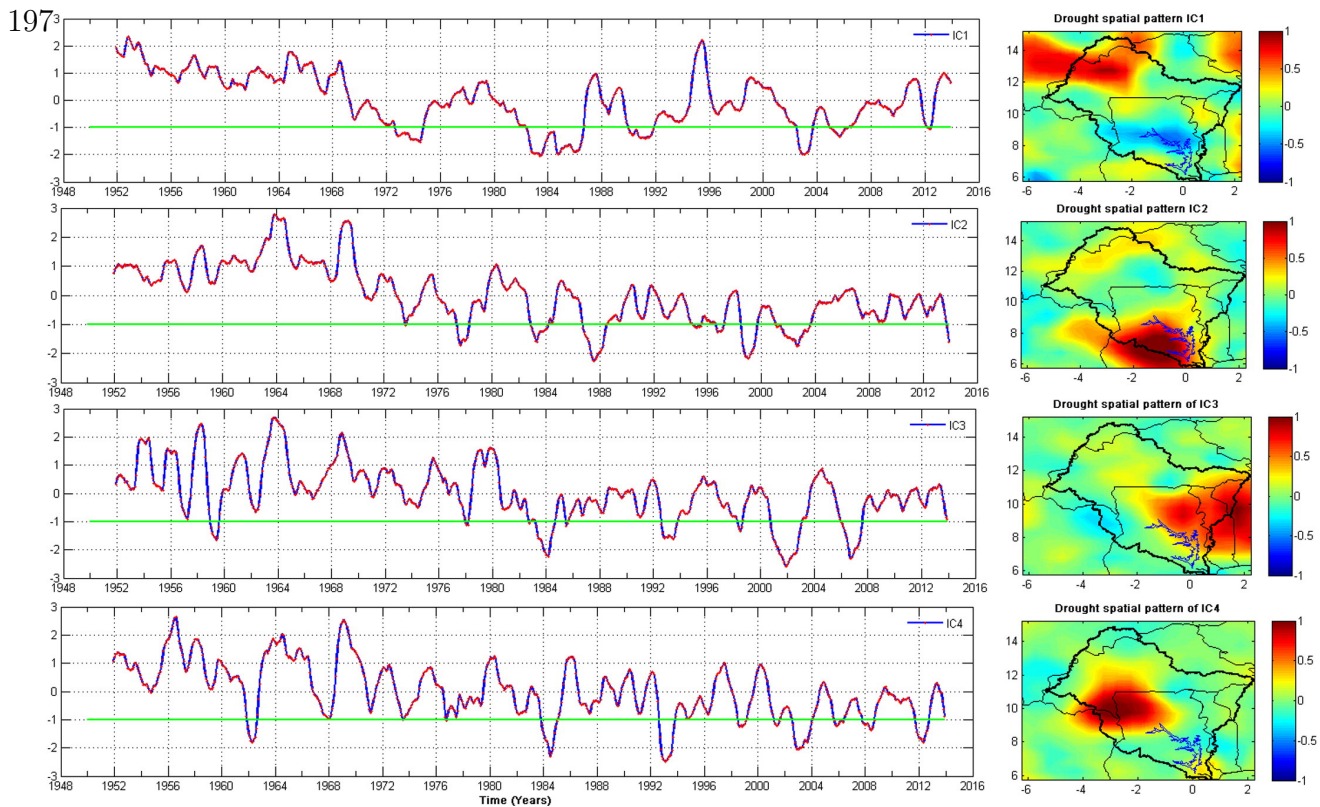


Fig. 8. ICA-derived spatio-temporal hydrological drought patterns over the Volta basin using 24-month gridded SSI values. SSI values are computed using CPC-based soil moisture for the period 1950–2013. The variability of the ICA modes (i.e., the spatial and temporal drought patterns) for the decomposed SSI values within the basin are 8.6%, 8.2%, 7.3%, and 5.6% for IC1, IC2, IC3, and IC4, respectively. Actual SSI values for drought classification and categorisation are jointly derived from the localised spatial drought pattern (right) and its corresponding temporal evolutions (left). The green solid line shows the drought threshold based on McKee et al. (1993) description. (For interpretation of the references to color in this figure legend, the reader is referred to the web version of this article.)

Decadal Oscillation (PDO), North Atlantic Oscillation (NAO), and Arctic Oscillation (AO). In order to decrease the effects of strong inter-annual variability on the computed correlations (e.g., Awange et al., 2014), the temporal evolutions of SPI 12 and 24 months and the indices were smoothed using a 12-month moving average filter. The summary of the correlation results (see, Tables 1 and 2) performed at 95% confidence level over the entire period of the SPI data show that at 12 and 24 months SPI scale, PDO has a statistically significant negative correlation of -0.39 and -0.38 , respectively while NAO has a statistically significant negative correlations of -0.28 and -0.28 , respectively with IC1 of Figs. 5 and 6. For the Lake area where we analyse further the results of 12 and 24 months SPI correlations with the three indices (see, Fig. 9), the PDO, NAO and AO all have statistically significant negative correlations of -0.25 , -0.24 , and -0.25 (see, Table 2) with IC4 of Fig. 6, respectively. Generally the extreme wet periods as indicated by SPI 12 and 24 months (Fig. 9) coincide with the negative phase of the three indices while the observed dry periods (i.e., IC2 and IC4 of Figs. 5 and 6), coincide with the positive phase of all the indices as well. The coupled relationship of ENSO and Indian Ocean Dipole (IOD) were identified as major cause of the 1983/1984 drought that spread across the continent (e.g., Bader and Latif, 2011; Giannini et al., 2003) while over the Sahel, ENSO, NAO, Atlantic Multi Decadal Oscillation (AMO), and IOD were reported as having strong relationship with precipitation at different time scales (Okonkwo, 2014). Further, Brown et al. (2010) showed the results of the response of African land surface phenology to large scale climate oscillations, indicating that over West Africa, cumulative NDVI correlated with PDO in the September–November period. However, in the current study, PDO, NAO, and AO are coupled ocean-atmosphere phenomena that are speculated as

contributing to observed low frequency wet/dry periods in Burkina Faso (i.e., IC1 of Figs. 5 and 6) and the lower Volta region in Ghana (i.e., IC2 and IC4 of Figs. 5 and 6). Diatta and Fink (2014) reported a negative correlation of -0.38 and -0.30 (both significant at 95% and 99% confidence levels) between PDO and rainfall indices of the Central Sahel (region including most parts of Burkina Faso) and West Sahel, respectively, somewhat consistent with our SPI drought temporal evolutions.

The physical causes of the PDO are not yet known and may be largely perceived as an irregular oscillation with unpredictable phase duration (Molion and Lucio, 2013). However, we highlight the PDO because it is a phenomenon that is not only characterised by low frequency variability but can also be employed for prospective future climate outlook. According to Molion and Lucio (2013) the PDO has been described as a long live ENSO episode with a cycle of 50 to 60 years, with each phase of the cycle lasting 25 to 30 years. In Fig. 9 (i.e., from the PDO time series), the period between 1950 and 1975 is characterised with the cold phase (CP) while 1977–1998 is characterised with a warm phase (WP). During the CP, it is observed that the PDO is associated with

Table 1
Correlations between ICA-decomposed SPI-12 month temporal drought evolutions and global climate indices. The correlation coefficient with asterisk is insignificant at the 95% significant level using the Student *t*-test.

S/N	ICs	PDO	NAO	AO
1	IC1	-0.39	-0.28	-0.18
2	IC2	-0.03^*	-0.21	-0.27
3	IC3	-0.18	-0.18	-0.18
4	IC4	-0.25	-0.24	-0.25

Table 2

Correlations between ICA-decomposed SPI-24 month temporal drought evolutions and remote climate indices. Correlation coefficients are all significant at the 95% significant level using the Student *t*-test.

S/N	ICs	PDO	NAO	AO
1	IC1	−0.38	−0.28	−0.18
2	IC2	−0.21	−0.21	−0.27
3	IC3	−0.18	−0.18	−0.18
4	IC4	−0.25	−0.24	−0.25

wet conditions while in contrast to the CP, extreme dry periods are observed during the WP of the PDO. It is noteworthy that the CP of PDO running since 1999 till date has recorded at least two La-Niña periods leading to flood and extreme wet conditions in 2007 and 2010 in the basin. This period has seen the TWS and the Lake Volta water level rise in late 2007 up to 7 m in 2010 due to increased rainfall, leading to the spilling of the reservoir for the first time after so many years in November 2010 (see, e.g., Ndehedehe et al., 2016; Owusu and Waylen, 2013). The PDO has also been reported as a mechanism associated with rainfall variability in the Sahel. For instance, Molion and Lucio (2013) reported a decline in rainfall during the WP of PDO in the Sahel. Given that each phase of the PDO cycle lasts for about 25–30 years, it can be inferred that the current phase of the PDO may bring significant wetter conditions to the Sahel (i.e., in Burkina Faso) and the southern part of the basin at large in the near future. Molion and Lucio (2013) maintains this same position and have suggested a further clarification by establishing the sea surface temperature (SST) patterns of the Pacific Ocean as the duration of each phase of the PDO may not be predictable owing to its dependence on large magnitude seismic events, which could be scarce and random. On the whole, the influence of PDO, NAO, and AO, on the observed drought temporal evolutions as indicated in their correlations (see Tables 1 and 2) further emphasizes the role of multiple dominant physical mechanisms in the climate extremes and variability of rainfall in the region (Druyan, 2011).

4.2.2. Decadal spatial rainfall patterns during 1950–2010

The decadal rainfall patterns as analysed using the MLRA confirm that the periods between 1950 and 1960 and 1960–1970 were

relatively wetter in the Volta basin as the mean annual amplitude and mean monthly rainfall respectively were relatively stronger than in other decades (Fig. 10). On a decadal-scale variability, our results are consistent with those of Nicholson et al. (2000) who showed that rainfall in the 1950s and 1960s were quite high as the mean regionally averaged rainfall were relatively high.

The observed increase in precipitation trends spreading mostly in the southern basin during 1980–1990 period appears to be the strongest increase since 1950 (Row 1, Fig. 10). While the annual rainfall patterns in the 1980s were relatively weak due to the extreme drought of the 1983/1984 (see, e.g., Figs. 2–3 and 5–6), strong annual rainfall patterns similar to those of the 1950s are observed in northern Togo and Benin between 1990 and 2000 and 2000–2010 periods (Row 2, Fig. 10). This seems to be a recovery in the annual rainfall patterns of those countries (Row 2, Fig. 10). The semiannual rainfall patterns seem rather weak in the last decades compared to the 1950s (Row 3, Fig. 10) while the mean rainfall shows a general decline at the southern basin as rainfall reduces from about 150 mm in the 1950–1960 period to 110 mm during 2000–2010 period (Rows 3 and 4, Fig. 10).

4.3. Terrestrial water storage changes

We also analysed the GRACE-derived TWS using ICA and MLRA approaches in order to relate observed drought patterns to water availability and the basin's hydrological behaviour. The annual amplitude of GRACE-derived TWS was removed using MLRA through parameterisation of the harmonic components. The residuals, which contain semi-annual signal and trends were thereafter statistically decomposed into temporal and spatial patterns using the ICA method. The annual amplitude of TWS coincides with the annual amplitudes of rainfall (not shown). The first independent component (IC) of TWS shows the variability around the Lake area and the converging points of the three rivers (i.e., the Black Volta, White Volta and Oti Rivers, cf. Fig. 1) that forms the Volta river system in Ghana (IC1, Fig. 11).

The other signals shown are those of Burkina Faso (IC2, Fig. 11), south east Ghana (IC3, Fig. 11), and northern Ivory Coast (IC4, Fig. 11). While the period between 2007 and 2010 indicate an increasing trend, the period between 2012 and 2014 show a decline in all sub-

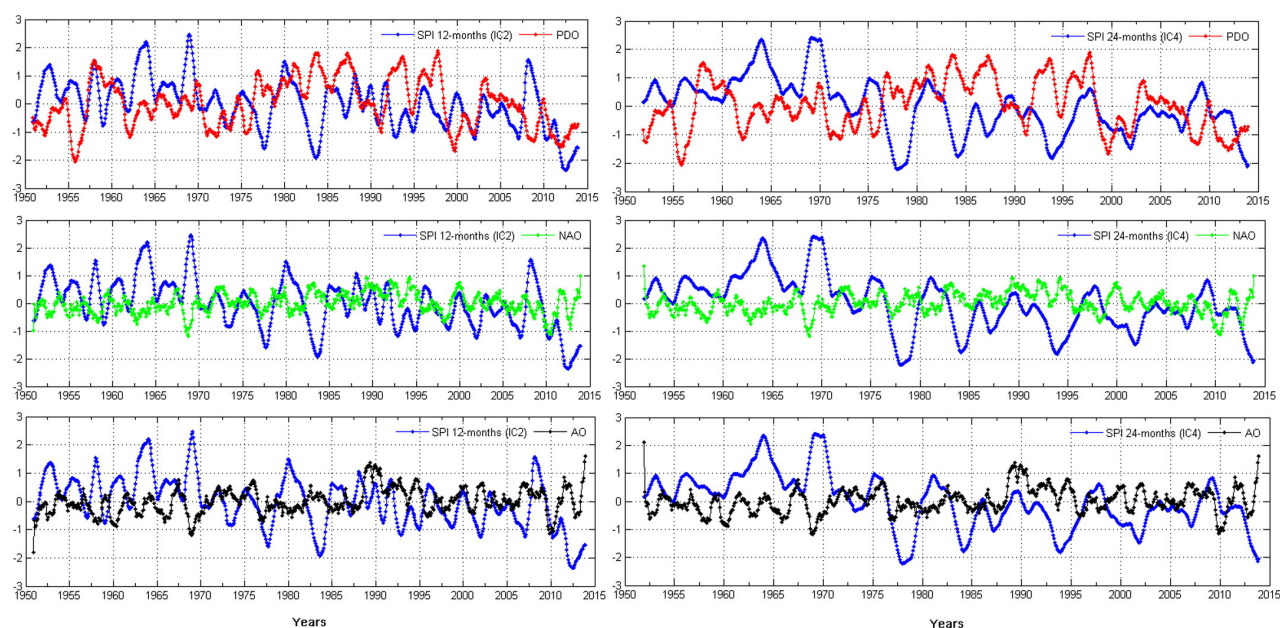


Fig. 9. Influence of global climate teleconnection indices (i.e., 1950 to 2014) on temporal evolutions of hydrological droughts (i.e., 12 and 24 months SPI). The temporal drought pattern of ICA mode 2 and ICA mode 4 shown in Fig. 5 and 6, respectively are correlated with PDO (top), NAO (middle), and AO (bottom).

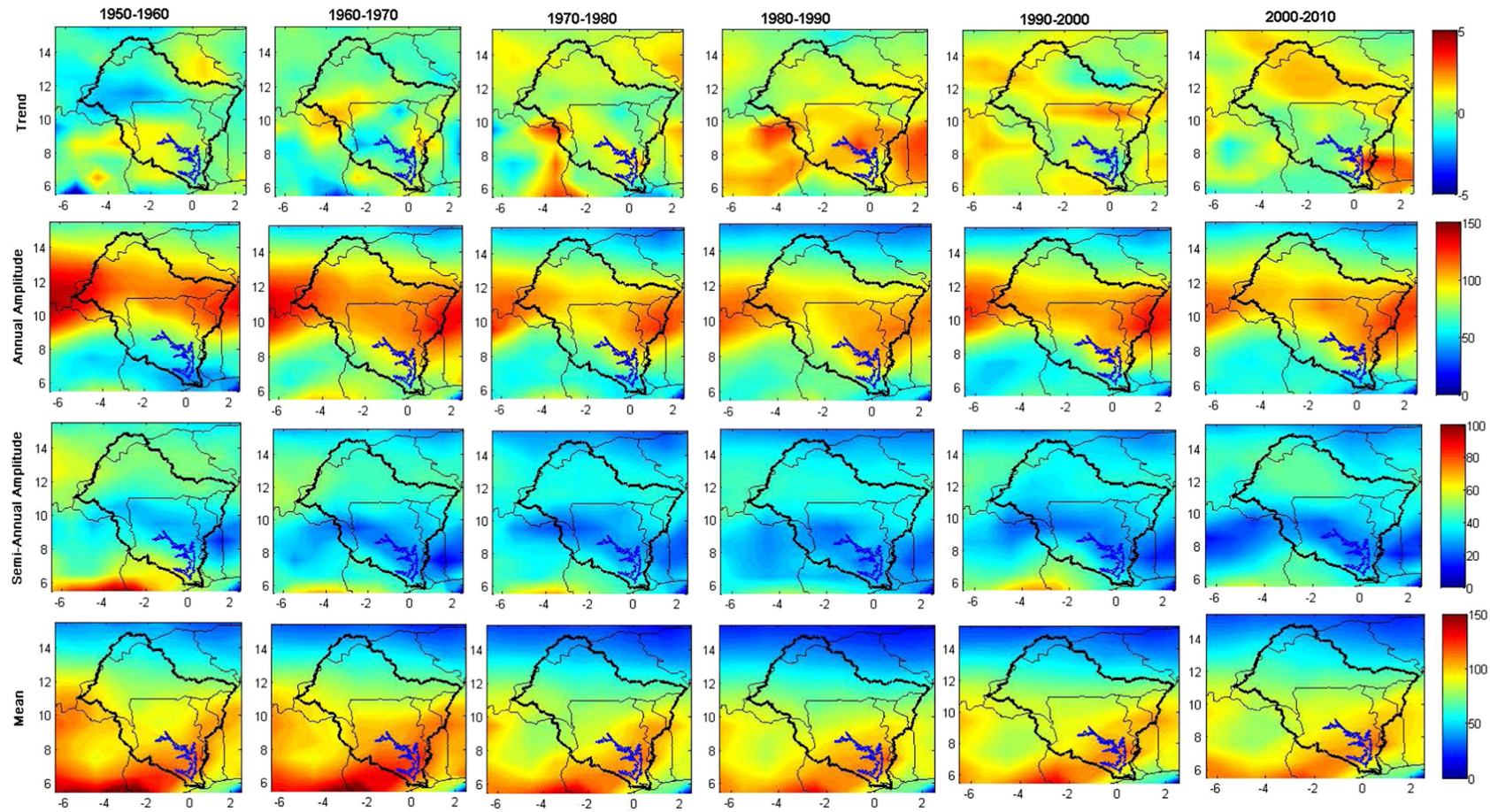


Fig. 10. Decadal rainfall (mm) patterns over the Volta basin (1950–2010). Row 1: Trends in precipitation. Row 2: Mean annual amplitude of precipitation. Row 3: Mean semi-annual amplitude of precipitation. Row 4: Decadal mean precipitation.

200

regions (i.e., IC1–IC4, Fig. 11). This observed pattern is stronger in IC1 of Fig. 11 due to the stronger loadings of its spatial patterns, possibly triggered by the presence of Lake Volta and the hydrology of the Volta river catchment in Ghana. Concerning the observed TWS signals in IC1 of Fig. 11, about 67% of the surface water resources in Ghana come from outside through the Volta river system, with Oti River contributing about 32% (11.2 km³) while the Black Volta and White Volta contribute 24% (8.3 km³) and 11% (3.9 km³), respectively (Andreini et al., 2002). These surface water contributions from outside of Ghana, which are major triggers of observed hydrological signals in IC1 of Fig. 11, drain more than two-thirds of Ghana, with Lake Volta being formed by the Akosombo dam through the impoundment of these surface waters as they flow downstream. Analysis of recent satellite altimetry data (not shown) over Lake Volta showed an increase of 2.31 ± 0.24 m/yr corresponding to a water volume change of 19.635 km³ during the period of 2007/08–2010/12 over the Lake while the period 2011/01–2015/09 showed a decline of 2.25 ± 0.10 m/yr coinciding with the period of observed decline in TWS change between 2012 and 2014 in Fig. 11. The 2007 La-Niña and the extreme wet condition of 2010 can be seen in the increasing trend in the observed TWS residual over the basin. The computed SPI, SRI, and MSDI in all aggregation scales over the basin (see, Fig. 2) also indicated similar increase between 2007 and 2010. This essentially demonstrates the utility of multiple standardised indicators to understand more vividly the sensitivity of lakes, reservoirs, and catchment systems to hydro-climatological and environmental changes. This apparently will largely support the management systems

of water resources and the assessment of any anthropogenic influence (if any). The current study did not analyse human footprints on the basin's TWS. However, conflicting positions regarding the scientific evidence of anthropogenic influence on the inflows to the lake (see, e.g., Friesen et al., 2005; Andreini et al., 2002) is a critical subject for future considerations.

4.4. Water availability and net precipitation over the Volta basin

The numerous water infrastructures, multiple sources of inflow into the Lake and the impact of water impoundments by the Akosombo dam in the Volta basin (e.g., Ahmed et al., 2014; Andreini et al., 2002) are just a few among the factors complicating the hydrology of the basin. The hydrology of the Volta basin is largely controlled by hydrological cycle components such as precipitation, runoff, and recharge and can be represented by the water balance equation

$$\frac{dS(t)}{dt} = P(t) - E(t) - R(t), \quad (10)$$

where P , E , R , and dS are precipitation, evapotranspiration, runoff, change in storage (i.e., TWS), and t the time, respectively. The yearly

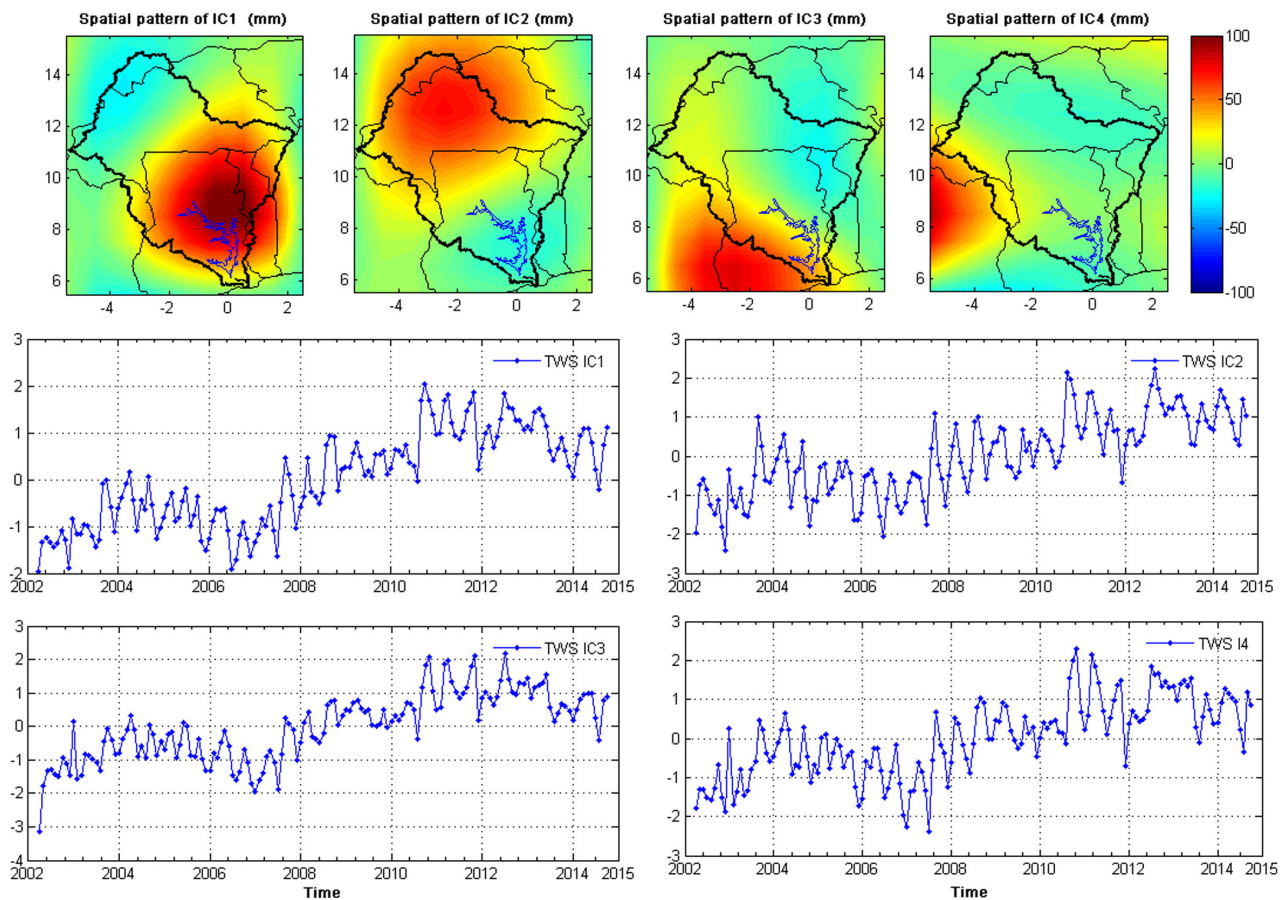


Fig. 11. The independent components (bottom) of GRACE-derived TWS (i.e., after removing the annual signals over the Volta basin) corresponding to spatial patterns (top), which are scaled using the standard deviation of the computed independent components of the GRACE data. These independent components are unitless since they have been standardised using their standard deviations.

water availability i.e., the net precipitation can be given as

$$P-E = \frac{dS(t)}{dt} + R(t). \quad (11)$$

Net precipitation is important as it can help describe water deficit in a given hydrological system. The observed trends in dS , P , E and the difference between P and E (i.e., $P-E$) were compared in order to understand the recent hydrological behaviour of the Volta basin. Rainfall indicated an insignificant decline of 1.25 ± 1.74 mm/yr during the 2002–2013 period while evapotranspiration showed a significant increase of 1.03 ± 0.59 mm/yr during the 2002–2014 period. TWS and $P-E$ over the basin indicated a significant increase of 16.24 ± 2.28 mm/yr and a decrease of 2.53 ± 1.22 mm/yr at 95% confidence level respectively. Averaged rainfall over the entire basin shows a correlation of 0.84 at the same 95% confidence level with evapotranspiration, indicating consistent behaviour especially in its variability (Fig. 12, top). The impact of the 2007 ENSO event and other years (e.g., 2003–2004, 2008, and 2010) with relatively strong annual amplitudes are obvious (Fig. 12, top). However, between 2011 and 2013, annual peak rainfall, which usually occurs in August barely reached 170 mm compared to the more than 200 mm recorded in the years between 2007 and 2010 (Fig. 12, top). The observed less pronounced annual peak rainfall between 2011 and 2013 coincides with the observed less pronounced annual net precipitation over the basin (Fig. 12, top and bottom). The year 2010 was quite wet over the Volta basin, leading to strong amplitudes of TWS change (Fig. 12, bottom) consistent with observed trends and amplitudes of water storage and the Lake Volta water level in previous studies (e.g., Ndehedehe et al., 2016; Ahmed et al., 2014). However, the amplitudes of observed TWS during 2011–2013 period (Fig. 12, bottom) may not necessarily be due to increased rainfall as that period suggests a hydrological drought period in the Lake Volta area (see, IC1 and IC4 of Figs. 5 and 6, respectively). Over the entire basin, at 6, and 12 months aggregation scales and with respect to the mean of 1980, SPI and MSDI indicate a severe drought condition in 2011 that terminated in 2012 with a resurgence in 2013 (Figs. 2 and 3). While we

attribute such changes in TWS during the period (2011–2013 in Fig. 12, bottom) to variations in lake level and river discharge, which has a non-linear relationship to rainfall as indicated earlier, apparently, from the statistical decomposition of TWS over the basin, the Lake Volta area, and the Oti river catchment area show a decline in observed residual TWS within the same period (IC1, Fig. 11). Consequently, the notion that the Volta basin may be predispose to drier conditions that could impact negatively on ecosystem services is affirmed, especially with lack of a significant positive trend in rainfall in the last decade.

5. Conclusions

In this study, we have examined the potentials of multiple drought indicators (SPI, SRI, SSI, and MSDI) and Gravity Recovery and Climate Experiment (GRACE) derived terrestrial water storage (TWS) to assess hydrological drought characteristics over the Volta basin. For the first time over the Volta basin, independent component analysis was employed to determine the space-time occurrence of hydrological drought in the basin. The influence of low frequency large scale oscillations on observed temporal evolutions of droughts over the basin was also investigated through correlation analysis. The results show that:

- At all monthly cumulations, SPI time series computed over the basin show a relatively weak correlation with SRI with extreme wet periods exhibiting some lagged or non-linear relationships, reflecting a relatively slow response of discharge to extreme wet condition, especially after a previous extreme dry period. Also, the observed regression fit and relationship between soil moisture and TWS in Fig. 4a makes it reasonable to employ soil moisture at longer time scales (e.g., 12 months) for a quantitative hydrological drought assessment over the Volta basin, complementing the limited availability of GRACE observations.
- The correlation between the two sets of MSDIs derived from combining precipitation/river discharge and precipitation/soil moisture indicates a significant value of 0.70 and show an improved skill in hydrological drought monitoring over the Volta basin. The SPI and

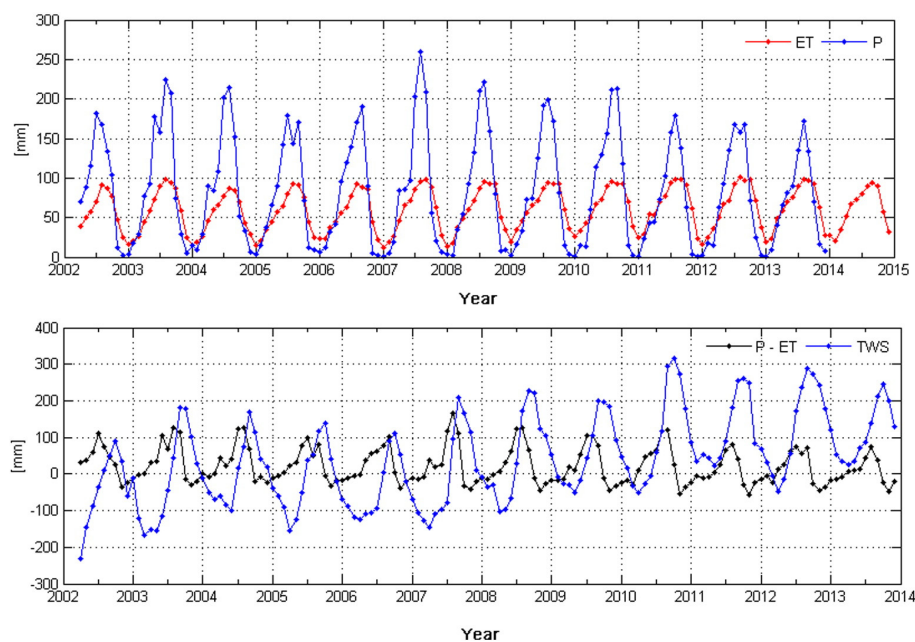


Fig. 12. Time series of averaged precipitation, evapotranspiration, and net precipitation over the Volta basin. Top: GPCC-based precipitation and Modis derived Evapotranspiration over the entire basin. Bottom: averaged GRACE-derived TWS changes and the corresponding precipitation minus evapotranspiration (net precipitation), a measure of water availability in basin.

202

SSI show a contrasting behaviour to SPI/SRI, indicating a correlation of 0.63 (i.e., at 12 month cumulation) and rather consistent in the observed dry and wet years.

- iii. The ICA-derived spatio-temporal hydrological drought patterns for the SPI and SSI are rather consistent and show Burkina Faso and the Lake Volta area as frequent drought zones. The spatial patterns of the observed drought signals are less patchy, and more meaningful as they are well localised while their corresponding temporal evolutions are generally consistent with previous drought records of the basin.
- iv. The statistically significant negative correlations of Pacific Decadal Oscillations (-0.39 and -0.25) with temporal evolutions of drought at Burkina Faso and Ghana suggest the possible influence of low frequency large scale oscillations in the observed wet and dry regimes over the basin. Besides the influence of Pacific Decadal Oscillation, the observed significant negative correlations of North Atlantic Oscillation, and Arctic Oscillation with the temporal evolutions of drought signals further regurgitates the role of multiple dominant physical mechanisms in the climate extremes and variability of rainfall in the region.
- v. The statistical decomposition of TWS (i.e., after removing the annual signal) indicate a decline in the Lake area and the Oti river catchment between 2012 and 2014, consistent with observed less pronounced annual peak rainfall and fluctuating drought conditions during the 2011–2013 period.

Finally, net precipitation shows a significant decline while a more recent hydrological drought condition at the Lake Volta area is observed during the 2011–2013 period. The notion that the Volta basin may be predisposed to drier conditions that could impact negatively on ecosystem services is affirmed, especially with the lack of a significant positive trend in rainfall in the last decade. The current study did not analyse human footprints on the basin's TWS. However, conflicting positions regarding the scientific evidence of anthropogenic influence on the inflows to Lake Volta should be relevant and topical issues for future considerations. This study has confirmed that drought varies spatially and temporally in its frequency, duration, and severity. Hence, our space-time approach and the use of multiple climate variables in drought assessment over the Volta basin contributes to a broad framework for hydrological drought monitoring that will complement existing methodologies while looking forward to increase in the records of GRACE observations. The results and analyses from this study are based mostly on satellite measurements and model-based data. Hence, the results should be interpreted with caution as we look forward to new studies that will rely on large scale in-situ data over the region.

Acknowledgments

Christopher E. Ndehedehe is grateful to Curtin University for his PhD funding through the Curtin Strategic International Research Scholarship (CSIRS) programme. The Authors are grateful to CSR, NOAA, and NASA for the data used in this study. The authors are also grateful to Water Research Institute of Ghana for the river discharge data of Akosombo station used in this study. Joseph Awange is grateful for the Brazilian Science Without Borders Program/CAPES Grant No. 88881.068057/2014-01 which supported his stay in UFPE Federal University of Pernambuco, Brazil. We also thank the editor and the three anonymous reviewers for their very useful comments, which helped improved the manuscript.

References

- Ahmed, M., Sultan, M., Wahr, J., Yan, E., 2014. The use of GRACE data to monitor natural and anthropogenic induced variations in water availability across Africa. *Earth-Sci. Rev.* 136, 289–300. <http://dx.doi.org/10.1016/j.earscirev.2014.05.009>.
- Ali, A., Lebel, T., 2009. The Sahelian standardized rainfall index revisited. *Int. J. Climatol.* 29, 1705–1714. <http://dx.doi.org/10.1002/joc.1832>.
- Andreini, M., Vlek, P., Giesen, N.V.D., 2002. Water sharing in the Volta basin. *Proceedings of the Fourth International FRIEND Conference. FRIEND, South Africa*, pp. 329–335.
- Awange, J., Forootan, E., Kuhn, M., Kusche, J., Heck, B., 2014. Water storage changes and climate variability within the Nile Basin between 2002 and 2011. *Adv. Water Resour.* 73, 1–15. <http://dx.doi.org/10.1016/j.advwatres.2014.06.010>.
- Awange, J., Forootan, E., Ferreira, V., Khandu, Andam-Akorful, S., Agutu, N., He, X., 2016. Uncertainties in remotely sensed precipitation data over Africa. *Int. J. Climatol.* 36, 303–323. <http://dx.doi.org/10.1002/joc.4346>.
- Bader, J., Latif, M., 2011. The 1983 drought in the West Sahel: a case study. *Clim. Dyn.* 36 (3–4), 463–472. <http://dx.doi.org/10.1007/s00382-009-0700-y>.
- Baur, O., Kuhn, M., Featherstone, W.E., 2009. GRACE-derived ice-mass variations over Greenland by accounting for leakage effects. *J. Geophys. Res. Solid Earth* 114 (B6). <http://dx.doi.org/10.1029/2008JB006239> B06407.
- Bazrafshan, J., Hejabi, S., Rahimi, J., 2014. Drought monitoring using the multivariate standardized precipitation index (MSPi). *Water Resour. Manag.* 28, 1045–1060. <http://dx.doi.org/10.1007/s11269-014-0533-2>.
- Becker, A., Finger, P., Meyer-Christoffer, A., Rudolf, B., Schamm, K., Schneider, U., Ziese, M., 2013. A description of the global land-surface precipitation data products of the Global Precipitation Climatology Centre with sample applications including centennial (trend) analysis from 1901 to present. *Earth System Science Data* 5 (1), 71–99.
- Bekoe, E.O., Logah, F.Y., 2013. The impact of droughts and climate change on electricity generation in Ghana. *Environ. Sci.* 1 (1), 13–24.
- Bloomfield, J.P., Marchant, B.P., 2013. Analysis of groundwater drought building on the standardized precipitation index approach. *Hydrol. Earth Syst. Sci.* 17 (12), 4769–4787. <http://dx.doi.org/10.5194/hess-17-4769-2013>.
- Boergens, E., Rangelova, E., Sideris, M.G., Kusche, J., 2014. Assessment of the capabilities of the temporal and spatiotemporal ICA method for geophysical signal separation in GRACE data. *J. Geophys. Res. Solid Earth* 119, 4429–4447. <http://dx.doi.org/10.1002/2013JB010452>.
- Bonaccorso, B., Bordin, I., Cancelliere, A., Rossi, G., Sutera, A., 2003. Spatial variability of drought: an analysis of the SPI in Sicily. *Water Resour. Manag.* 17 (4), 273–296. <http://dx.doi.org/10.1023/A:1024716530289>.
- Bonsor, H.C., MacDonald, A.M., 2011. An initial estimate of depth to groundwater across Africa. *British Geological Surveys Groundwater Science OR/11/067* (Retrieved from: <http://nora.nerc.ac.uk/id/eprint/17907>, Accessed 15th June 2015).
- Brown, M.E., de Beurs, K., Vrieling, A., 2010. The response of African land surface phenology to large scale climate oscillations. *Remote Sens. Environ.* 114 (10), 2286–2296. <http://dx.doi.org/10.1016/j.rse.2010.05.005>.
- Cardoso, J.-F., 1991. Super-symmetric Decomposition of the Fourth-order Cumulant Tensor, Blind Identification of More Sources Than Sensors Retrieved from: <http://perso.telecom-paristech.fr/cardoso/Papers/PDF/icassp91.pdf>. Accessed 15 January 2016.
- Cardoso, J.F., 1999. High-order contrasts for independent component analysis. *Neural Comput.* 11, 157–192.
- Cardoso, J.F., Souloumiac, A., 1993. Blind beamforming for non-Gaussian signals. *IEE Proceedings* 140 (6), 362–370.
- Cheng, M.K., Tapley, B.D., Ries, J.C., 2013. Deceleration in the earth's oblateness. *J. Geophys. Res.* 118, 1–8. <http://dx.doi.org/10.1002/jgrb.50058>.
- Common, P., 1994. Independent component analysis, a new concept? *Signal Process.* 36, 287–314.
- Crowley, J.W., Mitrovica, J.X., Bailey, R.C., Tamisiea, M.E., Davis, J.L., 2006. Land water storage within the Congo Basin inferred from GRACE satellite gravity data. *Geophys. Res. Lett.* 33 (19). <http://dx.doi.org/10.1029/2006GL027070> L19402.
- Diatta, S., Fink, A.H., 2014. Statistical relationship between remote climate indices and West African monsoon variability. *Int. J. Climatol.* 34 (12), 3348–3367. <http://dx.doi.org/10.1002/joc.3912>.
- Druryan, L.M., 2011. Studies of 21st-century precipitation trends over West Africa. *Int. J. Climatol.* 31 (10), 1415–1424. <http://dx.doi.org/10.1002/joc.2180>.
- Fan, Y., Dool, H.V., 2004. Climate prediction center global monthly soil moisture data set at 0.5 resolution for 1948 to present. *J. Geophys. Res.* 109. <http://dx.doi.org/10.1029/2003JD004345> D10102.
- Farahmand, A., AghaKouchak, A., 2015. A generalized framework for deriving nonparametric standardized drought indicators. *Adv. Water Resour.* 76, 140–145. <http://dx.doi.org/10.1016/j.advwatres.2014.11.012>.
- Fenoglio-Marc, L., Rietbroek, R., Grayek, S., Becker, M., Kusche, J., Stanev, E., 2012. Water mass variation in the Mediterranean and Black Seas. *J. Geodyn.* 59–60, 168–182.
- Ferreira, V., Asiah, Z., 2015. An investigation on the closure of the water budget methods over Volta Basin using multi-satellite data. *International Association of Geodesy Symposia*. <http://dx.doi.org/10.1007/1345-2015-137e>.
- Ferreira, V., Andam-Akorful, S.A., He, X., Xiao, R., 2014. Estimating water storage changes and sink terms in Volta Basin from satellite missions. *Water. Science and Engineering* 7 (1), 5–16. <http://dx.doi.org/10.3882/j.issn.1674-2370.2014.01.0028>.
- Forootan, E., Kusche, J., 2012. Separation of global time-variable gravity signals into maximally independent components. *J. Geod.* 86 (7), 477–497. <http://dx.doi.org/10.1007/s00190-011-0532-5>.
- Forootan, E., Awange, J., Kusche, J., Heck, B., Eicker, A., 2012. Independent patterns of water mass anomalies over Australia from satellite data and models. *Remote Sens. Environ.* 124, 427–443.

- 203 Rappart, F., Ramillien, G., Leblanc, M., Tweed, S.O., Bonnet, M.-P., Maisongrande, P., 2011. An independent component analysis filtering approach for estimating continental hydrology in the GRACE gravity data. *Remote Sens. Environ.* 115 (1), 187–204. <http://dx.doi.org/10.1016/j.rse.2010.08.017>.
- Friesen, J., Andreini, M., Andah, W., Amisigo, M.A., Giesen, N.V.D., 2005. Storage capacity and long-term water balance of the Volta Basin, West Africa. *Proceedings of Symposium S6 Held During the Seventh IAHS Scientific Assembly, Brazil* Retrieved from: <http://iahs.info/uploads/dms/13203.2220138-14520Foz20S6-2-1420Friesen.pdf>, Accessed 18 December 2015).
- Fukuda, Y., Yamamoto, K., Hasegawa, T., Nakaegawa, T., Nishijima, J., Taniguchi, M., 2009. Monitoring groundwater variation by satellite and implications for in-situ gravity measurements. *Sci. Total Environ.* 407 (9), 3173–3180. <http://dx.doi.org/10.1016/j.scitotenv.2008.05.018>.
- Giannini, A., Saravanan, R., Chang, P., 2003. Oceanic forcing of Sahel rainfall on interannual to decadal time scales. *Science* 302 (5647), 1027–1030. <http://dx.doi.org/10.1126/science.1089357>.
- Giesen, N.V.D., Andreini, M., Edig, A.V., Vlek, P., 2002. Competition for water resources of the Volta basin. *Regional Management of Water Resources*. 268, 199–205 (Retrieved from: <http://www.zef.de/fileadmin/template/Glowa/Downloads/>, Accessed 12 November 2014).
- Giesen, N.V.D., Liebe, J., Jung, G., 2010. Adapting to climate change in the Volta Basin. *West Africa. Curr. Sci.* 98 (8), 1033–1037.
- Greve, P., Orlowsky, B., Mueller, B., Sheffield, J., Reichstein, M., Seneviratne, S.L., 2014. Global assessment of trends in wetting and drying over land. *Nat. Geosci.* 7, 716–721. <http://dx.doi.org/10.1038/NGEO2247>.
- Gringorten, I.I., 1963. A plotting rule for extreme probability paper. *J. Geophys. Res.* 68 (3), 813–814.
- Hao, Z., AghaKouchak, A., 2013. Multivariate standardized drought index: a parametric multi-index model. *Adv. Water Resour.* (57), 12–18 <http://dx.doi.org/10.1016/j.advwatres.2013.03.009>.
- Hao, Z., AghaKouchak, A., 2014. A nonparametric multivariate multi-index drought monitoring framework. *J. Hydrometeorol* 15 (1), 89–101. <http://dx.doi.org/10.1175/JHM-D-12-0160.1>.
- Hayes, M.J., 2007. Drought indices. *Intermountain West Climate Summary* Retrieved from www.colorado.edu/climate/iwacs/archive/IWCS-2007-July-feature.pdf Accessed 9 December 2015.
- Hayes, M.J., Svoboda, M.D., Wilhite, D.A., Vanyarkho, O.V., 1999. Monitoring the 1996 drought using the standardized precipitation index. *Bull. Am. Meteorol. Soc.* 80, 429–438. [http://dx.doi.org/10.1175/1520-0477\(1999\)080b0429:MTDUTSN2.0.CO;2](http://dx.doi.org/10.1175/1520-0477(1999)080b0429:MTDUTSN2.0.CO;2).
- Hoekstra, A.Y., Mekonnen, M.M., 2012. The water footprint of humanity. *PNAS* 109 (9), 3232–3237. <http://dx.doi.org/10.1073/pnas.1109936109>.
- Joetzjer, E., Douville, H., Delire, C., Ciais, P., Decharme, B., Tytca, S., 2013. Hydrologic benchmarking of meteorological drought indices at interannual to climate change time-scales: a case study over the Amazon and Mississippi river basins. *Hydrol. Earth Syst. Sci.* 17 (12), 4885–4895. <http://dx.doi.org/10.5194/hess-17-4885-2013>.
- Jolliffe, I.T., 2002. *Principal component analysis*. Springer Series in Statistics, second ed. Springer, New York.
- Kasei, R., Diekkrüger, B., Leemhuis, C., 2010. Drought frequency in the Volta Basin of West Africa. *Sustain. Sci.* 5 (1), 89–97.
- Keys, P., van der Ent, R.J., Gordon, L.J., Hoff, H., Nikoli, R., Savenije, H.H.G., 2012. Analyzing precipitationsheds to understand the vulnerability of rainfall dependent regions. *Biogeosciences* 9, 733–746. <http://dx.doi.org/10.5194/bg-9-733-2012>.
- Keys, P., Barnes, E.A., van der Ent, R.J., Gordon, L.J., 2014. Variability of moisture recycling using a precipitationsheds framework. *Hydrol. Earth Syst. Sci.* 18, 3937–3950. <http://dx.doi.org/10.5194/hess-18-3937-2014>.
- Komusc, A.U., 1999. Using the SPI to analyze spatial and temporal patterns of drought in Turkey. *Drought Network News* 11 (1), 7–13.
- Kumar, R., Musuza, J.L., Loon, A.F.V., Teuling, A.J., Barthel, R., Broek, J.T., Mai, J., Samaniego, L., Attinger, S., 2015. Multiscale evaluation of the standardized precipitation index as a groundwater drought indicator. *Hydrol. Earth Syst. Sci.* 12, 7405–7436. <http://dx.doi.org/10.5194/hessd-12-7405-2015>.
- Kusche, J., Schmidt, R., Petrovic, S., Rietbroek, R., 2009. Decorrelated GRACE time-variable gravity solutions by GFZ, and their validation using a hydrological model. *J. Geod.* 83 (10), 903–913. <http://dx.doi.org/10.1007/s00190-009-0308-3>.
- Lacombe, G., McCartney, M., Forkuor, G., 2012. Drying climate in Ghana over the pe-riod 1960–2005: evidence from the resampling-based Mann-Kendall test at local and regional levels. *Hydrol. Sci. J.* 57 (8), 1594–1609. <http://dx.doi.org/10.1080/02626667.2012.728291>.
- Landerer, F.W., Swenson, S.C., 2012. Accuracy of scaled GRACE terrestrial water storage estimates. *Water Resour. Res.* 48 (4). <http://dx.doi.org/10.1029/2011WR011453> W04531.
- Li, B., Rodell, M., 2015. Evaluation of a model-based groundwater drought indicator in the conterminous U.S. *J. Hydrol.* 526, 78–88. <http://dx.doi.org/10.1016/j.jhydrol.2014.09.027>.
- Lloyd-Hughes, B., 2012. A spatio-temporal structure-based approach to drought characterisation. *Int. J. Climatol.* 32 (3), 406–418. <http://dx.doi.org/10.1002/joc.2280>.
- Long, D., Longuevergne, L., Scanlon, B.R., 2015. Global analysis of approaches for deriving total water storage changes from GRACE satellites. *Water Resour. Res.* 51 (4), 2574–2594. <http://dx.doi.org/10.1002/2014WR016853>.
- Loon, A.F.V., 2015. Hydrological drought explained. *WIREs Water* 2, 359–392. <http://dx.doi.org/10.1002/wat2.1085>.
- MacDonald, A.M., Bonsor, H.C., Dochartaigh, B.E.O., Taylor, R.G., 2012. Quantitative maps of groundwater resources in Africa. *Environ. Res. Lett.* 7. <http://dx.doi.org/10.1088/1748-9326/7/2/024009>.
- Masih, I., Maskey, S., Mussá, F.E.F., Trambauer, P., 2014. A review of droughts on the African continent: a geospatial and long-term perspective. *Hydrol. Earth Syst. Sci.* 18 (9), 3635–3649. <http://dx.doi.org/10.5194/hess-18-3635-2014>.
- McKee, T.B., Doeskin, N.J., Kieist, J., 1993. The relationship of drought frequency and duration to time scales. *Conference on Applied Climatology, American Meteorological Society, Massachusetts, Boston*, pp. 179–184 (Retrieved from: www.ccc.atmos.colostate.edu/relationshipofdroughtfrequency.pdf, Accessed 27 June 2014).
- McKee, T.B., Doeskin, N.J., Kieist, J., 1995. Drought monitoring with multiple time scales. *Conference on Applied Climatology, American Meteorological Society, Boston, Massachusetts* 233–236 (Retrieved from: www.southwestclimatechange.org/node/911, Accessed 13 July 2014).
- Mishra, A.K., Singh, V.P., 2010. A review of drought concepts. *J. Hydrol.* 391, 202–216. <http://dx.doi.org/10.1016/j.jhydrol.2010.07.012>.
- Molion, L.C.B., Lucio, P.S., 2013. A note on Pacific decadal oscillation, El Niño Southern oscillation, Atlantic multidecadal oscillation and the intertropical front in Sahel, Africa. *Atmospheric and Climate Sciences* 3, 269–274. <http://dx.doi.org/10.4236/acs.2013.33028>.
- Mu, Q., Zhao, M., Running, S.W., 2011. Improvements to a MODIS global terrestrial evapotranspiration algorithm. *Remote Sens. Environ.* 115 (8), 1781–1800. <http://dx.doi.org/10.1016/j.rse.2011.02.019>.
- Nalbantis, I., Tsakiris, G., 2009. Assessment of hydrological drought revisited. *Water Resour. Manag.* 23, 881–897. <http://dx.doi.org/10.1007/s11269-008-9305-1>.
- Ndehedehe, C., Awange, J., Agutu, N., Kuhn, M., Heck, B., 2016. Understanding changes in terrestrial water storage over West Africa between 2002 and 2014. *Adv. Water Resour.* 88, 211–230.
- Nichol, J.E., Abbas, S., 2015. Integration of remote sensing datasets for local scale assessment and prediction of drought. *Sci. Total Environ.* 505, 503–507. <http://dx.doi.org/10.1016/j.scitotenv.2014.09.099>.
- Nicholson, S.E., Some, B., Kone, B., 2000. An analysis of recent rainfall conditions in West Africa, including the rainy seasons of the 1997 El Niño and the 1998 La Niña Years. *J. Clim.* 13 (14), 2628–2640. [http://dx.doi.org/10.1175/1520-0442\(2000\)013b2628:AAORRCN2.0.CO;2](http://dx.doi.org/10.1175/1520-0442(2000)013b2628:AAORRCN2.0.CO;2).
- Nicholson, S.E., Some, B., Mccollum, J., Nelkin, E., Klotter, D., Berte, Y., Diallo, B.M., Gaye, I., Kpabebe, G., Ndiaye, O., Noukpozoukou, J.N., Tanu, M.M., Thiam, A., Toure, A.A., Traore, A.K., 2003. Validation of TRMM and other rainfall estimates with a high-density gauge datasets for West Africa Part I: validation of GPCP rainfall product and pre-TRMM satellite and blended products. *J. Appl. Meteorol.* 42, 1337–1354 [http://dx.doi.org/10.1175/1520-0450\(2003\)042C1337:VOTAOR3E2.0.CO;2](http://dx.doi.org/10.1175/1520-0450(2003)042C1337:VOTAOR3E2.0.CO;2).
- Odekunle, T.O., Eludoyin, A.O., 2008. Sea surface temperature patterns in the Gulf of Guinea: their implications for the spatio-temporal variability of precipitation in West Africa. *Int. J. Climatol.* 28, 1507–1517. <http://dx.doi.org/10.1002/joc.1656>.
- Oguntunde, P.G., Friesen, J., van de Giesen, N., Savenije, H.H., 2006. Hydroclimatology of the Volta River Basin in West Africa: trends and variability from 1901 to 2002. *Physics and Chemistry of the Earth, Parts A/B/C* 31 (18), 1180–1188. <http://dx.doi.org/10.1016/j.pce.2006.02.062>.
- Okonkwo, C., 2014. An advanced review of the relationships between Sahel precipitation and climate indices: a wavelet approach. *International Journal of Atmospheric Sciences* 2014. <http://dx.doi.org/10.1155/2014/759067> 11.
- Owusu, K., Waylen, P., 2009. Trends in spatio-temporal variability in annual rainfall in Ghana (1951–2000). *Weather* 64 (5), 115–119.
- Owusu, K., Waylen, P., 2013. The changing rainy season climatology of mid-Ghana. *Theor. Appl. Climatol.* 112 (3), 419–430. <http://dx.doi.org/10.1007/s00704-012-0736-5>.
- Owusu, K., Waylen, P., Qiu, Y., 2008. Changing rainfall inputs in the Volta basin: implications for water sharing in Ghana. *Geojournal* 71 (4), 201–210. <http://dx.doi.org/10.1007/s10708-008-9156-6>.
- Paeth, H., Fink, A., Pohl, S., Keis, F., Machel, H., Samimi, C., 2012. Meteorological characteristics and potential causes of the 2007 flood in sub-Saharan Africa. *Int. J. Climatol.* 31, 1908–1926. <http://dx.doi.org/10.1002/joc.2199>.
- Preisendorfer, R., 1988. *Principal component analysis in meteorology and oceanography*. Developments in Atmospheric Science 17. Elsevier, Amsterdam.
- Ramillien, G., Bouhours, S., Lombard, A., Cazenave, A., Flechtner, F.R., Schmidt, 2008. Land water storage contribution to sea level from GRACE geoid data over 2003–2006. *Glob. Planet. Chang.* 60 (3–4), 381–392. <http://dx.doi.org/10.1016/j.gloplacha.2007.04.002>.
- Rodríguez-Fonseca, B., Janicot, S., Mohino, E., Losada, T., Bader, J., Caminade, C., Chauvin, F., Fontaine, B., Garc'ia-Serrano, J., Gervois, S., Joly, M., Polo, I., Ruti, P., Roucou, P., Voldoire, A., 2011. Interannual and decadal SST-forced responses of the West African monsoon. *Atmos. Sci. Lett.* 12, 67–74. <http://dx.doi.org/10.1002/asl308>.
- Rouault, M., Richard, Y., 2003. Intensity and spatial extension of drought in South Africa at different time scales. *Water SA* 29 (4), 489–500.
- Santos, J.A.F., Pulido-Calvo, I., Portela, M.M., 2010. Spatial and temporal variability of droughts in Portugal. *Water Resour. Res.* 46 (3). <http://dx.doi.org/10.1029/2009WR008071> W03503.
- Schneider, U., Becker, A., Finger, P., Meyer-Christoffer, A., Ziese, M., Rudolf, B., 2014. GPCP's new land surface precipitation climatology based on quality-controlled in situ data and its role in quantifying the global water cycle. *Theor. Appl. Climatol.* 115 (1–2), 15–40. <http://dx.doi.org/10.1007/s00704-013-0860-x>.
- Shukla, S., Wood, A.W., 2008. Use of a standardized runoff index for characterizing hydrologic drought. *Geophys. Res. Lett.* 35 (2). <http://dx.doi.org/10.1029/2007GL032487> L02405.
- Sneeuw, N., Lorenz, C., Devaraju, B., Tourian, M., Riegger, J., Kunstmann, H., Bárdossy, A., 2014. Estimating runoff using hydro-geodetic approaches. *Surv. Geophys.* 35 (6), 1333–1359. <http://dx.doi.org/10.1007/s10712-014-9300-4>.
- Swenson, S., Wahr, J., 2007. Multi-sensor analysis of water storage variations of the Caspian Sea. *Geophys. Res. Lett.* 34 (16). <http://dx.doi.org/10.1029/2007gl030733>.

- 204 Swenson, S., Chambers, D., Wahr, J., 2008. Estimating geocenter variations from a combination of GRACE and ocean model output. *Geophys. Res. Lett.* 31, 1–4. <http://dx.doi.org/10.1029/2004GL019920>.
- Tapley, B., Bettadpur, S., Watkins, M., Reigber, C., 2004. The Gravity Recovery and Climate Experiment: mission overview and early results. *Geophys. Res. Lett.* 31, 1–4. <http://dx.doi.org/10.1029/2004GL019920>.
- Theis, F.J., Gruber, P., Keck, I.R., Meyer-bäse, A., Lang, E.W., 2005. Spatiotemporal blind source separation using double-sided approximate joint diagonalization. In *Proc. EUSIPCO 2005*.
- Tourian, M., Elmi, O., Chen, Q., Devaraju, B., Roohi, S., Sneeuw, N., 2015. A spaceborne multisensor approach to monitor the desiccation of Lake Urmia in Iran. *Remote Sens. Environ.* 156, 349–360. <http://dx.doi.org/10.1016/j.rse.2014.10.006>.
- Vicente-Serrano, S.M., 2006. Spatial and temporal analysis of droughts in the Iberian Peninsula (1910–2000). *Hydrol. Sci. J.* 51 (1), 83–97. <http://dx.doi.org/10.1623/hysj.51.1.83>.
- Wahr, J., Molenaar, M., Bryan, F., 1998. Time variability of the Earth's gravity field: hydrological and oceanic effects and their possible detection using GRACE. *J. Geophys. Res. Solid Earth* 103 (B12), 30205–30229. <http://dx.doi.org/10.1029/98jb02844>.
- Wouters, B., Schrama, E.J.O., 2007. Improved accuracy of GRACE gravity solutions through empirical orthogonal function filtering of spherical harmonics. *Geophys. Res. Lett.* 34 (23). <http://dx.doi.org/10.1029/2007GL032098>.
- Ziehe, A., 2005. *Blind Source Separation Based on Joint Diagonalization of Matrices With Applications in Biomedical Signal Processing*. Universitat Potsdam (PhD thesis; Retrieved from: <http://en.youscribe.com/catalogue/reports-and-theses/knowledge/blind-source-separation-based-on-joint-diagonalization-of-matrices-1424347>. Accessed 15 May 2015).

6 Hydrological controls on surface vegetation dynamics

This chapter is covered by the following publication ([Ndehedehe et al., 2017b](#)):

Christopher E. Ndehedehe, Joseph L. Awange, Michael Kuhn, and Nathan O. Agutu (2017). Hydrological controls on surface vegetation dynamics over Sub-Sahara Africa using GRACE satellite observations. *Revised and submitted to Journal of Arid Environments*.

Numerous studies in the past have used various remotely sensed precipitation and soil moisture products to investigate the water driven variability of surface vegetation. Because of the complex combination of environmental, social, and multiple strings of anthropogenic factors in Africa, these products are somewhat restricted as drivers of vegetation dynamics. For the first time in SSA (West Africa and the Congo basin), the water driven variability of surface vegetation (the normalised difference vegetation index used as a vegetation proxy) is investigated using TWS derived from GRACE satellite observations. This current contribution provides new perspectives on the response of surface vegetation to hydrological conditions in the region that will benefit the remote sensing community and foster a better understanding of eco-hydrological processes and interactions in African biophysical systems. Specifically, it presents GRACE observations as a suitable hydrological indicator in lieu of soil moisture for monitoring vegetation phenology in the dry tropics, complementing rainfall, which only provides an indirect observation of water availability. Several regional studies, including those at country-level have shown the sensitivity of ecosystems to intra-annual (seasonal variability in rainfall) and inter-annual (year to year variability) changes in rainfall. Such changes in rainfall presents not only challenges to economic development (e.g., food production), but raises concerns on the sustainability and survival of the region's remarkable biodiversity. However, as this study suggests, degradational transitions in land cover and climate variations are composite phenomena that will primarily determine the trajectory of prospective future changes in the vegetation system of SSA and how it responds to the hydrological cycle.

Hydrological controls on surface vegetation dynamics over Sub-Saharan Africa using GRACE satellite observations

Christopher E. Ndehedehe^{a,b,*}, Joseph L. Awange^a, Michael Kuhn^a, Nathan O. Agutu^{a,c}

^a*Department of Spatial Sciences, Curtin University, Perth, Western Australia, Australia.*

^b*Department of Geoinformatics and Surveying, University of Uyo, P.M.B. 1017, Uyo, Nigeria.*

^c*Department of Geomatic Engineering and Geospatial Information Systems JKUAT, Nairobi, Kenya.*

Abstract

A considerable number of independent case studies have shown the explicit role of rainfall and soil moisture as drivers of surface vegetation dynamics. However, the weak relationship exhibited by rainfall and soil moisture with vegetation productivity in some semi-arid and humid ecosystems of Africa due to a complex combination of social and environmental factors warrants further assessment of hydrological controls on surface vegetation changes. This study explores the utility of terrestrial water storage (TWS) derived from Gravity Recovery and Climate Experiment (GRACE) as a hydrological control on surface vegetation in Sub-Saharan Africa-SSA using monthly Normalized Difference Vegetation Index (NDVI) (2002 – 2013) as a vegetation proxy. Results indicate that the temporal relationships of NDVI with TWS over West Africa, and in catchment-specific cases (southern Mali and Lake Chad basin-LCB), be it monthly or annual scale, are generally slightly stronger than the widely reported rainfall-NDVI relationship. However, when the spatial relations of TWS-NDVI and rainfall-NDVI were evaluated at monthly and seasonal scales, rainfall shows a considerable and wider spread of significant correlations ($\rho < 0.05$) with surface vegetation greenness compared to TWS. Some locations in the semi-arid Sahel (e.g., north-east Nigeria, southern Chad, and West Sahel) exist nonetheless, where spatial correlation between NDVI and TWS is relatively higher and consistent as opposed to rainfall-NDVI correlations. A contemporary understanding of the water driven variability in surface vegetation in SSA indicates that (i) the preponderance of observed positive correlations of NDVI with TWS and rainfall are predominantly found in the Sudano-Sahelian ecosystems, where total NDVI variability is apparently the strongest (51.4%), and (ii) some of the Sahelian vegetation also show considerable and significant association with model-derived groundwater.

Keywords: NDVI, Sahel, Water, Rainfall, Vegetation, West Africa

*Corresponding author

Email address: christopherndehedehe@gmail.com (Christopher E. Ndehedehe)

1 **1. Introduction**

2 As it is with other terrestrial ecosystems of the world, changes in hydro-climatic conditions
3 represent a considerable challenge to the availability of water in Africa, leading to loss of bio-
4 diversity, desertification, and increased vulnerability of ecosystem services. These often cause
5 societal stress with implications on surface vegetation phenology and crop production in the
6 continent, as the vegetation system in the tropics are mostly restricted by water availability
7 (Zeng et al., 1999). Since mankind depends on healthy vegetation not only for the supply of
8 energy and food, but also for essential services such as regulating the climate system, storing
9 carbon, and hosting biodiversity (e.g., Trumbore et al., 2015; Zeng et al., 1999), the need to
10 examine the response of surface vegetation to changes in hydrological conditions is important.

11 To highlight the constraints of water on terrestrial ecosystems and regional land surface
12 phenology, soil moisture and rainfall products are commonly used (see, e.g., Guan et al., 2014;
13 Knauer et al., 2014; Chen et al., 2014; Zhou et al., 2014; Seghieri et al., 2012; Huber et al.,
14 2011; Do et al., 2005; Nicholson et al., 1990). Some recent reports have argued that rainfall
15 only provides an indirect observation of water availability (e.g., Chen et al., 2014; Yang et al.,
16 2014) while others have emphasized that uncertainties in regional precipitation estimates and
17 water budget indicators are major challenges in understanding vegetation response to water
18 constraints (e.g., A et al., 2015; Zhang et al., 2009). Globally, the impacts of climate change
19 on ecosystem productivity may trigger complex terrestrial ecosystem response to hydrological
20 conditions. In southwestern North America, for example, surface vegetation greenness is both a
21 function of dry season length and precipitation with the former playing a more significant role
22 in vegetation growth (Zhang et al., 2010). The length of rainy season in some African *hot spots*
23 does have strong non-linear impacts on tree fractional cover due to compound mechanisms of
24 hydrological cycle (Guan et al., 2014). But in dry tropical areas, a decrease in temperature was
25 found to be the strongest predictor of both leafing and reproductive phenophases in the Sahel
26 (Seghieri et al., 2012).

27 Region-specific case studies in West Africa (Fig. 1a) as summarised by Knauer et al. (2014)
28 agree that it is somewhat difficult to satisfactorily untangle the impact of precipitation on its
29 vegetation system due to a number of factors that include, e.g., extreme rainfall variability,
30 complex landscapes and hydrological processes. Accumulating evidence from considerable case
31 studies by Knauer et al. (2014) indicates that rainfall has not sufficiently explained changes in

32 surface vegetation greenness in West Africa. This has been attributed mostly to human influence
33 and the impacts of climate change (see, e.g., [Dardel et al., 2014](#); [Jamali et al., 2014](#); [Knauer et al.,](#)
34 [2014](#); [Boschetti et al., 2013](#); [Olsson et al., 2005](#); [Herrmann et al., 2005](#); [Li et al., 2004](#)). Whereas
35 model-derived soil moisture is restricted as a driver of vegetation dynamics in the African Sahel
36 (e.g., [Huber et al., 2011](#); [Do et al., 2005](#)), the complex formation of the African rainforest limits
37 satellite moisture observations in the study of vegetation water dynamics. Apparently, soil
38 moisture observations from remote sensing platforms maybe limited and largely restricted in
39 highly dense vegetation community, as plant tissues, which contain significant amount of water
40 weaken the intensity of the microwave signal (e.g., [Dirmeyer et al., 2004](#); [Njoku and Entekhabi,](#)
41 [1996](#)).

42 The morphological and physiological adaptations of Sahelian vegetation results in complex
43 water use mechanisms during the dry season (e.g., [Guan et al., 2014](#); [Seghieri et al., 2012](#); [Huber](#)
44 [et al., 2011](#)) and may further restrict soil moisture as a driver of vegetation dynamics. Although
45 it is arguably the most suitable indicator in understanding land surface phenology and the re-
46 sponse of plants to the changing climate system (see, e.g., [Chen et al., 2014](#); [Huber et al., 2011](#)),
47 satellite soil moisture observations may be restricted in landscapes where vegetation and plant
48 cover, overwhelmingly depend on soil water from the saturated zone. This limitation can be
49 attributed to large retrieval errors (e.g., [Högstrom et al., 2014](#)) and the fact that satellite soil
50 moisture observations are mostly restricted to the few centimeters of the top soil (e.g., [Yang](#)
51 [et al., 2014](#)). The root depth of most Sahelian vegetation, for instance, extends to the water ta-
52 ble region, which lies up to 40 m below the surface during the dry season ([Huber et al., 2011](#); [Do](#)
53 [et al., 2005](#)). This makes some of the Sahelian trees much less sensitive not only to inter-annual
54 changes in rainfall but also to changes in soil moisture (be it satellite or model-derived). In
55 addition, environmental, pedological (e.g., soil characteristics), and hydro-climatological condi-
56 tions amongst other factors contribute considerably to the diversity in local hydrology, creating
57 uncertainties in our knowledge of vegetation response to land surface conditions (e.g., soil wet-
58 ness). Under these conditions, both soil moisture and precipitation may largely be restricted as
59 hydrological controls for vegetation dynamics in the African Sahel.

60 To circumvent the limitations of soil moisture and precipitation to infer changes in vege-
61 tation water content as discussed above, Gravity Recovery and Climate Experiment (GRACE,
62 [Tapley et al., 2004](#)) terrestrial water storage (TWS; soil moisture, groundwater, surface water,
63 and canopy) data are emerging as an alternative product to (i) evaluate temporal and spatial
64 dynamics in soil moisture and groundwater at watershed scale (e.g., [Abiy and Melesse., 2017](#);

65 Famiglietti, 2014; Wouters et al., 2014, and the references therein) and (ii) to study the impact
66 of climate variability on vegetation water changes (see, A et al., 2015; Yang et al., 2014). Its use
67 in the data deficient SSA as a proxy for available plant/vegetation water however, has not been
68 reported. Because of the restrictions of soil moisture in water-limited ecosystems and the fact
69 that sub-surface water use during dry season exists in the Sahel region (see, e.g., Guan et al.,
70 2014; Huber et al., 2011), investigating the potential use of GRACE-derived TWS as a driver
71 of vegetation dynamics is essential. This study is critical and provides complementary perspec-
72 tives on water availability as a driver of vegetation dynamics. Whereas it further advances our
73 knowledge of African ecology and its biophysical systems, this study extends GRACE satellite
74 observations as a valuable tool for global terrestrial ecosystem assessment, especially in data
75 sparse regions of the world.

76 The main objective of this study is to investigate the potential of GRACE-derived TWS
77 as a hydrological control for observed changes in surface vegetation over West Africa based on
78 temporal and spatial relations. In this study, surface vegetation is characterised by Normalized
79 Difference Vegetation Index (NDVI). The relationships of TWS and rainfall with the leading
80 temporal modes of NDVI variability over West Africa are also explored. This study further uses
81 groundwater derived from WaterGap model (Döll et al., 2014) in addition to GRACE-derived
82 TWS to better understand regions whose vegetation systems are groundwater-dependent. The
83 response of NDVI to hydrological conditions (GRACE-derived TWS and WaterGap model-
84 derived groundwater, and rainfall) is analysed and studied with respect to dominant plant
85 covers (Fig. 1b) derived from the Moderate Resolution Imaging Spectroradiometer (MODIS)
86 land cover products.

87 **2. The vegetation system of West Africa and response to climate**

88 The coastal regions of West Africa with several hydrological networks (Fig. 1a) are heavily
89 forested ecosystems (Fig. 1b) with considerable amounts of annual rainfall (Fig. 1c) compared
90 to the semi-arid and arid ecosystems found in Sudano and Central Sahel belt, respectively.
91 Apparently, surface vegetation dynamics in West Africa is largely sensitive to water availability,
92 which is largely modulated by climate variability. The seasonal distribution of NDVI in the
93 region, for example, predominantly follows the climatic zones, with vegetation density decreasing
94 gradually from the humid tropical rainforest of the Guinea Coast and Equatorial countries
95 through the semi-arid Sahel region to the Sahara Desert (Fig. 1b and d). This diversity in
96 ecosystem and species richness and vegetation density (Figs. 1b and d) in the region is largely

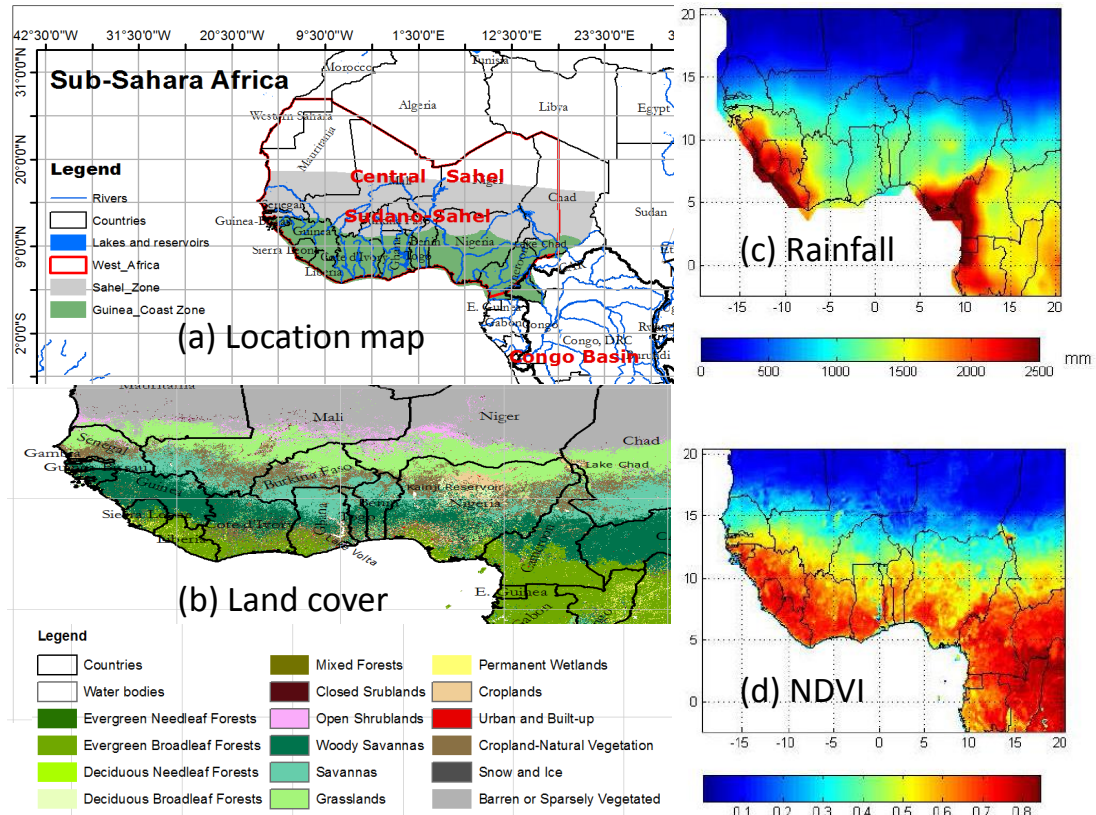


Figure 1: Study area showing countries and other sub-regions in Sub-Saharan Africa. (a) Location map showing countries of West Africa, Equatorial region/Congo basin, and hydrological units, (b) land cover map extracted from MODIS (MCD12Q1) Land Cover products (the data can be accessed using the spatial data access tool available at http://webmap.ornl.gov/ogcdown/dataset.jsp?ds_id=10004), (c) the annual rainfall, and (d) mean annual NDVI during the 2003 – 2013 period averaged over SSA.

97 driven by the migration of the tropical rainbelt, leading to over 2500 mm/yr of annual rainfall in
 98 the Guinea Coast and Equatorial countries (hereafter called coastal countries) and less than 500
 99 mm/yr in the Sahelian countries (Fig. 1c). Specifically, in the Central African Republic (CAR,
 100 see Fig. 1d) where several vegetation formations ranging from savannas, swamp forests, to other
 101 forests are found to be strongly correlated with rainfall (Gond et al., 2013). High NDVI values
 102 in almost all seasons except the period between September and December are predominant
 103 (Fig. 1d). Similarly, NDVI values are relatively high (about 0.8) and decreases (between 0.6
 104 and 0.7) towards the end of the year in the upland Congo basin where a considerable amount
 105 of Evergreen broadleaf forests are mostly embedded in swamps (Figs. 1b and d).

106 A quick assessment of NDVI distribution show that relatively strong NDVI values are
 107 observed in the coastal countries during the January-March (JFM), April-June (AMJ), and

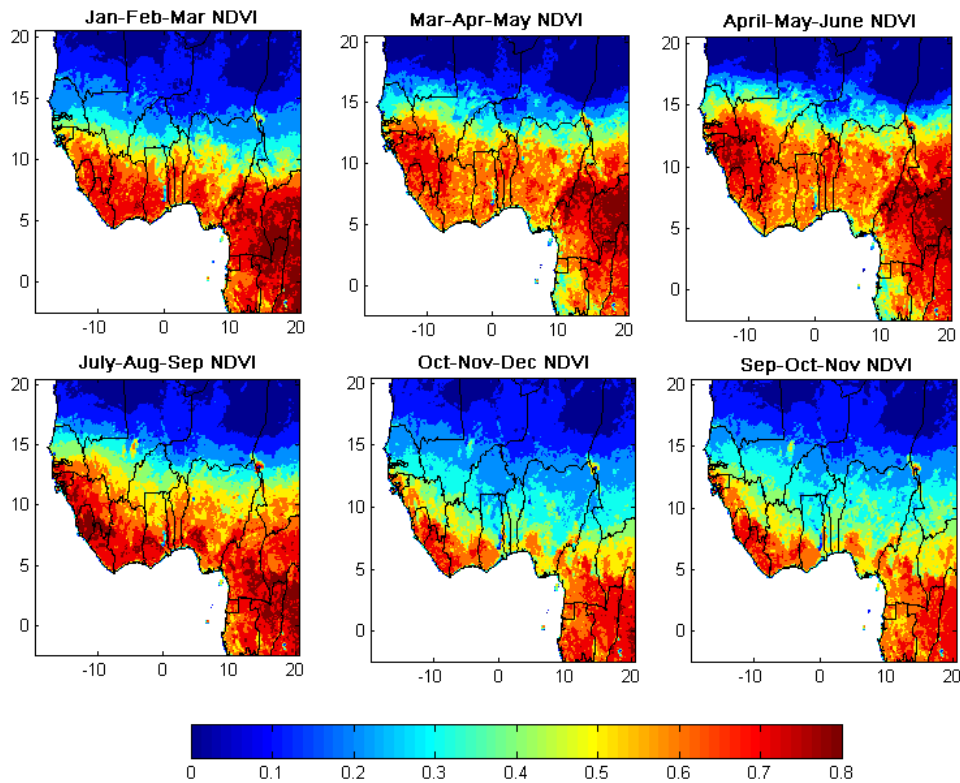


Figure 2: Average seasonal NDVI distribution over SSA for the period 2002 to 2013. The seasonal classifications are based on crop and rain seasons in SSA and are described as: January, February, and March-JFM; March, April, and May-MAM; April, May, and June-AMJ; July, August, and September-JAS; September, October, and November-SON; October, November, and December-OND.

108 July-September (JAS) periods (Fig. 2). Conversely, low NDVI values are observed during the
 109 September-November (SON) and October-December (OND) periods (Fig. 2). NDVI still os-
 110 cillates during dry seasons along the coastal countries of SSA. This can be seen, for example,
 111 in the JFM period in Liberia, Côte d'Ivoire, southern Ghana, and Cameroon where despite
 112 receiving relatively low rainfall during the period (dry season) indicate high NDVI values. This
 113 perhaps is due to the presence of permanent wetlands and huge Evergreen broadleaf forests that
 114 thrives in water logged soils (Fig. 1b). Consequently, rainfall may not be sufficient in monitoring
 115 vegetation conditions in such areas as the vegetation and forest formations are mostly sensitive
 116 to pedological conditions that are in the root zones. Apart from soil type, climate variability
 117 play key roles in the spatial and temporal distributions of surface vegetation in SSA.

118 3. Data

119 3.1. Normalised Difference Vegetation Index (NDVI)

120 The Normalized Difference Vegetation Index (NDVI) is sensitive to vegetation condition
121 and is associated with vegetation primary production and photosynthetically active radiation
122 (e.g., Tucker et al., 2005; Herrmann et al., 2005). Several studies have used it to monitor
123 changes in surface vegetation and water stress in plants (e.g., Dardel et al., 2014; Chen et al.,
124 2014; Jamali et al., 2014; Knauer et al., 2014; Boschetti et al., 2013; Olsson et al., 2005; Her-
125 rmann et al., 2005; Li et al., 2004; Nicholson et al., 1990). The monthly NDVI data used
126 in this study is an 8 km spatial resolution data prepared by the Global Inventory Modelling
127 and Mapping Studies (GIMMS) based on the Advanced Very High Resolution Radiometer
128 (AVHRR) (e.g., Tucker et al., 2005; Herrmann et al., 2005) and is available for download
129 (<http://ecocast.arc.nasa.gov/data/pub/gimms/>). The data has been corrected for cloud cover,
130 atmospheric water vapour, and residual sensor degradation and is suitable for vegetation studies
131 (see, e.g., Bégué et al., 2011; Herrmann et al., 2005; Tucker et al., 2005). The consistency of
132 the NDVI product used in this study in the region with three other AVHRR-NDVI datasets,
133 field measurements, and MODIS NDVI has already been assessed (Dardel et al., 2014). The
134 recent NDVI products (GIMMS-3g) used in this study are the monthly maximum composites
135 and covers the period of 2002 – 2013. It is used to analyse the variability in surface vegetation
136 greenness over SSA. The annual NDVI time series were derived by aggregating these monthly
137 maximum composites over SSA. It is re-projected and aggregated to a 1° x 1° grid before ap-
138 plying the spatial correlation with TWS and rainfall in order to maintain a common spatial
139 resolution with other data.

140 3.2. GRACE-derived terrestrial water storage (TWS)

141 Gravity Recovery and Climate Experiment (GRACE, Tapley et al., 2004) satellite mission
142 provides an integrated sum of changes in surface waters, catchment stores (e.g., groundwater, soil
143 moisture, etc.), and canopy based on the observations of the Earth's time variable gravity field.
144 GRACE observations have been extensively used to study the Earth's water storage changes at
145 regional, continental, and global scales (e.g., Ndehedehe et al., 2016b; Joodaki et al., 2014; Ramil-
146 lien et al., 2008; Swenson and Wahr, 2007; Wouters et al., 2014, and the references therein). In
147 this study, the GRACE Release-05 (RL05) spherical harmonic coefficients obtained from Center
148 for Space Research (CSR) (see, <http://icgem.gfz-potsdam.de/ICGEM/shms/monthly/csr-rl05/>)
149 covering the period of 2002 – 2014, are used to estimate TWS over the region on a 1° x 1° grid

150 following the approach of Wahr et al. (1998). Processing details follow the approach of Landerer
151 and Swenson (2012) and are only briefly summarised here. As opposed to GRACE applications
152 in studies of droughts, floods, and terrestrial water budget (see, e.g., Thomas et al., 2014; Reager
153 et al., 2014; Houborg et al., 2012; Sheffield et al., 2009; Yirdaw et al., 2008), it is employed here
154 as a tool for ecosystem assessment. Note that GRACE-derived TWS is simply referred to as
155 TWS in the manuscript.

156 3.3. *WaterGap global hydrology model (WGHM)*

157 The global hydrological model WaterGAP (Döll et al., 2014) is used to derive groundwater
158 component over SSA for the period 2002 – 2009. This model takes into account groundwater
159 recharge from surface water bodies in semi-arid and arid regions and groundwater depletion.
160 The relationship between groundwater and NDVI is examined using correlation analysis. The
161 WaterGAP model (version 2.2a) data used in this study has a spatial resolution of $1^\circ \times 1^\circ$ and
162 is downloaded from Center for Environment Systems Research (CESR) website.

163 3.4. *Precipitation from tropical rainfall measuring mission (TRMM)*

164 TRMM 3B43 (Huffman et al., 2007; Kummerow et al., 2000) based precipitation, cover-
165 ing the period 2002 – 2013 is used in this study to examine vegetation response to rainfall
166 variability. The data has a global coverage between 50°S and 50°N with a spatial resolu-
167 tion of $0.25^\circ \times 0.25^\circ$. The TRMM 3B43 data, which also includes the Global Precipita-
168 tion Climatology Center (GPCC) gauge dataset performs well in the region (see, e.g., Paeth
169 et al., 2012). Monthly TRMM precipitation were resampled to a $1^\circ \times 1^\circ$ grid before ap-
170 plying the spatial correlation in order to maintain a common spatial resolution with other
171 datasets such as the NDVI and GRACE-TWS solutions. The data is available at the National
172 Aerospace and Space Administration (NASA) Goddard Space Flight Center (GSFC) website
173 (<http://disc.gsfc.nasa.gov/datacollection/TRMM3B43-V7>
174 .shtml).

175 3.5. *MODIS land cover data*

176 The Moderate Resolution Imaging Spectroradiometer (MODIS) global land cover product
177 (MCD12Q1) version 005 with a spatial resolution of 500 m, contains multiple classification
178 schemes that describe different global land covers. This data, which covers the 2001 – 2007
179 period is used to study the response of vegetation formations to TWS and rainfall. The prin-
180 cipal global vegetation classification scheme of this product identifies 17 land cover types as

181 defined by the International Geosphere Biosphere Programme (IGBP) and is available online
 182 (http://webmap.ornl.gov/ogcdown/dataset.jsp?ds_id=10004). This data was extracted for the
 183 study area (latitudes 2.5°S to 20°N and longitudes 20°W to 20°E) and further processed using
 184 a geographic information system (GIS) framework in order to obtain a mask for the different
 185 vegetation formations and their transitions during the period of 2001 – 2007.

186 4. Methods

187 4.1. Multivariate analyses

188 To regionalise NDVI over SSA, independent component analysis (ICA), a fourth-order cu-
 189 mulant statistic, was employed (see, e.g., Ziehe, 2005; Cardoso and Souloumiac, 1993; Cardoso,
 190 1991; Common, 1994; Cardoso, 1999). This cumulant based statistics decomposes monthly grids
 191 of NDVI into spatial and temporal patterns as

$$\mathbf{X}_{NDVI} = \mathbf{B}\mathbf{E}^T, \quad (1)$$

192 where \mathbf{X} is the NDVI data matrix with rows and columns representing months and the NDVI
 193 grid values over SSA, respectively. \mathbf{B} contains the independent components (ICs) (also known
 194 as the NDVI temporal evolutions), which are scaled by its standard deviation and \mathbf{E}^T the NDVI
 195 spatial patterns, which are scaled by multiplying with the standard deviation of its corresponding
 196 ICs. The relationships of four leading temporal modes of NDVI regionalised over SSA with
 197 standardised anomalies of TWS and rainfall averaged over West Africa, the Sahel region, and
 198 the Congo basin area were further examined using correlation and regression analyses. Further
 199 details about the application of this method can be found in previous studies (e.g., Ndehedehe
 200 et al., 2016b, 2017a; Frappart et al., 2011; Ziehe, 2005).

201 After removing the harmonic components (i.e., annual and semi-annual signals) of the NDVI
 202 data, the residual part was compared with those of TWS and rainfall using the MLRA. This is
 203 done to examine which of TWS and rainfall reflects better the internal variabilities in NDVI.
 204 This was achieved by parameterizing the linear, annual, and semi-annual components of the
 205 data \mathbf{Y} , as (e.g., Ndehedehe et al., 2017b)

$$\mathbf{Y}_{NDVI/TWS/TRMM}(x, y, t) = \beta_0 + \beta_1 t + \beta_2 \sin(2\pi t) + \beta_3 \cos(2\pi t) + \beta_4 \sin(4\pi t) + \beta_5 \cos(4\pi t) + \varepsilon(t), \quad (2)$$

206 where (x, y) are grid locations, t is the time, β_0 is the constant offset, β_1 is the linear trend, β_2
 207 and β_3 accounts for the annual signal while β_4 and β_5 represents the semi-annual signal, and

208 $\varepsilon(t)$ is the random error term. These harmonic components were removed from the data (i.e.,
209 NDVI, TRMM, and TWS) in order to obtain the residual, which in this case includes the trend
210 component.

211 4.2. Correlation analyses and cumulative departures

212 The temporal relationship of NDVI with TWS and rainfall is examined using Pearson's
213 correlation coefficients (r). On the other hand, the association of surface vegetation with changes
214 in TWS and rainfall at monthly and seasonal scales (i.e., NDVI/TWS and NDVI/rainfall)
215 is illustrated by a grid by grid comparison. This is achieved by using correlation analyses
216 after re-projecting and aggregating NDVI and TRMM-based precipitation to a $1^\circ \times 1^\circ$ spatial
217 resolution as TWS. The cross-correlation method is used to determine the time lag in the data
218 when maximum correlation occurred. Furthermore, monthly anomalies for NDVI, TWS, and
219 TRMM-based precipitation were estimated by removing the long term mean. Thereafter, these
220 monthly anomalies were aggregated to yearly values and subsequently the cumulative departure
221 (e.g., [Weber and Stewart, 2004](#)) of each data was then computed. Cumulative departures of
222 these variables are helpful as a general indicator of trends, with the upward and downward
223 gradient indicating relatively a rise and fall, respectively.

224 5. Results and discussion

225 5.1. GRACE-derived TWS hydrological control on the temporal variations of NDVI

226 In this Section, the results of temporal variations, seasonal, and mean annual cycles of NDVI
227 are compared with those of TWS and rainfall. Specifically, the potential of TWS as an alternate
228 indicator to rainfall that can enhance the understanding of vegetation response to hydrological
229 conditions along different climatic belts in the region is discussed.

230 5.1.1. Mean annual cycles of NDVI, TWS, and rainfall

231 Comparing the cumulative annual departures (i.e., cumulative annual anomalies) of NDVI
232 with those of TWS and rainfall masked over West Africa, the temporal patterns of NDVI is
233 somewhat consistent with that of rainfall, both indicating a fall during the 2003 – 2005 period
234 (Fig. 3a-b). Further, NDVI showed a rise during 2005 – 2013 period in their cumulative annual
235 anomalies while TWS showed a fall between 2003 and 2007 and an increase during the 2007–2009
236 period (Fig. 3a). It seems that rainfall generally follows NDVI except for the anomalous years
237 of 2009 and 2011 (Fig. 3b). These cumulative annual departures provide an overview of the

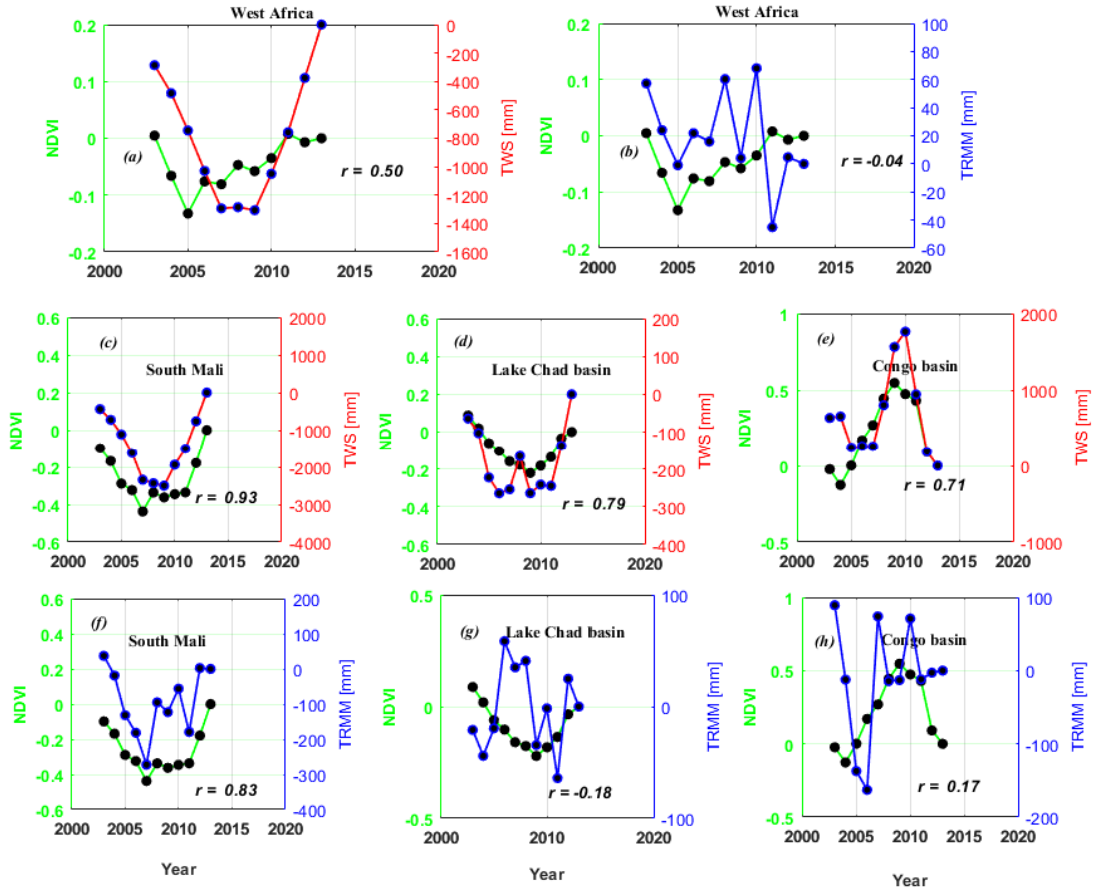


Figure 3: Comparison of cumulative annual departures of NDVI with those of TWS and TRMM based precipitation during the 2003 – 2013 period in SSA. (a)-(b) Cumulative annual departures (NDVI vs TWS and NDVI vs TRMM) over West Africa, (c)-(e) cumulative annual departures of NDVI with TWS, and (f)-(h) cumulative annual departures of NDVI with precipitation over the selected basins/catchments (southern Mali, Lake Chad and Congo basins).

238 eco-hydrological narrative of West Africa during the 2003 – 2013 period. In particular, the role
 239 of land use change on surface runoff (e.g., Descroix et al., 2009; Favreau et al., 2009; Séguis
 240 et al., 2004) and the impact of surface water schemes on hydrological regimes (e.g., Ndehedehe
 241 et al., 2017a) may result in complex hydrological processes that influences the NDVI-TWS
 242 relationship over West Africa. Other reports from some case studies identified hydrological
 243 drought in the Volta basin during the 2003 – 2007 period and increase in TWS and satellite
 244 derived altimetry water levels (2007–2011) that were more or less consistent with rainfall trends
 245 in the period (e.g., Ndehedehe et al., 2016c; Bekoe and Logah, 2013). GRACE-derived TWS
 246 integrates precipitation over time, and for West Africa, it comprises mainly surface waters (e.g.,

247 lakes and reservoirs), soil moisture, groundwater, and canopy. Since vegetation growth is mostly
248 restricted by soil wetness, it is therefore likely to respond faster to severe drought conditions,
249 unlike TWS where aquifer characteristics, seepages to groundwater, the extent of inundated
250 areas and other human interventions could create a lag of 1-2 years (e.g., Ndehedehe et al.,
251 2016a, 2017a; Ahmed et al., 2014). This relates to the point that the severity of a drought
252 may also depend on the amount of TWS present prior to rainfall deficits. In addition, the
253 cumulative annual departure of TWS between 2007 and 2009 could be an hibernation period
254 when the hydrology of the region is trying to reset owing to an improved rainfall condition
255 (Fig. 3b). Overall, the cumulative rise in TWS tend to mimic that of NDVI more closely (e.g.,
256 2009 – 2011 period) and indicates a modest and statistically significant association during the
257 whole period unlike rainfall (Figs. 3a-b). As TWS can act as a buffer for water availability
258 despite rainfall deficits, such relationship can be relied upon to evaluate the availability of water
259 (excess water or its deficit) for vegetation growth in terrestrial ecosystems.

260 Furthermore, the averaged annual time series of cumulative annual anomalies (NDVI, TWS,
261 rainfall) in selected catchment and river basins (south Mali, Lake Chad basin, and Congo basin)
262 were also evaluated since cumulative annual anomalies over West Africa may be dominated by
263 the tropical regions having very large NDVI, rainfall, and TWS values. The correlation results
264 (Table 1) for these region-specific cases suggest that dynamics in surface vegetation greenness is
265 more associated with TWS than rainfall (Figs. 3c-h). While the annual time series of rainfall and
266 TWS in southern Mali show significant relationships with NDVI, rainfall over the Lake Chad
267 and Congo basins show no statistically significant association with NDVI (Table 1). It appears
268 trends in evapotranspiration (Section 5.2) impact on land surface conditions and the response
269 of vegetation to rainfall in these river basins. But the annual cumulative departures of NDVI
270 and TWS in the Congo basin and West Africa showed considerable and modest associations,
271 respectively (Table 1).

272 5.1.2. Leading temporal evolutions of NDVI variability over SSA

273 The four leading temporal evolutions of NDVI variability (Fig. 4, right) are obtained from the
274 regionalisation of monthly NDVI grids over SSA. These temporal series of NDVI are associated
275 with spatial patterns (Fig. 4, left) that are distributed along different climatic domains. The
276 first NDVI mode indicates variability in the Sudano-Sahelian band while the second NDVI mode
277 shows a dipole pattern over the Central Sahel and Guinea Coast with an opposite phase to the
278 Guinea Coast during the September period (Fig. 4, left). This dipole, which corresponds to an

Table 1: Temporal correlations (r) of NDVI with TRMM and TWS in southern Mali, Lake Chad basin, Congo basin, and West Africa during the 2003–2013 period. Correlation coefficients are significant at the 95% significant level using the Student t-test except for those marked with *.

S/N	Temporal correlations	Southern Mali	Lake Chad basin	Congo basin	West Africa
1	NDVI vs TRMM (monthly)	0.72	0.73	0.70	0.68
2	NDVI vs TWS (monthly)	0.79	0.83	0.09*	0.74
3	NDVI vs TRMM (annual)	0.68	0.21*	0.09*	0.16*
4	NDVI vs TWS (annual)	0.79	0.58	0.42*	0.27
5	NDVI vs TRMM (annual cumulative)	0.83	-0.18*	0.17*	-0.04*
6	NDVI vs TWS (annual cumulative)	0.93	0.79	0.71	0.50

279 approximate phase shift of 0.5 years, is caused by the latitudinal displacement of the rainbelt,
 280 leading to inter-annual variability of rainfall towards the north and south of approximately
 281 latitude 10°N (Nicholson, 2009).

282 With respect to the SSA region (cf. Fig. 1a-b and d), changes in vegetation density and
 283 photosynthetic activity are found to be mostly concentrated around the Sudano-Sahel belt (IC1,
 284 Fig. 4, left) and the Central Sahel (IC2, Fig. 4, left), both accounting for approximately 51.4%
 285 and 15.1% of the total variance, respectively. The observed temporal evolutions of NDVI modes
 286 over the Sudano and Central Sahel indicate relatively strong annual and multi-annual variations,
 287 respectively (IC1 and IC2, Fig. 4, right). Generally, the first NDVI mode is consistent with the
 288 dominant patterns of rainfall and TWS in West Africa as shown in a recent study (Ndehedehe
 289 et al., 2016a). This presents a preliminary picture of both rainfall and TWS as drivers of water
 290 driven changes in surface vegetation over the Sudano-Sahel belt. As the main focus of this
 291 section is on the temporal assessment of the leading modes of NDVI with TWS, the relationship
 292 of the former with rainfall is also explored. Spatially averaged rainfall over West Africa is
 293 strongly associated with NDVI temporal evolutions in the Sudano-Sahel (IC1, Fig. 4 and Table
 294 2) compared to the relationship of averaged rainfall over the Central Sahel with NDVI (IC2,
 295 Fig. 4 Table 2). This shows a strong response of vegetation to rainfall in the Sudano and
 296 semi-arid Sahel regions. Over the Central Sahel (IC2, Fig. 4), the temporal variation of TWS
 297 showed a relatively strong association with NDVI while in the Sudano-Sahel area (IC1, Fig. 4),
 298 TWS showed slightly less agreement with NDVI when compared to rainfall (Table 2). Their
 299 coefficient of determination (R^2) show that TWS explains 47% while rainfall explains 59% of
 300 the annual signals in NDVI over the Sudano-Sahel belt (IC1, Fig. 4, Table 2). In the Central
 301 Sahel (IC2, Fig. 4, Table 2), TWS explains slightly higher portion of the variability in NDVI
 302 ($R^2=52\%$) than rainfall ($R^2=48\%$). This explicit relationship between TWS and vegetation

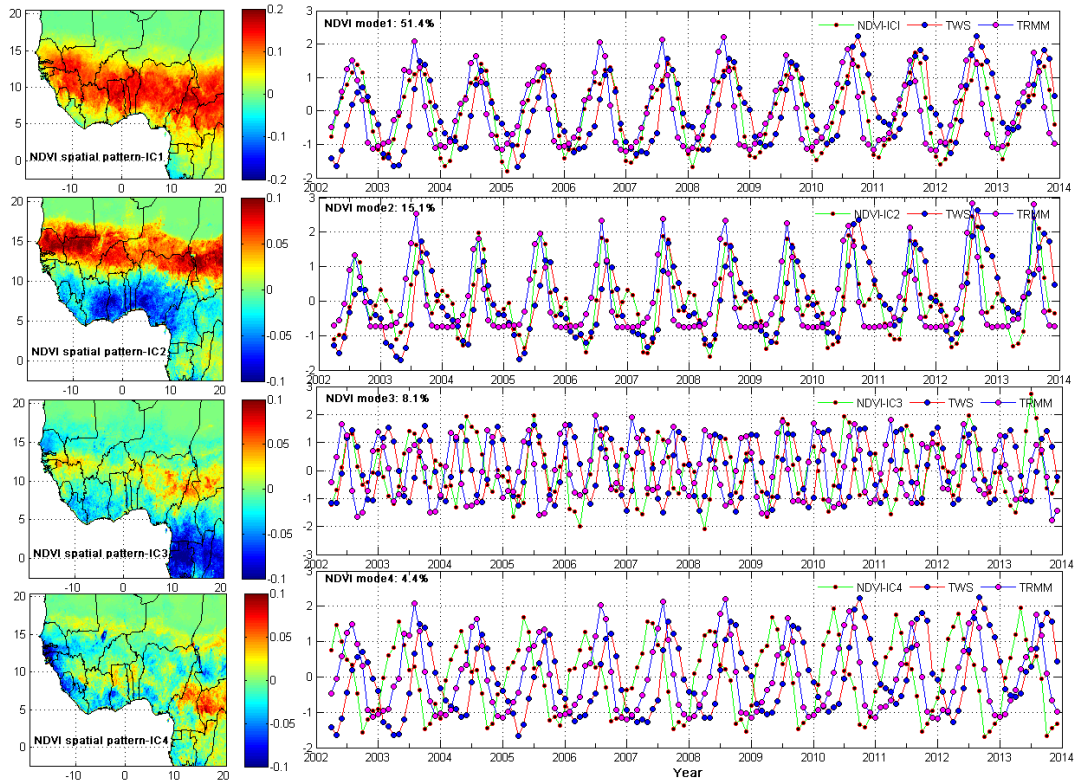


Figure 4: Statistical decomposition of NDVI over Sub-Saharan Africa using the ICA technique. The temporal evolutions (right) have been standardised using their standard deviations. The NDVI spatial patterns (left) are scaled using the standard deviation of the computed independent components (i.e., temporal evolutions). Averaged TWS and rainfall masked over West Africa and Central Sahel have been compared with the temporal evolutions of the first and second ICA modes of NDVI. Also, rainfall and TWS in the Congo basin area and West Africa are compared with the third and fourth ICA modes, respectively.

303 condition in the Central Sahel suggests that TWS could serve as a hydrological control for
 304 assessing vegetation response to changes in hydro-climatic conditions since it is a more direct
 305 measure of water availability in a given ecosystem, complementing precipitation that provides
 306 an indirect observation of water availability.

307 Notably, the Central Sahel is semi-arid, characterised by mostly grasslands, open shrub-
 308 lands, and croplands, with annual rainfall ranging from 700 mm to less than 200 mm during
 309 the studied period (cf. Figs. 1b and d). Given that the Central Sahel is characterised by high
 310 land surface temperatures since it is somewhat close to the Sahara Desert, vegetation growth
 311 and the green-up of plant cover in this region will be largely restricted by soil wetness and
 312 pedological conditions such as infiltration and water holding capacity. High evapotranspiration
 313 rates emanating from land surface temperatures decreases the amount of net precipitation (pre-

Table 2: Temporal relations (r/R^2) of NDVI with those of TRMM and TWS in SSA as observed in the independent modes of variability in Fig. 4. Correlation coefficients are significant at the 95% significant level using the Student t-test except for those marked with *.

S/N	Modes	NDVI vs TRMM		NDVI vs TWS	
		r	R^2	r	R^2
1	IC1	0.77	0.59	0.68	0.47
2	IC2	0.69	0.48	0.72	0.52
3	IC3	0.11*	0.00*	0.01	0.00*
4	IC4	0.32	0.10	-0.67	0.44

314 cipation minus evapotranspiration), and may contribute to the lower proportion of variability
 315 explained by rainfall. As TWS is likely to be driven by changes in soil wetness in such areas,
 316 GRACE-derived TWS changes become a more reliable and available surrogate for soil wetness,
 317 an ideal land surface state variable to examine the impacts of the climate system on vegetation
 318 changes. Nevertheless, the results for NDVI mode 1 indicate that rainfall is still a more viable
 319 driver of vegetation changes in the Sudano-Sahel region (IC1, Fig. 4). The impact of rainfall on
 320 temporal NDVI evolutions in the Sudano-Sahel belt may be justified given that it is largely an
 321 agricultural ecosystem (Fig. 1b) and interestingly, heavily dependent on rainfall. Exceptions to
 322 this may include some of the selected catchments where observed temporal relationships (NDVI
 323 vs rainfall) based on annual aggregations show otherwise (Fig. 3c-h).

324 Furthermore, the third mode of NDVI variability, accounting for 8.1% of the total variability
 325 indicates multi-annual vegetation changes in the Congo basin (IC3, Fig. 4). The fourth mode
 326 showed NDVI annual variability in some coastal countries with an opposite phase in the south
 327 of CAR and north of Cameroon (IC4, Fig. 4), and corresponds to 4.4% of the total variance. In
 328 the Congo basin area (cf. Fig. 1a), observed NDVI variability showed a rather poor relationship
 329 with TWS while averaged rainfall indicated a positive correlation (IC3, Fig. 4 and Table 2). As
 330 TWS somewhat acts as a low-pass filter of precipitation, this may also point towards a phase
 331 lag between TWS and NDVI (IC3, Fig. 4). But the last NDVI mode (IC4, Fig. 4) showed
 332 a statistically significant negative association with average TWS over West Africa and may
 333 be caused by a phase shift of 0.5 years. On the other hand, average rainfall over the same
 334 area indicated a positive association (Table 2). Other complementary perspectives that could
 335 contribute to complex environmental processes in the area may be related to land use change,
 336 surface albedo alterations, uncontrolled deforestation and bush burning, amongst other factors.
 337 Such assumptions, however, may be subject to further clarification.

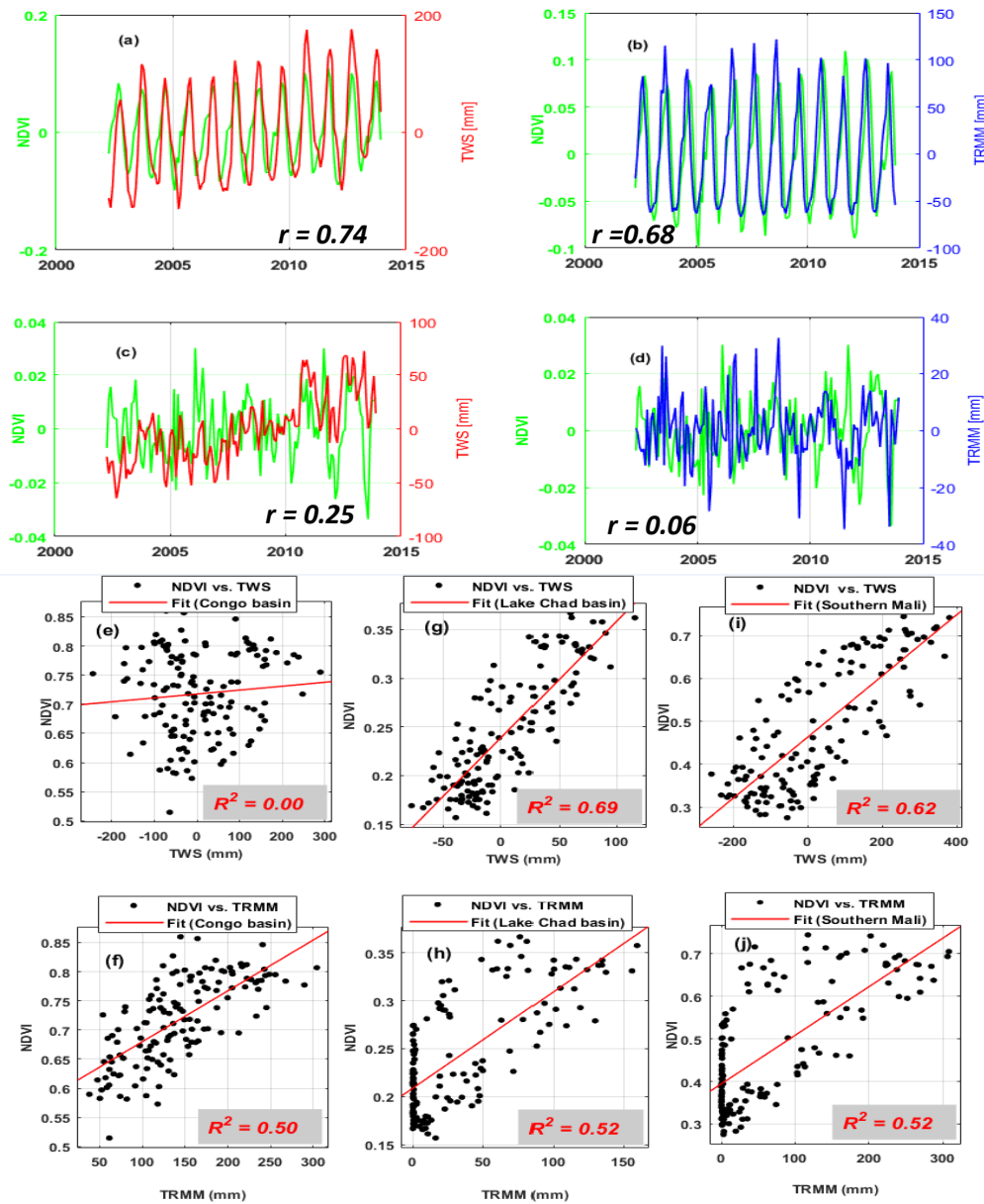


Figure 5: Comparing time series of temporal variations of NDVI, TWS, and rainfall averaged over West Africa and selected basins/catchment areas (Congo basin, Lake Chad basin, and southern Mali) after removing the mean of the period (2003 – 2013). (a-b) Monthly temporal relationship of NDVI with TWS and precipitation and (c-d) association of monthly residuals in NDVI with those of TWS and precipitation over West Africa. (e-j) Regression fits for NDVI with TWS and precipitation in the selected basins and catchment. The MLRA was used to estimate the residual parts of each data by separating the harmonic components (annual and semi-annual) from the data.

338 *5.1.3. The influence of TWS and rainfall on regional dynamics of surface vegetation*

339 To further evaluate the utility of TWS as a hydrological indicator that can be useful in un-
 340 derstanding the temporal variations of vegetation dynamics, the temporal variations of monthly,
 341 annual, and residual NDVI anomalies over West Africa and selected catchments were compared
 342 with those of TWS and precipitation. Temporal patterns of monthly TWS show a rather sim-
 343 ilar association with NDVI indicating a correlation of 0.74 while rainfall shows a correlation
 344 of 0.68 (Figs. 5a and b, Table 1). Also, the residuals of TWS showed some weak associations
 345 with NDVI compared to the residuals of rainfall that showed almost no association with that of
 346 NDVI (Figs. 5c and d). The MLRA results of Figs. 5a-b were compared with singular spectral
 347 analysis (Ghil et al., 2002) of NDVI, rainfall, and TWS time series over West Africa. Although
 348 the results of singular spectral analysis are not shown, overall, they are somewhat consistent
 349 with those of MLRA, indicating that temporal series of TWS are more associated with NDVI
 350 compared to rainfall. In Figs. 5e-j, both TWS and rainfall explained significant variability in
 351 observed NDVI over southern Mali, Lake Chad basin and Congo basin (except for TWS) with
 352 TWS in the Lake Chad basin explaining the highest variability ($R^2 = 69\%$). At the annual
 353 scales, TWS and rainfall averaged over West Africa to some degree are less associated with
 354 NDVI given their relatively low correlations with NDVI (Table 1). Because of the diversity in
 355 landscapes, climate patterns, and ecosystem structure, poor annual associations like this could
 356 result from data averaging and aggregation over the region. Similar analysis for selected catch-
 357 ments in SSA showed that TWS and rainfall have stronger associations with NDVI in southern
 358 Mali while only TWS is better associated with NDVI in Lake Chad basin (Table 1). Also, the
 359 ‘human-induced signal’ such as increase in cropping areas, land use change, and a reduction
 360 in fallow period as indicated by Dardel et al. (2014), in our view, could significantly affect the
 361 temporal evolutions of surface vegetation, leading to poor correlations of NDVI with TWS and
 362 rainfall.

363 Evaluating the monthly temporal patterns of NDVI with those of TWS and rainfall over
 364 SSA, it becomes rather apparent that the monthly and inter-annual variability of NDVI are both
 365 explained by TWS and rainfall (Figs. 5a-j). In particular, TWS appear to be more dependable
 366 than rainfall in its capacity to highlight the water-driven changes in the temporal evolutions
 367 of surface vegetation greenness in southern Mali and the Lake Chad basin (Figs. 5g and i).
 368 Over West Africa, the relationship is somewhat similar as TWS explains about 55% of the
 369 changes in monthly NDVI while rainfall explains about 46% (Figs. 5a, b and Table 1). This
 370 picture accentuates the relative capacity and potential of TWS as a hydrological state variable

371 for monitoring climatic influence on the temporal variations in surface vegetation greenness over
 372 West Africa. This narrative may change nonetheless, when the association between NDVI and
 373 TWS is evaluated based on a grid by grid comparison. Such changes maybe subject to the
 374 complexity in ecosystem interactions and environmental factors (e.g., irrigation, use of chemical
 375 fertilizers, etc.).

376 5.2. Spatial relations of GRACE-TWS, rainfall, and groundwater variability to NDVI

377 5.2.1. Response of monthly NDVI to hydrological conditions at pixel scale

378 NDVI shows relatively strong sensitivity to changes in TWS and rainfall mostly in the Sahel
 379 zone (i.e., Sudano and Sahel belt) (Fig. 6), consistent with the results in Section 5.1.2. Evalu-
 380 ating the pixel scale relationship, rainfall shows statistically significant correlations ($\alpha = 0.05$)
 381 with NDVI in about 90% of SSA (includes non-linear response) during the 2002 – 2013 period
 382 compared to TWS (70% of the region) (Figs. 6a-b). From the spatial distribution of the cor-
 383 relation coefficients, rainfall has a much wider spread of positive correlations than TWS. It is
 384 observed that woody savannas, croplands (natural vegetation), savannas, and grasslands (cf.
 385 Fig. 1b) are the dominant biomes in this Sahel zone where NDVI indicates a strong associa-
 386 tion with rainfall and TWS. Our contemporary understanding of the African eco-hydrological
 387 processes indicates that savannas, grasslands and agricultural biomes of the Sahel region are
 388 sensitive to TWS and rainfall conditions.

389 Looking closely, TWS in some parts of West Sahel (e.g., Gambia, Guinea, Guinea Bissau,
 390 southern Mali) and some *hot spots* in Lake Chad basin show stronger association with NDVI
 391 compared to rainfall (Figs. 6a-b). In the northern flank of Niger, the positive correlations in
 392 Fig. 6a indicates that NDVI still oscillates in some arid ecosystems and shows agreement with
 393 TWS unlike the non-linear response indicated by rainfall (Fig. 6b). This again highlights the
 394 potentials of GRACE-derived TWS as a hydrological control for ecosystem performance, at least
 395 in these region-specific cases. Plant cover ideally responds to land surface conditions. Hence,
 396 change in soil conditions and possible changes in land surface temperature in these ecosystems
 397 may play a major role in the observed association of NDVI with TWS and rainfall. We also
 398 found relatively strong positive correlations of NDVI with rainfall in Gabon and some areas
 399 of the Congo basin, where evergreen broadleaf forest and wetlands are largely predominant.
 400 Other coastal countries in West Africa (e.g., Liberia, Côte d'Ivoire, Sierra Leone, etc.) however,
 401 show relatively poor and negative correlations despite having almost similar climate patterns,
 402 vegetation and edaphic formations as the countries in the Congo basin.

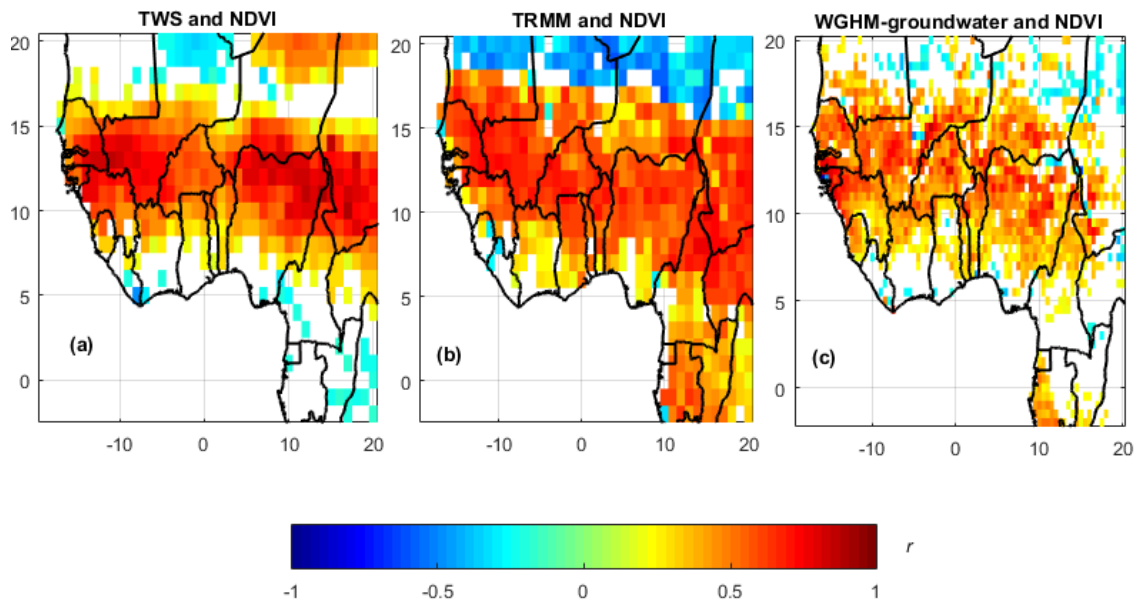


Figure 6: Correlations of monthly NDVI with (a) TWS (2002 – 2013), (b) TRMM-based precipitation (2002 – 2013), and (c) WGHM groundwater (2002 – 2009) over SSA.

403 An assessment of vegetation response to rainfall and TWS show some spatial limits and
 404 complexities. For example, be it rainfall or TWS, the correlations are either generally low or
 405 negative in humid (coastal areas) and extreme arid environments (Central Sahel). Apparently
 406 high correlations are mostly present in regions of considerable seasonal change (cf. IC1, Fig. 4)
 407 rather than regions with little seasonal change such as the tropical coastal regions. Also, rela-
 408 tively weak associations of TWS and rainfall with NDVI were found even in ecosystems with
 409 annual rainfall exceeding 2500 mm (areas with very little seasonal change as seen in IC1, Fig. 4)
 410 while those with annual rainfall less than 1000 mm (areas with considerable seasonal change-
 411 IC1, Fig. 4) indicated strong association with NDVI. The result of different vegetation having
 412 different water critical points may also account for this. The waterlogged soils of humid coastal
 413 SSA countries (e.g., Liberia, southern Côte d'Ivoire) may suggests that vegetation development
 414 is mostly a function of pre-existing soil conditions as argued earlier. Consequently for such
 415 ecosystems, rainfall is not primarily a factor for vegetation growth. Similar relationship is also
 416 observed with TWS in the coastal areas lying in the evergreen broadleaf forests, where there
 417 was no association with NDVI (Fig. 6a). This probably is due to the fact that TWS changes
 418 here are the result of a weak seasonal signal. But in the Sahel and Sudano belt, rainfall maybe
 419 perceived as a major indicator to NDVI, hence their strong agreement (Fig. 6b). However,

420 roots exploration, the adaptability and tolerance of plants to arid conditions and changes in
421 the composition of species richness may impact such relationship (e.g., [Chen et al., 2014](#); [Zhou
422 et al., 2014](#)).

423 The correlation results in Fig. 6c also indicate that WGHM-derived groundwater is well
424 associated with NDVI in southern Mali and much of the Sahel and Sudano belt. Based on the
425 response of NDVI to GRACE-TWS and groundwater (e.g., southern Mali, Senegal, Gambia,
426 south-west Guinea, northern Nigeria, etc.) in Figs. 6a and c, we argue that surface vegetation in
427 these ecosystems respond to water availability in all catchment stores, including groundwater.
428 [Huber et al. \(2011\)](#) had reported the restriction of soil moisture in the southern Sahel regions
429 with higher woody vegetation canopy. It is therefore more likely that TWS maybe the most
430 prominent driver(s) of vegetation dynamics in some parts of the Sahel. As the Sahel region is
431 well known for frequent droughts owing to the impact of climate variability (e.g., [Ndehedehe
432 et al., 2016b](#); [Nicholson et al., 1998](#)), roots exploration and the adaptability of some plants to
433 long dry periods validates such argument. Going by the response of NDVI to groundwater (e.g.,
434 Guinea Bissau, southern Mali, etc.) in Fig. 6c, TWS would be a substantive driver of vegetation
435 dynamics as it better represents the rooting depth of any vegetation, given its water column,
436 which extends to the unsaturated zone.

437 5.2.2. Seasonal relations of NDVI to TWS and rainfall

438 Seasonal variability of NDVI was also compared with TWS and rainfall in order to assess
439 their interrelationships. As NDVI correlations with rainfall during dry season introduces larger
440 bias ([Huber et al., 2011](#)), correlations were also undertaken for seasonal periods to provide a
441 more robust assessment. Correlations between NDVI and rainfall tend to be high in the Sahel
442 zone and some coastal countries during the OND, AMJ, SON, and MAM periods while very
443 little association is found in the JAS and JFM period (Fig. 7a). TWS on the other hand shows
444 the strongest relation in OND while other seasonal periods indicate significant relationships with
445 NDVI mostly in the Sahel zone except during the MAM period (Fig. 7b). Indeed, an overall
446 assessment of the relation of the monthly and seasonal NDVI with those of rainfall and TWS
447 (i.e., based on the respective grids) indicates that rainfall unarguably, provides a hydrological
448 control on NDVI phenology in much of the sub-continent. A similar relationship (i.e., NDVI and
449 rainfall) was observed by [Nicholson et al. \(1990\)](#) in the Sahel region, consistent with our result
450 here. However, rainfall is restricted in the growing season (e.g., JAS) as a driver of vegetation
451 dynamics unlike TWS (Fig. 7b). The seemingly poor performance of rainfall as a driver of

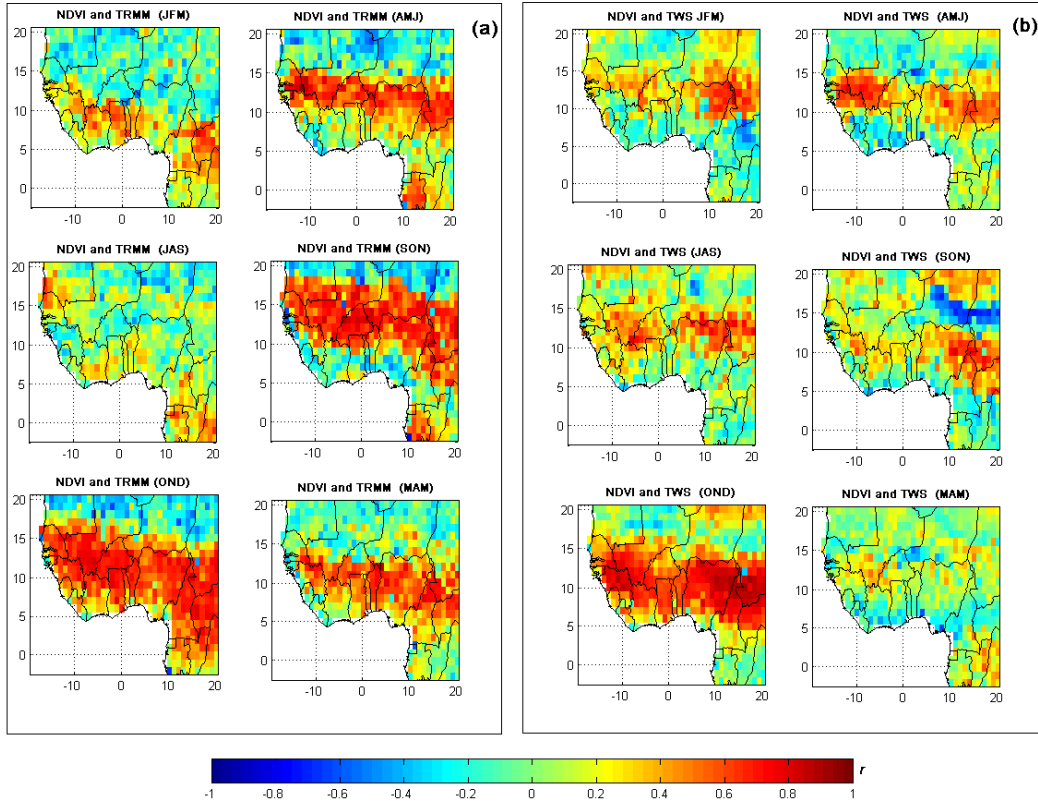


Figure 7: Correlations of NDVI with TRMM-based precipitation and TWS at pixel scale for the seasonal periods identified in Section 2. (a) Correlations between seasonal NDVI and rainfall and (b) correlations between seasonal NDVI and TWS. The seasonal classifications (i.e., JFM, AMJ, JAS, SON, OND, and MAM) is the same used in Fig. 2 and are also based on crop and rain seasons in SSA.

452 vegetation dynamics during the growing season is consistent with the findings of [Huber et al.](#)
 453 (2011) who also argued that the dry seasons introduce bias in the observed relationship (rainfall
 454 vs NDVI) because while NDVI still oscillates during such periods, rainfall does not. Rainfall
 455 certainly shows wider spread of positive correlations during the OND period (Fig. 7a) compared
 456 to TWS (Fig. 7b). Nonetheless, TWS has shown linear relationships (positive correlations)
 457 in some locations (e.g., northern Niger) where rainfall indicated negative correlations or no
 458 association. Although TWS is also strongly associated with NDVI in much of SSA similar to
 459 rainfall, some *hot spots* exists where NDVI, either at monthly or seasonal scales, demonstrates
 460 relatively strong and consistent sensitivity to TWS when compared to rainfall (Figs. 6 and 7).
 461 It is our view that these region-specific cases, which include West Sahel (e.g., southern Mali
 462 and Guinea) and the Lake Chad basin (e.g., north-east Nigeria and southern Chad), are typical
 463 examples of where TWS provides better hydrological controls for the water driven variability

464 in vegetation. In these region-specific cases, TWS may also serve as a strong complement
465 to rainfall for the mapping of hydrological impacts on surface vegetation, given the lack of
466 in-situ data and the bureaucracies involved in its acquisition in the region. TWS in these
467 landscapes would be more reliable than precipitation as soil moisture surrogate to monitor
468 water availability for the development of surface vegetation, since technically GRACE-derived
469 TWS changes would be mostly driven by soil wetness in the unsaturated soil moisture zone.
470 As argued by Yang et al. (2014) these zones are more readily affected by changes in climate
471 than the saturated zones. For the Lake Chad basin, for example, changes in TWS would largely
472 emanate from this catchment store (unsaturated zone and to some degree saturated zone during
473 extreme hydrological drought periods), as groundwater abstractions are unknown and water loss
474 is mostly through evapotranspiration (e.g., Ndehedehe et al., 2016b).

475 5.2.3. Lag response of NDVI to rainfall and TWS and the influence of land surface conditions

476 The observed relationship of NDVI with TWS in the specific *hot spots* identified in the
477 preceding section is further confirmed from the analysis of lagged correlation using the cross
478 correlation method. These results (i.e., the time lag for maximum correlations) apparently
479 show stronger correlation coefficients in the TWS-NDVI relationship (Fig. 8a) in these *hot spots*
480 when compared to NDVI-rainfall relationship (Fig. 8b). With an estimated time lag of 1 month
481 (Fig. 8c), the variability in surface vegetation greenness can fairly be predicted in the Lake Chad
482 basin using TWS. As indicated in Fig. 8c, TWS lags and leads NDVI by approximately one
483 month in the Sahel and Guinea coast zones, respectively. Apart from other arid ecosystems in
484 the Central Sahel where TWS also leads NDVI, probably due to plants adaptability, composition
485 and structure, NDVI shows generally, a lead of one month and to some degree a zero lag in the
486 Sahel zone. On the other hand, rainfall is more associated with NDVI in much of SSA than TWS
487 (Fig. 8b), and shows a one month lead except for areas where the biomes are predominantly
488 broadleaf forest, indicating a zero lag (Fig. 8d).

489 Unlike rainfall, TWS is a rather weak driver of vegetation dynamics in the Congo basin
490 (Figs. 6a, 7a, and 8a). The distribution of the cross correlation coefficients indicate no asso-
491 ciation between NDVI and TWS in large parts of the Congo basin (Fig. 8a). But trends in
492 TWS and ET are somewhat consistent with NDVI in extreme southern part of the Congo-DRC
493 region, unlike rainfall (Figs. 9a-d), suggesting the potential impacts of other factors on the
494 NDVI-TWS relationship in Congo basin. Apart from increased evapotranspiration (Fig. 9d)
495 and a likely human footprint, poor spatial relations of TWS with NDVI even at maximum

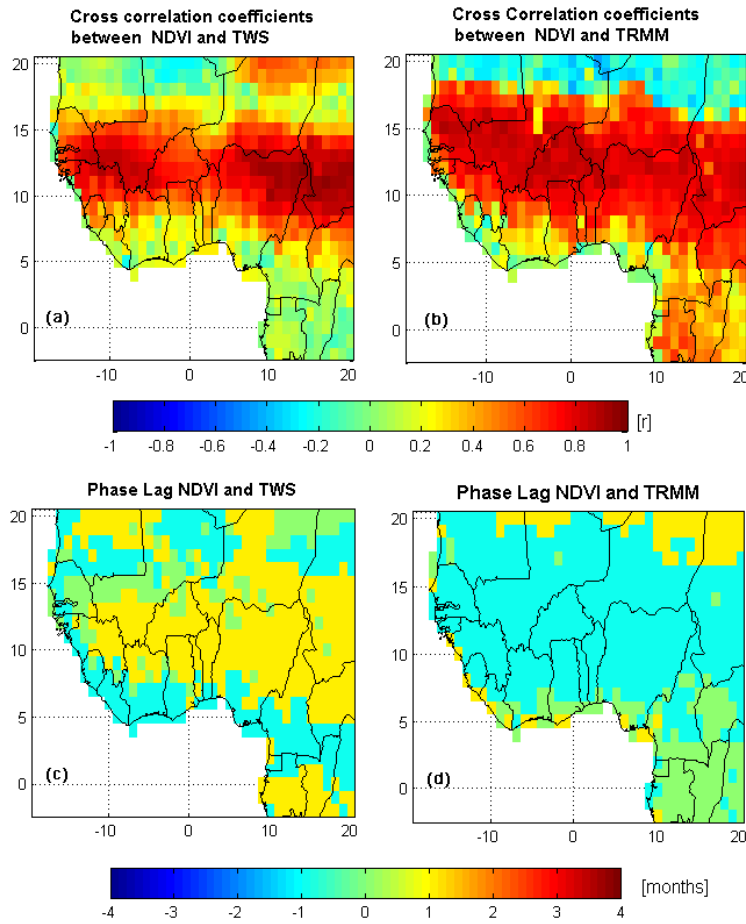


Figure 8: Maximum correlations of NDVI with TRMM-based precipitation and TWS for the common period (2002 – 2013). (a) Maximum correlations between NDVI and TWS (b) maximum correlations between NDVI and rainfall (c) time lag for which maximum correlation is observed between NDVI and GRACE-TWS and (d) time lag for which maximum correlation is observed between NDVI and rainfall.

496 correlations could be due to the fact that TWS in the Congo basin, is mostly driven by runoff
 497 as the multi-annual variation in TWS over the Congo basin is strongly associated with river
 498 runoff (not shown). Although no spatial relations exist between NDVI and TWS in the Congo
 499 basin (except weak positive correlations during the MAM period-Fig. 7b), the negative trends
 500 in TWS of the Congo basin, which agree with those of NDVI in the extreme southern part of the
 501 Congo-DRC region (Fig. 9a and c), suggest TWS can be used to monitor the impacts of climate
 502 change on vegetation dynamics. However, the negative trends in TWS around some sub-regions
 503 of the Congo basin was attributed to deforestation (Ahmed et al., 2014) and further confirms
 504 that a combination of land cover transitions and climatic variations impact on the hydrological

response of a drainage basin.

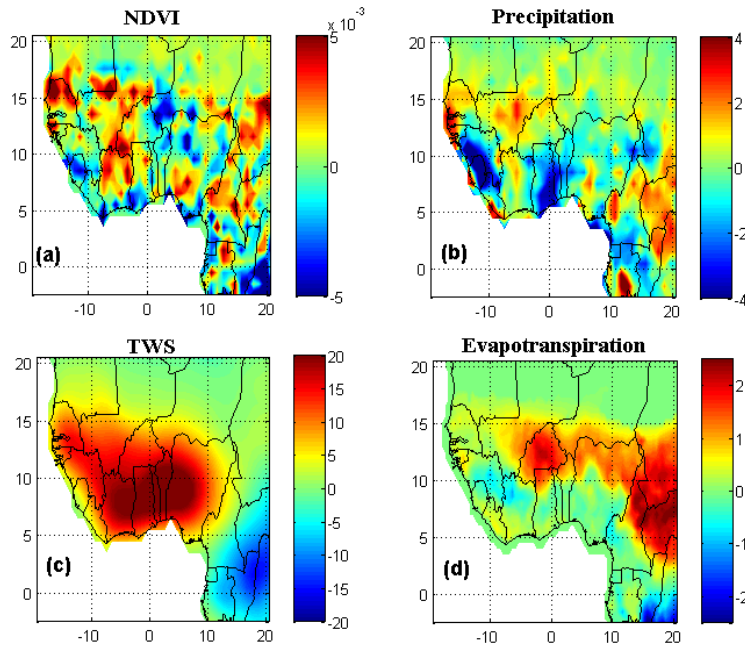


Figure 9: Spatial trends in (a) NDVI, (b) TRMM-based precipitation, (c) TWS, and (d) evapotranspiration during the 2002 – 2013 period. The trends in TRMM, TWS, and evapotranspiration are in mm/month.

505

506 In Fig. 9d, the Lake Chad basin show considerable increase in evapotranspiration. This
 507 increase in evapotranspiration in much of the basin is an indication of high evaporative demand
 508 (the rate of water loss from a wet surface). Reduced alimention and precipitation deficits in
 509 relation to large outgoing water flux such as evapotranspiration may lead to large water budget
 510 changes and hydraulic behaviour of the basin that impacts on NDVI-rainfall relationship. Given
 511 that atmospheric conditions regulate the life span of canopy phenology, and both leafing and
 512 reproductive phenophases of Sahelian ecosystems (e.g., Seghieri et al., 2012; Do et al., 2005),
 513 TWS would better account for plant water availability. This is largely because GRACE-TWS
 514 provides an overall picture of the water budget and accounts for available freshwater changes in
 515 the ecosystem, regardless of catchment and landscape effects (e.g., soil and vegetation types) that
 516 may have potential impact on hydrological processes. Add to this, widespread drought tolerant
 517 species resulting from extended and prolonged drought periods in the semi-arid ecosystems
 518 could lead to transformative relationship and changes in the composition of species richness.
 519 This creates a complex response of surface vegetation to hydrological conditions due to the
 520 mechanics of water use in the region (e.g., Huber et al., 2011). This, for example, is evident

521 in the Sahelian ecosystems that are considerably associated with groundwater (Fig. 6c). Thus,
 522 GRACE-derived TWS would be a more suitable hydrological indicator to highlight the impact
 523 of climate variability on vegetation dynamics in the basin and other ecosystems where similar
 524 relationship is observed.

525 5.2.4. The role of human activities

526 The influence of human-related disturbances of vegetation on the spatio-temporal relations
 527 of NDVI with TWS and rainfall in the humid SSA region was further investigated. One of such
 528 regions is the Guinea coast (e.g, southern Nigeria and Cameroon), where spatial relations of
 529 monthly NDVI time series with rainfall and TWS were relatively poor. The role of human ac-
 530 tivities is perhaps one of the most significant drivers of surface vegetation in non-industrialized
 531 regions where infrastructural development is rather unregulated and people in rural community
 532 depend heavily on forests for food, building materials, and other socio-economic reasons. The
 533 significant discrepancies in the observed spatial trends in NDVI and those of rainfall and TWS
 534 (Figs. 9a-c) are possible indications that human-induced activities (e.g., land cover transitions,
 535 reduction in fallow periods, etc) are also drivers of vegetation dynamics in the region. Observed
 536 changes in the MODIS-derived land cover show some transitions, for example, agricultural ex-
 537 pansion (insert A1-B1, Fig. 10). These transitions in land cover are somewhat related to the
 poor associations of NDVI with rainfall and TWS. Southern Nigeria faces an endemic loss of

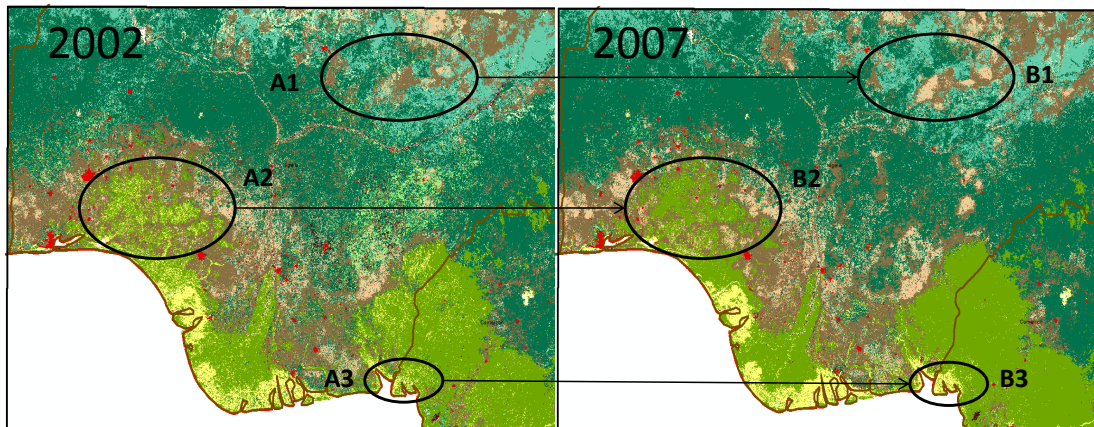


Figure 10: Graphical illustration of vegetation transition between 2002 and 2007 in the Lower Niger Delta of southern Nigeria and Cameroon (Latitudes 4.0°N–9.6°N and Longitudes 2.7°E–11.1°E) based on the classification schemes of MODIS global land cover product (MCD12Q1) version 005. Specific examples of transition highlighted in the top panel include agricultural (A1 to B1) biomes, Evergreen broadleaf forests (A2 to B2), and permanent wetlands (A3 to B3). Note that the legend for the land cover map in the top panel is the same as Fig. 1b.

538 vegetation cover and species richness as a result of forest transitions. This is illustrated in an
539 extended analysis of the land cover dynamics in southern Nigeria/Cameroon (hereafter lower
540 Niger Delta) based on the MODIS land cover data. Between 2002 and 2007, the lower Niger
541 Delta indicates a significant shift in land cover with obvious declines in the spatial extent (dis-
542 tribution) of savannas (4128 km²), deciduous broadleaf forests (3711 km²), permanent wetlands
543 (4341 km²), grasslands (13504 km²), and closed shrub lands (4152 km²). These observed forest
544 transitions and land cover changes are somewhat chronic and degradational. They are primarily
545 caused by urbanization, lack of forest management regulations, and infrastructure developments
546 such as the activities of oil companies and exploitation of forest resources for economic purposes
547 (e.g., [Onojeghuo and Blackburn, 2011](#); [James et al., 2007](#)).

548 In addition to the foregoing, Fig. 10 shows graphical illustrations of forest transition at the
549 lower Niger Delta, highlighting the increase in agricultural biomes (croplands) (location A1 to
550 B1), loss of permanent wetlands to Evergreen broadleaf forests and other plant covers (location
551 A2 to B2), and the increase in the density of permanent wetlands at the shores of Cameroon
552 (location A3 to B3). Amongst other factors highlighted in Section 5.2.1, an overall assessment
553 of vegetation response to TWS and rainfall in this study reveals that the loss of plant cover
554 resulting from human activities (e.g., deforestation, land use change, etc.) also contributes to
555 the observed poor correlations of NDVI with TWS and rainfall in much of the Guinea coast
556 zone. Based on a recent remotely-sensed assessments of land cover dynamics in the Niger Delta
557 region of Nigeria (see, [Ayanlade and Drake, 2016](#)), over 40% of the forest reserves have been
558 lost (1984 – 2011) mostly due to agricultural expansion and illegal selective logging on both
559 commercial and domestic scales while urban areas expanded by nearly 85% during the same
560 period. Prospective future changes in the vegetation system of humid tropical SSA forests maybe
561 largely controlled by the trajectory of human disturbance of the ecosystem and to some degree
562 the climate system. However, the weak response of vegetation to TWS anomalies and rainfall
563 variability in the humid SSA landscape, aligns with previous arguments (see, e.g., [Dardel et al.,](#)
564 [2014](#); [Knauer et al., 2014](#); [Boschetti et al., 2013](#); [Bégué et al., 2011](#); [Olsson et al., 2005](#); [Herrmann](#)
565 [et al., 2005](#)) on the overarching human-related perturbations on the vegetation system. This
566 further confirms the role of human activities not only in NDVI-rainfall relationship as reported
567 in the studies above, but also in the NDVI-TWS relationship.

568 **6. Conclusions**

569 This study provides an overview of the utility of Gravity Recovery and Climate Experiment
 570 (GRACE) derived terrestrial water storage (TWS) and rainfall as drivers of vegetation dynamics
 571 in Sub-Sahara Africa (SSA). This is achieved by using the Normalized Difference Vegetation
 572 Index (NDVI) as a surface vegetation proxy for the 2002 – 2013 period. The conclusions from
 573 the study are summarised as follows:

- 574 (1) The temporal relations of NDVI with those of TWS and rainfall in SSA suggest that the
 575 monthly and inter-annual variability of NDVI are both explained by TWS and rainfall in
 576 the semi-humid and arid ecosystems of Sub-Sahara Africa (SSA). But in region specific
 577 cases (southern Mali and Lake Chad basin), TWS explained more of the water-driven
 578 changes in the temporal evolutions of surface vegetation greenness than rainfall.
- 579 (2) TWS and rainfall are strongly associated with NDVI in the Sahel zone (Central and Su-
 580 dano) when the relationship is evaluated at pixel scale (spatial relations). Rainfall in
 581 particular shows stronger association with NDVI in much of SSA (except for some of the
 582 Guinea coast countries) than TWS. *Hot spots* also exists (e.g., north-east Nigeria and
 583 southern Chad) where NDVI, either at monthly or seasonal scales (i.e., spatial relations),
 584 demonstrates relatively strong and consistent sensitivity to TWS when compared to rain-
 585 fall.
- 586 (3) There are indications that some of the Sahelian vegetation also depend on groundwater as
 587 strong association between NDVI and WaterGap groundwater model have been observed.
 588 This relationship (NDVI vs groundwater) also coincides with some of the site-specific
 589 cases (mostly semi-arid) in (ii) above where NDVI shows consistent response to TWS
 590 than rainfall. Since NDVI still oscillates in these arid ecosystems despite having limited
 591 or highly variable rainfall, TWS provides better hydrological control for the water driven
 592 variability in surface vegetation.
- 593 (4) Human activities and degradational transitions in land cover due to infrastructure devel-
 594 opments, agricultural expansion, and lack of forest conservation policies amongst others
 595 impact on the response of surface vegetation to hydrological conditions in SSA. It is more
 596 likely that prospective future changes in the vegetation system of humid tropical SSA
 597 forests maybe largely controlled by the trajectory of human disturbance of the ecosystem.

598 **Acknowledgments**

599 Christopher E. Ndehedehe and Nathan O. Agutu are grateful to Curtin University for the
600 CSIRS funding that supported this work. The Authors are grateful to CSR, NASA, and NOAA
601 for the data used in this study. They are grateful to National Oceanic and Atmospheric Admin-
602 istration, National Aeronautics and Space Administration, and Center for Environment Systems
603 Research for all the data used in this study.

604 **References**

- 605 A, G., Velicogna, I., Kimball, J. S., and Kim, Y. (2015). Impact of changes in GRACE derived
606 terrestrial water storage on vegetation growth in Eurasia. *Environmental Research Letters*,
607 10(12):124024.
- 608 Abiy, A. Z. and Melesse., A. (2017). Evaluation of watershed scale changes in groundwater and
609 soil moisture storage with the application of {GRACE} satellite imagery data. *CATENA*,
610 153:50 – 60. doi:10.1016/j.catena.2017.01.036.
- 611 Ahmed, M., Sultan, M., J.Wahr, and Yan, E. (2014). The use of GRACE data to monitor
612 natural and anthropogenic induced variations in water availability across Africa. *Earth Science*
613 *Reviews*, 136:289–300. doi:10.1016/j.earscirev.2014.05.009.
- 614 Ayanlade, A. and Drake, N. (2016). Forest loss in different ecological zones of the Niger Delta,
615 Nigeria: evidence from remote sensing. *GeoJournal*, 81(5):717–735.
- 616 Bégué, A., Vintrou, E., Ruelland, D., Claden, M., and Dessay, N. (2011). Can a 25-year trend in
617 soudano-sahelian vegetation dynamics be interpreted in terms of land use change? a remote
618 sensing approach. *Global Environmental Change*, 21(2):413 – 420.
- 619 Bekoe, E. O. and Logah, F. Y. (2013). The impact of droughts and climate change on electricity
620 generation in Ghana. *Environmental Sciences*, 1(1):13–24.
- 621 Boschetti, M., Nutini, F., Brivio, P. A., Bartholom, E., Stroppiana, D., and Hoscilo, A.
622 (2013). Identification of environmental anomaly hot spots in West Africa from time series
623 of NDVI and rainfall. *ISPRS Journal of Photogrammetry and Remote Sensing*, 78:26 – 40.
624 doi:10.1016/j.isprsjprs.2013.01.003.
- 625 Cardoso, J.-F. (1991). Super-symmetric decomposition of the fourth-order cumulant ten-
626 sor, blind identification of more sources than sensors. Retrieved from:[http://perso.telecom-](http://perso.telecom-paristech.fr/~cardoso/Papers.PDF/icassp91.pdf)
627 [paristech.fr/~cardoso/Papers.PDF/icassp91.pdf](http://perso.telecom-paristech.fr/~cardoso/Papers.PDF/icassp91.pdf). Accessed 15 January 2016.
- 628 Cardoso, J. F. (1999). High-Order contrasts for Independent Component Analysis. *Neural*
629 *Computation*, 11:157–192.
- 630 Cardoso, J. F. and Souloumiac, A. (1993). Blind beamforming for non-gaussian signals. *IEE*
631 *Proceedings*, 140(6):362–370.

- 632 Chen, T., de Jeu, R., Liu, Y., van der Werf, G., and Dolman, A. (2014). Using satellite based
633 soil moisture to quantify the water driven variability in NDVI: A case study over mainland
634 Australia. *Remote Sensing of Environment*, 140:330 – 338. doi:10.1016/j.rse.2013.08.022.
- 635 Common, P. (1994). Independent component analysis, A new concept? *Signal Processing*,
636 36:287–314.
- 637 Dardel, C., Kergoat, L., Hiernaux, P., Mougin, E., Grippa, M., and Tucker, C. (2014). Re-
638 greening Sahel: 30 years of remote sensing data and field observations (Mali, Niger). *Remote*
639 *Sensing of Environment*, 140:350 – 364. doi:10.1016/j.rse.2013.09.011.
- 640 Descroix, L., Mahé, G., Lebel, T., Favreau, G., Galle, S., Gautier, E., Olivry, J.-C., Albergel,
641 J., Amogu, O., Cappelaere, B., Dessouassi, R., Diedhiou, A., Breton, E. L., Mamadou, I.,
642 and Sighomnou, D. (2009). Spatio-temporal variability of hydrological regimes around the
643 boundaries between Sahelian and Sudanian areas of West Africa: A synthesis. *Journal of*
644 *Hydrology*, 375(12):90–102. doi:10.1016/j.jhydrol.2008.12.012.
- 645 Dirmeyer, P. A., Guo, Z., and Gao, X. (2004). Comparison, validation, and transferability
646 of eight multiyear global soil wetness products. *Journal of Hydrometeorology*, 5:1011–1033.
647 doi:10.1175/JHM-388.1.
- 648 Do, F. C., Goudiaby, V. A., Gimenez, O., Diagne, A. L., Diouf, M., Rocheteau, A., and Akpo,
649 L. E. (2005). Environmental influence on canopy phenology in the dry tropics. *Forest Ecology*
650 *and Management*, 215(1–3):319 – 328. doi:10.1016/j.foreco.2005.05.022.
- 651 Döll, P., Müller Schmied, H., Schuh, C., Portmann, F. T., and Eicker, A. (2014). Global-
652 scale assessment of groundwater depletion and related groundwater abstractions: Combining
653 hydrological modeling with information from well observations and GRACE satellites. *Water*
654 *Resources Research*, 50(7):5698–5720.
- 655 Famiglietti, J. S. (2014). The global groundwater crisis. *Nature*, 4:945–948.
656 doi:10.1038/nclimate2425.
- 657 Favreau, G., Cappelaere, B., Massuel, S., Leblanc, M., Boucher, M., Boulain, N., and Leduc, C.
658 (2009). Land clearing, climate variability, and water resources increase in semiarid southwest
659 Niger: a review. *Water Resources Research*, 45:W00A16. doi:10.1029/2007WR006785.
- 660 Frappart, F., Ramillien, G., Leblanc, M., Tweed, S. O., Bonnet, M.-P., and Maisongrande,
661 P. (2011). An independent component analysis filtering approach for estimating continental

- 662 hydrology in the GRACE gravity data. *Remote Sensing of Environment*, 115(1):187 – 204.
663 doi:doi.org/10.1016/j.rse.2010.08.017.
- 664 Ghil, M., Allen, M. R., Dettinger, M. D., Ide, K., Kondrashov, D., Mann, M. E., Robertson,
665 A. W., Saunders, A., Tian, Y., Varadi, F., and Yiou, P. (2002). Advanced spectral methods
666 for climatic time series. *Reviews of Geophysics*, 40(1):3–1–3–41. doi:10.1029/2000RG000092.
- 667 Gond, V., Fayolle, A., Penneç, A., Cornu, G., Mayaux, P., Camberlin, P., Doumenge, C., Fauvet,
668 N., and Gourlet-Fleury, S. (2013). Vegetation structure and greenness in central africa from
669 modis multi-temporal data. *Philosophical Transactions of the Royal Society of London B:*
670 *Biological Sciences*, 368(1625). doi:10.1098/rstb.2012.0309.
- 671 Guan, K., Wood, E. F., Medvigy, D., Kimball, J., Pan, M., Caylor, K. K., Sheffield, J., Xu, X.,
672 and Jones, M. O. (2014). Terrestrial hydrological controls on land surface phenology of African
673 savannas and woodlands. *Journal of Geophysical Research: Biogeosciences*, 119(8):1652–1669.
674 doi:10.1002/2013JG002572.
- 675 Herrmann, S. M., Anyamba, A., and Tucker, C. J. (2005). Recent trends in vegetation dynamics
676 in the African Sahel and their relationship to climate. *Global Environmental Change*, 15(4):394
677 – 404. doi:10.1016/j.gloenvcha.2005.08.004.
- 678 Högestrom, E., Trofaier, A. M., Gouttevin, I., and Bartsch, A. (2014). Assessing seasonal
679 backscatter variations with respect to uncertainties in soil moisture retrieval in Siberian Tun-
680 dra regions. *Remote Sensing*, 6(9):8718–8738. doi:10.3390/rs6098718.
- 681 Houborg, R., Rodell, M., Li, B., Reichle, R., and Zaitchik, B. F. (2012). Drought indicators based
682 on model-assimilated Gravity Recovery and Climate Experiment (GRACE) terrestrial water
683 storage observations. *Water Resources Research*, 48(7):W07525. doi:10.1029/2011WR011291.
- 684 Huber, S., Fensholt, R., and Rasmussen, K. (2011). Water availability as the driver of vegetation
685 dynamics in the African Sahel from 1982 to 2007. *Global and Planetary Change*, 76(34):186
686 – 195. doi:10.1016/j.gloplacha.2011.01.006.
- 687 Huffman, G. J., Adler, R. F., Bolvin, D. T., Gu, G., Nelkin, E. J., Bowman, K. P., Hong, Y.,
688 Stocker, E. F., and Wolff, D. B. (2007). The TRMM Multisatellite Precipitation Analysis
689 (TMPA): Quasi-Global, Multiyear, Combined-Sensor Precipitation Estimates at Fine Scales.
690 *Journal Of Hydrometeorology*, 8:38–55. doi:10.1175/JHM560.1.

- 691 Jamali, S., Seaquist, J., Eklundh, L., and Ardö, J. (2014). Automated mapping of vegetation
692 trends with polynomials using NDVI imagery over the Sahel. *Remote Sensing of Environment*,
693 141:79 – 89. doi:10.1016/j.rse.2013.10.019.
- 694 James, G. K., Adegoke, J. O., Saba, E., Nwilo, P., and Akinyede, J. (2007). Sattelite-based
695 assessment of the extent and changes in the mangrove ecosystem of the Niger Delta. *Marine*
696 *Geodesy*, 30:249–267. doi: 10.1080/01490410701438224.
- 697 Joodaki, G., Wahr, J., and Swenson, S. (2014). Estimating the human contribution to ground-
698 water depletion in the Middle East, from GRACE data, land surface models, and well obser-
699 vations. *Water Resources Research*, 50(3):2679–2692. doi:10.1002/2013WR014633.
- 700 Knauer, K., Gessner, U., Dech, S., and Kuenzer, C. (2014). Remote sensing of vegeta-
701 tion dynamics in West Africa. *International Journal of Remote Sensing*, 35(17):6357–6396.
702 doi:10.1080/01431161.2014.954062.
- 703 Kummerow, C., Simpson, J., Thiele, O., Barnes, W., Chang, A. T. C., Stocker, E., Adler, R. F.,
704 Hou, A., Kakar, R., Wentz, F., Ashcroft, P., Kozu, T., Hong, Y., Okamoto, K., Iguchi, T.,
705 Kuroiwa, H., Im, E., Haddad, Z., Huffman, G., Ferrier, B., Olson, W. S., Zipser, E., Smith,
706 E. A., Wilhelm, T. T., North, G., Krishnamurti, T., and Nakamura, K. (2000). The status of
707 the Tropical Rainfall Measuring Mission (TRMM) after two years in orbit. *Journal of Applied*
708 *Meteorology*, 39(12):1965–1982. doi:10.1175/1520-0450(2001)040<1965:TSOTTR>2.0.CO;2.
- 709 Landerer, F. W. and Swenson, S. C. (2012). Accuracy of scaled GRACE terrestrial water storage
710 estimates. *Water Resources Research*, 48(4):W04531. doi:10.1029/2011WR011453.
- 711 Li, J., Lewis, J., Rowland, J., Tappan, G., and Tieszen, L. (2004). Evaluation of land perfor-
712 mance in Senegal using multi-temporal NDVI and rainfall series. *Journal of Arid Environ-*
713 *ments*, 59(3):463 – 480. doi:10.1016/j.jaridenv.2004.03.019.
- 714 Ndehedehe, C., Awange, J., Agutu, N., Kuhn, M., and Heck, B. (2016a). Understanding changes
715 in terrestrial water storage over West Africa between 2002 and 2014. *Advances in Water*
716 *Resources*, 88:211–230. doi:10.1016/j.advwatres.2015.12.009.
- 717 Ndehedehe, C. E., Agutu, N. O., Okwuashi, O. H., and Ferreira, V. G. (2016b). Spatio-temporal
718 variability of droughts and terrestrial water storage over Lake Chad Basin using independent
719 component analysis. *Journal of Hydrology*, 540:106– 128. doi:10.1016/j.jhydrol.2016.05.068.

- 720 Ndehedehe, C. E., Awange, J., Kuhn, M., Agutu, N., and Fukuda, Y. (2017a). Analysis of
721 hydrological variability over the Volta river basin using in-situ data and satellite observations.
722 *Journal of Hydrology: Regional studies*, 12:88–110. doi:10.1016/j.ejrh.2017.04.005.
- 723 Ndehedehe, C. E., Awange, J., Kuhn, M., Agutu, N., and Fukuda, Y. (2017b). Climate
724 teleconnections influence on West Africa's terrestrial water storage. *Hydrological Processes*,
725 31(18):3206–3224. doi: 10.1002/hyp.11237.
- 726 Ndehedehe, C. E., Awange, J. L., Corner, R., Kuhn, M., and Okwuashi, O. (2016c). On the
727 potentials of multiple climate variables in assessing the spatio-temporal characteristics of
728 hydrological droughts over the Volta Basin. *Science of the Total Environment*, 557-558:819–
729 837. doi:10.1016/j.scitotenv.2016.03.004.
- 730 Nicholson, S. (2009). A revised picture of the structure of the monsoon and land itcz over west
731 africa. *Climate Dynamics*, 32(7-8):1155–1171. doi:10.1007/s00382-008-0514-3.
- 732 Nicholson, S. E., Davenport, M. L., and Malo, A. R. (1990). A comparison of the vegetation
733 response to rainfall in the Sahel and East Africa, using normalized difference vegetation index
734 from NOAA AVHRR. *Climatic Change*, 17(2):209–241. doi:10.1007/BF00138369.
- 735 Nicholson, S. E., Tucker, C. J., and Ba, M. B. (1998). Desertification, drought, and surface
736 vegetation: An example from the West African Sahel. *Bulletin of the American Meteorological*
737 *Society*, 79(5):815 – 829. doi:10.1175/1520-0477(1998)079<0815:DDASVA>2.0.CO;2.
- 738 Njoku, E. G. and Entekhabi, D. (1996). Passive microwave remote sensing of soil moisture.
739 *Journal of Hydrology*, 184(1):101 – 129. doi:/10.1016/0022-1694(95)02970-2.
- 740 Olsson, L., Eklundh, L., and Ard, J. (2005). A recent greening of the Sahel-
741 trends, patterns and potential causes. *Journal of Arid Environments*, 63(3):556 – 566.
742 doi:0.1016/j.jaridenv.2005.03.008.
- 743 Onojeghuo, A. O. and Blackburn, G. A. (2011). Forest transition in an ecologically important
744 region: Patterns and causes for landscape dynamics in the Niger Delta. *Ecological Indicators*,
745 11(5):1437 – 1446. doi:10.1016/j.ecolind.2011.03.017.
- 746 Paeth, H., Fink, A., Pohle, S., Keis, F., Machel, H., and Samimi, C. (2012). Meteorological
747 characteristics and potential causes of the 2007 flood in sub-Saharan Africa. *International*
748 *Journal of Climatology*, 31:1908–1926. doi:10.1002/Joc.2199.

- 749 Ramillien, G., Bouhours, S., Lombard, A., Cazenave, A., Flechtner, F. R., and Schmidt (2008).
750 Land water storage contribution to sea level from GRACE geoid data over 2003-2006. *Global*
751 *and Planetary Change*, 60(3-4):381–392. doi:10.1016/j.gloplacha.2007.04.002.
- 752 Reager, J. T., Thomas, B. F., and Famiglietti, J. S. (2014). River basin flood potential inferred
753 using GRACE gravity observations at several months lead time. *Nature Geoscience*, 7(8):588–
754 592. doi:10.1038/ngeo2203.
- 755 Seghier, J., Carreau, J., Boulain, N., De Rosnay, P., Arjounin, M., and Timouk, F. (2012). Is
756 water availability really the main environmental factor controlling the phenology of woody
757 vegetation in the central Sahel ? *Plant Ecology*, 213(5):861–870. doi:10.1007/s11258-012-
758 0048-y.
- 759 Séguis, L., Cappelaere, B., Mils, G., Peugeot, C., Massuel, S., and Favreau, G. (2004). Simu-
760 lated impacts of climate change and land-clearing on runoff from a small Sahelian catchment.
761 *Hydrological Processes*, 18(17):3401–3413. doi:10.1002/hyp.1503.
- 762 Sheffield, J., Ferguson, C. R., Troy, T. J., Wood, E. F., and McCabe, M. F. (2009). Closing
763 the terrestrial water budget from satellite remote sensing. *Geophysical Research Letters*,
764 36(7):L07403.
- 765 Swenson, S. and Wahr, J. (2007). Multi-sensor analysis of water storage variations of the Caspian
766 Sea. *Geophysical Research Letters*, 34(16). doi:10.1029/2007gl030733.
- 767 Tapley, B., Bettadpur, S., Watkins, M., and Reigber, C. (2004). The Gravity Recovery and
768 Climate Experiment: Mission overview and early results. *Geophysical Research Letters*, 31:1–
769 4. doi:10.1029/2004GL019920.
- 770 Thomas, A. C., Reager, J. T., Famiglietti, J. S., and Rodell, M. (2014). A GRACE-based
771 water storage deficit approach for hydrological drought characterization. *Geophysical Research*
772 *Letters*, 41(5):1537–1545. doi:10.1002/2014GL059323.
- 773 Trumbore, S., Brando, P., and Hartmann, H. (2015). Forest health and global change. *Science*,
774 349(6250):814–818. doi:10.1126/science.aac6759.
- 775 Tucker, C. J., Pinzon, J. E., Brown, M. E., Slayback, D. A., Pak, E. W., Mahoney, R., Vermote,
776 E. F., and Saleous, N. E. (2005). An extended AVHRR 8-km NDVI dataset compatible
777 with MODIS and SPOT vegetation NDVI data. *International Journal of Remote Sensing*,
778 26(20):4485–4498. doi:10.1080/01431160500168686.

- 779 Wahr, J., Molenaar, M., and Bryan, F. (1998). Time variability of the Earth's gravity field:
780 Hydrological and oceanic effects and their possible detection using GRACE. *Journal of Geo-*
781 *physical Research-Solid Earth*, 103(B12):30205–30229. doi:10.1029/98jb02844.
- 782 Weber, K. and Stewart, M. (2004). Critical analysis of the cumulative rainfall departure concept.
783 *Ground Water*, 42(6):935–938. Retrieved from:<http://info.ngwa.org/gwol/pdf/042979908.pdf>
784 Accessed 25 March, 2016.
- 785 Wouters, B., Bonin, J. A., Chambers, D. P., Riva, R. E. M., Sasgen, I., and Wahr, J. (2014).
786 GRACE, time-varying gravity, Earth system dynamics and climate change. *Reports on*
787 *Progress in Physics*, 77(11):116801. doi:10.1088/0034-4885/77/11/116801.
- 788 Yang, Y., Long, D., Guan, H., Scanlon, B. R., Simmons, C. T., Jiang, L., and Xu, X. (2014).
789 GRACE satellite observed hydrological controls on interannual and seasonal variability in
790 surface greenness over mainland Australia. *Journal of Geophysical Research: Biogeosciences*,
791 119(12):2245–2260. doi:10.1002/2014JG002670.
- 792 Yirdaw, S. Z., Snelgrove, K., and Agboma, C. (2008). GRACE satellite observations of terrestrial
793 moisture changes for drought characterization in the Canadian Prairie. *Journal of Hydrology*,
794 356:84–92.
- 795 Zeng, N., Neelin, J. D., Lau, K.-M., and Tucker, C. J. (1999). Enhancement of interdecadal
796 climate variability in the Sahel by vegetation interaction. *Science*, 286(5444):1537–1540.
797 doi:10.1126/science.286.5444.1537.
- 798 Zhang, Q., Xu, C.-Y., Becker, S., Zhang, Z. X., Chen, Y. D., and Coulibaly, M. (2009). Trends
799 and abrupt changes of precipitation maxima in the pearl river basin, china. *Atmospheric*
800 *Science Letters*, 10(2):132–144. doi:10.1002/asl.221.
- 801 Zhang, X., Goldberg, M., Tarpley, D., Friedl, M. A., Morisette, J., Kogan, F., and Yu, Y. (2010).
802 Drought-induced vegetation stress in southwestern North America. *Environmental Research*
803 *Letters*, 5(2):024008.
- 804 Zhou, L., Tian, Y., Myneni, R. B., Ciais, P., Saatchi, S., Liu, Y. Y., Piao, S., Chen, H., Vermote,
805 E. F., Song, C., and Hwang, T. (2014). Widespread decline of congo rainforest greenness in
806 the past decade. *Nature*, 509(7498):86–90. doi:10.1038/nature13265.

807 Ziehe, A. (2005). Blind source separation based on joint diagonalization of matrices
808 with applications in biomedical signal processing. *PhD thesis, Universitat Potsdam*. Re-
809 trieved from:[http://en.youscribe.com/catalogue/reports-and-theses/knowledge/blind-source-](http://en.youscribe.com/catalogue/reports-and-theses/knowledge/blind-source-separation-based-on-joint-diagonalization-of-matrices-1424347)
810 [separation-based-on-joint-diagonalization-of-matrices-1424347](http://en.youscribe.com/catalogue/reports-and-theses/knowledge/blind-source-separation-based-on-joint-diagonalization-of-matrices-1424347). Accessed 15 May 2015.

7 Conclusion

Despite a highly polarized debate, global interest in the science of climate change and how its impacts natural systems is developing fast and receiving increasing attention. This is evident in the frequent discussions on greenhouse effect and its implications, which continue to predominate global science and policy agenda (e.g., the Paris Climate Agreement) on climate change. In West Africa, multiple lines of evidence have shown that drought events and other forms of reduced alimentation resulting from unmitigated climate change, represent significant and considerable negative impacts on agriculture/food security, hydro-power, economic development, and the region's remarkable biodiversity. These deleterious impacts have ripple effects on the socio-economic systems of the region. As most agricultural goods are produced in regions that are vulnerable to water-related impacts, this will have massive implications not just on the economy of West Africa but other regions of the world that indirectly consume the water resources of West Africa. Despite this strategic importance of West African countries to the global community, there are still considerable and prominent gaps however, in the knowledge of how global changes in climate impact on the region's water resources systems. Not only is hydrology poorly understood, large scale temporal and spatial dynamics in TWS, and a framework to characterize key hydrological metrics and extreme weather events are lacking in West Africa. As reported in this thesis, an increasing number of constraints, e.g., lack of robust investments in gauge measurements for meteorological and hydrological applications amongst other factors, combine to restrict the availability of in-situ observations for hydro-climatic research that addresses the aforementioned issues.

For most sub-regions of West Africa that are located in hydrologically unfavourable catchments and river basins, understanding the impacts of global climate on large scale dynamics of regional changes in terrestrial water system is therefore warranted. Essentially, this will, (i) support policy and risk management strategies, (ii) promote the need for management and sustainability of water resources, (iii) foster campaign on regional adaptation strategies in the event of extreme hydrological conditions, (iv) advance hydro-climatic research in terms of optimising climate and hydrological models, and (v) provide new perspectives on eco-hydrological processes in West Africa. As this thesis illustrates, opportunities for hydro-climatic research in West Africa that leverage on sustained investments in satellite geodetic programmes exist. The potentials of satellite gravity observations, gridded gauge and high spatial resolution satellite precipitation data in the region, are opportunities to further assess the representation of the land surface and atmospheric states in global reanalysis models, given the inherent problems of global climate models in simulating primary aspects of the West African

Monsoon. Specifically, the Gravity Recovery and Climate Experiment satellite mission is the latest of satellite geodetic mission that provides the opportunity to quantitatively assess monthly changes in terrestrial water storage over large spatial scales. As demonstrated in this thesis, these geodetic programmes (GRACE and radar altimetry missions) along with other satellite missions, and auxiliary data synthesized by forcing global land surface models with historical meteorological data (reanalysis) have ignited a plethora of scientific findings. These outcomes are not only informative but could be considerably useful for public policy and management decisions related to water resources.

This research found that unlike in West Africa where rainfall is the principal driver of GRACE-derived TWS, multi-annual changes in the Congo river discharge provide the dominant control on observed inter-annual variations in GRACE-derived TWS over the Congo basin, and show considerable association with global SST anomalies. Between 2002 and 2014, GRACE-derived TWS showed considerable increase over large portions of West Africa compared to the Congo basin where it decreased significantly, and coincided with warming of the land surface and the surrounding oceans. Further, despite declines in precipitation (2002 – 2014), GRACE-derived TWS increased significantly over the Volta basin with Lake Volta contributing about 41.6% to the observed increase in TWS. After removing the Lake's induced water storage, a strong decline in TWS over the lower Volta catchment that coincided with net precipitation loss (2002 – 2014) was observed between 2007 and 2011, confirming the impacts of reservoir systems on hydrological changes. Meanwhile, some parts of the Sahel have shown significant wetting (rainfall, soil moisture, and TWS) trends in the long term (1982 – 2015) and aligns with the ongoing narratives of rainfall recovery in the region. However, the hydrological conditions of the Congo basin are unfavourable, particularly in the key downstream areas of the Equatorial countries where long term drying was observed from the analysis of multi-resolution hydro-climatic data during the 1982 – 2015 period. Generally, the spatio-temporal analysis of various hydrological units confirm that hydrological conditions before the notorious drought episodes of the 1980's are relatively better than those of the last decade.

A new approach based on a fourth order cumulant statistics, the independent component analysis was employed to analyse the spatio-temporal variability of drought/wet events in the Volta and Lake Chad basins, where drought studies are lacking and mostly undocumented. This statistical-based framework introduced to support the regionalisation and characterisation of key hydrological metrics and extreme precipitation anomalies allows the evaluation of indices of oceanic variability and other low frequency climate signals that impacts on hydro-meteorological conditions in the region. Apart from its capability in regionalising drought signals, this framework showed that AMO, ENSO, PDO, and AMM *inter alia*, play key roles in the drought characteristics of the

Sahel region and the Gulf of Guinea countries. Interestingly, presumptive evidence from the thesis based on a range of multivariate techniques, indicated that ENSO and AMO are the two major climatic indices more likely to impact on the temporal and spatial distribution of West Africa's TWS, amongst others. As the hydrological system is innately connected to the climate and socio-ecological systems, this cumulant framework will enhance risk assessment and improve our understanding of dominant drivers of drought or the various processes leading to drought and its impacts.

Further, the novel potential of GRACE-derived TWS as a prominent driver of ecosystem performance provides new insight and complementary perspectives on African ecology. A contemporary understanding of the water driven variability in surface vegetation in West Africa from the thesis indicates that (i) TWS and rainfall are strongly associated with NDVI mostly in agricultural biomes and Sahelian ecosystems; (ii) some Sahelian vegetation are also groundwater-dependent; and (iii) climate variations and degradational transitions in land cover are found to be composite phenomena that will primarily determine the trajectory of prospective future changes in the vegetation system of West and Central Africa, and how it responds to changes in the hydrological cycle. It further confirms GRACE observations as a more reliable tool in the data deficient semi-arid region (Sahel) for studies of eco-hydrological processes, and advances our understanding of the impacts of climate variability on surface vegetation dynamics and catchment storage.

Overall, the findings of this thesis are instructive and outline not just well documented protocols in the practical monitoring and comprehensive assessment of terrestrial hydrology but novel perspectives on the water resources of West Africa. Considering that man-made reservoirs such as the Lake Volta impacts on the hydrological characteristics of the lower Volta catchment; the Volta basin water management authority, for instance, will have to consider new strategies to evaluate water budget closure, and freshwater availability and variability that incorporates the two-step procedure outlined in this thesis. The surface waters (e.g., lakes and reservoir systems) in West Africa are considerably sensitive to climate variability. This research acknowledges that apart from climatic drivers, various anthropogenic factors, especially in the era of the Anthropocene without doubt exacerbate the impact of climate variability on the region's terrestrial hydrology. However, the receding Lake Volta water levels and the near-desiccated Lake Chad are typical examples of the impacts of extreme climatic conditions that contributes to the ecological and evolutionary processes that shapes the stability of these lake's ecosystems. Generally, strong fluctuations in the water levels of these lakes (e.g., Lake Volta) and some reservoirs (e.g., Kainji), caused by strong inter-annual variability in rainfall in this tropical system are critical dimensions to the hydrological challenges that confronts the region. This will unavoidably continue to impact negatively on the national incomes and hydro-power potentials of

the host countries in the region. Beyond that, the long history of shared water resources and competition on available freshwater in the region, perhaps may result in local agitations, civil and interstate conflicts if extreme changes in climate (droughts) become more frequent and severe. Hydro-meteorological conditions in the Congo basin in the last three decades show that large portions of the region's TWS maybe stressed. This could be a major constraint amongst other factors, to the proposed and ambitious water transfer from the basin to nourish the Lake Chad catchment. However, the use of GRACE observations and outputs from hydrological models to evaluate the groundwater resources of the Lake Chad basin in future studies and water infrastructure development, are key initiatives that can be integrated with policy solutions for adaptation and sustainability. Finally, with the increasing sparsity of observational hydrological data, GRACE-follow on mission and the scheduled launch of Surface Water and Ocean Topography (SWOT) mission by 2020 will help in quantifying terrestrial water budget components and monitoring of aquifer system processes in the region.

References

- A, G., Velicogna, I., Kimball, J. S., and Kim, Y. (2015). Impact of changes in GRACE derived terrestrial water storage on vegetation growth in Eurasia. *Environmental Research Letters*, 10(12):124024.
- Agutu, N., Awange, J., Zerihun, A., Ndehedehe, C., Kuhn, M., and Fukuda, Y. (2017). Assessing multi-satellite remote sensing, reanalysis, and land surface models' products in characterizing agricultural drought in East Africa. *Remote Sensing of Environment*, 194(0):287–302. doi:10.1016/j.rse.2017.03.041.
- Ahmed, M., Sultan, M., J.Wahr, and Yan, E. (2014). The use of GRACE data to monitor natural and anthropogenic induced variations in water availability across Africa. *Earth Science Reviews*, 136:289–300. doi:10.1016/j.earscirev.2014.05.009.
- Alcamo, J., Döll, P., Henrichs, T., Kaspar, F., Lehner, B., Rösch, T., and Siebert, S. (2003). Global estimates of water withdrawals and availability under current and future 'business-as-usual' conditions. *Hydrological Sciences Journal*, 48(3):339–348. doi:10.1623/hysj.48.3.339.45278.
- Alcamo, J., Döll, P., Kaspar, F., and Siebert, S. (1997). Global change and global scenarios of water use and availability: An application of WaterGAP1.0. *Center for Environmental Systems Research (CESR), University of Kassel, Germany*. Retrieved from:<https://pdfs.semanticscholar.org/a788/80a9f9952f0e04bc88c7c5699ea9c9e0fa30.pdf> on 18th August 2016.
- Ali, A. and Lebel, T. (2009). The Sahelian standardized rainfall index revisited. *International Journal Of Climatology*, 29:1705–1714. doi:10.1002/joc.1832.
- Alley, W. M. and Konikow, L. F. (2015). Bringing GRACE down to earth. *Groundwater*, 53(6):826–829. doi:10.1111/gwat.12379.
- Allison, G., Cook, P., Barnett, S., Walker, G., Jolly, I., and Hughes, M. (1990). Land clearance and river salinisation in the western Murray Basin, Australia. *Journal of Hydrology*, 119(1):1 – 20. doi:10.1016/0022-1694(90)90030-2.
- Alsdorf, D., Beighley, E., Laraque, A., Lee, H., Tshimanga, R., O'Loughlin, F., Mah, G., Dinga, B., Moukandi, G., and Spencer, R. G. M. (2016). Opportunities for hydrologic research in the congo basin. *Reviews of Geophysics*, 54(2):378–409. doi:10.1002/2016RG000517.
- Alsdorf, D., Birkett, C., Dunne, T., Melack, J., and Hess, L. (2001). Water level changes in a large amazon lake measured with spaceborne radar in-

- terferometry and altimetry. *Geophysical Research Letters*, 28(14):2671–2674. doi:10.1029/2001GL012962.
- Alsdorf, D., Han, S.-C., Bates, P., and Melack, J. (2010). Seasonal water storage on the amazon floodplain measured from satellites. *Remote Sensing of Environment*, 114(11):2448 – 2456. doi:10.1016/j.rse.2010.05.020.
- Alsdorf, D., Lettenmaier, D., and Vrsmarty, C. (2003). The need for global, satellite-based observations of terrestrial surface waters. *Eos, Transactions American Geophysical Union*, 84(29):269–276. doi:10.1029/2003EO290001.
- Alsdorf, D. E. and Lettenmaier, D. P. (2003). Tracking fresh water from space. *Science*, 301(5639):1491–1494. doi:10.1126/science.1089802.
- Alsdorf, D. E., Rodriguez, E., and Lettenmaier, D. P. (2007). Measuring surface water from space. *Reviews of Geophysics*, 45(2):RG2002. doi:10.1029/2006RG000197.
- Andam-Akorful, S., Ferreira, V., Ndehedehe, C. E., and Quaye-Ballard, J. (2017). An investigation into the freshwater variability in West Africa during 1979 – 2010. *International Journal of Climatology*, 37(S1):333–349. doi:10.1002/joc.5006.
- Anyadike, R. N. C. (1992). Hydrological regions of West Africa: A preliminary survey based on moisture regimes. *Geografiska Annaler. Series A, Physical Geography*.
- Bader, J. and Latif, M. (2011). The 1983 drought in the West Sahel: A case study. *Climate Dynamics*, 36(3-4):463–472. doi:10.1007/s00382-009-0700-y.
- Balas, N., Nicholson, S. E., and Klotter, D. (2007). The relationship of rainfall variability in West Central Africa to sea-surface temperature fluctuations. *International Journal of Climatology*, 27(10):1335–1349.
- Barbe, L. L., Lebel, T., and Tapsoba, D. (2002). Rainfall variability in West Africa during the years 1950-90. *Journal of Climate*, 15(2):187–202. doi:10.1175/1520-0442(2002)015;0187:Rviwad;2.0.Co;2.
- Basu, M. (2009). West Africa flooding affects 600,000, U.N. reports. *CNN*. Retrieved from:<http://edition.cnn.com/2009/WORLD/africa/09/08/west.africa.flooding/index.html> on August 30, 2017.
- Bekoe, E. O. and Logah, F. Y. (2013). The impact of droughts and climate change on electricity generation in Ghana. *Environmental Sciences*, 1(1):13–24.
- Birkett, C. M. (1995). The contribution of TOPEX/POSEIDON to the global monitoring of climatically sensitive lakes. *Journal of Geophysical Research: Oceans*, 100(C12):25179–25204. doi:10.1029/95JC02125.

- Birkett, C. M. (2000). Synergistic remote sensing of Lake Chad: Variability of basin inundation. *Remote Sensing of Environment*, 72:218–236.
- Boone, A., Decharme, B., Guichard, F., Rosnay, P. D., Balsamo, G., Beljaars, A., Chopin, F., Orgeval, T., Polcher, J., Delire, C., Ducharne, A., Gascoin, S., Grippa, M., Jarlan, L., Kergoat, L., Mougin, E., Gusev, Y., Nasonova, O., Harris, P., Taylor, C., Norgaard, A., Sandholt, I., Oettle, C., Pocard-Leclercq, I., Saux-Picart, S., and Xue, Y. (2009). The AMMA Land Surface Model Intercomparison Project (ALMIP). *Bulletin of American Meteorological Society*, 90(12):1865–1880. doi:10.1175/2009BAMS27/86.1.
- Brauman, K. A., Richter, B. D., Postel, S., Malsy, M., and Flörke, M. (2016). Water depletion: An improved metric for incorporating seasonal and dry-year water scarcity into water risk assessments. *Elementa*, 4(83). doi:10.12952/journal.elementa.000083.
- Brown, C. and Lall, U. (2006). Water and economic development: The role of variability and a framework for resilience. *Natural Resources Forum*, 30(4):306–317.
- Carrao, H., Russo, S., Sepulcre-Canto, G., and Barbosa, P. (2016). An empirical standardized soil moisture index for agricultural drought assessment from remotely sensed data. *International Journal of Applied Earth Observation and Geoinformation*, 48:74 – 84. doi:10.1016/j.jag.2015.06.011.
- Castellazzi, P., Martel, R., Galloway, D. L., Longuevergne, L., and Rivera, A. (2016). Assessing groundwater depletion and dynamics using GRACE and InSAR: potential and limitations. *Groundwater*, 54(6):768–780. doi:10.1111/gwat.12453.
- Chen, J., Famiglietti, J. S., Scanlon, B. R., and Rodell, M. (2016). Groundwater storage changes: Present status from GRACE observations. *Surveys in Geophysics*, 37(2):397–417. doi:10.1007/s10712-015-9332-4.
- Chen, J. L., Wilson, C. R., Tapley, B. D., Longuevergne, L., Yang, Z. L., and Scanlon, B. R. (2010). Recent La Plata basin drought conditions observed by satellite gravimetry. *Journal of Geophysical Research: Atmospheres*, 115(D22):D22108. doi:10.1029/2010JD014689.
- Chen, T., de Jeu, R., Liu, Y., van der Werf, G., and Dolman, A. (2014). Using satellite based soil moisture to quantify the water driven variability in NDVI: A case study over mainland Australia. *Remote Sensing of Environment*, 140:330 – 338. doi:10.1016/j.rse.2013.08.022.
- Coe, M. T. and Foley, J. A. (2001). Human and natural impacts on the water resources of the Lake Chad basin. *Journal Of Geophysical Research*, 106(D4):3349–3356. doi:10.1029/2000JD900587.

- Conway, D., Persechino, A., Ardoin-Bardin, S., Hamandawana, H., Dieulin, C., and Mahé, G. (2009). Rainfall and water resources variability in Sub-Saharan Africa during the twentieth century. *Journal of Hydrometeorology*, 10(1):41–59. doi:10.1175/2008JHM1004.1.
- Cook, K. H. and Vizy, E. K. (2006). Coupled model simulations of the West African monsoon system: Twentieth- and twenty-first-century simulations. *Journal of Climate*, 19(15):3681–3703. doi:10.1175/JCLI3814.1.
- Corzo Perez, G. A., van Huijgevoort, M. H. J., Voß, F., and van Lanen, H. A. J. (2011). On the spatio-temporal analysis of hydrological droughts from global hydrological models. *Hydrology and Earth System Sciences*, 15(9):2963–2978. doi:10.5194/hess-15-2963-2011.
- Crowley, J. W., Mitrovica, J. X., Bailey, R. C., Tamisiea, M. E., and Davis, J. L. (2006). Land water storage within the Congo Basin inferred from GRACE satellite gravity data. *Geophysical Research Letters*, 33(19):L19402. doi:10.1029/2006GL027070.
- Dai, A., Qian, T., Trenberth, K. E., and Milliman, J. D. (2009). Changes in continental freshwater discharge from 1948 to 2004. *Journal of Climate*, 22(10):2773–2792. doi:10.1175/2008JCLI2592.1.
- Dardel, C., Kergoat, L., Hiernaux, P., Mougou, E., Grippa, M., and Tucker, C. (2014). Re-greening Sahel: 30 years of remote sensing data and field observations (Mali, Niger). *Remote Sensing of Environment*, 140:350 – 364. doi:10.1016/j.rse.2013.09.011.
- Descroix, L., Mahé, G., Lebel, T., Favreau, G., Galle, S., Gautier, E., Olivry, J.-C., Albergel, J., Amogu, O., Cappelaere, B., Dessouassi, R., Diedhiou, A., Breton, E. L., Mamadou, I., and Sighomnou, D. (2009). Spatio-temporal variability of hydrological regimes around the boundaries between Sahelian and Sudanian areas of West Africa: A synthesis. *Journal of Hydrology*, 375(12):90–102. doi:10.1016/j.jhydrol.2008.12.012.
- Diatta, S. and Fink, A. H. (2014). Statistical relationship between remote climate indices and West African monsoon variability. *International Journal of Climatology*, 34(12):3348–3367. doi:10.1002/joc.3912.
- Dirmeyer, P. A., Guo, Z., and Gao, X. (2004). Comparison, validation, and transferability of eight multiyear global soil wetness products. *Journal of Hydrometeorology*, 5:1011–1033. doi:10.1175/JHM-388.1.

- Döll, P., Müller Schmied, H., Schuh, C., Portmann, F. T., and Eicker, A. (2014). Global-scale assessment of groundwater depletion and related groundwater abstractions: Combining hydrological modeling with information from well observations and GRACE satellites. *Water Resources Research*, 50(7):5698–5720.
- Du, L., Tian, Q., Yu, T., Meng, Q., Jancso, T., Udvardy, P., and Huang, Y. (2013). A comprehensive drought monitoring method integrating MODIS and TRMM data. *International Journal of Applied Earth Observation and Geoinformation*, 23:245 – 253. doi:10.1016/j.jag.2012.09.010.
- Erfanian, A., Wang, G., Yu, M., and Anyah, R. (2016). Multimodel ensemble simulations of present and future climates over West Africa: impacts of vegetation dynamics. *Journal of Advances in Modeling Earth Systems*, 8. doi:10.1002/2016MS000660.
- Falkenmark, M. and Lundqvist, J. (1998). Towards water security: political determination and human adaptation crucial. *Natural Resources Forum*, 22(1):37–51. doi:10.1111/j.1477-8947.1998.tb00708.x.
- Falloon, P. and Betts, R. (2010). Climate impacts on european agriculture and water management in the context of adaptation and mitigation-the importance of an integrated approach. *Science of The Total Environment*, 408(23):5667 – 5687. doi:10.1016/j.scitotenv.2009.05.002.
- Famiglietti, J. S. (2014). The global groundwater crisis. *Nature*, 4:945–948. doi:10.1038/nclimate2425.
- Famiglietti, J. S., Cazenave, A., Eicker, A., Reager, J. T., Rodell, M., and Velicogna, I. (2015). Satellites provide the big picture. *Science*, 349(6249):684–685. doi:10.1126/science.aac9238.
- Famiglietti, J. S. and Rodell, M. (2013). Water in the balance. *Science*, 340(6138):1300–1301. doi:10.1126/science.1236460.
- Fan, Y. and Dool, H. V. (2004). Climate prediction center global monthly soil moisture data set at 0.5° resolution for 1948 to present. *Journal Of Geophysical Research*, 109:D10102. doi:10.1029/2003JD004345.
- Farnsworth, A., White, E., Williams, C. J., Black, E., and Kniveton, D. R. (2011). *Understanding the Large Scale Driving Mechanisms of Rainfall Variability over Central Africa, In African Climate and Climate Change: Physical, Social and Political Perspectives*, pages 101–122. Springer Netherlands, Dordrecht. doi:10.1007/978-90-481-3842-5_5.
- Favreau, G., Cappelaere, B., Massuel, S., Leblanc, M., Boucher, M., Boulain, N., and Leduc, C. (2009). Land clearing, climate variability, and water resources increase

- in semiarid southwest Niger: a review. *Water Resources Research*, 45:W00A16. doi:10.1029/2007WR006785.
- Ferreira, V. and Asiah, Z. (2015). An investigation on the closure of the water budget methods over Volta Basin using multi-satellite data. *International Association of Geodesy Symposia*. doi:10.1007/1345-2015-137.
- Fisher-Jeffes, L., Carden, K., Armitage, N. P., and Winter, K. (2017). Stormwater harvesting: Improving water security in South Africa's urban areas. *South African Journal of Science*, 113(1/2):4. doi:10.17159/sajs.2017/20160153.
- Fontaine, B. and Bigot, S. (1993). West African rainfall deficits and sea surface temperatures. *International Journal Of Climatology*, 13(3):271–285. doi:10.1002/joc.3370130304.
- Frappart, F., Calmant, S., Cauhopé, M., Seyler, F., and Cazenave, A. (2006). Preliminary results of ENVISAT RA-2-derived water levels validation over the Amazon basin. *Remote Sensing of Environment*, 100(2):252 – 264. doi:10.1016/j.rse.2005.10.027.
- Frappart, F., Hiernaux, P., Guichard, F., Mougin, E., Kergoat, L., Arjounin, M., Lavenu, F., Koit, M., Paturel, J.-E., and Lebel, T. (2009). Rainfall regime across the Sahel band in the Gourma region, Mali. *Journal of Hydrology*, 375(1–2):128–142.
- Freitas, A. (2013). Water as a stress factor in sub-Saharan Africa. *European Union Institute for Security Studies*, pages 1–4. Retrieved from:http://www.iss.europa.eu/uploads/media/Brief_12.pdf on 12 July, 2017.
- Funk, C., Peterson, P., Landsfeld, M., Pedreros, D., Verdin, J., Shukla, S., Husak, G., Rowland, J., Harrison, L., Hoell, A., and Michaelsen, J. (2015). The climate hazards infrared precipitation with stations a new environmental record for monitoring extremes. *Scientific Data*, 2:150066. doi:10.1038/sdata.2015.66.
- Giannini, A., Biasutti, M., Held, I. M., and Sobel, A. H. (2008). A global perspective on African climate. *Climate Change*, 90(7):359–383. doi:10.1007/s10584-008-9396-y.
- Giannini, A., Saravanan, R., and Chang, P. (2003). Oceanic forcing of Sahel rainfall on interannual to decadal time scales. *Science*, 302(5647):1027–1030. doi:10.1126/science.1089357.
- Gleeson, T., Wada, Y., and van Beek, M. F. P. B. . L. P. H. (2012). Water balance of global aquifers revealed by groundwater footprint. *Nature*, 488:197–200. doi:10.1038/nature11295.

Gleick, P. H. (1989). Climate change, hydrology, and water resources. *Reviews of Geophysics*, 27(3):329–344. doi:10.1029/RG027i003p00329.

Gleick, P. H. (1993). Water and conflict: Fresh water resources and international security. *International Security*, 18(1):79–112. doi:10.2307/2539033.

Gleick, P. H. (2000). The world's water: Biennial report on freshwater resources 2000-2001. *Island Press*. Washington, DC.

Goncàlves, J., Peterson, J., Deschamps, P., Hamelin, B., and Baba-Sy, O. (2013). Quantifying the modern recharge of the “fossil” Sahara aquifers. *Geophysical Research Letters*, 40:2673–2678. doi:10.1002/grl.50478.

Greve, P., Orłowsky, B., Mueller, B., Sheffield, J., Reichstein, M., and Seneviratne, S. L. (2014). Global assessment of trends in wetting and drying over land. *Nature Geoscience*, 7:716–721. doi:10.1038/NGE02247.

Grippa, M., Kergoat, L., Frappart, F., Araud, Q., Boone, A., de Rosnay, P., Lemoine, J. M., Gascoin, S., Balsamo, G., Ottl, C., Decharme, B., Saux-Picart, S., and Ramillien, G. (2011). Land water storage variability over West Africa estimated by Gravity Recovery and Climate Experiment (GRACE) and land surface models. *Water Resources Research*, 47(5):W05549. doi:10.1029/2009wr008856.

Hall, J. W., Grey, D., Garrick, D., Fung, F., Brown, C., Dadson, S. J., and Sadoff, C. W. (2014). Coping with the curse of freshwater variability. *Science*, 346(6208):429–430. doi:10.1126/science.1257890.

Heim, R. R. (2002). A review of twentieth-century drought indices used in the United States. *Bulletin of American Meteorological Society*, 83(8):1149–1165.

Hély, C., Bremond, L., Alleaume, S., Smith, B., Sykes, M. T., and Guiot, J. (2006). Sensitivity of African biomes to changes in the precipitation regime. *Global Ecology and Biogeography*, 15(3):258–270. doi:10.1111/j.1466-8238.2006.00235.x.

Henry, C., Allen, D. M., and Huang, J. (2011). Groundwater storage variability and annual recharge using well-hydrograph and GRACE satellite data. *Hydrogeology Journal*, 19:741–755. doi:10.1007/s10040-011-0724-3.

Hinderer, J., de Linage, C., Boya, J.-P., Gegout, P., Masson, F., Rogister, Y., Amalvict, M., Pfeffer, J., Littel, F., Luck, B., Bayerb, R., Champollion, C., Collard, P., Moigne, N. L., Diamentc, M., Deroussi, S., de Viron, O., Biancale, R., Lemoine, J.-M., Bonvalot, S., Gabalda, G., Bock, O., Genthon, P., Boucher, M., Favreau, G., Sguis, L., Delclaux, F., Cappelaere, B., Oi, M., Desclotresh, M., Galleh, S.,

- Laurent, J.-P., Legchenko, A., and Bouink, M.-N. (2009). The GHYRAF (Gravity and Hydrology in Africa) experiment: Description and first results. *Journal of Geodynamics*, 48:172–181. doi:10.1016/j.jog.2009.09.014.
- Houborg, R., Rodell, M., Li, B., Reichle, R., and Zaitchik, B. F. (2012). Drought indicators based on model-assimilated Gravity Recovery and Climate Experiment (GRACE) terrestrial water storage observations. *Water Resources Research*, 48(7):W07525. doi:10.1029/2011WR011291.
- Hua, W., Zhou, L., Chen, H., Nicholson, S. E., Raghavendra, A., and Jiang, Y. (2016). Possible causes of the Central Equatorial African long-term drought. *Environmental Research Letters*, 11(12):124002. doi:10.1088/1748-9326/11/12/124002.
- Huntington, T. G. (2006). Evidence for intensification of the global water cycle: Review and synthesis. *Journal of Hydrology*, 319(14):83 – 95. doi:10.1016/j.jhydrol.2005.07.003.
- Hurkmans, R., Troch, P. A., Uijlenhoet, R., Torfs, P., and Durcik, M. (2009). Effects of climate variability on water storage in the Colorado River Basin. *Journal Of Hydrometeorology*, 10:1257–1270. doi:10.1175/2009JHM1133.1.
- IPCC (2015). Synthesis report. contribution of working groups i, ii and iii to the fifth assessment report of the Intergovernmental Panel on Climate Change [core writing team, r.k. pachauri and l.a. meyer (eds.)]. *Intergovernmental Panel on Climate Change, Switzerland*, page 151 pp. Retrieved from:https://ar5-syr.ipcc.ch/ipcc/ipcc/resources/pdf/IPCC_SynthesisReport.pdf on 16th January 2017.
- Janicot, S. (1992). Spatiotemporal variability of West African rainfall. part i: Regionalizations and typings. *Journal of Climate*, 5(5):489–497. doi:10.1175/1520-0442(1992)005<0489:SVOWAR>2.0.CO;2.
- Janicot, S. (1994). *The Recent West African Rainfall Variability Through Empirical and Modelling Investigations*, pages 135–149. Springer Berlin Heidelberg, Berlin, Heidelberg. doi:10.1007/978-3-642-79268-7_7.
- Jenkins, G. S., Adamou, G., and Fongang, S. (2002). The challenges of modeling climate variability and change in West Africa. *Climatic Change*, 52(3):263–286. doi:10.1023/A:1013741803144.
- Joly, M. and Voltaire, A. (2010). Role of the Gulf of Guinea in the inter-annual variability of the West African monsoon: what do we learn from CMIP3 coupled simulations? *International Journal of Climatology*, 30(12):1843–1856. doi:10.1002/joc.2026.

- Kasei, R., Diekkrüger, B., and Leemhuis, C. (2010). Drought frequency in the Volta Basin of West Africa. *Sustainability Science*, 5(1):89–97.
- Knauer, K., Gessner, U., Dech, S., and Kuenzer, C. (2014). Remote sensing of vegetation dynamics in West Africa. *International Journal of Remote Sensing*, 35(17):6357–6396. doi:10.1080/01431161.2014.954062.
- Konar, M., Evans, T. P., Levy, M., Scott, C. A., Troy, T. J., Vrssmarty, C. J., and Sivapalan, M. (2016). Water resources sustainability in a globalizing world: who uses the water? *Hydrological Processes*, 30(18):3330–3336. doi:10.1002/hyp.10843.
- Koster, R. D., Dirmeyer, P. A., Guo, Z., Bonan, G., Chan, E., Cox, P., Gordon, C. T., Kanae, S., Kowalczyk, E., Lawrence, D., Liu, P., Lu, C.-H., Malyshev, S., McAvaney, B., Mitchell, K., Mocko, D., Oki, T., Oleson, K., Pitman, A., Sud, Y. C., Taylor, C. M., Verseghy, D., Vasic, R., Xue, Y., and Yamada, T. (2004). Regions of strong coupling between soil moisture and precipitation. *Science*, 305(5687):1138–1140. doi:10.1126/science.1100217.
- Kuylenstierna, J. L., Bjrklund, G., and Najlis, P. (1997). Sustainable water future with global implications: everyone’s responsibility. *Natural Resources Forum*, 21(3):181–190. doi:10.1111/j.1477-8947.1997.tb00691.x.
- Lammers, R. B., Shiklomanov, A. I., Vrssmarty, C. J., Fekete, B. M., and Peterson, B. J. (2001). Assessment of contemporary Arctic river runoff based on observational discharge records. *Journal of Geophysical Research: Atmospheres*, 106(D4):3321–3334. doi:10.1029/2000JD900444.
- Laux, P. (2009). Statistical modeling of precipitation for agricultural planning in the Volta Basin of West Africa. *Doctoral dissertation, Mitteilungen/Institut fr Wasserbau, Universitt Stuttgart*, 179(198). Retrieved from:elib.uni-stuttgart.de/opus/volltexte/2009/4016/pdf/Dissertation-Laux.pdf. on 25 July, 2014.
- Lebel, T. and Ali, A. (2009). Recent trends in the Central and Western Sahel rainfall regime (1990-2007). *Journal of Hydrology*, 375(12):52 – 64. doi:10.1016/j.jhydrol.2008.11.030.
- Lebel, T., Cappelaere, B., Galle, S., Hanan, N., Kergoat, L., Levis, S., Vieux, B., Descroix, L., Gosset, M., Mougin, E., Peugeot, C., and Seguis, L. (2009). AMMA-CATCH studies in the Sahelian region of West-Africa: An overview. *Journal of Hydrology*, 375(1–2):3 – 13.
- Lebel, T., Delclaux, F., Le Barbé, L., and Polcher, J. (2000). From GCM scales to hydrological scales: rainfall variability in West Africa. *Stochastic Environmental Research and Risk Assessment*, 14(4):275–295. doi:10.1007/s004770000050.

- Leblanc, M., Leduc, C., Razack, M., Lemoalle, J., Dagorne, D., and Mofor, L. (2003). Applications of remote sensing and GIS for groundwater modelling of large semiarid areas: example of the Lake Chad Basin, Africa. *Hydrology of the Mediterranean and Semiarid Regions*, (278):186–191. proceedings of the international symposium held at Montpellier, April 2003.
- Leduc, C., Bromley, J., and Schroeter, P. (1997). Water table fluctuation and recharge in semi-arid climate: some results of the HAPEX-Sahel hydrodynamic survey (Niger). *Journal of Hydrology*, 188(188–189):123 – 138. doi:10.1016/S0022-1694(96)03156-3.
- Leduc, C., Favreau, G., and Schroeter, P. (2001). Long-term rise in a Sahelian water-table: the continental terminal in south-west Niger. *Journal of Hydrology*, 243(1–2):43 – 54. doi:10.1016/S0022-1694(00)00403-0.
- Lee, H., Beighley, R. E., Alsdorf, D., Jung, H. C., Shum, C., Duan, J., Guo, J., Yamazaki, D., and Andreadis, K. (2011). Characterization of terrestrial water dynamics in the Congo Basin using GRACE and satellite radar altimetry. *Remote Sensing of Environment*, 115(12):3530 – 3538. doi:10.1016/j.rse.2011.08.015.
- Lee, H., Jung, H. C., Yuan, T., Beighley, R. E., and Duan, J. (2014). Controls of terrestrial water storage changes over the Central Congo Basin determined by integrating Palsar ScanSar, Envisat Altimetry, and Grace data. *Remote Sensing of the Terrestrial Water Cycle, Geophysical Monograph*, 206:117–129. doi:10.1002/9781118872086.ch7/pdf.
- Lemoalle, J., Bader, J.-C., Leblanc, M., and Sedick, A. (2012). Recent changes in Lake Chad: Observations, simulations and management options (19732011). *Global and Planetary Change*, 8081:247 – 254. doi:10.1016/j.gloplacha.2011.07.004.
- Lettenmaier, D. P. (2005). Observations of the global water cycle global monitoring networks. in *Encyclopedia of Hydrological Sciences*, 5, edited by M G Anderson.:2719–2732. John Wiley & Sons, Ltd.
- Li, B. and Rodell, M. (2015). Evaluation of a model-based groundwater drought indicator in the conterminous U.S. *Journal of Hydrology*, 526:78 – 88. doi:10.1016/j.jhydrol.2014.09.027.
- Li, K., Coe, M., Ramankutty, N., and Jong, R. D. (2007). Modeling the hydrological impact of land-use change in West Africa. *Journal of Hydrology*, 337(3–4):258 – 268. doi:10.1016/j.jhydrol.2007.01.038.
- Li, K. Y., Coe, M. T., and Ramankutty, N. (2005). Investigation of hydrological variability in West Africa using land surface models. *Journal of Climate*, 18(16):3173–3188. doi:10.1175/JCLI3452.1.

- Long, D., Scanlon, B. R., Longuevergne, L., Sun, A. Y., Fernando, D. N., and Save, H. (2013). GRACE satellite monitoring of large depletion in water storage in response to the 2011 drought in Texas. *Geophysical Research Letters*, 40(13):3395–3401. doi:10.1002/Grl.50655.
- Long, D., Shen, Y., Sun, A., Hong, Y., Longuevergne, L., Yang, Y., Li, B., and Chen, L. (2014). Drought and flood monitoring for a large karst plateau in southwest china using extended GRACE data. *Remote Sensing of Environment*, 155:145 – 160. doi:10.1016/j.rse.2014.08.006.
- Losada, T., Rodríguez-Fonseca, B., Janicot, S., Gervois, S., Chauvin, F., and Ruti, P. (2010). A multi-model approach to the Atlantic Equatorial mode: impact on the West African monsoon. *Climate Dynamics*, 35(1):29–43. doi:10.1007/s00382-009-0625-5.
- Lovett, J. C., Midgley, G. F., and Barnard, P. (2005). Climate change and ecology in africa. *African Journal of Ecology*, 43(3):167–169. doi:10.1111/j.1365-2028.2005.00598.x.
- Malhi, Y. and Wright, J. (2004). Spatial patterns and recent trends in the climate of tropical rainforest regions. *Philosophical Transactions of the Royal Society of London*, 359:311329. doi:10.1098/rstb.2003.1433.
- McCabe, M. F., Rodell, M., Alsdorf, D. E., Miralles, D. G., Uijlenhoet, R., Wagner, W., Lucieer, A., Houborg, R., Verhoest, N. E. C., Franz, T. E., Shi, J., Gao, H., and Wood, E. F. (2017). The future of Earth observation in hydrology. *Hydrology and Earth System Sciences*, 21(7):3879–3914. doi:10.5194/hess-21-3879-2017.
- McKee, T. B., Doeskin, N. J., and Kieist, J. (1993). The relationship of drought frequency and duration to time scales. *Conference on Applied Climatology, American Meteorological Society, Boston, Massachusetts*, pages 179–184. Retrieved from:www.ccc.atmos.colostate.edu/relationshipofdroughtfrequency.pdf. Accessed 27 June, 2014.
- Mishra, A. K., Ines, A. V., Das, N. N., Khedun, C. P., Singh, V. P., Sivakumar, B., and Hansen, J. W. (2015). Anatomy of a local-scale drought: Application of assimilated remote sensing products, crop model, and statistical methods to an agricultural drought study. *Journal of Hydrology*, 526:15 – 29. doi:10.1016/j.jhydrol.2014.10.038.
- Mohino, E., Janicot, S., and Bader, J. (2011). Sahel rainfall and decadal to multi-decadal sea surface temperature variability. *Climate Dynamics*, 37:419–440. doi:10.1007/s00382-010-0867-2.

- Moore, P. and Williams, S. D. P. (2014). Integration of altimetry lake levels and GRACE gravimetry over Africa: Inferences for terrestrial water storage change 2003-2011. *Water Resources Research*, 50:9696–9720. doi:10.1002/2014WR015506.
- Mpelasoka, F., Awange, J. L., and Zerihun, A. (2018). Influence of coupled ocean-atmosphere phenomena on the greater horn of africa droughts and their implications. *Science of The Total Environment*, 610611:691 – 702. doi:10.1016/j.scitotenv.2017.08.109.
- Nahmani, S., Bock, O., Bouin, M.-N., Santamara-Gmez, A., Boy, J.-P., Collilieux, X., Mtivier, L., Isabelle Panet, P. G., de Linage, C., and Wppelmann, G. (2012). Hydrological deformation induced by the West African Monsoon: Comparison of GPS, GRACE and loading models. *Journal of Geophysical Research-Solid Earth*, 117(B5). doi:10.1029/2011JB009102.
- Nakaegawa, T., Kitoh, A., and Hosaka, M. (2013). Discharge of major global rivers in the late 21st century climate projected with the high horizontal resolution MRI-AGCMs. *Hydrological Processes*, 27(23):3301–3318. doi:10.1002/hyp.9831.
- Ndehedehe, C., Awange, J., Agutu, N., Kuhn, M., and Heck, B. (2016a). Understanding changes in terrestrial water storage over West Africa between 2002 and 2014. *Advances in Water Resources*, 88:211–230. doi:10.1016/j.advwatres.2015.12.009.
- Ndehedehe, C. E., Agutu, N. O., and Okwuashi, O. (2017a). Is terrestrial water storage a useful indicator in assessing the impacts of climate variability on crop yield in semi-arid ecosystems? *Manuscript in final stage of acceptance for publication in Ecological Indicators*.
- Ndehedehe, C. E., Agutu, N. O., Okwuashi, O. H., and Ferreira, V. G. (2016b). Spatio-temporal variability of droughts and terrestrial water storage over Lake Chad Basin using independent component analysis. *Journal of Hydrology*, 540:106– 128. doi:10.1016/j.jhydrol.2016.05.068.
- Ndehedehe, C. E., Awange, J., Kuhn, M., and Agutu, N. (2017b). Hydrological controls on surface vegetation dynamics over Sub-Sahara Africa using GRACE satellite observations. *Manuscript revised and submitted to Journal of Arid Environments*.
- Ndehedehe, C. E., Awange, J., Kuhn, M., Agutu, N., and Fukuda, Y. (2017c). Analysis of hydrological variability over the Volta river basin using in-situ data and satellite observations. *Journal of Hydrology: Regional studies*, 12:88–110. doi:10.1016/j.ejrh.2017.04.005.

- Ndehedehe, C. E., Awange, J., Kuhn, M., Agutu, N., and Fukuda, Y. (2017d). Climate teleconnections influence on West Africa's terrestrial water storage. *Hydrological Processes*, 31(18):3206–3224. doi: 10.1002/hyp.11237.
- Ndehedehe, C. E., Awange, J. L., Agutu, N. O., and Okwuashi, O. (2017e). Changes in hydro-meteorological conditions over Sub-Sahara Africa (1980–2015) and links to global climate. *Manuscript revised and resubmitted to Global and Planetary Change*.
- Ndehedehe, C. E., Awange, J. L., Corner, R., Kuhn, M., and Okwuashi, O. (2016c). On the potentials of multiple climate variables in assessing the spatio-temporal characteristics of hydrological droughts over the Volta Basin. *Science of the Total Environment*, 557-558:819–837. doi:10.1016/j.scitotenv.2016.03.004.
- Ngom, F., Tweed, S., Bader, J.-C., Saos, J.-L., Malou, R., Leduc, C., and Leblanc, M. (2016). Rapid evolution of water resources in the Senegal delta. *Global and Planetary Change*, 144:34 – 47. doi:10.1016/j.gloplacha.2016.07.002.
- Nicholson, S. (2005). On the question of the recovery of the rains in the West African Sahel. *Journal of Arid Environments*, 63(3):615–641. doi:10.1016/j.jaridenv.2005.03.004.
- Nicholson, S. (2013). The West African Sahel: a review of recent studies on the rainfall regime and its interannual variability. *ISRN Meteorology*, 2013(453521):1–32. doi:10.1155/2013/453521.
- Nicholson, S. and Grist, J. (2001). A conceptual model for understanding rainfall variability in the West African Sahel on interannual and interdecadal timescales. *International Journal Of Climatology*, 21:1733–1757. doi:10.1002/joc.648.
- Nicholson, S. E., Some, B., and Kone, B. (2000). An analysis of recent rainfall conditions in West Africa, including the rainy seasons of the 1997 El Niño and the 1998 La Nia years. *Journal of Climate*, 13(14):2628–2640. doi:10.1175/1520-0442(2000)013;2628:AAORRC;2.0.CO;2.
- Niu, J., Chen, J., and Sun, L. (2015). Exploration of drought evolution using numerical simulations over the Xijiang (West River) basin in South China. *Journal of Hydrology*, 526:68 – 77. doi:10.1016/j.jhydrol.2014.11.029.
- Nka, B. N., Oudin, L., Karambiri, H., Paturel, J. E., and Ribstein, P. (2015). Trends in floods in West Africa: analysis based on 11 catchments in the region. *Hydrology and Earth System Sciences*, 19(11):4707–4719. doi:10.5194/hess-19-4707-2015.
- Nkiaka, E., Nawaz, N. R., and Lovett, J. C. (2017). Analysis of rainfall variability in the logone catchment, Lake Chad basin. *International Journal of Climatology*, 37(9):3553–3564. doi:10.1002/joc.4936.

- Oettli, P., Sultan, B., Baron, C., and Vrac, M. (2011). Are regional climate models relevant for crop yield prediction in West Africa? *Environmental Research Letters*, 6(1):014008. doi:10.1088/1748-9326/6/1/014008.
- Ojo, O., Gbuyiro, S. O., and Okoloye, C. U. (2004). Implications of climate variability and climate change for water resources availability and management in West Africa. *GeoJournal*, 61(2):111–119. doi:10.1007/s/10708-004-2863-8.
- Okwuashi, O. and Ndehedehe, C. (2017). A prototype alternative methodology for modelling future urban land use change with remote sensing data using logistic regression based cellular automata. *Manuscript accepted for publication in Journal of Land Use Science*.
- Otto, F. E. L., Jones, R. G., Halladay, K., and Allen, M. R. (2013). Attribution of changes in precipitation patterns in african rainforests. *Philosophical Transactions of the Royal Society of London B: Biological Sciences*, 368(1625). doi:10.1098/rstb.2012.0299.
- Owusu, K. and Waylen, P. (2009). Trends in spatio-temporal variability in annual rainfall in Ghana (1951-2000). *Weather*, 64(5):115–119.
- Paeth, H., Fink, A., Pohle, S., Keis, F., Machel, H., and Samimi, C. (2012). Meteorological characteristics and potential causes of the 2007 flood in sub-Saharan Africa. *International Journal of Climatology*, 31:1908–1926. doi:10.1002/Joc.2199.
- Panthou, G., Vischel, T., and Lebel, T. (2014). Recent trends in the regime of extreme rainfall in the central sahel. *International Journal of Climatology*, 34(15):3998–4006. doi:10.1002/joc.3984.
- Paolino, D. A., III, J. L. K., Kirtman, B. P., Min, D., and Straus, D. M. (2012). The impact of land surface and atmospheric initialization on seasonal forecasts with ccs. *Journal of Climate*, 25(3):1007–1021. doi:10.1175/2011JCLI3934.1.
- Petropoulos, G. P., Ireland, G., and Barrett, B. (2015). Surface soil moisture retrievals from remote sensing: Current status, products, and future trends. *Physics and Chemistry of the Earth, Parts A/B/C*, 83–84:36 – 56. doi:10.1016/j.pce.2015.02.009.
- Phillips, T., Nerem, R. S., Fox-Kemper, B., Famiglietti, J. S., and Rajagopalan, B. (2012). The influence of ENSO on global terrestrial water storage using GRACE. *Geophysical Research Letters*, 39:L16705. doi:10.1029/2012GL052495, 2012.
- Piao, S., Ciais, P., Huang, Y., Shen, Z., Peng, S., Li, J., Zhou, L., Liu, H., YuecunMa, Ding, Y., Friedlingstein, P., Liu, C., Tan, K., Yu, Y., Zhang, T., and Fang, J. (2010).

The impacts of climate change on water resources and agriculture in China. *Nature*, 467:43–51. doi:10.1038/nature09364.

Pierre, C., Grippa, M., Mougin, E., Guichard, F., and Kergoat, L. (2016). Changes in Sahelian annual vegetation growth and phenology since 1960: A modeling approach. *Global and Planetary Change*, 143:162 – 174. doi:10.1016/j.gloplacha.2016.06.009.

Prudhomme, C., Giuntoli, I., Robinson, E. L., Clark, D. B., Arnell, N. W., Dankers, R., Fekete, B. M., Franssen, W., Gerten, D., Gosling, S. N., Hagemann, S., Hannah, D. M., Kim, H., Masaki, Y., Satoh, Y., Stacke, T., Wada, Y., and Wisser, D. (2014). Hydrological droughts in the 21st century, hotspots and uncertainties from a global multimodel ensemble experiment. *Proceedings of the National Academy of Sciences*, 111(9):3262–3267. doi:10.1073/pnas.1222473110.

Reager, J. T., Thomas, B. F., and Famiglietti, J. S. (2014). River basin flood potential inferred using GRACE gravity observations at several months lead time. *Nature Geoscience*, 7(8):588–592. doi:10.1038/ngeo2203.

Reason, C. J. C. and Rouault, M. (2006). Sea surface temperature variability in the tropical southeast Atlantic Ocean and West African rainfall. *Geophysical Research Letters*, 33(21):L21705. doi:10.1029/2006GL027145.

Reichle, R. H., Koster, R. D., Lannoy, G. J. M. D., Forman, B. A., Liu, Q., Mahanama, S. P. P., and Tour, A. (2011). Assessment and enhancement of MERRA land surface hydrology estimates. *Journal of Climate*, 24(24):6322–6338. doi:10.1175/JCLI-D-10-05033.1.

Rienecker, M. M., Suarez, M. J., Gelaro, R., Todling, R., Bacmeister, J., Liu, E., Bosilovich, M. G., Schubert, S. D., Takacs, L., Kim, G.-K., Bloom, S., Chen, J., Collins, D., Conaty, A., da Silva, A., Gu, W., Joiner, J., Koster, R. D., Lucchesi, R., Molod, A., Owens, T., Pawson, S., Pegion, P., Redder, C. R., Reichle, R., Robertson, F. R., Ruddick, A. G., Sienkiewicz, M., and Woollen, J. (2011). MERRA: NASA’s modern-era retrospective analysis for research and applications. *Journal of Climate*, 24(14):3624–3648. doi:10.1175/JCLI-D-11-00015.1.

Rijsberman, F. R. (2006). Water scarcity: Fact or fiction? . *Agricultural Water Management*, 80(1–3):5 – 22. doi:10.1016/j.agwat.2005.07.001.

Rodell, M., Houser, P. R., Jambor, U., Gottschalck, J., Mitchell, K., Meng, K., Arsenault, C. J., Cosgrove, B., Radakovich, J., Bosilovich, M., Entin, J. K., Walker, J. P., Lohmann, D., and Toll, D. (2004). The global land data assimilation system. *Bulletin of American Meteorological Society*, 85(3):381–394. doi:10.1175/BAMS-85-3-381.R.

- Rost, S., Gerten, D., Bondeau, A., Lucht, W., Rohwer, J., and Schaphoff, S. (2008). Agricultural green and blue water consumption and its influence on the global water system. *Water Resources Research*, 44(9):W09405. doi:10.1029/2007WR006331.
- Rouault, M. and Richard, Y. (2003). Intensity and spatial extension of drought in South Africa at different time scales. *Water SA*, 29(4):489–500.
- Roudier, P., Sultan, B., Quirion, P., and Berg, A. (2011). The impact of future climate change on West African crop yields: What does the recent literature say? *Global Environmental Change*, 21:1073–1083. doi:10.1016/j.gloenvcha.2011.04.007.
- Sanogo, S., Fink, A. H., Omotosho, J. A., Ba, A., Redl, R., and Ermert, V. (2015). Spatio-temporal characteristics of the recent rainfall recovery in West Africa. *International Journal of Climatology*, 35(15):4589–4605. doi:10.1002/joc.4309.
- Scanlon, B. R., Reedy, R. C., Stonestrom, D. A., Prudic, D. E., and Dennehy, K. F. (2005). Impact of land use and land cover change on groundwater recharge and quality in the southwestern US. *Global Change Biology*, 11(10):1577–1593. doi:10.1111/j.1365-2486.2005.01026.x.
- Schewe, J., Heinke, J., Gerten, D., Haddeland, I., Arnell, N. W., Clark, D. B., Dankers, R., Eisner, S., Fekete, B. M., Colón-González, F. J., Gosling, S. N., Kim, H., Liu, X., Masaki, Y., Portmann, F. T., Satoh, Y., Stacke, T., Tang, Q., Wada, Y., Wisser, D., Albrecht, T., Frieler, K., Piontek, F., Warszawski, L., and Kabat, P. (2013). Multimodel assessment of water scarcity under climate change. *PNAS*, 111(9):3245–3250,. doi:10.1073/pnas.1222460110.
- Schuol, J. and Abbaspour, K. C. (2006). Calibration and uncertainty issues of a hydrological model (SWAT) applied to West Africa. *Advances in Geosciences*, 9:137–143. doi:adv-geosci.net/9/137/2006/.
- Séguis, L., Cappelaere, B., Milsis, G., Peugeot, C., Massuel, S., and Favreau, G. (2004). Simulated impacts of climate change and land-clearing on runoff from a small Sahelian catchment. *Hydrological Processes*, 18(17):3401–3413. doi:10.1002/hyp.1503.
- Senay, G. B., Velpuri, N. M., Bohms, S., Demissie, Y., and Gebremichael, M. (2014). Understanding the hydrologic sources and sinks in the Nile Basin using multisource climate and remote sensing data sets. *Water Resources Research*, 50(11):8625–8650. doi:10.1002/2013WR015231.
- Sheffield, J., Ferguson, C. R., Troy, T. J., Wood, E. F., and McCabe, M. F. (2009). Closing the terrestrial water budget from satellite remote sensing. *Geophysical Research Letters*, 36(7):L07403.

- Sheffield, J. and Wood, E. F. (2008). Global trends and variability in soil moisture and drought characteristics, 1950–2000, from observation-driven simulations of the terrestrial hydrologic cycle. *Journal of Climate*, 21(3):432–458. doi:10.1175/2007JCLI1822.1.
- Sheffield, J., Wood, E. F., Chaney, N., Guan, K., Sadri, S., Yuan, X., Olang, L., Amani, A., Ali, A., Demuth, S., and Ogallo, L. (2014). A drought monitoring and forecasting system for Sub-Saharan African water resources and food security. *Bulletin of the American Meteorological Society*, 95(6):861–882. doi:10.1175/BAMS-D-12-00124.1.
- Shiferaw, B., Tesfaye, K., Kassie, M., Abate, T., Prasanna, B., and Menkir, A. (2014). Managing vulnerability to drought and enhancing livelihood resilience in sub-Saharan Africa: technological, institutional and policy options. *Weather and Climate Extremes*, 3(0):67 – 79. doi:10.1016/j.wace.2014.04.004.
- Shiklomanov, I. A. (2000). Appraisal and assessment of world water resources. *Water International*, 25(1):11–32. doi:10.1080/02508060008686794.
- Sultan, B. and Gaetani, M. (2016). Agriculture in West Africa in the twenty-first century: Climate change and impacts scenarios, and potential for adaptation. *Frontiers in Plant Science*, 7:1262. doi:10.3389/fpls.2016.01262.
- Swenson, S. and Wahr, J. (2007). Multi-sensor analysis of water storage variations of the Caspian Sea. *Geophysical Research Letters*, 34(16). doi:10.1029/2007gl030733.
- Tapley, B., Bettadpur, S., Watkins, M., and Reigber, C. (2004). The Gravity Recovery and Climate Experiment: Mission overview and early results. *Geophysical Research Letters*, 31:1–4. doi:10.1029/2004GL019920.
- Thiemig, V., Rojas, R., Zambrano-Bigiarini, M., and Roo, A. D. (2013). Hydrological evaluation of satellite-based rainfall estimates over the Volta and Baro-Akobo Basin. *Journal of Hydrology*, 499:324 – 338. doi:10.1016/j.jhydrol.2013.07.012.
- Thomas, A. C., Reager, J. T., Famiglietti, J. S., and Rodell, M. (2014). A GRACE-based water storage deficit approach for hydrological drought characterization. *Geophysical Research Letters*, 41(5):1537–1545. doi:10.1002/2014GL059323.
- Tiwari, V. M., Wahr, J., and Swenson, S. (2009). Dwindling groundwater resources in northern india, from satellite gravity observations. *Geophysical Research Letters*, 36(18):L18401. doi:10.1029/2009GL039401.
- Todd, M., Andersson, L., Ambrosino, C., Hughes, D., Kniveton, D. R., Mileham, L., Murray-Hudson, M., Raghavan, S., Taylor, R., and Wolski, P. (2011). *Climate*

Change Impacts on Hydrology in Africa: Case Studies of River Basin Water Resources, In *In African Climate and Climate Change: Physical, Social and Political Perspectives*, pages 123–153. Springer Netherlands, Dordrecht. doi:10.1007/978-90-481-3842-5_5.

Tourian, M., Schwatke, C., and Sneeuw, N. (2017). River discharge estimation at daily resolution from satellite altimetry over an entire river basin. *Journal of Hydrology*, 546:230 – 247. doi:10.1016/j.jhydrol.2017.01.009.

Tucker, C. J., Dregne, H. E., and Newcomb, W. W. (1991). Expansion and contraction of the Sahara Desert from 1980 to 1990. *Science*, 253(5017):299 – 300. doi:10.1126/science.253.5017.299.

van Huijgevoort, M. (2014). Hydrological drought: Characterisation and representation in large-scale models. *PhD thesis, Wageningen University, Wageningen, NL*. Retrieved from:<http://library.wur.nl/WebQuery/wda/2057611> Accessed 1st February, 2017.

Van Loon, A. F., Stahl, K., Di Baldassarre, G., Clark, J., Rangelcroft, S., Wanders, N., Gleeson, T., Van Dijk, A. I. J. M., Tallaksen, L. M., Hannaford, J., Uijlenhoet, R., Teuling, A. J., Hannah, D. M., Sheffield, J., Svoboda, M., Verbeiren, B., Wagener, T., and Van Lanen, H. A. J. (2016). Drought in a human-modified world: reframing drought definitions, understanding, and analysis approaches. *Hydrology and Earth System Sciences*, 20(9):3631–3650. doi:10.5194/hess-20-3631-2016.

Vicente-Serrano, S. M. (2006). Spatial and temporal analysis of droughts in the Iberian Peninsula (19102000). *Hydrological Sciences Journal*, 51(1):83–97. doi:10.1623/hysj.51.1.83.

Vicente-Serrano, S. M., Beguería, S., Lorenzo-Lacruz, J., Camarero, J. J., López-Moreno, J. I., Azorin-Molina, C., Revuelto, J., Morán-Tejeda, E., and Sanchez-Lorenzo, A. (2012). Performance of drought indices for ecological, agricultural, and hydrological applications. *Earth Interactions*, 16(10):1–27. doi:10.1175/2012EI000434.1.

Vörösmarty, C., Askew, A., Grabs, W., Barry, R. G., Birkett, C., Dll, P., Goodison, B., Hall, A., Jenne, R., Kitaev, L., Landwehr, J., Keeler, M., Leavesley, G., Schaake, J., Strzepek, K., Sundarvel, S. S., Takeuchi, K., and Webster, F. (2001). Global water data: A newly endangered species. *EOS, Transactions American Geophysical Union*, 82(5):54–58. doi:10.1029/01EO00031.

Vörösmarty, C. J., Douglas, E. M., Green, P. A., and Revenga, C. (2005). Geospatial indicators of emerging water stress: An application to africa. *Ambio*.

- Vörösmarty, C. J., Green, P., Salisbury, J., and Lammers, R. B. (2000). Global water resources: Vulnerability from climate change and population growth. *Science*, 289(5477):284–288. doi:10.1126/science.289.5477.284.
- Wagner, S., Kunstmann, H., Brdossy, A., Conrad, C., and Colditz, R. (2009). Water balance estimation of a poorly gauged catchment in West Africa using dynamically downscaled meteorological fields and remote sensing information. *Physics and Chemistry of the Earth*, 34:25–235. doi:10.1016/j.pce.2008.04/.002.
- Wald, L. (1990). Monitoring the decrease of Lake Chad from space. *Geocarto International*, 5(3):31–36. doi: 10.1080/10106049009354266.
- Washington, R., James, R., Pearce, H., Pokam, W. M., and Moufouma-Okia, W. (2013). Congo Basin rainfall climatology: can we believe the climate models? *Philosophical Transactions of the Royal Society of London B: Biological Sciences*, 368(1625). doi:10.1098/rstb.2012.0296.
- Wild, M., Grieser, J., and Schär, C. (2008). Combined surface solar brightening and increasing greenhouse effect support recent intensification of the global land-based hydrological cycle. *Geophysical research letters*, 35(L17706):L17706–1–L17706–5. doi:10.1029/2008GL034842.
- WMO (2013). WMO statement on the status of the global climate in 2012. *World Meteorological Organization*, WMO No.1108. Retrieved from:www.wmo.int/pages/prog/wcp/wcdmp/documents/WMO1108.pdf. on 15th June, 2015.
- WMO (2015). The climate in Africa:2013. *World Meteorological Organization*, WMO No.1147. Retrieved from:http://www.wmo.int/pages/prog/wcp/wcdmp/documents/1147_EN.pdf. on 26th January, 2017.
- Wouters, B., Bonin, J. A., Chambers, D. P., Riva, R. E. M., Sasgen, I., and Wahr, J. (2014). GRACE, time-varying gravity, Earth system dynamics and climate change. *Reports on Progress in Physics*, 77(11):116801. doi:10.1088/0034-4885/77/11/116801.
- Yang, D., Ye, B., and Kane, D. L. (2004). Streamflow changes over siberian yenisei river basin. *Journal of Hydrology*, 296(1–4):59 – 80. doi:10.1016/j.jhydrol.2004.03.017.
- Yang, Y., Long, D., Guan, H., Scanlon, B. R., Simmons, C. T., Jiang, L., and Xu, X. (2014). GRACE satellite observed hydrological controls on interannual and seasonal variability in surface greenness over mainland Australia. *Journal of Geophysical Research: Biogeosciences*, 119(12):2245–2260. doi:10.1002/2014JG002670.

Yirdaw, S. Z., Snelgrove, K., and Agboma, C. (2008). GRACE satellite observations of terrestrial moisture changes for drought characterization in the Canadian Prairie. *Journal of Hydrology*, 356:84–92.

Zhang, D., Zhang, Q., Werner, A. D., and Liu, X. (2016). GRACE-based hydrological drought evaluation of the Yangtze River Basin, China. *Journal of Hydrometeorology*, 17(3):811–828. doi:10.1175/JHM-D-15-0084.1.

Zhou, L., Tian, Y., Myneni, R. B., Ciais, P., Saatchi, S., Liu, Y. Y., Piao, S., Chen, H., Vermote, E. F., Song, C., and Hwang, T. (2014). Widespread decline of congo rainforest greenness in the past decade. *Nature*, 509(7498):86–90. doi:10.1038/nature13265.

Every reasonable effort has been made to acknowledge the owners of copyright material. I would be pleased to hear from any copyright owner who has been omitted or incorrectly acknowledged.

Christopher E. Ndehedehe

Appendix A Copyright permission statements

This is a confirmation that I have obtained, where necessary, permission from the copyright owners to use any third party copyright material reproduced in the thesis (e.g., unpublished letters), or to use any of my own published/accepted work (e.g., journal articles) in which the copyright is held by another party (e.g. publisher, co-author). These permissions, are all attached and exclude [Ndehedehe et al. \(2017c\)](#), of which permission to reuse is not required as it is an open access article published under the terms of the Creative Commons Attribution-Non Commercial-No Derivatives License (CC BY NC ND, <http://creativecommons.org/licenses/BY-NC-ND/4.0/>).

Christopher E. Ndehedehe
Department of Spatial Sciences
Curtin University, Bentley,
Western Australia,
Australia

**ELSEVIER LICENSE
TERMS AND CONDITIONS**

Jun 19, 2017

This Agreement between Mr. Christopher Ndehedehe ("You") and Elsevier ("Elsevier") consists of your license details and the terms and conditions provided by Elsevier and Copyright Clearance Center.

License Number	4132031037304
License date	Jun 18, 2017
Licensed Content Publisher	Elsevier
Licensed Content Publication	Advances in Water Resources
Licensed Content Title	Understanding changes in terrestrial water storage over West Africa between 2002 and 2014
Licensed Content Author	Christopher Ndehedehe, Joseph Awange, Nathan Agutu, Michael Kuhn, Bernhard Heck
Licensed Content Date	Feb 1, 2016
Licensed Content Volume	88
Licensed Content Issue	n/a
Licensed Content Pages	20
Start Page	211
End Page	230
Type of Use	reuse in a thesis/dissertation
Portion	full article
Format	both print and electronic
Are you the author of this Elsevier article?	Yes
Will you be translating?	No
Order reference number	
Title of your thesis/dissertation	Remote Sensing of West Africa's Water Resources Using Multi-Satellites and Models
Expected completion date	Aug 2017
Estimated size (number of pages)	270
Elsevier VAT number	GB 494 6272 12
Requestor Location	Mr. Christopher Ndehedehe Department of Spatial Sciences Curtin University Kent Street, Bentley Perth, Western Australia 6102 Australia Attn: Mr. Christopher Ndehedehe

INTRODUCTION

1. The publisher for this copyrighted material is Elsevier. By clicking "accept" in connection with completing this licensing transaction, you agree that the following terms and conditions apply to this transaction (along with the Billing and Payment terms and conditions established by Copyright Clearance Center, Inc. ("CCC"), at the time that you opened your Rightslink account and that are available at any time at <http://myaccount.copyright.com>).

GENERAL TERMS

2. Elsevier hereby grants you permission to reproduce the aforementioned material subject to the terms and conditions indicated.

3. Acknowledgement: If any part of the material to be used (for example, figures) has appeared in our publication with credit or acknowledgement to another source, permission must also be sought from that source. If such permission is not obtained then that material may not be included in your publication/copies. Suitable acknowledgement to the source must be made, either as a footnote or in a reference list at the end of your publication, as follows:

"Reprinted from Publication title, Vol /edition number, Author(s), Title of article / title of chapter, Pages No., Copyright (Year), with permission from Elsevier [OR APPLICABLE SOCIETY COPYRIGHT OWNER]." Also Lancet special credit - "Reprinted from The Lancet, Vol. number, Author(s), Title of article, Pages No., Copyright (Year), with permission from Elsevier."

4. Reproduction of this material is confined to the purpose and/or media for which permission is hereby given.

5. Altering/Modifying Material: Not Permitted. However figures and illustrations may be altered/adapted minimally to serve your work. Any other abbreviations, additions, deletions and/or any other alterations shall be made only with prior written authorization of Elsevier Ltd. (Please contact Elsevier at permissions@elsevier.com). No modifications can be made to any Lancet figures/tables and they must be reproduced in full.

6. If the permission fee for the requested use of our material is waived in this instance, please be advised that your future requests for Elsevier materials may attract a fee.

7. Reservation of Rights: Publisher reserves all rights not specifically granted in the combination of (i) the license details provided by you and accepted in the course of this licensing transaction, (ii) these terms and conditions and (iii) CCC's Billing and Payment terms and conditions.

8. License Contingent Upon Payment: While you may exercise the rights licensed immediately upon issuance of the license at the end of the licensing process for the transaction, provided that you have disclosed complete and accurate details of your proposed use, no license is finally effective unless and until full payment is received from you (either by publisher or by CCC) as provided in CCC's Billing and Payment terms and conditions. If full payment is not received on a timely basis, then any license preliminarily granted shall be deemed automatically revoked and shall be void as if never granted. Further, in the event that you breach any of these terms and conditions or any of CCC's Billing and Payment terms and conditions, the license is automatically revoked and shall be void as if never granted. Use of materials as described in a revoked license, as well as any use of the materials beyond the scope of an unrevoked license, may constitute copyright infringement and publisher reserves the right to take any and all action to protect its copyright in the materials.

9. **Warranties:** Publisher makes no representations or warranties with respect to the licensed material.

10. **Indemnity:** You hereby indemnify and agree to hold harmless publisher and CCC, and their respective officers, directors, employees and agents, from and against any and all claims arising out of your use of the licensed material other than as specifically authorized pursuant to this license.

11. **No Transfer of License:** This license is personal to you and may not be sublicensed, assigned, or transferred by you to any other person without publisher's written permission.

12. **No Amendment Except in Writing:** This license may not be amended except in a writing signed by both parties (or, in the case of publisher, by CCC on publisher's behalf).

13. **Objection to Contrary Terms:** Publisher hereby objects to any terms contained in any purchase order, acknowledgment, check endorsement or other writing prepared by you, which terms are inconsistent with these terms and conditions or CCC's Billing and Payment terms and conditions. These terms and conditions, together with CCC's Billing and Payment terms and conditions (which are incorporated herein), comprise the entire agreement between you and publisher (and CCC) concerning this licensing transaction. In the event of any conflict between your obligations established by these terms and conditions and those established by CCC's Billing and Payment terms and conditions, these terms and conditions shall control.

14. **Revocation:** Elsevier or Copyright Clearance Center may deny the permissions described in this License at their sole discretion, for any reason or no reason, with a full refund payable to you. Notice of such denial will be made using the contact information provided by you. Failure to receive such notice will not alter or invalidate the denial. In no event will Elsevier or Copyright Clearance Center be responsible or liable for any costs, expenses or damage incurred by you as a result of a denial of your permission request, other than a refund of the amount(s) paid by you to Elsevier and/or Copyright Clearance Center for denied permissions.

LIMITED LICENSE

The following terms and conditions apply only to specific license types:

15. **Translation:** This permission is granted for non-exclusive world **English** rights only unless your license was granted for translation rights. If you licensed translation rights you may only translate this content into the languages you requested. A professional translator must perform all translations and reproduce the content word for word preserving the integrity of the article.

16. **Posting licensed content on any Website:** The following terms and conditions apply as follows: Licensing material from an Elsevier journal: All content posted to the web site must maintain the copyright information line on the bottom of each image; A hyper-text must be included to the Homepage of the journal from which you are licensing at <http://www.sciencedirect.com/science/journal/xxxxx> or the Elsevier homepage for books at <http://www.elsevier.com>; Central Storage: This license does not include permission for a scanned version of the material to be stored in a central repository such as that provided by Heron/XanEdu.

Licensing material from an Elsevier book: A hyper-text link must be included to the Elsevier homepage at <http://www.elsevier.com>. All content posted to the web site must maintain the copyright information line on the bottom of each image.

Posting licensed content on Electronic reserve: In addition to the above the following clauses are applicable: The web site must be password-protected and made available only to bona fide students registered on a relevant course. This permission is granted for 1 year only. You may obtain a new license for future website posting.

17. **For journal authors:** the following clauses are applicable in addition to the above:

Preprints:

A preprint is an author's own write-up of research results and analysis, it has not been peer-reviewed, nor has it had any other value added to it by a publisher (such as formatting, copyright, technical enhancement etc.).

Authors can share their preprints anywhere at any time. Preprints should not be added to or enhanced in any way in order to appear more like, or to substitute for, the final versions of articles however authors can update their preprints on arXiv or RePEc with their Accepted Author Manuscript (see below).

If accepted for publication, we encourage authors to link from the preprint to their formal publication via its DOI. Millions of researchers have access to the formal publications on ScienceDirect, and so links will help users to find, access, cite and use the best available version. Please note that Cell Press, The Lancet and some society-owned have different preprint policies. Information on these policies is available on the journal homepage.

Accepted Author Manuscripts: An accepted author manuscript is the manuscript of an article that has been accepted for publication and which typically includes author-incorporated changes suggested during submission, peer review and editor-author communications.

Authors can share their accepted author manuscript:

- immediately
 - via their non-commercial person homepage or blog
 - by updating a preprint in arXiv or RePEc with the accepted manuscript
 - via their research institute or institutional repository for internal institutional uses or as part of an invitation-only research collaboration work-group
 - directly by providing copies to their students or to research collaborators for their personal use
 - for private scholarly sharing as part of an invitation-only work group on commercial sites with which Elsevier has an agreement
- After the embargo period
 - via non-commercial hosting platforms such as their institutional repository
 - via commercial sites with which Elsevier has an agreement

In all cases accepted manuscripts should:

- link to the formal publication via its DOI
- bear a CC-BY-NC-ND license - this is easy to do
- if aggregated with other manuscripts, for example in a repository or other site, be shared in alignment with our hosting policy not be added to or enhanced in any way to appear more like, or to substitute for, the published journal article.

Published journal article (JPA): A published journal article (PJA) is the definitive final record of published research that appears or will appear in the journal and embodies all value-adding publishing activities including peer review co-ordination, copy-editing, formatting, (if relevant) pagination and online enrichment.

Policies for sharing publishing journal articles differ for subscription and gold open access articles:

Subscription Articles: If you are an author, please share a link to your article rather than the full-text. Millions of researchers have access to the formal publications on ScienceDirect, and so links will help your users to find, access, cite, and use the best

available version.

Theses and dissertations which contain embedded PJAs as part of the formal submission can be posted publicly by the awarding institution with DOI links back to the formal publications on ScienceDirect.

If you are affiliated with a library that subscribes to ScienceDirect you have additional private sharing rights for others' research accessed under that agreement. This includes use for classroom teaching and internal training at the institution (including use in course packs and courseware programs), and inclusion of the article for grant funding purposes.

Gold Open Access Articles: May be shared according to the author-selected end-user license and should contain a [CrossMark logo](#), the end user license, and a DOI link to the formal publication on ScienceDirect.

Please refer to Elsevier's [posting policy](#) for further information.

18. **For book authors** the following clauses are applicable in addition to the above: Authors are permitted to place a brief summary of their work online only. You are not allowed to download and post the published electronic version of your chapter, nor may you scan the printed edition to create an electronic version. **Posting to a repository:** Authors are permitted to post a summary of their chapter only in their institution's repository.

19. **Thesis/Dissertation:** If your license is for use in a thesis/dissertation your thesis may be submitted to your institution in either print or electronic form. Should your thesis be published commercially, please reapply for permission. These requirements include permission for the Library and Archives of Canada to supply single copies, on demand, of the complete thesis and include permission for Proquest/UMI to supply single copies, on demand, of the complete thesis. Should your thesis be published commercially, please reapply for permission. Theses and dissertations which contain embedded PJAs as part of the formal submission can be posted publicly by the awarding institution with DOI links back to the formal publications on ScienceDirect.

Elsevier Open Access Terms and Conditions

You can publish open access with Elsevier in hundreds of open access journals or in nearly 2000 established subscription journals that support open access publishing. Permitted third party re-use of these open access articles is defined by the author's choice of Creative Commons user license. See our [open access license policy](#) for more information.

Terms & Conditions applicable to all Open Access articles published with Elsevier:

Any reuse of the article must not represent the author as endorsing the adaptation of the article nor should the article be modified in such a way as to damage the author's honour or reputation. If any changes have been made, such changes must be clearly indicated. The author(s) must be appropriately credited and we ask that you include the end user license and a DOI link to the formal publication on ScienceDirect.

If any part of the material to be used (for example, figures) has appeared in our publication with credit or acknowledgement to another source it is the responsibility of the user to ensure their reuse complies with the terms and conditions determined by the rights holder.

Additional Terms & Conditions applicable to each Creative Commons user license:

CC BY: The CC-BY license allows users to copy, to create extracts, abstracts and new works from the Article, to alter and revise the Article and to make commercial use of the Article (including reuse and/or resale of the Article by commercial entities), provided the user gives appropriate credit (with a link to the formal publication through the relevant DOI), provides a link to the license, indicates if changes were made and the licensor is not

represented as endorsing the use made of the work. The full details of the license are available at <http://creativecommons.org/licenses/by/4.0>.

CC BY NC SA: The CC BY-NC-SA license allows users to copy, to create extracts, abstracts and new works from the Article, to alter and revise the Article, provided this is not done for commercial purposes, and that the user gives appropriate credit (with a link to the formal publication through the relevant DOI), provides a link to the license, indicates if changes were made and the licensor is not represented as endorsing the use made of the work. Further, any new works must be made available on the same conditions. The full details of the license are available at <http://creativecommons.org/licenses/by-nc-sa/4.0>.

CC BY NC ND: The CC BY-NC-ND license allows users to copy and distribute the Article, provided this is not done for commercial purposes and further does not permit distribution of the Article if it is changed or edited in any way, and provided the user gives appropriate credit (with a link to the formal publication through the relevant DOI), provides a link to the license, and that the licensor is not represented as endorsing the use made of the work. The full details of the license are available at <http://creativecommons.org/licenses/by-nc-nd/4.0>. Any commercial reuse of Open Access articles published with a CC BY NC SA or CC BY NC ND license requires permission from Elsevier and will be subject to a fee.

Commercial reuse includes:

- Associating advertising with the full text of the Article
- Charging fees for document delivery or access
- Article aggregation
- Systematic distribution via e-mail lists or share buttons

Posting or linking by commercial companies for use by customers of those companies.

20. Other Conditions:

v1.9

Questions? customercare@copyright.com or +1-855-239-3415 (toll free in the US) or +1-978-646-2777.

**JOHN WILEY AND SONS LICENSE
TERMS AND CONDITIONS**

Jun 19, 2017

This Agreement between Mr. Christopher Ndehedehe ("You") and John Wiley and Sons ("John Wiley and Sons") consists of your license details and the terms and conditions provided by John Wiley and Sons and Copyright Clearance Center.

License Number	4132370127574
License date	Jun 19, 2017
Licensed Content Publisher	John Wiley and Sons
Licensed Content Publication	International Journal of Climatology
Licensed Content Title	An investigation into the freshwater variability in West Africa during 1979-2010
Licensed Content Author	S. A. Andam-Akorful, V. G. Ferreira, C. E. Ndehedehe, J. A. Quaye-Ballard
Licensed Content Date	Feb 14, 2017
Licensed Content Pages	1
Type of use	Dissertation/Thesis
Requestor type	Author of this Wiley article
Format	Print and electronic
Portion	Full article
Will you be translating?	No
Title of your thesis / dissertation	Remote Sensing of West Africa's Water Resources Using Multi-Satellites and Models
Expected completion date	Aug 2017
Expected size (number of pages)	270
Requestor Location	Mr. Christopher Ndehedehe Department of Spatial Sciences Curtin University Kent Street, Bentley Perth, Western Australia 6102 Australia Attn: Mr. Christopher Ndehedehe
Publisher Tax ID	EU826007151
Billing Type	Invoice
Billing Address	Mr. Christopher Ndehedehe Department of Spatial Sciences Curtin University Kent Street, Bentley Perth, Australia 6102 Attn: Mr. Christopher Ndehedehe
Total	0.00 AUD
Terms and Conditions	

TERMS AND CONDITIONS

This copyrighted material is owned by or exclusively licensed to John Wiley & Sons, Inc. or one of its group companies (each a "Wiley Company") or handled on behalf of a society with which a Wiley Company has exclusive publishing rights in relation to a particular work (collectively "WILEY"). By clicking "accept" in connection with completing this licensing transaction, you agree that the following terms and conditions apply to this transaction (along with the billing and payment terms and conditions established by the Copyright Clearance Center Inc., ("CCC's Billing and Payment terms and conditions"), at the time that you opened your RightsLink account (these are available at any time at <http://myaccount.copyright.com>).

Terms and Conditions

- The materials you have requested permission to reproduce or reuse (the "Wiley Materials") are protected by copyright.
- You are hereby granted a personal, non-exclusive, non-sub licensable (on a stand-alone basis), non-transferable, worldwide, limited license to reproduce the Wiley Materials for the purpose specified in the licensing process. This license, **and any CONTENT (PDF or image file) purchased as part of your order**, is for a one-time use only and limited to any maximum distribution number specified in the license. The first instance of republication or reuse granted by this license must be completed within two years of the date of the grant of this license (although copies prepared before the end date may be distributed thereafter). The Wiley Materials shall not be used in any other manner or for any other purpose, beyond what is granted in the license. Permission is granted subject to an appropriate acknowledgement given to the author, title of the material/book/journal and the publisher. You shall also duplicate the copyright notice that appears in the Wiley publication in your use of the Wiley Material. Permission is also granted on the understanding that nowhere in the text is a previously published source acknowledged for all or part of this Wiley Material. Any third party content is expressly excluded from this permission.
- With respect to the Wiley Materials, all rights are reserved. Except as expressly granted by the terms of the license, no part of the Wiley Materials may be copied, modified, adapted (except for minor reformatting required by the new Publication), translated, reproduced, transferred or distributed, in any form or by any means, and no derivative works may be made based on the Wiley Materials without the prior permission of the respective copyright owner. **For STM Signatory Publishers clearing permission under the terms of the [STM Permissions Guidelines](#) only, the terms of the license are extended to include subsequent editions and for editions in other languages, provided such editions are for the work as a whole in situ and does not involve the separate exploitation of the permitted figures or extracts**, You may not alter, remove or suppress in any manner any copyright, trademark or other notices displayed by the Wiley Materials. You may not license, rent, sell, loan, lease, pledge, offer as security, transfer or assign the Wiley Materials on a stand-alone basis, or any of the rights granted to you hereunder to any other person.
- The Wiley Materials and all of the intellectual property rights therein shall at all

times remain the exclusive property of John Wiley & Sons Inc, the Wiley Companies, or their respective licensors, and your interest therein is only that of having possession of and the right to reproduce the Wiley Materials pursuant to Section 2 herein during the continuance of this Agreement. You agree that you own no right, title or interest in or to the Wiley Materials or any of the intellectual property rights therein. You shall have no rights hereunder other than the license as provided for above in Section 2. No right, license or interest to any trademark, trade name, service mark or other branding ("Marks") of WILEY or its licensors is granted hereunder, and you agree that you shall not assert any such right, license or interest with respect thereto

- NEITHER WILEY NOR ITS LICENSORS MAKES ANY WARRANTY OR REPRESENTATION OF ANY KIND TO YOU OR ANY THIRD PARTY, EXPRESS, IMPLIED OR STATUTORY, WITH RESPECT TO THE MATERIALS OR THE ACCURACY OF ANY INFORMATION CONTAINED IN THE MATERIALS, INCLUDING, WITHOUT LIMITATION, ANY IMPLIED WARRANTY OF MERCHANTABILITY, ACCURACY, SATISFACTORY QUALITY, FITNESS FOR A PARTICULAR PURPOSE, USABILITY, INTEGRATION OR NON-INFRINGEMENT AND ALL SUCH WARRANTIES ARE HEREBY EXCLUDED BY WILEY AND ITS LICENSORS AND WAIVED BY YOU.
- WILEY shall have the right to terminate this Agreement immediately upon breach of this Agreement by you.
- You shall indemnify, defend and hold harmless WILEY, its Licensors and their respective directors, officers, agents and employees, from and against any actual or threatened claims, demands, causes of action or proceedings arising from any breach of this Agreement by you.
- IN NO EVENT SHALL WILEY OR ITS LICENSORS BE LIABLE TO YOU OR ANY OTHER PARTY OR ANY OTHER PERSON OR ENTITY FOR ANY SPECIAL, CONSEQUENTIAL, INCIDENTAL, INDIRECT, EXEMPLARY OR PUNITIVE DAMAGES, HOWEVER CAUSED, ARISING OUT OF OR IN CONNECTION WITH THE DOWNLOADING, PROVISIONING, VIEWING OR USE OF THE MATERIALS REGARDLESS OF THE FORM OF ACTION, WHETHER FOR BREACH OF CONTRACT, BREACH OF WARRANTY, TORT, NEGLIGENCE, INFRINGEMENT OR OTHERWISE (INCLUDING, WITHOUT LIMITATION, DAMAGES BASED ON LOSS OF PROFITS, DATA, FILES, USE, BUSINESS OPPORTUNITY OR CLAIMS OF THIRD PARTIES), AND WHETHER OR NOT THE PARTY HAS BEEN ADVISED OF THE POSSIBILITY OF SUCH DAMAGES. THIS LIMITATION SHALL APPLY NOTWITHSTANDING ANY FAILURE OF ESSENTIAL PURPOSE OF ANY LIMITED REMEDY PROVIDED HEREIN.
- Should any provision of this Agreement be held by a court of competent jurisdiction to be illegal, invalid, or unenforceable, that provision shall be deemed amended to achieve as nearly as possible the same economic effect as the original provision, and the legality, validity and enforceability of the remaining provisions

of this Agreement shall not be affected or impaired thereby.

- The failure of either party to enforce any term or condition of this Agreement shall not constitute a waiver of either party's right to enforce each and every term and condition of this Agreement. No breach under this agreement shall be deemed waived or excused by either party unless such waiver or consent is in writing signed by the party granting such waiver or consent. The waiver by or consent of a party to a breach of any provision of this Agreement shall not operate or be construed as a waiver of or consent to any other or subsequent breach by such other party.
- This Agreement may not be assigned (including by operation of law or otherwise) by you without WILEY's prior written consent.
- Any fee required for this permission shall be non-refundable after thirty (30) days from receipt by the CCC.
- These terms and conditions together with CCC's Billing and Payment terms and conditions (which are incorporated herein) form the entire agreement between you and WILEY concerning this licensing transaction and (in the absence of fraud) supersedes all prior agreements and representations of the parties, oral or written. This Agreement may not be amended except in writing signed by both parties. This Agreement shall be binding upon and inure to the benefit of the parties' successors, legal representatives, and authorized assigns.
- In the event of any conflict between your obligations established by these terms and conditions and those established by CCC's Billing and Payment terms and conditions, these terms and conditions shall prevail.
- WILEY expressly reserves all rights not specifically granted in the combination of (i) the license details provided by you and accepted in the course of this licensing transaction, (ii) these terms and conditions and (iii) CCC's Billing and Payment terms and conditions.
- This Agreement will be void if the Type of Use, Format, Circulation, or Requestor Type was misrepresented during the licensing process.
- This Agreement shall be governed by and construed in accordance with the laws of the State of New York, USA, without regards to such state's conflict of law rules. Any legal action, suit or proceeding arising out of or relating to these Terms and Conditions or the breach thereof shall be instituted in a court of competent jurisdiction in New York County in the State of New York in the United States of America and each party hereby consents and submits to the personal jurisdiction of such court, waives any objection to venue in such court and consents to service of process by registered or certified mail, return receipt requested, at the last known address of such party.

WILEY OPEN ACCESS TERMS AND CONDITIONS

Wiley Publishes Open Access Articles in fully Open Access Journals and in Subscription journals offering Online Open. Although most of the fully Open Access journals publish open access articles under the terms of the Creative Commons Attribution (CC BY)

License only, the subscription journals and a few of the Open Access Journals offer a choice of Creative Commons Licenses. The license type is clearly identified on the article.

The Creative Commons Attribution License

The [Creative Commons Attribution License \(CC-BY\)](#) allows users to copy, distribute and transmit an article, adapt the article and make commercial use of the article. The CC-BY license permits commercial and non-

Creative Commons Attribution Non-Commercial License

The [Creative Commons Attribution Non-Commercial \(CC-BY-NC\)License](#) permits use, distribution and reproduction in any medium, provided the original work is properly cited and is not used for commercial purposes.(see below)

Creative Commons Attribution-Non-Commercial-NoDerivs License

The [Creative Commons Attribution Non-Commercial-NoDerivs License](#) (CC-BY-NC-ND) permits use, distribution and reproduction in any medium, provided the original work is properly cited, is not used for commercial purposes and no modifications or adaptations are made. (see below)

Use by commercial "for-profit" organizations

Use of Wiley Open Access articles for commercial, promotional, or marketing purposes requires further explicit permission from Wiley and will be subject to a fee.

Further details can be found on Wiley Online

Library <http://olabout.wiley.com/WileyCDA/Section/id-410895.html>

Other Terms and Conditions:

v1.10 Last updated September 2015

Questions? customercare@copyright.com or +1-855-239-3415 (toll free in the US) or +1-978-646-2777.

**ELSEVIER LICENSE
TERMS AND CONDITIONS**

Jun 19, 2017

This Agreement between Mr. Christopher Ndehedehe ("You") and Elsevier ("Elsevier") consists of your license details and the terms and conditions provided by Elsevier and Copyright Clearance Center.

License Number	4132031397751
License date	Jun 18, 2017
Licensed Content Publisher	Elsevier
Licensed Content Publication	Journal of Hydrology
Licensed Content Title	Spatio-temporal variability of droughts and terrestrial water storage over Lake Chad Basin using independent component analysis
Licensed Content Author	Christopher E. Ndehedehe, Nathan O. Agutu, Onuwa Okwuashi, Vagner G. Ferreira
Licensed Content Date	Sep 1, 2016
Licensed Content Volume	540
Licensed Content Issue	n/a
Licensed Content Pages	23
Start Page	106
End Page	128
Type of Use	reuse in a thesis/dissertation
Portion	full article
Format	both print and electronic
Are you the author of this Elsevier article?	Yes
Will you be translating?	No
Order reference number	
Title of your thesis/dissertation	Remote Sensing of West Africa's Water Resources Using Multi-Satellites and Models
Expected completion date	Aug 2017
Estimated size (number of pages)	270
Elsevier VAT number	GB 494 6272 12
Requestor Location	Mr. Christopher Ndehedehe Department of Spatial Sciences Curtin University Kent Street, Bentley Perth, Western Australia 6102 Australia Attn: Mr. Christopher Ndehedehe
Total	0.00 AUD

INTRODUCTION

1. The publisher for this copyrighted material is Elsevier. By clicking "accept" in connection with completing this licensing transaction, you agree that the following terms and conditions apply to this transaction (along with the Billing and Payment terms and conditions established by Copyright Clearance Center, Inc. ("CCC"), at the time that you opened your Rightslink account and that are available at any time at <http://myaccount.copyright.com>).

GENERAL TERMS

2. Elsevier hereby grants you permission to reproduce the aforementioned material subject to the terms and conditions indicated.

3. Acknowledgement: If any part of the material to be used (for example, figures) has appeared in our publication with credit or acknowledgement to another source, permission must also be sought from that source. If such permission is not obtained then that material may not be included in your publication/copies. Suitable acknowledgement to the source must be made, either as a footnote or in a reference list at the end of your publication, as follows:

"Reprinted from Publication title, Vol /edition number, Author(s), Title of article / title of chapter, Pages No., Copyright (Year), with permission from Elsevier [OR APPLICABLE SOCIETY COPYRIGHT OWNER]." Also Lancet special credit - "Reprinted from The Lancet, Vol. number, Author(s), Title of article, Pages No., Copyright (Year), with permission from Elsevier."

4. Reproduction of this material is confined to the purpose and/or media for which permission is hereby given.

5. Altering/Modifying Material: Not Permitted. However figures and illustrations may be altered/adapted minimally to serve your work. Any other abbreviations, additions, deletions and/or any other alterations shall be made only with prior written authorization of Elsevier Ltd. (Please contact Elsevier at permissions@elsevier.com). No modifications can be made to any Lancet figures/tables and they must be reproduced in full.

6. If the permission fee for the requested use of our material is waived in this instance, please be advised that your future requests for Elsevier materials may attract a fee.

7. Reservation of Rights: Publisher reserves all rights not specifically granted in the combination of (i) the license details provided by you and accepted in the course of this licensing transaction, (ii) these terms and conditions and (iii) CCC's Billing and Payment terms and conditions.

8. License Contingent Upon Payment: While you may exercise the rights licensed immediately upon issuance of the license at the end of the licensing process for the transaction, provided that you have disclosed complete and accurate details of your proposed use, no license is finally effective unless and until full payment is received from you (either by publisher or by CCC) as provided in CCC's Billing and Payment terms and conditions. If full payment is not received on a timely basis, then any license preliminarily granted shall be deemed automatically revoked and shall be void as if never granted. Further, in the event that you breach any of these terms and conditions or any of CCC's Billing and Payment terms and conditions, the license is automatically revoked and shall be void as if never granted. Use of materials as described in a revoked license, as well as any use of the materials beyond the scope of an unrevoked license, may constitute copyright infringement and publisher reserves the right to take any and all action to protect its copyright in the materials.

9. Warranties: Publisher makes no representations or warranties with respect to the

licensed material.

10. **Indemnity:** You hereby indemnify and agree to hold harmless publisher and CCC, and their respective officers, directors, employees and agents, from and against any and all claims arising out of your use of the licensed material other than as specifically authorized pursuant to this license.

11. **No Transfer of License:** This license is personal to you and may not be sublicensed, assigned, or transferred by you to any other person without publisher's written permission.

12. **No Amendment Except in Writing:** This license may not be amended except in a writing signed by both parties (or, in the case of publisher, by CCC on publisher's behalf).

13. **Objection to Contrary Terms:** Publisher hereby objects to any terms contained in any purchase order, acknowledgment, check endorsement or other writing prepared by you, which terms are inconsistent with these terms and conditions or CCC's Billing and Payment terms and conditions. These terms and conditions, together with CCC's Billing and Payment terms and conditions (which are incorporated herein), comprise the entire agreement between you and publisher (and CCC) concerning this licensing transaction. In the event of any conflict between your obligations established by these terms and conditions and those established by CCC's Billing and Payment terms and conditions, these terms and conditions shall control.

14. **Revocation:** Elsevier or Copyright Clearance Center may deny the permissions described in this License at their sole discretion, for any reason or no reason, with a full refund payable to you. Notice of such denial will be made using the contact information provided by you. Failure to receive such notice will not alter or invalidate the denial. In no event will Elsevier or Copyright Clearance Center be responsible or liable for any costs, expenses or damage incurred by you as a result of a denial of your permission request, other than a refund of the amount(s) paid by you to Elsevier and/or Copyright Clearance Center for denied permissions.

LIMITED LICENSE

The following terms and conditions apply only to specific license types:

15. **Translation:** This permission is granted for non-exclusive world **English** rights only unless your license was granted for translation rights. If you licensed translation rights you may only translate this content into the languages you requested. A professional translator must perform all translations and reproduce the content word for word preserving the integrity of the article.

16. **Posting licensed content on any Website:** The following terms and conditions apply as follows: Licensing material from an Elsevier journal: All content posted to the web site must maintain the copyright information line on the bottom of each image; A hyper-text must be included to the Homepage of the journal from which you are licensing at <http://www.sciencedirect.com/science/journal/xxxxx> or the Elsevier homepage for books at <http://www.elsevier.com>; Central Storage: This license does not include permission for a scanned version of the material to be stored in a central repository such as that provided by Heron/XanEdu.

Licensing material from an Elsevier book: A hyper-text link must be included to the Elsevier homepage at <http://www.elsevier.com>. All content posted to the web site must maintain the copyright information line on the bottom of each image.

Posting licensed content on Electronic reserve: In addition to the above the following clauses are applicable: The web site must be password-protected and made available only to bona fide students registered on a relevant course. This permission is granted for 1 year only. You may obtain a new license for future website posting.

17. **For journal authors:** the following clauses are applicable in addition to the above:

Preprints:

A preprint is an author's own write-up of research results and analysis, it has not been peer-reviewed, nor has it had any other value added to it by a publisher (such as formatting, copyright, technical enhancement etc.).

Authors can share their preprints anywhere at any time. Preprints should not be added to or enhanced in any way in order to appear more like, or to substitute for, the final versions of articles however authors can update their preprints on arXiv or RePEc with their Accepted Author Manuscript (see below).

If accepted for publication, we encourage authors to link from the preprint to their formal publication via its DOI. Millions of researchers have access to the formal publications on ScienceDirect, and so links will help users to find, access, cite and use the best available version. Please note that Cell Press, The Lancet and some society-owned have different preprint policies. Information on these policies is available on the journal homepage.

Accepted Author Manuscripts: An accepted author manuscript is the manuscript of an article that has been accepted for publication and which typically includes author-incorporated changes suggested during submission, peer review and editor-author communications.

Authors can share their accepted author manuscript:

- immediately
 - via their non-commercial person homepage or blog
 - by updating a preprint in arXiv or RePEc with the accepted manuscript
 - via their research institute or institutional repository for internal institutional uses or as part of an invitation-only research collaboration work-group
 - directly by providing copies to their students or to research collaborators for their personal use
 - for private scholarly sharing as part of an invitation-only work group on commercial sites with which Elsevier has an agreement
- After the embargo period
 - via non-commercial hosting platforms such as their institutional repository
 - via commercial sites with which Elsevier has an agreement

In all cases accepted manuscripts should:

- link to the formal publication via its DOI
- bear a CC-BY-NC-ND license - this is easy to do
- if aggregated with other manuscripts, for example in a repository or other site, be shared in alignment with our hosting policy not be added to or enhanced in any way to appear more like, or to substitute for, the published journal article.

Published journal article (JPA): A published journal article (PJA) is the definitive final record of published research that appears or will appear in the journal and embodies all value-adding publishing activities including peer review co-ordination, copy-editing, formatting, (if relevant) pagination and online enrichment.

Policies for sharing publishing journal articles differ for subscription and gold open access articles:

Subscription Articles: If you are an author, please share a link to your article rather than the full-text. Millions of researchers have access to the formal publications on ScienceDirect, and so links will help your users to find, access, cite, and use the best

available version.

Theses and dissertations which contain embedded PJAs as part of the formal submission can be posted publicly by the awarding institution with DOI links back to the formal publications on ScienceDirect.

If you are affiliated with a library that subscribes to ScienceDirect you have additional private sharing rights for others' research accessed under that agreement. This includes use for classroom teaching and internal training at the institution (including use in course packs and courseware programs), and inclusion of the article for grant funding purposes.

Gold Open Access Articles: May be shared according to the author-selected end-user license and should contain a [CrossMark logo](#), the end user license, and a DOI link to the formal publication on ScienceDirect.

Please refer to Elsevier's [posting policy](#) for further information.

18. **For book authors** the following clauses are applicable in addition to the above: Authors are permitted to place a brief summary of their work online only. You are not allowed to download and post the published electronic version of your chapter, nor may you scan the printed edition to create an electronic version. **Posting to a repository:** Authors are permitted to post a summary of their chapter only in their institution's repository.

19. **Thesis/Dissertation:** If your license is for use in a thesis/dissertation your thesis may be submitted to your institution in either print or electronic form. Should your thesis be published commercially, please reapply for permission. These requirements include permission for the Library and Archives of Canada to supply single copies, on demand, of the complete thesis and include permission for Proquest/UMI to supply single copies, on demand, of the complete thesis. Should your thesis be published commercially, please reapply for permission. Theses and dissertations which contain embedded PJAs as part of the formal submission can be posted publicly by the awarding institution with DOI links back to the formal publications on ScienceDirect.

Elsevier Open Access Terms and Conditions

You can publish open access with Elsevier in hundreds of open access journals or in nearly 2000 established subscription journals that support open access publishing. Permitted third party re-use of these open access articles is defined by the author's choice of Creative Commons user license. See our [open access license policy](#) for more information.

Terms & Conditions applicable to all Open Access articles published with Elsevier:

Any reuse of the article must not represent the author as endorsing the adaptation of the article nor should the article be modified in such a way as to damage the author's honour or reputation. If any changes have been made, such changes must be clearly indicated. The author(s) must be appropriately credited and we ask that you include the end user license and a DOI link to the formal publication on ScienceDirect.

If any part of the material to be used (for example, figures) has appeared in our publication with credit or acknowledgement to another source it is the responsibility of the user to ensure their reuse complies with the terms and conditions determined by the rights holder.

Additional Terms & Conditions applicable to each Creative Commons user license:

CC BY: The CC-BY license allows users to copy, to create extracts, abstracts and new works from the Article, to alter and revise the Article and to make commercial use of the Article (including reuse and/or resale of the Article by commercial entities), provided the user gives appropriate credit (with a link to the formal publication through the relevant DOI), provides a link to the license, indicates if changes were made and the licensor is not

represented as endorsing the use made of the work. The full details of the license are available at <http://creativecommons.org/licenses/by/4.0>.

CC BY NC SA: The CC BY-NC-SA license allows users to copy, to create extracts, abstracts and new works from the Article, to alter and revise the Article, provided this is not done for commercial purposes, and that the user gives appropriate credit (with a link to the formal publication through the relevant DOI), provides a link to the license, indicates if changes were made and the licensor is not represented as endorsing the use made of the work. Further, any new works must be made available on the same conditions. The full details of the license are available at <http://creativecommons.org/licenses/by-nc-sa/4.0>.

CC BY NC ND: The CC BY-NC-ND license allows users to copy and distribute the Article, provided this is not done for commercial purposes and further does not permit distribution of the Article if it is changed or edited in any way, and provided the user gives appropriate credit (with a link to the formal publication through the relevant DOI), provides a link to the license, and that the licensor is not represented as endorsing the use made of the work. The full details of the license are available at <http://creativecommons.org/licenses/by-nc-nd/4.0>. Any commercial reuse of Open Access articles published with a CC BY NC SA or CC BY NC ND license requires permission from Elsevier and will be subject to a fee.

Commercial reuse includes:

- Associating advertising with the full text of the Article
- Charging fees for document delivery or access
- Article aggregation
- Systematic distribution via e-mail lists or share buttons

Posting or linking by commercial companies for use by customers of those companies.

20. Other Conditions:

v1.9

Questions? customer care@copyright.com or +1-855-239-3415 (toll free in the US) or +1-978-646-2777.

**ELSEVIER LICENSE
TERMS AND CONDITIONS**

Jun 19, 2017

This Agreement between Mr. Christopher Ndehedehe ("You") and Elsevier ("Elsevier") consists of your license details and the terms and conditions provided by Elsevier and Copyright Clearance Center.

License Number	4132030452922
License date	Jun 18, 2017
Licensed Content Publisher	Elsevier
Licensed Content Publication	Science of The Total Environment
Licensed Content Title	On the potentials of multiple climate variables in assessing the spatio-temporal characteristics of hydrological droughts over the Volta Basin
Licensed Content Author	Christopher E. Ndehedehe, Joseph L. Awange, Robert J. Corner, Michael Kuhn, Onuwa Okwuashi
Licensed Content Date	Jul 1, 2016
Licensed Content Volume	557
Licensed Content Issue	n/a
Licensed Content Pages	19
Start Page	819
End Page	837
Type of Use	reuse in a thesis/dissertation
Portion	full article
Format	electronic
Are you the author of this Elsevier article?	Yes
Will you be translating?	No
Order reference number	
Title of your thesis/dissertation	Remote Sensing of West Africa's Water Resources Using Multi-Satellites and Models
Expected completion date	Aug 2017
Estimated size (number of pages)	270
Elsevier VAT number	GB 494 6272 12
Requestor Location	Mr. Christopher Ndehedehe Department of Spatial Sciences Curtin University Kent Street, Bentley Perth, Western Australia 6102 Australia Attn: Mr. Christopher Ndehedehe
Total	0.00 AUD

INTRODUCTION

1. The publisher for this copyrighted material is Elsevier. By clicking "accept" in connection with completing this licensing transaction, you agree that the following terms and conditions apply to this transaction (along with the Billing and Payment terms and conditions established by Copyright Clearance Center, Inc. ("CCC"), at the time that you opened your Rightslink account and that are available at any time at <http://myaccount.copyright.com>).

GENERAL TERMS

2. Elsevier hereby grants you permission to reproduce the aforementioned material subject to the terms and conditions indicated.

3. Acknowledgement: If any part of the material to be used (for example, figures) has appeared in our publication with credit or acknowledgement to another source, permission must also be sought from that source. If such permission is not obtained then that material may not be included in your publication/copies. Suitable acknowledgement to the source must be made, either as a footnote or in a reference list at the end of your publication, as follows:

"Reprinted from Publication title, Vol /edition number, Author(s), Title of article / title of chapter, Pages No., Copyright (Year), with permission from Elsevier [OR APPLICABLE SOCIETY COPYRIGHT OWNER]." Also Lancet special credit - "Reprinted from The Lancet, Vol. number, Author(s), Title of article, Pages No., Copyright (Year), with permission from Elsevier."

4. Reproduction of this material is confined to the purpose and/or media for which permission is hereby given.

5. Altering/Modifying Material: Not Permitted. However figures and illustrations may be altered/adapted minimally to serve your work. Any other abbreviations, additions, deletions and/or any other alterations shall be made only with prior written authorization of Elsevier Ltd. (Please contact Elsevier at permissions@elsevier.com). No modifications can be made to any Lancet figures/tables and they must be reproduced in full.

6. If the permission fee for the requested use of our material is waived in this instance, please be advised that your future requests for Elsevier materials may attract a fee.

7. Reservation of Rights: Publisher reserves all rights not specifically granted in the combination of (i) the license details provided by you and accepted in the course of this licensing transaction, (ii) these terms and conditions and (iii) CCC's Billing and Payment terms and conditions.

8. License Contingent Upon Payment: While you may exercise the rights licensed immediately upon issuance of the license at the end of the licensing process for the transaction, provided that you have disclosed complete and accurate details of your proposed use, no license is finally effective unless and until full payment is received from you (either by publisher or by CCC) as provided in CCC's Billing and Payment terms and conditions. If full payment is not received on a timely basis, then any license preliminarily granted shall be deemed automatically revoked and shall be void as if never granted. Further, in the event that you breach any of these terms and conditions or any of CCC's Billing and Payment terms and conditions, the license is automatically revoked and shall be void as if never granted. Use of materials as described in a revoked license, as well as any use of the materials beyond the scope of an unrevoked license, may constitute copyright infringement and publisher reserves the right to take any and all action to protect its copyright in the materials.

9. Warranties: Publisher makes no representations or warranties with respect to the

licensed material.

10. **Indemnity:** You hereby indemnify and agree to hold harmless publisher and CCC, and their respective officers, directors, employees and agents, from and against any and all claims arising out of your use of the licensed material other than as specifically authorized pursuant to this license.

11. **No Transfer of License:** This license is personal to you and may not be sublicensed, assigned, or transferred by you to any other person without publisher's written permission.

12. **No Amendment Except in Writing:** This license may not be amended except in a writing signed by both parties (or, in the case of publisher, by CCC on publisher's behalf).

13. **Objection to Contrary Terms:** Publisher hereby objects to any terms contained in any purchase order, acknowledgment, check endorsement or other writing prepared by you, which terms are inconsistent with these terms and conditions or CCC's Billing and Payment terms and conditions. These terms and conditions, together with CCC's Billing and Payment terms and conditions (which are incorporated herein), comprise the entire agreement between you and publisher (and CCC) concerning this licensing transaction. In the event of any conflict between your obligations established by these terms and conditions and those established by CCC's Billing and Payment terms and conditions, these terms and conditions shall control.

14. **Revocation:** Elsevier or Copyright Clearance Center may deny the permissions described in this License at their sole discretion, for any reason or no reason, with a full refund payable to you. Notice of such denial will be made using the contact information provided by you. Failure to receive such notice will not alter or invalidate the denial. In no event will Elsevier or Copyright Clearance Center be responsible or liable for any costs, expenses or damage incurred by you as a result of a denial of your permission request, other than a refund of the amount(s) paid by you to Elsevier and/or Copyright Clearance Center for denied permissions.

LIMITED LICENSE

The following terms and conditions apply only to specific license types:

15. **Translation:** This permission is granted for non-exclusive world **English** rights only unless your license was granted for translation rights. If you licensed translation rights you may only translate this content into the languages you requested. A professional translator must perform all translations and reproduce the content word for word preserving the integrity of the article.

16. **Posting licensed content on any Website:** The following terms and conditions apply as follows: Licensing material from an Elsevier journal: All content posted to the web site must maintain the copyright information line on the bottom of each image; A hyper-text must be included to the Homepage of the journal from which you are licensing at <http://www.sciencedirect.com/science/journal/xxxxx> or the Elsevier homepage for books at <http://www.elsevier.com>; Central Storage: This license does not include permission for a scanned version of the material to be stored in a central repository such as that provided by Heron/XanEdu.

Licensing material from an Elsevier book: A hyper-text link must be included to the Elsevier homepage at <http://www.elsevier.com>. All content posted to the web site must maintain the copyright information line on the bottom of each image.

Posting licensed content on Electronic reserve: In addition to the above the following clauses are applicable: The web site must be password-protected and made available only to bona fide students registered on a relevant course. This permission is granted for 1 year only. You may obtain a new license for future website posting.

17. **For journal authors:** the following clauses are applicable in addition to the above:

Preprints:

A preprint is an author's own write-up of research results and analysis, it has not been peer-reviewed, nor has it had any other value added to it by a publisher (such as formatting, copyright, technical enhancement etc.).

Authors can share their preprints anywhere at any time. Preprints should not be added to or enhanced in any way in order to appear more like, or to substitute for, the final versions of articles however authors can update their preprints on arXiv or RePEc with their Accepted Author Manuscript (see below).

If accepted for publication, we encourage authors to link from the preprint to their formal publication via its DOI. Millions of researchers have access to the formal publications on ScienceDirect, and so links will help users to find, access, cite and use the best available version. Please note that Cell Press, The Lancet and some society-owned have different preprint policies. Information on these policies is available on the journal homepage.

Accepted Author Manuscripts: An accepted author manuscript is the manuscript of an article that has been accepted for publication and which typically includes author-incorporated changes suggested during submission, peer review and editor-author communications.

Authors can share their accepted author manuscript:

- immediately
 - via their non-commercial person homepage or blog
 - by updating a preprint in arXiv or RePEc with the accepted manuscript
 - via their research institute or institutional repository for internal institutional uses or as part of an invitation-only research collaboration work-group
 - directly by providing copies to their students or to research collaborators for their personal use
 - for private scholarly sharing as part of an invitation-only work group on commercial sites with which Elsevier has an agreement
- After the embargo period
 - via non-commercial hosting platforms such as their institutional repository
 - via commercial sites with which Elsevier has an agreement

In all cases accepted manuscripts should:

- link to the formal publication via its DOI
- bear a CC-BY-NC-ND license - this is easy to do
- if aggregated with other manuscripts, for example in a repository or other site, be shared in alignment with our hosting policy not be added to or enhanced in any way to appear more like, or to substitute for, the published journal article.

Published journal article (JPA): A published journal article (PJA) is the definitive final record of published research that appears or will appear in the journal and embodies all value-adding publishing activities including peer review co-ordination, copy-editing, formatting, (if relevant) pagination and online enrichment.

Policies for sharing publishing journal articles differ for subscription and gold open access articles:

Subscription Articles: If you are an author, please share a link to your article rather than the full-text. Millions of researchers have access to the formal publications on ScienceDirect, and so links will help your users to find, access, cite, and use the best

available version.

Theses and dissertations which contain embedded PJAs as part of the formal submission can be posted publicly by the awarding institution with DOI links back to the formal publications on ScienceDirect.

If you are affiliated with a library that subscribes to ScienceDirect you have additional private sharing rights for others' research accessed under that agreement. This includes use for classroom teaching and internal training at the institution (including use in course packs and courseware programs), and inclusion of the article for grant funding purposes.

Gold Open Access Articles: May be shared according to the author-selected end-user license and should contain a [CrossMark logo](#), the end user license, and a DOI link to the formal publication on ScienceDirect.

Please refer to Elsevier's [posting policy](#) for further information.

18. **For book authors** the following clauses are applicable in addition to the above: Authors are permitted to place a brief summary of their work online only. You are not allowed to download and post the published electronic version of your chapter, nor may you scan the printed edition to create an electronic version. **Posting to a repository:** Authors are permitted to post a summary of their chapter only in their institution's repository.

19. **Thesis/Dissertation:** If your license is for use in a thesis/dissertation your thesis may be submitted to your institution in either print or electronic form. Should your thesis be published commercially, please reapply for permission. These requirements include permission for the Library and Archives of Canada to supply single copies, on demand, of the complete thesis and include permission for Proquest/UMI to supply single copies, on demand, of the complete thesis. Should your thesis be published commercially, please reapply for permission. Theses and dissertations which contain embedded PJAs as part of the formal submission can be posted publicly by the awarding institution with DOI links back to the formal publications on ScienceDirect.

Elsevier Open Access Terms and Conditions

You can publish open access with Elsevier in hundreds of open access journals or in nearly 2000 established subscription journals that support open access publishing. Permitted third party re-use of these open access articles is defined by the author's choice of Creative Commons user license. See our [open access license policy](#) for more information.

Terms & Conditions applicable to all Open Access articles published with Elsevier:

Any reuse of the article must not represent the author as endorsing the adaptation of the article nor should the article be modified in such a way as to damage the author's honour or reputation. If any changes have been made, such changes must be clearly indicated. The author(s) must be appropriately credited and we ask that you include the end user license and a DOI link to the formal publication on ScienceDirect.

If any part of the material to be used (for example, figures) has appeared in our publication with credit or acknowledgement to another source it is the responsibility of the user to ensure their reuse complies with the terms and conditions determined by the rights holder.

Additional Terms & Conditions applicable to each Creative Commons user license:

CC BY: The CC-BY license allows users to copy, to create extracts, abstracts and new works from the Article, to alter and revise the Article and to make commercial use of the Article (including reuse and/or resale of the Article by commercial entities), provided the user gives appropriate credit (with a link to the formal publication through the relevant DOI), provides a link to the license, indicates if changes were made and the licensor is not

represented as endorsing the use made of the work. The full details of the license are available at <http://creativecommons.org/licenses/by/4.0>.

CC BY NC SA: The CC BY-NC-SA license allows users to copy, to create extracts, abstracts and new works from the Article, to alter and revise the Article, provided this is not done for commercial purposes, and that the user gives appropriate credit (with a link to the formal publication through the relevant DOI), provides a link to the license, indicates if changes were made and the licensor is not represented as endorsing the use made of the work. Further, any new works must be made available on the same conditions. The full details of the license are available at <http://creativecommons.org/licenses/by-nc-sa/4.0>.

CC BY NC ND: The CC BY-NC-ND license allows users to copy and distribute the Article, provided this is not done for commercial purposes and further does not permit distribution of the Article if it is changed or edited in any way, and provided the user gives appropriate credit (with a link to the formal publication through the relevant DOI), provides a link to the license, and that the licensor is not represented as endorsing the use made of the work. The full details of the license are available at <http://creativecommons.org/licenses/by-nc-nd/4.0>. Any commercial reuse of Open Access articles published with a CC BY NC SA or CC BY NC ND license requires permission from Elsevier and will be subject to a fee.

Commercial reuse includes:

- Associating advertising with the full text of the Article
- Charging fees for document delivery or access
- Article aggregation
- Systematic distribution via e-mail lists or share buttons

Posting or linking by commercial companies for use by customers of those companies.

20. Other Conditions:

v1.9

Questions? customer@copyright.com or +1-855-239-3415 (toll free in the US) or +1-978-646-2777.

**JOHN WILEY AND SONS LICENSE
TERMS AND CONDITIONS**

Sep 03, 2017

290

This Agreement between Mr. Christopher Ndehedehe ("You") and John Wiley and Sons ("John Wiley and Sons") consists of your license details and the terms and conditions provided by John Wiley and Sons and Copyright Clearance Center.

License Number	4181460239921
License date	Sep 03, 2017
Licensed Content Publisher	John Wiley and Sons
Licensed Content Publication	Hydrological Processes
Licensed Content Title	Climate teleconnections influence on West Africa's terrestrial water storage
Licensed Content Author	Christopher E. Ndehedehe, Joseph L. Awange, Michael Kuhn, Nathan O. Agutu, Yoichi Fukuda
Licensed Content Date	Jul 21, 2017
Licensed Content Pages	19
Type of use	Dissertation/Thesis
Requestor type	Author of this Wiley article
Format	Print and electronic
Portion	Full article
Will you be translating?	No
Title of your thesis / dissertation	Remote Sensing of West Africa's Water Resources Using Multi-Satellites and Models
Expected completion date	Aug 2017
Expected size (number of pages)	270
Requestor Location	Mr. Christopher Ndehedehe Department of Spatial Sciences Curtin University Kent Street, Bentley Perth, Western Australia 6102 Australia Attn: Mr. Christopher Ndehedehe
Publisher Tax ID	EU826007151
Billing Type	Invoice
Billing Address	Mr. Christopher Ndehedehe Department of Spatial Sciences Curtin University Kent Street, Bentley Perth, Australia 6102 Attn: Mr. Christopher Ndehedehe
Total	0.00 AUD
Terms and Conditions	

TERMS AND CONDITIONS

This copyrighted material is owned by or exclusively licensed to John Wiley & Sons, Inc. or one of its group companies (each a "Wiley Company") or handled on behalf of a society with which a Wiley Company has exclusive publishing rights in relation to a particular work (collectively "WILEY"). By clicking "accept" in connection with completing this licensing transaction, you agree that the following terms and conditions apply to this transaction

(along with the billing and payment terms and conditions established by the Copyright Clearance Center Inc., ("CCC's Billing and Payment terms and conditions"), at the time that you opened your RightsLink account (these are available at any time at <http://myaccount.copyright.com>).

Terms and Conditions

- The materials you have requested permission to reproduce or reuse (the "Wiley Materials") are protected by copyright.
- You are hereby granted a personal, non-exclusive, non-sub licensable (on a stand-alone basis), non-transferable, worldwide, limited license to reproduce the Wiley Materials for the purpose specified in the licensing process. This license, **and any CONTENT (PDF or image file) purchased as part of your order**, is for a one-time use only and limited to any maximum distribution number specified in the license. The first instance of republication or reuse granted by this license must be completed within two years of the date of the grant of this license (although copies prepared before the end date may be distributed thereafter). The Wiley Materials shall not be used in any other manner or for any other purpose, beyond what is granted in the license. Permission is granted subject to an appropriate acknowledgement given to the author, title of the material/book/journal and the publisher. You shall also duplicate the copyright notice that appears in the Wiley publication in your use of the Wiley Material. Permission is also granted on the understanding that nowhere in the text is a previously published source acknowledged for all or part of this Wiley Material. Any third party content is expressly excluded from this permission.
- With respect to the Wiley Materials, all rights are reserved. Except as expressly granted by the terms of the license, no part of the Wiley Materials may be copied, modified, adapted (except for minor reformatting required by the new Publication), translated, reproduced, transferred or distributed, in any form or by any means, and no derivative works may be made based on the Wiley Materials without the prior permission of the respective copyright owner. **For STM Signatory Publishers clearing permission under the terms of the [STM Permissions Guidelines](#) only, the terms of the license are extended to include subsequent editions and for editions in other languages, provided such editions are for the work as a whole in situ and does not involve the separate exploitation of the permitted figures or extracts,** You may not alter, remove or suppress in any manner any copyright, trademark or other notices displayed by the Wiley Materials. You may not license, rent, sell, loan, lease, pledge, offer as security, transfer or assign the Wiley Materials on a stand-alone basis, or any of the rights granted to you hereunder to any other person.
- The Wiley Materials and all of the intellectual property rights therein shall at all times remain the exclusive property of John Wiley & Sons Inc, the Wiley Companies, or their respective licensors, and your interest therein is only that of having possession of and the right to reproduce the Wiley Materials pursuant to Section 2 herein during the continuance of this Agreement. You agree that you own no right, title or interest in or to the Wiley Materials or any of the intellectual property rights therein. You shall have no rights hereunder other than the license as provided for above in Section 2. No right, license or interest to any trademark, trade name, service mark or other branding ("Marks") of WILEY or its licensors is granted hereunder, and you agree that you shall not assert any such right, license or interest with respect thereto
- NEITHER WILEY NOR ITS LICENSORS MAKES ANY WARRANTY OR REPRESENTATION OF ANY KIND TO YOU OR ANY THIRD PARTY, EXPRESS, IMPLIED OR STATUTORY, WITH RESPECT TO THE MATERIALS OR THE ACCURACY OF ANY INFORMATION CONTAINED IN THE MATERIALS, INCLUDING, WITHOUT LIMITATION, ANY IMPLIED WARRANTY OF MERCHANTABILITY, ACCURACY, SATISFACTORY

QUALITY, FITNESS FOR A PARTICULAR PURPOSE, USABILITY, INTEGRATION OR NON-INFRINGEMENT AND ALL SUCH WARRANTIES ARE HEREBY EXCLUDED BY WILEY AND ITS LICENSORS AND WAIVED BY YOU.

- WILEY shall have the right to terminate this Agreement immediately upon breach of this Agreement by you.
- You shall indemnify, defend and hold harmless WILEY, its Licensors and their respective directors, officers, agents and employees, from and against any actual or threatened claims, demands, causes of action or proceedings arising from any breach of this Agreement by you.
- IN NO EVENT SHALL WILEY OR ITS LICENSORS BE LIABLE TO YOU OR ANY OTHER PARTY OR ANY OTHER PERSON OR ENTITY FOR ANY SPECIAL, CONSEQUENTIAL, INCIDENTAL, INDIRECT, EXEMPLARY OR PUNITIVE DAMAGES, HOWEVER CAUSED, ARISING OUT OF OR IN CONNECTION WITH THE DOWNLOADING, PROVISIONING, VIEWING OR USE OF THE MATERIALS REGARDLESS OF THE FORM OF ACTION, WHETHER FOR BREACH OF CONTRACT, BREACH OF WARRANTY, TORT, NEGLIGENCE, INFRINGEMENT OR OTHERWISE (INCLUDING, WITHOUT LIMITATION, DAMAGES BASED ON LOSS OF PROFITS, DATA, FILES, USE, BUSINESS OPPORTUNITY OR CLAIMS OF THIRD PARTIES), AND WHETHER OR NOT THE PARTY HAS BEEN ADVISED OF THE POSSIBILITY OF SUCH DAMAGES. THIS LIMITATION SHALL APPLY NOTWITHSTANDING ANY FAILURE OF ESSENTIAL PURPOSE OF ANY LIMITED REMEDY PROVIDED HEREIN.
- Should any provision of this Agreement be held by a court of competent jurisdiction to be illegal, invalid, or unenforceable, that provision shall be deemed amended to achieve as nearly as possible the same economic effect as the original provision, and the legality, validity and enforceability of the remaining provisions of this Agreement shall not be affected or impaired thereby.
- The failure of either party to enforce any term or condition of this Agreement shall not constitute a waiver of either party's right to enforce each and every term and condition of this Agreement. No breach under this agreement shall be deemed waived or excused by either party unless such waiver or consent is in writing signed by the party granting such waiver or consent. The waiver by or consent of a party to a breach of any provision of this Agreement shall not operate or be construed as a waiver of or consent to any other or subsequent breach by such other party.
- This Agreement may not be assigned (including by operation of law or otherwise) by you without WILEY's prior written consent.
- Any fee required for this permission shall be non-refundable after thirty (30) days from receipt by the CCC.
- These terms and conditions together with CCC's Billing and Payment terms and conditions (which are incorporated herein) form the entire agreement between you and WILEY concerning this licensing transaction and (in the absence of fraud) supersedes all prior agreements and representations of the parties, oral or written. This Agreement may not be amended except in writing signed by both parties. This Agreement shall be binding upon and inure to the benefit of the parties' successors, legal representatives, and authorized assigns.
- In the event of any conflict between your obligations established by these terms and conditions and those established by CCC's Billing and Payment terms and conditions,

these terms and conditions shall prevail.

293

- WILEY expressly reserves all rights not specifically granted in the combination of (i) the license details provided by you and accepted in the course of this licensing transaction, (ii) these terms and conditions and (iii) CCC's Billing and Payment terms and conditions.
- This Agreement will be void if the Type of Use, Format, Circulation, or Requestor Type was misrepresented during the licensing process.
- This Agreement shall be governed by and construed in accordance with the laws of the State of New York, USA, without regards to such state's conflict of law rules. Any legal action, suit or proceeding arising out of or relating to these Terms and Conditions or the breach thereof shall be instituted in a court of competent jurisdiction in New York County in the State of New York in the United States of America and each party hereby consents and submits to the personal jurisdiction of such court, waives any objection to venue in such court and consents to service of process by registered or certified mail, return receipt requested, at the last known address of such party.

WILEY OPEN ACCESS TERMS AND CONDITIONS

Wiley Publishes Open Access Articles in fully Open Access Journals and in Subscription journals offering Online Open. Although most of the fully Open Access journals publish open access articles under the terms of the Creative Commons Attribution (CC BY) License only, the subscription journals and a few of the Open Access Journals offer a choice of Creative Commons Licenses. The license type is clearly identified on the article.

The Creative Commons Attribution License

The [Creative Commons Attribution License \(CC-BY\)](#) allows users to copy, distribute and transmit an article, adapt the article and make commercial use of the article. The CC-BY license permits commercial and non-

Creative Commons Attribution Non-Commercial License

The [Creative Commons Attribution Non-Commercial \(CC-BY-NC\) License](#) permits use, distribution and reproduction in any medium, provided the original work is properly cited and is not used for commercial purposes.(see below)

Creative Commons Attribution-Non-Commercial-NoDerivs License

The [Creative Commons Attribution Non-Commercial-NoDerivs License](#) (CC-BY-NC-ND) permits use, distribution and reproduction in any medium, provided the original work is properly cited, is not used for commercial purposes and no modifications or adaptations are made. (see below)

Use by commercial "for-profit" organizations

Use of Wiley Open Access articles for commercial, promotional, or marketing purposes requires further explicit permission from Wiley and will be subject to a fee.

Further details can be found on Wiley Online Library

<http://olabout.wiley.com/WileyCDA/Section/id-410895.html>

Other Terms and Conditions:

v1.10 Last updated September 2015

Questions? customercare@copyright.com or +1-855-239-3415 (toll free in the US) or +1-978-646-2777.

Appendix B Statements of contribution by others

This thesis consists of eight peer-reviewed journal papers (please note that from the list below, the revised versions of paper 3 is currently under review in *Global and Planetary Change* while paper 7 has been submitted to *Journal of Arid Environments*). Here, the author and coauthor's contributions for all of these papers are indicated.

To Whom It May Concern,

I, Christopher E. Ndehedehe, designed the study, built the analytical framework, processed the data using my own software/algorithm, interpreted the numerical results, and wrote the entire manuscripts. Others (supervisors-A/Prof Joseph Awange and Dr Robert Corner; collaborators-Prof. Bernhard Heck and Yoichi Fukuda, A/Prof. Michael Kuhn and Vagner G. Ferreira, Dr Onuwa Okwuashi, and Nathan Agutu) provided technical comments that improved the quality of the manuscripts and proof read some of the papers before a final submission for peer-review. All of the above hold for the following publications listed below (papers 1-7);

- (1) **Christopher Ndehedehe**, Joseph Awange, Nathan Agutu, Michael Kuhn, and Bernhard Heck (2016). Understanding changes in terrestrial water storage over West Africa between 2002 and 2014. *Advances in Water Resources*, 88, 211–230, dx.doi.org/10.1016/j.advwatres.2015.12.009.
- (2) **Christopher E. Ndehedehe**, Joseph Awange, Michael Kuhn, Nathan Agutu, and Yoichi Fukuda (2017). Influence of climate teleconnections on West Africa's terrestrial water storage. *Hydrological Processes*, 31(18), 3206–3224, dx.doi.org/10.1002/hyp.11237.
- (3) **Christopher E. Ndehedehe**, Joseph L. Awange, Nathan O. Agutu, and Onuwa Okwuashi (2017). Changes in hydro-meteorological conditions over Sub-Saharan Africa (1980 – 2015) and links to global climate. *Revised and resubmitted to Global and Planetary Change*.
- (4) **Christopher E. Ndehedehe**, Joseph L. Awange, Michael Kuhn, Nathan O. Agutu, and Yoichi Fukuda (2017). Analysis of hydrological variability over the Volta river basin using in-situ data and satellite observations. *Journal of Hydrology: Regional Studies*, 12, 88–110, dx.doi.org/10.1016/j.ejrh.2017.04.005.
- (5) **Christopher E. Ndehedehe**, Nathan Agutu, Onuwa Okwuashi, Vagner G.

Ferreira (2016). Spatio-temporal variability of droughts and terrestrial water storage over Lake Chad Basin using independent component analysis. *Journal of Hydrology*, 540, 106 – 128, dx.doi.org/10.1016/j.jhydrol.2016.05.068.

- (6) **Christopher E. Ndehedehe**, Joseph L. Awange, Robert J. Corner, Michael Kuhn and Onuwa Okwuashi (2016). On the potentials of multiple climate variables in assessing the spatio-temporal characteristics of hydrological droughts over the Volta Basin. *Science of the Total Environment*, 557 – 558, 819 – 837, dx.doi.org/10/.1016/j.scitotenv.2016.03.004.
- (7) **Christopher E. Ndehedehe**, Joseph L. Awange, Michael Kuhn, and Nathan O. Agutu (2017). Hydrological controls on surface vegetation dynamics over Sub-Sahara Africa using GRACE satellite Observations. *Revised and submitted to Journal of Arid Environments*.

And, I, Christopher E. Ndehedehe, wrote some parts of the manuscript, proof read and edited the whole manuscript, and provided some technical contributions and interpretations that improved the quality of the manuscript. The first author, Dr S.A. Andam-Akorful, did the computations, interpreted a considerable part of the results, and wrote most parts of the manuscripts while the second author, A/Prof V.G. Ferreira, designed the study and also contributed to numerical results. The fourth author, Dr. J.A. Quaye-Ballard, provided comments that improved the manuscript only during the first and second rounds of revision before a final re-submission. This applies to the publication below (paper 8);

- (8) S.A. Andam-Akorful, V.G. Ferreira **C.E. Ndehedehe** & J.A. Quaye-Ballard (2017). An investigation into the freshwater variability in West Africa during 1979–2010. *International Journal of Climatology*, 37(S1), 333–349, dx.doi.org/10.1002/joc.5006.

Christopher E. Ndehedehe _____

I, as a Co-Author, endorse that this level of contribution by the candidate indicated above is appropriate

Joseph L. Awange _____

Michael Kuhn _____

Bernhard Heck _____

Yoichi Fukuda _____

V.G. Ferreira _____

Robert J. Corner _____

Onuwa Okwuashi _____

S.A. Andam-Akorful _____

J.A. Quaye-Ballard _____

Nathan O. Agutu _____

List of Figures

1.1	The spatial and temporal changes of Lake Chad’s surface area as shown by Landsat imageries for 1973, 1987, 2003, and 2013. The blue lines on the map (left) show the river networks within the basin. The present Lake Chad shows two segmented pools with the northern pool completely dried up during drought periods (right). Map is adapted from Ndehedehe et al. (2016b).	11
-----	--	----

List of Tables

1.1	Published peer-reviewed journal papers (i.e., during the candidature) adapted for the thesis and the respective chapters and thesis objectives they cover. The full bibliographic details of all papers have been provided in the list of publications above.	21
-----	---	----